THE INFLUENCE OF SEDIMENT BUDGET ON GEOMORPHIC ACTIVITY OF THE TASMAN GLACIER, MOUNT COOK NATIONAL PARK, NEW ZEALAND.

A thesis submitted in partial fulfilment
of the requirements of the Degree of
Doctor of Philosophy

University of Canterbury

1989

Martin Kirkbride

FRONTISPIECE Detail of the lower Tasman Glacier in 1890, mapped by Thomas Brodrick. Note the surveyed ice levels, the extent of the debris cover, and the position of the terminus.

with 2 items in back pocket

ABSTRACT

Previous studies of sediment transport by valley glaciers have emphasised the dependence of rates of transport on glacier dynamics, in turn a function of climatic environment. Very few studies have considered cases where it is the debris in transport that plays a major role in affecting the dynamics of the glacier.

This study of the Tasman Glacier explains the interdependence of ice and debris fluxes in a tectonically-active maritime alpine environment. Glaciological monitoring has allowed the construction of a model of Twentieth-Century glacier behaviour. A model of medial moraine dynamics has been formulated from theoretical and empirical studies of debris in transport. Feedbacks between glacier flow structure, sediment routeways, supraglacial debris accumulation, ablation, glacier thickness and gradient have resulted in a positive sediment budget in the lower glacier and the growth of a 20 km^2 debris mantle. Insulation of underlying ice by the debris mantle has led to the preservation of a 7 km long ice tongue which would have ablated away within the last century without the protective mantle. The flow structure of the glacier has been radically affected by debris mantle spread and changes to the ablation gradient, causing slow downwasting and reduced surface gradient with no terminal retreat.

Studies of clast shape have revealed that much debris supplied to the terminus of the Tasman Glacier has been modified by water action rather than by glacial action. It is concluded that sediment transfer in the lower glacier is dominantly by fluvial transport in englacial conduits rather than by truely glacial transport. The implication is that much rounded debris found in older moraines was modified during high-level transport through the glacier.

Twentieth-Century negative mass balance has resulted in the formation of thermokarst lakes at valley glacier termini in the region. Growth and coalescence of these lakes has heralded the onset of the first phase of rapid terminal retreat for at least 5,000 years in the Godley Valley. Commencement of rapid retreat of the Tasman Glacier is imminent. The two-phase pattern of slow downwasting of debris-mantled glacier tongues followed by rapid retreat of a calving terminus with rapid glacio-lacustrine deposition provides an analogy to the mechanism of retreat from Late Pleistocene and early Holocene ice maxima. The size and persistence of the proglacial lakes allows them to act as major sediment traps. Their rapid formation during deglaciation marked an important

transition from net aggradation to net degradation of proglacial outwash plains at the end of the Pleistocene, leading to a phase of terrace-forming incision of rivers downstream of the lakes. The formation of similar lakes in front of the modern glaciers is in progress and may mark a comparable threshold in river regime.

Reconstructions of the Tasman Glacier have been made for various stages of the Neoglacial period. The implications of processes of ice ponding by an outwash head and preservation during negative balance phases over a 5,000 year period have been investigated. Neoglacial fluctuations are minor compared to nearby glaciers with no extensive supraglacial debris mantles. The terminus has become ponded behind an aggrading proglacial fan and resulting changes in the flow structure have increased the potential for supraglacial debris accumulation. The glacier terminus may have become progressively less sensitive to climatic oscillations since c.5,000 B.P. It is concluded that there has been a non-climatic evolution of glacier morphology due to feedbacks in the glacier-debris dynamic system.

It is concluded that in regions of high debris mass flux, glaciers of this type have complex responses to climatic change governed by lag responses and thresholds which are not controlled directly by climate. The strongly-positive sediment budgets in the lower parts of glaciers and in proglacial areas is a major cause of this complexity. Climatic interpretations of moraine sequences must therefore be made with caution.

TABLE OF CONTENTS.

CHAPTER 7: CONCLUSIONS AND OVERVIEW.

LIST OF FIGURES

LIST OF TABLES.

Chapter 2

Chapter 3

Chapter 4

Chapter 5

CHAPTER 1: INTRODUCTION.

1.1 OBJECTIVES AND SCOPE

The thesis is a study of the relationship of valley glaciers to the tectonic and climatic environment of the Southern Alps. Glacier volumes in general are responsive to climatic fluctuations operating over many timescales. Problems are associated with difficulties in the precise dating of former glacial, and therefore climatic, events. Glaciological attention has traditionally focused on the dynamics of modern glaciers and on their response to climatic impulses. More recently, the advent of numerical modelling has made possible advances in the field of palaeoglaciology. The traditional division between glacial geomorphologists and pure (theoretical) glaciologists is now being bridged by more integrated approaches to long-standing problems of landform development.

Tectonic influences on glacial processes have hardly been examined. Indeed, there is not even a methodological framework around which to work: tectonic geomorphology itself remains a young and rapidly-developing field. A major obstacle is presented by difficulties of separating tectonic influences from more immediately obvious climatically-induced influences on glaciers.

The scope of this thesis is to present a case study of a region for which a detailed chronology of glacier fluctuations spans c.12,000 years, and where the environment is tectonically active. This has not hitherto been considered as a possible factor in palaeoenvironmental interpretations of glacier fluctuations. As well as considering the possible tectonic influences, this study investigates the effects of high erosion rates and abundant debris production on the dynamics of valley glaciers, and thereby upon the geomorphic development of glacierized catchments.

The objectives of the study are the following:

1. to establish a dynamic model explaining the form and observed changes of the Tasman Glacier, particularly with respect to glacial debris transport;

2. to assess the role of modern valley glaciers on landform genesis in the Mount Cook region;

3. to interpret Holocene landform development in the light of present-day glacier dynamics;

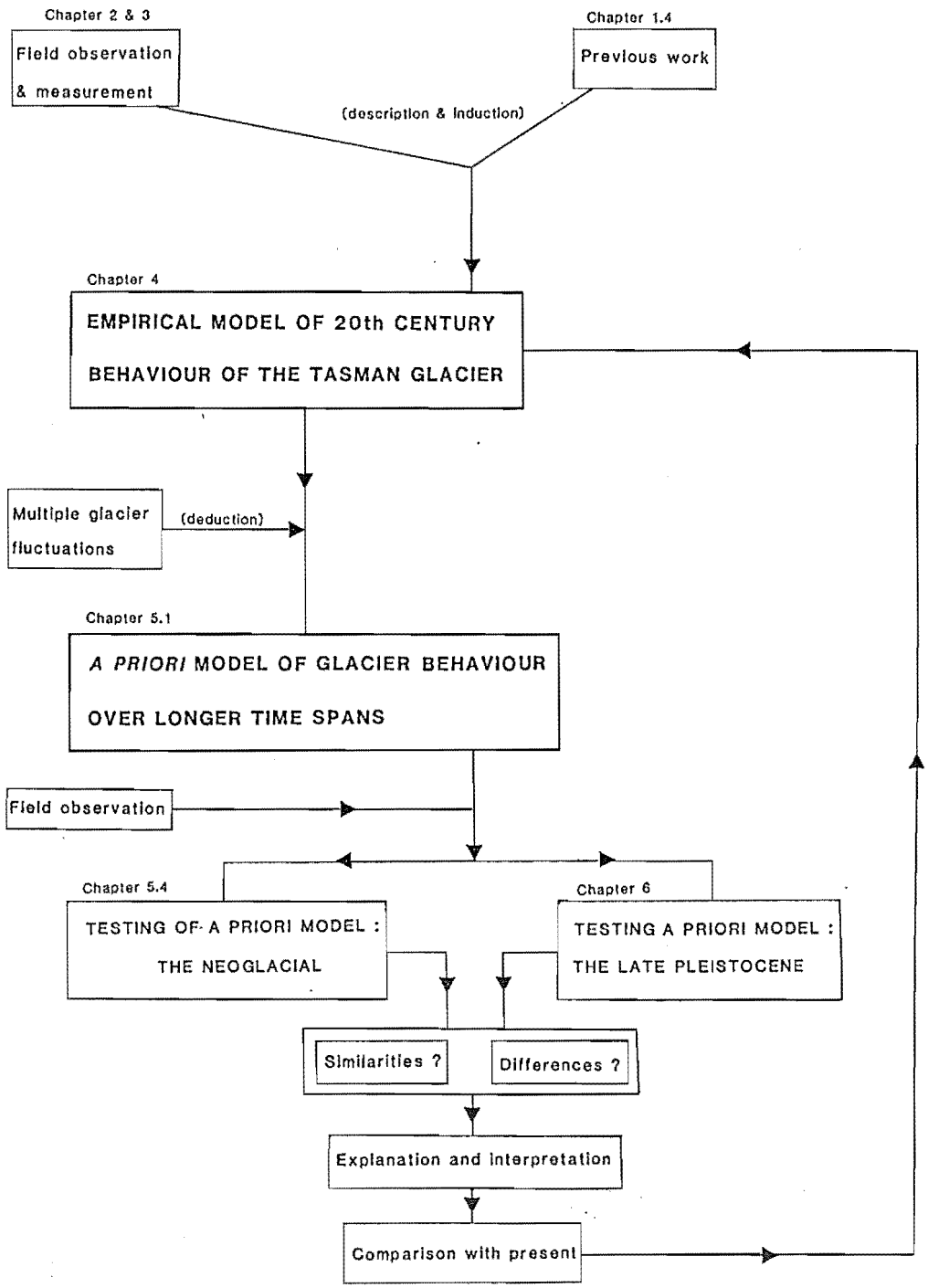

FIG. 1.1 Flow diagram of the structure of the thesis, and the applications of models on different timescales.

4. to assess the wider temporal and spatial context of observations made in the Mount Cook area.

1.2 THESIS STRUCTURE

The general structure of the thesis is based on the formulation of an empirical model of recent glacier behaviour, which later forms an a priori model for testing on two longer timescales (Fig 1.1). Inputs to the model are general: they are geological environment, climate, physical process, and time. These are discussed under Section 1.3 (Methodology). Emphasis is not shared equally between all timescales, but necessarily has an inverse relationship with time from the present, reflecting decreasing resolution of the model over time. The timescales on which testing is made are hierarchical, in that each depends on the results derived from preceding tests.

Initial investigation is directed to the formulation of an empirical model explaining the current morphology of Tasman Glacier in terms of its dynamics on a timescale of 10^2 years, a period corresponding to the period of scientific observation of the glacier. Chapters 2, 3, and 4 formulate this model.

Chapter 2 (Glaciology) presents information on the flow and mass balance of the Tasman Glacier, to quantify the ice mass flux. Particular emphasis is placed on the ablation zone.

Chapter 3 is a study of the debris transport system of the Tasman Glacier, dealing in turn with the sources, transport paths, quantitative flux, and sedimentological modification of debris in the glacier system. Information from other glaciers in the area is used to supplement that from Tasman Glacier.

Chapter 4 synthesises glaciological and debris transport information to establish a behavioural model. The first half of the chapter deals with conditions favouring formation of a supraglacial debris mantle: the second half describes the processes of destruction of the debris-mantled glacier tongue under negative mass balance conditions.

The next two chapters test the model of glacier behaviour over longer timescales.

Chapter 5 formulates an a priori model for multiple glacier fluctuations, extending the empirical model of Chapter 4. The behaviour of the glacier during the Neoglacial period (c.5,000 BP to the present) is predicted from the a priori model, and tested using glacial geological

evidence. The recent behaviour of the glacier is thereby placed in the broader temporal context of the last 5,000 years.

Chapter 6 applies the a **priori** model to a 10^4 year timescale, corresponding to the Late Pleistocene period. Again, the predicted behaviour of the glacier is tested using available glacial geological evidence. Deviations from the predicted behaviour are discussed in terms of the model inputs.

Chapter 7 concludes the thesis with a discussion of the role played by both climatic change and by tectonic factors on the glacier dynamic system over different timescales. The main conclusions are presented and directions for further research suggested.

1.3 METHODOLOGY

The response of glaciers to mass-balance change is magnified with distance towards the terminus, so that relatively small changes in accumulation cause relatively large volume changes in the lower parts of a glacier (Paterson 1981: Ch 12). Evidence of former mass-balance change is therefore commonly sought in depositional landforms around the margins of ablation zones. Examination of ablation-zone processes is therefore the focus of the thesis, as demanded by the methodological framework.

In the model of glacier behaviour, the glacier dimensions (volume and morphology) and mass flux are the outputs. The inputs are environmental parameters of geology (lithology, tectonics and structure) and climate (temperature and precipitation regimes) which interact to give the topography and glaciological environment (Andrews 1972; Golubev & Kotlyakov 1978) of the field area.

This methodological framework reduces the complexities of the real world to a small number of variables and invariate conditions. Climate varies spatially between the windward and leeward flanks of the Southern Alps, and on timescales (relevant to this study) between hours and millenia. Geological variability is less tangible: spatial variability is expressed as variability in lithology and rock mass strength; temporal variability as changes in regional stress, strain, and uplift rates. Geological change is so much slower that, within the time constraints of the study, the geological input is treated as a fixed (steady-state) environmental condition. The study therefore focuses on climatically-induced effects within a prescribed lithological and tectonic setting.

Given the aims of the study, the purpose of the model is mainly

explanatory. The resolution and potential applicability of the model decreases with time from the present day. This is due partly to the decreasing availability of detailed information of glacier dynamics, and partly to the changing input conditions on which the model is based. The quality of data sources is important. At each timescale, available data sources are summarised:

1. Current behaviour of Tasman Glacier. Measurements of glacier activity made within the last century are synthesised into a model of Twentieth-Century glacier dynamics, within known environmental conditions. Data sources are direct measurement, verbal and graphical description, and remote measurement from aerial photographs. Information about rates of process activity is available, and data are sufficiently detailed to enable the formulation of a rigorous empirically-based model.

2. The Neoglacial period. The extension of the model of current behaviour to the longer timescale aims to explain and interpret the significance of Neoglacial glacier fluctuations. Data sources are landform characteristics, distribution, and absolute and relative dating of till deposits. Information on process rate may be inferred from proxy data and by analogy. Resolution of the model is therefore moderate.

3. The Late Pleistocene. The application of the model to earlier sediment-landform associations aims to aid the interpretation of glacier fluctuations and their effect on landform evolution. Data sources are landform distribution and description, and model resolution is relatively very poor.

A dynamic approach to landform evolution has advantages over previous studies of glacial history in the region. There is potential for accounting for the sensitivity of individual glaciers to environmental change (Brunsden & Thornes 1979). Individual response and relaxation paths may be inferred. Previous work has commonly assumed a very direct and simple climate-glacier link. In other areas of geomorphology, a growing awareness of intrinsic and extrinsic threshold conditions (Schumm 1979) has resulted in a re-evaluation of many climate-landform relationships. This poses the question of whether or not the glacial environment may also, in some cases at least, exhibit a similar complexity if approached with an appropriate method.

A sediment budget approach is adopted as an appropriate framework to place an emphasis on debris transport, as much as on glacier dynamics. The concept of a budget implies a system of inputs, throughputs (flux), and outputs. Several routeways through the system are possible, as well as

storages within the system. The structure of Chapters 2 and 3 derives from the systems approach, whereas Chapters 4 onward deal with the consequences of the system rather than with its component parts. The budget theme is not applied rigorously, with quantification at all stages. Rather it acts as a framework to give structure and direction to the thesis.

1.4 LITERATURE REVIEW

The purpose of this review is to critically appraise the current state of knowledge of the origins, character, transport processes and glaciological effects of glacially-transported debris. A strong emphasis is placed on debris in the high-level transport zone (sensu Boulton & Eyles 1979), and secondarily on basal transport, rather than on glacial deposits, for which an extensive literature and many detailed reviews already exist (eg. Goldthwait 1975; Dreimanis 1976; Schluchter 1979; Evenson et al 1983; Eyles 1979, 1983; Dreimanis 1989).

The review is restricted to work directly concerned with the relationships between debris in transport and glacier ice. The literature is large, and for the sake of coherence some topics are reviewed in detail in relevent chapters of the thesis rather than in this section. Mention of this is made at the relevent points in this review.

1.4.1 Motivation for the study of debris transport

Interest in glacially-transported debris stems from the earliest studies of glaciers themselves. The statement of Agassiz (1840: p.55) that;

"Up to the present they (moraines) have not been paid the attention they deserve and have been mentioned only incidentally in most of the published works"

may still hold true, even though his assertion that;

"...they constitute the most important feature of glaciers"

will appeal more to the modern glacial geologist than to the pure glaciologist.

Attention has focused on glacial debris in transport for several reasons. Early interest developed in the Nineteenth Century before direct measurements of ice flow had been made. Supraglacial debris was used by several early glaciologists to interpret the flow pattern of glaciers. De Saussure (cited in Agassiz 1840) believed medial moraines were

concentrations of debris formed by ice flow towards the centre of glaciers. Agassiz (1840) criticised this interpretation, recognising that medial moraines formed at ice-stream confluences, but interpreted their gradual downglacier merging with lateral moraines as indicative of greater velocity at the glacier margins than along the centre. Direct measurement of ice flow eventually corrected these misunderstandings.

Toward the end of the Nineteenth Century, exploration of Alaska and the Yukon Territories lead to the discovery of many large glaciers with extensive covers of supraglacial debris. These glaciers became modern analogues for the stagnation, melt-out of debris, and decay of the margins of the Laurentide ice sheet, a topic attracting considerable attention over a period of several decades (eg. Russell 1892; Salisbury 1894; Tarr & Martin 1914; Flint 1929, 1942; Ray 1935; Flint & Demorest 1942; 1943; Sharp 1948, 1949; Hartshorn 1952; Gravenor & Kupsch 1959; Clayton 1964, 1967).

Subsequent interest in supraglacial debris has been relatively minor, perhaps because glaciological interest shifted emphasis to problems of ice dynamics and subglacial processes. In two areas of research has an interest in supraglacial debris been maintained. First, studies of medial moraines (Loomis 1970; Small & Clark 1974; Eyles & Rogerson 1977, 1978a, b; Small et al 1979; Gomez & Small 1986) and lateral moraines (Small 1983) have been concerned with controls of moraine form. Second, the scientific exploration of the glaciers of Asia has created a new interest in the debris covers of valley glaciers in that region (Kick 1962, 1985, 1986; Kraus 1966; Nakawo 1979; Yafeng 1980; Nakawo et al 1986; Wanatabe et al 1986; Bozhinskiy et al 1986).

Occasions have arisen where economic use of glacierized catchments has necessitated an understanding of sediment dynamics. Classical Norwegian work was inspired by a need to investigate the lifespan of turbines for hydro-electric power generation. Measurement of sediment transport by glacial outwash (Østrem 1975) has provided valuable information about subglacial erosion rates and sediment production (Kjeldsen 1981, cited in Drewry 1986; Hooke et al 1985). Similar studies have been carried out elsewhere in Norway (Liestol 1967; Corbel 1962; Rekstad 1911-1912, all cited in Drewry 1986), in the USSR (Chernova 1981), in Iceland (Boulton 1974), in Alaska (Corbel 1962, cited in Drewry 1986), and in New Zealand (Hicks et al, in press). In heavily glacierized regions, glacial deposits have been used as indicators of mineral provenance. The reconstuction of glacier flowlines to identify debris sources is the basis of these studies

(eg Stephens et al 1983). In the Caucasus, Bozhinskiy et al (1986) investigated the dynamics of a supraglacial debris mantle with a view to artificially controlling glacier run-off for irrigation purposes.

Academic interest in glacial transport and erosion rates has resulted in concentrated study when economic incentives have existed for developing an understanding of sediment sources and dynamics. A lack of such incentives in general has resulted in only a small number of detailed studies worldwide, so that general statements and comparisons are difficult to make.

1.4.2 Geographical distribution of debris-mantled and glacial ice.

The Tasman Glacier has a more extensive cover of supraglacial debris than most glaciers reported in the literature. Indeed, an abundance of supraglacial debris is characteristic of many glaciers in the Southern Alps (Chapter 4.1). This section reviews the distribution of debris-mantled glaciers and related features which have been reported in the literature. Glacier ice-cored and debris-mantled forms are varied in their genesis. A simple five-fold division of origins is used to map the distribution of features shown in Fig 1.2.

Extensive debris-covered ice masses occur through 160° of latitude and in all continents of the world except for Africa. Thus, at a general level, conditions promoting the burial of glacier ice by debris may occur wherever climatic conditions allow glacier ice itself to accumulate. The only climatic controls are therefore those which govern the global distribution of glaciers. At a smaller spatial scale, environmental conditions favouring supraglacial debris accumulation within any region are more varied and complex.

Most reported occurrences of debris-covered glacier ice are from regions of high relief, especially from convergent plate boundaries with associated fold mountains. By inference, a control on high-level transport zone debris concentration is exerted by topographic relief, especially in regions of tectonically-shattered bedrock (see Section 4.1.1.1). Exceptions include debris-covered ice shelves (Swithinbank 1988) where debris freezes to the glacier sole at the grounding line, and margins of polar and subpolar glaciers where a basal freezing-on mechanism aids the elevation of basal sediment to the glacier surface.

The global distribution of debris-covered glacier ice therefore predominantly reflects geological controls, which act through the creation of regions of steep topography and supply of debris to glacier surfaces

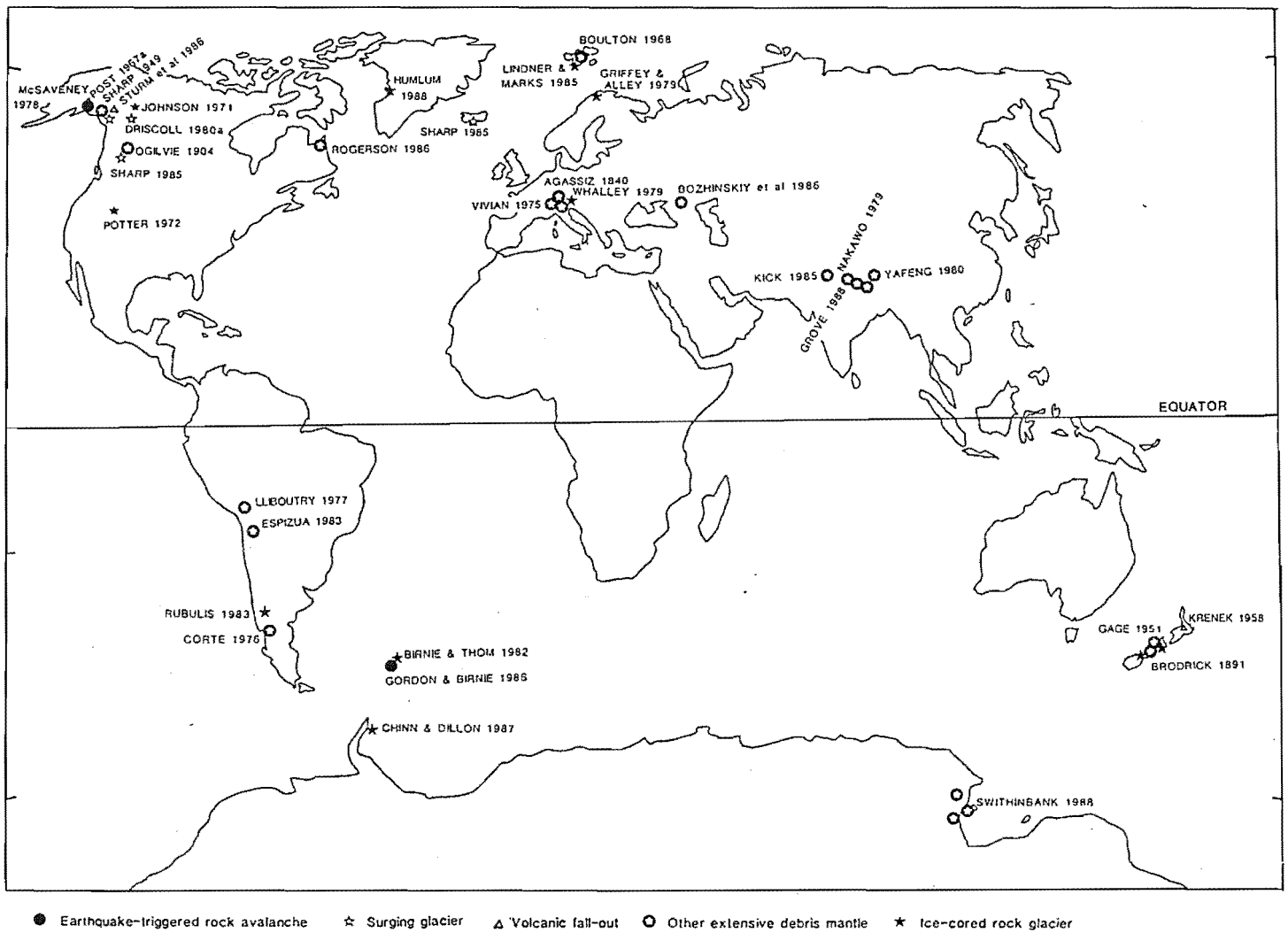

FIG. 1.2 Global distribution of glacier-ice-cored landforms and extensive supraglacial debris mantles reported in the literature.

from rock faces.

1.4.3 The origins and mechanisms of emplacement of supraglacial debris.

Mechanisms which cause rock debris to be concentrated upon glacier surfaces are numerous and their importance is, volumetrically, highly variable. The complexity is compounded when the diversity of sediment sources, entrainment processes, reworking processes, and all possible combinations of these processes is considered. Any attempt at classification would involve imposition of somewhat arbitrary and artificial boundaries, and is avoided in this study. Instead, published examples are described.

Extraglacial sources have long been recognised as providing abundant debris for supraglacial transport. Most extensive (10^5 to 10^7 m^2 or larger) debris mantles probably accumulate by "multitudinous small rockfalls and debris-filled snow avalanches" (McSaveney 1975 p.361), representing one extreme of a magnitude- frequency spectrum for debris supply processes. Such a "uniformitarian" origin of debris mantles was recognised by Agassiz (1840) in the European Alps, and subsequently by many authors in different regions. Examples include Alaska (Tarr 1908, cited by Flint 1942; Ellis & Calkin 1983), Canada (Ogilvie 1904; Odell 1948; Johnson 1974; Rogerson et al 1986), South America (Corte 1976a; Espizúa 1983), Europe (Vivian 1975), Scandinavia (Ackert 1984); the sub-Antarctic (Birnie 1978; Gordon & Birnie 1986), the Himalaya (Nakawo 1979; Nakawo et al 1986), the Caucasus (Bozhinskiy et al 1986), and New Zealand (Brodrick 1891; McSaveney 1975). Variants of the "uniformitarian" supply of supraglacial debris are glaciers avalanching over a cliff and reforming at the base as cones of ice and debris, continuing to flow as reconstituted glaciers. The process is particularly effective at supplying debris directly to the glacier surfaces where reconstitution takes place in ablation zones (Vivian 1975). Debris in the basal transport zone above avalanching ice-cliffs enters the high-level transport zone of the reconstituted portion. Ogilvie (1904) described the avalanche-reconstitution process giving rise to debris-mantled ablation zones in British Columbia, and contrasted these with nearby glaciers where he found neither reconstitution nor supraglacial debris mantles. Other documented examples are given by Rabassa et al (1978, cited by Rubulis 1983); Espizúa 1983; Rogerson et al 1986; and Aniya (1988). A large number of other examples occur incidentally in photographs in the glaciological

literature. Such glaciers have no particular name in the English language literature to describe the formational characteristics of their debris mantles, but they have been termed "Turkestan-type" glaciers by Kalesnik (1937, cited by Glazyrin 1975).

At the opposite end of the magnitude-frequency spectrum are glaciers whose debris mantles are emplaced in catastrophic events, usually as large rock avalanches (Voight 1978). The inclusion of snow, ice and dust in mobile rock masses, and the low frictional co-efficient of glacier surfaces, aids flow and spreading of rock avalanches so that they are capable of blanketing large areas with relatively thin sheets of debris (McSaveney 1978). Rock avalanching is favoured by high topographic relief and steep slopes, though the trigger mechanism of many events is conjectural. An earthquake trigger is well documented for rock avalanches in the Alaskan earthquake of 1964 (Post 1967b). In other cases an earthquake origin is probable (Tarr & Martin 1914; Whitehouse & Griffiths 1983). Relatively minor earthquakes have also been observed to release rock avalanches (Gordon et al 1978), whereas large earthquakes sometimes fail to trigger significant slope failures (Post 1967b). Therefore inferences of an earthquake origin must remain conjectural in the absence of direct observations (eg. discussion between Tuthill, 1966, and Post 1967a). Post (1967b) noted that several rock avalanches in Alaska have fallen without a direct earthquake trigger.

Other mechanisms leading to catastrophic slope failure include priming by the unloading of valley sides following deglaciation (Johnson 1974) and triggering by intense rainfall (Whitehouse & Griffiths 1983). Grove (1972) noted a correlation between rockfall hazard and climatic deterioration in Norway, and Porter & Orombelli (1981) suggest that large rock avalanches in the Mont Blanc region may have been more frequent during colder periods. However the triggers of many large rock avalanches are not obvious and may result from a complex threshold of slope stability being crossed by gradual action of many combined influences.

Catastrophic emplacement of supraglacial debris mantles may also result from volcanic activity. Documented examples include fall-out of 7.5 cm of ash onto glaciers on Mt Ruapehu, New Zealand, from a 1945 eruption (Krenek 1958), and the mantling of Drift Glacier, Alaska, by up to 5 m of sand and ash from the 1967 eruption of Mt Redoubt (Sturm et al 1986).

Much attention has been paid to the transport of supraglacial debris derived from subglacial entrainment and elevated and exposed by ablation. A review of the processes of entrainment and elevation is presented by

Chinn & Dillon (1987). In general, supraglacial debris of this origin is found as "shear moraines" (Bishop 1957) or "inner moraines" (Weertman 1961) in polar and sub-polar glaciers. They are formed where debris is entrained by some combination of regelation beneath sliding ice or by basal freezing due to seasonal migrations of the freezing zone at the soles of polythermal glaciers (Boulton 1970). Large volumes of debris may be entrained in these ways and elevated due to compressive ice flow behind a terminal obstruction. Obstructions may be formed thermally by a cold-based ice margin, or rheologically by the grounding of a "semi-rigid" zone of thin, less plastic ice near the terminus (Holdsworth 1969; Chinn & Dillon 1987). The distribution of strain within the upwarped ice has been debated, some authors inferring dislocation and thrusting along a discrete fault plane while others envisage a narrow zone of intense plastic deformation and differential shear. Whichever mechanism operates, each has the result of generating outcropping debris bands transverse to the glacier flow direction.

"Upthrusting" has been inferred to explain the extensive mantling of Late Pleistocene glaciers and ice sheets by englacially-derived debris (Tarr 1908, cited by Flint 1942; Rich 1943; Shaw & Archer 1979). The surface expression of outcropping debris bands has been described from Svalbard (Boulton 1967, 1968; Drozdowski 1977), Baffin Island (Goldthwait 1951; Hooke 1973; Hudleston 1976), Greenland (Bishop 1957; Goldthwait 1960; Swinzow 1962), South Georgia (Sugden et al 1987) and Antarctica (Hollin & Cameron 1961; Souchez 1967; Chinn & Dillon 1987). In high polar environments the areal extent of supraglacial debris is limited by the absence of a redistributing agent and the frozen nature of the debris. In lower (sub-polar) latitudes with available melt and rain water, a variety of mass flow processes cause the downslope redistribution of debris away from the outcrop of englacial debris bands, and extensive sheets of flow tills are formed (Boulton 1966, 1967; Drozdowski 1977; Lawson 1979, 1982).

The transfer of basally-derived debris to the surfaces of temperate glaciers has been explained hypothetically by Posamentier (1978). His model involves the seasonal change in ice velocity through icefalls, creating cyclic fluctuations in longitudinal strain rate resulting in the elevation of the basal transport zone in the hinges of large folds and/or by reverse faulting. It seems unlikely to the present author that seasonal velocity changes could generate the stress gradients necessary to explain deformation on such a scale in so short a space of time. It is uncertain whether or not variants of the "upshearing" process operate in wholly

temperate (warm-based) glaciers. Gomez & Small (1986) describe the passive elevation of basally-derived debris along the flowlines of an tributary glacier over-riding the main glacier, and do not invoke debris elevation along a "shear plane" or "shear zone".

Glacier flow structure is an important influence on the distribution of supraglacial debris where the debris sources lie above the equilibrium line altitude. Debris is buried by snowfall in the accumulation zone and incorporated englacially, and routeways taken by the debris then depend entirely on the strain distribution within the glacier (Boulton 1978; Boulton & Eyles 1979). Ablation eventually causes the emergence of englacial debris below the equilibrium line. Glazyrin (1975) formulated a mathematical model to describe this transport routeway in relation to glacier mass balance, and concluded that a complete cover of debris on the lower glacier can only form if a glacier is retreating. Glazyrin's model includes important simplifying assumptions, particularly an assumed absence of agents which redistribute supraglacial debris after it has emerged from englacial transport. Lateral movements of debris is known to be an important influence on the morphology of medial moraines (Loomis 1970; Small & Clark 1974; Eyles & Rogerson 1977; Small et al 1979) and the downglacier spread and coalescence of medial moraines to form a continuous debris cover has been reported from many regions (eg Agassiz 1840; Lliboutry 1964; Rampton 1970 Fig 2; Vivian 1975: Eyles & Rogerson 1978a; Rogerson et al 1986; Bozhinskiy et al 1986). A thorough review of medial moraine classifications and dynamics is presented in Chapter 3.2.

Glaciers with histories of repeated surging often display lobes of intensely folded ice, in which supraglacial moraines are compressed into accordian-like tight folds. This seems to be especially common in piedmont glacier lobes where longitudinal compression is accommodated by lateral extension. Post (1972) illustrates how medial moraines on Bering Glacier, Alaska, are folded so tightly that they form an extensive debris mantle.

Glacier ice may become debris covered by a multitude of processes in addition to those described above. In fact, wherever slow-moving glacier ice exists it is prone to burial by whatever contemporaneous debris-transport processes are active on surrounding ice-free surfaces. Burial by aggrading fluvial deposits are capable of burial by much thicker debris than is usually achieved by melt-out processes, which are largely self-regulating (Bozhinsiy et al 1986). Deposition by supraglacial streams and/or in supraglacial lakes (Morawski 1989) has been documented in modern environments (eg Sara 1968; Johnson 1971, 1974; Maizels 1977) and invoked

to explain Pleistocene facies associations (eg Flint 1942; Rich 1943; Shaw & Archer 1979; Gravenor et al 1984; Fleischer 1986; Levson & Rutter 1989;. Supraglacial aeolian deposition has received attention mainly through its importance in providing datable tephra layers, pollen, and other microparticles in ice cores, thus allowing palaeoenvironmental interpretations to be made (eg Thomson 1977; Keyes et al 1977; Dansgaard et al 1982; Thomson et al 1984; Thomson & Thomson 1987). Aeolian deposition of sufficient volume to have a glaciological significance is only likely to occur from volcanic activity, as described above.

1.4.4 Relationships between supraglacial debris, mass balance and ice movement.

The retardation of ice melt beneath debris was recognised in the earliest studies of glaciers (Agassiz 1840). Several early workers independently observed debris insulation (eg Ogilvie 1904; Wright & Priestly 1922). Lewis (1940) and Warren Wilson (1953) recognised that thin debris increases ablation, and Sharp (1949) qualitatively identified sensible heat transfer as an important component of sub-debris ice melt. Swithinbank (1950) recognised that a thin debris layer enhances melt rate and qualitatively discussed heat transfer as being dependent on the thermal conductivity of the debris and on its porosity and moisture content. Østrem (1959) carried out experimental work on ice melt under artificial debris patches up to 28 cm thick on Isfallsglaciaren, Sweden, and found that debris less than 1 cm thick enhanced melting while thicker debris retarded it. A 20 cm layer caused a 78% reduction in melting. In a classic paper, Østrem (1965) measured temperature profiles through the debris cover of ice-cored moraines at several times of the year in order to define the ablation season. Melt rates were not calculated from the temperature data however. Østrem's 1959 test plots were repeated and he found an 85% reduction of melting under 40 cm of debris. McKenzie (1969) estimated the rate and duration of conductive heat flow through the debris of an ice-cored kame terrace in Alaska, based on a small number of incomplete temperature profiles. McSaveney (1975) suggests that McKenzie's calculations are gross underestimates due to the temperature profiles used and to the neglect of advective heat transfer. Drewry (1972) found that for debris between 10 and 125 mm thick, grain size was important in controlling the stability of debris on the flanks of dirt cones. He developed a model of a steady-state system of dirt cone dynamics characterised by negative feedbacks between cone geometry and ablation.

Loomis (1970) showed how <4-7 mm of debris on Kaskawulsh Glacier increased ice melt and debris >1 cm thick retarded melting. McSaveney (1975) studied the effects of the 1964 Sherman Glacier rock avalanche on glacier mass balance and found earlier work (eg Marangunic 1972) tended to underestimate melt rates beneath.

Conductive and advective heat flow was calculated from two temperature profiles in 1.1 and 2.0 m thickness of debris and the results extrapolated for the whole deposit. A less thorough approach by Carrara (1975) measured temperatures at two depths in each of three profiles in wasting ice-cored moraines in Baffin Island, but did not use the data to compute melt rates. Nakawo (1979) made crude estimates of sub-debris melting of G-2 Glacier in Nepal using no data at all. Driscoll (1980) derived melt-rate curves for ice-cored debris on the Klutlan Glacier, Yukon, from 15 temperature profiles measured at 7 sites and assuming a steady heat flow throughout a 90 day ablation season. Driscoll (1980) does not list his calculated melt rates except as the time taken for ice-cores of various ages to melt.

The first detailed modelling of the process of sub-debris ice melt was undertaken by Kraus (1966) using an energy balance approach. Kraus applied his findings to the explanation of glacier surface micro-relief. Subsequent modelling by Nakawo & Young (1981) identified the accurate determination of thermal resistance as a key problem in field studies. Nakawo & Young (1982) tested the model on Peyto Glacier, making assumptions that all heat flow was conductive and that temperature gradients were linear, therefore avoiding the need to measure debris temperatures. Nakawo & Takahashi (1982) simplified the model to avoid the need for detailed meteorological data. Although the model is suitable for short-term estimates under thin (12 to 94 mm) debris layers, the approach of McSaveney (1975) is more appropriate for longer-term calculations on thick debris. Subsequently, Bozhinskiiy et al (1986) presented a mathematical model describing the time-dependent dynamics of debris mantle growth, and tested the model on Djankuat Glacier in the Soviet Caucasus.

On the scale of an entire glacier, much less information is available about the glaciological effects of supraglacial debris. Although most work revolves around ablational effects, which are reviewed below, an interesting hypothesis was put forward by Tarr & Martin (1914), termed the "Earthquake Advance Theory". The hypothesis was that an increase in glacier mass caused by the sudden addition of snow, ice and rock debris caused glaciers to advance in the years following the 1899 St. Elias

earthquake in Alaska. The hypothesis was tested by Post (1967b) using the known mass of rock avalanches which fell on Martin River Glacier in the 1964 Alaskan earthquake. Post concluded that no significant effect on ice dynamics could be measured or predicted. McSaveney (1975) suggested that observed advances following the 1899 earthquake may instead have resulted from the uplift of the St. Elias Mountains by 14 metres during the earthquake. The Earthquake Advance Theory has subsequently gained little credence among glaciologists.

Ablational effects of supraglacial debris have been demonstrated to significantly affect glacier behaviour. The distribution of ablation beneath a debris cover varies inversely with the thickness of the debris (Østrem 1959). Debris mantles typically thicken towards the distal and lateral margins. Available measurements indicate that this holds true for mantles of both a rock avalanche origin (McSaveney 1975, 1978) and of a uniformitarian origin (Ogilvie 1904; Sharp 1947, 1949; Glazyrin 1975; Nakawo 1979; Rubulis 1983; Nakawo et al 1986; Bozhinskiy et al 1986; Wanatabe et al 1986; Chinn & Dillon 1987), but for different reasons. In the former case thickening results from marginal strain, deceleration, and shear during the flow of fluidised rock avalanches (McSaveney 1978), in the latter case it is due to the longer time period over which melt-out of debris has taken place at slower-moving marginal locations on a glacier. However, no study has systematically explained the thickness variation of a uniformitarian debris mantle. Additions of material from the basal transport zone is also a cause of thickening of supraglacial debris around glacier margins (Flint & Demorest 1942).

The effect of an areal variation in debris cover thickness on the distribution of ice ablation has been used to explain or to infer the changing long profiles of stagnant glaciers (Rich 1943; Flint & Demorest 1942; Hartshorn 1952, 1958; Kaye 1960; Clayton 1967; Shaw & Archer 1979). Retardation of ablation beneath debris also controls the morphological development of the margins of slow-moving polar and sub-polar glaciers (Boulton 1967, 1968).

The increase in glacier ablation at lower altitudes, termed the ablation gradient (Schytt 1967), is reduced or even reversed where thick debris covers the glacier surface (Rogerson et al 1986). As ice flow is lessened, ablation becomes the dominant influence on changes in glacier surface profiles (Hastenrath 1987), and debris-induced variations become more significant. Nevertheless, existing data on the ablation gradients of debris-covered glaciers are minimal. No study has yet integrated the

effect of ice movement upon the areal pattern of ablation and glacier thinning under a debris mantle.

A possible reason is the assumption which pervades the literature that glacier ice must necessarily be stagnant to become extensively debris-covered by uniformitarian processes. (For a discussion of uses of the term "stagnant", see Mannerfelt 1981). Implicit in this assumption, though rarely stated, is that even low ice velocities are capable of evacuating a supraglacial debris cover to give an unmantled ice surface. The idea can be traced to the early reconstructions of the pattern of wastage of the margins of the Laurentide and Fennoscandian ice sheets, and appears to be a case of the interpretation preceding the evidence. Thus, many authors have categorically stated that a glacier is "stagnant" without any direct measurement of ice motion being available (Russell 1892; Flint 1929, 1942; Flint & Demorest 1942; Rich 1943; Odell 1948; Gravenor & Kupsch 1959; Clayton 1964; Tuthill 1966; Porter 1975a; Shaw & Archer 1979; Pickard 1983, 1984; Nakawo et al 1986; Wanatabe et al 1986). In these cases, the presence of abundant supraglacial debris is equated directly with "stagnant" ice, rather than ice motion being inferred from glacier gradient. In many cases the ice probably is effectively stationary, and in other cases measurements demonstrate this (Nakawo 1979). However, ice movement has also been measured in parts of glaciers which are extensively debris-covered (Brodrick 1891; Ogilvie 1904; Lliboutry 1977). Therefore it is insufficient to assume that a debris mantle corresponds to stagnant ice.

A second assumption which is implicit in many papers is that the accumulation of supraglacial debris indicates negative mass balance. There are supporting observations of the spreading of supraglacial debris coincident with glacier thinning and/or retreat. However, only Glazyrin (1975) has investigated the dynamics of the process, but in little detail. Observations of debris-mantled glaciers whose surfaces are level with the crests of lateral moraines (Brodrick 1891; Small 1983), and the formation of large lateral moraines by supraglacial dumping (Osborn 1978; Rothlisberger & Schneebeli 1979) suggest that some glaciers maintain (or formerly maintained) abundant quantities of supraglacial debris under equilibrium or positive mass balance conditions.

Persistent debris mantles have existed on some glaciers since observations began, usually 100 to 200 years ago. Extensive debris mantles reduce the ablation rate to the extent that such glaciers typically have a lower accumulation area ratio than unmantled glaciers (Grove 1988; Aniya

et al 1988).

The response of glaciers to climatic change is, in general, complicated by the presence of an extensive supraglacial debris cover. Ogilvie (1904) may have been the first to realise this, when he observed that the magnitude of the advances of glaciers in part of the Canadian Rockies was related to the thickness and extent of their supraglacial debris cover. In New Zealand, Speight (1940) was puzzled by his observations of thinning in the middle and lower reaches of the Tasman Glacier contemporaneous with a small advance of the terminus. His observations of ice movement beneath the debris mantle caused him to question Flint's (1929) hypothesis of stagnation. Speight (1940; p.143) hypothesised that

"Some connection between low speed on low gradient and the wasting process probably exists..."

Lacking field measurements, he was unable to explain his observations in terms of the relationships between debris cover thickness, ablation rate, and ice velocity. Subsequently, there has been little improvement on the early ideas about the effects of debris mantles of uniformitarian origins.

Progress has mostly been related to the effects of supraglacial rock avalanche deposits on glacier dynamics, inspired especially by the 1964 Alaska earthquake. For the first time, there existed the data to make comparisons between the behaviour of several glaciers before and after the emplacement of debris mantles, and between mantled and unmantled glaciers in the same region. Several studies have predicted that the change in ablation gradient caused by a debris mantle may reduce or reverse a prevailing negative mass balance trend, or may enhance positive balance independently of climatic influences (Post 1967b; McSaveney 1975; Rogerson et al 1986). Actual monitoring lends general support to these predictions (Post 1967b; McSaveney 1975; Porter & Orombelli 1981) though it has proved difficult to predict accurately the magnitudes (as well as the directions) of mass balance changes and translate these to a rate or distance of glacier advance or retreat.

1.4.5 Summary and conclusions of the literature review.

The review identifies those areas of research which have received concentrated study and those where much remains to be discovered.

1. The effect of a debris cover on ablation of an underlying ice surface are well-documented for small debris thicknesses over time periods

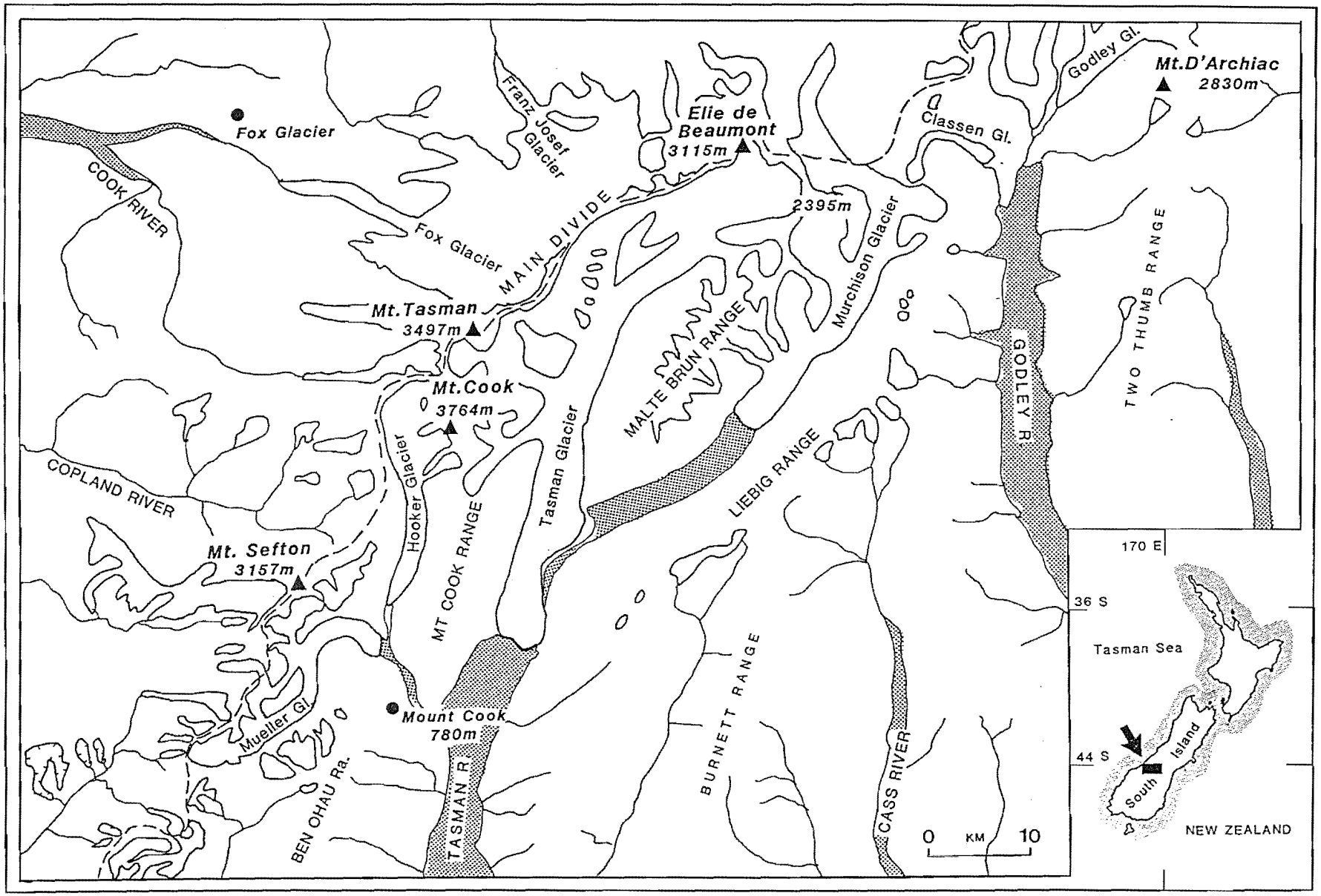

FIG. 1.3 Location map of the study area.

of a few hours.

2. The effect of thick debris covers (decimetres to metres) on ablation is less well documented. Few studies exist so that that there are no established relationships between debris thickness and ablation rate at a wide range of latitudes and altitudes. With the exception of the valuable work of Østrem (1959, 1965) and Bozhinskiy et al (1986), the lack of debris temperature data monitored over a whole year limits our understanding of annual variations of thermal gradients, moisture movements, active layer thicknesses, and debris layer heat storage effects.

3. The origins of supraglacial debris cover are varied and well-documented. However, detailed studies of the emplacement mechanisms are few, and have only been conducted for rock avalanches and for "up-sheared" marginal debris aprons and "inner moraines". Particularly, there has been no systematic study of the origins and mass balance relationships of debris mantles formed by uniformitarian processes, or of the possible range of magnitude-frequency combinations of debris supply processes.

4. The effects of extensive debris covers on glacier dynamics (rather than the reverse relationship) are poorly documented, with the exception of rock avalanche effects over periods of decades. Long-term effects on climate-glacier relationships may be expected from the known ablational effects of supraglacial debris.

The Tasman Glacier and neighbouring glaciers in the Mount Cook region provide the opportunity to resolve some of these problems and to add to the overall understanding of the debris-ice system.

1.5 THE STUDY AREA

Mount Cook National Park (Fig 1.3) covers an area of 800 km^2 of the highest peaks of the Southern Alps. The area is a suitable field location for the study, possessing the following advantages:

1. Well preserved and dated Holocene moraine sequences;

2. Direct glaciological observations spanning a hundred years, including glacier velocities, ablation and geophysical information.

3. Contrasting debris-mantled and unmantled glaciers in the same region;

4. Relatively straightforward access to study locations.

1.5.1 Geology.

The region lies entirely within the Torlesse terrane, comprising Carboniferous to Cretaceous greywackes deposited in a large submarine fan system (Findlay & Spörli 1984; Waterhouse 1985). Lithologies include indurated, poorly-sorted polymict sandstones interbedded with polymict siltstones and mudstones (Waterhouse 1966; Field 1976; Spörli & Lillie 1974; Findlay & Spörli 1984). Fine-grained lithologies include black, red and green argillites related to minor episodes of submarine volcanism. These lithologies are more common in the south and east of the area than in the west.

Metamorphic grade increases in a north-westerly direction (Gair 1967). Prehnite-pumpellyite facies cover most of the area south and east of the Mount Cook Range, but to the north and west grade increases through pumpellyite-actinolite facies in the Hooker Valley to greenschist facies across the Main Divide. The trend results from uplift from progressively greater depths closer to the Divide, the axis of uplift lying in a zone between the Main Divide and the range-bounding Alpine Fault to the west. The age of metamorphism is ascribed to the Rangitata Orogeny by Grindley (1963). Its effect has been to indurate the sediments and to impart a distinctive west-dipping schistosity to rocks on and west of the Main Divide.

The structural complexity of the region is a result of deformation in two orogenic episodes. The earlier Rangitata Orogeny of Cretaceous age is was responsible for the formation of a regional system of kilometre-scale steeply plunging folds which dominate the areas mapped by Lillie (1962a,b, 1964), Lillie & Gunn (1964); Waterhouse (1972, 1985) and Findlay & Spörli (1984). The origin of the folds has been debated, opinions variously describing them by a recumbent fold model (Lillie 1964; Waterhouse 1972) or by deformation at a dextral oblique-slip plate boundary (Waterhouse 1972; Findlay & Spörli 1984). Structures formed during the later Kaikoura Orogeny (Tertiary to the present) are characterised by more brittle deformation at a higher crustal level than that at which currently-exposed Rangitata structures were formed (Waterhouse 1985). Large strike-parallel north-easterly trending faults have been mapped through the region (Spörli & Lillie 1974; Findlay & Spörli 1984; Waterhouse 1985). The parallelism of structures together with poor exposure beneath gravel and ice-filled valleys has hindered the identification and mapping of these structures. Current uplift rates have been inferred from geomorphic evidence to increase towards the Main Divide from about 4 to 8 mma^{-1} in the Mount Cook

region (Wellman 1979).

In general, the geology of the study area is characterised by a small number of lithologies with no distinctive marker horizons on a regional scale. Past and present tectonism has imparted a distinct north-west-south-east structural grain, delineated by the metamorphic fabric in the west, and by major fault lines and fold axes throughout the area. At a smaller scale, the geological history has resulted in an abundance of well-indurated lithologies with a dense joint network.

1.5.2 Climate.

The South Island of New Zealand lies in the zone of mid-latitude westerly airflow and is characterised by a humid mesothermal climate. The mountain barrier of the Southern Alps, perpendicular to the dominant wind direction, causes high orographic precipitation especially on western range fronts. Highest rainfall totals of up to 12,000 mma^{-1} occur west of the Main Divide, with minor peaks over eastern ranges (Griffiths & McSaveney 1983). The proportion of annual precipitation which falls as snow increases with altitude. At Ivory Glacier, 1400-1800 m altitude and 60 km to the north-west, snowfall comprises 25% of annual precipitation, and at 1550 m in the Craigeburn Range (140 km to the north-west) 36% falls as snow (McCracken 1980, cited by Whitehouse 1987).

Long-term climatic records from Mount Cook village are summarised in Fig 1.4. Sporadic climate data from Ball Hut, Hooker Hut and Tasman Saddle (Fig 1.5) indicate the climatic variability in valley-floor locations at different altitudes. The village has a mean annual temperature of 9.1°C, mean January and July temperatures being 15° and 5°C respectively. Frosts occur on >25 days in July. Snow lies at 780 m elevation for 20-30 days of the year on average, though inter-annual variations are large. Mean annual precipitation at Mount Cook Village is 4,071 mma^{-1}, with an even distribution throughout the year, but with a slight summer maximum. At higher elevations, snowpack increases from Autumn (April or May) until early summer (November). Snowpack thicknesses of 10 m have been recorded on the upper Tasman Glacier (Anderton 1975: Fig 14). No temperature data is available from high altitude locations.

1.5.3 Geomorphology.

A regional geomorphology of the Southern Alps is presented by Whitehouse (1987), who identifies three geomorphic regions with regard to tectono-climatic environment. The study area straddles Whitehouse's axial

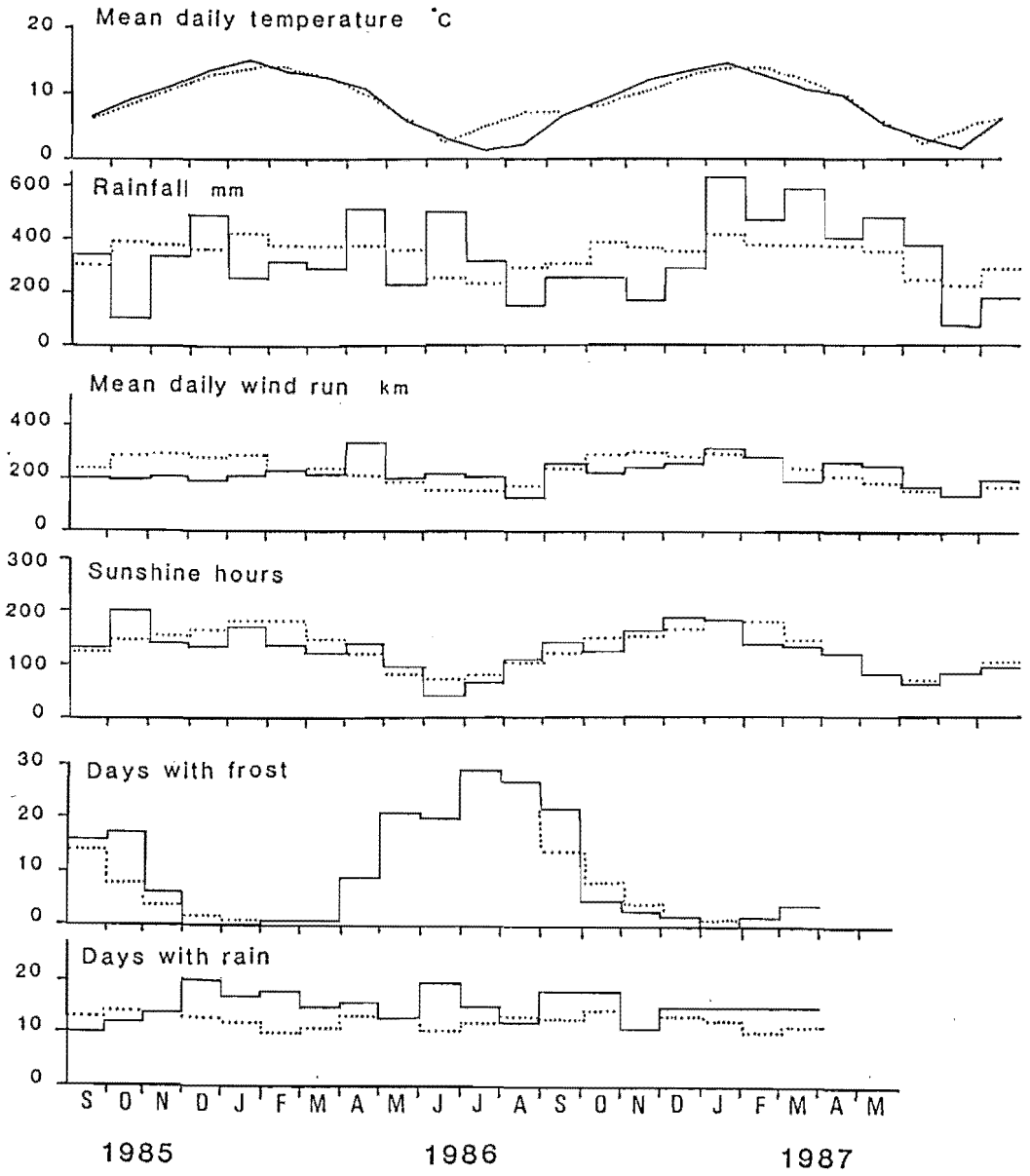

FIG. 1.4 Climatic data from Mount Cook village.
(Dotted lines are long-term means).

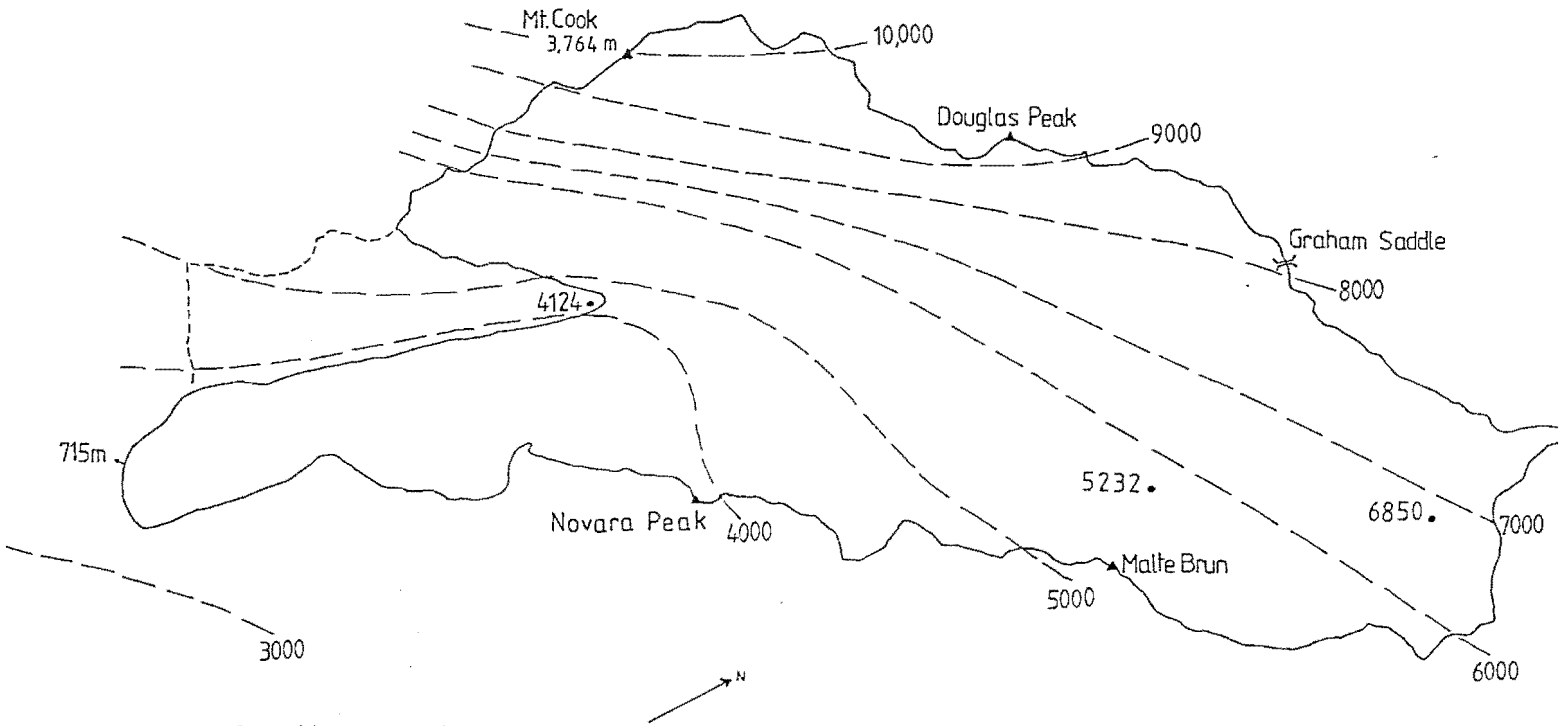

FIG. 1.5 Interpolated isohyets from Mount Cook National Park.

and eastern regions, where glacial processes and rapid mass-wasting of slopes predominate. Range crests are generally accordant at around 2500-3000 m on the Main Divide, and 2000-2700 m in more easterly ranges. Highest elevations lie close to the Main Divide (Mount Cook, 3764 m). North-easterly trending ranges are separated by deeply-incised glacial valleys to give a relative relief of 1000-2000 m between valley floors and summit levels. The main valleys trend sub-parallel to the regional geological strike.

The present distribution of glaciers is a function of the intersection of the accordant summit levels with a north-westerly dipping glaciation limit (Porter 1975a; Chinn & Whitehouse 1980). The largest glaciers drain the Main Divide, where there is the greatest topographic elevation above the glacier equilibrium line altitude (ELA). As ELA rises to the south-east at a gradient of 70 m km^{-1} and summit elevations decrease slightly, glaciers become smaller and confined to cirques at progressively higher elevations. Beyond a distance of c.20 km from the Main Divide, glaciers do not exist in the Mount Cook area under present climatic conditions.

Evidence of periods of more extensive glaciation are preserved in moraines within the Tasman watershed. These have been mapped and dated by several workers. Late Pleistocene moraines are located around the south end of Lakes Tekapo and Pukaki (Mansergh 1973; Mathews 1967; Porter 1975a). Holocene moraines occur north of Lake Pukaki (Speight 1940; Porter 1975a) and around the margins of present glaciers (Burrows 1973; Burrows & Gellatly 1982; Gellatly 1985; Gellatly et al 1985; Burrows 1989) and in eastern cirques (McGregor 1967; Birkeland 1982). The Holocene glacial chronology is reviewed in detail in Chapter 6.

Other geomorphic research in the area has been concerned with debris cone hazard, especially in the vicinity of Mount Cook village, and with the causes and extent of erosion (Whitehouse 1982). Studies relevant to this research but conducted over a wider area than the Mount Cook area include the mapped distribution of large rock avalanche deposits (Whitehouse 1983) and their frequency (Whitehouse & Griffiths 1983); the development and refinement of rock weathering rind dating on the Torlesse sandstones (Chinn 1981; Whitehouse et al 1986); the understanding of talus development (Whitehouse & McSaveney 1983); and the quantitative assessment of denudation rates in alpine catchments in the region (McSaveney 1978; Hicks et al, in press).

CHAPTER 2: GLACIOLOGY.

2.1 ICE FLOW

2.1.1 Theory

Existing theories of ice flow are reviewed, to allow the estimation of flow parameters for use in the analysis of velocity measurements. The following sections therefore discuss general theories of glacier movement in the particular context of the Tasman Glacier.

2.1.1.1 Internal deformation of ice.

The classic papers by Glen (1952, 1958) and Nye (1952a, 1959) established the relationship between strain rate, $\dot{\varepsilon}$, and shear stress, τ, for polycrystalline ice. This has subsequently been widely applied as a general flow law for glacier ice. The law states that

$$\dot{\varepsilon} = A\tau^n \qquad (1)$$

where $\dot{\varepsilon}$ = strain rate, τ = shear stress, A is a constant and n the flow law exponent. The basal shear stress of a glacier cannot usually be measured in the field, but is derived from the equation

$$\tau_b = \rho g h \sin \alpha \qquad (2)$$

where ρ = ice density, generally taken to be 0.91 gcm^3, g = acceleration due to gravity (9.81 $ms^{-1}s^{-1}$), h = ice thickness and = α glacier surface slope (Glen 1952).

For the accurate calculation of ice deformation, it is necessary to attach accurate values to the parameters in the shear stress and flow law equations, particularly to the values of A and n. Ice density and the gravitational constant are well established. Glacier slope is easily measured in the field or from topographic maps. Ice depths may be estimated by geophysical surveys or measured in boreholes. Seismic and gravity surveys have been carried out on the Tasman Glacier by Broadbent (1973) and Claridge (1983) who also used electrical resistivity. These studies provide data on ice thicknesses at several transects of the valley glaciers and their termini in the field area. Broadbent's (1973) profiles have been remeasured using a surface impedence meter (Thiel 1986) which found good agreement with Broadbent's ice depths (Ruddell, pers. comm.).

For valley glaciers, equation (2) must be modified to account for the friction exerted by the valley sides. Instead of using ice depth, a parameter approximating to the hydraulic radius R is applied, where R = CSA/P (where CSA is the cross-sectional area of the glacier and P is the

length of the ice-substrate contact, or "wetted perimeter": Nye 1952a p.85). The average basal shear stress per unit area of glacier bed, τ_{av}, is then

$$\tau_{av} = \rho g(A/P)\sin\alpha \quad (3)$$

The ice velocity, U_0, at the glacier surface due to internal deformation of the glacier is

$$U_0 = \frac{2hA(\tau_{av})^n}{(n+1)} \quad (4)$$

and the mean velocity through the cross-section due to internal deformation, U_{av}, is

$$U_{av} = \frac{2hA(\tau_{av})^n}{(n+2)} \quad (4a)$$

The adjustment to the denominator in equation (4a) was made by Booth (1986) and, though not explained, is an attempt to convert Paterson's equation to one which gives the mean rather than the surface velocity. The change from (n + 1) to (n + 2) assumes that, if n approximates to 3, the mean velocity is about 80% of the maximum in a vertical velocity profile. In other words, most of the deformation takes place near the glacier base. This is a reasonable approximation of reality because shear stress (and therefore deformation or strain rate) increases with depth.

Equations (4) and (4a) involve the two constants A and n in Glen's flow law (equation 1). A great deal of effort has been expended by glaciologists in trying to determine the variation in these parameters under different conditions of stress and temperature. A review of this subject is presented by Paterson (1981).

The exponent n is commonly assumed to have a value of 3 (eg Mathews 1967, Booth 1986). It has been determined experimentally to range from c.1 to c.4.5. The value is primarily a function of the ice fabric, in that increasing values of n reflect an increasing alignment of basal glide planes among ice crystals (Andrews 1975 p.35-36). The strain history of the glacier is an important influence. The "constant" n is likely to vary spatially over any glacier. A detailed study of ice crystallography and stress/strain relations is beyond the scope of this study, so a value of n = 2.8 has been selected from the literature for use in this study.

This value was determined from borehole deformation on the Salmon Glacier in British Columbia, Canada (Mathews 1959). The Salmon Glacier is the closest approximation to the Tasman Glacier, that the present author has been able to find, on which a value of n was worked out from field data. The climate (and therefore ice temperature), glacier size, depth,

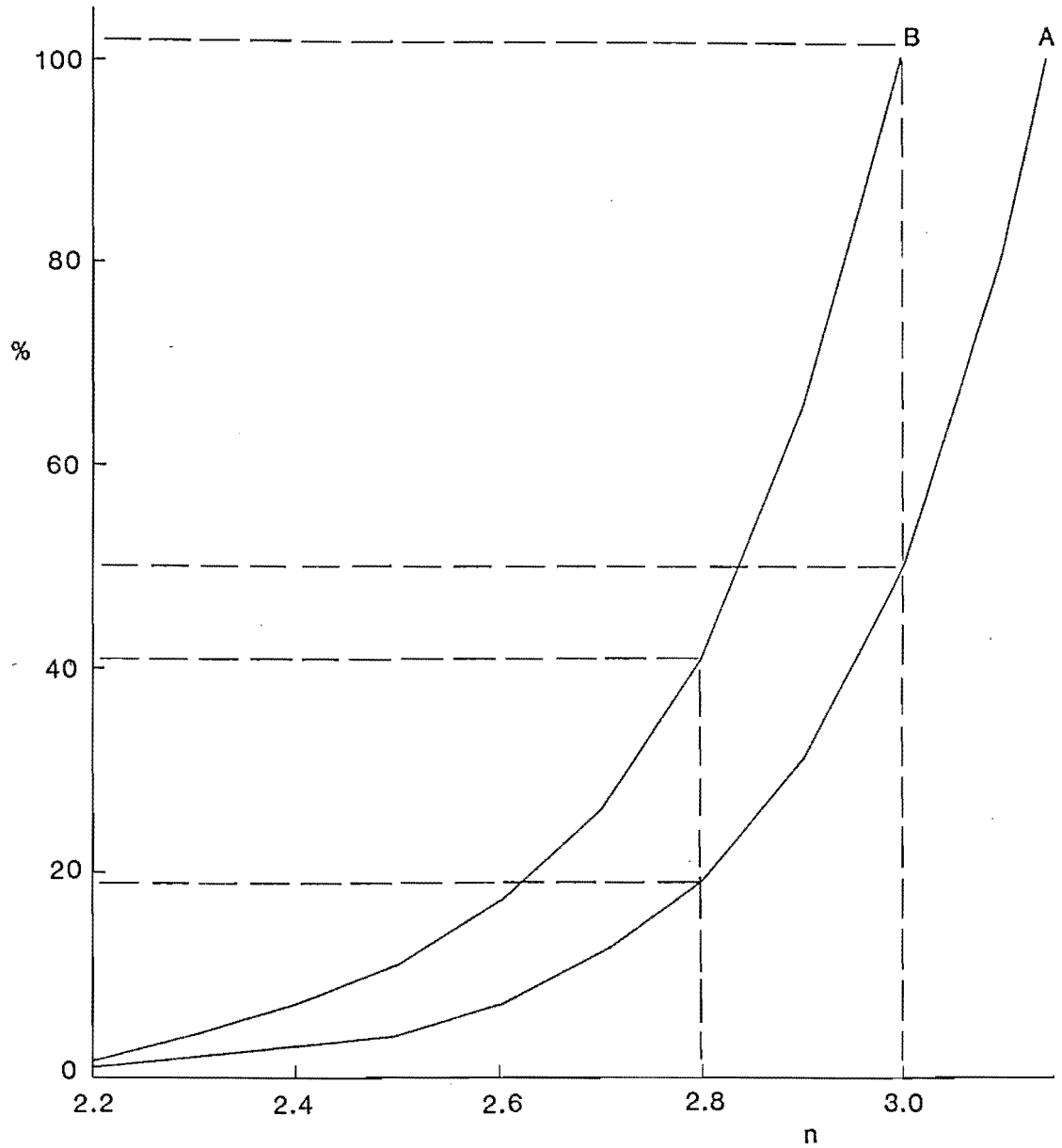

FIG. 2.1 The effect of values of the flow-law exponent n (x-axis) on the percentage of measured surface velocity which is accounted for by ice deformation (y-axis). A = Malte Brun transect in 1973, when h = 480 m, τ_{av} = 154 kN/m^2. B = Ball Hut transect in 1973, when h = 600 m, τ_{av} = 112 kN/m^2. Note the overestimate of deformation at Ball Hut if n = 3.

Site	Date	T_b (kNm^{-2})
Celmisia Flat	1890	21
	1973	14
	1986	14
Ball Hut	1890	135
	1973	112
	1986	105
De la Beche	1890	202
	1973	154
	1986	150

TABLE 2.1 Basal shear stresses of the Tasman Glacier.

efficient heat transfer (Marcus et al. 1985) and the ice of the glacier may be treated as isothermal, and typical of other maritime glacial environments (Golubev & Kotlyakov 1978). This restricts the possible values of A considerably. However, for different values of n at 0^0c, various authors have found that A varies over five orders of magnitude. Given the value of n already selected, reasonable values of A lie in the range of 4.8 to $8.85 \times 10^{-15} sec^{-1} kPa^{-n}$. For the stress range 50 to 130 kPa values of 5.1 to $5.5 \times 10^{-15} sec^{-1} kPa^{-n}$ have been determined, and the mean of these values, $5.3 \times 10^{-15} sec^{-1} kPa^{-n}$, has been used for the Tasman Glacier (Paterson 1981 Tables 3.1 and 3.2).

2.1.1.2 Basal sliding of temperate glaciers.

Basal sliding refers to a velocity discontinuity between the glacier sole and its substrate. It occurs where the glacier sole is at its melting point, and is therefore usually associated with temperate (warm-based) glaciers (Paterson 1981). Following the hypotheses of Weertman (1957), two basic processes of basal sliding were recognised and have subsequently been substantiated by direct observations (Kamb & LaChappelle 1964).

1) Regelation occurs where pressure-melting on the upstream side of subglacial hummocks allows meltwater to flow down the pressure gradient to the lee-side, where lower pressures cause refreezing to take place. A net transfer of ice downglacier is the result. The process is most effective on small bedrock obstacles which allow heat to be conducted from the stoss to lee side.

2) Enhanced ice flow is caused by increased pressure melting on the upstream side of substrate irregularities. The process is more effective where obstacles are large so that the increased strain affects a greater volume of ice.

A combination of these two processes has given rise to the concept of **controlling obstacle size**, which refers to the size of substrate irregularities at which the ice velocity due to regelation equals that due to enhanced pressure melting. The controlling obstacle size has been regarded as the limiting factor governing sliding rates, leading to complex mathematical modelling of the sliding process (eg. Weertman 1964b; Lliboutry 1968, 1978; Nye 1969b, 1970; Kamb 1970; Morland 1976).

Observations at the base of glaciers have confirmed that basal sliding occurs, but it has never been possible to accurately model or predict rates of sliding theoretically (eg. Kamb & LaChappelle 1964; Hodge 1974). This is partly due to the difficulty of quantitatively describing bed

roughness and hardness, but also to the complexity of sliding processes, for example where gravel-rich ice occurs at the glacier sole, where subglacial hydrology is not well understood, and where cavitation occurs (Boulton & Vivian 1973; Engelhardt et al 1978; Iken et al 1979; Hallet 1979).

Budd et al (1979) showed experimentally that a steady sliding velocity resulted from of a constant normal load and shear stress. The velocity was approximately proportional to the shear stress and inversely proportional to the normal load and bed roughness. They concluded that thick glaciers with low shear stresses will tend to have slower sliding velocities than thinner, steeper glaciers. They suggest that basal sliding will be the dominant component of glacier velocity in temperate glaciers less than 173m thick, and internal deformation will predominate in thicker glaciers. A further conclusion is that enhanced pressure melt (rather than regelation) is the controlling mechanism of basal sliding. Budd et al (1979) derived a flow law for basal sliding which greatly underestimated actual velocities. They suggested that this was due to the effects of the englacial water table, which reduces the effective normal load of the glacier. When this was taken into account, predicted sliding rates were much faster and a 220 m thick glacier with a shear stress of 150 kPa and a water table at a height of 0.25 of the glacier thickness will slide at a rate of 200 ma^{-1}, which compares quite reasonably with observed rates.

The presence of a gravel substrate (rather than bedrock) beneath much of the Tasman Glacier (Broadbent 1973) does not correspond with Budd et al's (1979) assumptions. The lack of information on the internal hydrology of the Tasman Glacier also precludes the use of a Budd-type flow law, given the importance of the effect of the water table on the normal load exerted by the glacier on its bed. Instead, the rate of basal sliding has been calculated by subtracting the velocity due to internal deformation from the measured surface velocity of the glacier, both of which can be calculated or measured relatively accurately compared to basal sliding velocity.

2.1.1.3 The significance of a deformable substrate.

Geophysical surveys suggest that most of the lower tongue of the Tasman Glacier rests on about 200m of gravel. There is a significant shear stress at the glacier sole, so that deformation of the glacier substrate may possibly account for a part of the measured velocity at the surface.

Beneath Breidamerkùrjökull (a temperate sliding glacier), Boulton

(1979) observed one locality where 90% of the movement at the glacier sole was due to deformation in 75 cm of sandy till beneath the glacier. Only 10% was due to the sliding of the glacier over its bed.

A flow law for glacier-bed deformation was proposed by Boulton & Jones (1979). They concluded that the exceptionally low-gradient surface profiles of Late Pleistocene glacier lobes in the Northern Hemisphere could be explained by substrate deformation under conditions of high pore-water pressures in fine-grained sediments. By applying their model to various glacier-bed conditions, Boulton & Jones (1979) concluded that a 40 km long glacier moving over relatively permeable (free-draining) gravels would not cause significant substrate deformation under mass-balance conditions likely to be found in nature. This conclusion suggests that substrate deformation is not likely to be a significant component of measured ice velocities of the Tasman Glacier unless significant amounts of fine-grained sediment occur within the underlying gravels. Such a case has not been shown by the geophysical surveys, though more precise techniques would probably need to be employed.

Boulton & Hindmarsh (1987) presented flow laws for subglacial till which depend on the relative pressures of subglacial water and of the ice overburden. Subglacial till deformation is predicted at positive effective bed pressures, or under unstable conditions of zero or negative effective pressures.

Exposures of Late Pleistocene tills (Chapter 6) show that the expanded piedmont lobe which formerly occupied the Tasman Valley may have had substrate conditions conducive to till deformation.

2.1.2 Tasman Glacier: surface flow rates.

2.1.2.1 Previous measurements of ice velocities on the Mount Cook glaciers.

Although glaciological research in New Zealand has been of a piecemeal nature, data on flow rates measured on the Mount Cook glaciers covers a period of nearly 100 years.

Brodrick's surveys. T.N. Brodrick, District Surveyor of Canterbury, made the earliest glaciological measurements in New Zealand. His reports of 1891, 1894, and 1906 provide records which were made with repeatability in mind. The four main glaciers in the area were surveyed. The most complete record is for the Mueller Glacier (Brodrick 1891; 1906) for which a slowing of ice velocity near the terminus was recorded between 1889 and 1906. No subsequent measurements have been made on this glacier.

Surveys were carried out to measure the movement of eighteen stakes drilled into the Tasman Glacier along two transects (Fig.2.2). The measurement period ranged from three days to one month during mid-summer 1890. The results are shown in Table 2.2.

N.Z. Geological Survey, 1957-1966. As part of a broader mass balance programme, velocities were measured by the NZGS. Some of the results are presented by Goldthwait & McKellar (1962), the rest were not published. No attempt was made to repeat Brodrick's earlier transects, although some later measurement points correspond approximately to earlier ones. Seasonal velocity variations near Malte Brun hut were detected for the first time. No measurements were made on the lower reaches of the glacier.

Ministry of Works and Development surveys, 1971-1973. Mass balance studies were continued by the MOWD (Anderton 1975). Ice depths were estimated by geophysical survey at three transects (Fig 2.3) allowing ice discharge to be estimated. Annual ice velocities were measured.

This thesis presents new measurements of ice velocity. Previous results were adjusted using measured seasonal variations in velocity to provide data which are standardised as annual flow rates. Comparisons with earlier measurements allow long-term trends to be identified over a time period which compares well with some of the longer glacier records in the world.

2.1.2.2 1985-1986 field surveys.

Selection of transects.

Several factors were considered when deciding where to measure ice velocities on the Tasman Glacier, and on what arrangement of markers to use.

1) All fixed points and glacier surface markers had to be accessible to a person on foot carrying a heavy load.

2) Fixed points had to be visible from existing trigonometric stations to allow absolute elevations (reduced levels) to be calculated.

3) The survey was designed to allow easy repeatability in the future, which some previous surveys have not adequately considered (eg Skinner's (1964) siting of fixed points on moraine crests). To this end, all fixed points were located on stable bedrock sites where possible and permanently marked with rock bolts (Appendix 1). Where possible, existing Trig. points marked on NZMS1 Sheet 79 were located and used.

4) Velocities were measured along transects where depths and velocities had previously been measured, to allow ice discharges and

TABLE 2.2 Summary of measured ice velocities on the Tasman Glacier.

Source & location		Days between surveys	Velocity Mean	Velocity Max.	No. markers	Season
Brodrick (1891)						
line D 1890		32	144.5	166.8	8	Sr
line C 1890		32	74.9	103.0	10	Sr
McKellar (unpubl.)						
Malte Hut 1958		187	167.4	186.9	4	W-Sp
Malte Hut 1960		212	171.0	191.4	4	W-Sp
Mc Kellar (unpubl.)						
Lower end of	66/4	249	47.4	{ 70.8	1	W-Sp-Sr
Tasman ice	66/5	249		{ 24.0	1	W-Sp-Sr
	66/6	249	40.0	{ 39.8	1	W-Sp-Sr
	66/7	249		{ 40.2	1	W-Sp-Sr
	66/8	249	32.9	{ 41.6	1	W-Sp-Sr
	66/9	249	___	{ 24.1	1	W-Sp-Sr
mean		249	40.1		6	W-Sp-Sr
Anderton (1975)						
Malte Hut 1972-73		367	235.0	244.2	3	all year
Ball Hut 1971-72		229	80.0	87.9	4	Sp-Sr-A
Ball Hut 1972-73		407	54.4	61.0	6	Sp-Sr-A
This study						
De la Beche 1985-86		173	255.3	270.4	5	Sr
De la Beche 1986		213	240.9	248.5	5	W-Sp
mean			241.5	249.9		all year
Ball Hut 1986		211	87.2	98.1	7	W-Sp
Celmisia Flat 1986		210	1.5	3.3	7	W-Sp

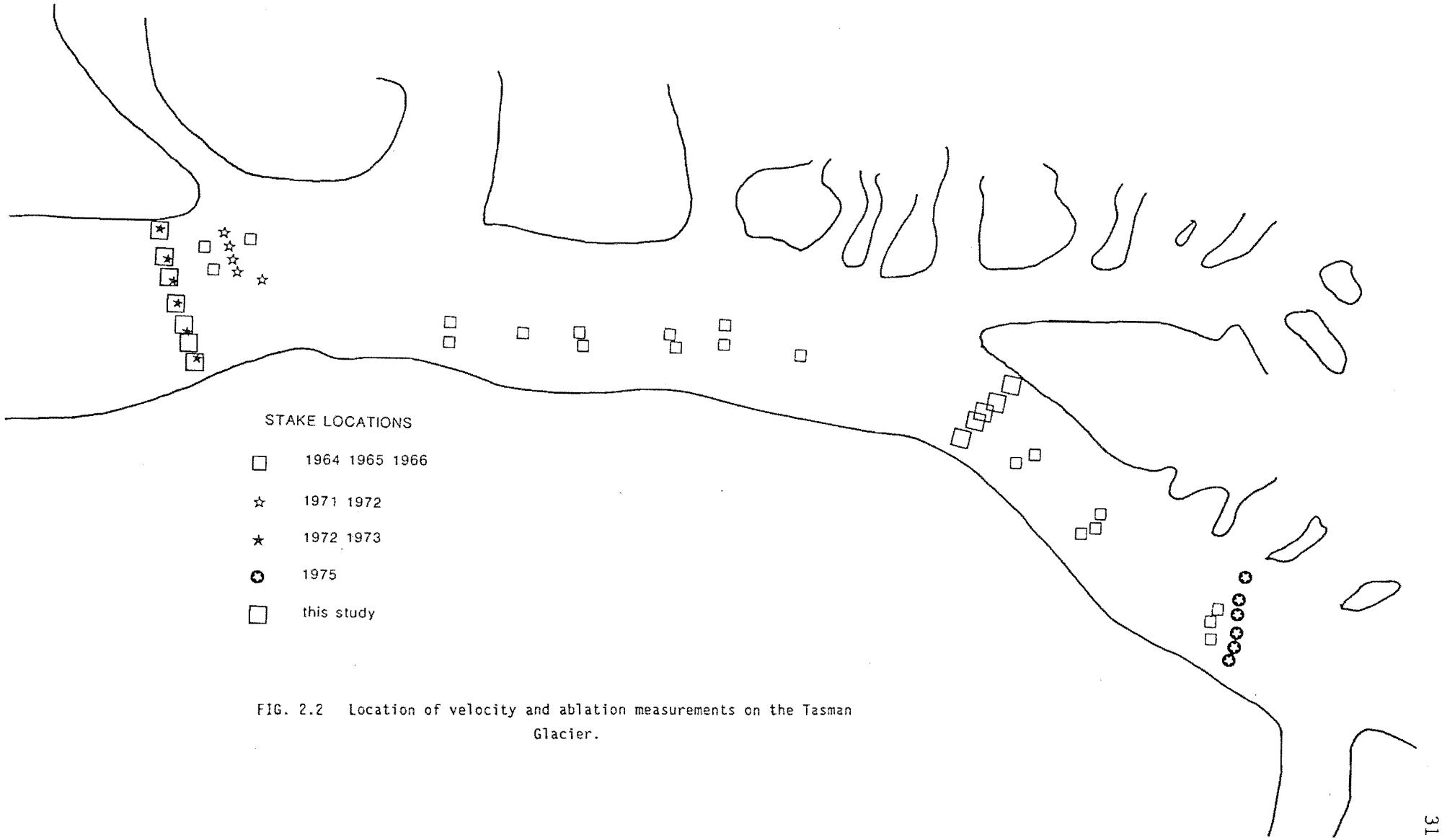

FIG. 2.2 Location of velocity and ablation measurements on the Tasman Glacier.

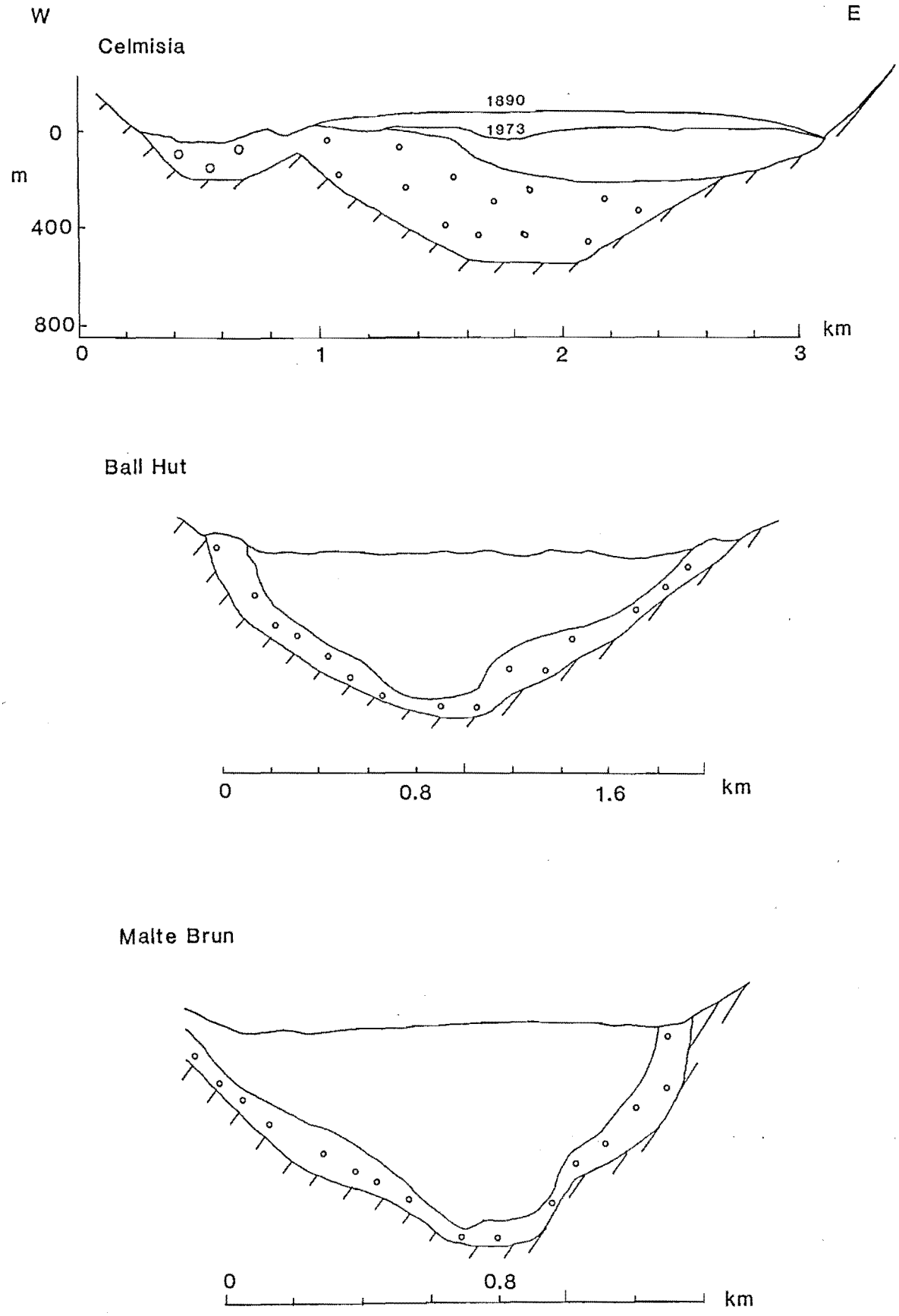

FIG. 2.3 Cross-sections of study transects, estimated from gravity and seismic surveys by Broadbent (1973). Ice surfaces in 1973 are shown except where stated otherwise. See Fig M1 for transect locations.

changes over time to be calculated. Surface markers were therefore arranged in lines perpendicular to the glacier axis.

Three transects were selected. Full details of the locations of fixed points, the base lines used, and the calculations are presented in Appendix 1 and 2.

Celmisia Flat. Ice flow had not previously been measured within 9 km of the terminus. A transect near Celmisia Flat (on the Ball Hut road) was established 2 km from the terminus, to supplement measurements from aerial photographs (Chapter 2.1.2.3), and to coincide with a geophysical survey line of Broadbent (1973) and Claridge (1983).

Ball Hut. A transect at this site was established to coincide with another geophysical survey line and to allow direct comparisons with earlier velocity measurements (Brodrick 1891; Anderton 1975) and glacier surface levels (Skinner 1964). A disadvantage of the site is the strong longitudinal gradient in ice flow which makes it important to duplicate precisely the positions of previous velocity measurements. This was made possible by reference to Brodrick's unpublished field notes (held in DOSLI archives, Christchurch) and Fig. 4 of Skinner (1964).

De la Beche. The removal of the old Malte Brun Hut and the collapse of the moraine walls at that site made it impractical to maintain a line of ablation stakes for several months continuously at the site used by Anderton (1975) with the techniques available. A line of stakes was established 2.5 km downstream from the 1971-1973 line, where the glacier width and slope were the same as at the old Malte Brun site. The glacier cross-section at Malte Brun (Anderton 1975 Fig.18) is similar to the cross-section at the 1985-1986 transect. No tributary glaciers join the Tasman between the 1971-1973 line and the line used in this study. Two new fixed points had to be established for the survey (Appendix 1).

Survey methods.

The location and reduced level of each marker on the glacier surface was fixed by intersecting angles from two fixed points using a Wild T-1A theodolite. Distances between fixed points and markers were measured using a Wild DI4-L Electronic Distance Meter (EDM) and up to nine prisms to give a range of 7 km (though in practice no distances greater than 4.5 km were measured).

All locations were converted to co-ordinates using Lands and Survey Department computor programmes. Reduced levels have a precision of ± 250 mm. The E.D.M. measurements were much more precise than theodolite data (±5 mm against ±30" over distances of several km). Errors in the positions

TABLE 2.3 Seasonal variation in ice velocities

Marker	summer velocity as % annual velocity	Winter velocity as % annual velocity	Winter velocity as % summer velocity
P2	109	94	92
P3	104	97	96
P4	106	95	94
P5	101	97	95
P7	105	95	91
Mean	105 %	96 %	94 %

TABLE 2.4
Transect 3: De la Beche 1360 m
Survey dates 23-25/11/85, 16-17/5/86, and 16/12/86
Period between surveys: (a) Nov '85 to May '86 = 174 days
(b) May to Dec '86 = 213 days.
Total period = 387 days

Marker	Movement (m) (a)	(b)	Ice velocity (a) (md^{-1})	(b) (md^{-1})	mean (md^{-1})	(ma^{-1})
P2	128.15	136.77	0.74	0.64	0.68	249.90
P3	121.64	138.49	0.70	0.65	0.67	245.43
P4	122.97	135.68	0.71	0.64	0.67	243.95
P5	117.53	136.66	0.67	0.64	0.66	239.74
P7	114.74	127.52	0.66	0.60	0.63	228.49
Mean			0.70	0.63	0.66	241.48

TABLE 2.5
Transect 2: Ball Hut 960 m
Survey dates 13-14/5/86 and 10/12/86
Interval between surveys = 211 days

Marker	Movement (m)	Ice velocity (ma^{-1})
F1	37.79	72.64
P1	46.39	89.17
P4	45.58	87.61
P2	---	---
P3	47.21	90.75
F2	51.05	98.13
F3	47.14	90.61
F4	42.38	81.46
Mean		87.20

TABLE 2.6
Transect 1: Celmisia Flat 772 m
Survey dates: 12-13/5/86 and 8/12/86
Interval between surveys = 210 days

Marker	Movement (m)	Ice velocity (ma^{-1})
F1	1.19	2.07
F2	0.49	0.85
F3	0.69	1.20
F4	1.85	3.21
F5	1.70	2.95
F6	1.90	3.30
F7	0.66	1.45
Mean		2.15* (1.53)*

TABLE 2.7 Adjusted ice velocities at Malte Brun and Ball Hut transects

Location		U_s (measured)	U_0 (calc)	U_0 (adj)	U_{sl} (calc)	U_{sl} (adj)	U_{sl}/u_s (vel ratio)
Malte Brun	1890	500	150	185	350	315	0.63
	1973	244	56	75	188	169	0.69
	1986	270	49	71	221	199	0.74
Ball Hut	1890	167	58	69	109	98	0.59
	1973	61	29	32	51	29	0.47
	1986	98	19	27	79	71	0.72

of individual markers on the glacier are less than ± 400 mm.

A preliminary survey using only the theodolite was made in November 1985 at the De la Beche transect. This allowed a six-month (summer) flow rate to be calculated between November 1985 and May 1986. In May and December 1986 complete surveys were made of all three transects, and results from these surveys have been adjusted to annual flow rates according to the measured seasonal variation in ice velocity at De la Beche (Table 2.3) The results of the velocity measurements are shown in Tables 2.4 to 2.6, and seasonally-adjusted velocities in Table 2.7.

2.1.2.3 Aerial photographic survey of boulder movements.

The stable parts of the supraglacial debris mantle on the lower glacier have many large boulders on the surface which are visible on low-level aerial photographs. Some of the boulders have been identified on photographs taken 29 years apart: mistaken identification is avoided by recognising groups of boulders whose local distribution is unique. In the case of large boulders, the shape of individuals is sometimes recognisable on different photographs.

The movement of twenty-five boulders was determined by plotting the positions of each one on a transparent overlay on vertical aerial photographs. Photographs taken in 1957, 1971, and 1986 were used because the time interval between each set was sufficient to allow boulders to move far enough to reduce measurement errors, and because these photographs have better definition than other sets (eg 1965, 1973). Each set was adjusted to exactly the same scale. The scale was determined by measuring six distances between identifiable ground features from the photographs at the altitude of the glacier surface, and measuring the same distances on the NZMS 1 topographic map. The mean of the six scales calculated in this way was 1:12,950 with a range of 1:12,749 to 1:13,218, a variation of less than ±2%. This figure was checked by measuring the ground distance between boulders 18 and 19 (Fig 2.4) in 1987. The ground distance of 71 m compared with 5.4mm measured with a graduated magnifying eyepiece from the 1986 aerial photographs, giving a scale of 1:13,148. Taking these two independent measures into account, a scale of 1:13,000 was used for the area shown in Fig 2.4. There is an altitudinal range of about 50 m in this area which introduces a 1.25% error to the photograph scale.

The distance between the position of each boulder plotted on the overlay for each date was measured to the nearest 0.5 mm, which represents

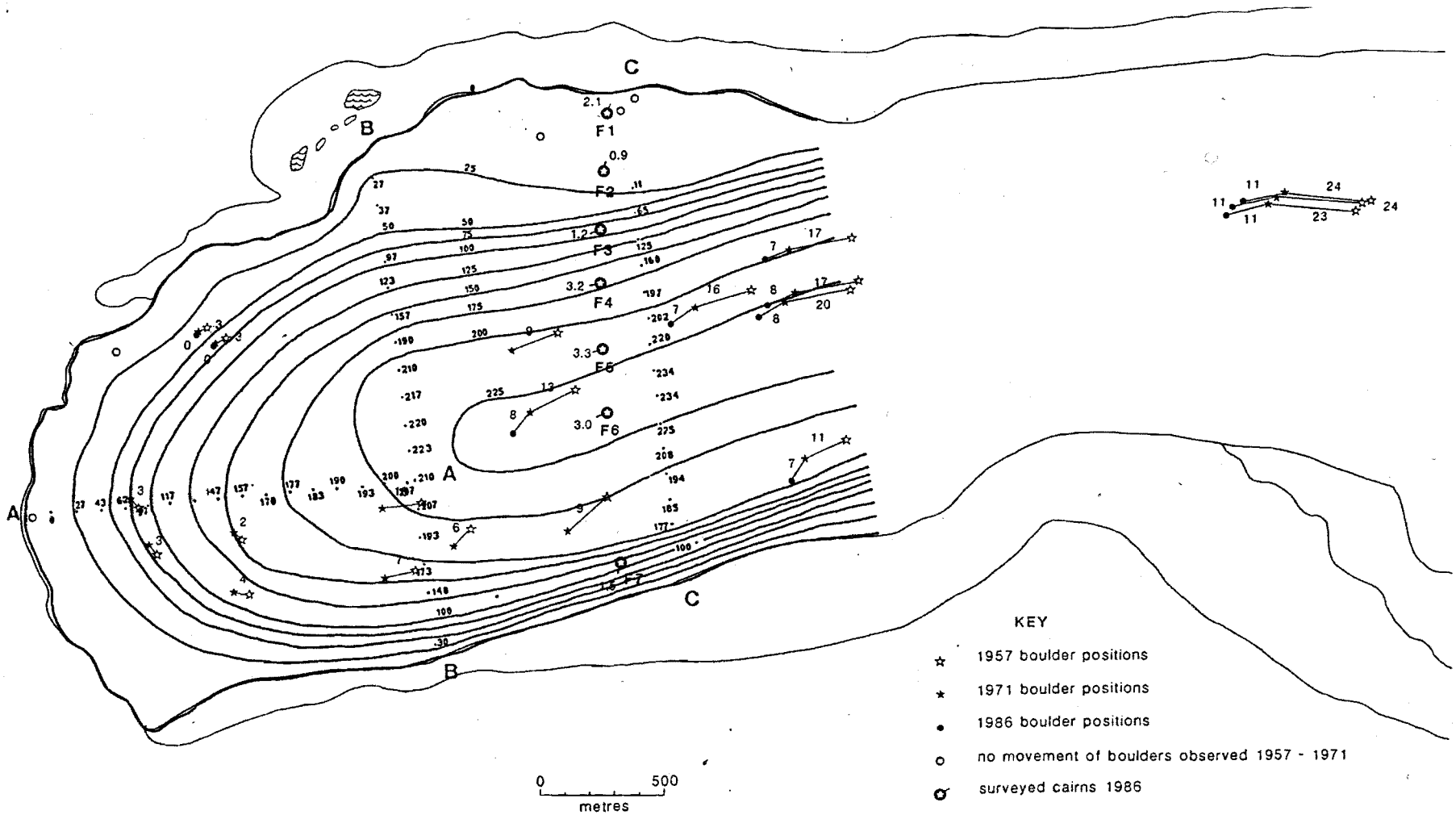

FIG. 2.4 Boulder vectors on the lower Tasman Glacier measured from aerial photographs, and vectors of surveyed cairns in 1986. OVERLAY: ice thickness estimates by Broadbent (1973) and Claridge (1983).

6.5 m on the ground. The flow rate of the glacier in ma^{-1} at each point is then simply calculated by

$$(13 \times S_{map})/(t_2-t_1) \qquad (5)$$

where S_{map} is the map distance in mm between successive positions of the same boulder, t_2 is the date of the later photograph, and t_1 is the date of the earlier photograph. The measurement error is about $\pm$0.5mm which gives an error of $\pm$0.5 ma^{-1} over an interval of 13 years.

The growth of thermokarst lakes since the early 1970s has removed several boulders from view, so the distribution of measured flow rates for 1957-1971 is more extensive than for 1971-1986.

The results are shown in Table 2.8 and are plotted on Fig 2.4. These can be interpreted in terms of ice velocities, flow vectors, and of the causes of observed changes.

Ice velocities.

The velocities are generally low, with a down-glacier decline from about 24 ma^{-1} at 4.5km from the terminus to zero at the terminus in the 1957-1971 period. The highest velocities are in the glacier centre, and correspond to the deepest parts of the glacier determined by Broadbent (1973) and Claridge (1983). Flow rates declined by about 40-60% between the two measurement periods, as confirmed by the movements of surveyed markers in 1986 (see Section 2.1.2.2 above). By 1986 much of the terminus was almost stationary.

Flow vectors.

The main flow of the glacier is in a south-easterly direction around the bulge in the eastern lateral moraine (Fig 2.4). Upstream of this bulge, flow is aligned more directly down-glacier. Within 1km of the terminus flow converges on the zone of thermokarst erosion, indicating that flow is in response to local topography rather than to the (very slight) general downvalley gradient. A trend towards greater divergence of flow vectors is shown by a comparison of the 1957-1971 and the 1971-1986 movements, indicating that as the glacier slows, the influence of local effects become more marked. Flow vectors of the 1986 surveyed markers (see 2.1.2.2 above) confirm the longer-term trend.

Causes of the observed trends: what is "stagnant" ice ?

Various definitions of "stagnant" ice have been proposed by glaciologists, none of which are universally applicable (Clapp 1904; Cook 1924; Flint 1929; Ahlmann 1948; Hooke 1977; Mannerfelt 1981). The debris-covered area of the Tasman Glacier was described as "stagnant" by Porter (1975a). The present author regards the glacier as "stagnant" only

TABLE 2.8
Movement of surface boulders measured from aerial photographs.

Boulder	1957-1971 movement (m)	1957-1971 rate (ma^{-1})	1971-1986 movement (m)	1971-1986 rate (ma^{-1})
1	332	24	163	11
2	332	24	169	11
3	325	23	169	11
4	241	17	98	7
5	241	17	117	8
6	254	20	117	8
7	221	16	104	7
8	156	11	98	7
9	0	0	0	0
10	0	0	0	0
11	0	0	0	0
12	124	9	-	-
13	182	13	117	8
14	124	9	-	-
15	85	6	-	-
16	137	10	-	-
17	104	7	-	-
18	39	3	0	0
19	46	3	0	0
20	26	2	-	-
21	52	4	-	-
22	39	3	-	-
23	46	3	-	-
24	0	0	0	0
25	0	0	0	0

TABLE 2.9 Estimated sliding velocities compared to measured flow rates

Location		Estimated U_{SL} (a)	Nearest measured flow rate (b)	% difference if (a)>(b)
Ball Hut	1890	109	92	-16%
	1973	51	40	-20%
	1986	79	73	-8%
De la Beche	1986	221	228	--

when it is not moving. Most of the debris-mantled tongue is moving in response to stress patterns relating to the down-valley slope and (increasingly) to ablation around thermokarst zones. A definition of "stagnant ice" based on absolute flow rate (eg. Hooke 1977) is preferred to one based on movement of the basal layer of the glacier (eg. Mannerfelt 1981).

Adopting the above definition, a zone of stagnant ice now exists on the Tasman Glacier which extends 350 m out from the lateral moraine at marker F2 (Fig 2.4) and perhaps to 1km above the terminus on the glacier centre line. The "stagnant" zones of the glacier are largely determined by the effect of subglacial topography on surface slope during thinning. The relationship between zones where flow vectors in the 1971-1986 period respond primarily to local influences and the subglacial topography is shown in Fig 2.4 (overlay). It is clear that the "stagnant" ice occurs almost entirely on the subglacial shelves around the ice margin. The data does not reveal whether or not there is a marked velocity discontinuity (a "shear plane" sensu Weertman 1957) bordering these zones, but their absence on aerial photographs and the low velocity gradients make their existence extremely unlikely near the terminus. However, 1957 aerial photographs (Fig M1) show evidence of shear zones on the eastern glacier margin bordering the Murchison embayment.

2.1.2.4 Spatial and temporal trends in ice velocity on the lower Tasman Glacier

Fig 2.5 synthesises available velocity data into an interpretation of the Twentieth Century variation in velocity over the lower 10 km of the Tasman Glacier. A general decrease in velocity is apparent. The longitudinal velocity gradient has decreased in the lower 4 km of the glacier, in contrast to an increased gradient (greater compression) between 10 and 7 km above the terminus. Short-lived increases in surface velocity are inferred by comparison with observations of other glaciers in the region (Section 2.1.3.3).

2.1.3 Ice discharges of the Tasman Glacier.

Measurements of the velocity at the glacier surface are not in themselves adequate for understanding the dynamics of the glacier. They give only an approximate indication of the presence or absence of basal sliding and of the total ice discharge through a cross-section of the valley. The shape of the vertical velocity profile and the ice discharge

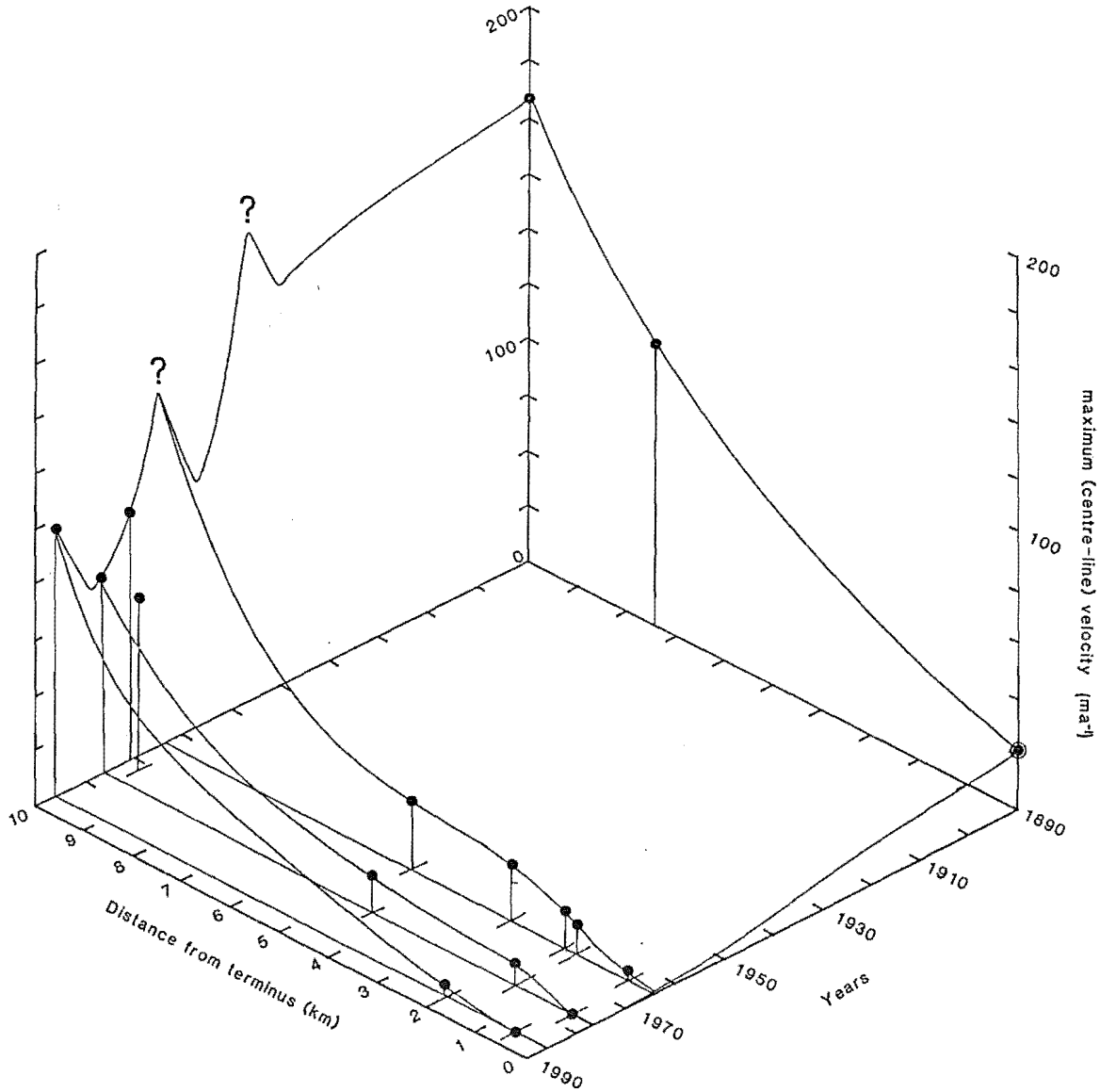

FIG. 2.5
Spatial and temporal distribution of velocity of the lower Tasman Glacier. 1890 data from Brodrick (1891), post-1965 data on the lower 5 km of the glacier from boulder movements, data at 10 km from surveys by Anderton (1975) and this study. Note inferred fluctuations at 10 km which have not affected the terminus (see text).

must be estimated if the discharge of debris in transport is also to be calculated.

It is possible to make reasonably precise calculations of the ice discharge at the three cross-sections of the Tasman Glacier where ice velocities have been measured and ice depths estimated. The ice discharge Q is the product of the average velocity U of ice through the cross-section in a unit of time and of the cross-sectional area A, thus:

$$Q = UA \qquad (6)$$

The calculation of the parameters in this equation is not always easy and depends on many assumptions, especially concerning the behaviour of ice under stress as discussed above (Section 2.1.1).

2.1.3.1 Calculation of mean velocity at each transect.

Ice flow is treated as a combination of processes of internal deformation and of basal sliding. Since the theoretical understanding of deformation is better developed than that of basal sliding, the former is treated in more detail and the latter is quantified by inference rather than by calculation.

The internal deformation of the glacier at each cross-section was calculated using equation (4a) on p.23c, which gives the mean velocity due to internal deformation through the cross-section, U_{av} (Booth 1986), or by using equation (4) on p.23c, which gives the surface velocity due to deformation, u_0 (Nye 1952a; Paterson 1981).

The velocity due to basal sliding of the glacier, U_{sl} is calculated from

$$U_{sl} = U_s - U_0 \qquad (7)$$

A check of the sliding velocity is provided by comparing calculated values of U_{sl} with measured flow rates close to the valley sides, because the latter will approximate to actual rates of basal sliding. All measured velocities have been located at points at least several tens of metres in from the glacier margins so that the calculated rates should always be less than the measured rates. The comparisons with available data (Table 2.9) show that two of the calculated rates are actually greater than the nearest measured rates by 8% and 16% respectively. This suggests that the equations used to calculate ice deformation have underestimated the plasticity of the ice, though whether this error originates in the shear stress (τ_{av}) or the flow law parameters (A and/or n) is not known. However, an error of up to perhaps 20% in the calculations is not surprising given the rather simplistic approach which has been adopted. An

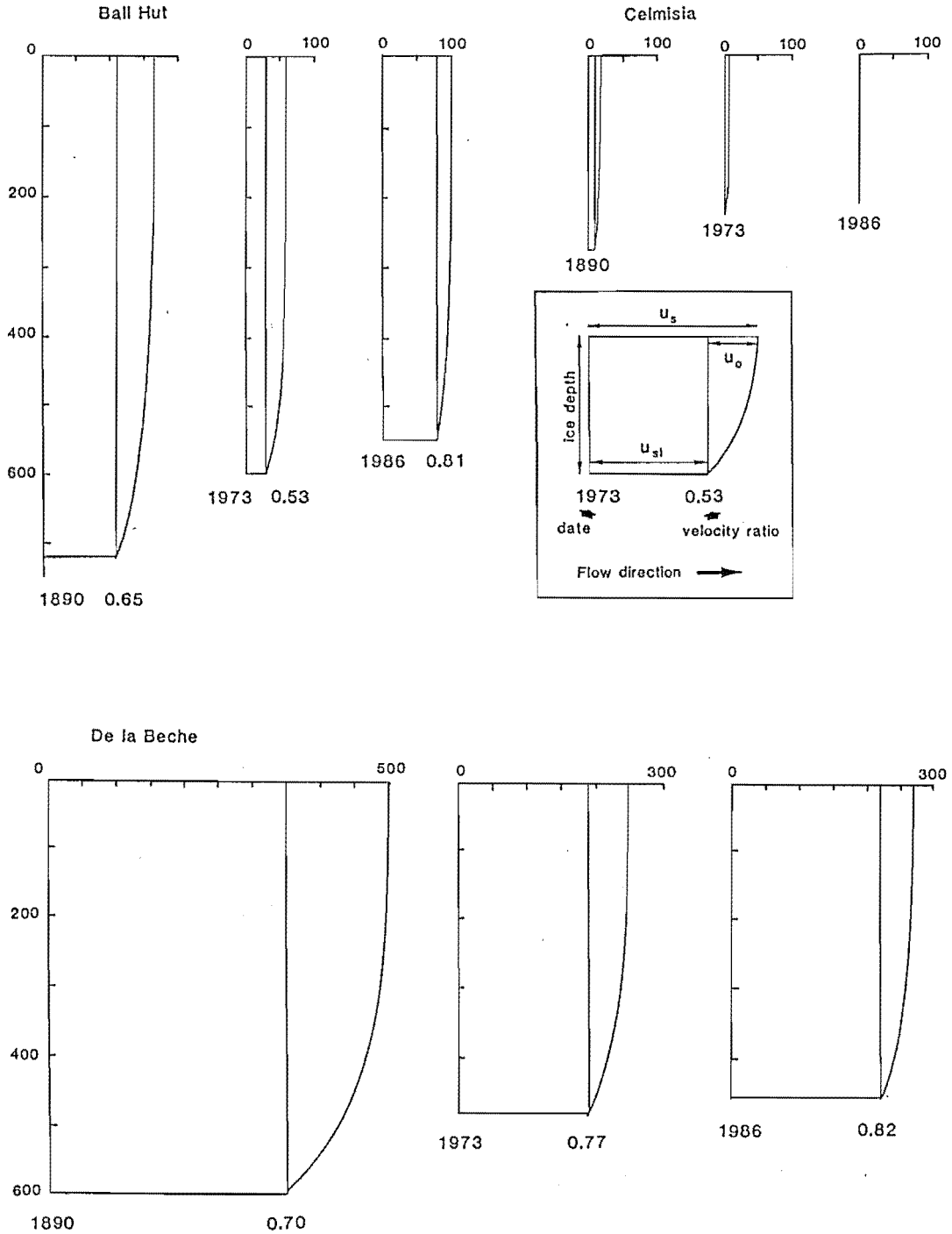

FIG. 2.6 Vertical velocity profiles for the Tasman Glacier.

adjustment of -10% has been made to the calculated rates of basal sliding, and therefore also of internal deformation, used in the following calculations of ice discharge. Fig 2.6 shows calculated vertical velocity profiles at each cross-section.

2.1.3.2 Cross-sectional areas of the study transects.

The cross-sectional area of the glacier at each transect was calculated from the seismic profiles of Broadbent (1973) (Fig 2.3). From these profiles, the cross-sectional areas for 1890 and 1986 were calculated using the ice-surface elevations and glacier widths from these years. The hydraulic radius (Equation 3 p.23c) was also measured from the cross-sections.

2.1.3.3 Ice discharges: results.

The calculated ice discharges through each cross-section are shown in Table 2.10. Their magnitudes and changes over space and time (Fig 2.7) allow the following conclusions to be drawn.

1). Ice discharge reduces towards the glacier terminus, and at the terminus Q = 0 by definition. The rate of reduction down the glacier has remained constant over time (Table 2.11) even though ice discharges have been greatly reduced. Thus, the relative amounts of ice passing through each cross-section has varied by only a small amount. A minor exception is that as the ice near the terminus has approached zero velocity over time the ice discharge has been proportionately reduced, and this trend is expected to continue.

2). Similarly, the proportionate reduction in ice discharge at each cross-section over time has been constant between sites (Table 2.12 and Fig 2.7 inset). Thus, the 1973 ice discharge was 37% of the 1890 value at Malte Brun, and 31% of the 1890 value at both Ball Hut and Celmisia Flat. Differences emerge when the increase in ice discharge in the 1980s is considered. Both Malte Brun and Ball Hut show increased discharges, whereas the discharge past Celmisia Flat continued to decline. Field observations of the distribution of the rise in ice surface elevation along the glacier margins (Chapter 2.2.6.1) reveal that the recent positive mass balance trend has yet to affect ice levels at Celmisia Flat, while the glacier surface has risen and flow has accelerated since the 1973 measurements at the other two transects.

3). Space-time trends in ice discharge follow from similar trends in ice velocity and cross-sectional area. In the Tasman Glacier, the dominant

TABLE 2.10 Calculation of ice velocities and discharges of the study cross-sections.

Site		U_S (ma^{-1})	U_{SL} (ma^{-1}) (a)	U_{SL} (ma^{-1}) (b)	U_O (ma^{-1}) (a)	U_O (ma^{-1}) (b)	U_{av} (ma^{-1})	$U_{SL} + U_O$ (ma^{-1})	CSA (m^2)	Q (m^3a^{-1})
Malte Brun	1890	500	350	315	150	185	148	463	622,850	2.884×10^8
	1973	244	188	169	56	75	60	229	470,600	1.078×10^8
	1986	270	221	199	49	71	57	256	434,200	1.112×10^8
Ball Hut	1890	167	109	98	58	69	55	153	791,500	1.211×10^8
	1973	80*	51	46	29	34	27	61	625,000	3.813×10^7
	1986	98	79	71	19	27	22	93	552,850	5.141×10^7
Celmisia Flat	1890	20?	--	10^X	0.1	10^X	8^X	18	371,950	6.695×10^6
	1973	11**	11	7.5^Y	0	3.5	0.8^{YY}	8.3	257,500	2.137×10^6
	1986	3.3	3.3	1.0^Z	0	2.3	0.5^{ZZ}	1.5	237,370	3.561×10^5

* mean of 1971-72 and 1972-73 velocities of boulders X1/4, X1/5, P3 and P4
** mean of velocities of boulders 7 and 13, 1957-71 and 1971-86.
X estimate from assumed velocity ratio of 0.5
Y mean of velocities of boulders 8 and 14, 1957-71 and 1971-86.
YY estimate from comparison with 1986 velocity ratio.
Z velocities of 1986 survey show $0.9 < U_{SL} < 1.2$
ZZ (mean velocity of 1986 markers) - U_{SL}

U_S = maximum measured surface velocity.
U_O = maximum calculated surface velocity due to internal deformation
U_{av} = mean calculated surface velocity due to internal deformation
U_{SL} = velocity due to basal sliding, assuming U_{SL} is constant across a cross-section.

TABLE 2.11 Spatial trends in ice discharge ie. standardised with respect to time.

Site	1890	1973	1986
Malte Brun	100	100	100
Ball Hut	42	35	46
Celmisia Flat	2	2	0.4

TABLE 2.12 Temporal trends in ice discharge ie. standardised with respect to space.

Year	Malte Brun	Ball Hut	Celmisia Flat
1890	100	100	100
1973	37	31	31
1986	39	42	6

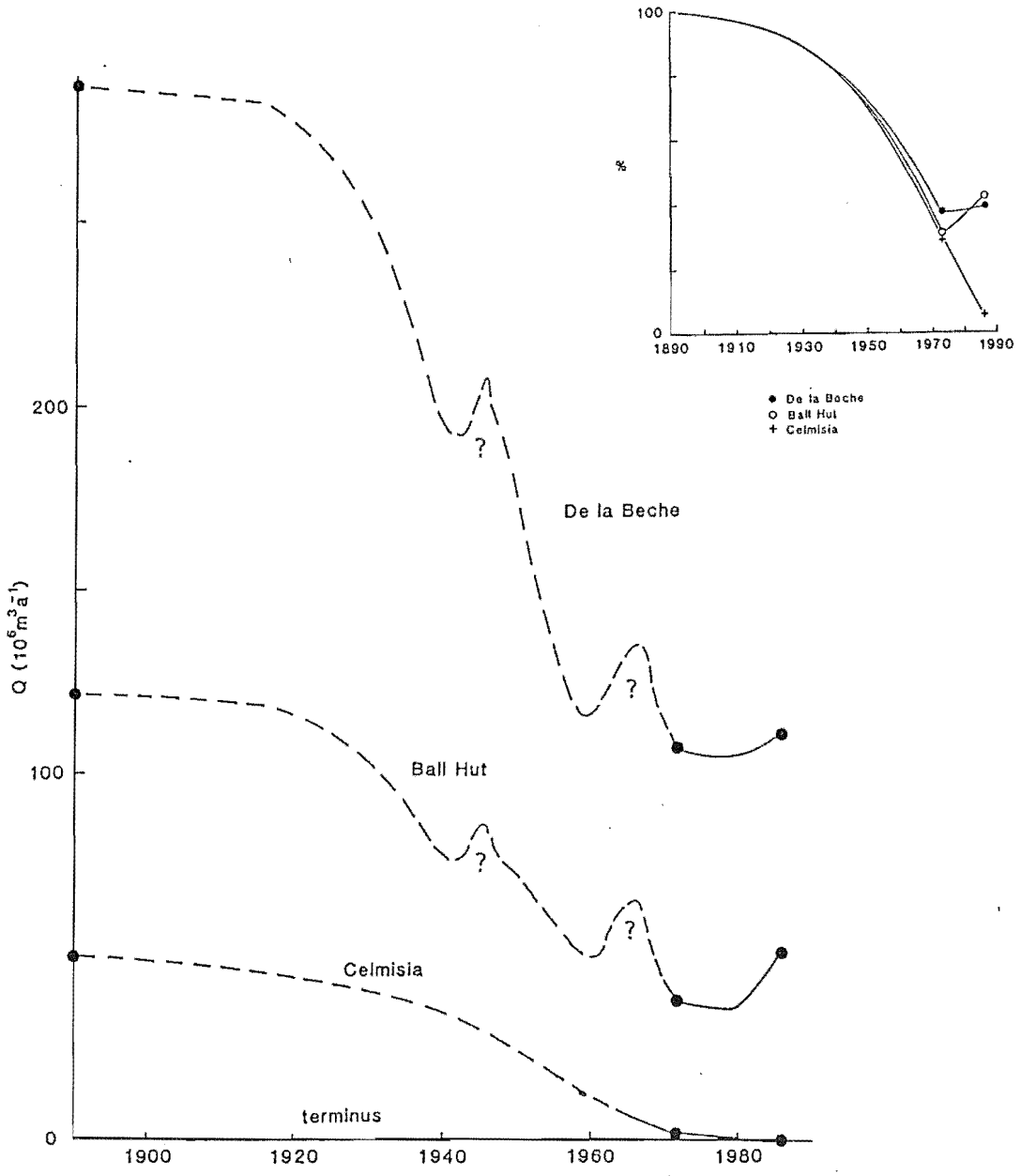

FIG. 2.7 Temporal variation in ice discharge at each transect. Interpolated peaks are explained in the text.
INSET: Variation in ice discharge at each transect as a proportion of their respective 1890 values (1890 = 100%).

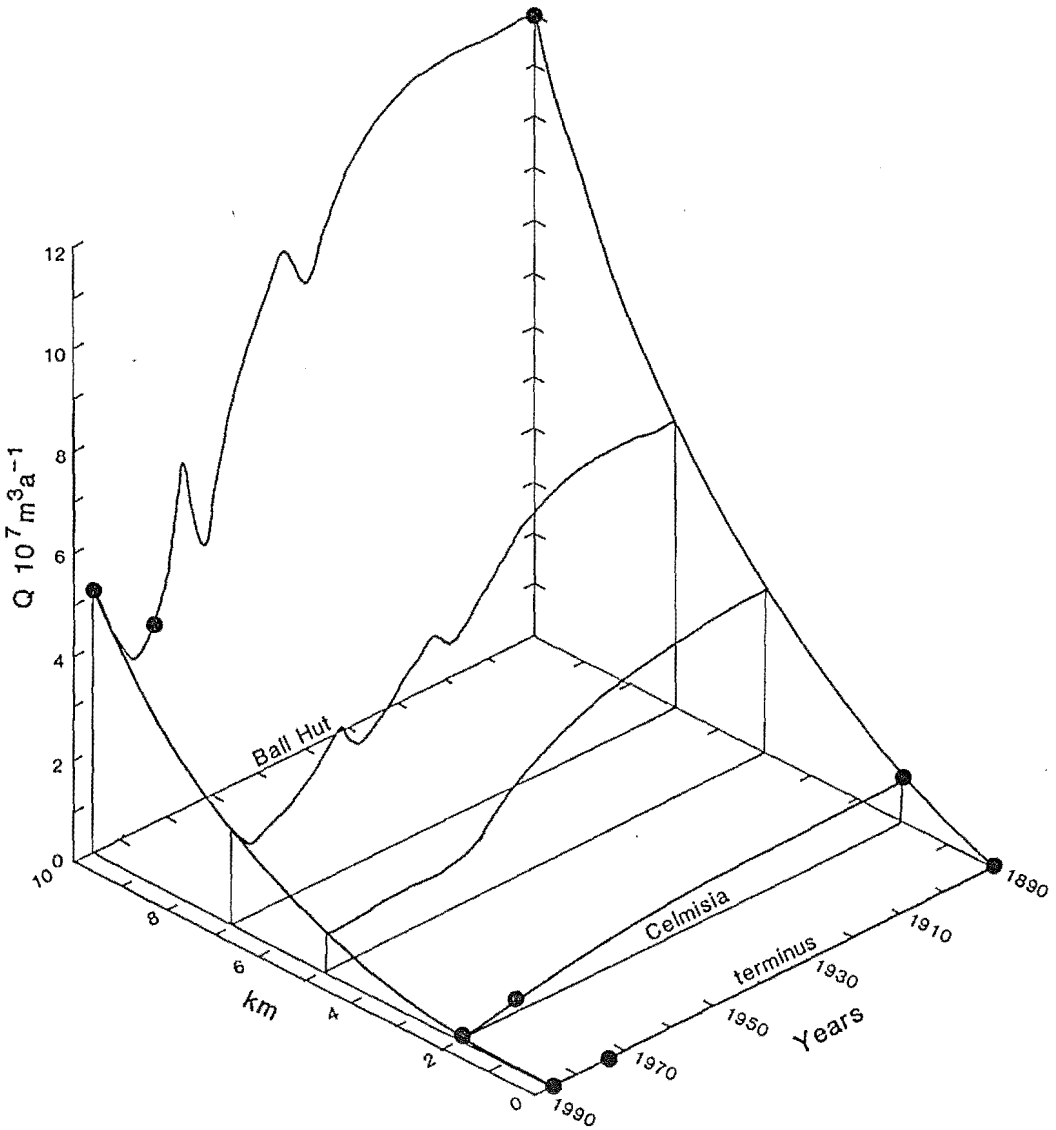

FIG. 2.8 Spatial and temporal distribution of ice discharge of the lower Tasman Glacier. 1890 data calculated from Brodrick (1891), 1973 data from Anderton (1975), 1986 data this study. Note inferred decrease in discharge fluctuations towards the terminus (see text).

influence on ice discharge is the change in ice velocity, because proportionately greater changes in velocity have occurred since 1890 than in cross-sectional area. This conclusion is implicit in the earlier findings that ice in the lower tongue has slowed without retreat of the terminus. A basic difference exists between the Tasman and the Fox and Franz Josef Glaciers in this respect, in that the two Westland glaciers have responded to mass balance changes by rapidly changing the cross-sectional area of the lower tongues to the point where rapid retreat or advance of the terminus has taken place.

The variation in ice discharge in the lower 10 km of the Tasman Glacier over the last century is presented in Fig 2.8. Although there are few data points, the interpretation of discharge variations is inferred from fluctuations of the termini of the Fox and Franz Josef Glaciers. The 1986-87 rise in surface level at Ball Hut is the first recorded rise this century, and corresponds to an advance of the Westland Glaciers of similar or slightly greater magnitude to advances in the mid 1960s and 1940s (Sara 1968, 1970; Soons 1971; Wardle 1973). Given the coincidence of a current advance of the Westland glaciers with the rise in ice level at Ball Hut, it is suggested here that a similar coincidence has occurred and gone unrecorded in the past. The historical record of glacier fluctuations at Mount Cook includes very few surveys, and the interpretations made by Gellatly (1985c) do not consider the possibility of unrecorded short-term events.

The present increase in ice discharge has yet to affect the Celmisia Flat transect and it is possible that earlier positive fluctuations similarly had no effect since they probably were of smaller magnitude than the present one. Fluctuations in ice discharge since 1890 have been of a sufficiently small magnitude to allow the long, low-gradient lower tongue of the Tasman to have had a damping effect on the passage of climatically-induced kinematic waves (Chapter 2.2). The amplitudes of the ice-discharge peaks in Fig 2.8 are therefore shown attenuating towards the terminus, and neither the 1940s nor the 1960s peak is likely to have affected the lower 2 km of the glacier, just as the present peak has as yet failed to do.

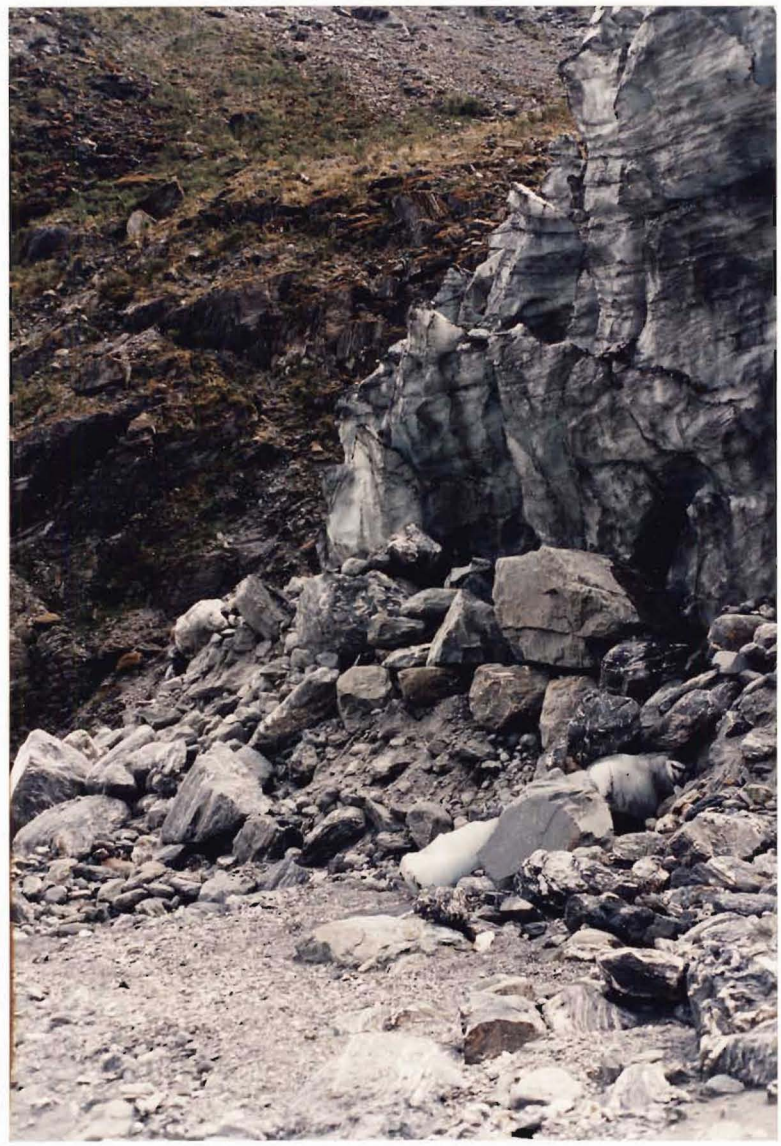

FIG. 2.9 The terminus of the Fox Glacier, advancing at a rate of up to 1 metre per day and forming a small push moraine. (December 1987)

2.2 MASS BALANCE

2.2.1 Theory.

Mass balance studies deal with changes in the mass of a glacier over time and space, usually expressed volumetrically as an advance or retreat of the terminus or a rise or fall of the surface. Standard mass balance terms are defined by Anonymous (1969). Glaciers gain mass through the accumulation of snow, the zone where there is a net annual accumulation being the accumulation zone. Mass is lost through ablation, the zone of net annual loss being the ablation zone. The two zones are separated by the equilibrium line, at which there is no net annual mass change. Ice flow redistributes mass from the accumulation to the ablation zone at a rate corresponding to the rates of accumulation and ablation. Thus a glacier is a system in inputs, transfer and outputs of mass which attempts to balance its mass budget to maintain an equilibrium (steady state volume and mass flux) with respect to prevailing climate. A detailed summary of measurement techniques and terminology is given by Østrem & Stanley (1969).

2.2.2 Accumulation.

Snow surveys in the accumulation zone of the Tasman Glacier were conducted in the 1960s and 1970s (McKellar, 1965, 1966; Anderton 1975). Specific balances were calculated, but the density of measurement sites was insufficient to make precise estimates of area-averaged accumulation. A value of 6850 mm (water equivalent) of annual precipitation at Tasman Saddle Hut was estimated (Anderton 1975). No accumulation measurements have been made for this study.

2.2.3 Ablation of the Tasman Glacier.

The term "ablation" is used in glaciology to include all processes by which snow and ice are lost from the glacier (Paterson 1981 p.43; Anonymous 1969). Drewry (1986 p.264) summarises the main processes of mass loss as including melting of the glacier surface and sole, evaporation and wind removal of snow. The mechanical removal of ice by rainwater erosion (Marcus et al 1985) and ice-cliff avalanching (Alean 1985; Röthlisberger 1987) has also been observed and may be important in individual cases. The broad definition of the term is adopted in this study, so that it is necessary to use terms such as "basal melt" or "ice-cliff calving" to refer to specific processes of mass loss from the glacier.

This usage is at variance with that of some authors, who exclude calving mechanisms and even direct surface melting (Pickard 1984 p.449). It should also be noted that ablation of ice should not be confused with the aeolian removal of rock or soil debris, also termed ablation (Whitten and Brooks 1985).

2.2.3.1 Previous studies.

Despite many observations of glaciers in New Zealand since the late Nineteenth and early Twentieth Centuries (Brodrick 1891, 1894, 1906; Harper 1934, 1935; Gage 1951; Harrington 1952; Skinner 1964; Sara 1968; Gellatly 1985a), only Bell (1910) made direct measurements of ablation (on the Franz Josef Glacier) before the late 1950s. Only in 1957 was a monitoring program commenced on the Tasman Glacier. This was continued intermittently until 1968. Preliminary results were reported by Goldthwait and McKellar (1962), and subsequent data are reported in unpublished reports (McKellar 1962, 1965, 1966, 1967, all unpubl.). Data relevent to the present study from McKellar's reports appears in Appendix 3 .

The main conclusions of this phase of research were that the magnitude of ice loss on the Tasman Glacier was much greater than had previously been assumed, and the melt rates associated with different seasons and synoptic conditions were recorded. The drawbacks of the study were that the measurement periods were either one or two days or were about one year. The lack of intermediate length periods restricted the amount of information on the seasonal variation in ablation rate. Complete records of surface melt were obtained for the years 1964-65 and 1965-66 for sites at 10 and 18 different altitudes respectively, allowing two annual ablation gradients to be constructed (Fig 2.12, Section 2.2.3.4)

In 1971 further mass-balance work was carried out by Ministry of Works and Development staff (Anderton 1975). Surface melt was measured at transects below Ball Hut and near Malte Brun Hut in the period 1971-1973. Accumulation studies made about this time are described in Chapter 2.2.2. The main results of these studies were to determine ice discharges at the two transects, but the detailed mass balance of the glacier could not be determined with the available data. Measurements of surface melt confirmed the findings of earlier workers that ice losses were great at lower altitudes.

2.2.3.2. 1985-1987 measurement of bare-ice ablation.

A main requirement of this study is to determine the amount of surface melting occurring at various points on the glacier surface. From these basic data, seasonal and synoptic variations in melt rate, and the seasonal and annual ablation gradients have been determined.

Measurement sites at c.960 m and c.1360 m altitude were selected. The lower site corresponds to transects of 1890 and 1972-73 and allows direct comparisons to be made. Between three and six stakes were maintained at this site throughout the study, and were located around the glacier centre line on strips of clean ice between areas of supraglacial debris. The upper site was chosen because of accessibility from huts and because it lies on the same reach of the glacier as several earlier measurement sites. Eight stakes were put in a line across the glacier. Six were maintained through the 1985-86 year and five through the 1986-87 year. The vertical separation of 400 m between sites was considered adequate for calculating ablation gradients based on only the two sites, given the good correlation of ice loss with altitude for the 1964-66 results (McKellar 1966).

A significant effect on melt rates due to reflected incoming radiation from the valley sides was expected. The significance of this effect was tested using the line of stakes at the upper site. The clustering of the stakes in the glacier centre at the lower site minimised this effect and comparisons are made with stakes in the equivalent (central) position at the upper site.

2.2.3.3 Results.

Results of the measurement of surface melt on the Tasman Glacier over two years are presented in Tables 2.13 and 2.14. The seasonal and annual ice losses are described below for each site, using data which have been adjusted to compensate for the measurement errors discussed in Appendix 4.

Ball Hut site. Melt rate (Fig 2.10) varies seasonally in a consistent pattern. Although melting was not taking place on the one mid-winter visit to the site in August 1986, some synoptic conditions cause melting at this elevation in any month of the year (Marcus et al. 1985; Hay & Fitzharris 1988). Melt rates in the winter of 1986 nevertheless were very low. A loss of 60 mm of ice was recorded between 13 May and 17 August at Stake 3, at a rate of 0.4 mmd^{-1}. The early spring melting was 260 mm of ice at 27 mmd^{-1} between 17 August and 13 September. The ablation season would thus appear

TABLE 2.13 Glacier ablation at Ball Hut (c.960 m).

Period	Measurement interval	Mid-point date	Ablation (cm) measured	Ablation (cm) adjusted	Ablation rate (mm d^{-1})
1985-86 Ablation season.					
26/09 - 3/10	7	30/09	19.6	19.6	28.0
3/10 - 10/11	38	22/10	>155.4	>172.5	>45.4
13/11 - 29/11	16	21/11	116.5	117.0	73.1
29/11 - 17/12	18	8/12	167.6	190.2	105.7
17/12 - 16/01	30	1/01	300.0?	300.0?	100.0?
16/01 - 5/02	20	26/01	174.8	193.2	96.6
5/02 - 21/02	16	13/02	98.2	99.9	62.4
21/02 - 18/03	25	6/03	153.8	162.6	65.0
18/03 - 2/04	15	26/03	74.3	74.3	49.5
2/04 - 7/05	35	19/04	143.8	156.4	44.7
7/05 - 13/05	6	10/05	9.7	10.7	17.8
1986 Winter.					
13/05 - 17/08	96		163.0	183.4	1.9
17/08 - 13/09	27	31/08	26.0	26.0	1.0
1986-87 Ablation season.					
13/09 - 15/10	32	29/09	62.9	62.9	19.6
15/10 - 11/11	27	28/10	140.7	151.9	56.3
11/11 - 7/12	26	24/11	160.2	179.4	69.0
7/12 - 18/12	11	12/12	125.6	129.0	117.3
18/12 - 6/01	19	28/12	183.8	214.3	112.8
6/01 - 29/01	23	17/01	227.3	262.5	114.1
29/01 - 15/02	17	7/02	133.8	137.1	80.6
15/02 - 6/03	19	25/02	117.0	120.8	63.6
6/03 - 20/03	14	13/03	>83.0	>99.6	>71.1
20/03 - 17/04	28	3/04	125.8	132.1	47.2
17/04 - 25/04	8	21/04	35.0	35.0	43.8
25/04 - 9/05	14	2/05	47.0	47.0	33.6

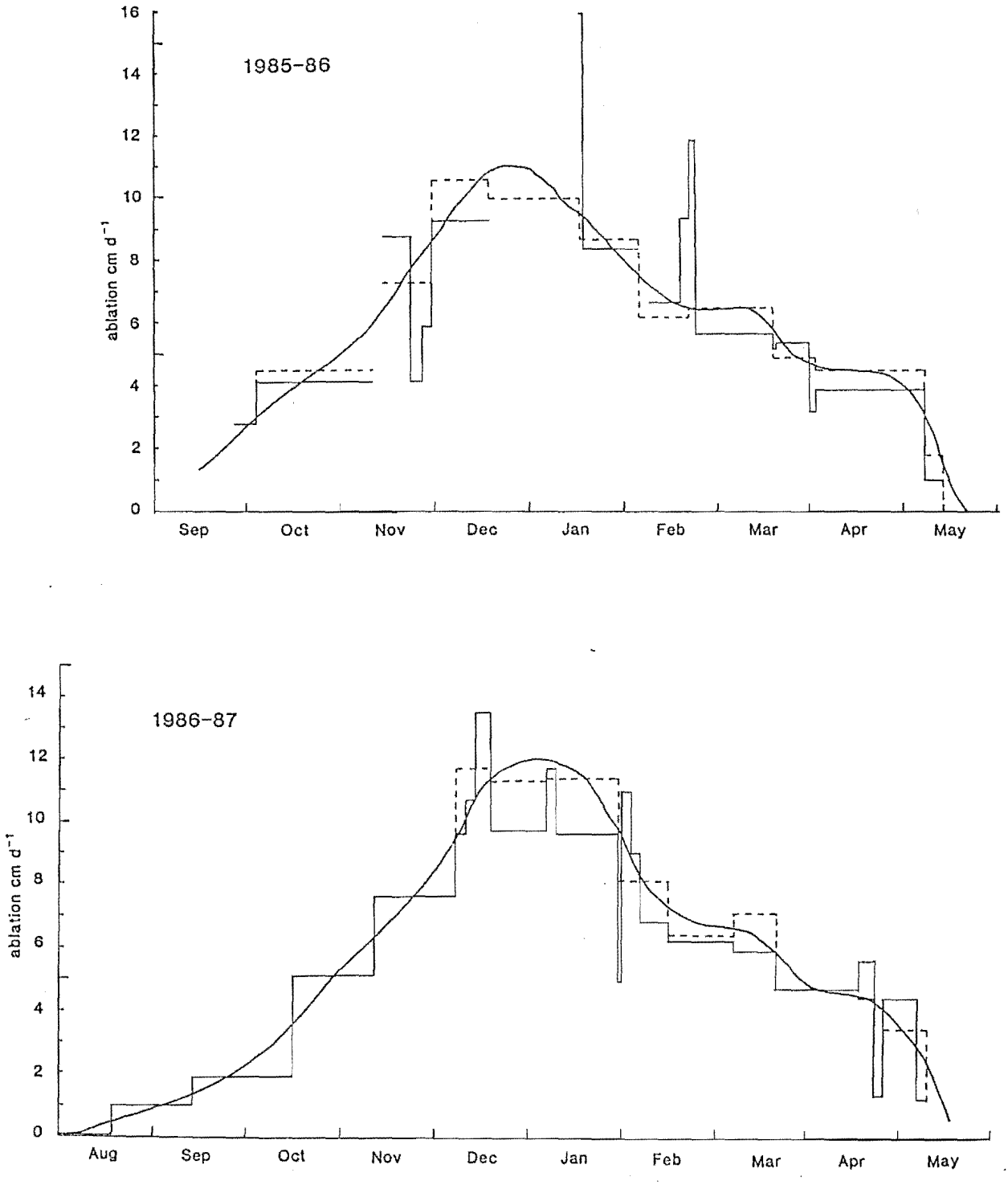

FIG. 2.10 Bare-ice ablation at Ball Hut (960 m a.s.l.) Solid lines = measured stake emergence, dashed lines = adjusted ablation rate, taking into account melt-subsidence of stakes (Appendix 4). Curve indicates estimated seasonal variation in ablation.

TABLE 2.14 Glacier ablation at De la Beche (c.1360 m).

All measurements are from poles 3, 4, and 5 in the glacier centre except for the period 12/11/86 to 12/12/86 which includes 3 and 5.

Period	Measurement interval	Mid-point date	Ablation (cm) measured	Ablation (cm) adjusted	Ablation rate (mm d^{-1})
1985-86 Ablation season					
11/11 - 25/11	14	18/11	55.5	55.5	39.6
25/11 - 21/12	26	8/12	155.0	171.3	65.9
21/12 - 17/01	27	4/01	146.8	160.4	59.4
17/01 - 5/02	19	27/01	153.0	169.1	89.0
5/02 - 22/02	17	13/02	90.3	90.3	53.1
22/02 - 19/03	25	7/03	118.0	122.1	48.8
19/03 - 1/04	13	25/03	45.7	45.7	35.1
1/04 - 16/05	45	23/04	134.7	144.1	32.0
1986 Winter.					
16/05 - 14/09	121		0.0?	0.0?	0.0?
1986-87 Ablation season.					
14/09 - 15/10	31	29/09	0.0?	0.0?	0.0?
15/10 - 12/11	28	29/10	66.7	66.7	23.8
12/11 - 12/12	30	27/11	130.0	137.5	45.8
12/12 - 7/01	28	26/12	189.3	205.6	73.4
7/01 - 1/02	25	19/01	200.0	240.0	96.0
1/02 - 7/03	35	18/02	167.2	168.5	48.1
7/03 - 20/03	13	13/03	55.5	62.4	48.0
20/03 - 23/04	34	6/04	117.0	120.8	35.5
23/04 - 8/05	15	1/05	31.3	31.3	20.9

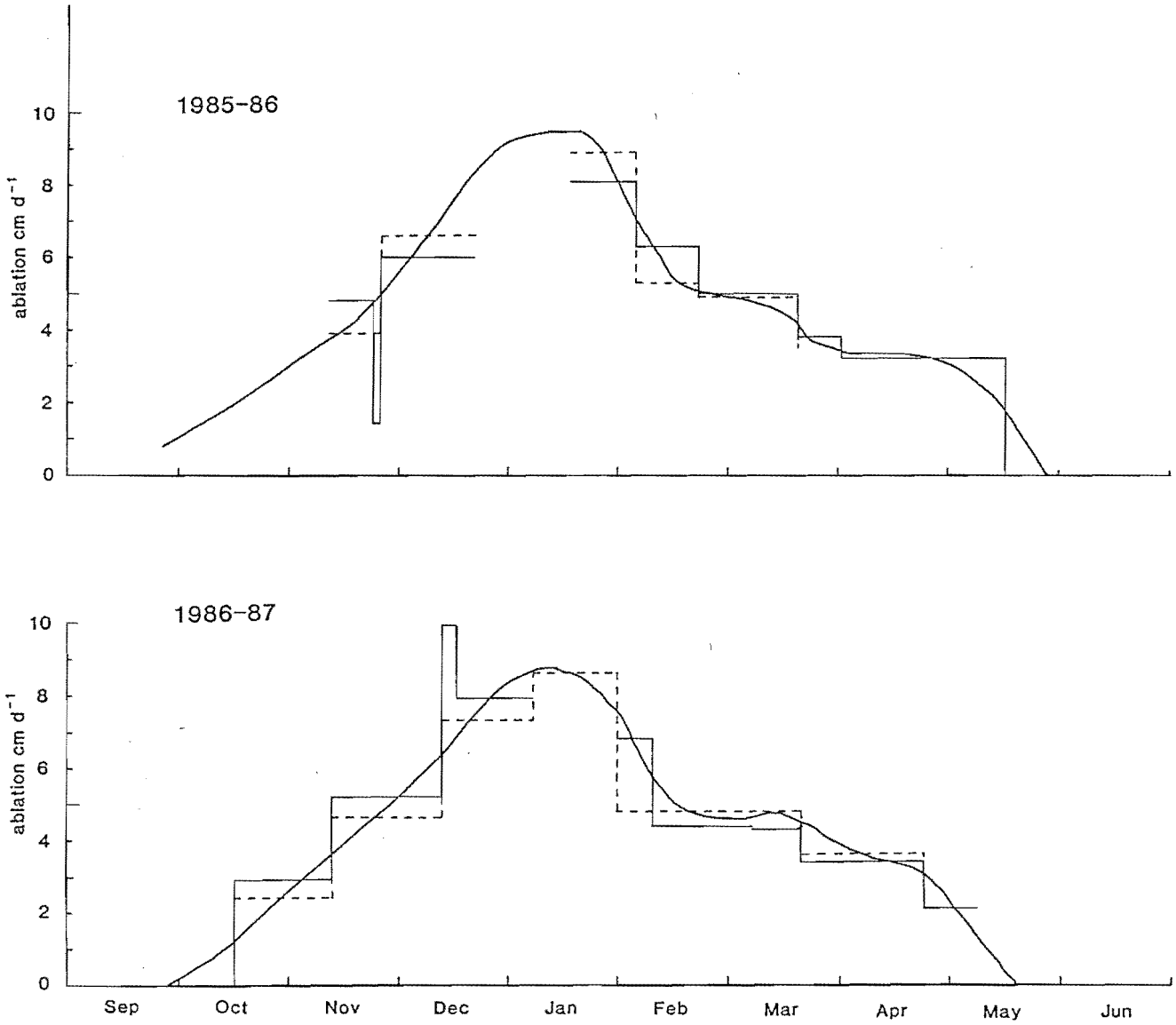

FIG. 2.11 Bare-ice ablation at De la Beche (1360 m a.s.l.). Notation as for Fig. 2.10.

to commence in the second half of August, if 1986 were a typical year. The earliest measurements at the site in September 1985 recorded a melt rate of 28 mmd^{-1} over a 7 day period, suggesting a slightly later start to the ablation season, but broadly similar to the results from the following year.

After the start of the ablation season, melt rates increase abruptly and linearly through October and November before the melt rate curve flattens to a peak rate which may occur between mid-December and mid-January, depending on short-term synoptic conditions at this time of the year. Peak melt rates coincide with the warmest temperatures and greatest daily insolation of the year.

A rapid decline in melt rates commences in the second half of January and continues until mid- to late February. A secondary peak then occurred in both years of measurement, possibly due to fine weather in late summer in both years when high levels of insolation were received by the glacier.

Following the secondary peak, a further rapid decline in rate lasts from late April until the arrival of the earliest winter snow at the site. In 1986 this occurred in a strong southerly storm on 19 May, when snow fell to as low as 500 m and remained on the glacier at the Ball Hut site throughout the winter until late September. No melting was observed on 19 May, and mid-May is regarded as the end of the 1985-86 ablation season. No similar snowfall occurred in the early winter of 1987; a winter marked by very little snow until September. Cessation of melt was not observed. It is likely that intermittent melting occurring throughout the winter.

The above observations suggest that the length of the ablation season at 960 m elevation is about 250 days.

The measured apparent ice loss against ablation stakes at Ball Hut was 16.027 m for the 1985-86 year and 16.421 m for the 1986-87 year. When these values are adjusted for melt subsidence of the stakes (Appendix 4) annual ice losses for the two years were 17.041 m and 17.716 m respectively. The measured ice melt apparently underestimates the true melt by 6 to 7%

<u>De la Beche site.</u> (Fig 2.11). The commencement of the ablation season at 1360 m elevation was not measured in the spring of 1985. In 1986, no melting was taking place beneath 50 cm of snow in mid-September, but a melt rate of 24 mmd^{-1} was recorded over one month in late October and early November. It appears that the melt season commences at this site in late September to early October. McKellar (1966) reports melting of the

ice surface beneath saturated snowpack in late winter.

From the onset of melt the trend of the melt rate is very similar to that near Ball Hut. Similar features include the rapid increase in melt rates through October and November; the peak in late December to mid-January; the rapid decline to a secondary peak or plateau in March; and the subsequent decrease until melting ceases in May.

The length of the ablation season at 1360 m elevation is about 225 days: only 10% shorter than at 960 m. The difference in ice loss between the two sites reflects differences in melt rate more than differences in the length of the melt season.

Apparent ice loss at the De la Beche site was measured at 9.462 m in 1985-86 and 9.720 in 1986-87. When adjusted for stake subsidence, the true ice loss is 10.299 m and 10.478 m of ice respectively. Apparent rates underestimate true rates by 7 to 8%, a similar difference as at the Ball Hut site.

The timing of the increases, peaks and decreases in the melt rate curve is identical at the two sites in both years. The secondary peak in late summer has not previously been reported.

2.2.3.4 Ablation gradients.

The ablation gradient (Schytt 1967) is the rate of change of surface ablation with altitude. The significance of this parameter is that characteristic ablation gradients are found in different climatic environments. Glaciers with high mass fluxes tend to have high ablation gradients and characterise maritime environments (Andrews 1972; Golubev & Kotlyakov 1978; Kuhn 1984).

Previous work on the Tasman Glacier has allowed three ablation gradients to be constructed (Fig 2.12). The gradients for 1964-65 and 1965-66 are based on 12-month measurements of ice loss at 10 and 17 points respectively, in the altitudinal range of 1040 m to 1630 m. The 1972-73 gradient is based on 12-month measurements at only two altitudes, but there is no reason to suspect that the gradient is erroneous as a result even though it is much lower than the earlier examples. Schytt (1967) reviewed ablation gradients over a 20-year period on Storglaciaren in Sweden and found that ablation gradients varied by up to 20% from year to year: the variability of the more limited data from the Tasman Glacier is similar.

The present study allows a fourth and fifth annual ablation gradient to be constructed from the measurements of surface melt. The results (Fig

2.12) compare closely with the gradients from the 1960s although the total loss of ice at each altitude is 10% to 20% greater. Annual ablation gradients of the Tasman Glacier are in the range -0.95 to -1.85 m per 100 m altitude per year, with an average of -1.52 m per 100 m. These gradients are very high by world standards. For comparison, Andrews (1972) lists 13 ablation gradients from around the world which range from -0.1 to -1.1 m per 100 m per year.

2.2.3.5 Losses from bare ice surfaces.

The altitude-area curve for the Tasman Glacier (Fig 2.13) has been calculated by Chinn (unpublished). Using each of the annual ablation gradients shown in Fig 2.12, the total annual ice loss from each altitude-area class was calculated by multiplying the mid-point altitude of each class width by the ice loss at that altitude in each year. The ice losses of each altitude class were summed to give the annual total over the whole altitudinal range of the bare-ice surface of the glacier (Table 2.16).

Corrections have been applied to the basic result for the following reasons. First, the totals in Table 2.16 assume that the ablation zone lies between 914 m and 1828 m throughout. Second, they assume that the ablation zone was free of supraglacial debris. The lower limit of debris-free ice lay at 1000 m in 1965 and at 960 m in 1986. This limit lies 2 km upstream of the 914 m contour in 1986: 4 km^2 of the glacier above 914 m is debris-mantled, where melt rates are reduced. An estimated 5% reduction in melt rate beneath the debris (from Chapter 2.2.4) is applied to adjust the ice loss total over this area.

The firn line lies at an altitude of 1730 m on average, or 100 m below the arbitrary 1828 m limit of the calculation. Ice loss in this area is small and no adjustment to account for this discrepency is significant.

Finally, the debris cover of the Rudolf ice stream reduces ice loss over a 3 km^2 part of the ablation zone. Again applying a 5% reduction to the ablation rate for the altitudinal range of this zone (between 1067 m and 1676 m), the resulting reduction in the ice loss is only 0.3% of the total for the glacier above 914 m, and is therefore insignificant.

The annual ice losses above the up-glacier margin of the debris mantle are presented for each year for which an ablation gradient is available in Table 2.15. The average annual ice loss from the clean-ice surface of the glacier corresponds to a mean water discharge of 8.9 cumecs.

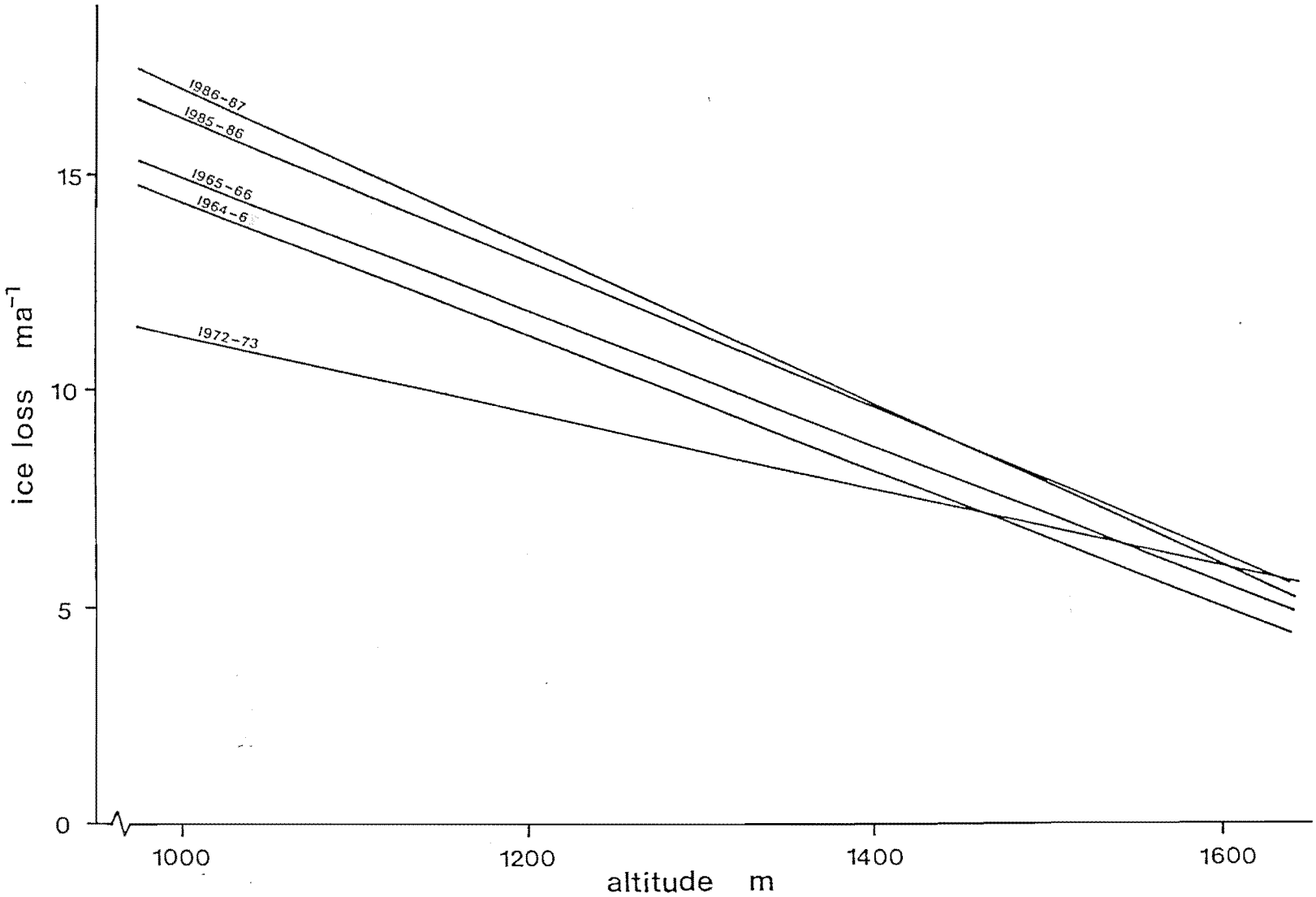

FIG. 2.12 Ablation gradients of the Tasman Glacier. 1964-5 and 1965-6 data from McKellar (1966), 1972-3 data from Anderton (1975), 1985-6 and 1986-7 data this study. Mean gradient = -1.52 m/100 m altitude.

Altitude		Area	Cumulative	Area (km^2)			
Feet	Metres	km^2	%	Darwin Gl	Rudolf Gl.	Mid/upper Tasman	Hochstetter/ Ball Gl.
<3000	<914	12.2044		0	0	1.4845	10.7199
			14.8				
3-4000	914-1219	16.9862		0	0	8.3403	8.6459
			35.4				
4-5000	1219-1524	8.1216		0	1.3317	6.2660	0.5239
			45.2				
5-6000	1524-1828	7.9036		1.0044	1.3317	4.8470	0.7205
			54.8				
6-7000	1828-2134	12.4668		1.4628	2.5982	6.6154	1.7904
			69.9				
7-8000	2134-2438	16.2218		1.4410	2.2050	7.7508	4.8250
			89.6				
8-9000	2438-2743	7.0519		0.8733	1.3537	2.7727	2.0522
			98.1				
>9000	>2743	1.5718		0	0.2183	0.7423	0.6112
			1.9				
TOTALS				4.7815	9.0386	38.7790	29.8890

GLACIER TOTAL AREA = 82.5 km^2

TABLE 2.15 Area-altitude data for Tasman Glacier and tributaries.

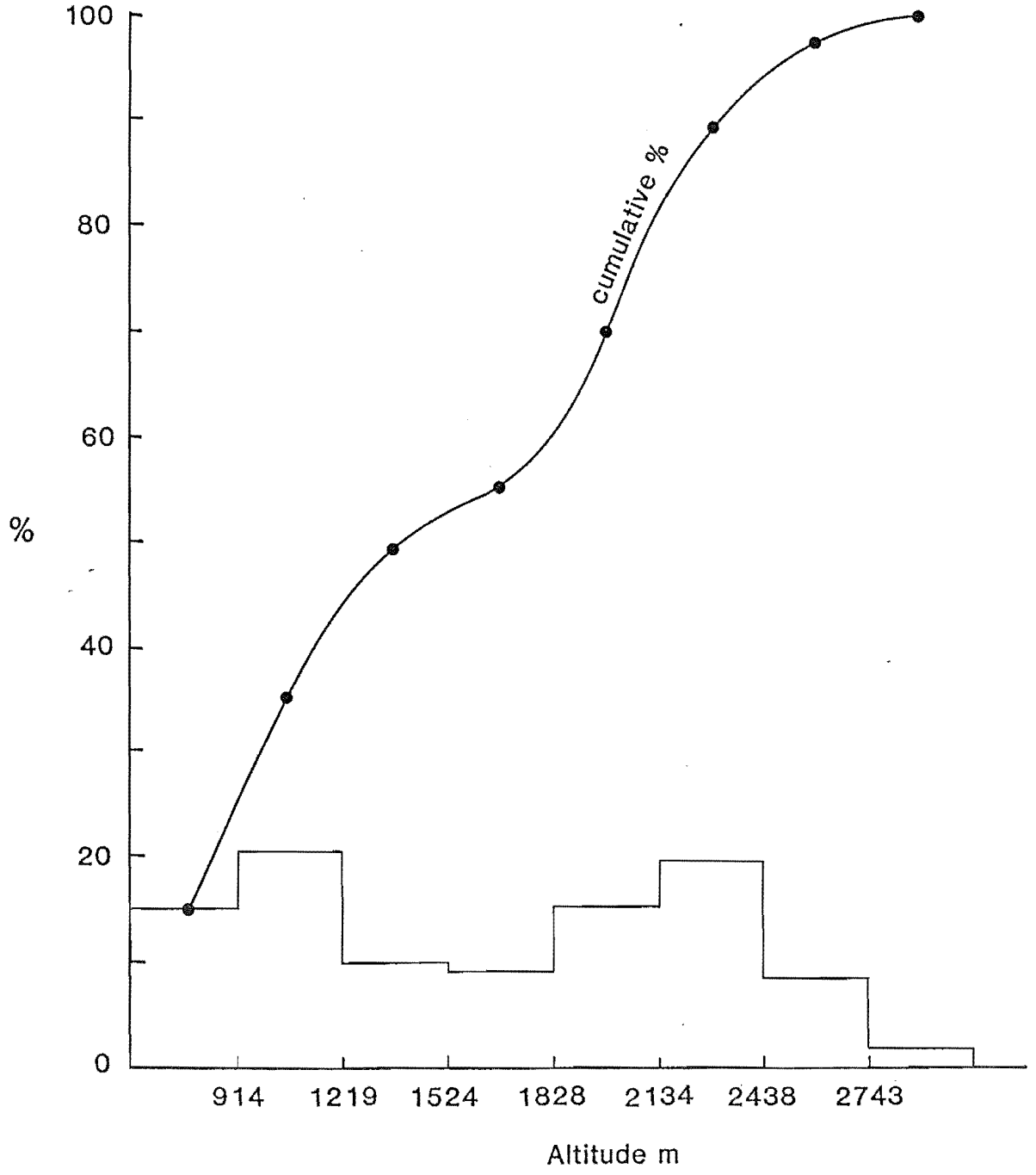

FIG. 2.13 Area-altitude curve for the Tasman Glacier, based on unpublished data (provided by T. Chinn).

2.2.4 Ablation beneath a debris layer.

2.2.4.1 Previous studies

A detailed review of previous studies of sub-debris ice melt is presented in Chapter 1.4.4. Detailed modelling of the process (eg Kraus 1966; Nakawo & Young 1981, 1982; Nakawo & Takahashi 1983) is applicable only for short-term estimates under thin (12 to 94 mm) debris layers. The approach of McSaveney (1975) is more appropriate for longer-term calculations on thick debris.

The annual ice melt beneath a debris layer may be calculated if the following parameters are known (McSaveney 1975):

1) the vertical thickness of the debris layer

2) the average thermal gradient through the debris layer during the ablation season

3) the thermal conductivity of the debris layer

4) the length of the ablation season

5) the amount of annual rainfall and its seasonal distribution.

Calculations of heat transfer by both conduction and advection may be based on this information. The relative importance of each process depends largely on the regional climate. McSaveney (1975) found that conduction supplied 94% of the heat causing melting beneath debris on the Sherman Glacier, Alaska, and advection supplied only 6% with other processes being negligible. Bozhinskiiy et al (1986) calculated that percolating water carried enough heat to melt 5 cm of ice annually beneath the 1 m thick debris mantle of Djankuat Glacier in the Caucasus. Other workers have not calculated the advective contribution to ice melt (McKenzie 1969; Carrara 1975; Driscoll 1980b) and all previous studies have had to assume the length of the ablation season or infer it from meteorological records.

2.2.4.2 Calculation of heat flow.

The following calculations follow closely those of McSaveney (1975). His basic postulates are adopted, namely

1) the debris layer approximates to a thin planar sheet

2) heat flow is in response to a temperature gradient normal to the plane of the sheet

3) the debris cover may be treated as a uniform aggregate of isotropic thermal conductivity.

4) ablation of ice is due to heat flow across the ice-debris interface, therefore it is the thermal conductivity and gradient close to

this interface which are important (cf McKenzie 1969).

Heat flow by conduction.

To calculate melt by conductive heat flow, information on the thermal conductivity and temperature gradient within the debris layer is needed.

Thermal conductivity: the thermal conductivity is a function of three variables.

a) Thermal conductivity of the parent rock: although there is a paucity of information on thermal conductivities of rocks, the accurate estimation of this property is crucial to the calculation of heat flow (Nakawo & Young 1981). A compilation of the conductivities of 43 lithologies by Clark (1966 Table 21-2) allowed McSaveney (1975) to select a value of 2.3 $Wm^{-2}deg^{-1}$ for greywacke. This value is the mean of an unspecified number of rocks of granitic composition. Bozhinskiiy et al (1986 Table 3) selected a value of 2.8 $Wm^{-2}deg^{-1}$ for granite, a value closely comparable to those listed by Clark (1966). Other studies (eg Driscoll 1980b) have based estimates of thermal conductivity on published values for soils.

b) Porosity of the debris layer. The thermal conductivity of the debris layer (k_m) is the mean of the conductivities of the parent rock type and any institial media, weighted by volume. Thus in a dry layer,

$$k_m = k_g(1-p) + k_a p \qquad (8)$$

where k_g and k_a are the thermal conductivities of rock and air respectively, and p = porosity (Bozhinskiiy et al 1986). Similarly, in a saturated layer,

$$k_m = k_g(1-p) + k_w p \qquad (8a)$$

where k_w refers to the thermal conductivity of water. McSaveney (1975 Fig 26) showed that thermal conductivity is more sensitive to porosity than to water content. The realistic range of porosity and water content in a debris mantle is small; McSaveney (1975 p.141) suggests the range 1.5 to 2.0 $Wm^{-2}deg^{-1}$ is probable given the characteristics of porous, well-drained soils and less porous, poorly-drained soils. Other authors have adopted Kersten's measurements of soil thermal conductivities (Kersten 1966; McKenzie 1969; Driscoll 1980b). McKenzie used a value of 1.5 $Wm^{-2}deg^{-1}$ and Driscoll a value of 0.8 $Wm^{-2}deg^{-1}$ for supraglacial debris. While McKenzie's estimate is close to those of McSaveney (1975) and Bozhinskiiy et al (1986), that of Driscoll (1980b) is very low. How realistic Driscoll's estimate of thermal conductivity is cannot be determined since Driscoll presents no information about rock type, sorting

or porosity of the till. Given the origin of the debris on the Klutlan ice-cored moraines (Watson 1980) the present author presumes that a thermal conductivity of 0.8 $Wm^{-2}deg^{-1}$ is a significant underestimate. It is based on the thermal conductivities of well-sorted (and therefore more porous) sands and sandy tills (Driscoll 1980b Table 4) which are dissimilar to much of the bouldery Klutlan debris illustrated by Watson (1980 Fig 3).

No direct measurement of porosity was made in any of the above studies, or on the Tasman Glacier. The range of estimates is based on theoretical conditions of particle sorting and packing (Table 2.16). A porosity of 30% was assumed for the Tasman debris mantle, because the observed clogging of the basal part of the debris layer reduces the porosity below that of more openwork aggregates (cf Bozhinskiiy et al 1986 p.259).

c) Water content. Although most studies assume that the debris remains dry where mean annual temperatures are below freezing (Carrara 1975; Bozhinskiiy et al 1986), Nakawo & Young (1981) found that thermal conductivity increases rapidly when the water content of the debris exceeds 1%. They also noted how initially dry Ottawa sand rapidly became saturated and remained saturated during melting of subjacent ice. This supports the contention of McSaveney (1975) that the debris should be treated as a saturated soil as long as the ice substrate is melting. Observations on the Tasman Glacier reveal that the basal layer of the debris mantle is moist throughout the spring, summer and autumn. Only in mid-August 1986 was it observed to be dry, during a period of cold anticyclonic weather with no melting of bare ice at 960 m. The freezing front on this occasion extended to at least 2 m depth within the debris mantle. All other observations from ten months of the year show melting at the ice-debris interface. The accumulation of silt and mud at the ice surface (Chapter 4.1) favours the retention of moisture at the interface throughout the ablation season (Nakawo & Young 1981). The calculation of the thermal conductivity therefore assumes a constant saturation of water of thermal conductivity = 0.6 $Wm^{-2}deg^{-1}$ (cf 0.56 $Wm^{-2}deg^{-1}$ for pure water).

Taking into account the observed and assumed properties of the debris mantle, the thermal conductivity of the layer is calculated to be

$$k_m = (2.3 \times 0.7) + (0.6 \times 0.3)$$
$$= 1.8\ Wm^{-2}deg^{-1}$$

This is identical to the value arrived at by McSaveney (1975) for

a) Theoretical cases (Fraser 1935)

	% loose	% packed
Mixed spheres of 3 sizes	30-38	-
Standard sand	39	34
Uniform spheres	40-43	37
Uniform crushed quartz	48	41

b) Published estimates

Deposit	% porosity	Source
Rock avalanche	30 ± 20	McSaveney 1975
Supraglacial debris	45	Nakawo 1979
Supraglacial debris	40-45	Bozhinskiiy et al 1986
Protalus ramparts	33	Ballantyne & Kirkbride 1987

TABLE 2.16 Porosities of rock debris aggregates.

K debris ($W\ m^{-2}\ deg$)	K parent lithology ($W\ m^{-2}\ deg$)	Porosity %	Moisture content %	Method	Source
1.50	1.50 Ottawa Sand	?	?	K assumed to = K of Ottawa Sand	McKenzie 1969
1.80	2.30 Greywacke	30 ± 20 assumed	100	K estimated from published values	McSaveney 1975
0.79	?	?	?	K assumed, after Kersten (1969)	Driscoll 1980b
2.23	Ottawa Sand	?	17-22	mean of 4 field determinations	Nakawo & Young 1981
1.46	Ottawa Sand	?	8-17	mean of 2 field determinations	Nakawo & Young 1982
1.78	Ottawa Sand	?	?	mean of 6 field determinations	Nakawo & Young 1982
1.60	2.80 Granite	40 - 45 assumed	0	K estimated from published values	Bozhinskiiy *et al* 1986

TABLE 2.17 Published estimates of thermal conductivities (K) of coarse aggregates.

bouldery greywacke debris on the Sherman Glacier, and to the mean of six calculations by Nakawo & Young (1982) for an unspecified lithology. Published estimates of thermal conductivity are shown in Table 2.17.

Thermal gradients in the debris mantle.

The thermal gradient of a debris layer fluctuates diurnally and seasonally. Bozhinskiiy et al (1986) calculated that diurnal fluctuations affect the upper 0.16 m of the debris layer on Djankuat Glacier, and seasonal fluctuations affect the upper 1.5 m. Fluctuations on an annual scale penetrate to 3.1 m depth. However, at high latitudes and altitudes only rarely does the thermal gradient allow downward heat flow by conduction (Østrem 1965; Carrara 1975). In temperate areas a downward heat flow vector is strongly established and melting occurs wherever the ice-debris interface lies at depths shallower than the depth of penetration of the annual warm wave. In such cases, it is necessary to determine an average temperature gradient during the ablation season to remove diurnal and synoptically-induced fluctuations.

Ideally, this requires continuous monitoring of subsurface temperatures. Practical difficulties prevented this approach in this study, though attempts were made to dig through the debris mantle to bury thermistors. Instead, a digital thermometer was used to measure temperatures in freshly-dug pits in debris-mantle sections exposed by the backwasting of ice walls. The advantages in terms of allowing data to be gathered from many sites balanced the disadvantages of the lack of longer-term records at a single site.

Temperature gradients were measured on four occasions in April and May 1987 and in early May 1988, using an electronic digital thermometer with a copper-covered sensor. This period is when bare-ice melt rates approximate to the mean melt rate for the ablation season (Figs 2.10 and 2.11) and it is assumed that sub-surface melt rates follow the same seasonal trend. The rate of heat flow through debris is sufficiently responsive to surface temperature changes to make this assumption reasonable (Bozhinskiiy et al 1986), and most of the measured temperature profiles indicate steady-state heat flow. Other (deeper) profiles show warm waves at several depths which are probably a response to either diurnal or synoptically-induced changes in surface temperature being propagated through the debris layer. In such cases an average thermal gradient over the profile is assumed, because the time period under consideration is of a much longer interval than the probable frequency of the warm waves.

Fifteen temperature profiles (Fig 2.14) were measured in debris ranging in thickness from 19 ± 3 cm to 300 ± 10 cm (Fig 2.15). The number of point measurements of temperature in each profile varies from five in thinner debris to twelve in greater thicknesses. The vertical spacing of measurements was closer in the lower part of each profile than in the upper part, since it is the gradient in the basal layers that is important. In all cases the ice surface was seen to be melting and therefore was at 0°C. Temperatures were measured by inserting the probe horizontally at least 10 cm into the debris. Measurements were made on exposures shaded from direct sunlight as far as possible, in order to minimise the effects of local heating. Each measurement was made to 0.1°C, with a true precision (due to instrument calibration and sensitivity) of ± 0.5°C.

Measured profiles are shown in Fig 2.14, and the thermal gradients used in heat flow calculations in Table 2.18. Melting caused by conduction has been estimated using the relationship between thermal gradient, thermal conductivity, and melt rate (Fig 2.16).

Heat flow by advection.

In addition to the conductive heat flux described above, heat is transferred with the movement of fluids through the debris mantle. Both wind and water are potentially significant in advective heat transfer. Field observations suggest that turbulent eddies due to surface winds affect the uppermost 10 to 30 cm of debris, depending on the porosity and packing at the debris surface. At localities where the debris mantle consists of coarse openwork boulders, eddies have been felt in holes several metres deep, but such sites are relatively rare on the debris mantle. In the light of observations from all parts of the debris mantle, it is doubtful that turbulent heat transfer significantly affects the melting of ice beneath thicknesses of debris greater than about 20-30 cm, and the process is therefore regarded as being of negligible importance.

Water, with its high heat capacity compared to ice and rock, is capable of significant heat transfer. The amount of melting that this causes is calculated (following McSaveney 1975) from measured debris temperatures and rainfall records combined with the length of the ablation season. An assumption made in the calculation is that the temperature of water percolating through the debris mantle will equilibriate with that of the debris. Thus, if warm rain falls on cool debris, heat lost from the rainwater will warm the debris and be transferred by conduction according to the prevailing thermal gradient. Conversely, cool rain falling on warm

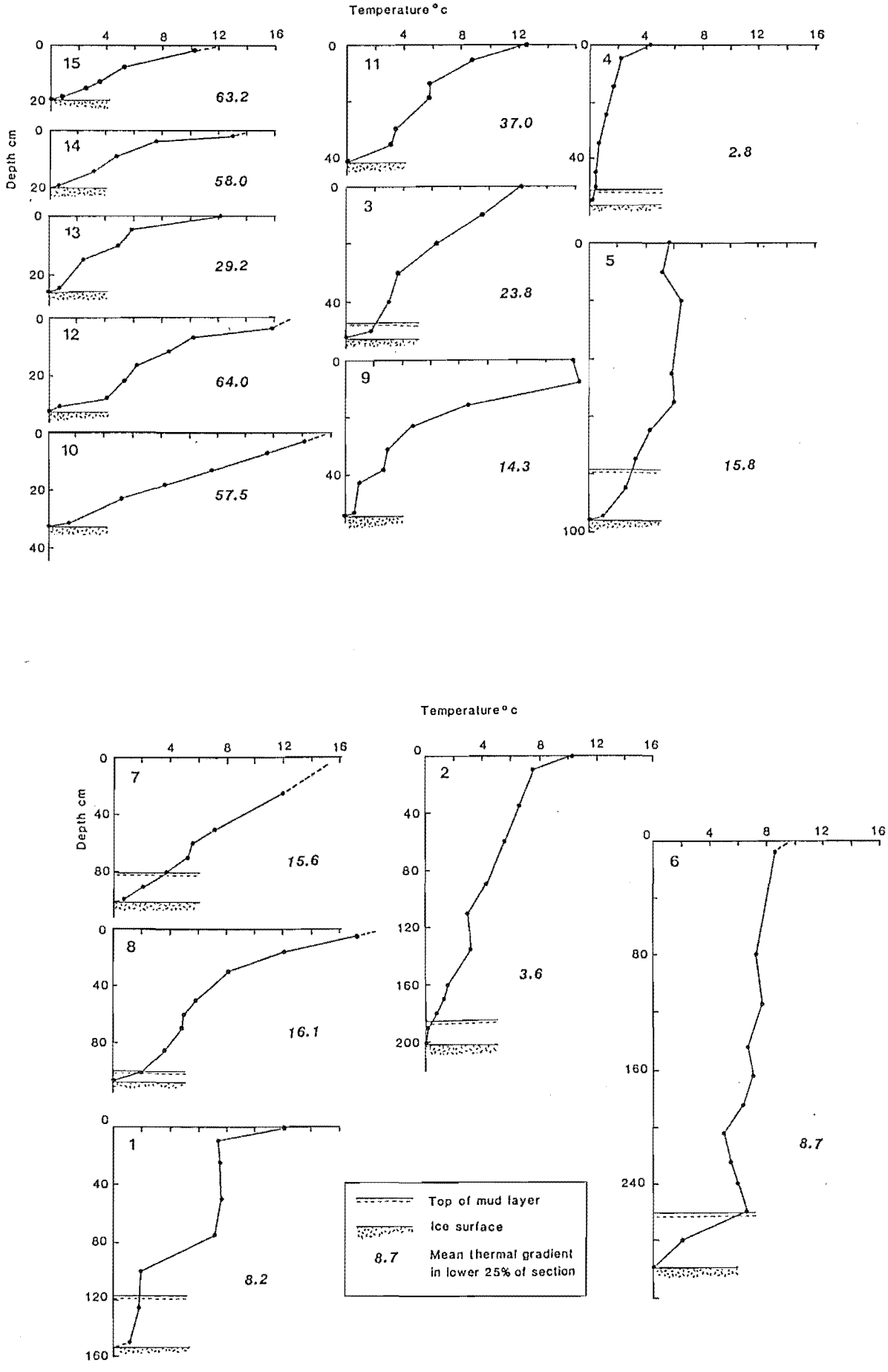

FIG. 2.14 Temperature profiles in the debris cover of the Tasman Glacier. Site number given in top left of each graph.

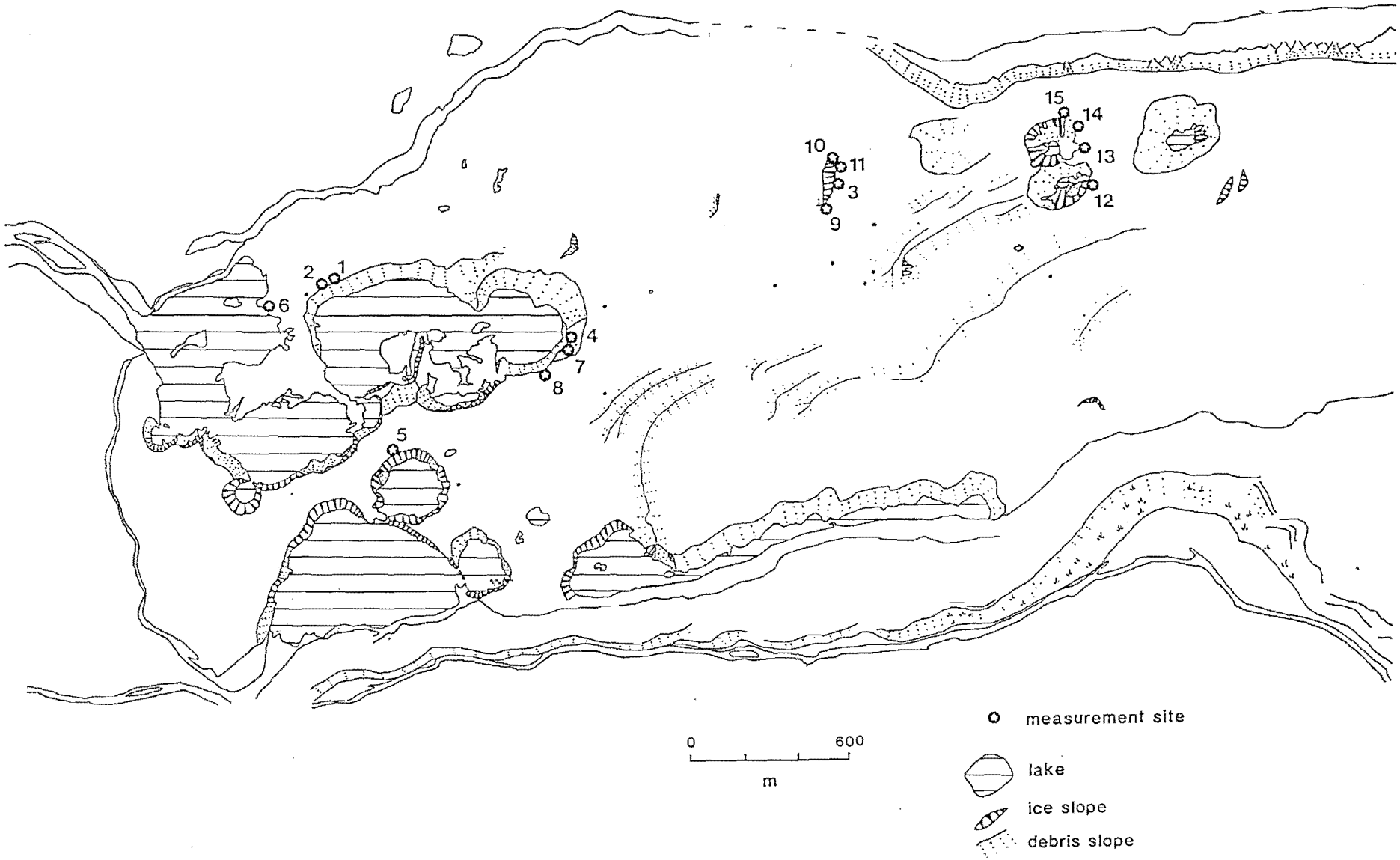

FIG. 2.15 Location of temperature measurements in the debris mantle.

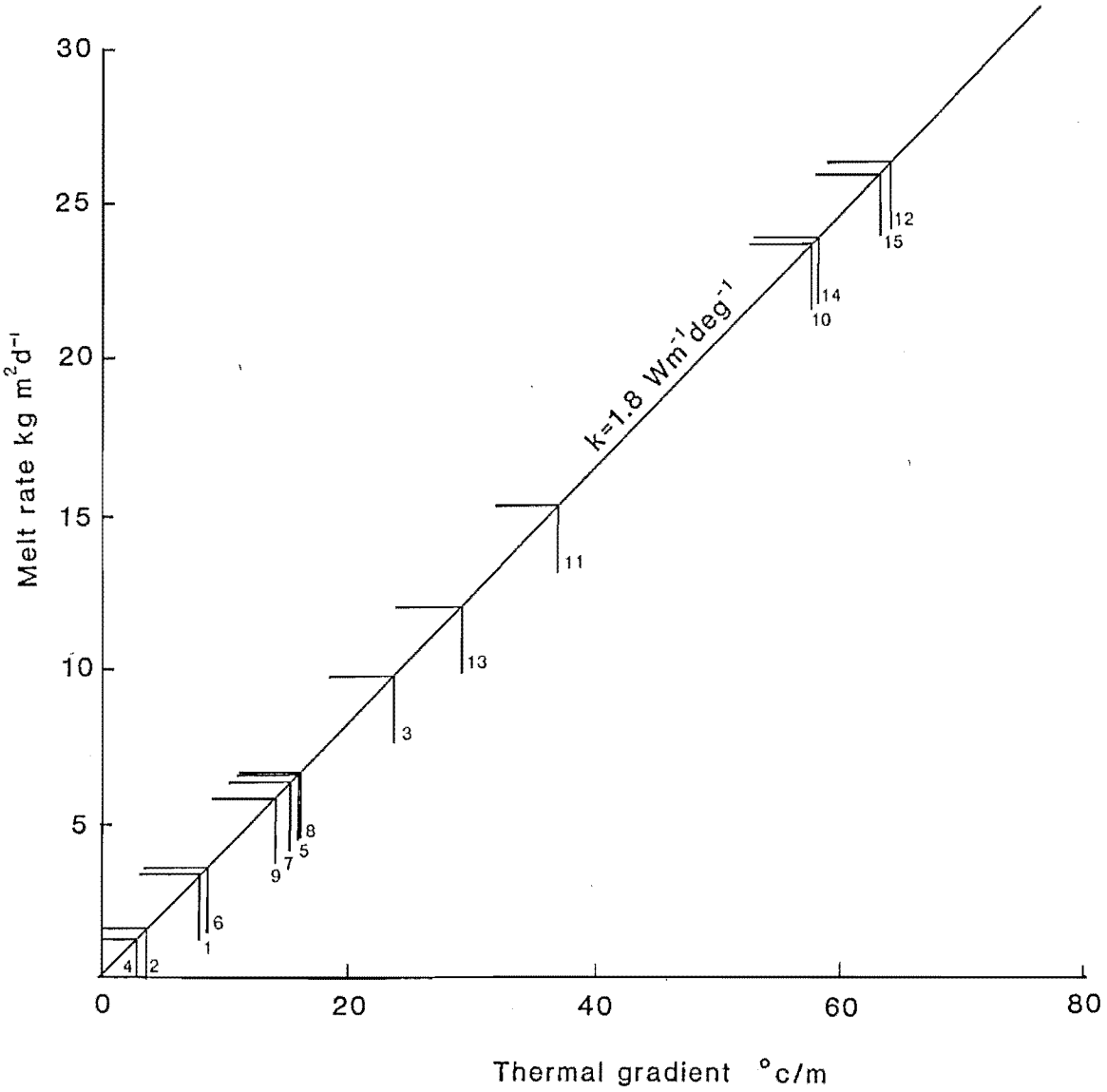

FIG. 2.16 Relationship between thermal gradient and melt rate for a thermal conductivity of k = 1.8 $Wm^{-1}deg^{-1}$. Numbers refer to measurement sites.

Profile	Depth (cm)	Temperature gradient (°Cm^{-1}) (a) Mud layer	(b) Lower 25%	(c) Lower 50%	Melt rate Kgm^{-1}d^{-1}	Annual loss (10 month season) kgm^{-2}	Ice lowering (m)
1	152	7.4	8.2		3.4	1020	1.11
2	210	3.6	3.6		1.6	480	0.52
3	52	48.0	23.8		9.8	2940	3.21
4	56	8.0	2.8		1.2	360	0.39
5	96	17.2	15.8		6.6	1980	2.16
6	300	10.5	8.7	4.8	3.6	1080	1.18
7	100	15.0	15.6		6.4	1920	2.04
8	105	42.0	16.1		6.7	2010	2.19
9	54		14.3		5.9	1770	1.93
10	33		57.5		23.8	7140	7.79
11	41		37.0		15.3	4890	5.00
12	32		64.0		26.4	7920	8.64
13	26		29.2		12.1	3630	3.49
14	20		58.0		23.9	7170	7.82
15	19		63.2		26.0	7800	8.51

TABLE 2.18 Debris-mantle temperature gradients and estimated ablation due to conduction.

Advection: with mean monthly rainfall of 360mm

Profile	Depth of mud (cm)	Mean temperature (°C)	Monthly ice melt (Kgm^{-2})	Annual melt in 10 month season (kgm^{-2})	Ice lowering (m)
1	35	1.3	5.86	59	0.064
2	25	0.5	2.26	23	0.025
3	5	1.2	5.41	54	0.059
4	5	0.2	0.90	9	0.010
5	18	1.6	7.22	72	0.078
6	40	2.1	9.47	95	0.104
7	20	1.9	8.57	86	0.094
8	10	1.1	4.96	50	0.054
9	0	1.0*	4.51	45	0.049
10	0	2.3*	10.38	104	0.113
11	trace	1.8*	8.12	81	0.088
12	trace	2.5*	11.28	113	0.123
13	0	1.0*	4.51	45	0.049
14	0	1.5*	6.77	68	0.074
15	0	1.5*	6.77	68	0.074

TABLE 2.19 Calculation of sub-debris ablation due to advective heat transfer.

debris will acquire heat until their temperatures are equal. In both cases, by the time the percolating water reaches the ice-debris interface it will be close to a thermal equilibrium with the debris. The temperature of percolating water is therefore estimated to equal the mean temperature in the lowermost 25% of the debris layer. Where this zone is clogged by saturated illuviated mud (Chapter 4.1), the mean temperature in the mud layer is used in the calculation.

The rainfall in the Tasman Valley is uniformly distributed throughout the year (Chapter 1.5.2). The mass of water which falls on the lower tongue of the glacier is therefore the monthly total multiplied by the 10 months of the ablation season. The amount of ice melted is then

$$Q_I = \frac{tc_w m_w}{Q_w} \qquad (9)$$

where Q_I is the amount of ice melted (in kg m^{-2} month), c_w, m_w, and Q_w are the specific heat capacity of water (4186 x 10^3 kJ kg), the mass of water (kg month), and the latent heat of fusion (334 kJ kg) respectively, and t is the water temperature in degrees centigrade.

Estimates of advective heat transfer and ice melt have been made for each of the fifteen sites at which temperature profiles were measured. The results (Table 2.19, Fig 2.17) show a wide scatter but indicate that advective heat transfer is one to two orders of magnitude less than conductive heat transfer. The relative contribution of advective heat flow appears to increase with greater debris thicknesses.

The sub-debris melt rate at each measurement site is the sum of melting caused by conductive and advective heat flow (Table 2.20).

2.2.4.3 Ice losses beneath the debris mantle.

The relationship between annual ice loss and debris thickness (Fig 2.17) can be used to calculate the total ice loss beneath the debris mantle. Over 150 measurements of debris thickness were made at ice wall exposures on the lower 10 km of the glacier. The debris thickness is locally highly variable due to slumping and reworking, so a large number of point measurements is necessary to allow general trends in thickness to be identified. Good exposure above ice walls along the eastern margin and around the terminal lakes show that the debris thickness is on average 1.5 times thicker at the margin than in the glacier centre. Cursory examination of other localities where exposure was very limited do not refute this, and it is applied as a general relation over the whole debris mantle.

Profile %	Depth (cm)	Conductive loss $kgm^{-2}a^{-1}$	ma^{-1} (ice)	%	Advective loss $kgm^{-2}a^{-1}$	ma^{-1} (ice)	%	Total $kgm^{-2}a^{-1}$	ma^{-1} (ice)
6	300	1080	1.18	92	95	0.104	8	1175	1.28
2	210	480	0.52	95	23	0.025	5	503	0.55
1	152	1020	1.11	94	59	0.064	6	1079	1.17
8	105	2010	2.19	98	50	0.054	2	2060	2.24
7	100	1920	2.09	96	86	0.094	4	2006	2.18
5	96	1980	2.16	92	72	0.078	8	2158	2.24
4	56	360	0.39	98	9	0.010	2	369	0.40
9	54	1770	1.53	97	45	0.049	3	1815	1.58
3	52	2940	3.21	98	54	0.059	2	2994	3.27
11	41	4590	5.00	98	81	0.088	2	4671	5.09
10	33	7140	7.79	99	104	0.113	1	7244	7.90
12	32	7920	8.64	99	113	0.123	1	8033	8.76
13	26	3630	3.99	99	45	0.049	1	3675	4.04
14	20	7170	7.82	99	68	0.074	1	7238	7.89
15	19	7800	8.51	99	68	0.074	1	7868	8.58

TABLE 2.20 Calculation of specific ice losses beneath the debris mantle.

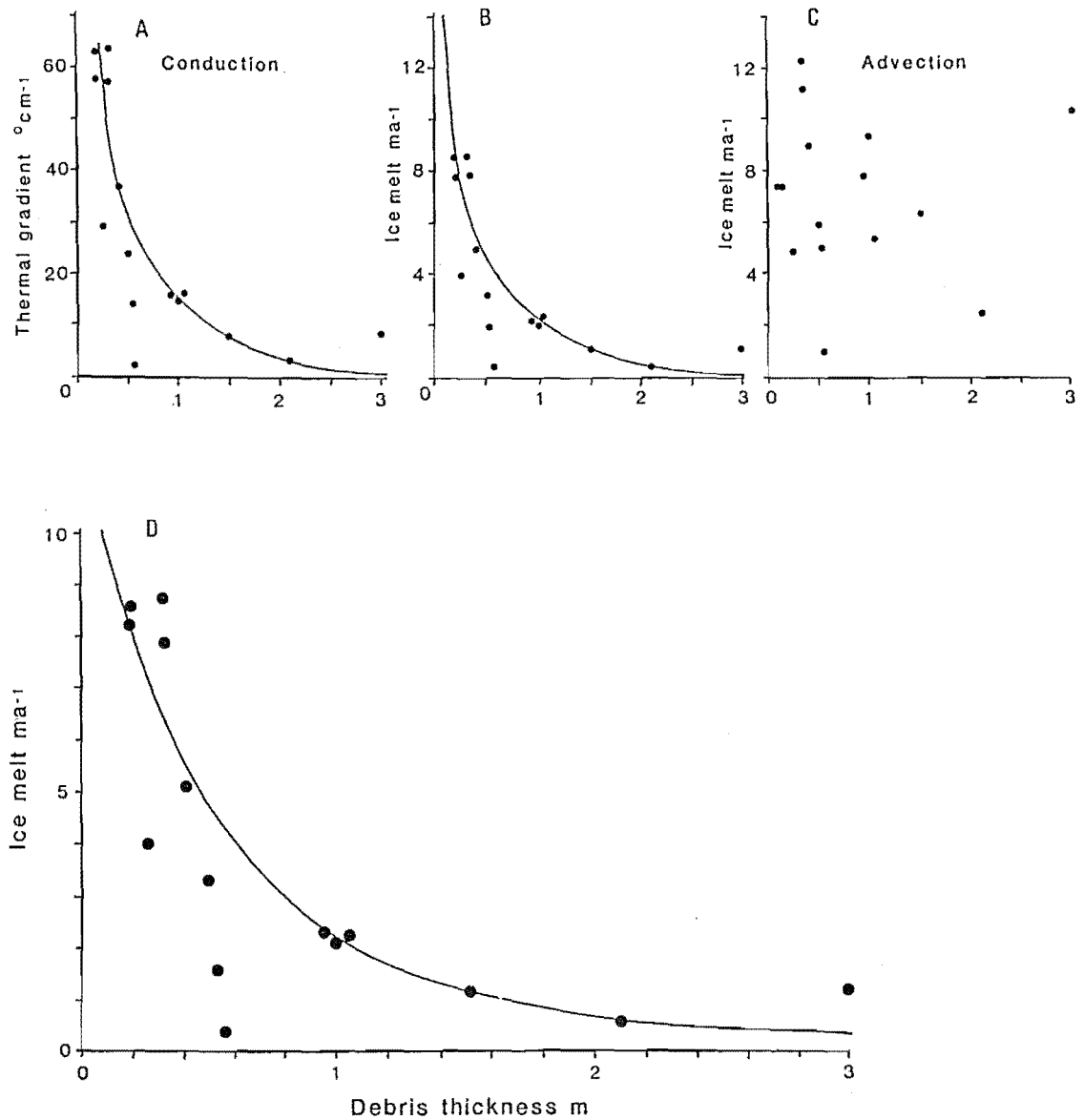

FIG. 2.17 Relationships between debris thickness (x-axis) and; (A) thermal gradient (B) conductive melt rate (C) advective melt rate (D) total ablation.

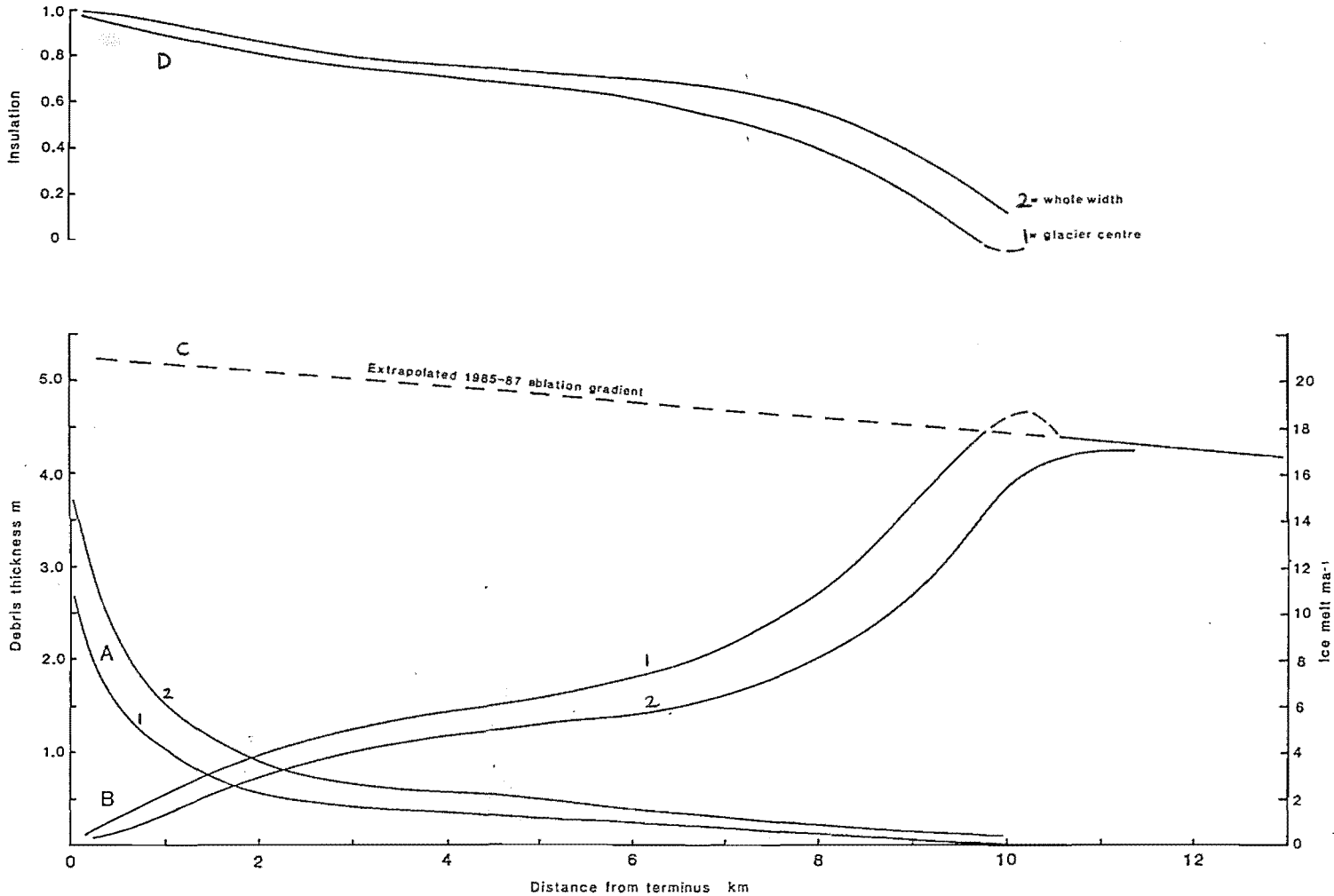

FIG. 2.18 (A) Variation in debris thickness over the lower 10 km of the Tasman Glacier. A1 = centre line of glacier A2 = average for whole width of glacier. (B) Ablation gradient with respect to horizontal distance. (C) Bare-ice ablation gradient extrapolated from measurements at Ball Hut and De la Beche. (D) Insulation index: D1 = (C - B1) / C : D2 = (C - B2) / C

By combining the profile of centre-line debris thickness with the ice loss / debris thickness relationship, an ablation curve for the centre line of the debris-covered tongue is generated (Fig 2.18). Because all the temperature profiles were measured in the lower 4 km of the glacier, ice loss beneath the debris has been adjusted for altitude using the extrapolated bare-ice ablation gradient (Fig 2.12). This adjustment is small over the 200 m altitudinal range of the debris mantle.

Fig 2.18 shows the effect of the increase in debris thickness on ablation near the terminus. At the terminus itself, ice loss is only c.1% of the melt rate of bare ice at the same altitude. Between 10 and 4 km from the terminus the linearly-thickening debris mantle causes an asymptotic decrease in ice melt, corresponding to the curve of Fig 2.17. Over the entire area of the debris mantle, annual ablation is c.68% of the ablation of bare ice in the same altitudinal range. The ice loss from this area is calculated from Fig 2.18 to be 104 x 10^6 $m^3a^{-1}$with an average specific loss of 5.8 ma^{-1}.

Exposed ice-walls melt at rates similar to the bare-ice rate at the relevent altitude. On the basis of mean ice-wall height, a backwasting rate of 20 ma^{-1}, and an aerial photograph-based estimate of total ice-wall length, ice-wall backwasting causes a mean lowering of 10 ma^{-1} over 5% of the debris-mantled area. This amounts to a loss of 9.0 x 10^6 m^3a^{-1}. Thus the total ice loss from the Tasman Glacier surface downstream from Ball Hut is 113 x 10^6 m^3a^{-1}.

2.2.5.Total ice loss from the Tasman Glacier.

The total annual loss from the Tasman Glacier is simply the sum of the surface losses of the debris-mantled area and the bare-ice area of the ablation zone (Sections 2.2.4.3 and 2.2.3.5).

A figure of 4.4 x 10^8 m^3a^{-1} of water (4.4 x 10^{11} kga^{-1}) is calculated to be released by the Tasman Glacier. This represents 40% of the annual discharge of water from the catchment, the remainder being run-off from rainfall and seasonal snowmelt. From the hydrological budget of the catchment, the estimated water discharge of the (ungauged) Tasman River is 48 m^3s^{-1}. This compares well with the measured discharge of the Hooker River (Griffiths 1981) and observations of their relative sizes.

2.2.6 Mass balance trends on the Tasman Glacier.

No quantitative assessment of mass balance was intended in this study, nor has it been possible in previous studies designed for the purpose (Anderton 1975). Nevertheless, it is possible to observe whether the glacier is in a state of positive, equilibrium, or negative balance at various times over the last century.

The ultimate expression of change in mass balance is the adjustment of glacier volume to a new equilibrium with climatic conditions. This adjustment usually manifests itself in changes in both ice thickness and glacier length. The dynamics of such changes are highly complex (Paterson 1981). The response time of a glacier to mass-balance change usually exceeds the frequency of such changes: as a result, at any point in time, different parts of a glacier are at different stages of adjustment to different climatic impulses, whose individual effects may be difficult to separate. Observed trends in glacier volume and mass flux may therefore be difficult to interpret in terms of their climatic triggers.

Nevertheless, glaciers with high mass fluxes adjust relatively quickly to climatic impulses and problems of interpretation are lessened.

2.2.6.1 Changes in surface elevation on the Tasman Glacier.

The position of the terminus of the Tasman Glacier has changed very little over the 130 years of observations (Gellatly 1985c). Although this has led to the impression that the Tasman Glacier is unresponsive to short-term climatic changes (Gellatly 1985c), this is probably untrue because all other glaciers in the region have fluctuated (Hessell 1983; Salinger et al 1983). Corresponding changes in volume probably have occurred on the Tasman Glacier. Fluctuations in the position of the terminus are not an appropriate indicator of ice volume variations for this glacier. The alternative is to measure surface elevations, which are controlled by ice thickness (Harper 1934; Skinner 1964).

The changes in the surface elevation at glacier cross-sections reflect imbalance between the mass loss from the glacier (ablation) and recharge by mass redistribution (ice flow). Thus,

$$\Delta h = Q_i - A_i \qquad (10)$$

where h = surface elevation, Q_i = ice discharge, A_i = ablational ice loss. Under negative balance, $Q_i < A_i$, Δh is negative and the ice surface lowers. Conversely, where positive balance prevails, $Q_i > A_i$, Δh is positive and the ice surface rises. It is important to note that because the change in elevation represents an imbalance between ice discharge and

ablation, at lower ice discharges Δ h is increasingly a function of specific balance (Hastenrath 1987). It is meaningless to infer changes in ablation rate from changes in surface elevation wherever ice is moving.

The composite structure of the glacier, with many tributaries feeding a trunk ice stream, complicates the relationship between mass balance and ice level because different tributaries respond at different rates to a regional change in mass balance, due to differences in velocity and rate of diffusion of kinematic waves. Also, the extent to which a rise or fall in an ice stream affects adjacent ice streams is unknown.

For the purposes of describing surface elevation changes as a mass balance indicator over the last century, the dominant ice stream feeding the lower tongue of the glacier (the Hochstetter) has been examined in detail. More information is available for this ice stream than for any other part of the Tasman Glacier. More limited observations from other parts of the glacier are subsequently compared with those from the Hochstetter ice stream.

Twentieth-Century surface change.

Most observations of surface level change on the Tasman Glacier have been in the Ball Hut area. Cross-profiles of surface levels at this point are show in Fig 2.19.

More data from a variety of sources (Brodrick 1891; Harper 1934; 1946; Skinner 1964; Gellatly 1985; this study) has been used to construct a trend surface showing the spatial and temporal variation in centre-line elevation over the lower 10 km of the Tasman Glacier (Fig 2.20). Although the distribution of observations is rather irregular, the necessary interpolation is made with reasonable confidence, given that the variation illustrated in Fig 2.20 is over decades, during which short-term fluctuations are not detectable, and that changes have been very great.

Fig 2.20 shows a gradual change from a convex-up long profile in 1890 to a concave-up profile at present. The convex profile is characteristic of a glacier ablation zone in equilibrium or positive mass balance. The centre-line elevation is above the level of the western lateral moraine crest in 1890, consistent with Brodrick's observations of deposition on the crest and distal slope of this moraine (Brodrick 1891). The transition during negative balance to a concave long profile without terminal retreat is unusual. Indeed, the author has been unable to find any reference to a similar trend over a similar time period for any glacier in the world.

The rate of surface lowering has been variable over time and space.

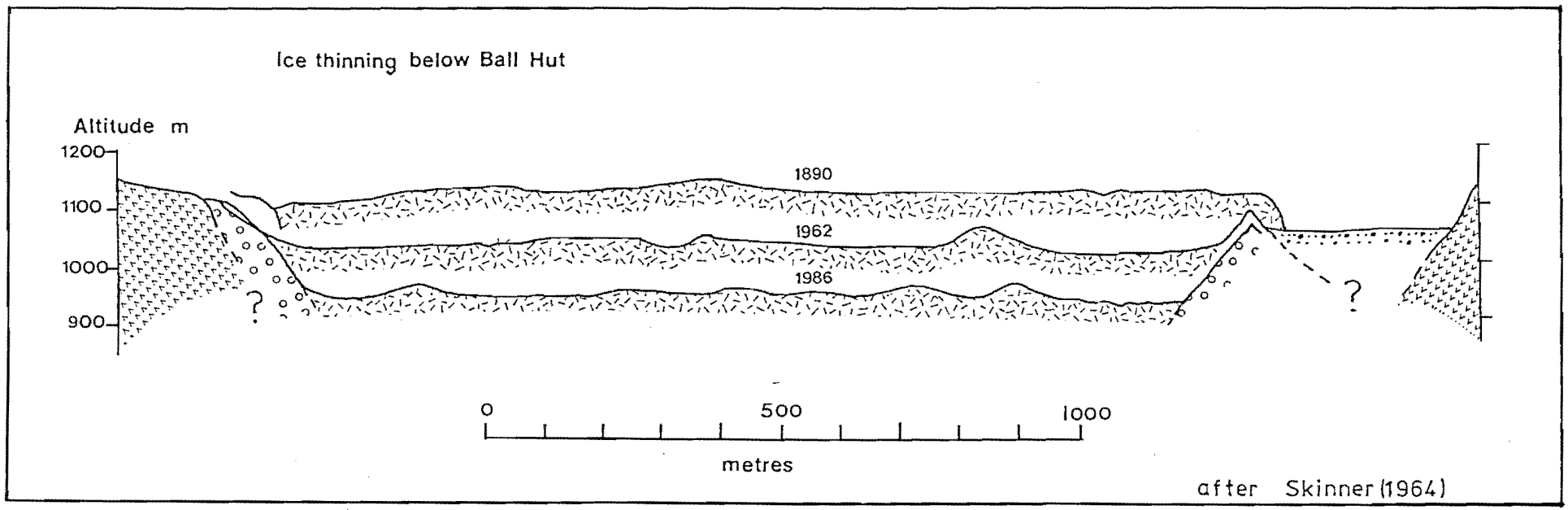

FIG. 2.19 Cross-profiles of the Tasman Glacier at Ball Hut. Data from Brodrick (1891), Skinner (1964) and this study.

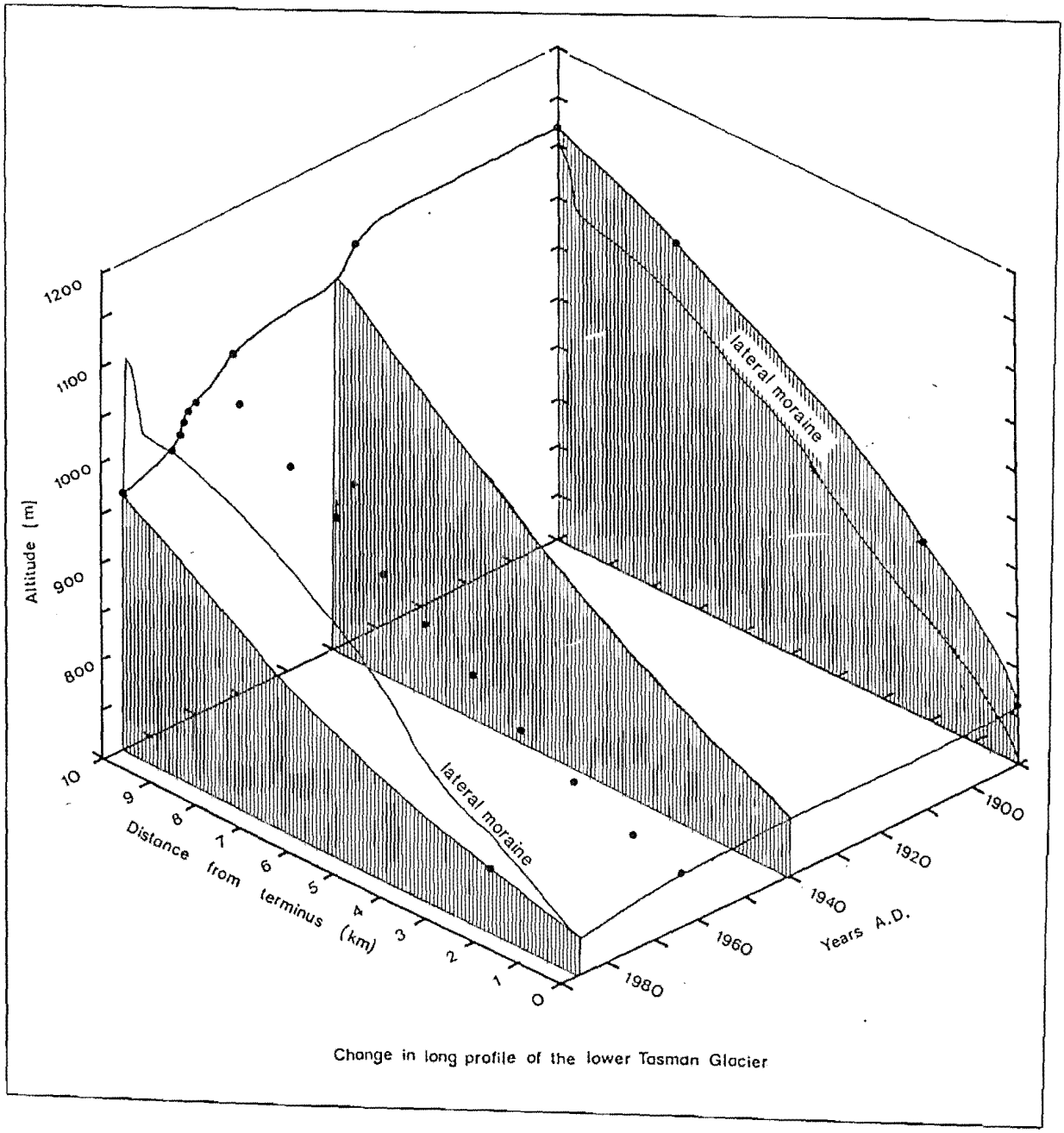

FIG. 2.20 Spatial and temporal variation in ice levels of the lower Tasman Glacier. The western lateral moraine crest in 1890 is shown for comparison. Data sources are listed in the text.

Little change in elevation was detected until the second decade of the Twentieth Century (Gellatly 1985c), after which ice levels decreased at Ball Hut at a variable rate. Lowering appears to have been especially rapid during the 1930s and 1970s. The possibility of other phases of rapid lowering (or indeed of rising ice levels) cannot be dismissed given the sporadic distribution of observations. Only the long-term trend is reliably illustrated by the existing record.

The elevation of the terminus has decreased by a relatively small amount, with the most rapid rate of lowering having occurred prior to 1965 (Fig 2.20). The overall gradient of the lower tongue of the glacier has correspondingly declined from 1°57′ in 1890 to 1°33′ at present. Concomitant with the convex to concave transition in long profile has been a similar transition in the cross-profile at the Celmisia transect, 2 km above the terminus (Fig 2.3).

1985-87 surface elevation change.

Surveyed ice levels across the three study transects show seasonal and annual changes in ice levels. The Celmisia and Ball Hut transects include the Hochstetter ice stream, the De La Beche transect includes ice streams draining the upper Tasman Glacier. The calculation of the change in elevation over time of a point on the glacier surface, corrected for ice flow and surface slope, is given in Appendix 5. The results of the calculations are summarised in Table 2.21.

The seasonal components of annual surface change were measured at De la Beche only. Table 2.21 shows that

$$\Delta h_w = 0.6\,\Delta h_s \qquad (11)$$

where Δh_w and Δh_s are the winter and summer ice-level changes respectively. The net effect is an annual change of Δh = + 2.7 m.

No summer elevation changes were measured at the Ball Hut transect, so the relation between Δh_w and Δh_s has been estimated from the greater ablation at Ball Hut. For Ball Hut, Equation (11) becomes

$$\Delta h_w = 0.75\Delta h_s \qquad (12)$$

to allow a net change in elevation to be calculated (Table 2.21). Although the summer decrease in elevation is greater, it appears that the net change in glacier surface level in 1986 was a rise of about 1.98 m. Although the actual amount of increase is dependent on the estimated relation in Equation (12), independent evidence supporting a rising ice surface exists in observations of marginal crevassing occurring between late 1985 and mid 1987, and of steep repose slopes at the ice margins as they rose against the moraine-wall talus aprons (Fig 2.21).

TABLE 2.21 Change in surface elevation of the Tasman Glacier in 1986.

Marker	(a) Elevation of marker (m asl)		(b) Elevation change of marker =d (m)	(c) Horizontal movement =l (m)	(d) Glacier surface slope = α	(e) Elevation change of glacier $h=d+(l.\tan\alpha)$	(f) Annual change in elevation
	12-13/5/86	8-9/12/86	Celmisia				
F1	801.1	801.0	- 0.1	1.19	0	as for (b)	- 0.17
F2	779.5	778.9	- 0.7	0.49	0	"	- 1.22
F3	767.8	767.4	- 0.4	0.69	0	"	- 0.69
F4	764.3	763.8	- 0.5	1.85	0	"	- 0.87
F5	764.8	764.2	- 0.6	1.70	0	"	- 1.04
F6	772.6	771.6	- 1.0	1.90	0	"	- 1.74
F7	755.9	755.2	- 0.7	0.66	0	"	- 1.22
Means			- 0.6				- 0.99
	12-13/5/86	8/12/86	Ball Hut				
F1	977.6	978.4	+ 0.8	37.79	2.3^0	+ 2.32	+ 1.00
P1	960.2	964.0	+ 3.8	46.39	"	+ 5.66	+ 2.45
P4	955.9	959.3	+ 3.4	45.58	"	+ 5.23	+ 2.26
P3	964.9	968.8	+ 3.9	47.21	"	+ 5.79	+ 2.50
F2	975.9	978.8	+ 2.9	51.05	"	+ 4.95	+ 2.14
F3	966.9	970.5	+ 3.6	47.14	"	+ 5.49	+ 2.38
F4	980.6	981.4	+ 0.8	42.38	"	+ 2.50	+ 1.08
Means						+ 4.56	+ 1.98
	23-25/11/85	16-17/5/86	De la Beche				
P2	1373.2	1362.1	- 11.1	128.15	3.83^0	- 2.51	
P3	1371.4	1360.2	- 11.2	121.64	3.83^0	- 3.05	
P4	1369.2	1357.2	- 12.0	122.97	3.83^0	- 3.76	
P5	1370.6	1357.4	- 13.2	117.53	4.00^0	- 4.98	
P7	1371.2	1356.7	- 14.8	114.74	5.17^0	- 4.43	
Means						- 3.75	
	16-17/5/86	16/12/86	De la Beche				
P2	1362.1	1356.4	- 5.7	136.77	4.50^0	+ 5.06	
P3	1360.2	1355.5	- 4.7	138.49	4.50^0	+ 6.20	
P4	1357.2	1352.1	- 5.1	135.68	4.50^0	+ 5.58	
P5	1357.4	1351.9	- 5.5	136.67	4.67^0	+ 5.66	
P7	1356.7	1351.7	- 4.7	127.52	5.83^0	+ 8.33	
Means						+ 6.17	

Annual change in elevation at De la Beche = $\frac{-3.75}{174} + \frac{6.17}{213} \times 365$

= + 2.71 m

FIG. 2.21 View down the western margin of the Tasman Glacier immediately downstream of the Haast Glacier confluence, February 1987. Debris mantled ice of the Tasman Glacier (left) is rising and over-riding avalanche snow from the previous winter (right). Height of ice-marginal bank is approximately 5 metres.

At the Celmisia transect, no seasonal adjustment to measured ice levels has been necessary because the elevation of marker F6 was determined in February 1986, as well as in May and December. Table 2.21 shows that the ice level at this site continued to decline throughout the 10.5 month measurement period to give an annual change of Δh = -2 m.

2.2.6.2. Glacier response to negative mass balance.

Observed trends in ice velocity, discharge, and surface elevation are now related to the Twentieth Century mass balance history of the glacier.

Records of the terminal fluctuations of the nearby Franz Josef Glacier (Sara 1968; Soons 1971; Hessell 1983) and Stocking Glacier (Salinger et al 1983) give indications of the magnitudes and timing of glacier volume changes in the Mount Cook region have experienced (Fig 2.22). The terminal position of each of these glaciers is sensitive to short-term climatic changes on the timescale of several years, and therefore this record forms a reference against which the observed behaviour of the Tasman Glacier can be compared.

A general negative mass-balance trend during this century is evident, punctuated by short-lived readvances in the 1940s and 1960s. More recently, the Franz Josef Glacier has been advancing since 1984 and the Fox Glacier since 1985. Climatic triggers of positive and negative balance fluctuations of these glaciers should also have affected the Tasman Glacier, in spite of the lack of recorded volume increases there. The response of the Tasman Glacier to mass balance changes must involve terminal stability of the glacier and the pattern of ice thinning described above.

In Chapter 4.1, an explanation of the unusual pattern of thinning of the lower Tasman Glacier is proposed, which relates the distribution of ice loss to the evolution of the debris mantle. The dynamics of debris mantle growth are complex, and the principles are developed in Chapter 4.

2.2.6.3. Glacier response to positive mass balance.

Increases in ice-surface elevation, flow velocity and ice discharge have been measured at the De la Beche and Ball Hut transects but not at Celmisia Flat. The 1985-87 positive balance fluctuation on the Tasman Glacier is the first recorded this century, and corresponds to the advances since 1984-85 of the Fox and Franz Josef Glaciers in Westland. These advances are of similar or slightly greater magnitude to those of

the 1940s and 1960s (Suggate 1952; Sara 1970; Wardle 1973; Soons 1971), so that increased ice discharges on the Tasman Glacier also should have occurred to a similar extent at these times.

In the ablation zones of glaciers, where flow is compressive, adjustment to positive balance fluctuations takes place by the propagation of kinematic waves. (See Paterson 1981 Chapter 12 for a discussion of wave dynamics). The time taken for a wave to reach the terminus and cause an advance (the response time) is a function of the relationship between strain rate and wave velocity. Paterson (1981) demonstrates how on glaciers with low surface gradients kinematic waves are diffused (attenuated) more than on steeper glaciers. This affects the response both by increasing the response time and by increasing the mass-balance impulse necessary to cause a response of the terminus.

Steeper, faster flowing glaciers such as the Franz Josef (Gunn 1965; McSaveney & Gage 1968) and Fox Glaciers will respond to smaller mass balance increases than will the Tasman Glacier and will respond more quickly. This has given rise to the notion that the Tasman Glacier is "unresponsive" (Gellatly 1985c). Although true in a relative sense, the measured rises in ice discharges on the Tasman Glacier indicates that kinematic waves have been propagated from the Grand Plateau and the Tasman Saddle accumulation zones at least as far as the Ball Hut and De la Beche transects, both involving distances of 9 km from their respective ice divides. The Franz Josef and Fox Glaciers were both 13 km long when their termini began to advance. The surface level of the Tasman Glacier has risen to a point about 3 km downstream of Ball Hut in February 1987, giving a wave propagation of about 12 km. It appears that the time taken for a wave to travel 13 km (the length of the Fox and Franz Josef Glaciers) down the Tasman Glacier is similar to or only slightly greater than the response times of the Westland glaciers. This is to be expected given the flow rates of >500 ma^{-1} for the Hochstetter Icefall and 230-270 ma^{-1} for the upper Tasman ice streams (Chapter 2.1), velocities comparable to those of the Westland glaciers. The "unresponsiveness" of the Tasman Glacier therefore appears to be due to the length and low gradient of the slow-moving lower tongue, in which kinematic waves are effectively diffused and the terminus (in the Twentieth Century at least) remains unaffected.

Fig 2.8 is an interpretation of the spatial and temporal change in ice discharge on the lower tongue of the Tasman Glacier since 1890. Interpolations are made on the basis of the inferred but unrecorded

positive fluctuations on this part of the glacier. The diffusion of kinematic waves in the lower tongue is illustrated for the 1940s, 1960s and 1980s positive balance periods.

2.2.6.4. Glacier fluctuations elsewhere in the Southern Alps.

Documented glacier fluctuations elsewhere in the Southern Alps (Harper 1935; Gage 1951; Harrington 1952; Sara 1968, 1970; Anderton & Chinn 1978; Hessell 1983; Salinger et al 1983; Gellatly 1985c; Bishop & Forsyth 1988) show that trends have been regionally consistent over the century of observations.

Observed fluctuations of glaciers in the Mount Cook area are summarised by Gellatly (1985c). Between 1892 and 1888 there was a general recession, the magnitude of which varied locally. Glacier volumes remained fairly constant from the time of Brodrick's (1890) surveys, small terminal fluctuations being observed on the Stocking Glacier (Salinger et al 1983), the Mueller Glacier, and on tributaries of the Tasman and Murchison Glaciers (Gellatly 1985c). No evidence of an advance of the termini of these glaciers was recorded, though Speight (1940) reported on the steepness of the frontal debris-covered slope of the Tasman Glacier. Valley glaciers in the Godley Valley began to retreat between 1892 and 1914. There was a prolonged stillstand between 1905 and 1940, though some glaciers thinned without any recorded terminal retreat (Gellatly 1985c). Between 1914 and 1935 several tributaries to the Murchison Glacier had become separated from the trunk glacier. The Godley Valley glaciers began to retreat around 1920, and the rate of retreat has increased in the last 3 decades.

Glaciers in the Rakaia Valley may have been retreating before those in the Mount Cook area (Gage 1951). The Lyell Glacier had retreated 800 m in the 45 years before 1911, then changed little until after 1933. Similarly, the Ramsay Glacier retreated 200 m and thinned by 20 m between visits by Haast in 1865 and Speight in 1910. Little change in the position of the terminus then occurred until after 1932. By 1949 a thinning of 60 m had occurred. Since then a retreat of 1.5 km has continued.

The well-documented Franz Josef Glacier has experienced a general retreat since 1895, punctuated by minor readvances in 1907-9, the 1920s, 1947-50, 1963-68, and 1984 to the present (Suggate 1952; Sara 1970; Soons 1971; Hessell 1983; Brazier et al in prep.). The Fox and Stocking Glaciers follow similar trends (Sara 1970; Salinger et al 1983) (Fig 2.22).

Evidence from aerial photographs of the central Southern Alps taken

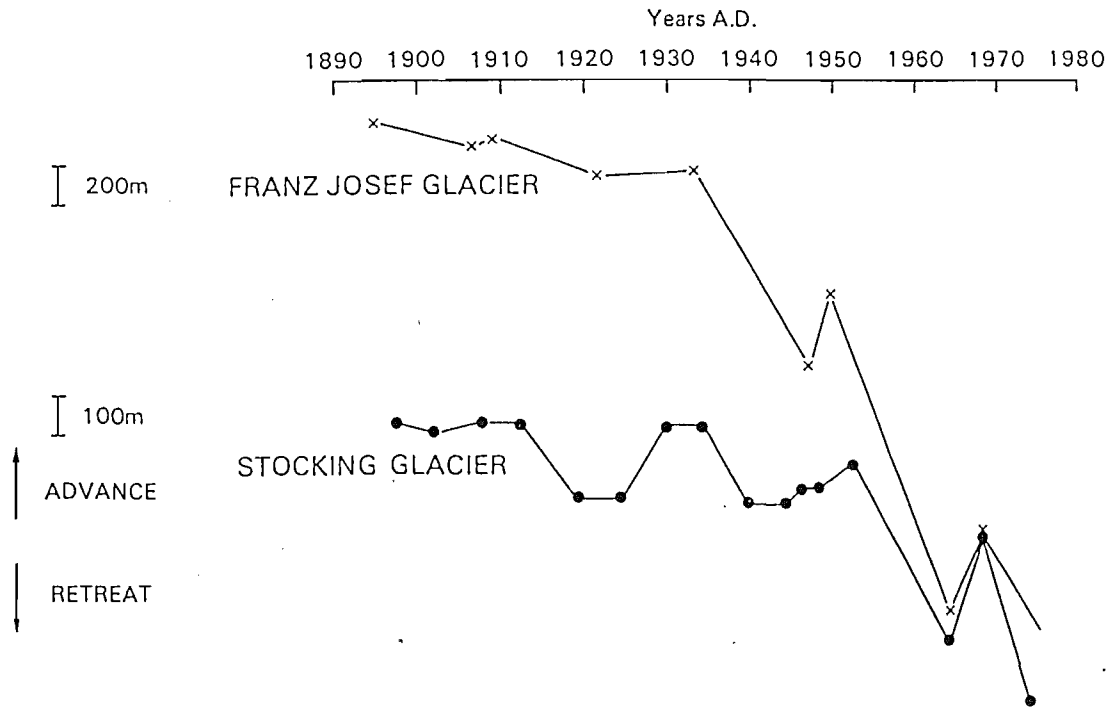

FIG. 2.22 Documented fluctuations of the Franz Josef and Stocking Glaciers, from data compiled by Salinger et al (1983).

in February 1986 indicates that most valley glaciers in the region have positive mass balance. The lateral margins of many glaciers are well-defined, rising above the base of adjacent moraine wall talus aprons, and the surfaces of some glaciers show a greater degree of crevassing than on photographs taken in the mid 1960s and early 1970s.

In summary, the measured thickening of the Tasman Glacier is part of a mass balance trend affecting all glaciers in the region. Differences in Twentieth Century glacier retreat between debris-mantled and unmantled glacier are described in Chapter 4.

2.3 CONCLUSIONS OF CHAPTER 2.

1. Velocities and mass fluxes of the Tasman Glacier are large in comparison with other mid-latitude glaciers. Such a high-energy glacier system is characteristic of maritime environments.

2. Ablation rates are high and ablation gradients correspondingly steep. Ice loss reaches a maximum of 17 to 18 ma^{-1} of ice at 960 m, and decreases by an average of 1.5 m per 100 m altitude.

3. An extensive debris mantle wedges to >2 m thick near the terminus, and reduces ablation of underlying ice by an average of 68% Conduction supplies most heat for melting beneath the debris layer.

4. Twentieth-Century change has been great. The glacier has thinned by up to 160 m and ice discharge reduced by 31-37% between 1890 and 1973. The terminus has become almost stationary by 1986, but has not retreated.

5. Present thinning of the lower glacier appears to be a response to mass-balance change which occurred at least 40 years ago. Above 7 km from the terminus, ice levels rose during 1985-87 in common with a regional positive mass balance trend. Previous positive fluctuations have probably passed undetected.

CHAPTER 3. THE GLACIAL-DEBRIS TRANSPORT SYSTEM

Chapter 2 described the Tasman Glacier in terms of the supply, transfer and loss of ice. Chapter 3 uses these data in a study of the transport of rock debris through the system. The chapter is in three parts.

1. The sources of debris are described and the processes of debris production are discussed. The purpose is to identify the different processes by which debris is supplied to the glacier and to assess qualitatively the relative importance of each.

2. The glacial debris transport routes are identified and the relationships with glaciological and morphological controls are analysed. Mechanisms governing the morphology of supraglacial debris accumulations are presented. This section allows the significance of changes in the extent of the supraglacial debris cover to be assessed in terms of mass balance changes. The principles developed here form the basis for a detailed study of the debris mantle in Chapter 4.

3. Discharges of debris through three measured cross-sections of the glacier are calculated using glaciological data from Chapter 2. Spatial and temporal variations in debris discharge are interpreted and discussed. The results are used to derive a denudation rate for the Grand Plateau cirque on the eastern side of Mount Cook.

3.1 DEBRIS SOURCES

3.1.1 Subglacial erosion and entrainment.

Implicit in most texts on geomorphology is the concept that glaciers which slide over their beds are highly erosive. The field evidence supporting this premise is vast: landforms from the scale of striae and chattermarks to roche moutonees, to the scale of valley forms or vast areas of areal scouring all attest the effectiveness of ice as an eroding agent. The diversity of such forms is reflected in the varied approaches to the study of subglacial processes. From geomorphic description of large-scale landforms, and from the study and modelling of micro-scale processes at the glacier bed have arisen ambitious attempts to relate the two (eg. Boulton 1974; Sugden 1978). Drewry (1986 p.33) comments that the understanding of physical relationships operating at the ice-substrate interface still are insufficiently understood to allow more than general relationships to be formulated. No quantitative framework for the study

of glacier erosion exists, nor have the temporal relationships between erosion and changing glacier dimensions been investigated in detail.

Given the state of theory and the difficulty collecting data from the subglacial environment, the following discussion of the Tasman Glacier is limited to describing conditions favouring subglacial erosion and their likely occurrence or non-occurrence below the glacier. Qualitative statements may then be made about the effectiveness of various processes in the light of very limited field observations. Of unknown importance is the boundary condition of a deformable glacier bed (Boulton 1979). The possible significance of this with regard to the Tasman is discussed.

3.1.1.1 Subglacial Erosion.

Ice erodes bedrock by crushing and fracture and by abrasion. The process is the essentially the same, the difference being a matter of scale (Sharp & Gomez 1986). Crushing and fracture of rock by the weight of overlying ice appears to be an effective process even though the compressive strength of rock usually far exceeds the loads exerted by glaciers. The point contacts of clasts embedded in the glacier sole may give rise to locally concentrated stresses able to cause crescentic gouges and chattermarks in the rock substrate. At the temperatures and confining pressures of the subglacial environment, and with the high stress imparted by sliding ice, rock tends to be brittle rather than ductile. Repeated loading cycles by the passage of several clasts over a given point on the substrate is thought to be an effective means of bringing about brittle fatigue failure at lower loads than might be expected in the prevailing stress regime. This may especially be the case where clasts roll, rather than slide, across the substrate (Drewry 1986). By implication the effectiveness of bedrock fracture may not be directly related to the ice overburden pressure at the time of failure. At a scale of tens to hundreds of metres, variations in pressure across the ice-bedrock interface cause spatial differences in stress conditions. Modelling of this situation by Morland & Boulton (1975) has shown that fracture is most likely to occur in cavities which may open in the lee of bedrock hummocks. Failure is facilitated by microcracks which exploit crystallographic and cleavage weaknesses in loaded bedrock, eventually leading to semi-continuous shear surfaces. Various combinations of these processes produce fragments which may simultaneously or subsequently be entrained by the glacier.

Abrasion includes all processes of "wear" by sliding ice. Although it

has been shown experimentally that pure ice can cause significant wear of the substrate (Budd et al 1979), it is generally accepted that rock debris greatly increases abrasive wear by providing tools which plough grooves in the bed. The exact nature of the process involves the concentration of elastic strain at the point contacts (asperities) of clasts on the substrate. The release of stress causes the impact of asperity against rock surface, which produces rock chips. The repeated build-up and release of stress in this manner causes a jerky path of the abrading tool as it cuts the groove or striation. A simple mathematical formulation of the problem presented by Drewry (1986 p.50-51) shows the dependence of abrasion on sliding velocity, normal load, and on the yield stresses of the tools and the substrate. On a larger scale, the debris concentration in the basal ice is significant: Hallet (1981) suggests that maximum abrasion occurs at volume concentrations of 10 to 30%. Hallet's model of abrasion proposes that the force pressing a clast against the substrate is directly related to the glacier sliding velocity, therefore the effectiveness of abrasion is primarily a function of sliding velocity and basal debris concentration. This differs from the model of Boulton (1974), which suggests that clast velocity at the bed (and therefore the force it exerts) depends largely on clast size and geometry. Away from a critical optimum clast size, regelation around the clasts increases the passage of ice around the clasts and the relative velocity between ice and clasts is increased. The Hallet and Boulton theories differ in the factors seen as most important for producing the effective contact force at the bed: Hallet proposes that abrasion rates are independent of ice pressure and depend on the ice flow towards the bed and on sliding velocity. Boulton suggests that the contact force is the sum of the buoyant weight of the clast in ice and of the net weight of the overlying ice column. The conflict remains unresolved, though Drewry's (1986) review favours the Hallet model as being probably more applicable. However, ice thickness and sliding velocity are related (Chapter 2).

From these reviews it is apparent that subglacial crushing and fracture is favoured by greater ice thicknesses (normal load) and sliding velocities (shear stress), and by irregular substrates which set up spatial pressure variations. Abrasion is favoured by either deeper ice (Boulton) or greater sliding velocities (Hallet), or some combination of the two. Both fracture and abrasion are enhanced by clasts embedded in the glacier sole and by supply of these tools to replace those lost by wear.

3.1.1.2 Subglacial entrainment

The products of glacier-bed erosion may be entrained (incorporated into ice) in several ways, thereby allowing further erosion to occur. Regelation is the process by which ice, close to its pressure melting point, deforms over and around obstacles inducing melting on the high-stress (upstream) side and refreezing on the low-stress (downstream) side. Regelation ice of several centimetres thickness is accreted to the glacier sole downstream from the obstacle and small rock fragments may become incorporated. This is also a basic process of glacier "sliding" (chapter 2) and has been confirmed by direct observation (eg. Kamb & LaChappelle 1964). Lliboutry (1964) describes a "hydraulic jack" effect whereby opening of subglacial cavities allows ice in the lee of bedrock obstacles to pluck debris away with it.

Other entrainment processes described in the literature are, by their nature, not likely to operate below the Tasman Glacier. These processes require changing thermal conditions at the ice-bedrock interface, and include ice-debris accretion (Weertman 1961) and block incorporation (Moran et al. 1980).

3.1.1.3 Subglacial erosion and entrainment by the Tasman Glacier.

There is no direct access to the bed of the Tasman Glacier, and no direct measurements of subglacial erosion rate. Any information must be gained by inference from the glaciological parameters favouring erosion. From the above review, a qualitative assessment of various parameters is made in Table 3.1 in terms of the likely effects of each parameter in encouraging or discouraging subglacial erosion. Quantitative values for the Tasman Glacier are based on calculations presented in Chapter 2, and these are compared to the published ranges of each parameter from glaciers worldwide.

It is concluded that the glaciological conditions of the Tasman Glacier favour both high rates of abrasion and of crushing and fracture. The Tasman Glacier approaches the upper extremes of observed normal loads and shear stresses, therefore both fracture and abrasion will be effective regardless of the validity of the contrasting abrasion models of Boulton and Hallet. Sliding velocities are high, but experimental work by Budd et al (1979) indicates higher values do not correlate to greater normal load or basal shear stress, for reasons which are not understood. However, if Budd et al's predictions are accepted, an estimate of abrasion rate is possible. From Budd et al (1979: Table 2), for a normal load of 4000 kPa

TABLE 3.1 Factors favouring subglacial erosion in temperate valley glaciers.

Parameter	Fracture and crushing	Abrasion	Tasman Glacier	World Range
Normal load N (ice depth)	favoured by higher values of N	important in Boulton model	up to 5000 kPa (up to 550 m)	500-5000 kPa (Budd 1979)
Basal shear stress	favoured by higher values of	important in Hallet model	up to 150 kPa (1986) up to 200 kPa (1890)	50-200 kPa (Budd 1979)
Sliding velocity U_{sl}	favoured by higher values	important in Hallet model	c.70 ma^{-1} (Ball Hut 1973) c.200 ma^{-1} (Malte Brun)	0-10^3 ma^{-1} (Drewry 1986)
Bed roughness	favoured by bed roughness setting up pressure variations	may be enhanced on stoss sides of bed irregularities	(no data)	extremely variable
Cavitation	favoured by stresses set up in cavities (Morland & Boulton 1975)	ice-bedrock decoupling prevents abrasion	evidence of occurence	common under sliding glaciers
Bedrock jointing	facilitates fracture and removal	(not relevant)	Selby M_s= 26-70	extremely variable
Basal debris concentration	favoured by presence of "tools"	optimised by 10-30% volume concentration (Hallet 1981)	(no data)	abundant debris in temperate glaciers

and a shear stress of 130 kPa an abrasion rate of 5.0 mma^{-1} is estimated. These stress conditions approximate to those in ice streams draining from the Tasman Saddle area. Budd et al's experiment involved ice with no initial debris content and therefore no abrasive tools, so the abrasion rate of 5 mma^{-1} may be regarded as a minimum. An erosion rate of the glacier bed by crushing, fracture and abrasion may therefore be as much as 10 mma^{-1}.

Variations in surface slope and ice thickness cause significant variations in normal and shear stress. However, the lack of established relationships between stress, ice thickness, ice velocity, bed roughness, and erosion rate make it impossible to estimate the zone of greatest erosion or the spatial extent of deposition. The effects of Twentieth Century thinning and velocity reduction on the amount and distribution of erosion should be a trend towards less erosion and more deposition.

Empirical evidence of subglacial erosion supports the deductive reasoning that rates are generally high. Three lines of evidence give some indication of subglacial process.

1. Abundant surfaces of striated bedrock occur above the present glacier on slopes stable enough not to have collapsed following glacier thinning. Fine examples occur to the north and south of the Beetham Valley.

2. A striated boulder on a medial moraine bore clear evidence that ice had slid over it. Abrasion on the upper surfaces and deposition of $CaCO_3$ on the lee side (Figure 3.1) indicate basal sliding and lee-side cavitation associated with pressure melting and regelation around the obstacle. This mechanism preferentially enriches meltwater in $CaCO_3$ which is reprecipitated in lee-side cavities (Hallet 1976; 1979a; Souchez & Lorrain 1975).

3. Coarse-grained bubble-free ice, which has undergone regelation at the glacier sole (Hambrey & Muller 1978), outcrops at the glacier surface along ice-stream junctions and in abundance within 1 km of the glacier terminus. No detailed mapping of ice-crystallographic types was undertaken, but the general distribution shows an association of regelation ice with zones where ice formerly in contact with the glacier bed would be expected to outcrop (Hambrey, pers. comm. Tasman Glacier 1986).

In summary, both field evidence and deductive reasoning indicate that the Tasman Glacier is likely to be highly erosive of its bed, whether this be bedrock or gravel. The extent of erosional and depositional zones is

FIG. 3.1 Boulder on a medial moraine of the ice stream draining Tasman Saddle. Calcium carbonate (arrowed) has been deposited in a subglacial cavity in the lee of the pronounced step in the rock surface. Striations show the points of detachment and reattachment of ice sliding over the boulder.

not known, nor are changes in any of these variables with changing ice discharge. Tentative comparisons with the experimental work of Budd et al (1979) suggest an erosion rate of the glacier bed of perhaps 10 mma^{-1} close to the equilibrium line.

3.1.2. Extraglacial (subaerial) erosion and entrainment.

The strong maritime influences on this area of high relief favour the mechanical weathering of rock by ice crystal growth. The influence of other processes is probably slight.

The geology of the Mount Cook area was reviewed in Chapter 1. Gross rock mass properties result from interactions between original lithotype, metamorphic grade, and tectonic history. The regional metamorphism of Torlesse Sandstones to prehnite-pumpellyite grade (Findlay & Spörli 1984) gives high intact rock mass strengths (IRMS) (sensu Addison 1981). The tectonic history suggests that up to 30 km of uplift has occurred since the early Jurassic, and >5 km since the late Miocene (Adams 1979). Erosion of the uplifting massif has released the large confining pressures on the rock mass. Jointing of the rock is well-developed as a result, giving moderate to low discontinuous rock mass strengths (DRMS). A similar response is evident in argillite lithologies, the difference being the fissility of these rocks as a result of finer grain sizes and response to deep burial in comparison to the massive, coarser, poorly sorted sandstones. In consequence the argillites form flatter and smaller clasts during weathering, the exception being in areas of greater induration associated with higher metamorphic grade (Chlorite Subzone 2 of Gair 1967). Sandstone and argillite far exceed any other lithologies in outcrop extent in the Tasman, Murchison and Godley Valleys. In the Hooker and Mueller Valleys, schists of Chlorite Subzone 2 outcrop along western valley sides.

The importance of intact and discontinuous rock mass strengths on the efficiency of frost-weathering has not been studied systematically, perhaps because the weathering process itself is not fully understood. The effects of frost on soils (eg. Higginbottom & Fookes 1971; Washburn 1979) and of rock properties on slope stability (eg. Fookes et al. 1971; Hoek & Bray 1981) and glacial erosion patterns (Addison 1981) have received attention, but the effects of rock mass properties on frost action remain poorly understood. A qualitative discussion of this topic in the maritime glacial environment of South Georgia was made by Gordon & Birnie (1986). They identified the main influences on bedrock weathering on the island as

being low discontinuous rock mass strength due to the ubiquitous closely-spaced open joints favouring moisture penetration for frost-weathering. A conclusion that physical processes predominate is implicit.

To assess the susceptibilities of the main lithologies to frost weathering it is necessary to examine in more detail the geomechanical factors which define the overall rock mass strengths. Selby's (1980) rock mass strength classification is based on a variety of lithological characteristics (Table 3.2). Although the properties of the intact rock mass account for only 20-25% of the overall rock mass strength, these properties are important in defining the relative effects of macrogelivation (frost-weathering producing coarse clasts) and microgelivation (frost weathering causing granular disintegration) (Tricart 1956). Porous and poorly indurated lithologies quickly disintegrate to constituent grains due to freezing of pore water. Well-indurated lithologies, conversely, allow moisture to penetrate only along open joints. Frost-wedging produces clasts whose sizes are a direct function of joint spacing. This difference explains many characteristics of periglacial regoliths (Ballantyne 1984). The high degree of induration of the Torlesse Group rocks, especially the sandstone lithofacies, strongly favours the production of coarse frost-shattered detritus, and the abundance of talus aprons and blockfields on ice-free mountain sides is ample evidence of this. Finer-grained regoliths are common in localities where joint spacing is extremely high, as in many argillite beds and fault zones.

The weathering of susceptible argillites can reduce the rock mass to a residual soil which forms soft slope mantles. These are rapidly eroded and do not form significant sources for glacially-transported material even though they are widespread, though localised according to lithology.

Selby's (1980) classification lends much weight to DRMS: up to 70% of the rock mass strength is influenced by joints and related phenomena. The field area has two main types of bedrock discontinuity:

1). Tectonic faults, on many scales, formed as a response to regional crustal stresses. Major faults cross the field area with a generally NNE-SSW trend. Several large faults have been mapped to the margins of the area but not into the structurally-complex regions around the Main Divide (Spörli and Lillie 1974). Major faults, such as the Ostler Fault, extend through the area (Chapter 1); however many appear to trend sub-parallel to strike and are difficult to identify in the field (Waterhouse 1985), while others lie beneath river gravels in the main valleys and have not been

TABLE 3.2 Rock mass strength properties and ratings (Selby 1980: Table 6)

	1	2	3	4	5
Weathering	unweathered r: 10	slightly weathered r: 9	moderately weathered r: 7	highly weathered r: 5	completely weathered r: 3
Spacing of joints	> 3 m r: 30	3–1 m r: 28	1–0.3 m r: 21	300–50 mm r: 15	< 50 mm r: 8
Joint orientations	Very favourable. Steep dips into slope, cross joints interlock r: 20	Favourable. Moderate dips into slope r: 18	Fair. Horizontal dips, or nearly vertical (hard rocks only) r: 14	Unfavourable. Moderate dips out of slope r: 9	Very unfavourable. Steep dips out of slope r: 5
Width of joints	< 0.1 mm r: 7	0.1–1 mm r: 6	1–5 mm r: 5	5–20 mm r: 4	> 20 mm r: 2
Continuity of joints	none continuous r: 7	few continuous r: 6	continuous, no infill r: 5	continuous, thin infill r: 4	continuous, thick infill r: 1
Outflow of groundwater	none r: 6	trace r: 5	slight < 25 l/min/ 10 m² r: 4	moderate 25–125 l/min/ 10 m² r: 3	great > 125 l/min/ 10 m² r: 1
Total rating	100–91	90–71	70–51	50–26	< 26

mapped (Lillie 1962a, 1962b; Spörli et al. 1974; Findlay & Spörli 1984).

Faulting increases the density of discontinuities in the rock mass through cataclasis in brittle lithologies. The DRMS is thereby reduced and water penetrates more easily. These modifications are localised to fault zones themselves, many of which form gullies where they intersect slopes at a high angle. In extreme cases, fault crushing has the effect of destroying the IRMS, allowing granular disintegration of the fine-grained "crush-rocks".

2). Joint pattern is the most important influence on coarse debris production. Joints define primary planes of weakness which disrupt the intact rock mass strength and allow water to penetrate. Regardless of IRMS, the joint spacing and penetration will determine the rock mass strength as a whole, and therefore the stable angle of rock slopes.

Rockfall scars show open joints on failure surfaces which had several tens of metres of overburden prior to failure. Further evidence of joint penetration is provided by site investigations for anchor points for the Hooker River foot bridge at S79/765347. There, open joints penetrated at least 5 metres into massive sandstone forming a steep bluff undercut by the river. My observations, while not extending to systematic measurement of joint geometry, suggest that joint orientations are variable throughout the area and that joint spacing ranges from centimetres to metres. Generally there are several sets of intersecting joints: often one or two major sets are intersected at high angles by two or more minor sets. Where metamorphic grade is higher in the north-west of the area, one set becomes dominant and sub-parallels to the foliation in schistose lithologies. Such a pattern is characteristic of Westland valleys, but is not widespread to the east of the Main Divide.

In the Tasman Valley, dominant joint sets, where they occur, tend to parallel the trend of the main valley. This is especially so on the eastern side of the glacier, giving rise to the steep slabby rock faces of the Malte Brun Range and to the wall above the glacier at Beetham Corner (Fig.3.2). It is not clear whether this joint trend is a result of glacial incision or whether it preceded (and has therefore been exploited by) glacierization. (For a discussion of this problem see Addison 1981). West of the glacier, joint geometry is less simple and several sets occur with little or no systematic relationship to topography.

In summary, jointing is strongly developed throughout the field area and of great significance in reducing rock-mass strengths and allowing moisture penetration. Although the spacing and orientation of joints is

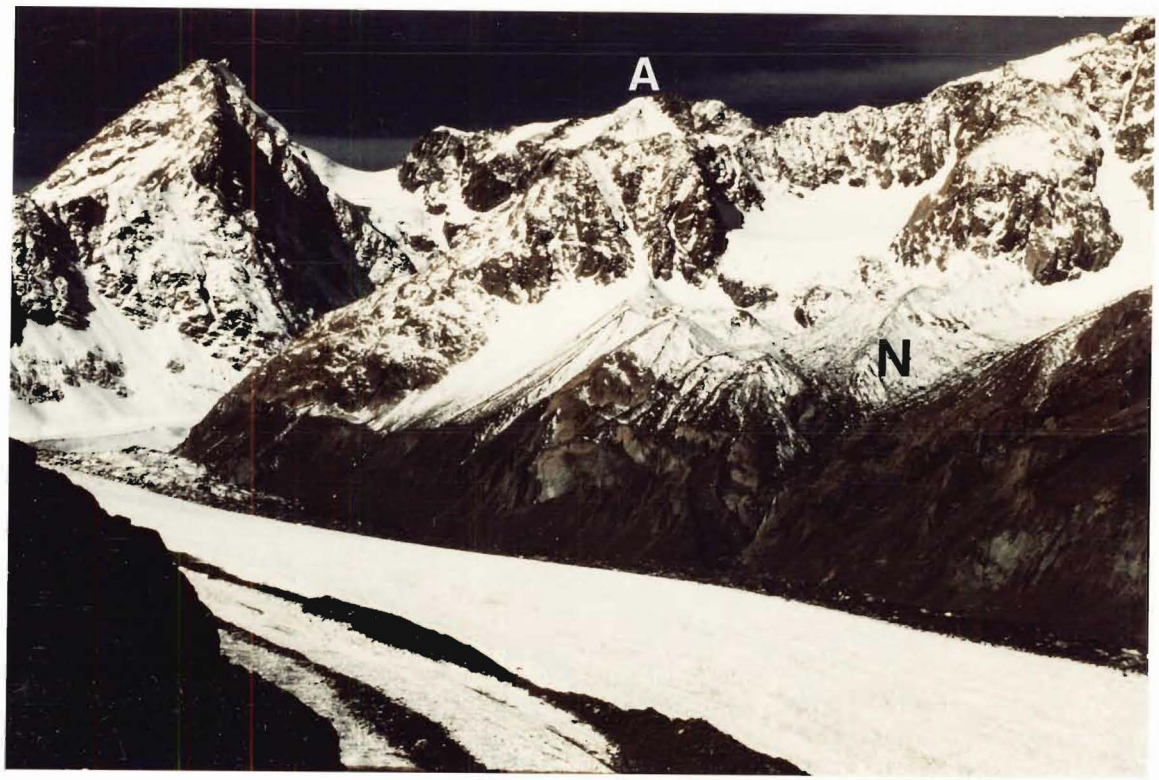

FIG. 3.2 (A) The eastern valley side above the Tasman Glacier at the old Malte Brun Hut site. Arrow indicates bedrock exposed by erosion of lateral moraines in the last 50 years. N = Neoglacial moraine of Turnbull Glacier, A = Mt. Annan.

(B) The eastern valley side at Beetham corner. Bedrock exposed by lateral moraine collapse bears a marked trimline. Zone of toppling failure is arrowed (T), while moraines survive in protected locations (M).

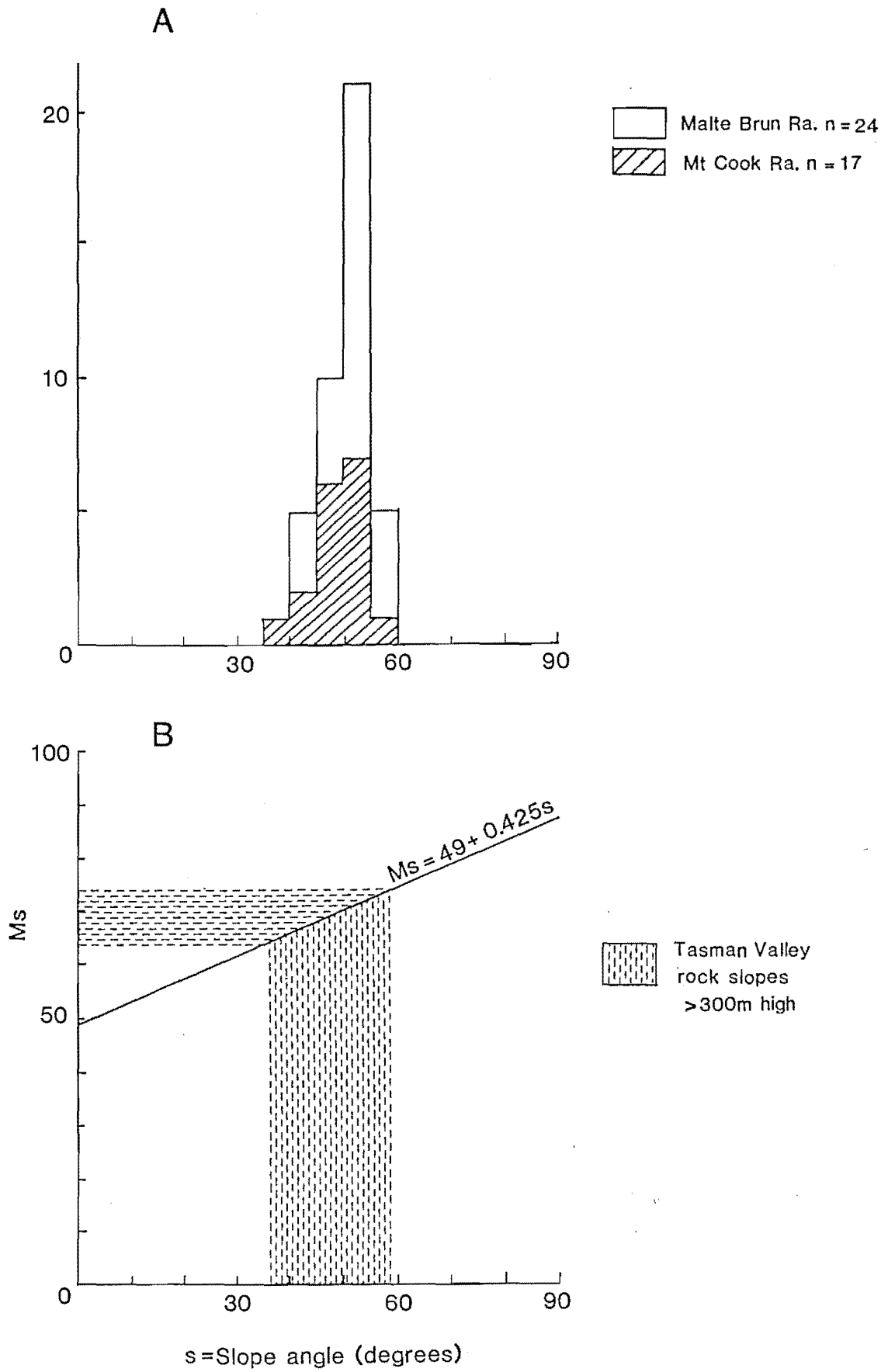

FIG. 3.3 (A) Histogram of angles of 41 300 m high rock slope segments in the Mount Cook and Malte Brun Ranges.

(B) Inferred rock-mass strength values (Ms) based on the measured slope angles, using the relationship derived by Selby (1980).

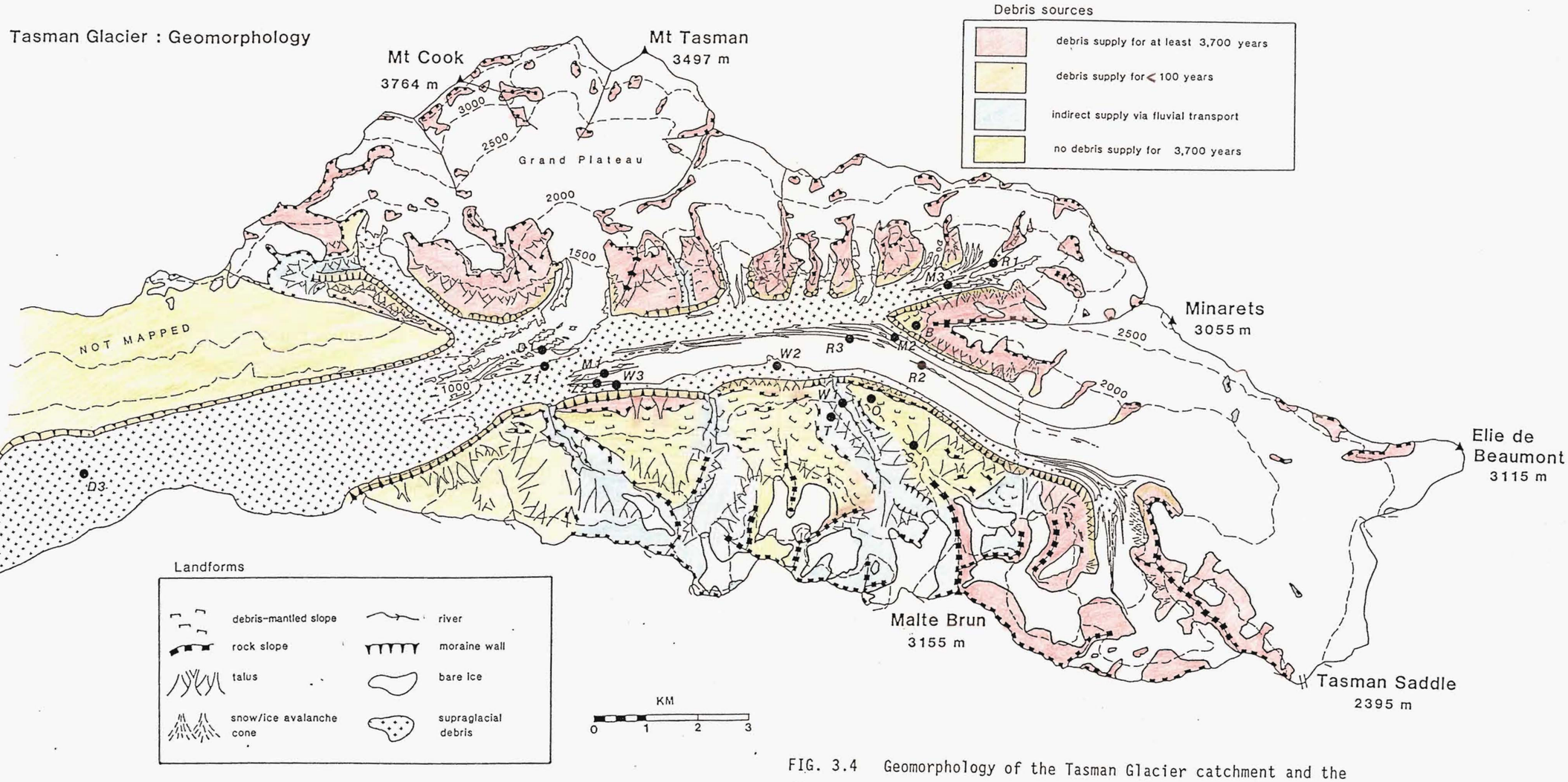

FIG. 3.4 Geomorphology of the Tasman Glacier catchment and the distribution of supraglacial debris. Slopes are classified in terms of landform (symbols), and in terms of their contribution of sediment to the Tasman Glacier (colours). Map drawn at 1 : 25,000 scale from 1965, 1971, and 1986 aerial photographs and from Brodrick's 1890 map.

regionally variable, joint patterns allow only weak to moderate rock-mass strengths (Fig 3.3B).

Slope angles of 41 rock surfaces were measured from NZMS 1 series topographical maps enlarged to 1:40,000 scale (Fig 3.3A). Rock slopes were first identified on aerial photographs, then 305 m (1000 feet) high segments were selected on the steepest slopes. The corresponding overall rock mass strength value is Ms = 70 (Fig 3.3B). This value is the maximum rock strength for the field area, since the sample is limited to the steepest (and therefore strongest) slopes.

Slope angles in the Mount Cook Range were compared with those in the Malte Brun Range to test for differences between the two groups. On an a **priori** basis, it might be expected that the generally more stable-looking and weathered rock slopes of the Malte Brun Range, with an apparently wider joint spacing, may maintain steeper angles than those in the Mount Cook Range. A Mann-Whitney two-sample test (U Statistic) reveals that the steepest rock slope segments in the Malte Brun Range are indeed steeper at a 0.01 significance level. This does not necessarily mean that overall mountain slope angles differ: it merely suggests variation in the controls on rock mass strength (Table 3.2). That this variation is primarily due to the geometry of planes of weakness is likely, but remains an hypothesis.

3.1.3. Debris sources of the Tasman Glacier.

There are four broad sources of rock debris being supplied to the glacier (Fig 3.4):

a) subglacial erosion and entrainment

b) direct rockfall and rock avalanche above and below the equilibrium line from bedrock sources.

c) reworking of older deposits, especially lateral moraines.

d) fluvial transport from ice-free tributary valleys.

The relative importance these sources is difficult to determine, and possible changes during glacier thinning and can only be qualitatively assessed.

The extraglacial sources of the Tasman Glacier are dominantly rockfalls above the firn-line (Fig 3.4). Fluvial sediment is derived from valleys of the Malte Brun Range (Fig 3.5). Moraine walls exposed by Twentieth-Century glacier thinning (Skinner 1964; this study, Chapter 2) provide debris to the lower tongue, but this supply feeds a narrow marginal zone bordering the base of the moraine walls and apparently is not transported away from this apron.

Subglacially-eroded debris is unmeasurable on the glacier. The suspended sediment load of the Tasman River is very high, by analogy with the Hooker River (Griffiths 1981), and implies that much of the fine material produced by abrasion is flushed through the glacial drainage system. Much fine material is also englacial, indicating entrainment of basally-derived debris. The relative volumes of material washed rapidly through the system to those entrained by the glacier are unknown.

Debris inputs to the glacier surface above the equilibrium line have not increased significantly this century. Examination of early photographs of the glacier show that very few "new" outcrops have been exposed by glacier thinning in the accumulation zones of the Tasman Glacier. Most outcrops have increased in area as the glacier surface has dropped, but the total area of rock faces around the Tasman Glacier is so great that the increase in source areas over the last century is probably not significant. The reason is that in the accumulation zones outcrops exposed by glacier thinning are covered by snow and ice above the main bergschrunds, and are subaerially exposed for only a few weeks in late summer if at all.

In contrast, debris sources below the equilibrium line have increased in area significantly. Many are formed from unconsolidated drift deposited by glacial and slope processes, in addition to steep rock-faces above the glacier. The major change in debris input this century is the exposure of these unstable slopes to mass wasting. Divergent flow vectors in the ablation zone have tended to restrict debris from these sources to the narrow apron below the retreating moraine walls, except where tributary ice-streams carry the debris to a more central position on the glacier. This transposition is important on the Godley Glacier (Fig 3.24), but also occurs at the Tasman Glacier tributaries.

Mass-wasting of lateral moraines in the middle reaches of the Tasman Glacier has caused moraine walls to be eroded down to bedrock. This is especially noticeable near the Beetham Valley where till is plastered onto steep rock faces (Fig.3.2). Although the newly-exposed rock faces have also begun to collapse, the rate of debris supply to the glacier will be reduced as the supply from the eroding lateral moraine is exhausted. Downvalley, where the lateral moraines are separated from the valley sides, debris supply from retreating moraine walls is likely to continue while a reservoir of till remains. The greater size of lateral moraines downglacier means that debris will continue to be supplied to the margins of the lower glacier for decades after the supply at higher elevations is

Tasman Glacier April 1971

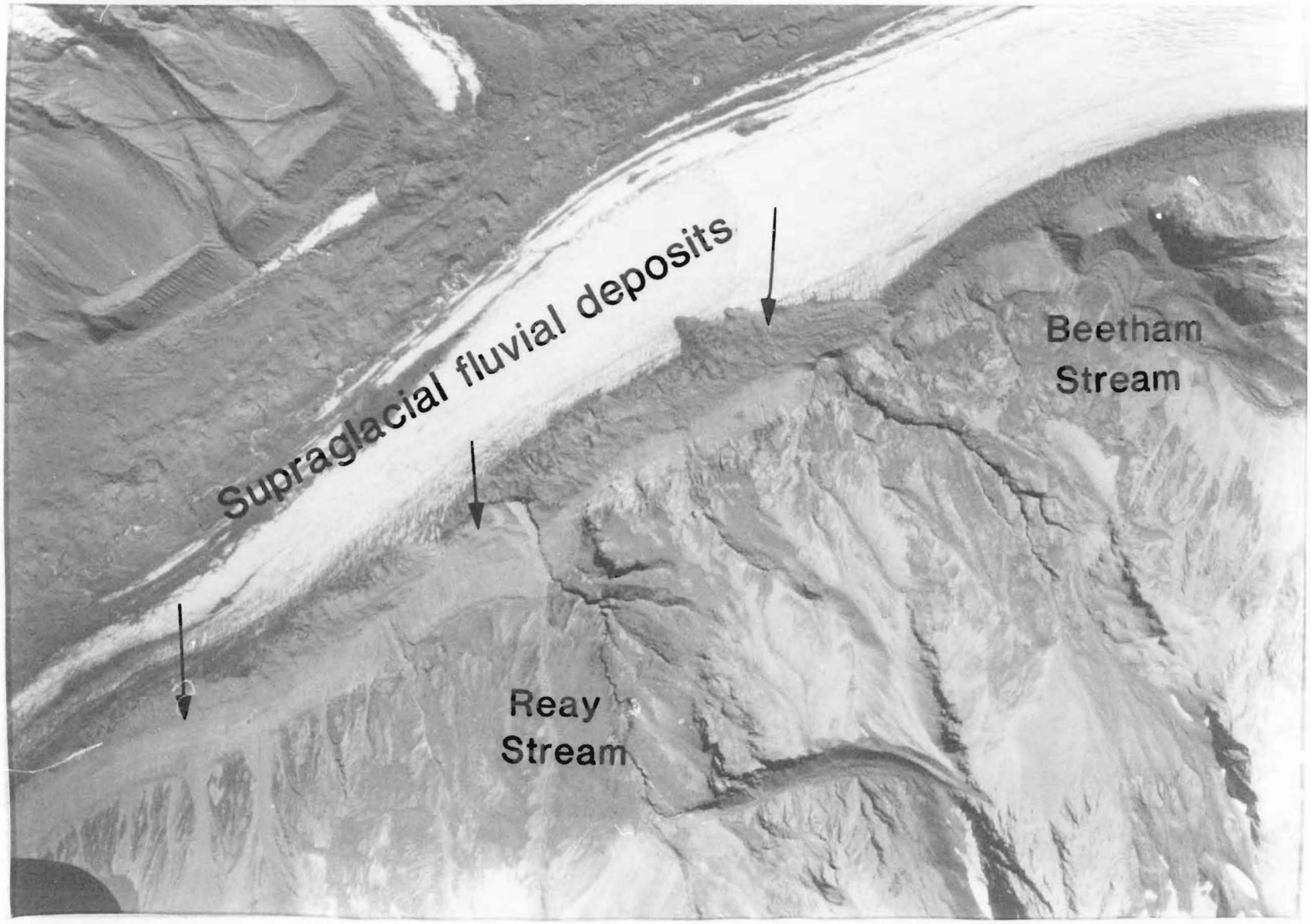

Figure 3.5

exhausted. The increase in the volume of the debris reservoir, together with slower ice flow towards the terminus, means the potential for the accumulation of a thick marginal supraglacial apron of debris is very great.

Sediment washed in by streams is a significant supply of debris along the eastern margin of the glacier (Fig 3.5). Rivers draining the largely ice-free valleys of the Malte Brun Range transport abundant coarse bedload into ice caves in the glacier margin. An unknown proportion of this debris outcrops in large supraglacial accumulations in a lateral position, as well as forming a medial moraine lower down the glacier (Section 3.4) Observations of Beetham Stream at all times of the year show that this coarse debris enters the glacier during summer floods. Winter and summer base flows appear to be insufficiently competent to transport the volumes and grades of material on the glacier.

3.1.4 Conclusions of Chapter 3.1.

1) Subglacial erosion rates of the Mt. Cook valley glaciers are inferred to be high, possibly up to 10 mma^{-1}.

2) Extraglacial debris sources are varied, but the products of physical weathering predominate. Rockfall above the equilibrium line is the dominant supplier of debris to high-level glacial transport, and has been relatively insensitve to changes in glacier size over the last century.

3) Contributions from below-equilibrium line sources have increased during 20th Century glacier thinning, but the flow structure of the Tasman Glacier does not favour entrainment from these sources. Debris supply from valley sides and moraine walls below the equilibrium line is sensitive to changes in glacier size.

4) An unknown, but probably significant, discharge of fluvial sediment enters englacial transport from ice-free valleys in the Malte Brun Range.

3.2 GLACIER TRANSPORT PATHS.

3.2.1 Background

The distribution of debris in glaciers reflects trajectories that particles follow through glaciers from the various sources. The geometry of transport paths within any glacier depends on three main factors:

1. The locations of points of entrainment. Debris eroded from the glacier bed generally remains in ice close to the sole in temperate glaciers (the basal transport zone of Boulton & Eyles, 1979). Debris supplied to the accumulation zone is buried by snow and enters englacial transport. Debris supplied to the glacier surface below the equilibrium line remains in supraglacial transport. Englacial and supraglacial debris together are contained in the high-level transport zone.

2. Glacier flow lines. A glacier of simple structure with no tributaries transports debris from its source along flow lines which generally converge and have downward vectors in the accumulation zone and which generally diverge and have upward vectors in the ablation zone. Debris in transport above the equilibrium line therefore tends to move towards the centre of a glacier cross-section, and below the equilibrium line tends to move outwards towards the glacier margins.

3. Glacier flow structure. A composite glacier such as the Tasman Glacier includes many ice streams, each with its own set of debris sources and transport paths. Ice flow is laminar, so the transport zones of each ice stream maintain their individuality after confluence with other ice streams, although lateral moraines-in-transport unite as medial moraines.

The general model of transport-path geometry proposed by Boulton & Eyles (1979) is shown in Figure 3.6. The model distinguishes between a basal traction zone and a high-level transport zone. The former is defined by the occurrence of interparticle and particle-bed contacts causing the abrasion and fracture of debris. Large amounts of very fine debris (<1 phi size range) is produced, and rounded and striated clasts characterise this zone (Boulton 1978). The high-level transport zone debris is modified little during transport. The distinction between the two zones is based on process-form relationships define characteristic sedimentological properties of the debris in each zone.

Studies of characteristics of debris from each transport zone (Boulton 1978; Boulton & Eyles 1979) have been made on glaciers where the distinction between zones was clear, in that all debris in high-level transport was from rockfalls onto the glacier surface, and was highly

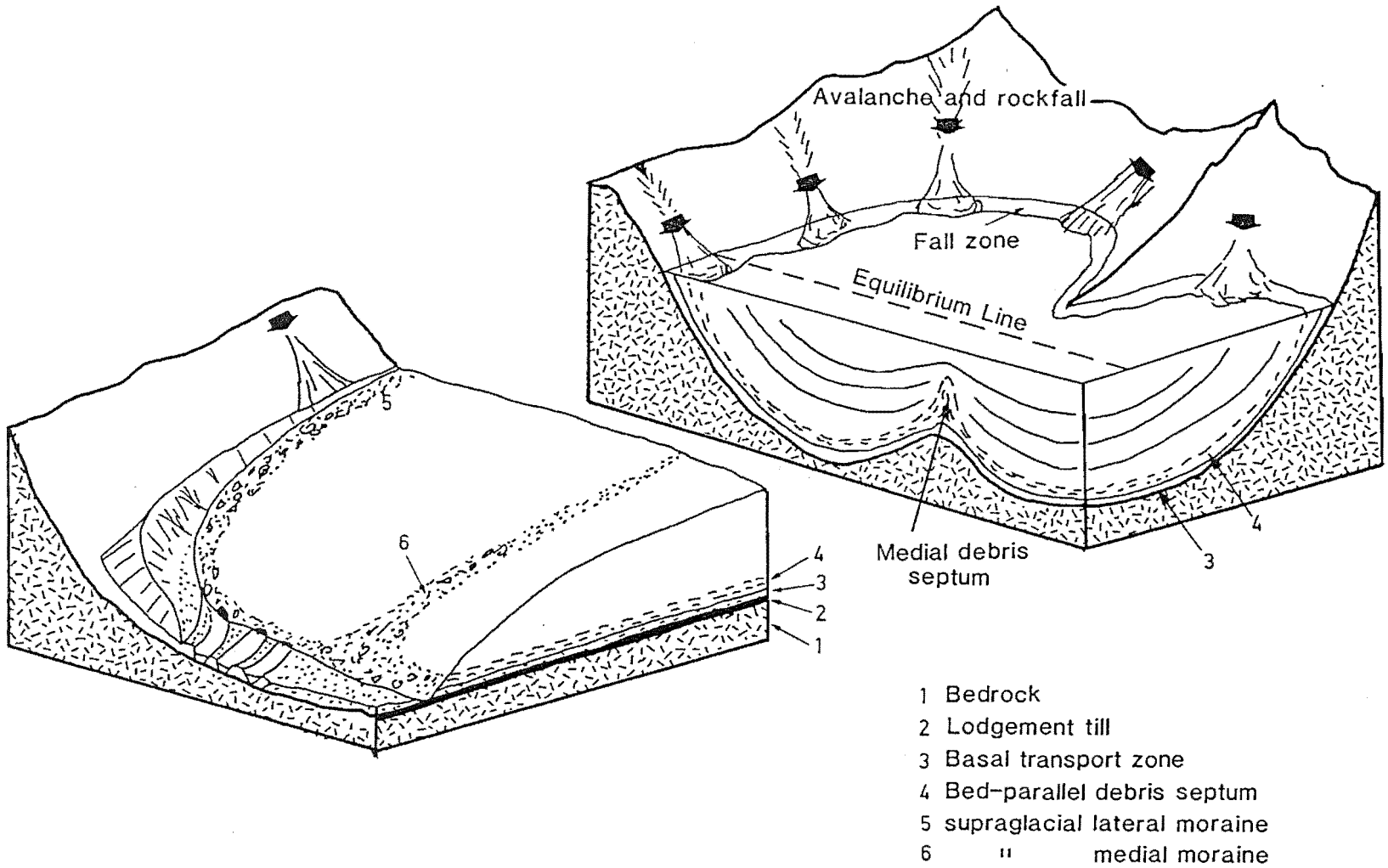

FIG. 3.6 Terminology of elements of the glacier transport system, their geometry and relationships to debris sources and depostional landforms (from Boulton & Eyles 1979).

angular. A significant input of debris to the Tasman Glacier is fluvially-transported (Section 3.1). In addition, the length and low gradient of the glacier and the abundance of water favour fluvial reworking of debris while in glacial transport. The sedimentological effects of these processes are examined in Section 3.4. They do not affect the distinction between basally-transported and high-level debris, but introduce variety into high-level zone debris.

The distribution of debris in a glacier is inhomogeneous: debris sources and flow structure tend to concentrate rock debris into planar geometries (debris septa) or into discrete bodies of various geometries (lenses, ellipses etc.). The overall concentration of debris in transport is the sum of the volumes of each transport zone. Quantification is difficult, so the following sections attempt to explain the dynamics of each zone to allow the total amount of debris in transport to be calculated.

3.2.2. The Basal Transport Zone

The distribution of debris within the lower few tens of metres of glaciers is traditionally divided into two facies, the dispersed and the stratified facies. The basis for this distinction are texture, debris concentration, and structure (Lawson 1979).

The dispersed facies contain relatively coarse, angular particles in ice in a zone typically up to 10 m thick. Debris concentrations are generally higher than in the superjacent englacial facies but less than in the subjacent stratified facies. No traction occurs in this zone: debris is concentrated by downward flow vectors from higher-level zones. Debris concentrations in this zone of Matanuska Glacier vary from 0.04% to 8.4% (Lawson 1979). Volumetrically, the dispersed facies debris contains much less debris than the stratified facies below.

The stratified facies may be regarded as the basal transport zone proper. It occupies the lower 3 to 15 m of Matanuska Glacier and comprises layered and irregular debris bands of greater and lesser lateral continuity. A sharp contact separates the stratified from dispersed facies. Intense folding and shearing characterise the zone of stratified facies, and abrasion, fracture and crushing cause increased rounding and comminution of debris particles. Debris may be derived from high-level transport by downward flow vectors, or from primary glacier-bed erosion and entrainment. The basal-traction zone (Boulton 1978) corresponds to the zone of intense shear and abrasion.

Thicknesses of, and debris concentrations in, the basal transport zones of glaciers are extremely variable and difficult to explain or predict (Drewry 1986 p.100). Given the lack of exposure of basal ice of the Tasman Glacier, this creates a major problem in estimating the glacier's basal debris load. However, this problem becomes much less serious if it is accepted that the basal ice of the Tasman Glacier is entirely at pressure-melt point (Chapter 2.1). Thick basal transport zones depend on cold and polythermal basal temperature regimes (Pessl & Frederick 1981) (Fig 3.7). This reflects the efficiency of subglacial entrainment processes the 0°C isotherm migrates at the glacier sole (Weertman 1961; Moran et al 1980). The destruction of particles in basal transport by abrasion and their removal by lodgement is also greatly reduced where basal melting is absent. The limited thickness of the basal transport zone in temperate glaciers is also reported by Boulton (1974, 1978, 1979), who suggests that the zone of abrasion and comminution near the temperate glacier sole rarely exceeds several decimetres.

Debris concentrations within this narrow zone are highly variable. Fig 3.7 shows a range from 5% to 55% with a mean of 28 %, from 12 sites. Lawson (1979) shows that the technique used to estimate debris concentration influences the value obtained. Local influences exert an important control, and great variability occurs within a small area of a single glacier. Based on published data from elsewhere, the overall basal debris concentration of the Tasman Glacier is probably about 30%.

The thickness of the basal transport zone is not visible on the main trunk of the Tasman Glacier, so an estimate has been made simply by taking the average of published figures listed for temperate glaciers (1.1 m, the mean of 18 values, Pessl & Frederick (1981).

An independent check of these estimates is provided by exposures of basal melt-out till in the Murchison Embayment on the eastern margin of the Tasman Glacier (Fig 3.8). The stratigraphy, structure and texture of these tills are described elsewhere (Chapter 5.3). They are interpreted as having been deposited in the last three decades from stationary ice, so that the thickness of the till unit may be compared directly with the estimate of basal debris load made above. The estimated basal debris content of the glacier is sufficient to deposit a till unit by the melting of stationary ice of an average thickness of 31 cm. Thicknesses range from 40cm to 150cm. The estimate is therefore of the correct order, given that the Murchison embayment till is in a favourable location for concentrating of debris at the glacier sole prior to melt-out (Chapter 5).

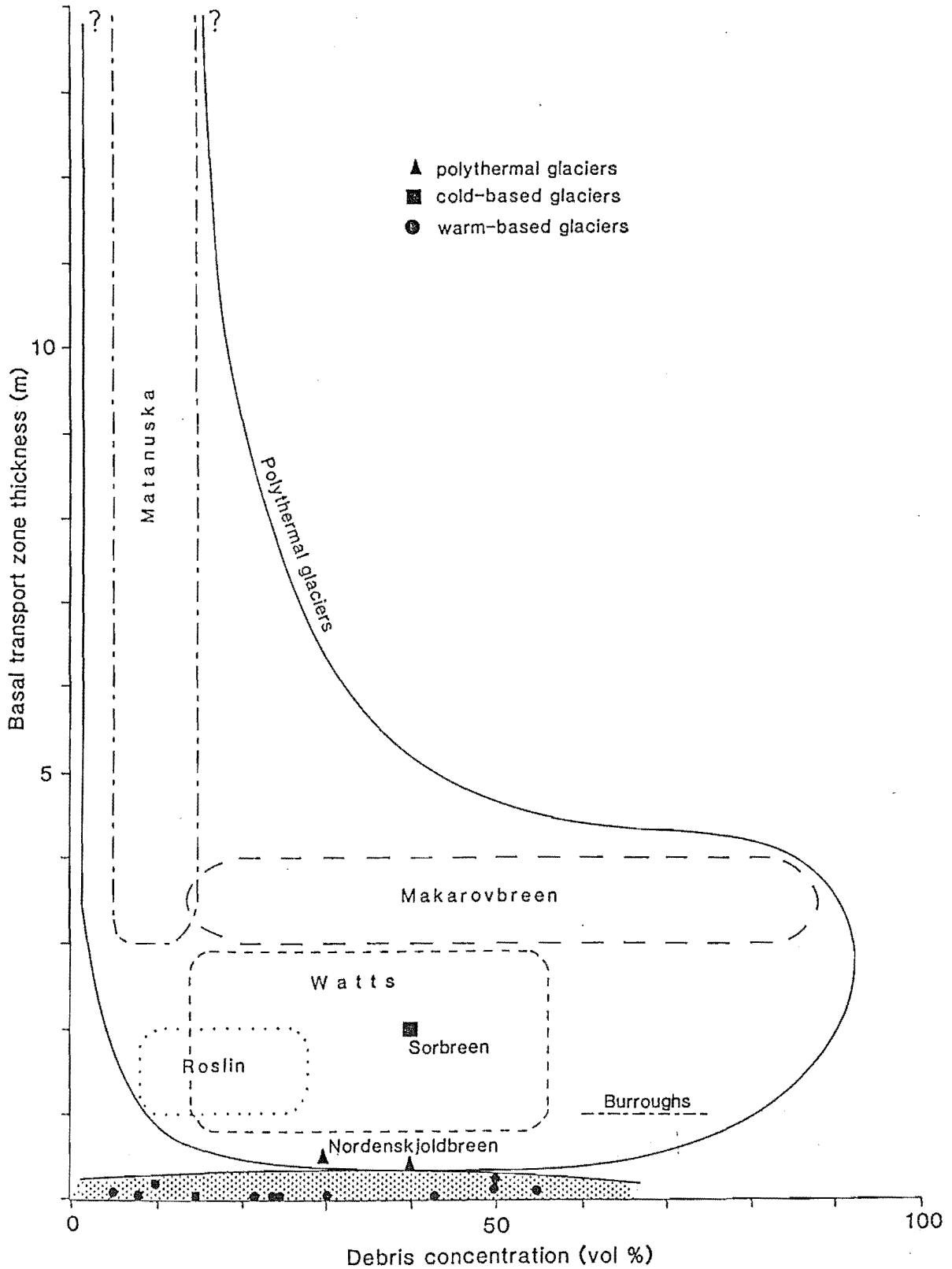

FIG. 3.7 Basal transport zone thicknesses and debris concentrations for cold-based, polythermal, and warm-based glaciers. Data from Pessl & Frederick (1981).

FIG. 3.8 Exposure of basal melt-out till in the Murchison Embayment of the Tasman Glacier. The till was probably deposited during ice retreat in the last 30 years. Pack is about 50 cm high.

Several tributary glaciers have ice-cliffs which reveal complete cross-sections where the thickness, orientation and elevation of debris septa within the glacier are visible. These provide general information about the disposition of debris in transport, but they cannot be regarded as representative of the trunk stream where conditions at the glacier bed are very different.

Un-named glacier at S79/874 526 (Fig 3.9). The snout of this glacier was visited in February 1987. The advancing, bulging ice cliff at the terminus was over-riding a small bedrock outcrop which "moulded" the glacier sole sliding over it. Up to 5 cm thickness of "true" basal debris occured in discontinuous lenses and clusters of fine silt to pebble sizes in regelation ice at the glacier sole. Pebbles were angular to sub-rounded in shape, suggesting that abraded clasts were mixed with newly-entrained plucked clasts. A small number of larger clasts appeared to be lodged between the ice and substrate. Above the thin basal zone, several dirt bands outcropped over a vertical height of up to 20 m in a broadly synclinal structure paralleling the "wetted perimeter" of the glacier. Although very dirty with washed material on the surface, these bands contained very dispersed angular clasts and greater concentrations of sandy material characteristic of the high-level transport zone. Tight to isoclinal folding of the dirt bands and ice foliation were most probably related to deformation during passage through the ice-falls above. Melt-out of debris from the steep snout fed rockfalls onto the completely debris-covered snow and ice avalanche-fed reconstituted glacier. The small amount of traction-modified debris to unmodified high-level zone debris was striking.

Shelf Glacier, Mount Sefton S79/710360 (Fig 3.10). The huge ice-cliffs of this glacier provide a cross-section above the equilibrium line. Debris is heavily concentrated in a basal zone several metres thick, but the site was inaccessible. Most of the debris is probably contained in discontinuous bed-parallel debris septa fed by rockfalls from the 300 m high summit rock faces of Mount Sefton. It is not possible for basally-derived debris to reach the observed levels within the glacier over the short distance available and in an accumulation zone. Similar debris septa in glaciers which are not truncated as spectacularly as this would find their way along convergent flow lines to the basal-traction zone, provided the debris source was well above the equilibrium line.

FIG. 3.9 Avalanche-reconstitution of the Kaufman Glacier flowing from Mt. Haidinger. Note the blanket of debris on the reconstituted avalanche cone, and the abundant supply of ice-avalanche material. The terminus of the (un-named) glacier to the north (right) is described in Section 3.2.2

FIG. 3.10 Telephotograph of the Shelf Glacier, Mt. Sefton. Avalanches from the ice cliff supply ice and debris to the Mueller Glacier. Discontinuous bed-parallel debris septa are visible. Lying above ELA, the densification of firn to ice is visible as a colour change from white to blue with depth.

Stocking (Tewaewae) Glacier S79/747373. The terminal ice-cliff was observed from Sefton Bivouac in October 1987. Again, relatively debris-free blue ice overlay bed-parallel and basal debris septa occupying the lowermost 2 to 3 metres of the glacier. Lack of safe access prevented any assessment of the sedimentology. Again, it is unlikely that basally-derived debris could form the bed-parallel septa.

Similar observations have been made on other glaciers in the Hooker and Tasman Valleys. Without exception, debris is concentrated in basal zones extending from a few centimetres to three metres in thickness. Closer inspection (where possible) reveals that the debris is much less concentrated than the superficial dirtiness of the ice surface would suggest, even on very steep faces. A general conclusion is that most of the apparently "basal" debris is high-level transport zone material forming bed-parallel debris septa. The sample of observed glaciers is rather in terms of size and morphology, and these observations may not apply to the trunk ice streams of the Tasman Glacier.

Nevertheless, the evidence presented in this section suggest that the Tasman Glacier is likely to have a relatively thin basal transport zone of perhaps 0.5 to 1.5 metres, with a debris concentration of about 30%. The supply of debris to the basal transport zone is probably great, to compensate for its removal by abrasion, lodgement, and meltwater at the glacier sole.

3.2.3. The High-Level Transport Zone.

The high-level transport zone (HLTZ) contains all rock debris in transport that has not been modified by traction at or near the glacier sole. The zone includes debris from a wide variety of sources and in transport in accumulations of various geometries within and upon the glacier. To quantify debris discharges, the sources, geometries and volumes of individual debris bodies must be understood in relation to the overall debris distribution in the glacier.

3.2.3.1 Terminology.

High-level transport paths have been defined by Boulton & Eyles (1979), whose terminology is adopted in this study. The genesis of englacial debris geometries derived from supraglacial sources is shown in Figure 3.6. The terms medial debris septum and bed-parallel debris septum refer to planar bodies of dispersed englacial debris whose geometry is described in relation to the sides and base of the glacier. This simple

classification assumes that frequent small debris inputs feed the septa, which are consequently continuous features on the scale of the whole glacier even though they may be discontinuous on scales of less than 100 m. (Gomez & Small 1986). The emergence of a medial debris septum in the ablation zone feeds a medial moraine on the glacier surface (Fig 3.6): similarly, emergence of bed-parallel septa near the glacier margins feeds lateral moraines-in-transport (Small 1983).

3.2.3.2 The high-level transport zone: a review.

Most work on HLTZ debris has been concerned with medial moraine genesis. Traditionally regarded as accumulations of debris along a medial axis formed by the juxtaposition of lateral moraines-in-transport at an ice-stream confluence (eg. Agassiz 1840; Sharp 1960), recent work has shown that medial moraines may form from combinations of several processes.

Two classifications of medial moraines exist. The earlier was proposed by Eyles & Rogerson (1978b). The basis for their classification is the relationship between the point of emergence of the moraine and the firn-line position. This allows two main and one minor type of moraine to be identified:

1. "Ablation-dominant type" is formed by debris collecting on the glacier surface in the accumulation zone and being ingested by burial under subsequent winters' snow. The debris passes through englacial transport, and lateral compression creates a medial debris septum. The emergence of the septum in the ablation zone gives rise to the medial moraine.

2. "Ice-stream interaction type" forms where the confluence of ice streams below the firn line generates a medial moraine from the joining of two supraglacial lateral moraines.

3. "Avalanche type" moraines are regarded as minor. They form by infrequent rockfalls leaving discrete deposits on the glacier surface.

This classification is useful when aerial photograph data are available, but provides little insight into understanding moraine dynamics. The distinction between the two main types is not based on any difference in process, and the ablation-dominant type is usually only an ice-stream interaction type whose source lies above the equilibrium line. It has also been shown that some glaciers have medial moraines dominated by the avalanche type (Rogerson et al 1986), which in turn are often a form of ablation-dominant moraines.

A second classification has been proposed by Small et al. (1979) using equilibrium-line position and the presence or absence of crevasse-ingestion of debris. This allows a fourfold division of medial moraines fed by continuous small rockfalls. The classification is used to explain the effect of debris supply and differential ablation on moraine morphology following the work of Small & Clark (1974). Their study also attempts to relate inhomogeneous englacial debris concentrations to "beaded" moraines instead of the simple continuous moraine. "Waxing" and "waning" stages of the moraine are identified by the effect of the exhaustion of the englacial feeder on morphology, allowing moraine height to decrease downglacier, as suggested by Loomis (1970). An "equiliibrium" moraine relief is also described by Loomis, in which moraine relief remains constant downglacier. The relative importance of ablation and compression in determining moraine morphology has been debated (Eyles 1976: Small & Clark 1976) and this debate highlights the inadequacies of each model in accounting for the range of processes which affect medial-moraine genesis and morphology. An appeal for more account to be made of debris sources (Gomez & Small 1986) suggests that an extended classification of medial moraines is required.

This is especially so where basally-derived sediments are incorporated into surface medial moraines. Eyles & Rogerson (1977) depart from a purely morphological approach to explain this observation as resulting from upward "shearing" of debris where a tributary ice-stream over-rides the main glacier, thus elevating debris from the basal traction zone along the suture between the two ice-streams. A similar structural interpretation is made by Gomez & Small (1986) (Fig 3.11), though they suggest that the debris is elevated passively within ice of the over-riding tributary. The dominant structural influence on moraine morphology at the confluence is replaced by ablation effects as the flow rates of the tributary and the main ice stream become equal downglacier.

The sedimentology of medial moraines reflects relative inputs of traction zone and high-level transport zone debris. The distinction between the two transport zones based on the character of the debris is blurred by the inclusion into high-level transport of debris with inherited characteristics of basal transport. Most commonly, coarse angular debris reflecting "periglacial" weathering processes is found (Eyles & Rogerson 1978a; this study, Chapter 3.4). The grain sizes of moraine debris reflect the joint spacing of source outcrops feeding the moraine, and little subsequent comminution by frost action occurs (Boulton

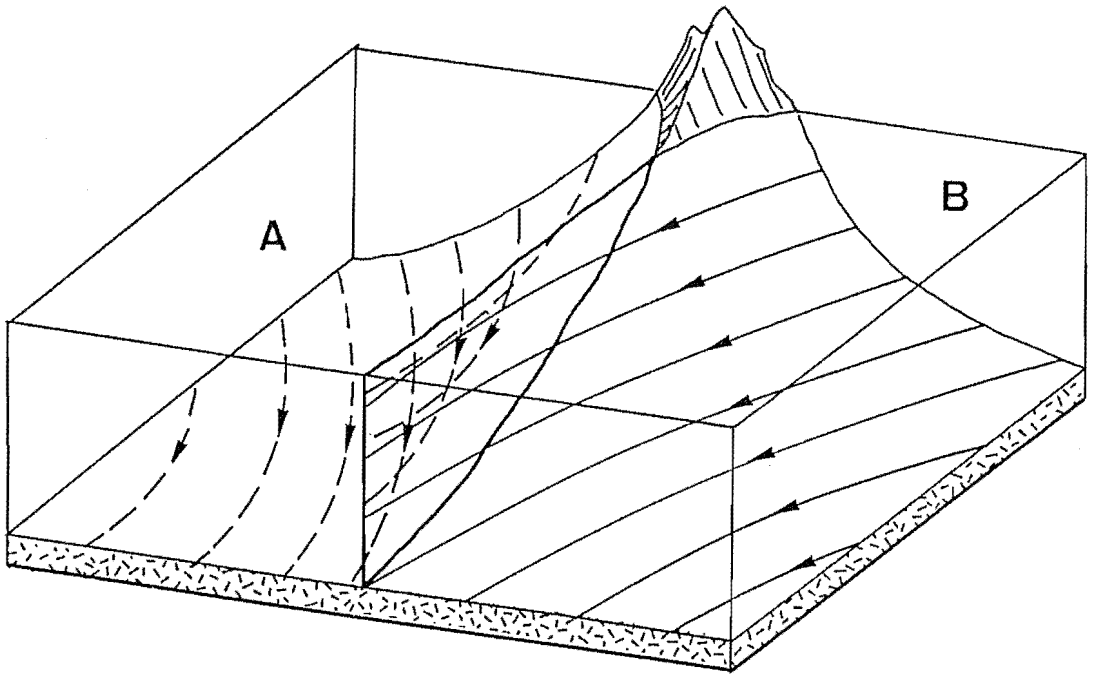

FIG. 3.11 Elevation of basal ice to the glacier surface along flowlines at an ice-stream confluence in an ablation zone (based on observations of the Haut Glacier d'Arolla, Switzerland, by Gomez & Small 1986). This flowline geometry explains the emergence of abraded debris along the junction of the Hochstetter (A) and Haast (B) ice streams of the Tasman Glacier, where (A) is apparently also over-riding (B) (Fig 3.14).

1978). The proportion of debris showing characteristics of traction is therefore an essential observation in interpreting the genesis of a medial moraine.

Lateral moraines-in-transport are similar in origin to some medial moraines in that they are the supraglacial expression in the ablation zone of englacial debris bodies, or represent direct inputs to the glacier ablation zone surface. In the field area, they contain debris of more diverse origins than described by Small (1983), because the products of many extraglacial processes can be entrained by the glacier in these zones. These are described more fully in the following classification.

The range of debris-body geometries and sources found in large valley glaciers in the field area is not adequately represented in previous classifications of glacial debris. These classifications emphasise the position of the moraine debris source relative to the equilibrium line. While this is an obvious feature on aerial photographs, it does not affect the genesis of the moraine and appears to be peripheral to the main issue. The sources of the moraine's debris should also be considered: that is, the absolute and relative contributions of rockfalls and avalanche events of all magnitudes and frequencies, and of debris eroded from the glacier bed.

The aims of this study suggest that a classification of high-level transport zone debris should place the greatest emphasis on:

1. the magnitudes and frequencies of debris inputs to the glacier, and
2. the distinction between extraglacial and subglacial sources.

Other features of the moraine, such as morphology, are treated as a means to the end of interpreting the moraine genesis in terms of the above criteria. Subsequently, moraine morphology is investigated as an indicator of mass balance change. The classification which follows attempts to include these findings within the limitation imposed by a lack of detailed field checking of many sites.

3.2.3.3 An expanded classification of high-level transport zone debris.

The morphology of a supraglacial debris body is a product of the volume of debris, its mode of transport to the glacier, the flow structure of the glacier below the debris source, and the effects of the debris body on ablation of ice beneath it. Any classification therefore needs to reflect the relative importance of these effects given the reasons for attempting the classification in the first place. For a study of glacier

sediment transport, the discharge of debris through the glacier transport zones is considered to be of prime importance. Accordingly, this classification is based around the frequency of inputs of different volumes of debris.

The postulate is made that the two-dimensional geometry of a supraglacial deposit reflects its former three-dimensional form during previous stages of englacial transport. Two other considerations that the classification recognises are that:

1). Rock debris is transported passively within glacier ice but may undergo downslope mass movement on the glacier surface.

2). Glacier flows allow spatial variation in moraine geometry to be substituted for temporal variation as a deposit moves along a glacier flow line.

Each type of debris accumulation on the glacier surface is classified by an upper case letter on the basis of magnitude. The observed continuum of magnitudes is simplified into three scales as defined in Table 3.3. These groups are:

1) C type and AC type moraines, fed by continuous small rockfalls and rock/snow/ice avalanches.

2) E type and AE type moraines, fed by episodic small to large rockfalls and rock/snow/ice avalanches.

3) R type moraines, fed by single catastrophic rockfall or rock avalanche events.

Each category is inferred from its degree of continuity along a glacier flow line, which introduces a dependence on local variations in flow rate on and between glaciers. Because glacier flow rates vary through an order of magnitude, whereas debris volumes vary through at least six orders, such variation is of limited significance.

The second letter is a subscript and indicates whether the debris source lies above or below the equilibrium line, and is regarded as of secondary importance. The subscript "$_A$" denotes a source above the equilibrium line, the subscript "$_B$" one below. Moraines including debris from both above or below the equilibrium line, or of indeterminate source location, have a subscript $_{AB}$.

A number is used for moraines where identification of the relative proportions of basal-traction zone and high-level transport zone debris is possible;

Debris source	Symbol	Diagnosis
Continuous supply	C	Moraine has unbroken outcrop along flow line.
Episodic supply	E	Moraine is more or less beaded due to separate events from same source.
Catastrophic event	R	Deposit is single discrete unit unrelated to other deposits.
Ice/snow avalanches	A	Symbol used in combination with C or E types, eg. AC and AE.

TABLE 3.3 Classification of moraines according to episodicity of debris supply.

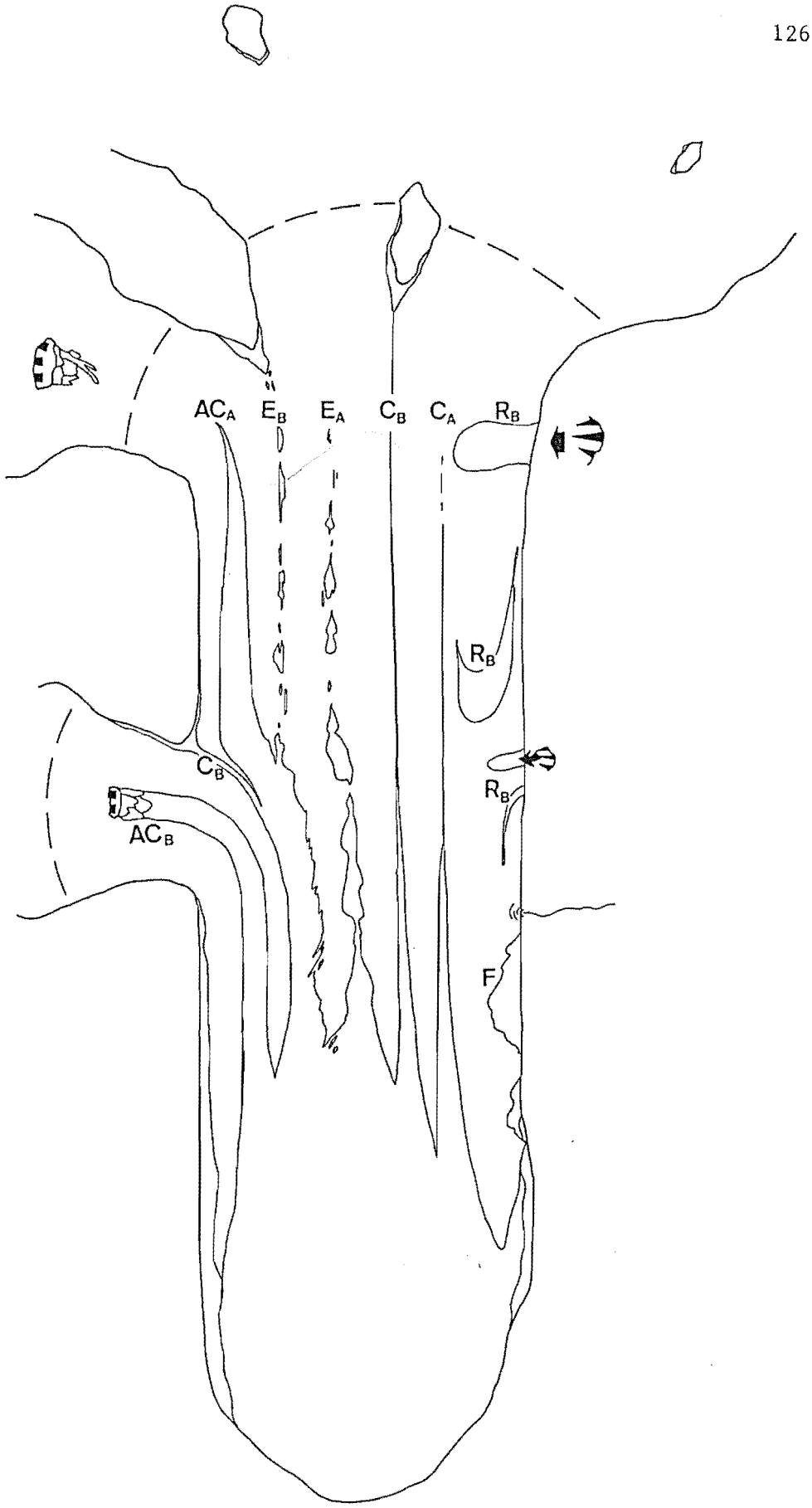

FIG. 3.12 Schematic vertical view of the moraine types classified in Table 3.4.

Geometry	Debris Source	Identification
C		High-frequency low-magnitude debris inputs which give rise to a continuous moraine in which individual inputs cannot be distinguished.
C_A	basal/supraglacial	Ingestion above the equilibrium line forms a continuous debris septum which may or may not have bed contact. Outcrop below equilibrium line feeds a medial whose subsequent morphology depends on ablation and flow structure. No surface contact with debris source.
C_B	basal/supraglacial	Continuous moraine fed by direct supraglacial input and/or emergent traction zone debris. Moraine has surface contact with supraglacial source. May or may not be fed by debris septum.(Field checking necessary).
E		Lower frequency and higher magnitude of debris inputs allows ice flow to separate individual events to form a beaded moraine whose geometry reflects the magnitude-frequency distribution of the inputs.
E_A	supraglacial	Ingestion above the equilibrium line forms discontinuous debris septum which may or may not have bed contact. Outcrop forms a beaded moraine. Strongly compressive ice flow forms a set of arcuate up-glacier dipping lenses and the moraine has a "nested spoons" form.
E_B	supraglacial	Debris is entirely supraglacial and has surface contact with source. Otherwise as for Ea.
R		Low-frequency high-magnitude input forms a debris body which is not confined to a single flow line and often overlaps other medial moraines. Does not form a related series of deposits in transport, i.e. the frequency is less than the maximum age of ice in the glacier. The source location is often unidentifiable.
R_A	supraglacial	Ingestion above equilibrium line forms deforming debris body whose geometry reflects total strain since ingestion.
R_B	supraglacial	Debris source lies below equilibrium line but no contact between deposit and source occurs, therefore often indistinguishable from Ra. Shape partly reflects run-out distance of the rock avalanche.
A	ice avalanche	Englacially- and basally-transported debris is reworked by ice cliff collapse and reconstitution.
A_A	basal + englacial	Ingestion below fall zone followed by emergence forms a moraine whose character is classified by C or E above. AC forms are most common.
A_B	basal + englacial	As above, except moraine is supraglacial immediately below ice cliff source. Forms as a lag deposit after the melting of ice avalanche talus.
F	englacial/supraglacial	Fluvially-transported debris which has entered the glacier via side streams and is transported englacially to emerge as irregular deposits of rounded, sorted debris. Only occurs below equilibrium line on glaciers bordered by ice-free side valleys.

TABLE 3.4 Classification of supraglacial debris bodies in transport. (To be used in conjunction with Figure 3.12).

1 = supraglacial debris source

2 = basal debris source

3 = combined supraglacial and basal debris sources

no number = indeterminate source(s).

The debris source is often difficult to identify on aerial photography, so field checking is always necessary before the numerical character can be assigned.

The full classification is presented in Table 3.4 and Figure 3.12.

3.2.3.4 Transport paths of the Tasman Glacier.

Three zones are recognised in the transport paths of the Tasman Glacier. Each includes various types of debris which may be subdivided in terms of variations in geometry or sedimentology (Table 3.5).

The composite structure of the glacier creates a complex system of englacial and supraglacial transport paths. The cover of supraglacial debris varies between ice streams depending on the proportion of steep rock walls and ice cliffs to ice-covered area in each tributary source (Fig 3.4). Thus, the Rudolf Glacier is completely covered by debris a short distance below the firn line, and the Hochstetter ice stream becomes debris-mantled 2 km below the base of the ice-fall as englacial debris melts out at the glacier surface. In contrast, the ice streams draining the relatively gentle and contiguous firn basins around Tasman Saddle remain largely free of supraglacial debris. These ice streams only become debris-covered when compression upstream of the tributary Hochstetter ice stream aids the emergence of englacial debris septa.

The location of debris inputs relative to the firn line is important (Glazyrin 1975; Boulton 1978). The Rudolf Glacier has abundant rockfall sources above and below the firn line, in contrast to the Tasman Saddle ice stream whose sources lie predominantly above the firn line. Two structural factors aiding debris emergence are intense longitudinal compression below ice-falls (Chapter 4.1) and ice-cliff avalanching and reconstitution (Fig 3.9), both of which are more influential in the Hochstetter and Rudolf tributaries than in the Tasman Saddle area.

Few exposures of the basal transport zone (including traction zone debris) are visible. No debris from this source seems to be elevated to the surface below ice-falls except at ice stream confluences (cf. Posamentier 1978). The mechanism proposed by Gomez & Small (1986) (Fig 3.11) explains the emergence of traction-zone debris as a narrow band outcropping along the junction between the Hochstetter and Haast ice

TABLE 3.5 Characteristics of glacier transport zones, as observed on the Tasman Glacier.

Transport zone	Debris character	Disposition of debris
Supraglacial	Frost-shattered, weathered, winnowed particles, large range of clast sizes.	Longitudinal and transverse surficial deposits, continuous mantle, generally thin
Englacial	Angular, unmodified clasts derived from supraglacial zone; rounded, streamlined and comminuted debris from basal zone (less common)	Upglacier-dipping transverse lenses, steeply dipping longitudinal septa; bed-parallel septa low concentration dispersed particles.
Basal	Rounded, streamlined and comminuted clasts; fines	Suspended dispersed particles (zone not observed at the glacier bed).

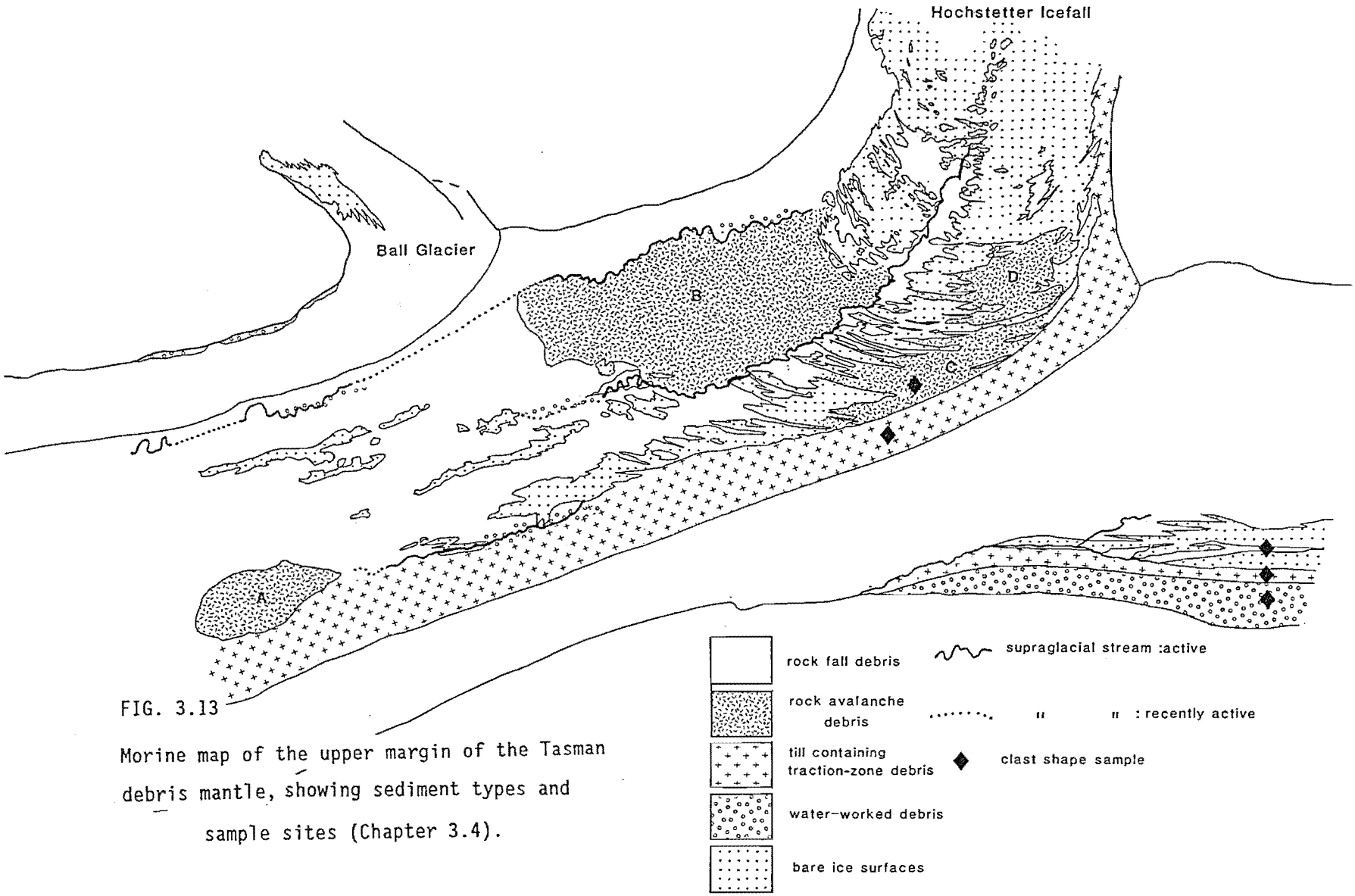

FIG. 3.13

Morine map of the upper margin of the Tasman debris mantle, showing sediment types and sample sites (Chapter 3.4).

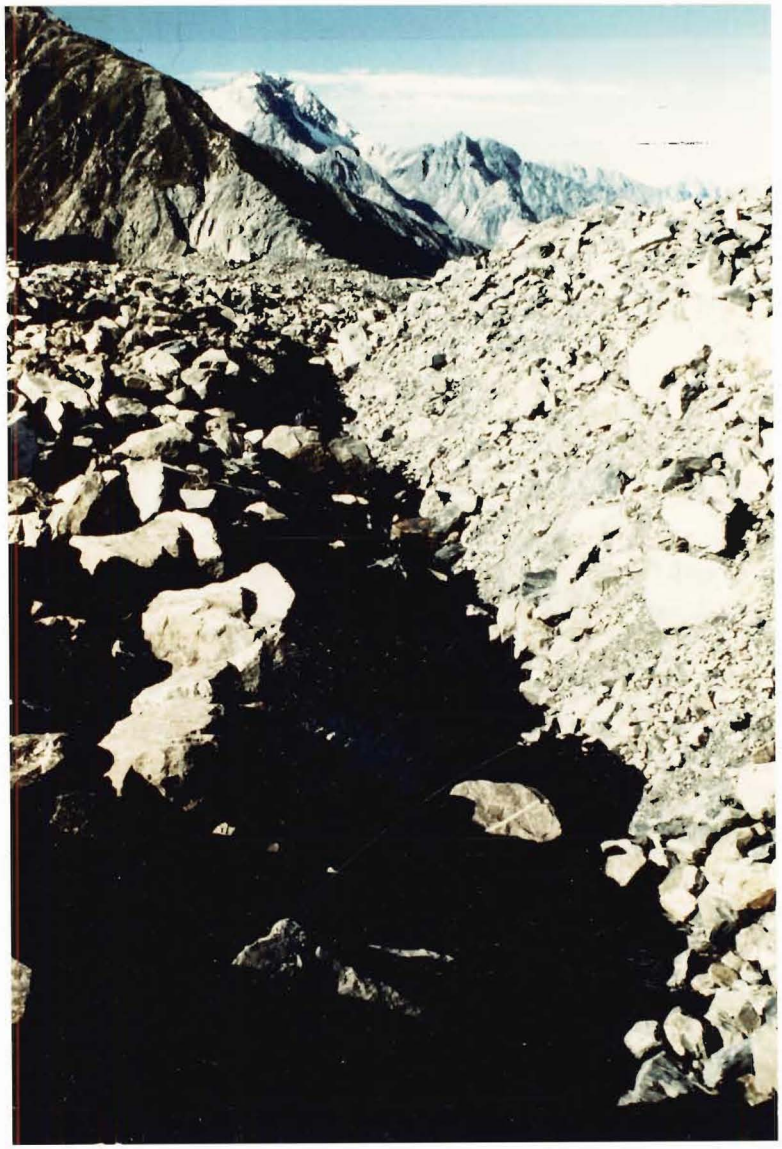

FIG. 3.14 Furrow marking the junction of the Hochstetter (to the right) and Haast (to the left) ice streams. The former flows faster than the latter at this point, and is apparently over-riding it. The furrow marks a shear zone between the two ice streams. Note the higher degree of weathering of supraglacial debris on the left than on the right.

streams (Fig 3.13). This debris is identified by the high proportion of sand and mud forming a matrix around rounded, striated clasts of a fresh, unweathered appearance. This contrasts with the characteristics of the surrounding debris mantle. Even though traction zone debris is limited in exposure, the observed outcrops are nevertheless sufficient evidence to indicate that longitudinal debris septa composed of dominantly abraded debris occur below all major ice stream confluences, especially where active tributaries are apparently overriding the trunk ice stream (Fig 3.14). In the terminal ice cliff of the Grey-Maud Glacier, in the Godley Valley, a distinct medial debris septum is exposed (Fig 4.16).

3.2.4 Medial-moraine evolution related to ice flow and ablation conditions.

During the period of European settlement in the Mount Cook area, the larger glaciers have become progressively more covered by supraglacial debris. The change from a largely debris-free to debris-covered glacier surface represents an important change in the routing of debris through the glacier. The feedbacks involved in this evolution are significant in terms of the dynamics of the lower glacier (Chapter 4). To understand the significance of the changes, it is necessary to understand the dynamics of the medial moraines which feed the debris blankets. This section is in four parts: (1) A discussion of medial moraines with no englacial debris feeder; (2) a review of existing steady-state models of medial moraine dynamics; (3) modification of these models to non-steady-state conditions; (4) comparison of the changes expected from the theoretical models with those observed in medial moraines in the field area.

3.2.4.1 Medial moraine evolution with no englacial feeder.

Where there is no supply of debris from within the glacier, all debris is supplied from above the glacier surface at a point source. The moraine discussed here is a type C_B with no englacial feeder (Table 3.4). The simplicity of this case allows both steady-state and non-steady state cases to be treated together.

If rockfalls at the moraine source were sufficiently small and infrequent to generate a debris cover thick enough to retard ice melt, the moraine would not develop relief. The debris would form a moraine lying flush with the surrounding ice surface, and the plan form would be straight and parallel-sided, unless there were strongly compressive flow (Fig 3.15).

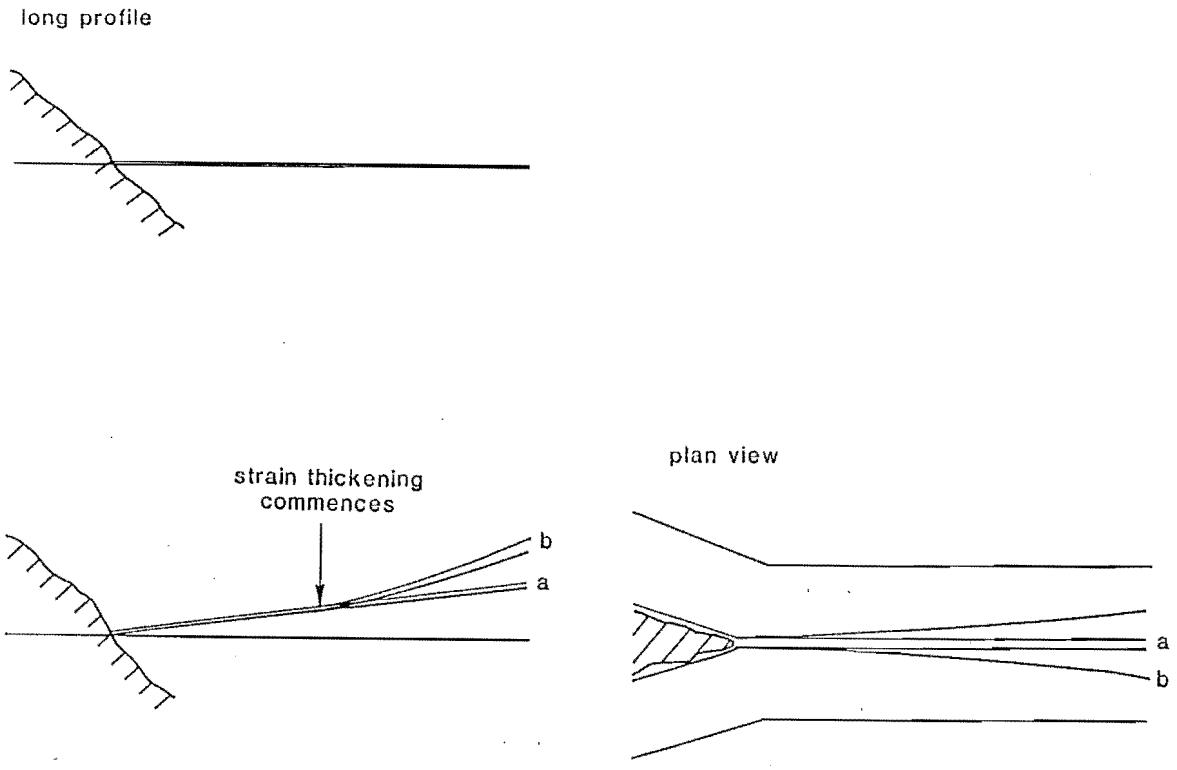

FIG. 3.15 (A) Medial moraine with no englacial feeder, where debris is insufficiently thick to retard ablation.

(B) Medial moraine with no englacial feeder, where debris is sufficiently thick to retard ablation. Profile (a) results where flow is uniform and differential ablation between the moraine crest and the surrounding glacier remains constant as the moraine is transported away from the debris source. Profile (b) results where compressive flow causes strain thickening in the debris cover and an increase in differential ablation.

(C) Plan views of medial moraines with no englacial feeder or lateral sliding of debris. (a) uniform flow (b) compressive flow.

If the debris cover were thick enough to retard ice melt, the other cases shown in Fig 3.15 would apply. Since no debris is added to the moraine from below, the debris thickness is simply a function of the rate of rockfall input relative to the ice velocity. Under uniform flow, the debris will have constant thickness downglacier. The moraine relief will therefore increase downglacier at a constant rate which is proportional to the differential ablation rate. These are the only conditions under which such a moraine will form, because all other conditions lead to thickening debris downglacier. This moraine corresponds to Type A of Small et al (1979), and can hardly be regarded as a "typical" case. This moraine type is steady-state because an equilibrium between ice flow, debris thickness and moraine relief is attained so that moraine relief, though increasing downglacier, remains constant at all points on the moraine (relative to fixed co-ordinates) over time.

With conditions of compressive flow, differential ablation, and no strain-thickening of debris, the moraine waxes downglacier at an increasing rate (Fig 3.15). This is because differential ablation is constant over time, so that moraine relief increases uniformly over time. Compressive flow causes unit increases in moraine relief to occur at decreasing distances downglacier, therefore the moraine has a concave long-profile.

In nature it is more likely that compressive flow will cause strain-thickening of the debris cover. Dispersed debris will not thicken sufficiently to retard ablation. However, the plan form of the moraine will be affected as shown in Fig. 3.15. A more continuous debris cover is likely to thicken under longitudinal compression. This may cause or enhance differential ablation, leading to an increase in moraine relief determined by the degree of ice compression and debris thickening. A non-steady state may develop as discussed below.

3.2.4.2 Englacially-fed medial moraine evolution in a steady state (Fig 3.16).

Medial moraine morphology is a function of the effects of differential ablation and of the longitudinal compression or extension of the glacier (Loomis 1970; Small & Clark 1974, 1976; Eyles & Rogerson 1977). Previous studies have been based entirely on short-term measurements and the moraine dynamics have been treated as a steady state, in which the size and morphology of the moraine is regarded as being in equilibrium with the prevailing ice flow and ablation at the time of the study. Thus, an

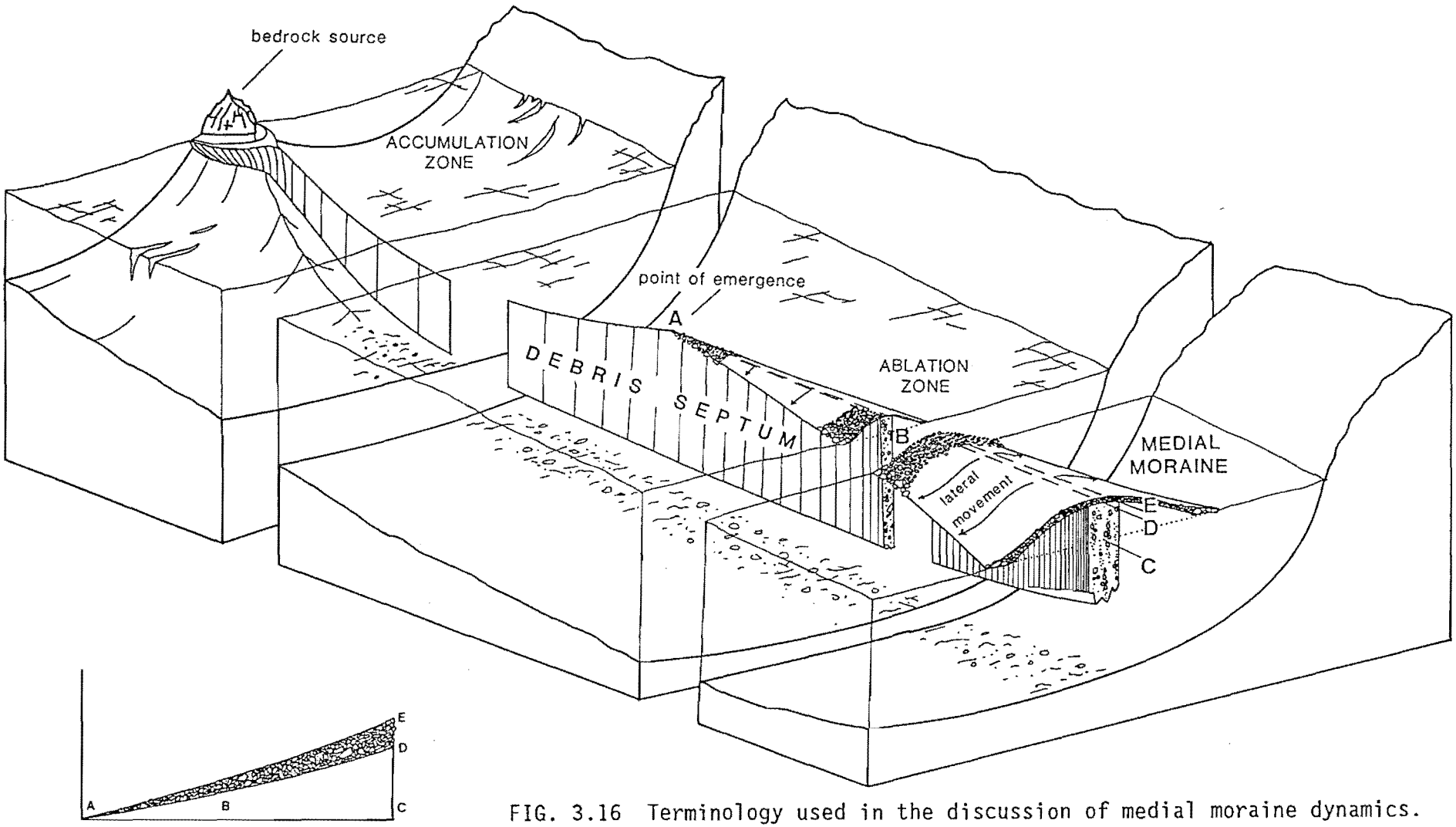

FIG. 3.16 Terminology used in the discussion of medial moraine dynamics. B = ice core; AE = moraine crest; AD = ice-debris interface; AC = level of surrounding ice surface; ADE = debris thickness profile; ACE = moraine profile. Arrows indicate lateral movement of debris away from the crest.

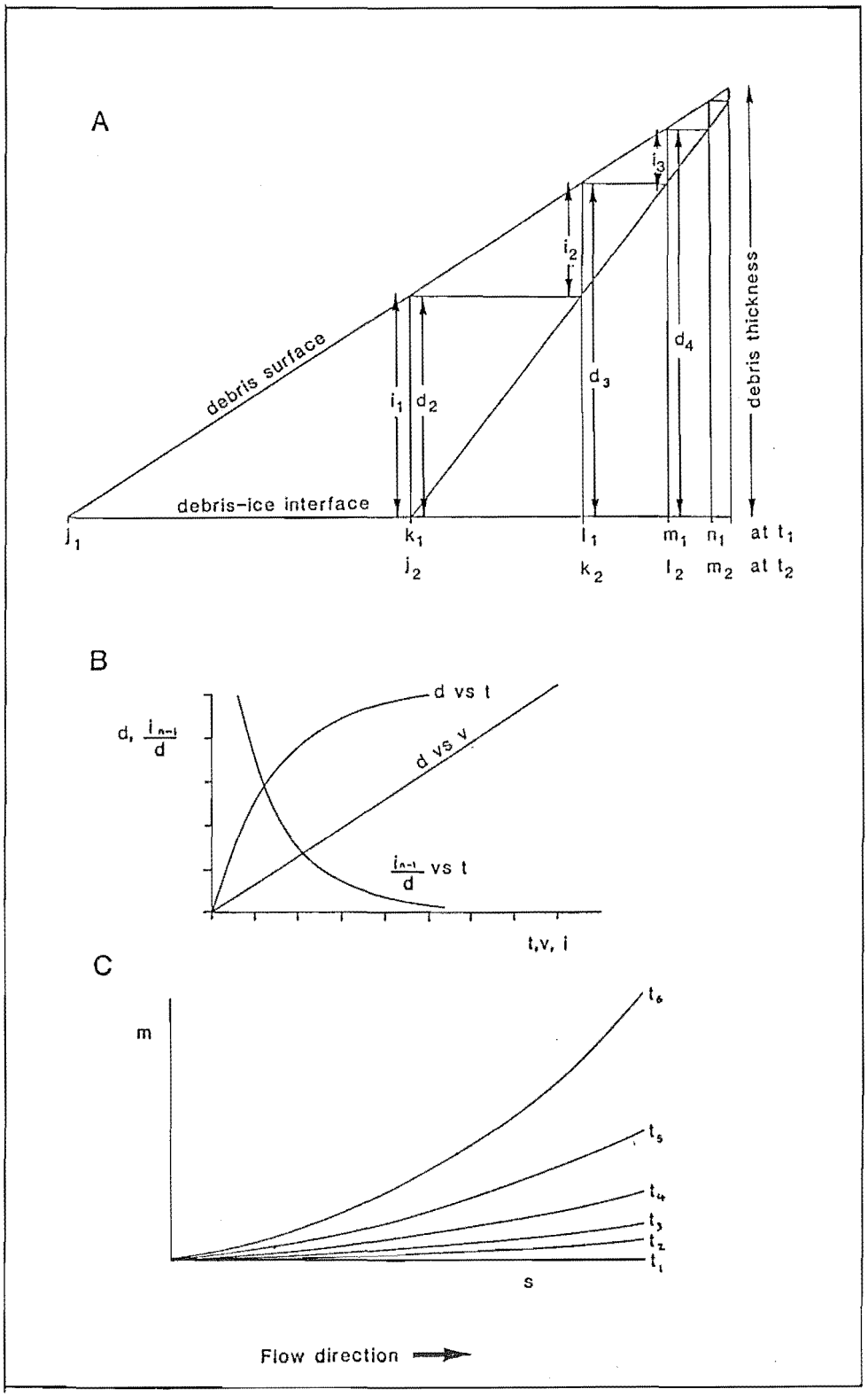

FIG. 3.17

(A) Hypothetical debris-thickness profile, relative to co-ordinates fixed in space. $i_{1...n}$ refers to increases in debris thickness and $d_{1...n}$ to debris thickness at different times and locations. See text for explanation and implications.

(B) Relationships governing the debris-thickness profile shown in (A).

(C) Moraine profiles resulting from the debris-thickness profile shown in (A). No lateral sliding of debris from moraine crests is assumed.

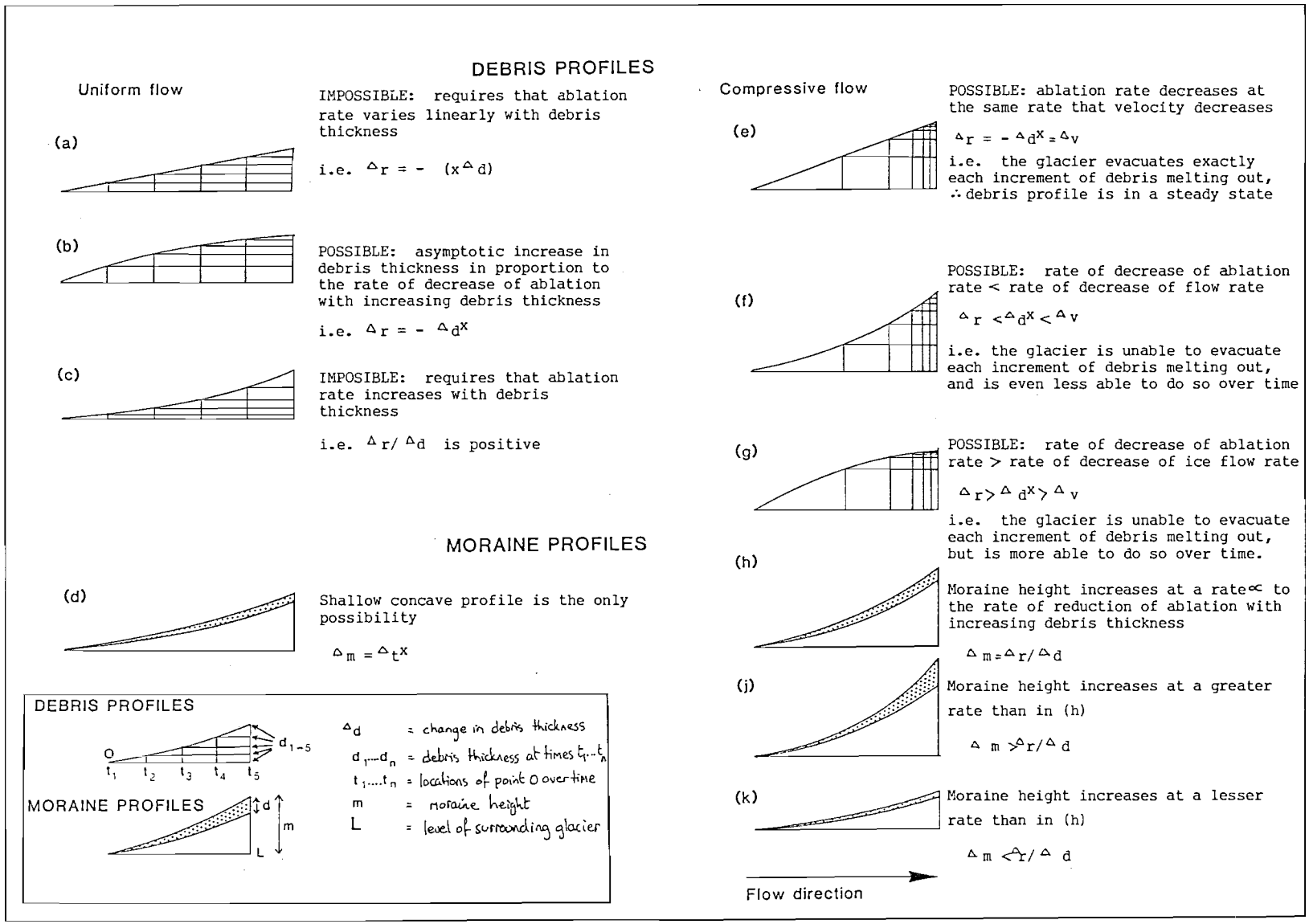

FIG. 3.18

Debris-thickness profiles and moraine profiles resulting from various combinations of flow conditions and rates of debris thickening. No lateral sliding of debris from moraine crests is assumed.

implicit dynamic equilibrium is contained in these models, with all of the main variables being mutually adjusted.

If a dynamic equilibrium and unvarying moraine relief over time are assumed, the rate of downglacier increase in moraine relief (the "waxing stage" of Small & Clark, 1974) depends on the rate of decrease in ablation beneath the moraine debris. In addition, the constancy of moraine relief over time demands that there is no net increase in debris thickness on the moraine crest over time so that differential ablation does not change at each point on the moraine. This would only be acheived by an unlikely balance between the rate of debris thickening and the rate of removal by ice flow and lateral sliding.

It must be stressed that this steady-state allows moraine relief to increase downglacier, but to remain constant relative to co-ordinates fixed in space. There is a throughput of material at each point on the moraine, of course.

A more rigorous condition of steady state is where the moraine relief is constant downglacier as well as over time. This can only occur if the ablation rate of the moraine crest is the same as that of the surrounding debris-free glacier surface. This can only be acheived if debris melting out at the moraine crest is removed. This normally occurs by sliding down the steepening flanks of the moraine ridge (Loomis 1970; Small & Clark 1974). However, many medial moraines have debris on the moraine crest which thickens over time, leading to the common situation of non-steady state conditions.

3.2.4.3 Englacially-fed medial moraine evolution in a non-steady state.

The dynamics of non-steady state moraine development are explained in Fig 3.17. To simplify matters, Fig 3.17A shows debris thickness increasing linearly with distance downglacier under compressive flow conditions. It is assumed that the moraine is fed by a vertical longitudinal debris septum of uniform debris concentration, that no strain thickening of the debris cover occurs, that no debris is removed from the moraine crest, and that the debris-ice interface is planar. The x-axis of Fig 3.17 represents distance downglacier, the y-axis debris thickness. The diagram is a downglacier profile of debris thickness at a point in time. Therefore the analysis initially deals with a C_A type moraine. The problem is treated as a two-dimensional one with variables of debris thickness, ablation rate, and ice velocity.

This profile of debris thickness is assumed not to change over time. Because the glacier beneath moves, there is a throughput (flux) of debris which does not alter this thickness profile. With this constraint, at any point (fixed in space) on the moraine, debris melts out at a rate sufficient to exactly replace the debris carried away from that point by glacier flow. For example, between times t_1 and t_2, point j_1 (which at t_1 is the point of emergence of the englacial debris septum) moves to k_1. Debris thickness at j_1 at t_1 was zero: by the time j_1 has moved to k_1, an increase in thickness of i_1 gives a total debris thickness of d_2.

In the same time interval, k_1 moves downglacier to l_1. At time t_1, debris thickness at k_1 was d_2: by the time k_1 has moved to l_1, an amount i_2 of debris has melted out to give a thickness $(d_2 + i_2) = d_3$. Similarly, l_1 moves to m_1 and i_3 of debris is added to give $(d_3 + i_3) = d_4$. In this way a flux of debris passes through the moraine, without altering the long profile of debris thickness. There is a steady-state with respect to debris.

The asymptotic decline of sub-debris ablation with increasing debris thickness (Fig 3.17B) is accommodated in Fig 3.17A by the smaller increments which are added to the debris column in a downglacier direction. The assumption of steady-state therefore requires that, in a downglacier direction, the sub-debris ablation rate must decrease at the same rate as glacier velocity. If this was not the case, the debris thickness at each point on the profile would change.

Although Fig 3.17A is a steady-state with respect to the debris flux through the moraine, the moraine as a whole (including the ice core) is in unsteady state (Fig 3.17C), because a constant downglacier rate of growth cannot be maintained. Debris thickness increases linearly downglacier, therefore differential ablation between the moraine crest and the surrounding glacier increases along the moraine. The relief of the moraine must also increase downglacier at an **increasing rate**. The point of emergence of the debris septum (the upglacier end of the medial moraine) does not migrate, so that the moraine crest steepens with respect to the surrounding glacier surface. In other words, the moraine "grows" over time as well as waxes downglacier. This is what is meant here by "unsteady state": the moraine is unable to maintain a constant relief over space and time. This indicates that a steady state of debris flux through the moraine does not correspond to a steady state of moraine morphology.

When some of the constraints on moraine evolution in Fig 3.17 are relaxed, the complexity of the interrelationships in moraine dynamics are

even more apparent. Fig 3.18 shows cases of uniform as well as compressive ice flow. Under uniform flow, the only debris thickness profile is an asymptotic increase, in proportion to the rate of decrease of ablation rate with increasing debris thickness. The only possible moraine long-profile is therefore concave.

Compressive flow is typical in ablation zones where medial moraines occur. Under such conditions, Fig 3.18B shows that the profile of debris thickness depends on the relative rates of downglacier decrease of ice velocity and the ablation rate of ice-covered debris. The debris thickness profile depends on the glacier's ability to evacuate each increment of debris added by melt-out in a unit of time. It has already been shown (Fig 3.17 and Fig 3.18e) that a linear profile results from a balance of debris supply and removal. If the glacier is unable to fully evacuate each increment of melting-out debris, the debris thickness will increase at a point on the moraine fixed in space (ie. a point not moving with respect to the ice). In addition to linearly-thickening debris, two other variations of this condition are possible:

1) the debris profile is concave-downglacier if compression (the rate of decrease in ice velocity) exceeds that of sub-debris ablation (Fig 3.18f).

2) the debris profile is convex if the rate of decrease of sub-debris ablation rate exceeds that of ice velocity (Fig 3.18g).

Cases (e), (f) and (g) all involve an increase in differential ablation downglacier. Each case generates a moraine whose relief increases exponentially downglacier and over time, as in case (d). The difference between each case lies in the rate at which these increases occur: debris profile (e) generates moraine profile (h), (f) gives (j), and (g) gives (k) in Fig 3.18B. Changes in moraine profiles over time are similar, and the general evolution is as for Fig 3.17C. Again, the difference lies in the rate of increase in moraine relief.

In summary, For a debris septum feeding a moraine with differential ablation between debris-covered and debris-free ice:

1. debris thickness increases downglacier but at different rates depending on the ablation rates and ice velocities;

2. moraine relief always increases exponentially downglacier and at any point on the moraine over time;

3. the increase in moraine relief is a function of debris thickness acting through its effect on differential ablation.

Transitions from steady-state to non-steady-state may result from

thickening of the debris cover, rather than in the thickness itself. From the above analysis, it is clear that thickening of the debris may result from compression in a moraine with no englacial feeder, or from a combination of compression and/or change in differential ablation due to englacial supply where a debris septum feeds the moraine.

3.2.4.4 Other factors in the model of medial-moraine evolution.

1. Lateral sliding of debris down moraine flanks.

The previous discussion assumed that all debris arriving at the moraine crest is added to the debris thickness and hinders ice melt. In nature, debris sliding down the flanks of the moraine as relief increases must also be considered (Loomis 1970; Small & Clark 1974; Small et al 1979).

Slope profiles of Small & Clark (1974 Fig. 3), Small et al (1979 Tables 2 and 3) and my observations of debris stability and slope angle (Table 3.6) suggest that as moraine relief increases, lateral slopes attain angles steep enough for debris movement at a very early stage. Subsequent increase in relief is associated with corresponding increase in width, which implies that debris removal from the crest remains approximately constant. Lateral sliding acts consistently down the length of the moraine if the slope remains constant. It reduces the rate of increase in debris thickness and moraine relief, but does not necessarily affect the overall form of the long profile, at least until growth of the moraine causes a marked increase in slope angle and sliding. It is doubtful whether sliding alone ever causes a downglacier change from waxing to waning stages of a medial moraine, and the model remains applicable in spite of the effect of sliding. The model of medial moraine morphology of Small et al. (1979) does not use sliding of debris alone to cause the eventual thinning of debris cover and inception of the waning stage of relief: it uses exhaustion of the englacial feeder in combination with sliding.

2. Compressional effects on morphology.

Following the work of Loomis (1970) and Small & Clark (1974), there was debate on the relative effects of ablation and compression on moraine morphology and height-width relationships (Eyles 1976; Small & Clark 1976). Which of the two influences is dominant at a particular point on the moraine may sometimes be difficult to determine. In other cases one effect is clearly dominant. As a general rule, strain dominates close to the moraine source but tends to be replaced by ablation with distance down

Angle	No.Obs	Debris characteristics	Source
39-43°		Continuous but mass moving cover on medial moraine	Kaskawulsh Glacier (Loomis 1970)
27-29°		Medial moraine	Gl. de Tsidjiore Nouve (Small and Clark 1974)
max = 41° mean = 35°	8	West medial moraine	Bas Gl. d'Arolla (Small et al. 1979)
max = 32° mean = 24°	8	East medial moraine	Bas Gl. d'Arolla (Small et al. 1979)
max = 38° mean = 29°	13	West medial moraine	Haut Gl. d'Arolla (Small et al. 1979)
max = 40° mean = 27°	16	East medial moraine	Haut Gl. d'Arolla (Small et al. 1979)
max = 47° mean = 33°	18	Continuous but mass moving debris mantle	Tasman Gl. This study
>35°		Clean ice walls	This study
20-30°		Stable debris mantle	This study

TABLE 3.6 Lateral slope angles of medial moraines.

the moraine (Eyles & Rogerson 1977). The influence of strain depends on the geometry of the ice-stream confluence at the moraine source (Anderton 1970).

3. Crevasse-recycling of debris.

A major feature of the medial-moraine model of Small et al. (1979) is that some moraines ingest debris into crevasses, to be subsequently melted-out further downglacier. I have seen this process frequently around the Tasman Glacier, but it is rather localised. I regard it as an exception to the general model rather than a basis for classification.

3.2.4.5 Summary of medial-moraine dynamics.

The previous sections discussed the mechanics which affect the morphology of medial moraines. Conclusions not previously reported in the literature have been reached.

A moraine nourished by an englacial debris septum may "grow" along its entire length over time under conditions of ice flow, ablation and debris supply which occur commonly in nature. Such evolution may be a function of negative mass balance, as many authors assume when describing how "wasting" or "stagnating" ice becomes covered in supraglacial debris (eg. Flint 1929, 1971).

What has previously not been recognised is that a medial moraine may progressively cover a glacier surface under equilibrium glacier mass balance. This is because moraine dynamics are rarely in equilibrium with glaciological conditions, but are controlled by local conditions of ice flow, ablation, and debris concentration along the moraine. Debris concentration is important in the model, and is largely independent of glacier mass balance. The model showed how moraines may develop with no impulse from changing glaciological conditions, but instead merely reflect debris delivery to, and its effect on, the ice surface.

Where removal of debris from the moraine crest by lateral sliding is insufficient to halt differential ablation, and where ice velocity is insufficient to remove all of the debris melting out at the surface, moraines will spread across the glacier surface regardless of other influences. Negative mass balance is not necessary to initiate this blanketing by debris. This spread of supraglacial debris retards ablation over a wide area of the lower glacier. If this trend were widespread, and because equilibrium mass balance requires that the accumulation of ice equals ablation, a significant reduction in ablation rate would require an increase in ablation area. Thus, the accumulation: ablation area ratio

would adjust through an advance of the glacier even though the glacier was in equilibrium mass balance.

Likewise, glacier mass balance can be maintained by increasing debris cover while snow supply diminishes. During this time, the glacier terminus may advance, retreat, or maintain the same position, depending on the the net result of these two opposing influences. Detailed discussion of the possible results of this effect follows in Chapter 4).

Even though the spread of supraglacial debris does not require glacier wastage, negative mass balance can promote moraine growth. Four effects are identified.

1. Glacier thinning has two effects: (a) it increases the area of exposed rock and moraine slopes above the glacier surface which in turn increase the supply of debris to the glacier; (b) each point on the glacier is reduced in altitude over time, causing warming and increased ablation. The 160 m thinning of the Tasman Glacier this century equates to an annual ablation increase of 15% to 20% per year since 1890.

2. Reduction in ice velocity reduces the ability of the glacier to evacuate debris melting out at the surface at increasing rates. It also reduces the rate of evacuation of rockfall debris from below source outcrops, leading to an decrease in the dispersion of supraglacial debris. Velocities of the Tasman have decreased by up to 40% since 1890 (Section 2.1.2.4).

3. Increased compression may occur under various conditions of positive or negative mass balance. Velocity gradients on the lower Tasman Glacier show an increase in longitudinal strain rate since 1890 during negative mass balance (Fig 2.5). By implication, other locations where steep icefalls feed a low-gradient tongue may also have experienced significant increases in compression.

The following section examines the field evidence for causes of the observed spread in supraglacial debris cover in the Mount Cook area during the Twentieth Century.

3.2.4.6 Observation and interpretation of medial moraines in the field area.

The general spread of supraglacial debris over the Twentieth Century is discussed with reference to three glaciers for which aerial photgraphs cover between 15 and 69 years of change (Figs 3.19 to 3.21). All types of moraine classified in Table 3.4 are present on these glaciers.

The morphological changes observed on the glaciers are summarised in

Table 3.7 and the causes of moraine evolution are suggested in the light of known glaciological changes in the area. Rock-avalanche moraines (type R) cannot be interpreted in terms of mass-balance change because their presence relates entirely to source-area failures. Types C and E moraines are considered because their morphology is sensitive to inherent dynamics and mass-balance trends.

Analysis of nineteen C and E type medial moraines (Table 3.8) reveals that there has been a general trend of moraine spreading on the study glaciers. The blanketing of the glacier surface by debris has been especially effective on the lower parts of the glaciers, with the spread of supraglacial debris becoming less towards the firn lines. However, the causes of moraine growth are varied and each example must be considered individually.

Tasman Glacier. (Fig 3.19)

The moraines of the middle Tasman Glacier all lie in an area where no significant longitudinal compression occurs north of the Rudolf confluence, as revealed by ice foliation and crevasse patterns. No reduction in ice velocity has been recorded in this reach between the photograph dates, although ice thickness has reduced by c.40-50m in keeping with the regional trend over this period (Chapter 2). Medial moraines emerge or have point sources close to the firn line, and field observation did not reveal any debris supplied from the basal traction zone. Morphological change has not been dramatic since a photograph by Du Faur, prior to 1914 (Du Faur 1914, Plate), though a general increase in moraine width occurs which reflects a slight but visible increase in source area exposure related to ice thinning. Below De la Beche corner, major morphological change occurs whose relationship to mass balance change is uncertain.

The Darwin Glacier C type medial moraines have also spread, and this may reflect increased compression behind the trunk ice stream as well as other influences.

Murchison Glacier. (Fig 3.20)

On the Murchison Glacier it is not possible to ascribe the observed spread of moraines to a specific cause since the glacier behaviour can only be inferred from nearby Tasman Glacier. It is hypothesised that changes due to inherent dynamics have been operating, but glacier thinning and velocity reduction has enhanced the spread of medial moraines. Tributaries may be more complex, and the disappearance of folding of the Mannering Glacier central medial moraine implies a decrease in

compression. This possibly relates to the passage of kinematic waves down the trunk and tributary glaciers at different times since the 1960s.

The Aida/ Murchison medial moraine illustrates overlap between moraine types, in this case due to large episodic debris inputs to a moraine generally fed by lower magnitude, higher frequency inputs. This has altered the morphology from an E_A type to a C_A type. The moraine has also widened considerably. (Fig 3.22).

Godley Glacier. (Fig 3.21)

The Godley Glacier contrasts with the Tasman and Murchison Glaciers, not in the changes which have taken place, but in their principal cause. Comparison of a 1917 photograph with later photographs shows the remarkable extent to which medial moraines have grown and coalesced. An important cause has been a large increase in the source area supplying debris to the glacier as lateral moraines have been exposed and collapsed, and as ice-fall tributaries have become detached from the trunk ice streams (Fig 3.23).

The flow structure of the glacier has exacerbated the result of these processes. Unlike the other two glaciers described, the Godley consists of two major tributaries of about equal ice discharge whose confluence is at point A in Fig 3.21. Most of the debris mantling the glacier by 1986 is derived from the huge medial moraine transported from this confluence (Fig 3.24). The moraine in turn is supplied by rockfall, debris flow and collapsing moraine walls on the north-east side of the Neish tributary, while the eastern tributary is fed by all these processes plus ice-cliff avalanching. There are many more sources of debris for this moraine, compared to published reports of moraine sources in other parts of the world. Without the major confluence, the discharge of debris from these sources would remain at the glacier margins due to the divergence of ablation zone flow vectors. Instead, the confluence leads the moraine to the central flow line of the trunk glacier from where a combination of lateral sliding, washing and compressional flow combine to distribute debris across the whole width of the glacier. The increase in the width of the main medial since 1917 is shown in Fig 3.22.

The detachment of ice-fall tributaries from the main trunk glacier has caused an abrupt change in high-level transport paths at these locations. Prior to detachment debris remained in englacial transport until exposed by ablation further down the glacier, but after detachment, ice-cliff avalanching transfers debris immediately to supraglacial transport. In 1917, six icefalls fed the upper Godley Glacier from the Main Divide (eg.

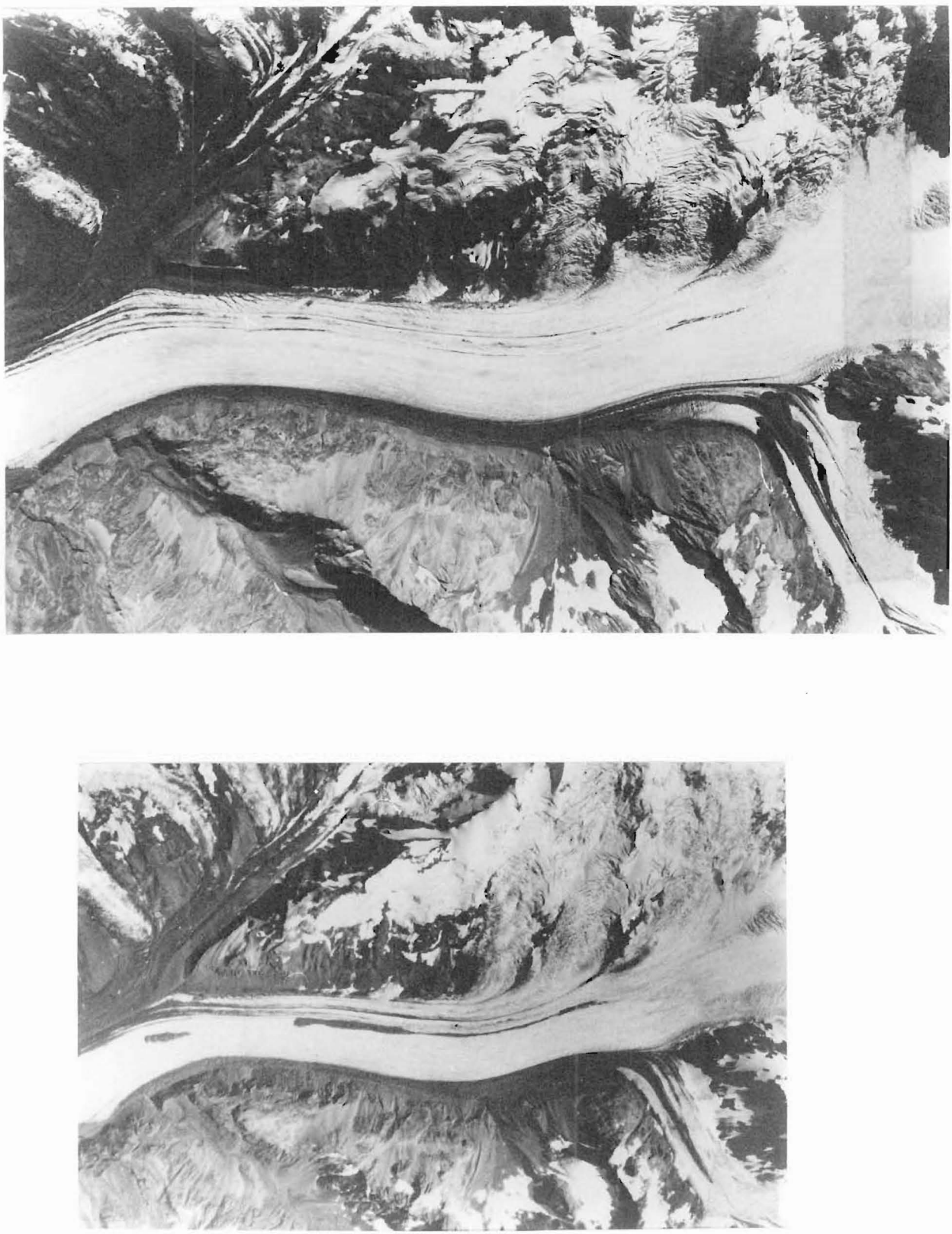

FIG. 3.19 Upper ablation zone of the Tasman Glacier, showing medial moraines in 1971 and 1986. Codes refer to Table 3.4 and Fig.3.12.

FIG. 3.20 Murchison Glacier in 1974 and 1986. Codes refer to Table 3.4 and Fig. 3.12.

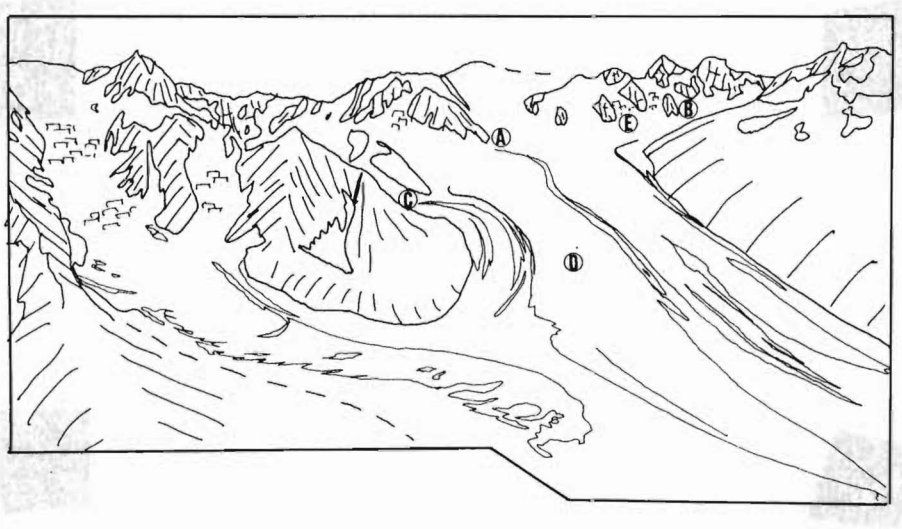

FIG. 3.21 Godley Glacier in 1917, 1971 and 1986. Codes refer to Table 3.4 and Fig. 3.12.

Moraine type	Location (ice stream)	Width change ?	Rate of width change ?	Source area change ?	Differential ablation change ?	Hypothesised main causes of changes
TASMAN GLACIER 1971-1986						
R_A	Anna ice stream	increase	----	----	----	5
E_A	Anna/Shirt Front	"	increase in lower part	----	increase	5
E_A	Shirt Front	"	"	----	increase in lower part	1,4,5
C_B	Ranfurly/ C. Knox	"	"	increase due to thinning	"	1,4,5
C_B	Pt 9142/ Ranfurly	"	none observable	increase	none observable	1
C_A	Haekel	"	increase	----	increase throughout	3,4,5
C_B	Haekel/ Hamilton	"	"	----	upglacier migration of onset	3,4,5
MURCHISON GLACIER 1974-1986						
R_A	Main trunk	----	----	----	----	5
R_B	Cooper's Mate	----	----	major failure	initiated over $10^4 m^2$ of Aida Glacier	-
C_A	Aida/ Murchison	increase	increase	----	----	1,3,5
C_A	Mannering (central)	"	decrease*	----	upglacier migration of onset	4,5
C_A	Mannering (west)	"	none observable	----	upglacier migration of onset	1
GODLEY GLACIER 1917-1971						
$C_{A/B?}$	Trunk (east)	increase to become lateral	?	----	onset throughout	1,3
C_A	Trunk (west)	increase to become indistinguishable	?	----	upglacier migration of onset	1,3
C_B	Confluence A	increase	increase	major increase	increase throughout	1,3
C_B	Neish icefall	increase	?	increase	onset throughout	1,3
C_B	Confluence C	increase to become indistinguishable	?	major increase	onset throughout	1,3
GODLEY GLACIER 1971-1986.						
$C_{A/B}$	Trunk (east)	now detached from glacier trunk as ice-cored lateral moraine				----
C_A	Trunk (west)	----------indistinguishable: part of debris mantle----------				
C_B	Confluence A	increase to merge with below	increase	increase	?	1,3
C_B	Neish icefall	increase to merge with above	increase	increase	increase	1,3
C_B	Confluence C	----------indistinguishable: part of debris mantle----------				

KEY 1 = source area increase due to thinning)
2 = ablation rate increase due to thinning) 1-4 are mass-balance induced changes
3 = reduced ice velocity)
4 = increased ice compression)
5 = inherent moraine dynamics (differential ablation)

TABLE 3.7 Observations of medial moraine evolution on the Tasman, Murchison and Godley glaciers.

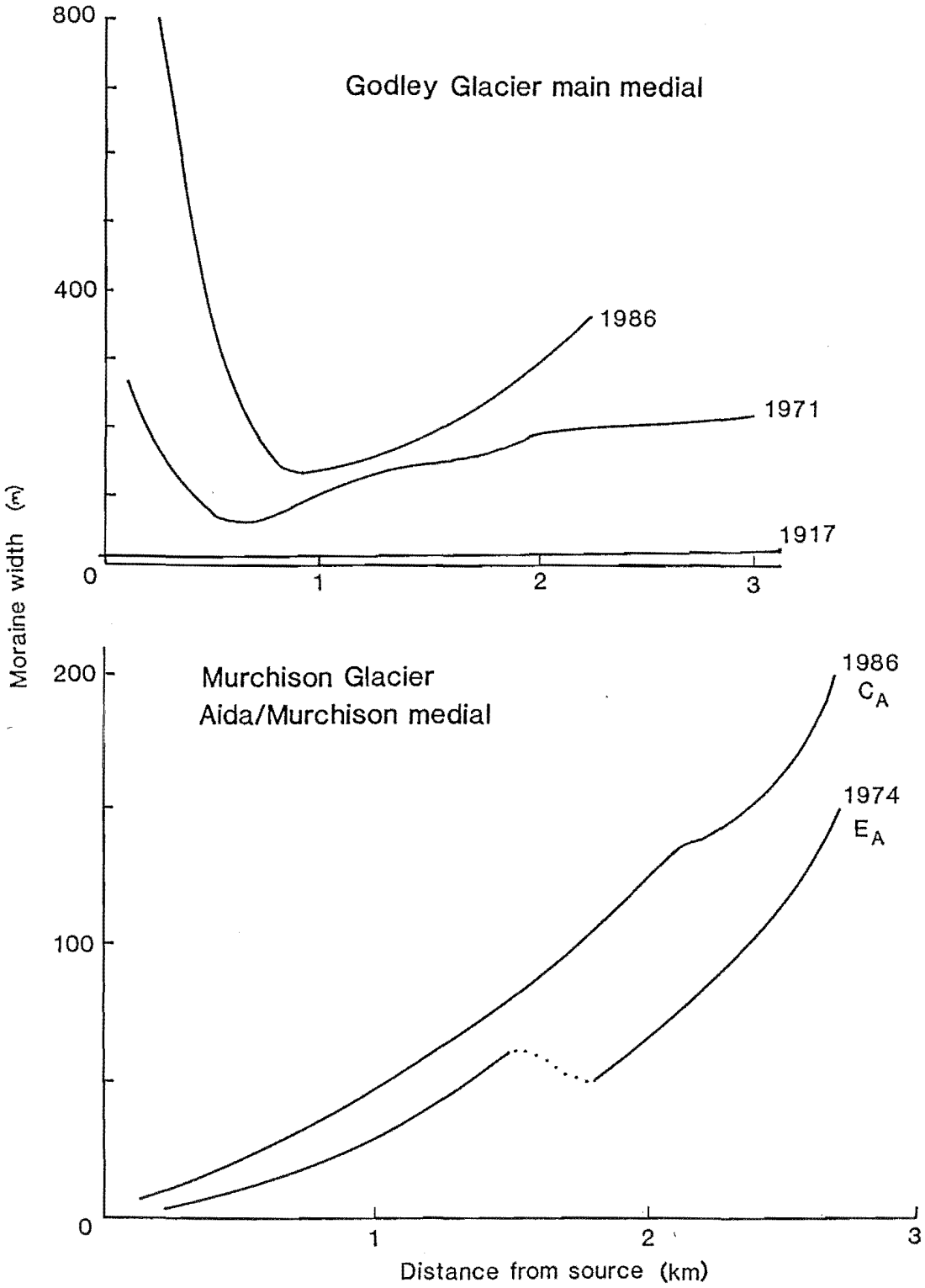

FIG. 3.22 Widths of medial moraines on the Godley and Murchison Glaciers.

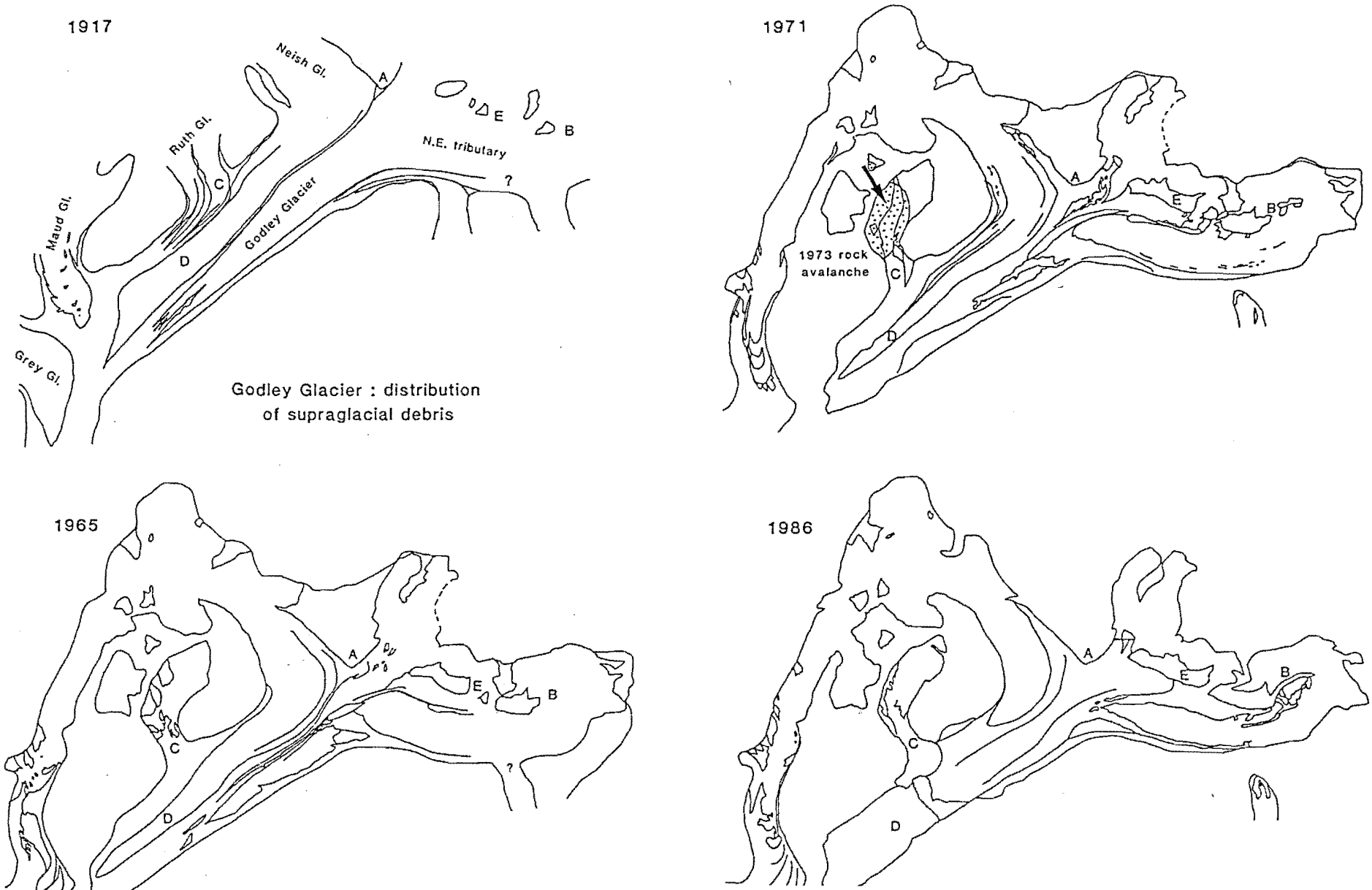

FIG. 3.23 Distribution of supraglacial debris on the Godley Glacier since 1917. Data from Williams (1967) and from aerial photographs. Letters A to D refer to same points as in Fig. 3.21.

FIG. 3.24 Oblique aerial photographs (April 1972) of the main medial moraine of the Godley Glacier. Lateral moraine in upper photograph now forms ice-cored moraine separated from the trunk ice stream.

(Photographs by T. Chinn).

A,E and B in Fig 3.21). By 1971, two had become detached, and by 1986 the icefall at B had vanished. A new medial moraine formed by ice-cliff avalanching is visible below the ice cliff. A similar case was reported from Alaska by Nielson & Post (1953), and such moraines must be common on composite alpine glaciers during thinning.

The Godley Glacier also differs from other glaciers in the area by being the only one where large ice-cored lateral moraines have formed. The thinning of the glacier since the middle of the century separated large rampart-like masses of debris-covered ice from the glacier along the valley sides (visible in the 1971 and 1986 aerial photographs, Figs 3.21 and 3.23). Widespread exposures of ice in these moraines suggest that they may be short-lived features suffering, rapid degradation of the ice core and backwasting of their proximal slopes (Fig 3.24). Similar features may be developing locally along the margins of the Tasman Glacier, though these are as yet at an early stage.

3.2.4 Conclusions of Chapter 3.2.

1) No conclusions about basal-transport-zone debris content can be drawn from field evidence. A thickness of c.1.1 m and a debris concentration of 30 % have been inferred from the literature.

2) The high-level transport zone is complex, reflecting the glacier flow structure. This has necessitated a re-appraisal of existing classifications of medial moraines.

3) Medial moraines are much more complex than described by previous authors. Theoretical considerations show that blanketing of a glacier surface by medial moraine growth is not necessarily induced by negative glacier mass balance but can occur under equilibrium or even positive mass balance conditions.

4) Nevertheless, the blanketing of a glacier surface by medial moraine growth may be initiated and will be enhanced by negative mass balance: this appears to be the case in the Mt. Cook area in the Twentieth Century.

5) Glacier morphology affects the susceptibility to blanketing by supraglacial debris during equilibrium and negative mass balance. Major confluences in the ablation zone are particularly effective for the formation of large medial moraines.

3.3 DEBRIS FLUXES AND EROSION RATES.

Sources, transport paths, and evolution of debris bodies carried by the glacier in basal and high-level transport zones have been examined qualitatively in previous sections. This information is now combined with glaciological data from Chapter 2 to quantify the transfers of rock debris in the Tasman Glacier, as far as the data will allow.

Three subsections examine:

1. the magnitudes and frequencies of rockfalls on to three glaciers in the study area;

2. the discharge of debris through three measured cross-sections of the Tasman Glacier;

3. the denudation rate of a high alpine cirque based on the debris flux of the glacier.

3.3.1 Rockfall magnitude and frequency estimates.

Between the firn line of the Tasman Glacier and the Rudolf Glacier confluence, several medial moraines transport debris for about 10 km to the upper margin of continuous debris mantle. Moraine of types C_A, C_B, E_A and E_B occur along the junctions between ice streams and can be traced upglacier to source outcrops. Using measured glacier velocities, the frequencies of rockfalls of different magnitudes can be estimated from these moraines.

Rockfall magnitudes were measured from the 1971 aerial photograph enlarged to 1 :25,000 scale. Lacking data on debris thickness, the area of supraglacial deposits was used as a surrogate for volume. Measurements were made by overlaying a template of different areas and shapes (Fig 3.25) on a map of moraine distribution (Fig 3.26). The closest approximation to the size and shape of each rockfall deposit was matched, and the areas recorded in classes of half-an-order-of-magnitude class width. The distances between deposits of each area class on each flow line were measured from the map, and converted to a time interval using the measured ice velocities (Fig 3.26).

The results (Tables 3.9 and 3.8) indicate that the record of rock falls preserved in the moraines spans only c.70 years, and up to 11 rock falls have occurred on any single flow line. The data are grouped to give an average rockfall magnitude and frequency distribution for the 11 source areas supplying the moraines.

A magnitude-frequency graph (Fig 3.27) indicates that rock falls of

Flow line	Distance between deposits (m)	Flow rate (ma^{-1})	Deposit age (years)	Deposit area (m^2)
AB	continuous	150-200	-	$<10^2$
B1 Ranfurly	1750	200	8.75	5×10^2
	2250	"	11.25	5×10^2
	2750	"	13.75	10^3
B2	1750	200	8.75	10^2
	2250	"	11.25	5×10^2
	2300	"	11.50	10^2
	2750	"	13.75	5×10^2
	3125	"	15.60	10^3
	3130	"	15.60	5×10^2
	3750	"	18.75	10^2
	3925	"	19.60	10^2
	4675	"	23.40	5×10^3
	4750	"	24.00	start of C_A moraine
BC	continuous moraine C_B from outcrop			$<10^2$
C1 Constance Knox	2100	230	9.1	10^2
	3075	"	13.4	10^2
	3075	"	13.4	5×10^2
	3100	"	13.5	5×10^2
	3425	"	14.9	5×10^2
	4800	"	20.9	10^2
	5050	"	22.0	10^3
	5175	"	22.5	10^3
	5675	"	24.7	10^3
	6000	"	26.1	5×10^3
	8000	upper margin of continuous mantle		
CD	3575	230	15.5	10^3
	4725	"	20.5	10^3
	6100	"	26.5	10^2
	6450	"	28.0	10^3
	6750	start of continuous moraine		
DE	3725	230	16.2	5×10^3
	4150	"	18.0	5×10^3
	4550	"	19.8	10^3
	4950	"	21.5	10^3
	5125	"	22.3	10^3
	5250	"	22.8	5×10^2
	5750	"	25.0	10^4
	6000	"	26.1	10^3
	6450	"	28.0	5×10^3
	6825	"	34.1	5×10^3
	6825	start of continuous moraine		
E1 Anna/ Hoch.Dome	2025	230	8.8	5×10^3
	7300	190	38.4	10^4
	7600	"	40.0	5×10^2
	7725	"	40.7	10^3
	9600	upper margin of continuous mantle		
EF	0	190	?	10^3
	1400 to 2150	150	?	$<10^2$
	3625	110	33.0	10^5
H1 Darwin	2250	80	28.0	5×10^4
H2	2500	"	31.25	10^4
H3	2675	"	33.4	10^4
H4	2950	"	36.9	5×10^4
H5	2825	"	35.3	10^4
H6	1050	"	13.1	5×10^3
H7	925	"	11.6	5×10^3
H8	750	"	9.4	10^3
J1	1250	<75	>16.7	10^4
J2	2375	75	31.7	5×10^4

TABLE 3.8 Approximate ages and areas of rock fall deposits in medial moraines on the Tasman Glacier. Data from 1971 aerial photographs enlarged to 1 : 25,000 scale. Flow lines refer to Fig 3.26.

TABLE 3.9 Recurrence interval of rock falls of each area class for each flow line.

Flow line	Area Category (m^2)	mean interval (years)
AB	$<10^2$	<20
B1	5×10^2	2.5
	10^3	>13.8
B2	$<10^2$	4.9
	5×10^2	5.2
	10^3	>15.6
	5×10^3	>23.4
BC	$<10^2$	<20
C1	$<10^2$	5.9
	5×10^2	>2.0
	10^3	>2.8
	5×10^2	17.0
CD	$<10^2$	11.4
	10^3	6.3
DE	5×10^2	>6.6
	10^3	2.7
	5×10^3	8.1
	10^4	>9.0
E1	5×10^2	>31.2
	10^3	>31.9
	5×10^3	>8.8
	10^4	>29.6
EF	$<10^2$	?
	10^5	>18.45
H	10^3	>9.4
	5×10^3	>4.4
	10^4	>11.8
	5×10^4	>18.5
J	10^4	>16.7
	5×10^4	>31.7

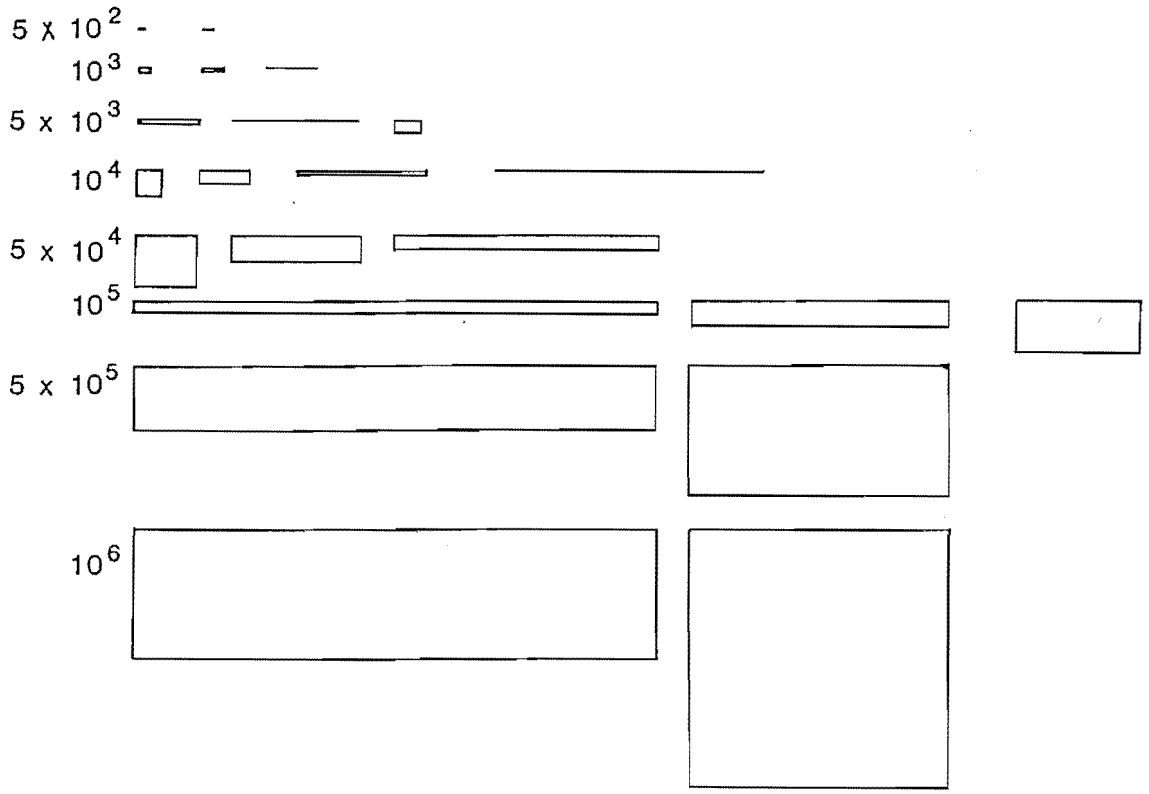

FIG. 3.25 Template used as an overlay on the 1971 map of medial moraines on the Tasman Glacier to estimate debris area. Figures are in m^2.

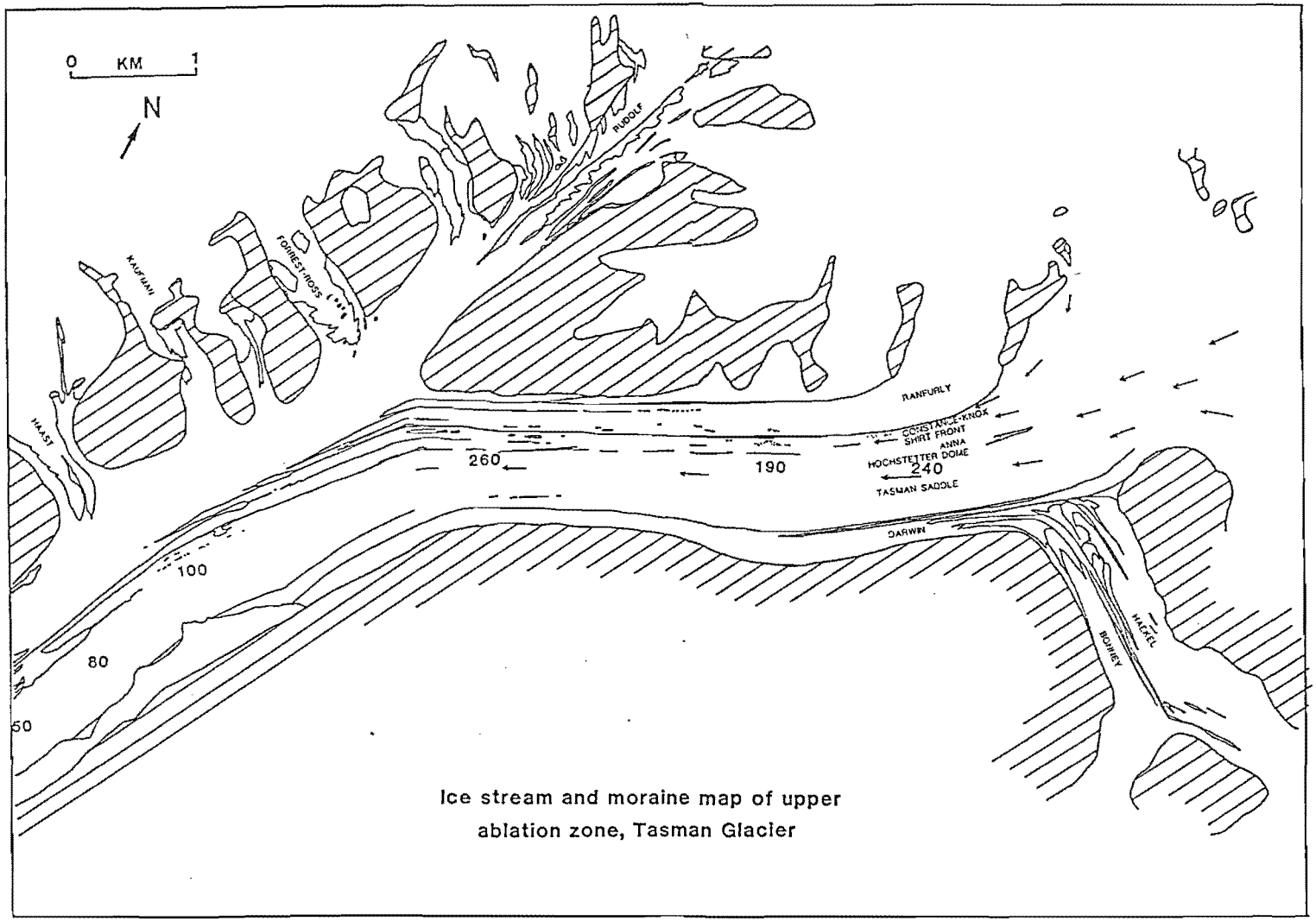

FIG. 3.26 Distribution of medial moraines and ice streams in 1971, used for the magnitude-frequency estimation. Arrows indicate flow direction only. Figures are flow velocities used in the calculation, estimated from deposit movements and from field surveys (Chapter 2).

$10^2 m^2$ occur more frequently than every 6 years, those of $10^5 m^2$ less frequently than every 30 years. A consistent relationship between rock fall magnitude and frequency exists. From this distribution, an estimate of the contribution of rock falls of each magnitude is made. In a 100-year period, the area of glacier surface covered by events of each magnitude (Table3.10) is proportionately greater for higher-magnitude rock falls. Larger events appear to be more significant than smaller events in supplying debris to the glacier.

There are several drawbacks with this analysis:

1) The use of deposit area as a surrogate for volume will weight the results in favour of thinner deposits. Larger rockfalls may give thicker deposits as well as a greater area of debris, and the magnitude-frequency distribution therefore underestimates the contribution of larger events.

2) Conversely, poor constraints on recurrence intervals may cause overestimates at higher magnitudes.

3) Moraines with sources above the firn line melt out progressively in the ablation zone (Section 3.2). The measurement of deposit areas on E_A type moraines may therefore be underestimates, if only part of the deposit is exposed at the glacier surface. However, no moraine sources lie more than 2 km above the firn line, and the septa feeding the moraines are expected to be shallow. The morphology of the medial moraines indicates that this is the case, and that septa are exhausted within a short distance of the earliest emergence of the moraines.

4) The moraines cover only c.70 years of supraglacial accumulation from limited source areas. Extrapolation to longer time periods and over a wider area creates uncertainties. For example, larger rockfalls with longer return periods have not been measured, and their recurrence can only be inferred. Extrapolation of Fig 3.27 suggests that a rock fall covering $10^6 m^2$ occurs every 60-80 years. Larger events have occurred recently in the Mount Cook area (Table 3.11) but they cannot be synthesised with the data from the Tasman Glacier alone.

If an earthquake origin for most large rock avalanches is accepted (Whitehouse & Griffiths 1983), the suggested 500-year recurrence interval of Richter magnitude 7 earthquakes on the Alpine Fault (Adams 1980) exceeds the oldest ice in the Tasman Glacier by c.200 years. This provides sufficient time for rock avalanches caused by one earthquake to be deposited at the glacier terminus well in advance of the succeeding earthquake. (The last large earthquake on the Alpine Fault is believed to have occurred c.500 years BP).

Area class (m^2)	100-year contribution (m^2)
$<10^2$	> 1,600
5×10^2	> 5,300
10^3	< 8,500
5×10^3	< 40,700
10^4	< 59,500
5×10^4	< 199,200
10^5	< 300,000

TABLE 3.10 Area of rock fall deposits likely to be contributed in 100 years, based on magnitude-frequency relations of the study outcrops

Date	Location	Basis for age estimate.
mid-1950s	Mt Hopkins, Richardson Glacier	1965 photo.
late 1950s	Darwin Glacier	Repeat photos = glacier flow rate
late 1950s	Bonney Glacier	Repeat photos = glacier flow rate
late 1960s	Mt Livingstone, Grey Glacier	1971 photo.
1973	Mt Wolseley, Ruth Glacier	Event between 1971 and 1974 photos.
1974	Moffat Peak, Classen Glacier	Event between 1971 and 1974 photos.
1979	Mt Vancouver, Linda Glacier	Observed.
Dec 1979	Cooper's Mate, Aida Glacier	Observed.
early 1980s	Mt Darwin, Tasman Glacier	Repeat photos = glacier flow rate
1984-88	Syme Ridge, Grand Plateau	Observed: repeated falls.
Sept 1986	Meteor Peak, Rudolf Glacier	Event between visits 1 week apart.

TABLE 3.11 Recent recorded rock falls of $>10^5$ m^2 in the Mount Cook area.

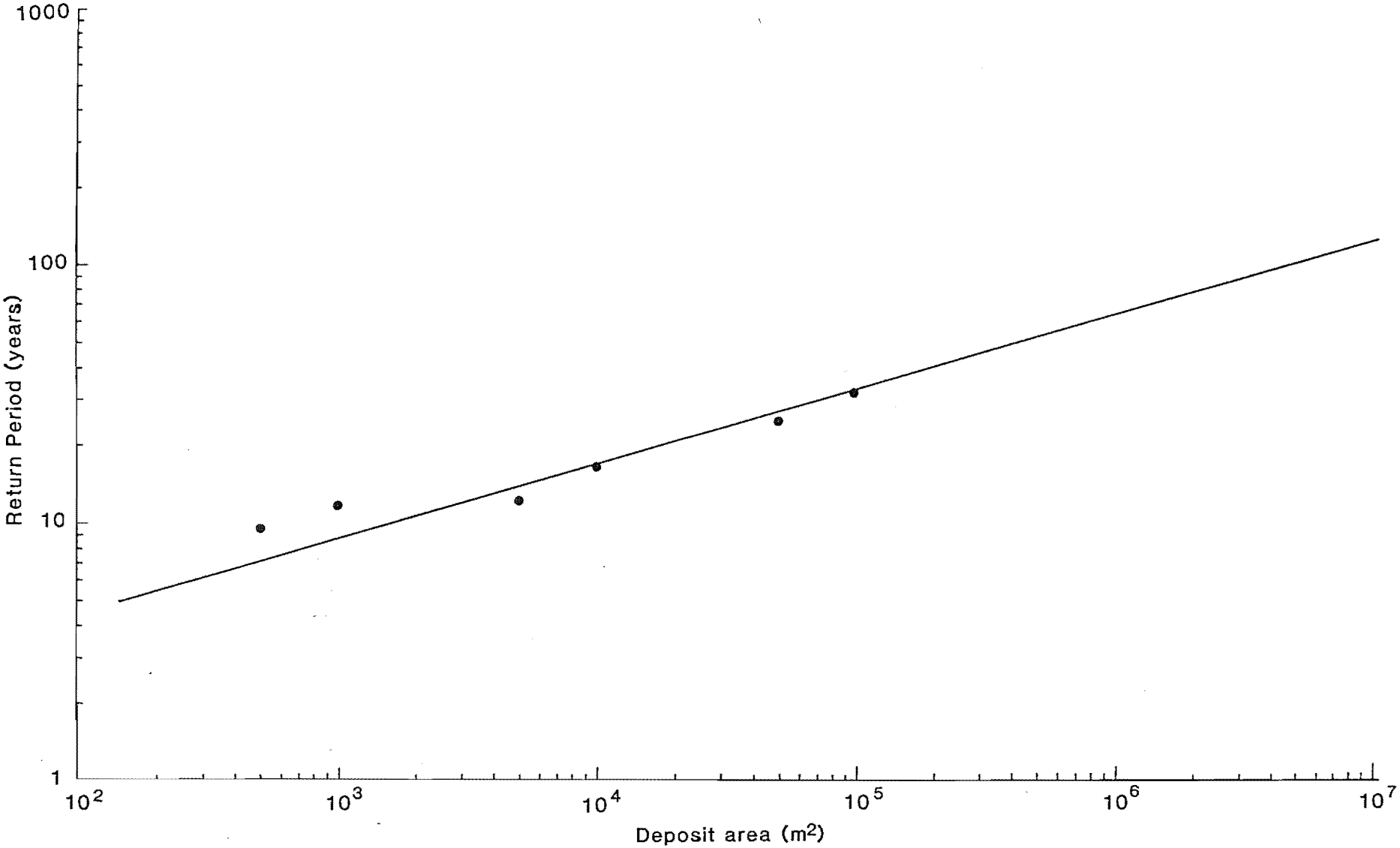

FIG. 3.27 Magnitude-frequency graph of rockfalls feeding medial moraines of the upper ablation zone.

In conclusion, within the (limited) range of deposit magnitudes currently transported supraglacially, larger magnitudes (covering c.10^4 to $10^5 m^2$) appear to provide most debris to the glacier. These magnitudes are small in relation to the whole magnitude-frequency spectrum. The measured magnitude-frequency distribution is incomplete, both in spatial and temporal dimensions, so it is impossible to assess the impact of infrequent large earthquakes on debris supply. Rock falls triggered by such events are not currently in supraglacial transport on the Tasman Glacier.

3.3.2 Debris discharges through measured cross sections.

3.3.2.1 Method.

The debris discharge Q_D through a cross-section of a glacier is given by

$$Q_D = Q_B + Q_E + Q_S \quad (13)$$

where Q_B, Q_E and Q_S are discharges of basal, englacial, and supraglacial transport zone debris respectively. Since debris discharge is related to ice discharge, the debris discharge through each cross-section is defined by the ice velocity, debris concentration, and cross-sectional area of each transport zone. Thus:

$$Q_B = c_B P U_{SL} h_b \quad (14)$$

$$Q_E = c_E A U \quad (15)$$

$$\text{and } Q_S = h_d W(1-p) U_{SURF} \quad (16)$$

where c_B, c_E are mean debris concentrations of the basal and englacial transport zones; P is the "wetted perimeter" of the glacier, A the cross-sectional area, and W the width covered by supraglacial debris; p is the void ratio of the debris cover; and U_{SL}, U, and U_{SURF} are the mean sliding velocity, mean velocity through the cross-section, and mean surface velocity through the cross-section respectively. Values of each of the parameters at each site and each time are summarised in Table 3.12. Sources and derivations of them are contained elsewhere in the thesis.

Errors associated with each parameter are difficult to assess given a lack of independent checks of most of them, and the simplistic calculation of ice discharges in Chapter 2. However, an independent check of sliding velocity at both Ball Hut and Malte Brun is available from measured ice-flow rates near the lateral margins of the glacier. Comparison with estimated figures shows that errors are less than 15%. The errors associated with the basal debris load are indicated by the standard error of the means of quoted values from other temperate glaciers. In general,

available indicators suggest that the likely range of values of debris discharge are within 25% of the estimates at Ball Hut. Less precisely constrained parameters in the calculations for the Malte Brun/ De la Beche and (especially) Celmisia Flat sites mean that debris discharges there are less precise than those at Ball Hut.

These results are relatively insensitive to the range of probable values of each variable. Although errors may affect the values used, the relative differences between values and their changes over space and time are confidently interpreted because any errors which may have arisen during calculation have been consistently applied.

3.3.2.2 Results.

Calculated debris discharges are presented in Table 3.12, and changes at each site over time are illustrated graphically in Figs 3.28 and 3.29.

Malte Brun/ De la Beche transect.

Most of the debris discharge through this cross-section is carried in the basal transport zone. Supraglacial transport has been negligible at <2% since 1890 at least (Fig 3.28). The most significant factor is a low englacial debris concentration due to the small area of debris sources feeding the high-level transport zone compared to the other major tributaries of the glacier. The consistently higher ice discharges and sliding velocities at this transect compared to Ball Hut is mirrored by the greater total debris discharges. This is in spite of the lower englacial debris concentration and debris discharge, due to the dominance of basal transport. The high proportion of debris carried in basal transport reflects the high sliding velocity, which accounts for an estimated 82% of the total flow rate through the cross-section (Chapter 2).

No major changes in the relative importance of each transport zone have occurred since 1890. However, the total debris discharge in 1986 was only 34% of the 1890 discharge, but the proportion is increasing under the present positive mass balance trend (Fig 3.29). The reduction in debris discharge has been proportionately slightly greater than that in ice discharge (c.30%). This reflects the reduced sliding velocity of this reach of the glacier since 1890 combined with the dominance of basal transport.

Ball Hut transect.

Basal transport predominates at this site despite the relatively high englacial debris concentration. However, factors such as the englacial

Site		Ice discharge (m^3a)	Englacial transport zone c_E (vol %)	Q_E (m^3a)	Supraglacial transport zone W (m)	h_d (m)	U_{SURF}	Q_S	Basal transport zone P (m)	U_{SL}	Q_B (m^3a)	Q_D (m^3a)
Malte Brun	1890	2.88×10^8	?0.0014	4,032	50	0.1	425	2125	2200	315	123,444	219,601
	1973	1.08×10^8	?0.0025	2,700	80	0.1	210	1680	1860	169	96,817	101,197
	1986	1.11×10^8	?0.0025	2,775	100	0.1	230	2300	1823	199	111,735	116,810
Ball Hut	1890	1.21×10^8	0.014	16,940	1900	0.05	144.5	13,728	2742	88	74,319	104,987
	1973	3.81×10^7	0.025	9,525	1790	0.1	80.0	14,320	2505	46	35,491	59,336
	1986	5.14×10^7	0.025	12,850	1780	0.15	87.2	23,282	2393	71	52,330	88,462
Celmisia	1890	6.70×10^6	?0.014	938	2300	0.39	?20	12,558	2189	?10	6,742	20,238
	1973	2.14×10^6	?0.025	535	2150	0.75	5.3	5982	2020	?7.5	4,666	11,183
	1986	3.56×10^5	?0.025	9	2108	0.78	1.5	1726	1989	?1.0	613	2,348

TABLE 3.12 Calculation of debris discharge for each transect and year.

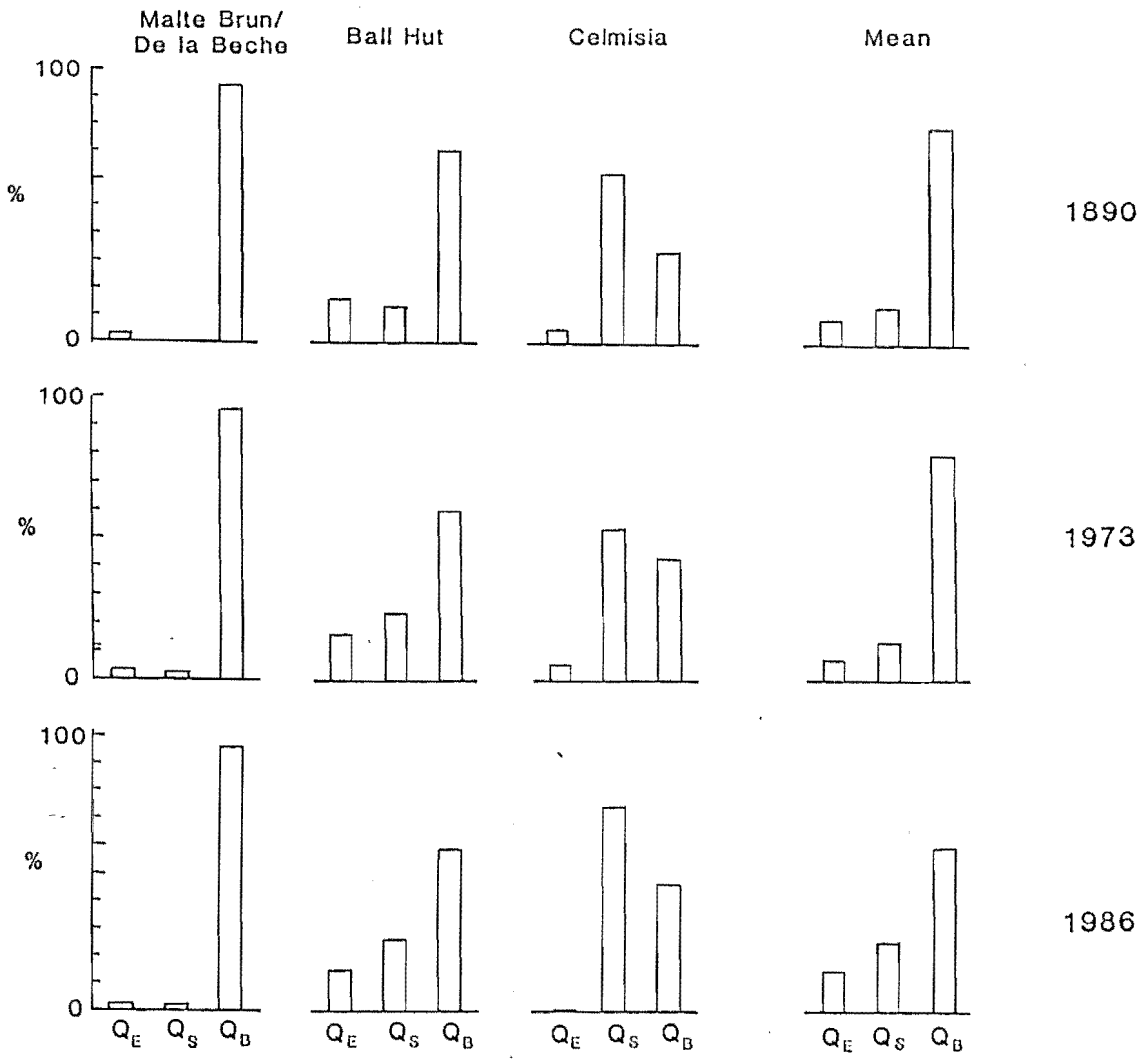

FIG. 3.28 Histograms of the proportion of debris transported in each of three transport zones through each study transect on the Tasman Glacier. Means for the whole glacier for each year are weighted with respect to the relative discharges through each transect. Q_E = englacial transport zone, Q_S = supraglacial transport zone, Q_B = basal transport zone. Total debris discharge through each transect in each year = 100 %

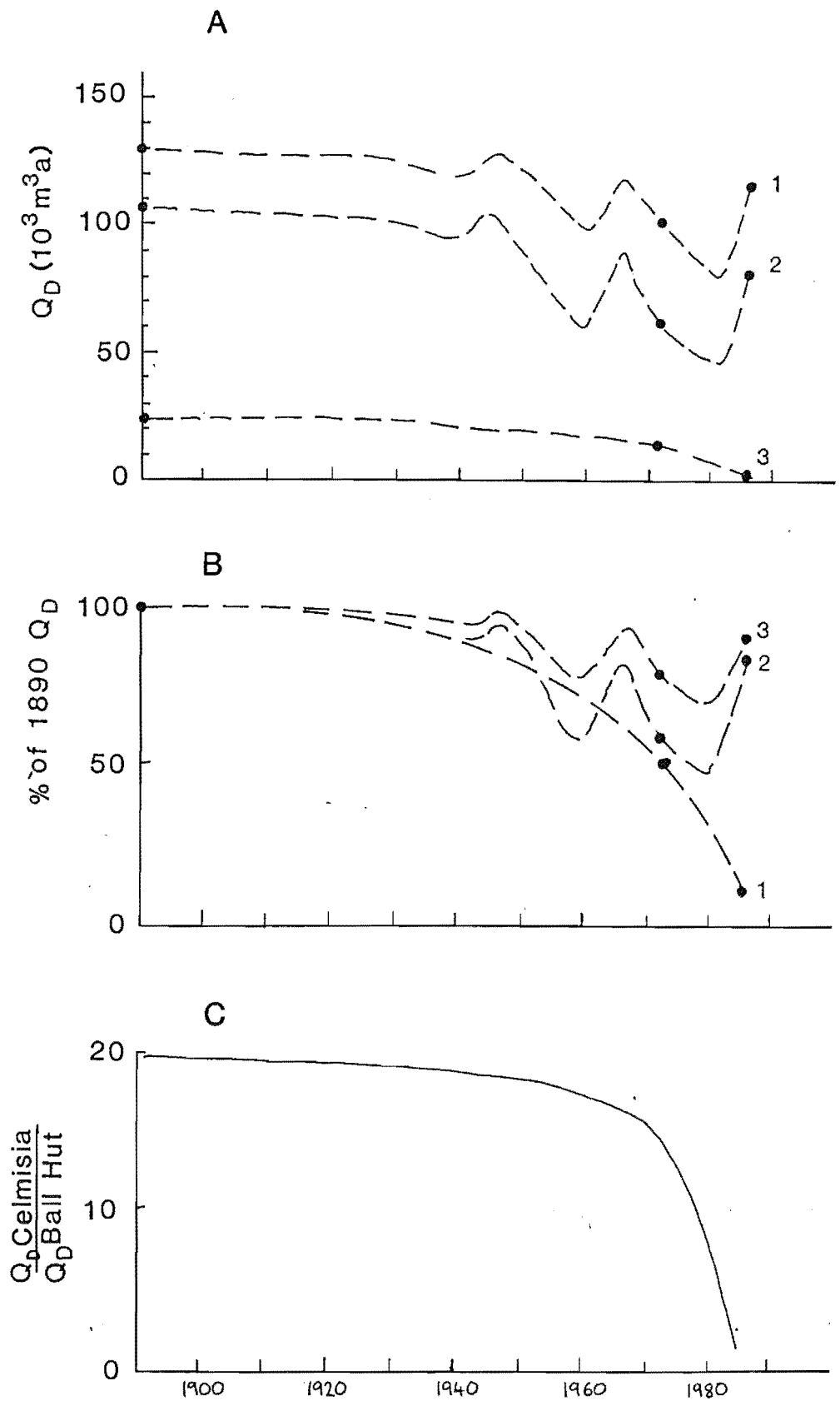

FIG. 3.29 (A) Debris discharge, Q_D, through each transect as a function of time. (B) Debris discharge over time as a proportion of the 1890 discharge through each transect. (C) Debris discharge through the Celmisia transect as a proportion of that through the Ball Hut transect and its temporal variation.

debris concentration, the valley shape factor (a high A/P value), and a relatively low velocity ratio of 58% favour a higher proportion of high-level transport compared to Malte Brun/ De la Beche. The extent of the supraglacial debris cover belies its low volumetric importance.

The proportion of the debris discharge carried by each transport zone has changed since 1890 in accordance with reduced sliding velocities and increased supraglacial cover. Fig 3.28 shows the general increase in the proportion of supraglacial debris discharge at the expense of basal debris discharge. The proportion of the total load carried by the englacial zone has not changed over the same time period. This conclusion rests partly on the assumption that the englacial debris concentration varies inversely with ice velocity, hence the higher concentrations in 1973 and 1986 than in 1890. However, if a constant debris concentration since 1890 is assumed, the englacial load would have accounted for 26% of the total: this is 11% different from the calculated proportion.

The total debris discharge in 1973 was 62% of the 1890 discharge, and in 1986 the proportion had increased to 72%. Increased ice velocities and ice thicknesses associated with the present positive mass-balance trend have recently brought about an increase in debris discharge, as they have at Malte Brun/ De la Beche.

Celmisia transect.

The data on which the following interpretations are made is scant. While the values given to each variable may be erroneous, the concepts revealed by quantification have merit. The inaccuracies derive mainly from the inadequacies of the flow-law based calculations at a cross-section where ice velocities and ice and debris discharges are very low. There may also be subglacial deformation of the gravel substrate.

Fig 3.28 illustrates changes involving reductions in the proportion of basally-transported debris between 1973 and 1986 as the ice velocity is reduced. To what extent this trend is the product of an over-simplified estimate of the basal transport zone discharge is debatable. At such low ice velocities, it is possible that substrate deformation accounts for a significant proportion of the measured flow rate (Boulton 1979). The velocity ratio at this site is little better than a guess and takes no account of the possible effects of subglacial deformation. However, the 1973 flow rate is believed to be too high to be explained by a deforming bed alone.

The reduction in ice velocity outweighs the post-1890 increase in volume of supraglacial debris in transport, so that supraglacial debris

discharge has declined throughout the measurement period. However, even if the uncertainties surrounding the englacial and basal debris discharges are taken into account, the supraglacial discharge has become relatively more important over time. (The data from which the supraglacial component has been calculated is relatively reliable). Total debris discharge has fallen rapidly this century due more to the effect of reduced ice velocity on ice discharge than to glacier thinning. The glacier has ceased to flow at the terminus and may do so soon at the Celmisia transect 2 km upvalley (Chapter 2). It is therefore expected that debris discharge will also reach zero within a few decades. The present positive fluctuation of the glacier has not had a discernible effect at this transect, in contrast to the other two which lie closer to their respective equilibrium lines.

3.3.2.3 Glaciological implications of debris-discharge variations.

Mass transfer in a glacier comprises two materials: ice/water and rock debris. The ice of the Tasman Glacier may ablate, but the rock debris is well below its melting point. The loss of ice due to melting cannot be mimicked by the loss of debris. While the difference in ice discharge between the Ball Hut and Celmisia transects can be explained by the flow structure and ablation of the glacier, a similar difference in debris discharge (Fig 3.29C) cannot. Conservation of mass demands that the debris which passes Ball Hut but does not reach Celmisia must either be deposited at the glacier sole, be washed out in the Tasman River, or remain in transport. An estimated 48% of the total debris discharge at Ball Hut is in the high-level transport zones, therefore a large volume of debris must be accumulating in the lower tongue of the glacier.

The relative debris discharges of the transport zones is strongly determined by the vertical profile of glacier velocity. The ratio of basal sliding to surface velocity (the velocity ratio) is especially important. Temperate glaciers with high ratios have correspondingly high basal debris discharges relative to the high-level zones, if other influences remain equal. The Tasman Glacier is an example. A high velocity ratio will also increase the total debris discharge because basal sliding causes higher ice velocities than in glaciers which do not slide.

Calculated supraglacial debris discharges are very variable over space and time. Comparison with discharges of six other temperate glaciers (Eyles 1979) with the Tasman Glacier shows that the latter has generally higher discharges, reflecting the high activity index and abundant debris sources. However, Table 3.13 shows that debris discharges near glacier

TABLE 3.13

Estimated debris discharges of supraglacial and basal transport zones near the termini of temperate glaciers.
(Icelandic data from Eyles, 1979).

a) Ice-cap outlets	B	S	B/S
Breidamerkùrjökull	26,000	2,000	13 : 1
Skaftafellsjökull	5,000	300	16.6 : 1
b) Valley glaciers			
Verkisjökull	750	400	1.87 : 1
Fjalljökull	300	825	1 : 2.75
Kviarjökull	500	1,250	1 : 2.5
Mosarjökull	1,500	200	7.5 : 1
c) Tasman Glacier			
Celmisia (1890)	6,742	12,558	1 : 1.86
Ball Hut (1890)	70,941	13,728	5.17 : 1
terminus (1986)	0	0	
Celmisia (1986)	459	1,726	1 : 3.76
Ball Hut (1986)	37,573	23,282	1 : 1.61

termini are spatially very variable making direct comparisons difficult. Of more interest is the comparison of the ratios of discharges of basal and supraglacial transport zones (B/S), which Eyles (1979) interprets as a function of available debris sources. The Tasman Glacier data show that there is a temporal variation in the B/S ratio superimposed on the spatial variation. The spatial trend is towards a higher proportion of supraglacial debris transport towards the terminus, with a temporal increase in the proportion during the Twentieth Century reflecting the changing glacier flow structure under negative mass balance. The B/S ratio at Celmisia Flat is most comparable with the Icelandic data, being located close to the terminus, and is similar to Eyles' (1979) figures for Icelandic valley glaciers.

Eyles's (1979) interpretations may therefore be extended by the observation that as total debris discharge approaches zero (over either time or space), the ratio of basal to supraglacial debris discharge is also reduced.

3.3.3 Erosion rates of high alpine cirques.

The data allow the denudation rate of the Grand Plateau to be calculated. This involves an assumption that the annual debris flux of the glacier is equal to the volume of material eroded from the catchment in the same year. It is then possible to divide the debris discharge by the source area of the catchment to derive the denudation rate for the cirque.

The validity of the result rests on (among other things) the assumption of an equivalence of erosion and transport rates. Debris is accumulating in the lower tongue of the glacier, therefore there is a discrepancy between the catchment erosion rate and the glacier debris discharge. The discrepancy increases towards the terminus, and the results of the previous section show that it has also increased during this century over the whole lower tongue. The problem is avoided by using data from 1890 for the calculation.

Ideally, the measured transect should be at the equilibrium line of the glacier. Although the Malte Brun transect fulfills this criterion, the debris concentrations and ice velocities of the Ball Hut transect are better known (the latter having been measured directly) and on balance make this the most suitable site. The discharge of the Hochstetter ice stream is used for the calculation.

3.3.3.1 Calculation of debris discharge.

Calculation of the debris discharge of the Hochstetter and Tasman Saddle ice streams are shown by Table 3.14. The same adjustments have been made to the parameters that were made for the debris-discharge calculations in Table 3.12. These involve

1) correction of the measured ice velocity for seasonal variation

2) calculation of sliding velocity and internal deformation of ice in the cross-section

3) use of the 1972 cross-sectional area (Broadbent 1973) adjusted to the surveyed ice level of 1890 (Brodrick 1891)

4) the lesser extent of the supraglacial debris cover in 1890 compared to the present (using Brodrick's map of 1890)

5) adjustment of englacial debris concentration (Appendix 6) for changing ice velocity.

Calculation of debris discharge from the upper Tasman Glacier is similar. However, the estimate of englacial debris concentration is less precise than for the Hochstetter ice stream. The estimate is made by comparing the area of source rock walls in the upper Tasman Glacier with that in the Grand Plateau: the much smaller area per unit of ice discharge gives an estimated debris concentration of 0.0014 % by volume in 1890.

3.3.3.2 Calculation of source area.

The area of the Grand Plateau cirque is 15.56 km^2, calculated from sheet 79 NZMS 1 topographic map (Sheet 79) enlarged to a scale of 1:50,000. The area above the base of the Hochstetter icefall is included. Below this, no debris was being supplied to the glacier surface in 1890, and it is assumed that no net gain or loss of debris occurs at the glacier bed between the base of the icefall and the study cross-section.

The area of the Tasman Glacier catchment above the firn line near the Malte Brun Hut site was calculated, from the same map, to be 35 km^2.

3.3.3.3 Calculation of denudation rate.

The specific annual sediment yield from Grand Plateau is 11,375 t km^2 a^{-1} giving a rate of vertical lowering of the land surface of 5.3 mma^{-1}. The corresponding values for the Tasman Saddle area are 16,313 t km^2 a^{-1} and 6.3 mma^{-1} (Table 3.14).

TABLE 3.14 Calculation of denudtion rates of the Grand Plateau and upper Tasman glacier.

Calculation of debris discharge : Ball Hut.

Cross-sectional area of ice stream in 1890		= 643,800 m^2	(1)
Ice velocities : mean surface velocity (stations 3 to 7 of Brodrick, 1890)		= 159 ma^{-1}	
: mean surface velocity with 10% seasonal adjustment		= 144 ma^{-1}	(2)
: mean velocity due to internal deformation *		= 46 ma^{-1}	(3)
: sliding velocity	(2)-(3)	= 98 ma^{-1}	(4)
Hydraulic radius (from Fig 2.3)		= 2,240 m	(5)
Glacier width (from Brodrick's map of 1890)		= 1,790 m	(6)
Supraglacial debris discharge	$Q_S = (2)h_d(1-p)(6)$	= 3,610 m^3a^{-1}	(7)
Englacial debris discharge	$Q_E = \frac{[(2)+(4)]}{2} c_E(1)$	= 10,906 m^3a^{-1}	(8)
Basal debris discharge	$Q_B = (4)h_B(5)c_B$	= 67,612 m^3a^{-1}	(9)
TOTAL DEBRIS DISCHARGE	$Q_D = (7)+(8)+(9)$	= 82,128 m^3a^{-1}	(10)

Calculation of denudation rate.

Volume of debris eroded in one year = annual debris discharge at Ball Hut		= 82,128 m^3a^{-1}	(10)
Area of source catchment		= 15.5632 km^2	(11)
Density of local bedrock		= 2.6 t m^3	(12)
SPECIFIC SEDIMENT YIELD	= [(10)x(12)]/(11)	= 13,720 t km^2 a^{-1}	
DENUDATION RATE	= 0.001[(10)/(11)]	= 5.28 mma^{-1}	

Calculation of denudation rate : Malte Brun.

Volume of debris eroded in one year = annual debris discharge (from table 3.12)	=	219,601 m^3 a^{-1}
Area of source catchment	=	35 km^2
Density of local bedrock	=	2.6 t m^2
SPECIFIC SEDIMENT YIELD	=	16,313 t km^2 a^{-1}
DENUDATION RATE	=	6.27 mm a^{-1}

3.3.3.5 Comparison with estimates of denudation and uplift rate in alpine environments.

a) Southern Alps of New Zealand.

A summary of sediment yields of 33 South Island rivers is presented by Griffiths (1981). A small amount of data from heavily glaciated catchments is available, notably the Hooker Valley, (Griffiths, 1981), and the Ivory Glacier (Hicks et al, in press).

The denudation rate of the Ivory Glacier cirque has been calculated using proglacial lake sedimentation rates to be 5.6 mma^{-1} (Hicks et al, in press). These authors conclude the presence of the small cirque glacier does not make the denudation significantly different from that of nearby largely ice-free basins. A yield of 14,900 t km^2 a^{-1} has been calculated. Griffiths (1981) gives a specific sediment yield of 3,538 t km^2 a^{-1} for the Hooker Valley, which converts to a denudation rate of 1.6 mma^{-1}.

There is a close correspondence between the estimated denudation rate of the Grand Plateau cirque (5.6 mma^{-1}) and of the upper Tasman Glacier (6.3 mma^{-1}) with the estimated uplift rate for the area of 5-6 mma^{-1} given by Wellman (1979). The rates are sufficiently similar to support the view of Adams (1980) that the axial Alps are in a steady state where rapid uplift is compensated by a correspondingly rapid rate of erosion. A similar interpretation may be made for the Himalayas, based on published rates (Brunsden et al. 1981; Saunders & Young 1983).

The denudation rate in this study supercedes the rate of "rockfall and snow avalanching" estimated from the Ball Hut transect by Whitehouse (1987).

b) Process rates from around the world.

The gross denudation of the Grand Plateau cirque is the sum of the sediment yields of rockfall/avalanching and subglacial erosion. A summary of estimates of these rates (Drewry 1986; Ballantyne & Kirkbride 1987) is presented for comparison in Table 3.15. Saunders & Young (1983) comprehensively review global process rates, including slope denudation. Modern rates of rock-wall denudation and glacial erosion do not appear to be significantly different. However, the sample of rockfall rates are biased by the inclusion of only the steepest slopes in any area. As slopes rarely consist entirely of steep rock-walls (even in alpine areas), the rates of glacial erosion are probably greater than the overall denudation of ice-free slopes.

The denudation rates from the Tasman Glacier appear to be similar to

TABLE 3.15A Published values of subglacial denudation rates.

(Data from Drewry 1986)

a) Estimates (Drewry 1986 Tables 6.2 and 6.3)

Glacier	Mean erosion rate (mma^{-1})	Source	Method
Muir, Alaska	19.0	Reid (1892)	1
Muir, Alaska	5.0	Corbel (1962)	1
Hidden, Alaska	30.0	Corbel (1962)	1
Engabreen, Norway	5.5	Rekstad (1911-12)	1
Engabreen, Norway	0.218	Kjeldsen (1981)	2
Storbreen, Norway	0.1	Liestol (1967)	1
Heilstugubreen, Norway	1.4	Corbel (1962)	1
Nigardsbreen, Norway	0.165	Kjeldsen (1981)	2
Erdalsbreen, Norway	0.610	Kjeldsen (1981)	2
Austre-Memurubre, Norway	0.313	Kjeldsen (1981)	2
Vesledalsbreen, Norway	0.073	Kjeldsen (1981)	2
Hoffellsjokull, Iceland	2.8-5.6 max	Thorarinsson (1939)	1
Kongsvegen, Svarlbard	1.0	Elverhoi et al. (1980)	1
St. Sorlin, France	2.2	Corbel (1962)	1
Imat, USSR	0.9	Chernova (1981)	1
Ajutor-3, USSR	0.7	Chernova (1981)	1
Fedchenko, USSR	2.9	Chernova (1981)	1
RGO, USSR	2.5	Chernova (1981)	1

b) Measured rates (Drewry 1986 Table 6.1)

Glacier	Abrasion rate (mma^{-1})	Ice velocity (ma^{-1})	Source
Argentiere, France	<36.0	250	Boulton (1974)
Breidamerkùrj., Iceland	3.75	15	"
"	3.40	20	"
"	0.90	20	"
"	3.00	10	"
"	1.00	10	"

but higher than most published rates. This presumably corresponds to the generally high energy levels and process rates in the area, notably uplift, relief, and glacier activity index. Furthermore, the susceptibility of the bedrock to erosion is probably greater in the Southern Alps than in the Norwegian areas cited in Table 3.15 which have given generally much lower rates.

3.3.4 Conclusions of Chapter 3.3.

3.3.1 Magnitudes and frequencies of rockfall inputs.

1) Rock falls covering areas of up to $10^5 m^2$ have contributed most debris to high-level transport of the Tasman Glacier over the last 70 years.

2) There is no evidence of debris supply by extreme events. If very large rock falls are earthquake-triggered, the absence of large supraglacial rock avalanches probably reflects the 500-year recurrence interval of large earthquakes in the region, compared to the maximum age of ice in the Tasman Glacier of c.300 years.

3) Extreme events probably have affected mass balance and glacier fluctuations during the Holocene even if they have not done so in the last few centuries.

3.3.2 Debris flux of the Tasman Glacier.

1) Debris discharges of the Tasman Glacier are high in comparison to valley glaciers elsewhere in the world.

2) Large spatial and temporal variations occur which primarily reflect changing glaciological conditions, but also changing debris supply.

3) There has been a significant Twentieth-Century trend to reduced debris discharges and a greater proportion of supraglacial transport.

4) The lower tongue of the glacier has had a positive sediment budget over the last century.

3.3.3 Denudation of the Grand Plateau and Tasman Saddle areas.

1) The Grand Plateau cirque is eroding at c.5.3 mma^{-1}, the Tasman Saddle area at c.6.3 mma^{-1}.

2) This rate does not refute the view that erosion rates in the Southern Alps are primarily a function of annual precipitation.

3) There is an approximate balance between uplift and denudation in the area of the Southern Alps with the highest relief.

3.4 EVOLUTION OF CLAST SHAPE DURING TRANSPORT THROUGH A GLACIERIZED VALLEY

3.4.1 Definition of clast shape properties.

According to Barrett (1980), the shape of a rock particle comprises three independent elements, namely form (the ratio of the long (a), intermediate (b), and short (c) orthogonal axes); roundness (the sense of smoothness of a particle as defined by the sharpness of the edges bounding the facets); and surface texture (the small-scale surface morphology superimposed on the facets and edges) (Fig 3.30). Commonly, it is the form and roundness of coarse particles which are studied, surface texture having no workable system of field measurement and a significance which is poorly understood.

Following Ballantyne (1982), form is described qualitatively with regard to the resistance to breakage of a clast. "Weak" forms are those with a high degree of flatness and/or elongation and which are susceptible to breakage parallel to the b-c plane. "Strong" forms are more equidimensional clasts with a correspondingly lower susceptibility to breakage.

3.4.2 Review of clast shape studies in glacial environments.

Interest in the genetic implications of the sedimentology of glaciogenic and periglacial deposits has focused attention on the use of clast shape both as a descriptive and as an interpretive tool. By using a variety of measurement techniques and analytical procedures (Barrett 1980) clast shape has been employed for three basic purposes.

1. To separate discrete environments by using shape as an indicator of different erosional processes. Clast form and roundness have proved an effective and simple way of distinguishing glaciogenic debris from periglacial regoliths (Seppälä 1976; Ballantyne 1982; Sutherland et al 1984; Ballantyne & Kirkbride 1986), subglacially-transported debris from supraglacial and englacial debris (Ogilvie 1904; Lindsay 1970; Reheis 1975; Boulton 1978; Domack et al 1980; Ballantyne 1982; Matthews & Petch 1982; Serebryanny & Orlov 1982; Anderson 1983; Dowdeswell et al 1985; Sharp 1985; Dowdeswell 1986; Vere & Matthews 198[illegible]; Matthews 1987), and supraglacial debris from water-worked debris (Sharp 1947, 1949; Slatt 1971; Matthews et al 1979; Rubulis 1983; Sharp 1985).

2. To interpret changes in clast shape process within a single

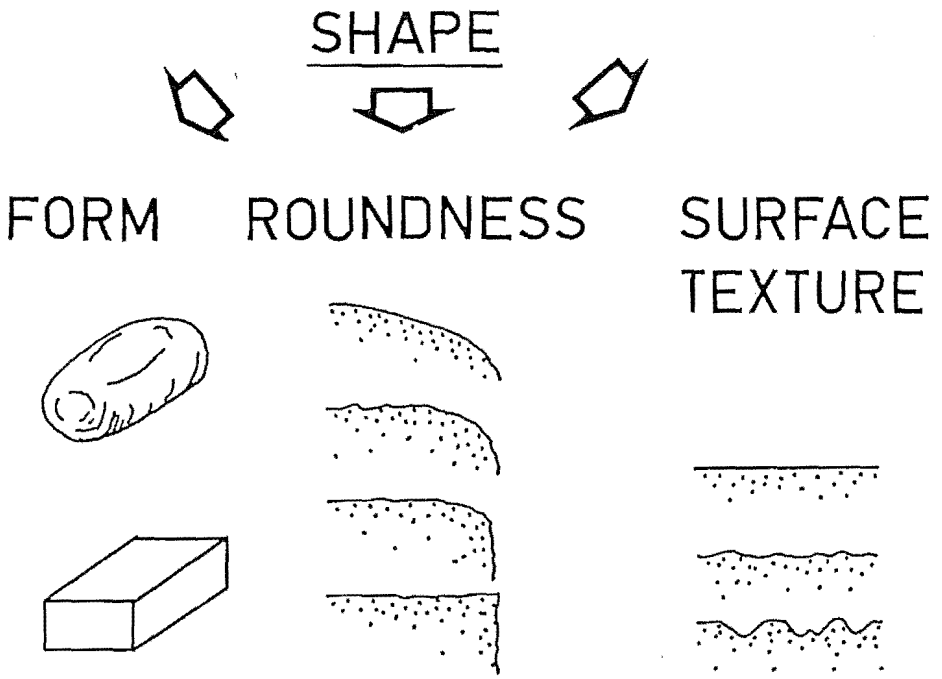

FIG. 3.30 The three elements of clast form (after Barrett, 1980).

environment. Progressive shape modification by subglacial processes has been documented (Drake 1972; Humlum 1981; Lister 1981), in contrast to the lack of modification during supraglacial transport (Sharp 1949; Boulton 1978; Eyles 1979).

3. As a relative dating tool, by using temporal changes in clast roundness due to weathering. Birkeland (1973) found this technique to be imprecise but Birkeland (1982), Dowdeswell (1982), Perttunen & Hirvas (1981), and Smyth (1984) achieved some success using different measurement techniques. Smyth concluded that roundness was time-dependent on a scale of decades.

Previous authors have employed shape measurements for narrowly defined purposes. This has lead to the distinction between "glacial" and "non-glacial" or "periglacial" environments (Seppälä 1976; Sutherland et al 1984; Ballantyne & Kirkbride 1986). The validity of this distinction is examined in this study, by using it as an a priori categorisation of sample sites which is subsequently tested and refined.

In spite of the abundance of studies there exists no systematic study of the progressive modification of shape within a glacierized catchment under conditions of good temporal and spatial control. This study attempts to synthesise measurements of clast shape at all stages of transport "history" in order to understand the location, abundance and rate of operation of shape-modifying processes.

The approach taken is

1. to identify appropriate quantitative indices of clast form and roundness in deposits of known origin:

2. to synthesise these sedimentological "fingerprints" with ancillary data into an empirical model of catchment sediment dynamics:

3. to assess the relative importance of transporting agents currently operating in the catchment:

4. to assess the significance of the results in terms of both established models of shape evolution and of the interpretation of ancient glaciogenic facies.

3.4.3 Relationships between clast shape and process.

From the above review, significant shape-modifying processes can be identified. The complexity surrounding the interpretation of clast shape in terms of formative processes is summarised in Table 3.16.

Form and roundness are independent properties, and it follows that a change in one may reflect a different process from a simultaneous change

PROCESS	FORM MODIFICATION	ROUNDNESS MODIFICATION
Microgelivation (granular disintegration)	none ?	INCREASE
Macrogelivation (frost shattering)	a) STRONGER FORMS b) WEAKER FORMS	DECREASE
Fall shattering	a) STRONGER FORMS b) weaker forms	DECREASE
Glacial abrasion	variable	INCREASE
Fluvial abrasion	variable	INCREASE
Subglacial crushing	STRONGER FORMS	DECREASE
Fluvial shattering	STRONGER FORMS	DECREASE

TABLE 3.16 The effect of erosional processes on clast shape properties. Upper case refers to major effect, lower case to subsidiary effect. In general, fracture processes destroy weak forms and increase angularity: abrasional processes dominantly affect roundness, which is increased.

(a) refers to fracture across the principal (a-b) plane.
(b) refers to fracture along the principal (a-b) plane.

in the other. For this reason, both have been measured for this study (cf. Ballantyne 1982; Matthews & Petch 1982). Furthermore, an observed change in one property may be the net result of several processes acting contemporaneously. In such a case it becomes difficult to separate the effects of each process and to interpret their relative significance. This is especially difficult for deposits whose clasts have complex transport histories involving multiple processes. For example, traction at the glacier sole involves abrasional rounding as well as crushing and fracture increasing sphericity: the two processes have independent effects (hence they are treated as separate processes, although Sharp & Gomez (1986) show that "abrasion" commonly refers to inter-granular brittle fracture). Furthermore, multiple processes may have coeval but opposite effects on a single shape property, for example abrasional rounding competing with the production of sharp edges by fracture. Does one measure the sharpest edge or the roundest edge of a freshly-crushed abraded clast? Each is the manifestation of a separate process, a problem which necessitates a clear definition of the process-shape relationships under investigation prior to sampling.

Further complexity derives from differences in the anisotropy of joint geometry within rock outcrops (Addison 1981), which defines the primary form of clasts produced by weathering (Drake 1970; Ballantyne 1982). In spite of these complexities, four generalisations may be made.

1. Bedrock weathering produces a variety of clast forms depending on joint geometry.

2. Fracture processes tend to destroy "weak" forms to produce a higher proportion of "strong" forms.

3. Fracture processes tend to increase clast angularity by producing sharp, freshly-broken edges.

4. Abrasional processes tend to increase clast roundness by preferential wear along clast edges. This occurs by some combination of inter- and intra-granular fracture and plastic deformation (Drewry 1986). Abrasional processes are not well understood and may vary according to lithology.

There should be sound independent evidence of the genesis of each deposit prior to "fingerprinting" the clast shape properties, due to dangers of misinterpreting process-shape relationships. For this reason a variety of ancillary evidence (locational, textural, geomorphological and chronological) has been used to determine the genesis and transport history of debris at each sample site (Table 3.17). In the Tasman Valley,

TABLE 3.17 Diagnostic features of deposit categories.

CATEGORY	MORPHOLOGY	SEDIMENTOLOGY		LOCATION/ASSOCIATION
		Clasts	Matrix	
"Extraglacial" categories				
O	Bedrock outcrops	in situ joint-bounded		Exposed bedrock
B	Slope mantle, no evidence of downslope movement	No exotic lithologies Autochthonous	None in upper part	Gentle slopes
S	Slope mantle, evidence of downslope movement (lobes, terraces, sorted stripes)	No exotic lithologies Autochthonous	Variable	Moderate to steep slopes with no rockfall source
T	Steep aprons or cones, typically 34-38°	Coarse, fall-sorted	None in upper part	Below obvious rockfall source
"Glacial" categories				
R	Fresh: lobate or digitate debris spread Old: ice-cored mounds	Coarse, poorly-sorted	None	On glacier below obvious rockwall source Within medial moraine or as isolated mound
M	Linear alignment parallel to glacier flow	Coarse, poorly-sorted	None	Up-glacier association with rock wall above or below firn line, ice-stream confluences
D	Areally-extensive supraglacial blanket	Coarse, poorly-sorted	Illuviated infill in lower part	Lower tongues of valley glaciers
Z	Occasionally forming medial moraines	Striated and faceted	infill of fines	Along major ice-stream confluences
"Fluvial" category				
W	Linear alignment along water courses, ice-cored hummocks	Moderately to poorly-sorted, occasional weak stratification	sandy, occasional stratification	Association with active or abandoned water courses

the use of weathering rinds (Chinn 1981; Whitehouse et al 1986) and glacier flow rates (Chapter 2.1) allows a degree of control to be established for clast ages.

3.4.4 Observations of modifying processes in the Tasman and Mueller Valleys

3.4.4.1 Weathering processes

Microgelivation (Tricart 1956)

Frost action causing the granular disintegration of rock is termed microgelivation. The process is effective and widespread on sandstones in the field area despite their high degree of induration, and causes the rounding of clast edges. Initial rounding occurs quickly, probably over a period of a few decades, and subsequent modification is limited and apparently independent of time (Fig 3.31).

Macrogelivation (Tricart 1956)

The fracture of rocks by frost action into joint-bounded clasts is termed macrogelivation. The densely-jointed nature of Torlesse Sandstones favours the production of coarse clasts whose initial form is a direct result of joint geometry. High-angle joint intersections tend to produce more equant clasts than reported elsewhere (Ballantyne 1982) but generally weak forms are produced.

3.4.4.2 Erosional processes

Fall shattering

The impact of a falling clast on bedrock, talus or ice surfaces causes fracturing usually across the principal (a-b) plane of the clast. This produces more equidimensional clasts (Ballantyne 1982) of high angularity. The effectiveness of macrogelivation in this region of steep relief gives rise to widespread aprons and cones of talus in the field area.

Downslope creep

Debris-mantled slopes of moderate angle undergo the gravitational creep of bouldery regoliths (Ballantyne 1984) which causes clast contacts and potential fracture, though shape modification by downslope creep is poorly documented.

Glacial abrasion

High basal debris loads (Chapter 3) and rapid rates of basal sliding of the Mount Cook glaciers (Chapter 2) favour the abrasion of large volumes of debris. Some of this material is entrained by the glaciers and eventually exposed along ice-stream confluences and near glacier termini.

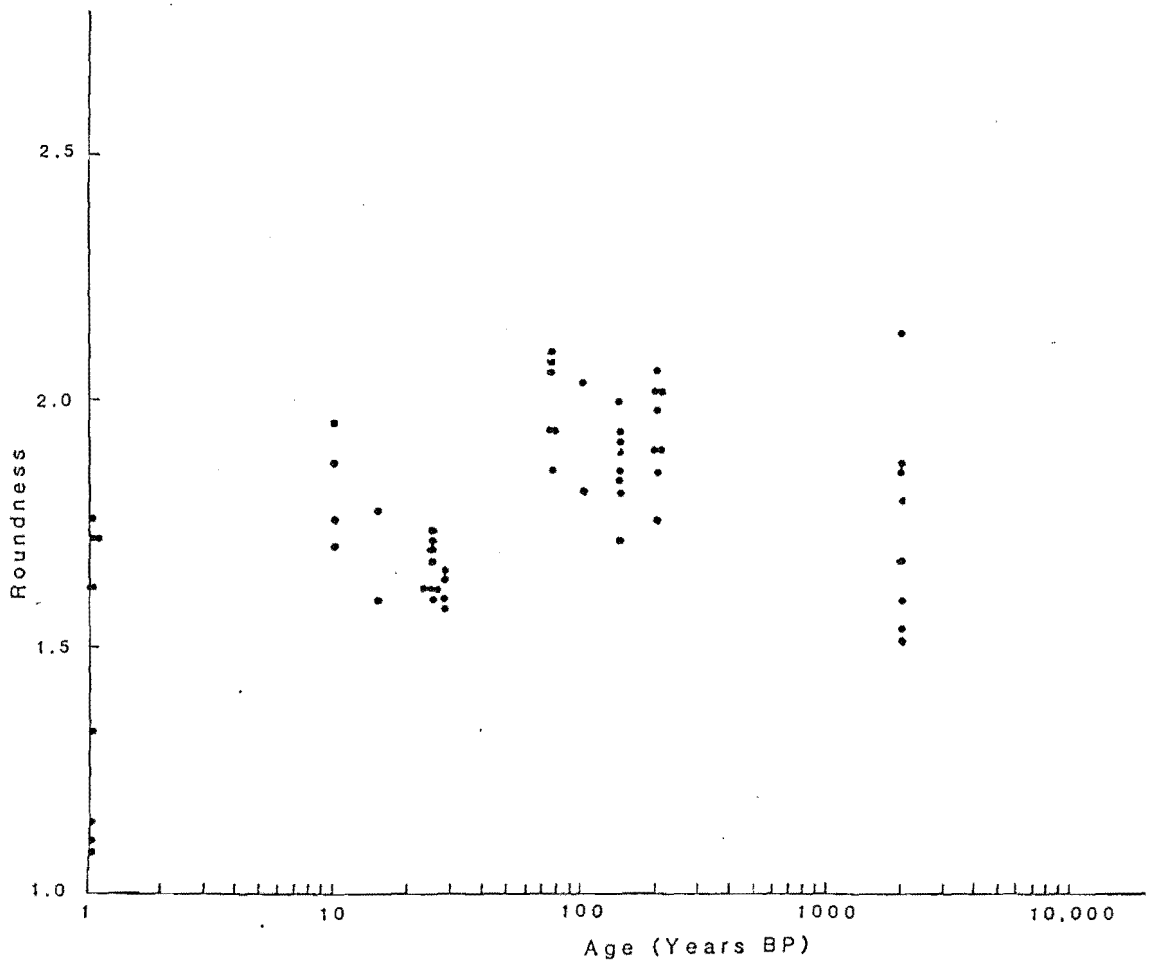

FIG. 3.31 Variation in clast roundness as a function of time for all samples subject to granular disintegration.

Glacial crushing

High stresses in the subglacial environment favour the brittle fracture of clasts (Drake 1972; Sharp & Gomez 1986; Drewry 1986). Fracture occurs within and between grains and within larger clasts. The latter causes the production of strong forms from weak ones, the former is classed as an abrasional process.

Fluvial abrasion

Abrasion is accepted as being effective at increasing clast roundness over relatively short distances (Gustavson 1974). However, the effects of fluvial abrasion on clast shape are difficult to isolate from downstream sorting effects. Although downstream fining has been widely reported (eg. Fahnestock 1963; Bluck 1964; Ballantyne 1978; Boothroyd & Nummedal 1978;) it is probably due to both abrasion and to size sorting (Gustavson 1974). Work on abrasional effects on clast form is lacking.

Fluvial shattering

Bluck (1964) identified a downstream increase in the proportion of weak forms over an alluvial fan surface due to the splitting of limestone fragments during transport. This also had the effect of reducing clast roundness. Elsewhere, a downstream increase in strong forms has been reported (Shan, cited by Smith 1985). It is usually difficult to ascribe downstream trends in clast form to a particular comminution process because of simultaneous size and shape sorting (Lane & Carlson 1954 ; Bradley et al 1972). The effects of fracture on clast shape during fluvial transport are therefore not well understood. Nevertheless, a reduction in roundness is intuitively probable and variable effects on form appear to be possible.

The distribution of deposits which could be distinguished in the field by characteristic sedimentological and morphological features is shown for particular locations in Figs 3.5, 3.13 and 3.32. The spatial operation of the processes outlined above is inferred to be very variable: some processes are ubiquitous, others are rather restricted spatially.

3.4.5 Measurement of form and roundness.

3.4.5.1 Sampling procedure.

The sampling procedure was to identify deposits whose origin was obvious from the location, morphology, and any relevant ancillary evidence. At least four samples of 50 clasts were measured on each

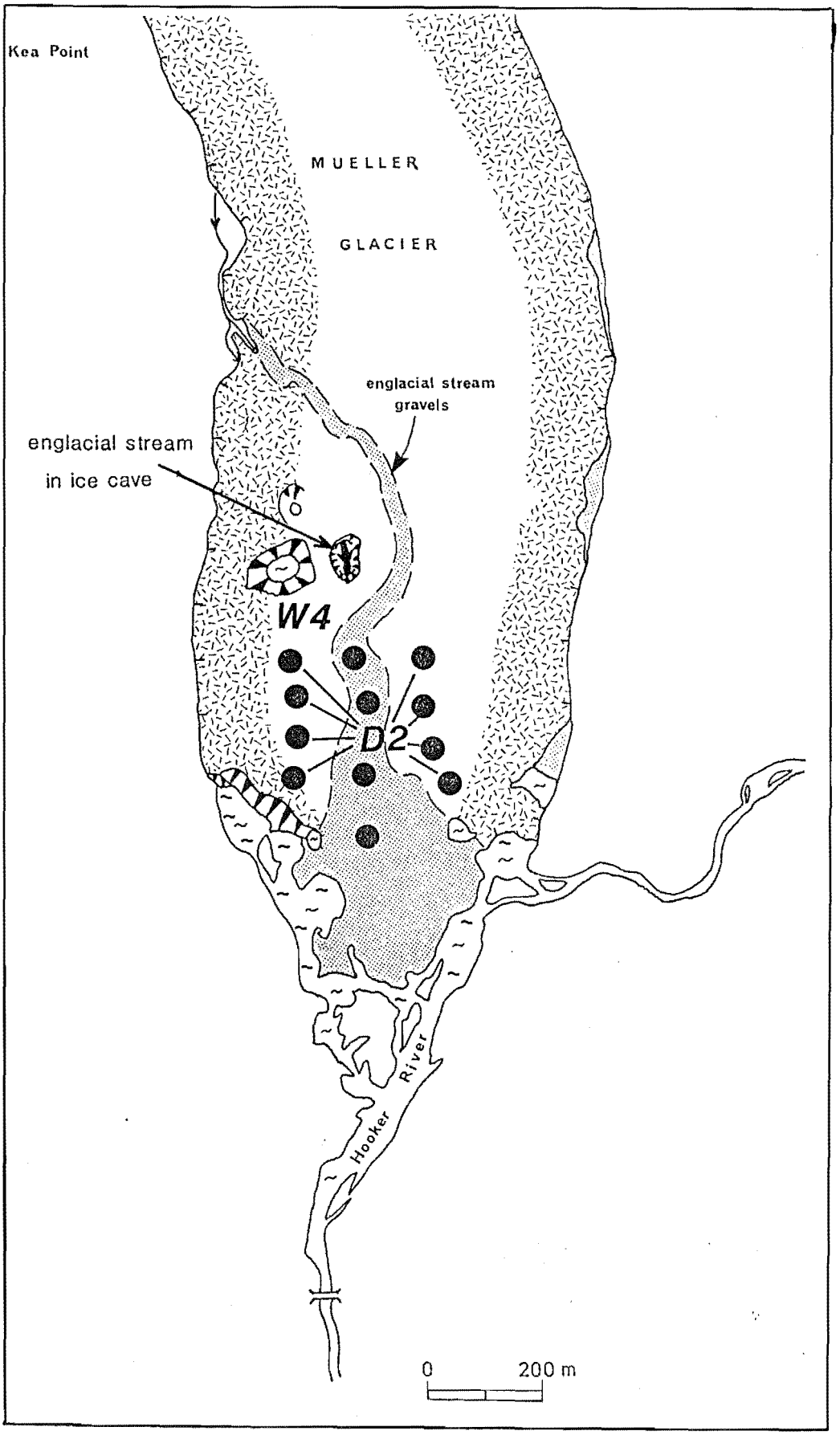

FIG. 3.32 Sample sites on the Mueller Glacier. D2 samples indicated, W4 samples located on fluvial gravels (stippled).

deposit, and in most cases more than one deposit in each category was sampled. A total of 88 samples from nine categories of deposit were measured.

Clast form description involved the measurement of the lengths of the three principal axes of each clast, here termed the a, b, and c axes respectively. Measurement was made to the nearest 5 mm, but on clasts larger than 500 mm in any axis the accuracy is estimated to be ± 25 mm. Various techniques for analysing form data have been employed in the past, primarily either simple axial ratios (eg. Sneed & Folk 1958) or a derived measure of overall sphericity (Krumbein 1941; Aschenbrenner 1956; Sneed & Folk 1958), or of a form property such as flatness (Wentworth 1922; Sneed & Folk 1958) or elongation (Sames 1966). Two measures of clast form are compared in this study.

1. Maximum projection sphericity (MPS) (Sneed & Folk 1958) gives approximately normally-distributed results, thus allowing parametric statistical analysis, is a relatively good discriminator, and is relatively uncomplicated to calculate (Barrett 1980).

2. The Sneed & Folk flatness index employed by Ballantyne (1982) concentrates on the short to long axial ratio, and therefore on the transitions from weak to strong clast forms. Despite some loss of information compared with sphericity measures, this enhances the distinctions between categories of deposits.

Particle roundness has previously been measured either by two-dimensional projections of corner geometry compared to circles of known radii (eg. Wadell 1932; Lees 1964; Barrett 1980), or by a subjective visual assessment of each particle with standard reference charts such as Krumbein (1941) and Powers (1953). The six-point chart of Powers (1953) was employed in this study for ease of data collection when dealing with a large number of samples (Fig 3.33). Roundness categories have been assigned numerical values (following Matthews & Petch 1982). The roundness scale is logarithmic, and favours discrimination at the less rounded (ie. angular) end of the scale. As such it is appropriate for sediments where angular material predominates. For consistency, the sharpest edge of any clast was used for roundness measurement and all measurements were made by a single operator.

3.4.5.2 Selection of sample sites

The criteria used to identify deposits of known genesis are indicated by Table 3.17, and the location of sample sites in Fig 3.4 and Table 3.18.

TABLE 3.18 Sample sites for form and roundness measurements.

Category	Symbol	Location	No. Samples
A). Extraglacial sites			
in situ bedrock	O	Malte Brun Range	4
in situ blockfield	B	De la Beche Ridge	4
debris-mantled slope	S	Malte Brun Range	4
rockfall talus	T	Beetham Valley	4
river gravels	W	Beetham Stream	4
B). Supraglacial sites			
rock avalanche debris	R	Rudolf Glacier	4
" " "		Tasman Glacier (De la Beche)	4
" " "		Tasman Glacier (Beetham)	4
medial moraine	M	Tasman Glacier (De la Beche)	4
" "		Tasman Glacier (Beetham)	4
" "		Rudolf Glacier	6
debris mantle	D	Tasman Glacier (Hochstetter)	4
" "		Tasman Glacier (Celmisia)	8
" "		Mueller Glacier	8
C). High-energy sites			
water-worked supra-glacial debris	W	Tasman Glacier (Langdale)	4
" " "		Tasman Glacier (Reay)	4
" " "		Mueller Glacier	4
traction-zone debris	Z	Tasman Glacier (Hochstetter)	6
" " "		Tasman Glacier (Reay)	4

Total number of sample sites.....92

CLASS	CRITERIA	ILLUSTRATION
Very Angular 1	Flat facets, "razor"-sharp facet edges	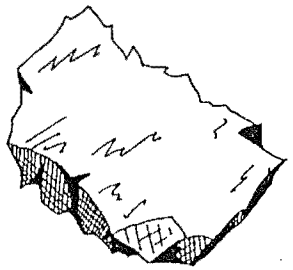
Angular 2	Flat facets, well-defined facet edges	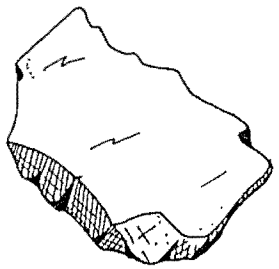
Sub Angular 3	Flat facets, blunt edges	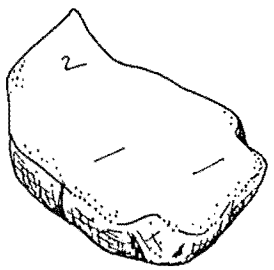
Sub Rounded 4	Blunt and rounded edges to facets	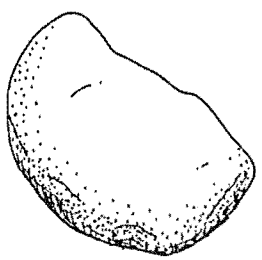
Rounded 5	Roughly-rounded clast, no distinct edges but facets still visible	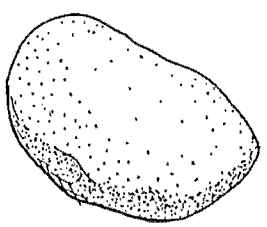
Well Rounded 6	Rounded, smooth surface, no facets or edges	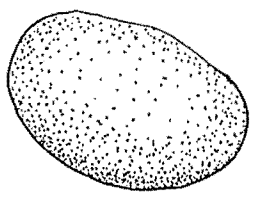

FIG. 3.33 Verbal and numerical definition of Power's roundness categories.

In most cases the interpretation of deposit genesis was straightforward. The water-worked deposits deserve further description because of the unusual supraglacial location of several samples.

On the Tasman Glacier water-worked debris occurs along the eastern margin of the glacier below the ice-free tributaries of the Malte Brun Range. The debris forms 0.25 km^2 of ice-cored mounds of moderate to poorly-sorted gravels which lack any striated clasts. The location indicates that the debris has been washed into the glacier from adjacent valleys and subsequently exposed at the glacier surface by ablation. No reference to similar deposits has been found in the literature.

Of particular interest are the Mueller Glacier samples in relation to the development of the englacial drainage system (Fig 3.32). Englacial drainage in the lower glacier occupies conduits whose base level has been controlled by a water table, defined by the moraine and outwash dam at the glacier terminus. The ice flow vectors in the lower tongue have an upward component, so that englacial conduits have been continuously migrating downwards relative to the ice in order to retain a hydraulic equilibrium. Three-dimensional avulsion and tunnel abandonment has caused a local switching of the conduit course and outlet position throughout this century. Abandoned gravel-filled conduits closed by ice flow have been exposed at the glacier surface sometime between 1906 and 1965 (from Brodrick's observations (1906) and from aerial photographs). Recently, surface lowering of the glacier has exposed the englacial stream in ice caves. Visits in 1986 and 1987 revealed discontinuous lenses and pods of rounded, stratified gravels within glacier ice at several levels above the active active channel (Fig 3.34), indicating conduit switching is of the order of several metres at a time. Samples for clast shape analysis were measured at four sites along the outcrop of the water-worked sediment.

3.4.6 Results

The shape data (Table 3.19) are presented as a roundness/form plot in Fig 3.35. Maximum projection sphericity and Ballantyne's flatness index are employed as comparative measures of form. Sphericity is found to be a relatively poor discriminator of strong and weak forms (cf Barrett 1980) because of the inclusion of the intermediate (b) axis in its calculation. By concentrating on the extreme axial lengths the flatness index highlights the differences between strong and weak forms.

FIG. 3.34 Lens of water-rounded gravel exposed in an englacial meltwater conduit in the Mueller Glacier. The lens is c.2.5 m thick and has an upglacier dip of c.25°. The matrix is granule to sand-size material.

CATEGORY	SITE	n	ROUNDNESS		SPHERICITY		c/a		% c/a < 0.4
			x	cv	x	cv	x	cv	
O	Malte Brun Range	4	1.16	0.30	0.54	0.26	0.31	0.42	77
B	De la Beche Ridge	4	1.64	0.30	0.56	0.27	0.37	0.38	73
S	Malte Brun Range	4	1.86	0.21	0.61	0.23	0.41	0.37	60
T	Beetham Valley	4	1.56	0.34	0.61	0.18	0.42	0.31	50
R1	Rudolf Glacier	4	1.71	0.27	0.62	0.21	0.41	0.36	51
R2	Tasman Glacier	4	1.64	0.30	0.59	0.24	0.37	0.41	62
R3	Tasman Glacier	4	1.62	0.30	0.64	0.20	0.43	0.35	46
M1	Tasman Gl. (Reay)	4	1.83	0.19	0.53	0.23	0.39	0.33	72
M2	Tasman Gl. (DLB)	4	1.69	0.30	0.57	0.25	0.37	0.38	54
M3	Rudolf Glacier	6	1.99	0.25	0.62	0.21	0.42	0.31	45
D1	Tasman Gl. (Hochstetter)	4	1.81	0.28	0.62	0.21	0.40	0.35	53
D2	Mueller Glacier	8	1.88	0.21	0.64	0.19	0.43	0.33	43
D3	Tasman Gl. (Celmisia)	8	1.94	0.19	0.63	0.19	0.43	0.33	48
Z1	Tasman Gl. (Hochstetter)	6	2.43	0.25	0.65	0.17	0.47	0.26	28
Z2	Tasman Gl. (Reay)	4	2.42	0.24	0.68	0.15	0.45	0.27	36
W1	Beetham Stream	4	3.29	0.21	0.68	0.16	0.47	0.28	30
W2	Tasman Gl. (Langdale)	4	2.76	0.24	0.70	0.13	0.49	0.22	18
W3	Tasman Gl. (Reay)	4	2.96		0.70	0.14	0.53	0.23	20
W4	Mueller Glacier	4	3.42	0.20	0.66	0.17	0.46	0.28	30

TABLE 3.19 Clast form properties for each sample site. n = number of samples per site. cv = co-efficient of variability (S.D./x) for each site. For explanation of deposit categories refer to Table 3.17.

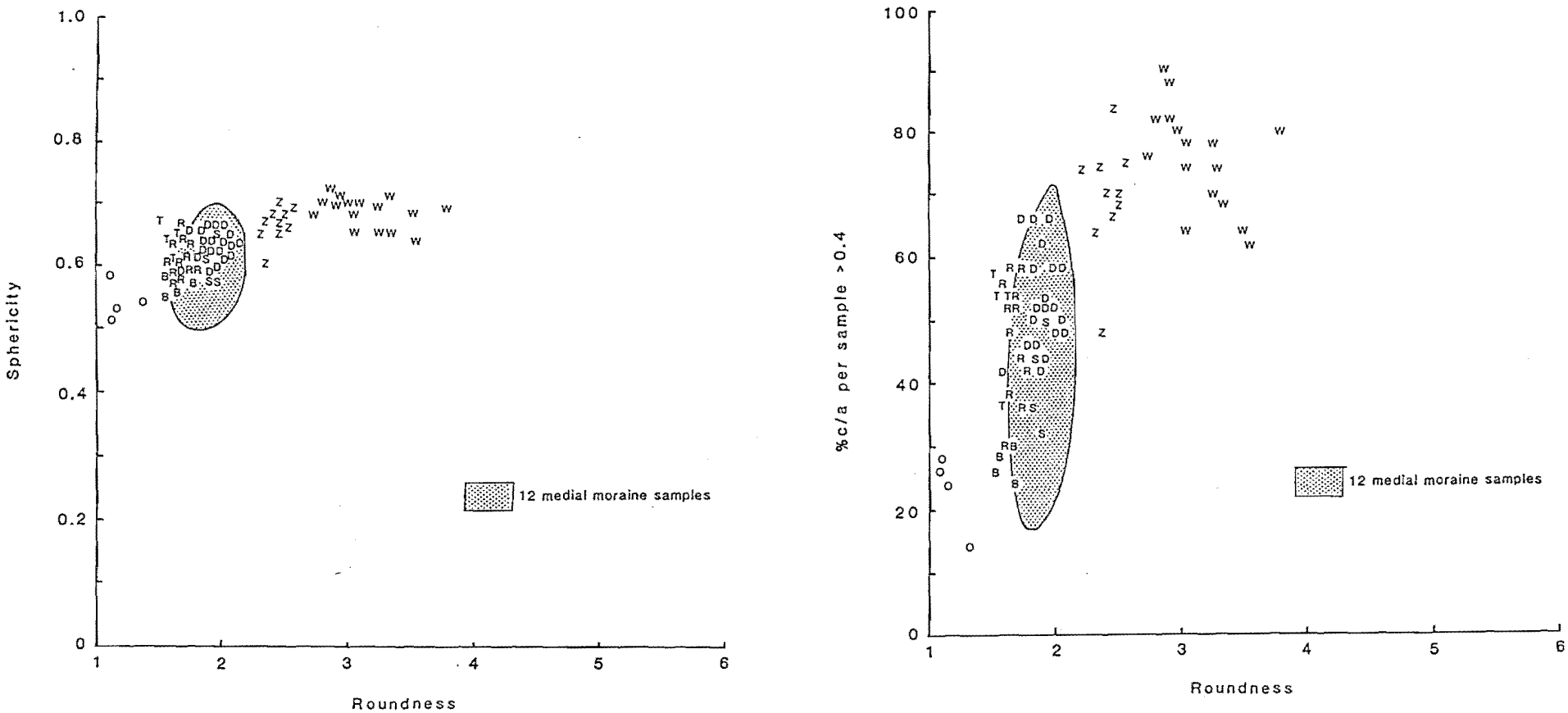

FIG. 3.35 Roundness-form plots for all 88 samples. Each letter represents a sample of 50 clasts. Shaded area represents distribution of 12 samples of 50 clasts each from medial moraines. Letters refer to deposit categories in Table 3.17. Left-hand graph: roundness-sphericity; right-hand graph: roundness-flatness.

3.4.6.1 Statistical analysis of clast shape.

For both form and roundness data, standard deviations within samples of 50 clasts are found to be greater than the variation between samples, indicating that there is a significant overlap between samples of clasts with different transport histories.

It is therefore necessary to test for statistical differences between the various categories of deposits. Samples from each site are treated as a group representative of that site, which means that any variability between samples at a site is treated as the natural variability within that category of deposit. The justification for this is that there is sufficient independent evidence for sample groupings (Table 3.17) without resorting to testing statistically for similarities within each deposit.

The means of each of the nineteen sites were tested against every other site to identify those groups of sites having similar shape properties. Barrett (1980) found that maximum projection sphericity measurements approximate to a normal distribution, allowing the parametric two-sample t-test to be employed. Both the flatness and roundness data (Fig 3.36) show skewed frequency distributions, so the non-parametric Mann-Whitney U-test is used to analyse these properties. The results of the tests are presented in matrix form in Tables 3.20 to 3.22. Groups of similar sites are indicated graphically in Figure 3.37 at the 0.05 significance level.

3.4.6.2 Clast shape characteristics of deposit categories.

Clast shapes may be described as varying from "primary" shapes through "immature" and into "mature" shapes, depending on the degree of modification compared to unweathered clasts picked out of bedrock outcrops. Several generalisations about the shape properties of different deposits may be made.

"Extraglacial" samples

Outcrop samples are the most immature. Generally very angular clasts are found and weak forms predominate (>70% of clasts have a c/a ratio of <0.4).

Blockfield samples differ from outcrop samples only in their slightly greater rounding due to granular disintegration. No change in clast form occurs.

The downslope creep of debris on slopes of 20-30^{o} significantly reduces the proportion of weak forms in some samples. Form remains rather variable nevertheless.

O	T	R3	R2	B	M2	R1	D1	M1	S	D2	D3	M3	Z2	Z1	W2	W3	W1	W4
O	.05	.05	.05	.05	.05	.05	.05	.05	.05	.01	.01	.01	.05	.01	.05	.05	.05	.05
	T	-	-	-	.10	.05	.05	.01	.05	.01	.01	.01	.05	.01	.05	.05	.05	.05
		R3	-	-	-	-	.05	.01	.05	.01	.01	.01	.05	.01	.05	.05	.05	.05
			R2	-	-	-	-	.01	.05	.01	.01	.01	.05	.01	.05	.05	.05	.05
				B	-	-	-	.01	.05	.01	.01	.01	.05	.01	.05	.05	.05	.05
					M2	-	-	.01	.05	.01	.01	.01	.05	.01	.05	.05	.05	.05
						R1	-	-	.05	.02	.01	.01	.05	.01	.05	.05	.05	.05
							D1	-	-	-	-	.01	.05	.01	.05	.05	.05	.05
								M1	-	-	-	-	.05	.01	.05	.05	.05	.05
									S	-	-	.01	.05	.01	.05	.05	.05	.05
										D2	-	.05	.01	.01	.01	.01	.01	.01
											D3	-	.01	.01	.01	.01	.01	.01
												M3	.01	.01	.01	.01	.01	.01
													Z2	-	.05	.05	.05	.05
														Z1	.01	.01	.01	.01
															W2	-	.05	.05
																W3	.10	.05
																	W1	-
																		W4

TABLE 3.20

Matrix of significance levels of differences in roundness between sample sites.

Letters refer to site locations (Fig $\frac{3.18}{\lambda}$) arranged in rank order.

O	B	M1	R2	S	M2	D1	R1	T	D3	R3	M3	D2	Z2	W1	W4	Z1	W3	W2
O	-	.05	.05	.05	.05	.05	.05	.05	.01	.05	.01	.01	.05	.05	.05	.01	.05	.05
	B	-	.10	.05	.05	.05	.05	.05	.01	.05	.01	.05	.05	.05	.05	.01	.05	.05
		M1	-	-	-	.10	-	.10	.10	.05	.10	.10	.05	.05	.05	.01	.05	.05
			R2	-	-	-	-	-	.05	.05	.01	.01	.05	.05	.05	.01	.05	.05
				S	-	-	-	-	.10	.05	.01	.02	.10	.05	.05	.01	.05	.05
					M2	-	-	-	-	-	-	-	.10	.05	.05	.01	.05	.05
						D1	-	-	-	-	-	-	-	.05	.05	.05	.05	.05
							R1	-	-	-	-	-	-	.05	.05	.01	.05	.05
								T	-	-	-	-	-	.05	.05	.01	.05	.05
									D3	-	-	-	-	.02	.01	.01	.01	.01
										R3	-	-	-	.05	.05	.01	.05	.05
											M3	-	-	.05	.10	.02	.01	.01
												D2	-	.05	.05	.01	.01	.01
													Z2	-	-	-	.10	.05
														W1	-	-	-	.10
															W4	-	-	.10
																Z1	-	.10
																	W3	-
																		W2

TABLE 3.21

Matrix of significance levels of differences in flatness index between sample sites.

Letters refer to site locations (Fig 3.18) arranged in rank order.

O	M1	B	M2	R2	S	R1	D1	D3	M3	R3	D2	T	Z2	W4	Z1	W1	W2	W3
O	-	-	-	.20	.10	.05	.05		.01	.02	.01	.01	.02		.01	.01	.01	.01
	M1	-	-	.20	.10	.05	.05		.01	.02	.01	.01	.01		.01	.01	.01	.01
		B	-	-	.01	.10	.10		.05	.05	.10	.01	.02		.01	.01	.01	.01
			M2	-	-	.20	.20		.05	.05	.10	.05	.02		.01	.01	.01	.01
				R2	-	-	-		.20	.20	-	.10	.05		.01	.01	.01	.01
					S	-	-		-	-	-	-	.20		.05	.05	.01	.01
						R1	-		-	-	-	-	.20		.05	.05	.01	.01
							D1		-	-	-	-	-		.10	.05	.02	.02
								D3										
									M3	-	-	-	-		.20	.20	.05	.05
										R3	-	-	-		.20	.20	.05	.05
											D2	-	-		.10	.05	.01	.01
												T	-		.20	.20	.05	.05
													Z2		-	-	.10	.10
														W4				
															Z1	-	-	-
																W1	-	-
																	W2	-
																		W3

TABLE 3.22

Matrix of significance levels of differences in sphericity between sample sites.

Letters refer to site locations (Fig 3.18) arranged in rank order.

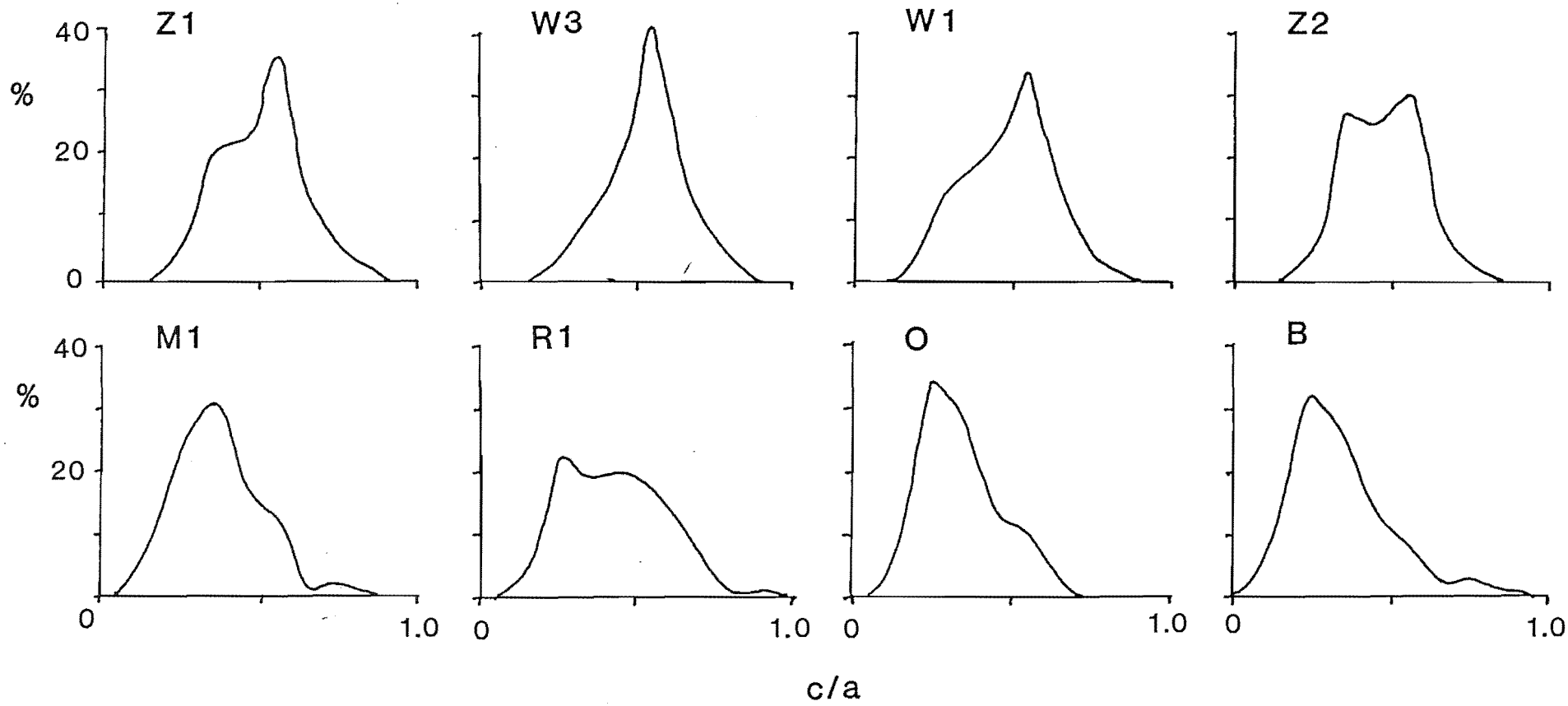

FIG. 3.36 Frequency distributions for c/a values of 8 selected samples of 50 clasts. For sample codes, see Table 3.17. The upper row shows approximately normal distributions characteristic of debris from high-energy transport, the lower row skewed distributions characteristic of relatively immature debris.

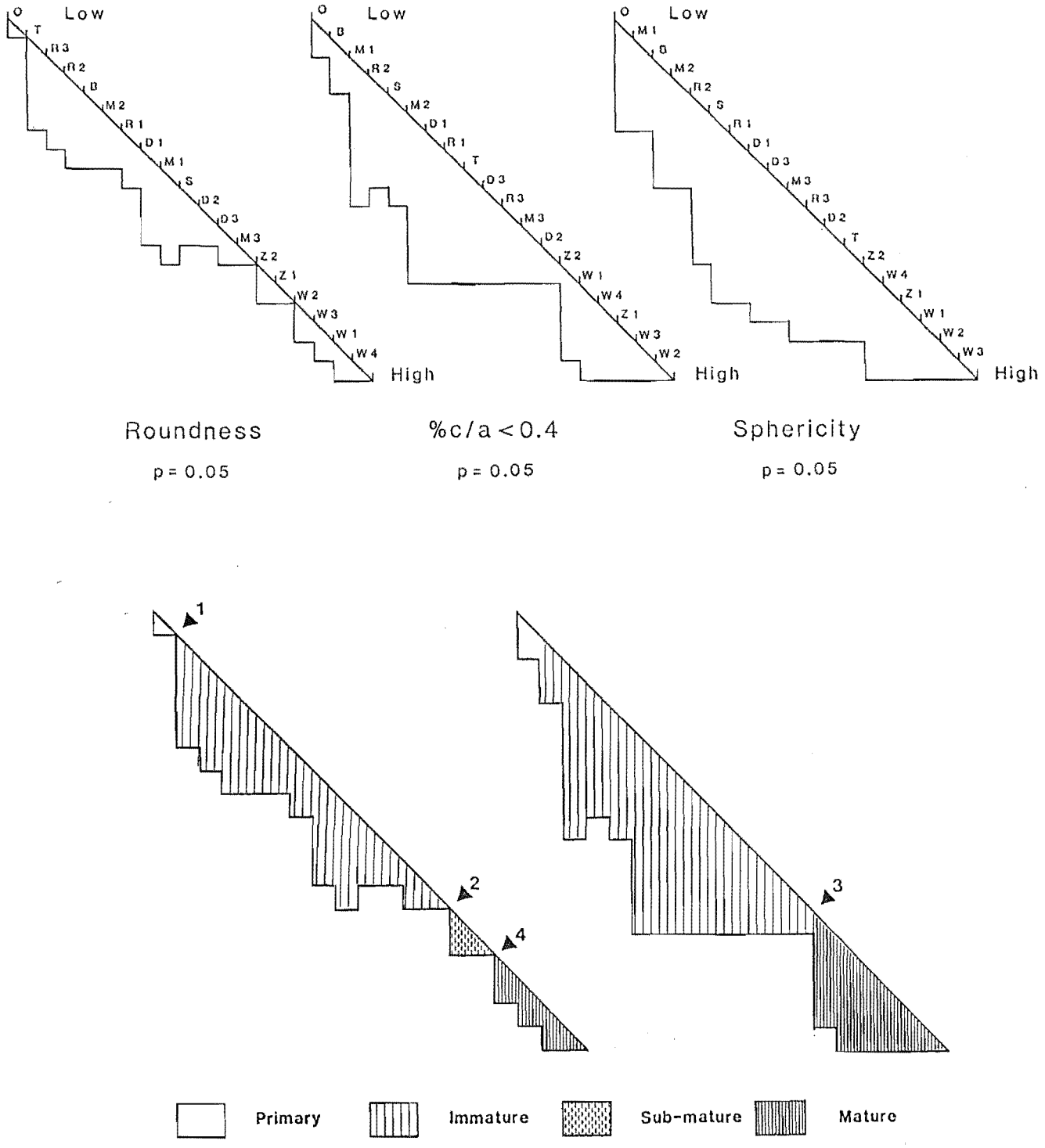

FIG. 3.37 Upper diagram: similarity diagrams for the 19 deposits sampled. Codes refer to site codes in Table 3.17 and sites are arranged in rank order. Each vertical bar links sample sites which are statistically indistinguishable at the given significance level (0.05).

Lower diagram: Interpretation of hiatuses in the similarity diagrams for Roundness and % c/a<0.4, in terms of clast shape maturity.

Talus samples show a significant reduction in weak forms (50% <0.4 c/a) but significant variation exists between samples, possibly due to less fracturing of rockfalls falling onto soft snow instead of hard talus in winter. No difference in roundness exists compared to other extraglacial categories.

"Glacial" samples

Rock avalanches, medial moraines and debris mantle samples all show similar characteristics of variable form and low roundness. All three represent different stages along the supraglacial transport pathway (Boulton & Eyles 1979:Fig 1). Minor differences are the slightly lower roundness of the relatively young rock avalanches and the reduction in the proportion of weak forms in the debris mantle. The greater age of the debris mantle samples compared to the medial moraines and rock avalanches suggests that either macrogelivation and/or corrasion within the debris mantle progressively destroys weaker forms.

Traction zone debris is significantly more rounded and devoid of weak forms compared to samples from high level transport zones, confirming the findings of previous researchers (Reheis 1975; Boulton 1978; Boulton & Eyles 1979; Ballantyne 1982). Traction-zone debris appears to be modified very rapidly and in terms of shape is distinct from all other categories except fluvially-worked debris. The presence of glacial striations on clasts is diagnostic of traction at the glacier sole, and distinguishes subglacial from fluvially-transported debris.

"Fluvial" samples

Water-worked debris has significantly greater rounding than traction zone debris. However, shape distinctions between the two may not be clear in all cases. Rounding occurs very rapidly (within one year) after clasts reach river channels. This is shown by the small amount of immature debris in seasonal supraglacial streams, and the rapid rounding of talus-derived clasts in Beetham Stream. No distinction can be made between debris washed into the glaciers (sample W1) and debris washed through the glaciers (samples W2 to W4).

Regression of form against roundness (Fig 3.38) gives a higher correlation co-efficient for a log-linear relationship than for a linear relationship. The correlation is highly significant ($p = 0.01$). The indication is that immature debris (predominantly low roundness and weak forms) is susceptible more to the modification of form rather than of roundness; the more mature the shape becomes, the more susceptible is roundness to modification than form. The regression is not used to infer

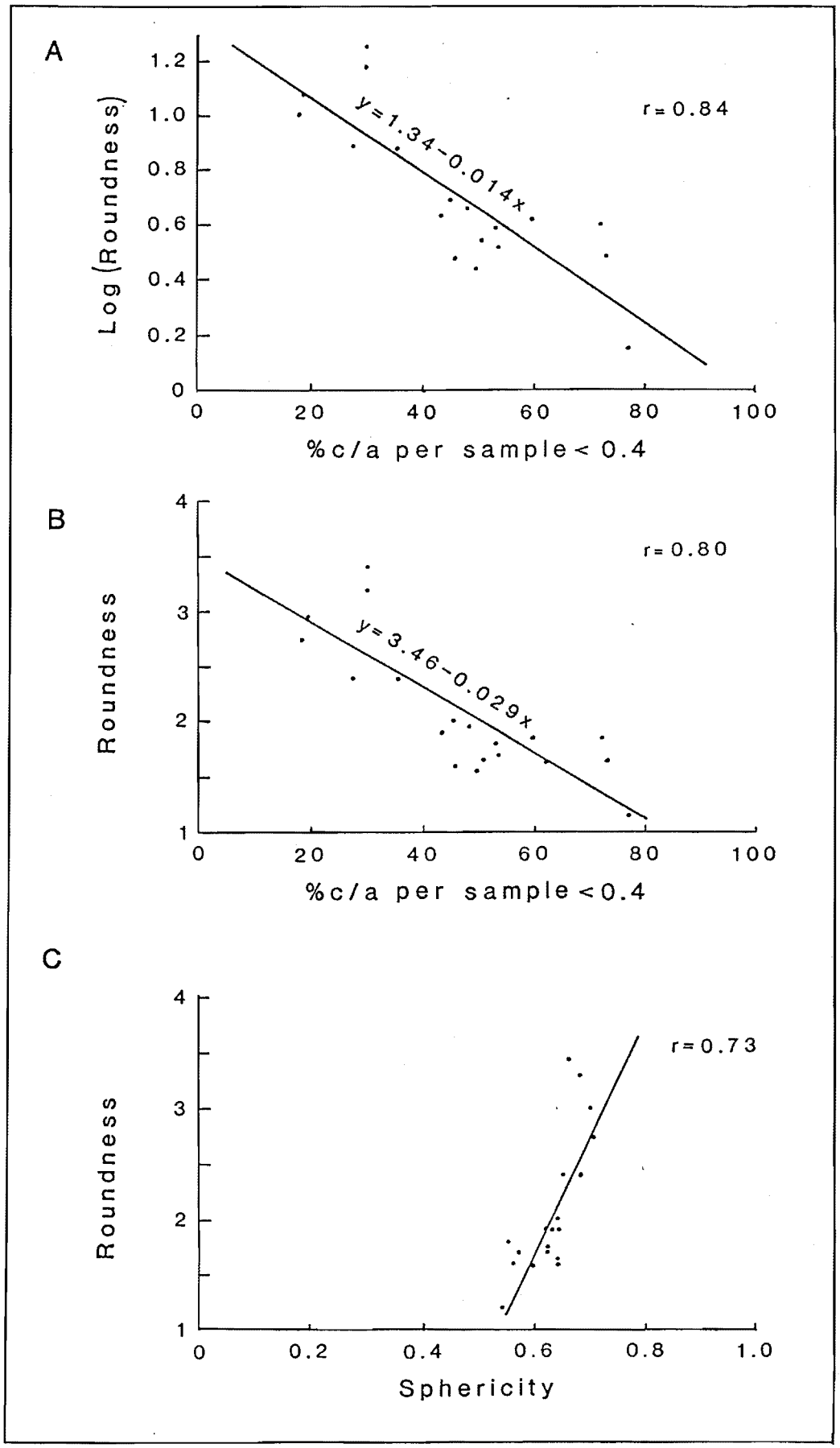

FIG. 3.38 Co-variance of clast roundness with different form properties for the 19 deposits sampled.

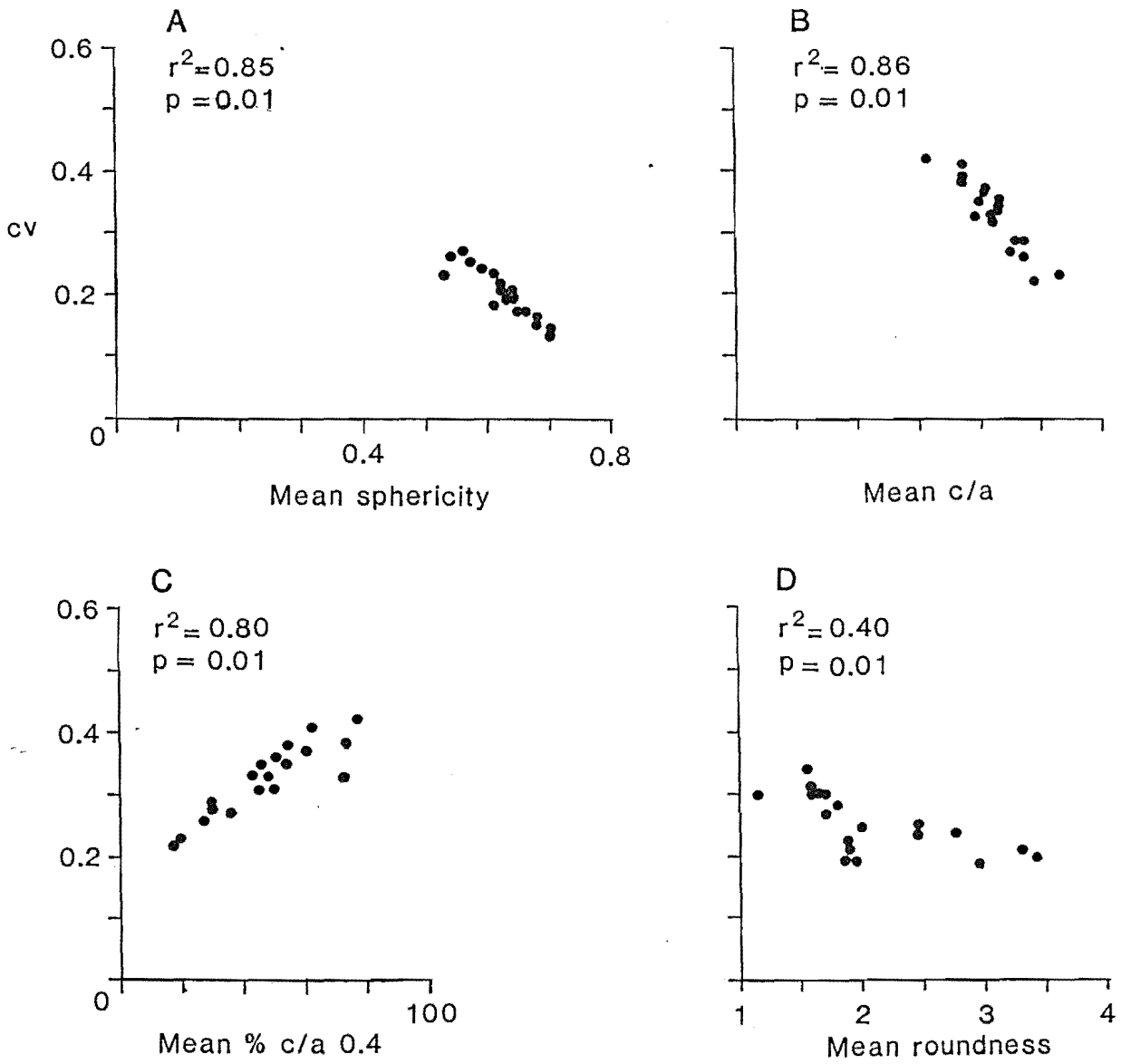

FIG. 3.39 Regression of co-efficients of variability against four clast shape properties for the 19 deposits sampled. Each dot represents between 4 and 8 samples of 50 clasts.

any causal relationship between the two variables and their independence is re-emphasised.

The variability of shapes within a sample is dependent on the degree of maturity of the deposit. Highly significant relationships exist between mean site sphericity and the mean site c/a ratio and their respective co-efficients of variability (Fig 3.39 A and B) Similarly, the proportion of clasts at each site with c/a < 0.4 systematically declines as the mean c/a ratio decreases (Fig 3.39 C). These relationships indicate that as shape maturity increases, the proportion of weak forms is systematically reduced and the deposits become increasingly shape-sorted.

A similar though weaker trend is evident in the roundness-variability graph (Fig 3.39 D). The scatter of points reflects processes operating at all stages of shape maturity that are variable in their effect on roundness. For example, fracture occurs throughout the transport system and reduces roundness, even in fluvial samples. The application of Powers' roundness scale to the sharpest edge of any clast probably contributes to the observed within-sample variability.

3.4.7 Interpretation

The shape properties presented in Table 3.19 and Fig 3.35 indicate general similarities between extraglacial and supraglacial samples and between subglacial and fluvial samples. This finding agrees with the accepted distinction between subglacially-transported and supraglacially-transported debris. However the traditional distinction between "glacial" and "non-glacial" debris implicitly assumes that supra-and englacial sediment volumes are minor compared to subglacial debris, so that "glacial" and "subglacial" debris have previously been used synonymously. The estimated sediment discharges at several glacier termini (Eyles 1979) supports this assumption for glaciers with few supraglacial debris sources.

This is not the case in the Tasman and Mueller Glaciers. The abundance of debris within the high-level transport zones (sensu Boulton 1978) provides a huge volume of debris on which water and frost can act to produce a wide range of clast shapes in high-level transport. This blurs the distinction between clasts of "glacial" and "non-glacial" origins in wet, debris-rich glaciers where a significant proportion of debris (much of it rounded) which is ultimately deposited at the glacier margins has never been in subglacial traction.

Furthermore, no assessment of the importance of shape-modifying

processes is possible without considering their distribution in space and in time. Observations of shape-modifying processes have shown that these vary in both their operational timescale (gradual versus episodic action) and in their spatial extent (compare the ubiquity of granular disintegration with the spatially-restricted distribution of water-worked sediment). A paradigm is needed which accounts for these considerations.

A cascading system approach (Chorley & Kennedy 1971) is adopted to describe the complexities of sediment dynamics in an appropriate way. The static representation of form-roundness fields (Fig 3.35) is converted to a dynamic system of clast shape evolution (Fig 3.40) by treating the roundness-form fields as subsystems separated by cascades, or thresholds. Changes in clast shape therefore have a direction with respect to shape thresholds and **maturity**, and only indirectly with respect to location and time. An advantage of this approach is that it allows for mature shapes to be attained very early during debris transport, but immature shapes may persist over long time periods and/or distances.

Each cascade represents a process transition reflected by an overall shape change. The corollary is that each subsystem (the roundness-form fields in Fig 3.35) is defined by the range of shapes a given process or combination of processes can produce. By substitution of observed spatial changes in clast shape by time, transport pathways through the valley and shape evolution can be interpreted. Major cascades are identified by the hiatuses in the statistical similarity between sample sites (Fig 3.37), and are used to define the shape fields (subsystems) in Fig 3.40.

Four cascades are recognised. Three occur with respect to clast roundness and one with respect to clast form. The relationships of these cascades to modifying processes are as follows.

1st Cascade

This represents the very rapid transition from primary (joint-bounded) shapes to sub-aerially weathered clasts showing some rounding. Primary shapes display a variety of forms which reflect variations in three-dimensional joint geometry, but roundness is initially minimal and highly sensitive to microgelivation over a period of a few years.

2nd Cascade

A second cascade marks the limit of rounding which is acheived by granular disintegration. The subsystem between the first and second cascade (here defining immature shapes) has a limited range of roundness because of the lack of an effective modifying process. Apart from microgelivation, fracture processes (fall shattering and macrogelivation)

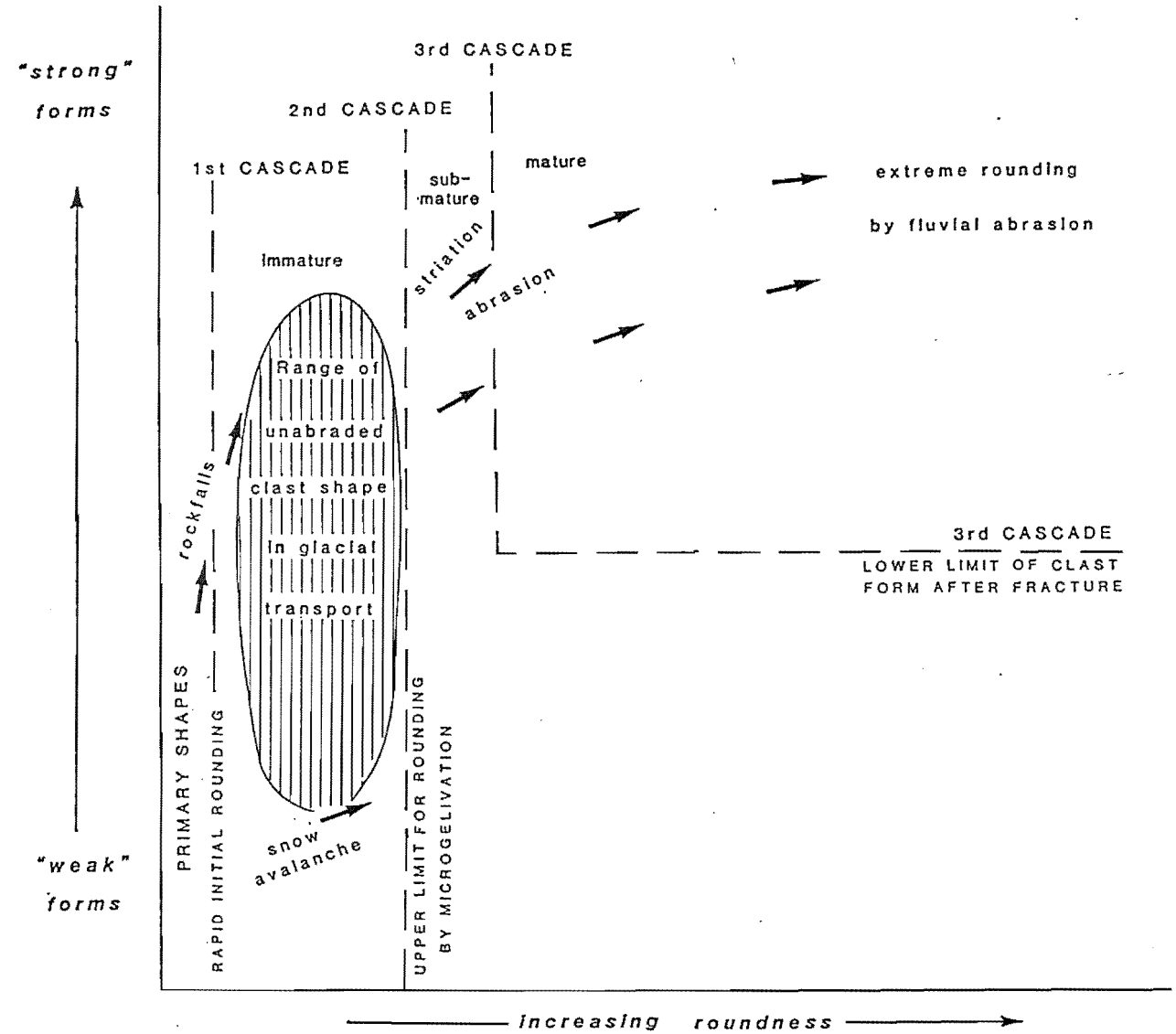

FIG. 3.40 Interpretation of roundness-form plots as a cascading system of transport histories and clast shape evolution.

dominate in this subsystem to produce the wide range of forms. Above the second cascade abrasive wear causes greater rounding and defines one boundary of the sub-mature subsystem.

3rd Cascade

The third cascade separates unabraded from abraded clasts and represents a form transition. Weak forms which occurred below this cascade are largely absent above it, indicating that any debris finding its way into the sub-glacial traction zone or into riverbeds is rapidly fractured and weak forms are destroyed. Pre-existing strong forms are less affected by the process transition across it.

4th Cascade

A threshold between the roundness acheivable by glacial abrasion and that achievable by fluvial abrasion defines the boundary between the sub-mature and mature subsystems. The maximum roundness in the sub-mature subsystem is interpreted as the effect on mean roundness of the competing effects of subglacial abrasion, which increases roundness, and cyclic fracture creating sharp edges (cf Drake 1972). Thus, glacial abrasion may be as effective a process as fluvial abrasion, but the rounding of traction-zone clasts is retarded to a greater extent by fracture than is the rounding of fluvially-transported debris. This cascade may not exist where sub-glacial transport has been over longer distances than has occured in the study area and more mature shapes may have developed.

3.4.8 Discussion: implications for till composition.

This study has so far interpreted clast shapes and their modifying processes as forming a cascading system. The following discussion considers the fluxes of debris of particular shape properties through the glacier in order to understand the relative importance of different transport processes.

Sedimentological maps of the debris mantles of the Tasman and Mueller Glaciers show that water-rounded debris covers <1% of the area of the Tasman debris mantle and <10% of that of the Mueller Glacier. Rounded debris is linearly distributed along conduit locations and medial moraines, in contrast to areally-distributed immature debris.

However, the flux of coarse mature debris is likely to account for a considerable proportion of the total debris flux. For example, the supraglacial debris discharge through the Celmisia Flat transect was 1700 m^3a^{-1} in 1986 (Chapter 3). For the debris discharge in englacial conduits to equal the supraglacial flux, only 4.7 m^3d^{-1} of coarse debris is

required to be carried in conduits through the transect. This amount would be concentrated in short periods of high water discharges, especially during heavy rainstorms. For example, 20 days in the year on which 85 m^3 crossed the transect in conduits would produce the required flux. Such a figure is considered possible given the size of the glacier, the abundance of available debris, and the availability of flowing water from ablation (Chapter 2) and rainfall (Griffiths & McSaveney 1983).

An important implication of this conclusion is that the composition of tills and moraines deposited marginal to very "wet" debris-rich glaciers will reflect the abundance of water-worked debris within the glacier. Several studies have described moraines containing much rounded debris which has variously been ascribed to the bulldozing of proglacial sediments (Slatt 1971) or to the deposition of subglacially-transported material (Matthews & Petch 1982; Serebyanny & Orlov 1982; Vere & Matthews 1986; Matthews 1987). Whilst these studies may well be correct in their interpretations, the possibility that water rounding in englacial and supraglacial locations may explain the observed distribution of rounded material has not been considered by the respective authors.

It has been suggested, on the basis of lithological provenance, that up to 90 % of the debris delivered to the terminal moraines of Alaskan valley glaciers may have been fluvially transported through the glacier from ice-free tributary valleys (Evenson & Clinch 1987). Hooke et al (1985) found that 95 % of the debris discharge in Bondhusbreen, Norway, is by water travelling through subglacial conduits. Only 5 % is transported in the basal transport zone of the glacier. Together with the findings of this study, this raises questions about the role of the glacier in terms of clast shape evolution in particular and of the sediment transport system in general. Although little rounded debris is usually visible in or on glacier tongues, consideration of the possible discharge of such debris has shown that even small amounts may reflect the dominance of water (rather than ice) as the major transporting medium in the distal reaches of the Tasman Glacier.

An important difference between the Alaskan case study and the New Zealand glaciers is that the latter have fewer and smaller ice-free valleys providing sources for pre-rounded material. Much of the rounded debris within the Mount Cook glaciers must originate from the reworking by water of the rockfall and rock avalanche-derived debris of the debris mantles. In such a case, the glacier tongue plays a significant though passive role as a reservoir for sediment eroded off mountain slopes. The

debris is concentrated in the distal part of the glacier via the high and low-level transport paths and is thus made available for reworking by ephemeral but powerful streams. The sharp transition from immature to mature forms across the break of slope between the terminal moraine of the Tasman Glacier and the outwash surface (FigM1) indicates that mature forms were transported out of englacial conduits rather than acquiring their form in the few metres distance from the glacier front.

The proportion of water-worked debris visibly increases downglacier in both the study glaciers. This suggests an alternative explanation of the distally-increasing proportion of rounded debris in Norwegian Neoglacial moraines (Matthews & Petch 1982). It is possible that this roundness "gradient" may reflect (in part at least) englacial water action, a possibility not considered by the authors. Similarly, the increase in rounded material in recent moraines at lower altitudes in the Jotunheim (Matthews 1987) may reflect the increased discharge of rain and meltwater in marginal englacial and supraglacial positions.

In summary, the evidence that this study presents indicates that the reworking of debris by water within the high-level transport zones of the glaciers is a significant process in determining the texture of proglacial deposits. Pre-rounding in this manner may explain observed variations in roundness in moraines reported in the literature. Ancient tills composed of a mixture of mature and immature clast shapes may therefore be diagnostic of a very wet, debris-rich glacial environment as well as allowing a sedimentological distinction to be made between till and rock avalanche deposits in such environments.

3.4.9 Conclusions

1. Significant modifications to clast shape occur during transport due to processes which are highly variable in their operational timescale and spatial extent.

2. Significant changes in shape tend to be episodic and localised, therefore shape evolution may appropriately be represented by a cascading system.

3. Clast form evolves to its maximum extent at a lower level of shape maturity than roundness. Form is a sensitive measure in less mature deposits and roundness is more sensitive in mature deposits. However each reflects separate processes and which aspect of shape is employed depends on the particular objectives of a study.

4. As maturity increases, the variability of clast shapes in a deposit

is reduced and shape sorting occurs. This is especially evident for clast form.

5. In the glaciers of the Southern Alps, the areal abundance of debris of given shape characteristics is not a reliable indicator of the flux of each type. The relative fluxes of mature and immature debris within a catchment must be understood, if only qualitatively, in order to understand the shape composition of glaciogenic deposits. Much rounded material in tills has been modified by water action during supraglacial and/or englacial transport.

CHAPTER 4: THE ORIGIN, SIGNIFICANCE AND DESTRUCTION OF SUPRAGLACIAL DEBRIS MANTLE WITH PARTICULAR REFERENCE TO THE TASMAN GLACIER

Chapters 2 and 3 were concerned with the glaciology and debris transport of the Tasman Glacier as a whole. Chapter 4 is a detailed investigation of factors favouring debris mantle formation, and of the effect of the mantle on the Tasman Glacier since 1890. Attention is focused on the dynamics of debris mantle formation and how debris mantles have influenced the nature of glacier retreat in the study area.

Information on glacier dynamics and debris transport, from Chapters 2 and 3, are applied to the specific case of the lower Tasman Glacier. Comparisons are made with other debris-mantled and unmantled glaciers in New Zealand, Europe and the Himalaya.

The aims of the chapter are:

1. to identify the environmental conditions which favour the growth and maintenance of supraglacial debris mantles in general;

2. to describe and model the relationships between the debris layer and the glacier beneath, in terms of the rates and distribution of ablation and the changes in glacier flow, and;

3. To determine the effects of the Tasman Glacier debris mantle on the mechanisms of glacier wastage during negative mass balance.

4.1 THE FORMATION OF SUPRAGLACIAL DEBRIS MANTLES

4.1.1 Physiography of debris-mantled glacier catchments.

The variety of different types of supraglacial debris mantles has been reviewed in Chapter 1.4. It was concluded that there is no clear distinction between debris-mantled and unmantled glaciers. A continuum of forms exists from glaciers whose ablation zones are almost entirely covered with rock debris to those with little or no supraglacial debris. Intermediate forms include all those glaciers with medial moraines which coalesce at a variety of distances above the terminus. Debris mantles originating as a single rock avalanche are yet another type, in which the debris cover is transient and is eventually deposited at the glacier terminus.

To identify environmental factors favouring debris mantle formation, it is necessary to examine the extremes of the continuum where characteristic features are best displayed. For the purposes of this

section, a distinction is made between debris-mantled and unmantled glaciers. Consideration of glaciers which represent end-members of the continuum indicates that two variables distinguish the two glacier types.

4.1.1.1. Source area relief.

Heavily debris-mantled glaciers share a common characteristic of high relative relief between the glacier accumulation zone and the general level of the surrounding ridge crests (Fig 4.1; Ogilvie 1904; Vivian 1975; Ellis & Calkin 1983; Gordon & Birnie 1986). Most debris mantles in the Mount Cook area are fed by frequent above-firn-line rockfalls (Chapter 3.1), so that as a first approximation the occurrence of a debris mantle is a function of the input and discharge of debris through the glacier. The long-profiles of glaciers suggest that debris-mantled termini are associated with a source-area relief of >700m.

4.1.1.2. Glacier long profile.

Fig 4.1 reveals a contrast between long profiles of debris-mantled and unmantled valley glaciers. Mantled glaciers all have concave long profiles, and by inference these glaciers have steep velocity gradients and strongly-compressive flow in their ablation zones. Unmantled glaciers typically have straight to convex profiles which result in a much lower velocity gradient and less compression in the lower tongue. Surface gradients in the ablation zone are generally less on debris-mantled glaciers than on unmantled glaciers. Compression is significant because greater longitudinal strain rates aid debris emergence (Section 4.1.4).

A graph of source area relief against debris-covered area (Fig 4.2) clearly separates the two types of glacier. Data from several glaciers outside New Zealand are included in Figs 4.1 and 4.2 to supplement the information from the study area. Within the debris-mantled group there is no relationship between the two variables due to the complexities of the flow structures and transport paths within individual glaciers. The omission of intermediate forms also contributes to the clear separation of the two glacier types.

The Glacier Blanc and Glacier Noir of the Dauphine Alps, France (Vivian 1975: p.146 and Fig 4.3), show a similar situation to the Westland glaciers. Here, debris-mantled and unmantled glaciers, with contrasting long-profiles, occur in adjacent valleys. There is no regional distinction between the two types of glacier, suggesting that the occurrence of debris mantles is not primarily controlled by a climatic effect. McSaveney (1975:

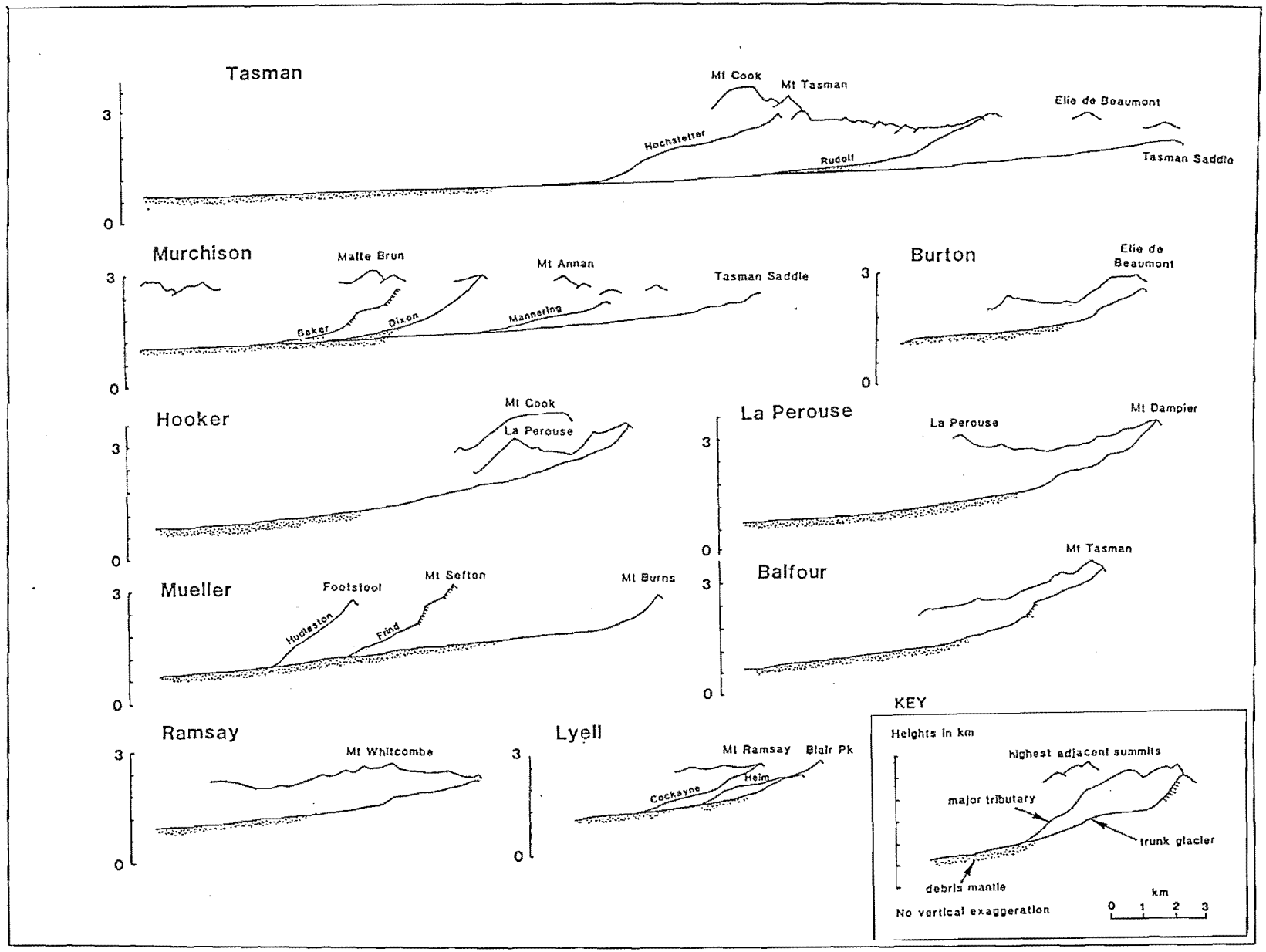

FIG. 4.1 Long-profiles of debris-mantled valley glaciers in the central Southern Alps. All drawn to same scale with no vertical exaggeration.

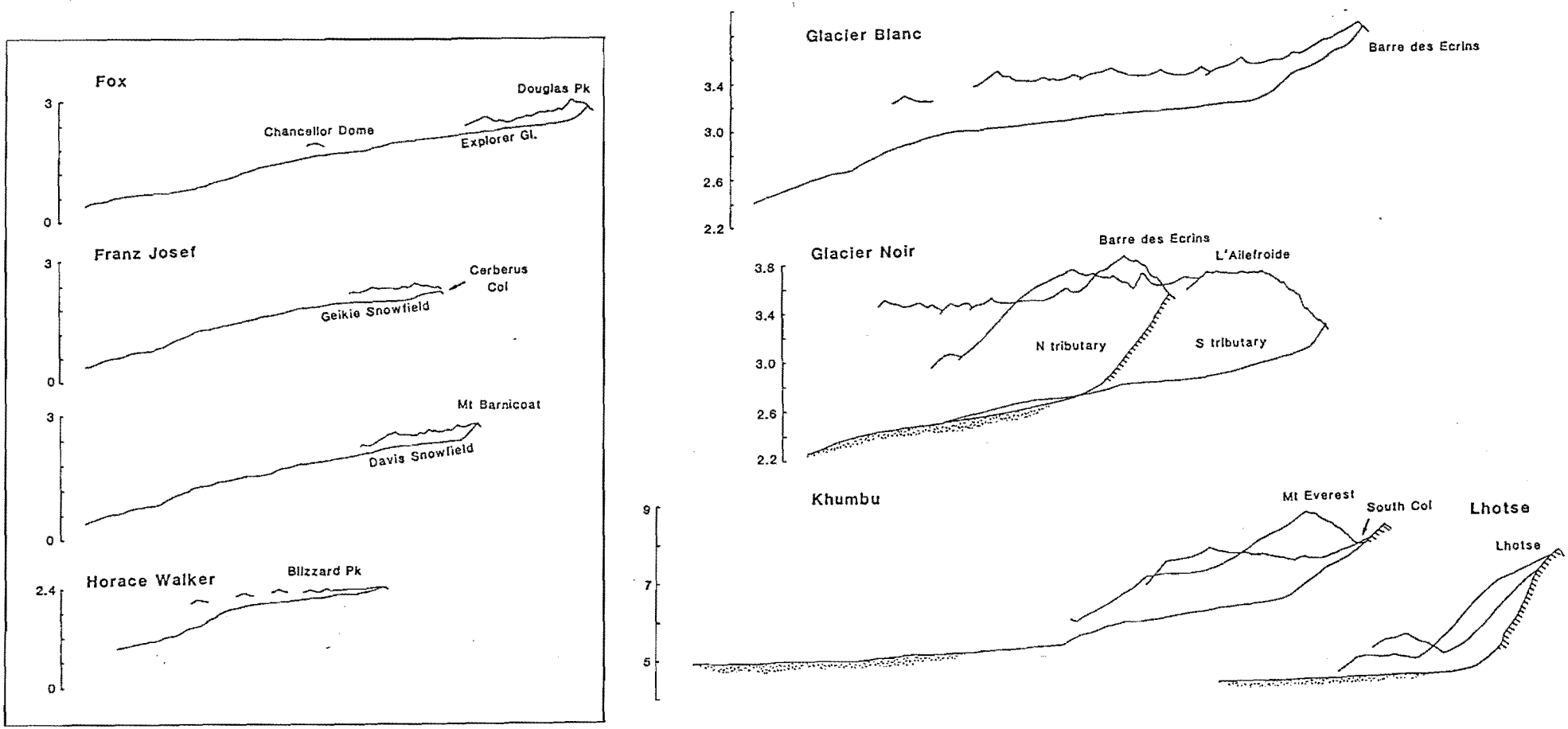

FIG. 4.1 (continued). (A) Long-profiles of glaciers with no debris mantles in the central Southern Alps. (B) Long-profiles of glaciers in the Dauphiné Alps, France (top) and the Khumbu region of Nepal (bottom). Note differences in scale between each group.

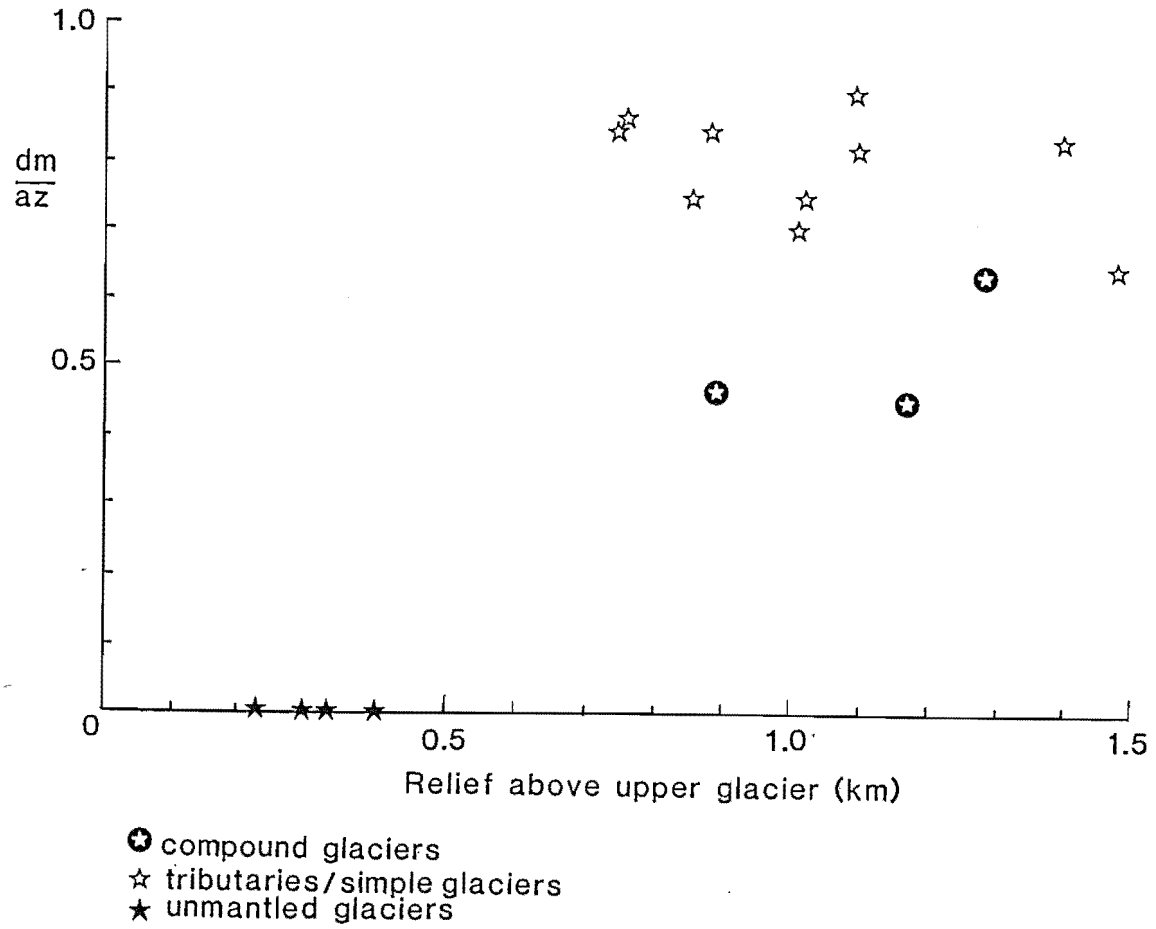

FIG. 4.2 Graph differentiating debris-mantled and unmantled glaciers on the basis of relief of surrounding ridges above accumulation zones (x-axis) and the ratio of the length of the debris-mantled tongue, dm, to the whole ablation zone, az, (y-axis).

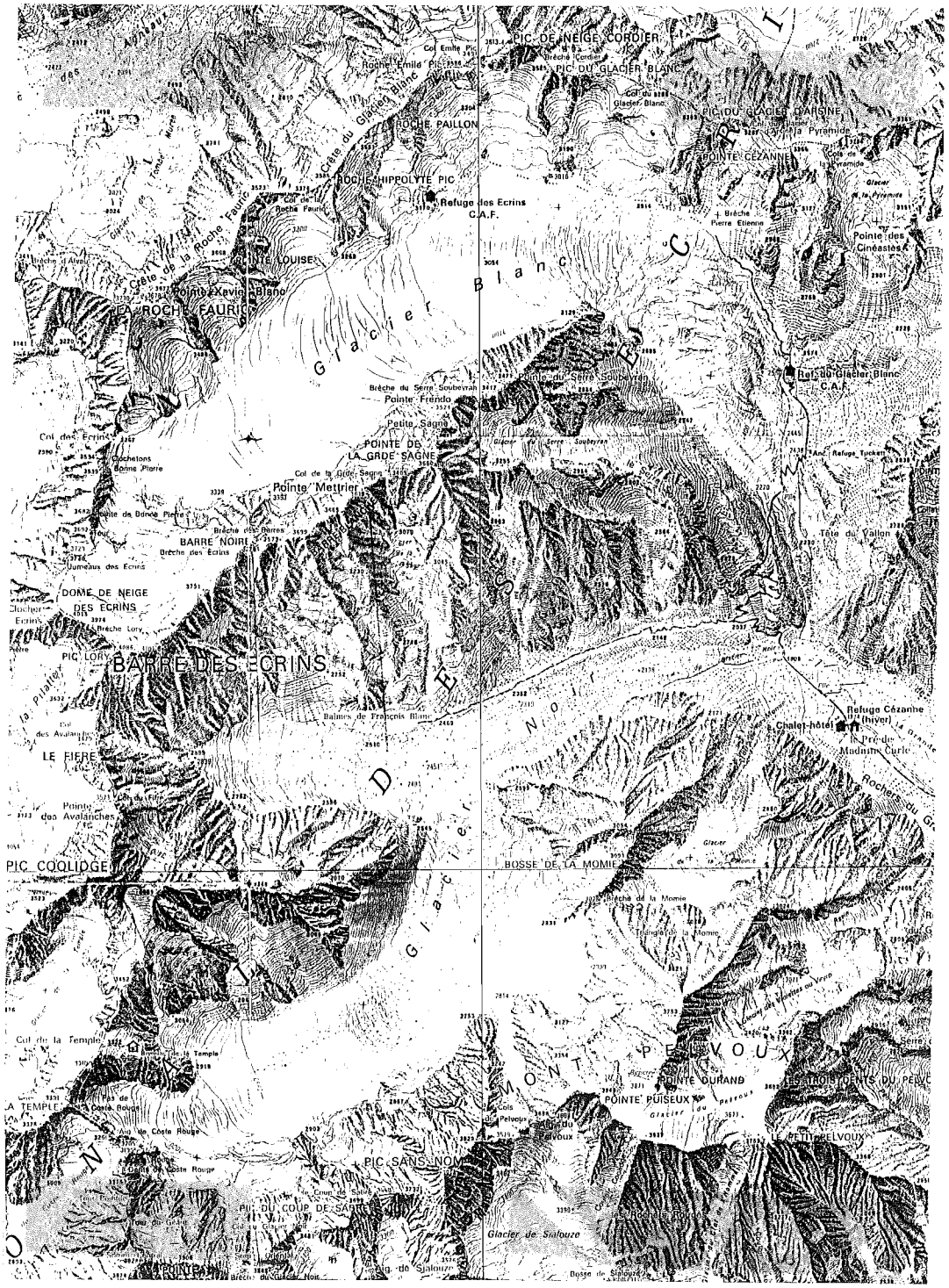

FIG. 4.3 Extract from Institut Geographique National Carte Touristique Sheet 241 (Massif des Ecrins, original scale 1 : 25,000) of the Dauphiné Alps, France. Note the contrasting relief of the accumulation zones of the debris-mantled Glacier Noir and the unmantled Glacier Blanc.

p.361) states that major glaciers west of the Main Divide lack continuous debris blankets. However, the distribution of debris-mantled glaciers in the central Southern Alps (Fig 4.4) shows that Fox and Franz Josef Glaciers are atypical in this respect.

4.1.2 Geological controls on glacier morphology.

The underlying factor which determines the occurrence of a debris mantle is considered to be the bedrock structure of the area. That climatic influences are secondary is supported by observations of debris-mantled glaciers over 160° of latitude and from maritime and continental regions (see literature review, Chapter 1.4).

The great length of several debris-mantled glaciers in the Mount Cook area is due to the confluence of major tributaries with the trunk glacier. The Tasman, Murchison, and Mueller Glaciers are examples (Fig 4.5). These glaciers are, in effect, a contiguous series of smaller glaciers which join "end-to-end". The reason is that the valley trends are parallel to the mountain ranges, reflecting preferential erosion along the strike of regional schistosity and of major strike-parallel faults (Lillie 1962a; Field 1976; Waterhouse 1985).

The large-scale pattern of ice flow is therefore fundamentally related to the structural "grain" of the bedrock, which has had a long-term influence on patterns of glacial erosion. Fig 4.4 (inset) shows the general flow directions of valley glaciers in the central Southern Alps. The strength of the mode is shown by the An 180 and An 360 statistics (Dale & Ballantyne 1980) to represent a weak clustering about a single mode, significant at the 0.05 level. A slight bimodality is introduced by the aspect control on snow accumulation. The minor north-easterly mode follows the direction of regional strike. The preferred orientation of glacier flow is unusual: more commonly large valley glaciers have a general regional flow pattern perpendicular to the axial trend of a mountain range.

The precipitation gradient is perpendicular to the range axes, so that an asymmetry of ice supply causes the glacier tongue to be re-supplied repeatedly by tributaries entering the ablation zone from one side only (Fig 4.5). The length of an ablation zone is not related to distance from the accumulation basins located furthest from the terminus. Instead, each ablation zone is actually a compound of ablation zones of several glaciers, which must be treated more-or-less independently. For example, the Mueller Glacier terminus receives all its ice from the slopes of Mt.

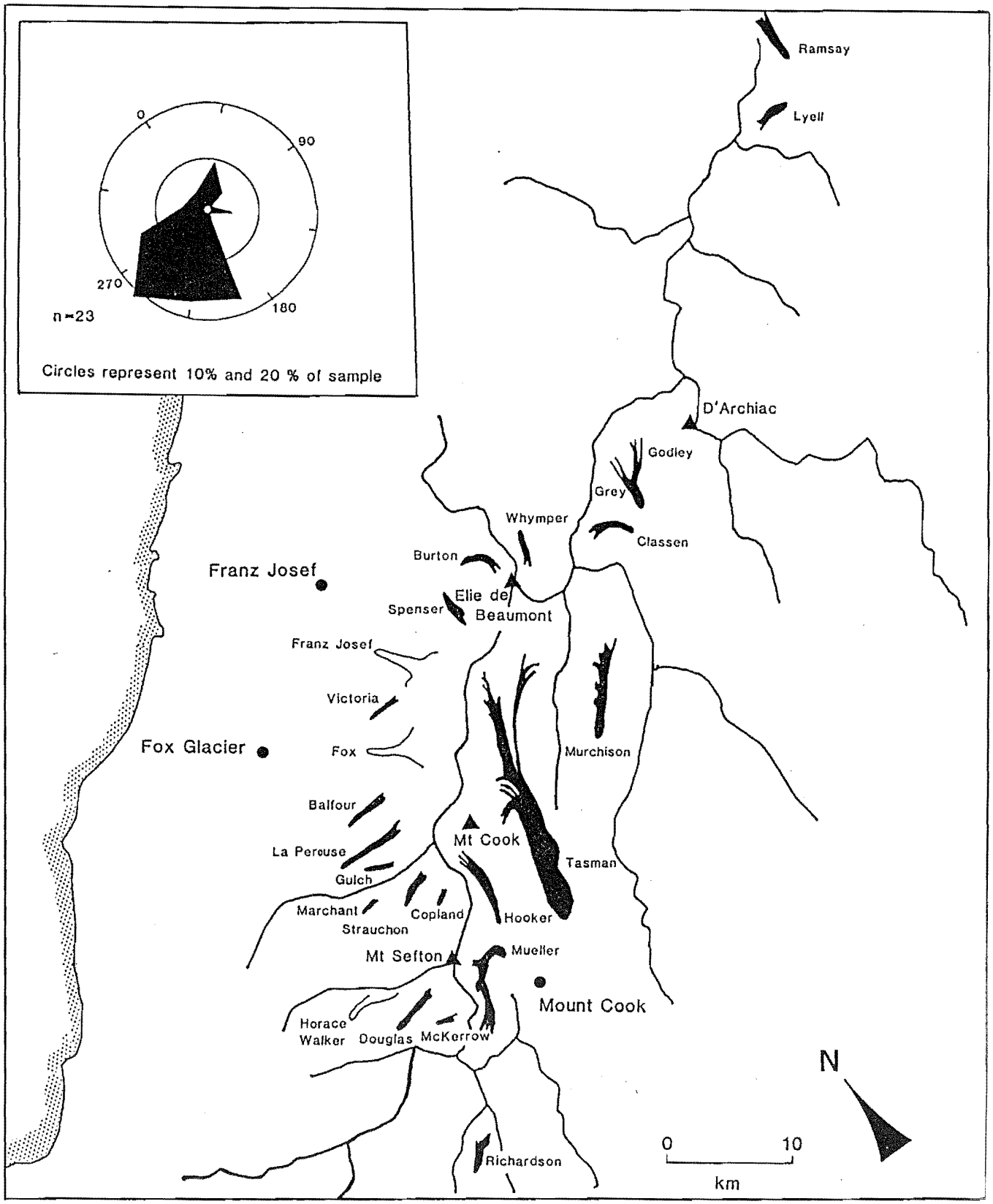

FIG. 4.4 Distribution of debris-mantled and unmantled valley glaciers in the central Southern Alps. Inset shows rose diagram of their general flow directions.

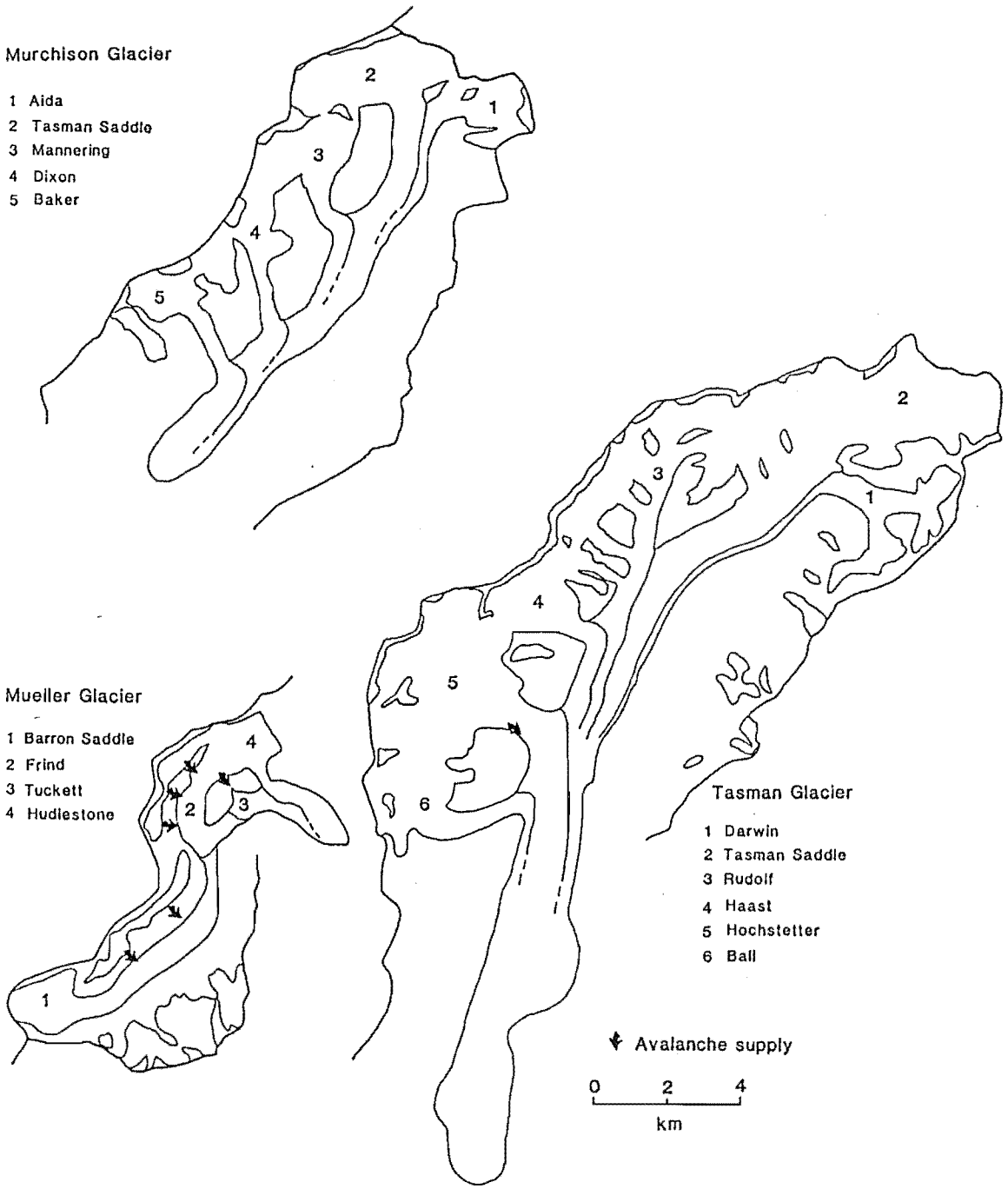

FIG. 4.5 Asymmetry of ice supply to three debris-mantled glaciers in the Mount Cook area. Prevailing wind direction is from north-west and precipitation decreases to the south-east.

Footstool and none from the head of the valley. Ice from the head of the valley flows only as far as the junction of the Frind Glacier (Fig 4.5). In such cases the term "confluence" is inappropriate because the separate tributaries do not flow alongside each other. The term "tributary junction" is preferred.

The significance of the asymmetry of ice supply to the debris-mantled tongues is twofold:

1. A large low-gradient ice tongue is maintained at low altitude despite high ablation. In the ablation zone, melt-out of englacial debris is rapid and low ice velocities allow supraglacial melt-out material to accumulate.

2. Tributaries are invariably steep ice falls or calving ice-cliffs. Both favour the emergence of debris at the glacier surface.

The case of the central Southern Alps emphasises the strong geological control on glacial erosion patterns which is responsible for glacier structures conducive to debris-mantle formation.

4.1.3 Tasman Glacier debris-mantle morphology and structure.

4.1.3.1 Relief

The debris mantle is fed by longitudinal debris septa and by transverse lenses of englacial debris with a steep up-glacier dip (Fig 4.6) These debris bodies emerge at the surface due to ablation. Their distribution causes differential ablation between the sporadic debris cover and bare ice surfaces which results in an increase in surface relief on the glacier. Most surface morphology on the Tasman Glacier can be explained by differential ablation rather than by compressive deformation of ice, because high ablation rates and abundant surface debris cause the rapid development of ice-cored topography of several tens of metres in relief over a period of only a few decades.

The evolution of relief in the debris mantle follows a pattern of initially increasing relief and instability of the debris cover, which gradually changes downglacier to a trend of decreasing relief and slope angles. Fig 4.7 presents observations of relief and lateral slope development along 4 transects across the debris mantle. The transects were measured in the field using an abney level, 100 m tape measure and compass.

Transect 4 crosses the up-glacier end of the debris mantle where strips of bare ice separate medial moraines. The moraines are well-defined and sharp-crested and inter-moraine areas are relatively gentle slopes

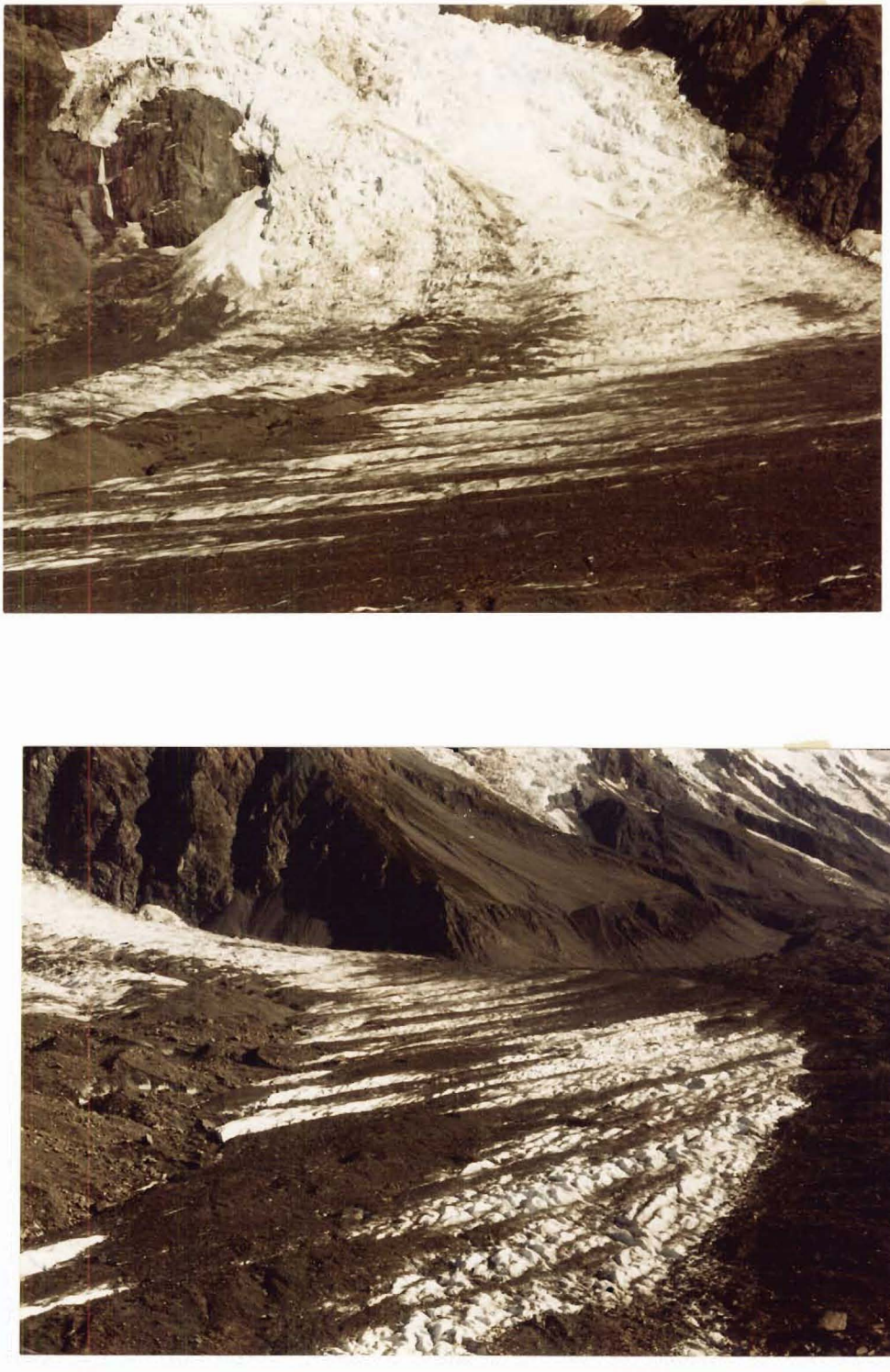

FIG. 4.6 Emerging lenses of rockfall debris (E_A moraines) at the base of the Hochstetter Icefall, and larger central rock avalanche deposit (R_A), feeding the debris mantle of the Tasman Glacier.

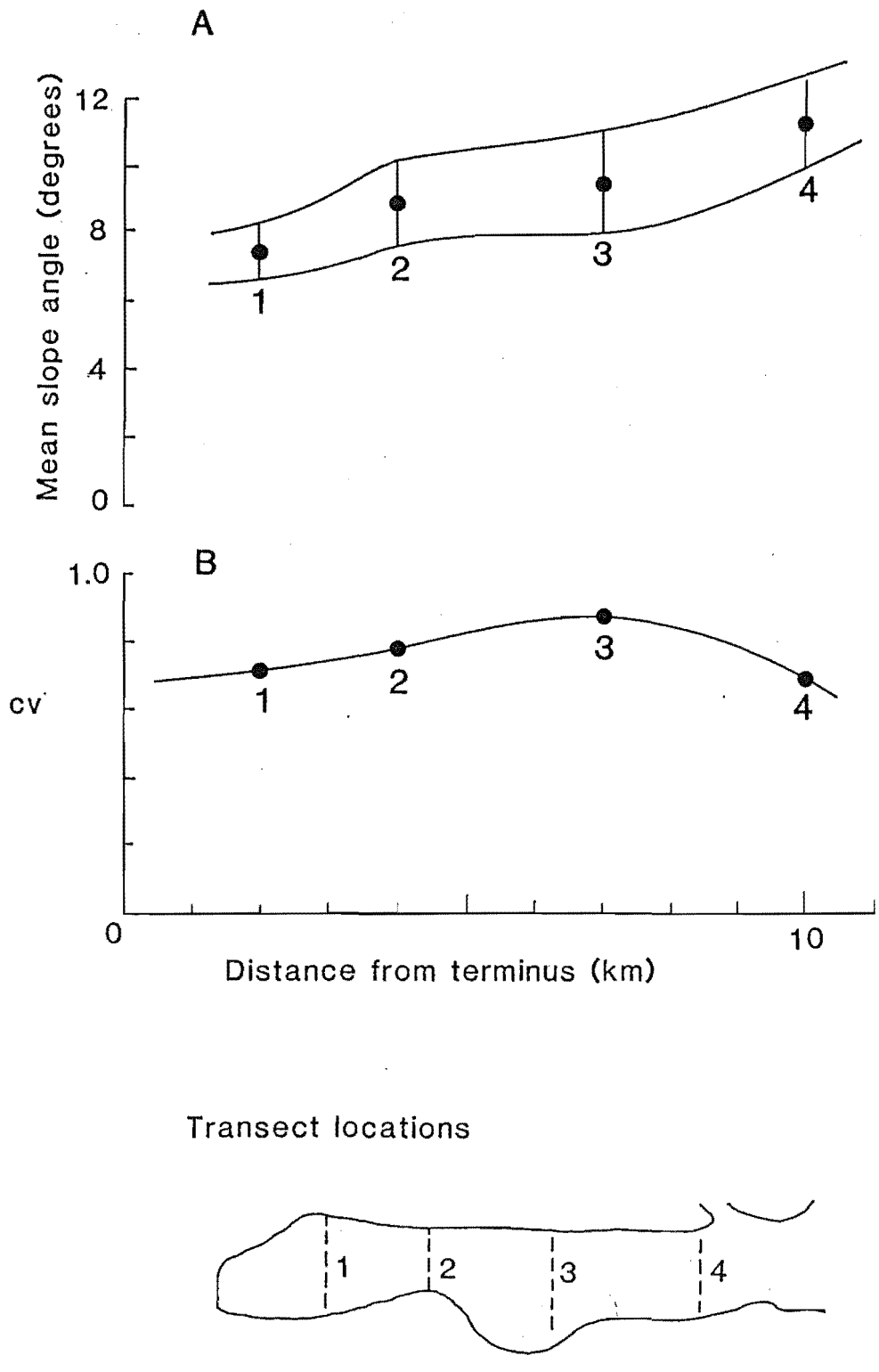

FIG. 4.7 Mean slope angles and their co-efficients of variability (cv) for four transects of the Tasman Glacier debris mantle.

FIG. 4.8 View of the stable zone of the Tasman Glacier debris-mantle in November 1985, with figure in right foreground for scale.

thinly covered with debris. Retardation of ablation is significant only in the vicinity of the medial moraines and close to the glacier margins. Slope angles average 11.4°.

Transect 3 lies 3 km downstream. Medial moraines have become broad-crested due to the effect on ablation of the lateral spreading of debris from the ridge crest. The relief between moraine crests and inter-moraine troughs is at a maximum on this transect. Meltwater erosion of the troughs accentuates their depth. Slope angles are less steep, averaging 9.5°, but are more variable than upstream. The western medial moraine in transect 4 has become indistinguishable from the lateral apron of ice-cored debris in transect 3.

Transect 2 lies a further 3 km downstream. This transect shows a marked decline in overall relief, in mean slope angle, and in the variability of slope angle. Lateral downslope movements of debris have caused a concentration of debris in inter-moraine troughs, and a correspondingly slower thickening of debris on the moraine crests to the point where debris thickness in the troughs eventually exceeds that on the crests. The earlier pattern of relatively low ablation rates on the crests has reversed, so that the relief has correspondingly declined and regular slopes of lower angle (averaging 9°) result.

Transect 1 lies 2 km downstream and 2 km above the glacier terminus. A continuation of the above trend is apparent. The form of the medial moraines is entirely lost at this location and relief-forming processes relate to thermokarst erosion (Section 4.2) and to ice deformation. The latter is probably responsible for the circular concentric ridges reported by Odell (1960), still visible on the glacier surface (Fig M1). Any strain-thickening of the debris mantle would also lead to an increase in differential ablation. However, sub-debris ablation rates are very low at this transect (Chapter 2.2.4) and the debris cover more evenly distributed than upstream. Thus relief takes much longer to form and is relatively subdued. The debris mantle has effectively become a thick, stable sheet of low relief (Fig 4.8).

These observations permit a distinction of three zones to be made within the debris mantle, which relate to relief development and to the distribution of ablation. Ablation in the lower tongue is controlled more by debris thickness than by altitude, so that these zones occur sequentially in the direction of glacier flow.

Zone of increasing instability

High ablation rates characterise this zone, and retarded ablation

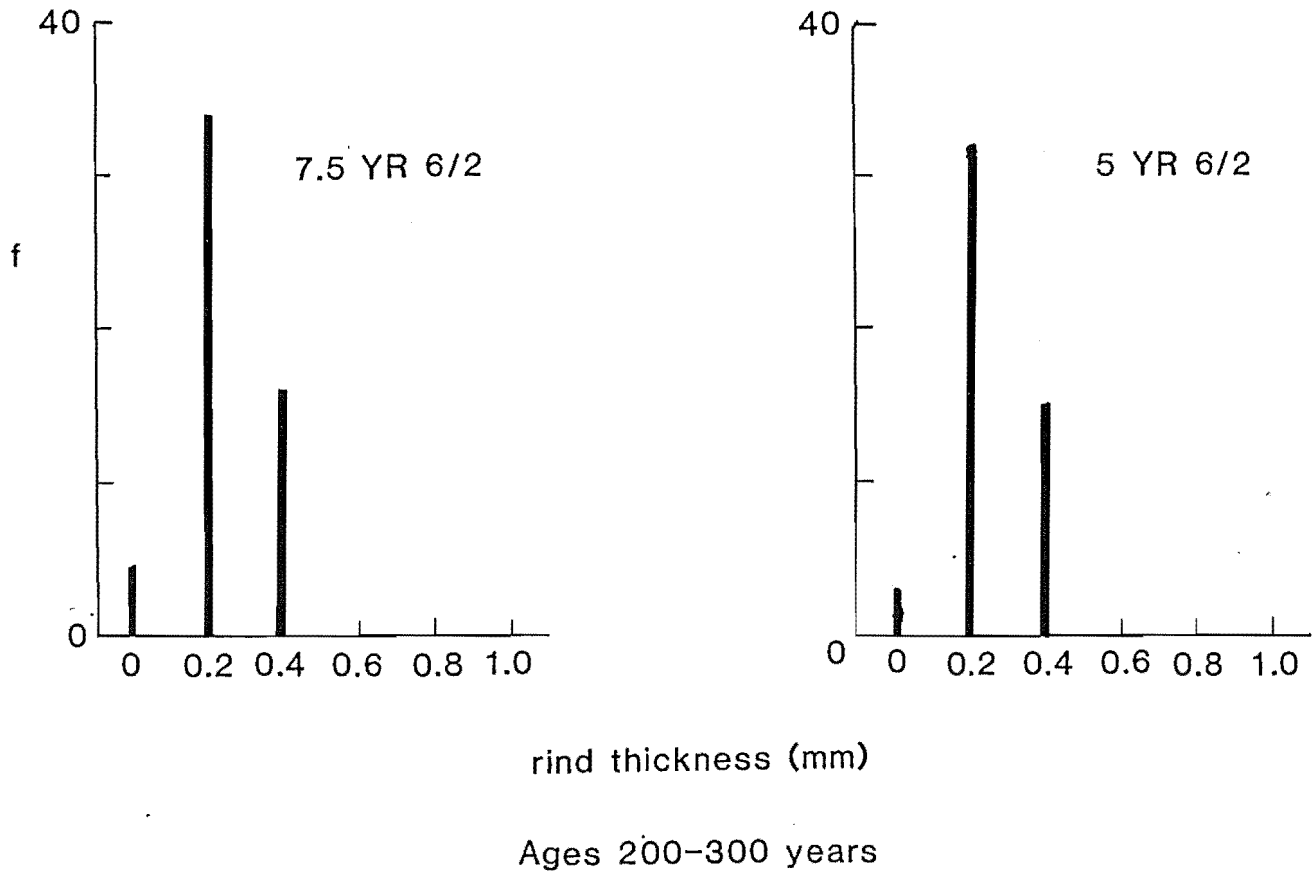

FIG. 4.9 Rock weathering-rind histograms from the stable zone of the Tasman debris mantle. Sample sites were at the north end of the proglacial lakes. Modal rind thicknesses of 0.2 mm suggest an age of 200-300 years using the calibration curve of Whitehouse et al (1986).

occurs dominantly on moraine crests. Differential ablation between moraine crests and intervening troughs is great, causing increasing relief and unstable slopes. Many bare ice walls occur where debris has slid downslope.

Zone of decreasing instability

Sliding and rolling of clasts down the lateral slopes of moraines cause a redistribution of surface debris thickness, so that thicker debris accumulates in troughs than on ridge crests. Although ablation is everywhere retarded by the debris cover, highest rates occur on ridge crests to cause a decrease in relief and an increasing uniformity of slope angles. Medial moraines thus appear to "die out" in this zone.

Zone of stability

Taken to its maximum development, debris redistribution results in a uniform debris blanket beneath which virtually no differential ablation occurs and where relief-forming processes are of minor importance. The result is a thick, stable and gently undulating debris mantle. That this zone occurs at all on the Tasman Glacier is due to the great length of the debris mantle and the low velocity of the lower glacier, which allow a long period for relief to evolve to a stable state. Weathering-rinds from the glacier centre near transect 1 (Fig 4.9) give ages of 200-300 years, indicative of the stability of the debris mantle. On most alpine valley glaciers, the terminus lies in zones 1 or 2 and a stable debris mantle does not have time to evolve.

4.1.3.2 Debris mantle geometry.

Predicted long-profiles of debris thickness on medial moraines (Fig 3.18) were concave, with thickness increasing downglacier at an increasing rate when there is no sliding of debris from moraine crests. On the debris mantle, zones of debris stability and relief development have been identified. When compared with the debris thickness profile (Fig 2.18), the rate of downglacier thickening increases in the zone of debris-mantle stability. An explanation is that as surface relief declines, lateral debris sliding ceases and the theoretical debris thickness profile becomes applicable. This occurs on the lower 2-3 km of the Tasman Glacier. Above this point, lateral redistribution of debris reduces the rate of downglacier thickening to a linear increase.

Thickening towards the terminus may be aided by two other processes: 1) emergence of ice with higher debris concentrations. Ice with dispersed facies debris (Chapter 3.2.2) outcrops in ice walls around the terminal

lakes of the Tasman Glacier;

2) emergence of englacial debris concentrated by the internal drainage of the glacier. Local thick (up to 5 m) accumulations of sorted sand and gravel (Fig 4.10) are interspersed in the coarser, blockier debris typical of most of the mantle. These deposits are similar to those described forming on the Mueller Glacier (Chapter 3.4.5.2).

4.1.3.3 Debris mantle texture and composition.

In vertical section, the debris mantle is coarse and unsorted except for a layer of mud at the base. Erosion of the mud layer by melt- and rain water means that the layer is absent under thin debris, but forms a coat several millimetres thick where the cover exceeds about 15-20 cm. Under thicker debris, the mud layer is also thicker, and 30 cm of interstitial mud has been measured in 2 m of debris. The mud is believed to be of two origins.

1) Mud and silt caps on clasts in openwork debris are interpreted as illuviated deposits, formed by the flushing of fines down through the debris mantle by rainwater (cf Locke 1986). The basal mud layer is deposited at the contact between the permeable debris cover and relatively impermeable ice. Aeolian erosion of dry lateral moraine walls has frequently been observed, and forms a source for the fine material.

2) Fine material derived from subglacial abrasion is accreted to the base of the debris mantle by ice melt. Englacial concentrations are low, but appear to increase within 1 km of the terminus, co-inciding with a thicker debris cover and mud layer. The thermal significance of the mud layer is discussed in Chapter 2.2.4.

Vertical movement of coarse clasts has been described elsewhere (eg McSaveney 1975). The emergence of large boulders from the Tasman Glacier debris mantle is indicated by caps of fresh gravel which, with time, are removed (Fig 4.11). Emergence may be due to differential ablation due to insulation of ice beneath large boulders, as McSaveney suggests. An alternative is suggested here. A column of >c.500 m of ice has ablated from beneath debris presently near the glacier terminus. Melting of this ice underneath a debris layer would have a similar effect on the debris as shaking a tray of poorly-sorted sand: crude sorting occurs and coarse particles are concentrated at the surface of the debris layer. The same process may explain metre-scale sorted circles which occur locally, in addition to a frost-sorting mechanism (Ballantyne 1979).

Fabrics within the debris mantle do not appear to reflect strain

FIG. 4.10 Lens of stratified, moderately well-sorted medium sand deposited in supraglacial pond, overlying coarse boulders of the debris mantle. Area of pond was c.30 x 20 m. Lower Tasman Glacier, August 1986.

FIG. 4.11 Gravel and sand cap on a boulder emerging from the debris mantle, March 1986.

history over the whole mantle, and are of no interpretive use. Much of the mantle has no clast preferred orientation. Zones of high strain have localised linear gutters of vertically-aligned platy clasts, but their relationship to directions of principal strain is unclear. Similar lineations are formed in zones of crevassing, as described elsewhere by Birnie (1978).

Compositionally, there are no distinctive lithologies in the Tasman Valley to aid provenance studies of supraglacial debris. The same may not be true of other valleys in the area (Brodrick 1891; Field 1976). The Tasman debris mantle consists of c.70 % sandstone and 30 % argillite. The outcrop of argillite is under-represented in the debris mantle because of the greater resistance to weathering of sandstone. There is a discernible downglacier reduction in the proportion of argillite in the debris mantle.

Of the minor debris-mantle features described, the vertical structure is of greatest significance because of its influence on the transfer of water, air and heat to the ice-debris interface (Chapter 2.2.4). Detailed study of other features has proved to be of little use, given the aims of the study.

4.1.4 A model of debris mantle dynamics related to ablation and ice flow.

4.1.4.1 Identification of key variables.

The key to understanding the effect of the debris mantle on the glacier tongue lies in understanding the distribution of downwasting and debris mantle spreading during the last hundred years (Fig 4.12). The pattern of downwasting has been described in Section 2.2.6, where it was shown that the amount of thinning has decreased towards the terminus and that the long-profile of the debris-mantled tongue has changed from a concave to a convex form since 1890.

The unusual pattern of thinning of the lower Tasman Glacier results from the distribution of ice loss during the evolution of the debris mantle. The dynamics of debris-mantle growth are complex: principles developed in Chapter 3 are here applied to the specific case of the lower glacier.

The down-glacier decrease in the amount of surface lowering which has occurred (Fig 2.20) is the reverse of the normal trend on glaciers under negative mass balance (Paterson 1981 p.251). The usual case involves more negative specific balance toward the terminus as ablational losses increase and replenishment of these losses by ice discharge decreases

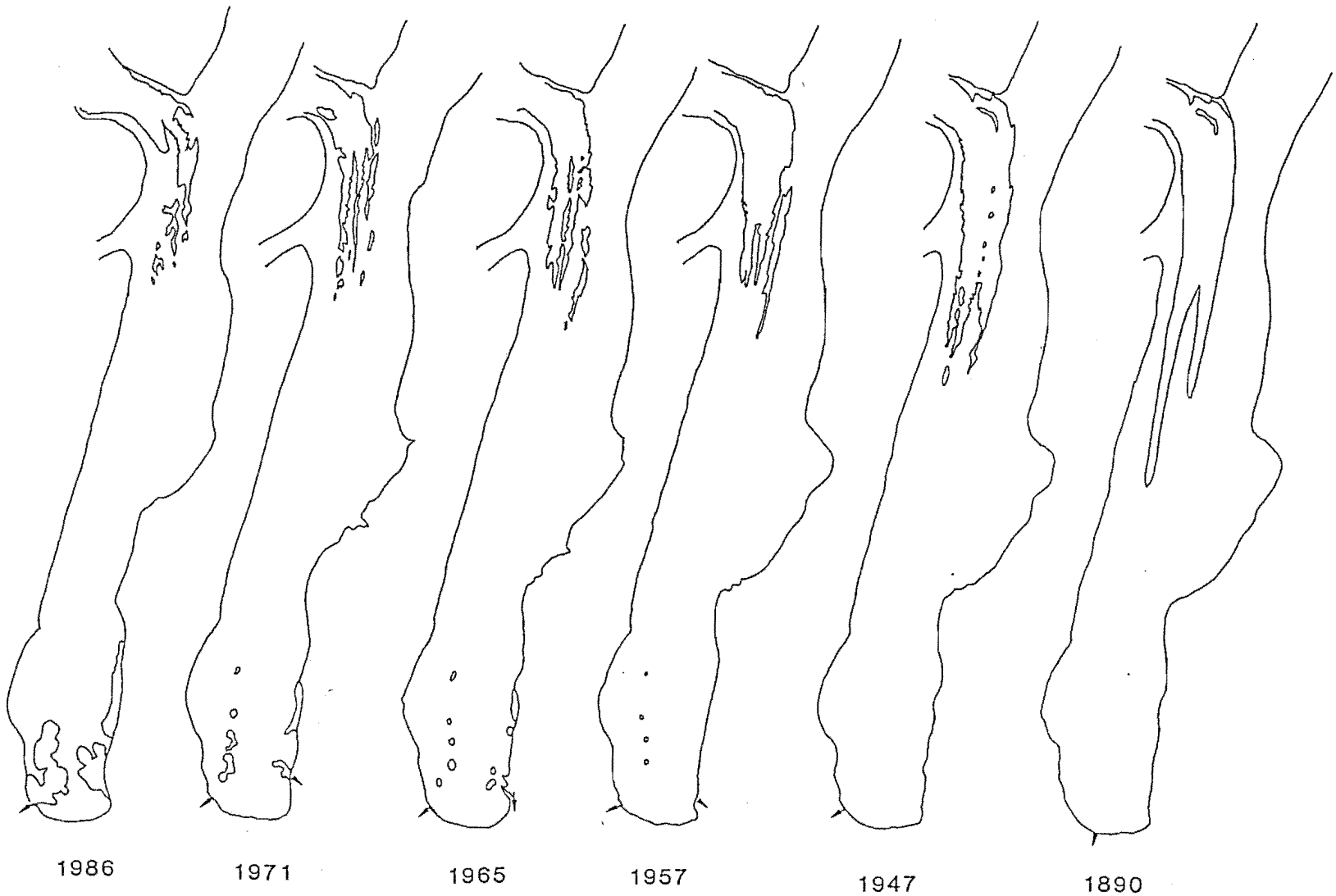

FIG. 4.12 Changing extent of the debris-mantle and proglacial lakes on the lower Tasman Glacier since 1890. Positions of outlet streams arrowed. Data from Brodrick's 1890 map (see Frontispiece), from 1947 oblique aerial photograph, and from vertical aerial photographs.

(Hastenrath 1987). At the terminus, recharge of ice is exactly equalled by ablation.

In the Tasman Glacier, ice discharge decreases towards the terminus as expected (Section 2.1.3). The increased thickness of the debris mantle reverses the ablation gradient (Section 2.2.4), because ablation is more a function of debris thickness than of altitude. This effect outweighs the downglacier decline in ice recharge (Table 4.1). Downstream from the Celmisia transect, only 18% of ablational loss is replaced by glacier flow. For the whole glacier downstream of Ball Hut 49% of the ablational loss is replaced. Despite this trend, the insulating effect of the debris mantle has been sufficient to cause a downstream decrease in glacier thinning.

Therefore to explain the distribution of surface lowering, the **absolute** mass flux at each site is more significant than the **relative** recharge. The extremely low ablation rate beneath thick debris cover means that the 1986 specific balance at the Celmisia transect is only -2 m even though ablation exceeds recharge by a factor of 4. For the whole glacier downstream of Ball Hut, the 1986 average specific balance is -3.4 m with ablation exceeding recharge by a factor of only 2.

The gradient of the debris-mantled area of the glacier has decreased because of the distribution of surface lowering. The transition from a convex to a concave profile causes an increase in the velocity gradient and therefore in compressive strain rate. The results of this are:

1. Increased compression causes ice thickening, all other factors remaining constant. In practice, on the Tasman Glacier changes in ablation and ice discharge dominate over this effect, so that compression has reduced the rate of thinning rather than caused thickening.

2. The emergence velocity (the vertical component of ice flow) increases correspondingly. Englacial particles whose trajectories follow flowlines in the glacier are elevated to the surface at points progressively further upglacier as compression increases. The upstream edge of the debris mantle migrates upglacier and the debris mantle spreads.

Changing emergence velocity during debris mantle evolution is important. Emergence velocity depends partly on horizontal ice velocity (Paterson 1981: Fig 5.2). It is affected by changes in velocity with no corresponding change in strain rate, as well as by changes in velocity and in strain rate. Fig 4.13 shows the combinations of horizontal velocity and the inclination of glacier flowlines (a surrogate for compressive strain

Transect	Distance above terminus (km)	Mean Specific balance below transect (ma^{-1})	Ice Discharge through transect ($m^3_a{}^{-1}$)	Recharge (%)
Ball Hut	10	-3.4	5.1×10^7	49
Celmisia	2	-2.0	3.6×10^5	18

TABLE 4.1 Specific balance and ice recharge in the lower Tasman Glacier.

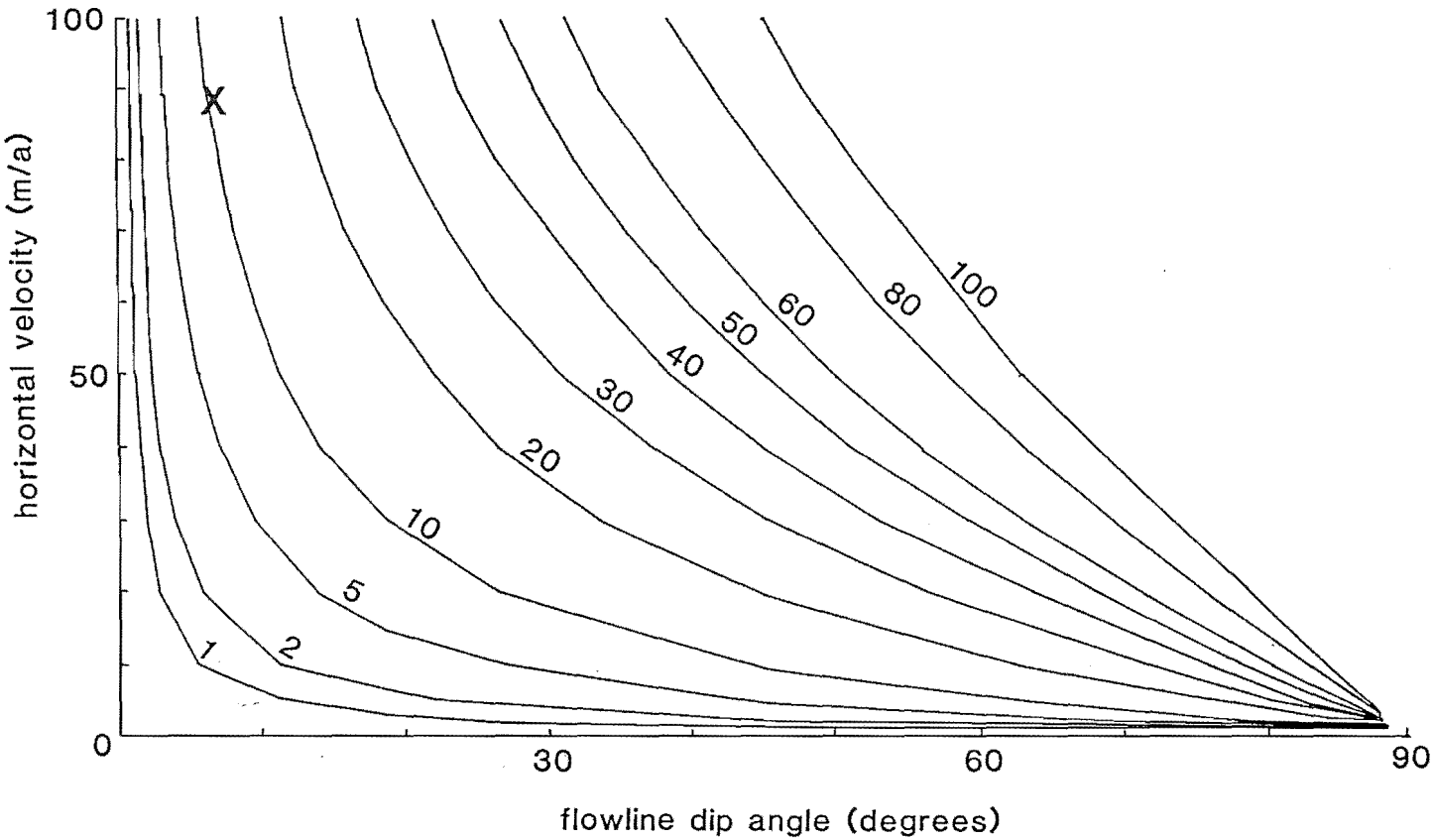

FIG. 4.13 Relationships between the dip of glacier flowlines (x-axis), horizontal ice velocity (y-axis), and emergence velocity (curves). Figures are emergence velocities in ma^{-1}. Based on equations given by Paterson (1981: p.61). X marks plot of Ball Hut in 1986.

rate) that give particular values of emergence velocity, and has been calculated from the equation given by Paterson (1981: p.61). The graph shows that very high emergence velocities (>40 ma^{-1}) are affected equally by changes in horizontal velocity and in flowline angle. Emergence velocities in nature are lower, values between 3 and 10 ma^{-1} being typical (Paterson 1981: p 64). At these values, emergence velocity is more sensitive to one variable than to another. At high horizontal velocities and low flowline inclinations emergence velocity is sensitive to changes in flowline inclination (ie longitudinal strain rate). Conversely, at low horizontal velocities, velocity is the dominant control.

The emergence velocity at Ball Hut is 10 ma^{-1} (Fig 4.13), a value which is high by world standards for non-surging glaciers. Glacier dynamics at Ball Hut make emergence velocity there especially sensitive to changes in compressive strain, such as has occurred during the change in long-profile caused by debris mantle spread. The increase in compression, acting through increased emergence velocity, propagates further debris mantle spread. A feedback loop therefore links these variables (Fig 4.14).

The emergence velocity under the distal end of the debris mantle is not known. However, since ice velocities there are only a few metres per year, the emergence velocity will be much less than at Ball Hut and will be affected mostly by changes in the glacier flow rate rather than in compression. The low values of flow and ablation limit the emergence of debris at the ice surface to a small fraction of that at the upstream margin of the mantle. There is therefore a transition with distance down the debris mantle in the variables which control particle emergence as well as in the supply of debris to the glacier surface.

4.1.4.2 Summary of the model.

A model of debris mantle evolution is proposed on the basis of the above discussion. Relationships governing the morphological development of a glacier tongue have been presented diagrammatically in Fig 4.14.

Ablation rate has been identified as the key variable in the system. For a (hypothetical) step-like decrease in ablation rate, a complex feedback system is initiated. The net effect is to cause a self-propagating upglacier spread of the debris mantle. This model is the key to understanding many observations of the behaviour of the Tasman Glacier. Application of the model to geomorphic observations is made in Chapters 5 and 6.

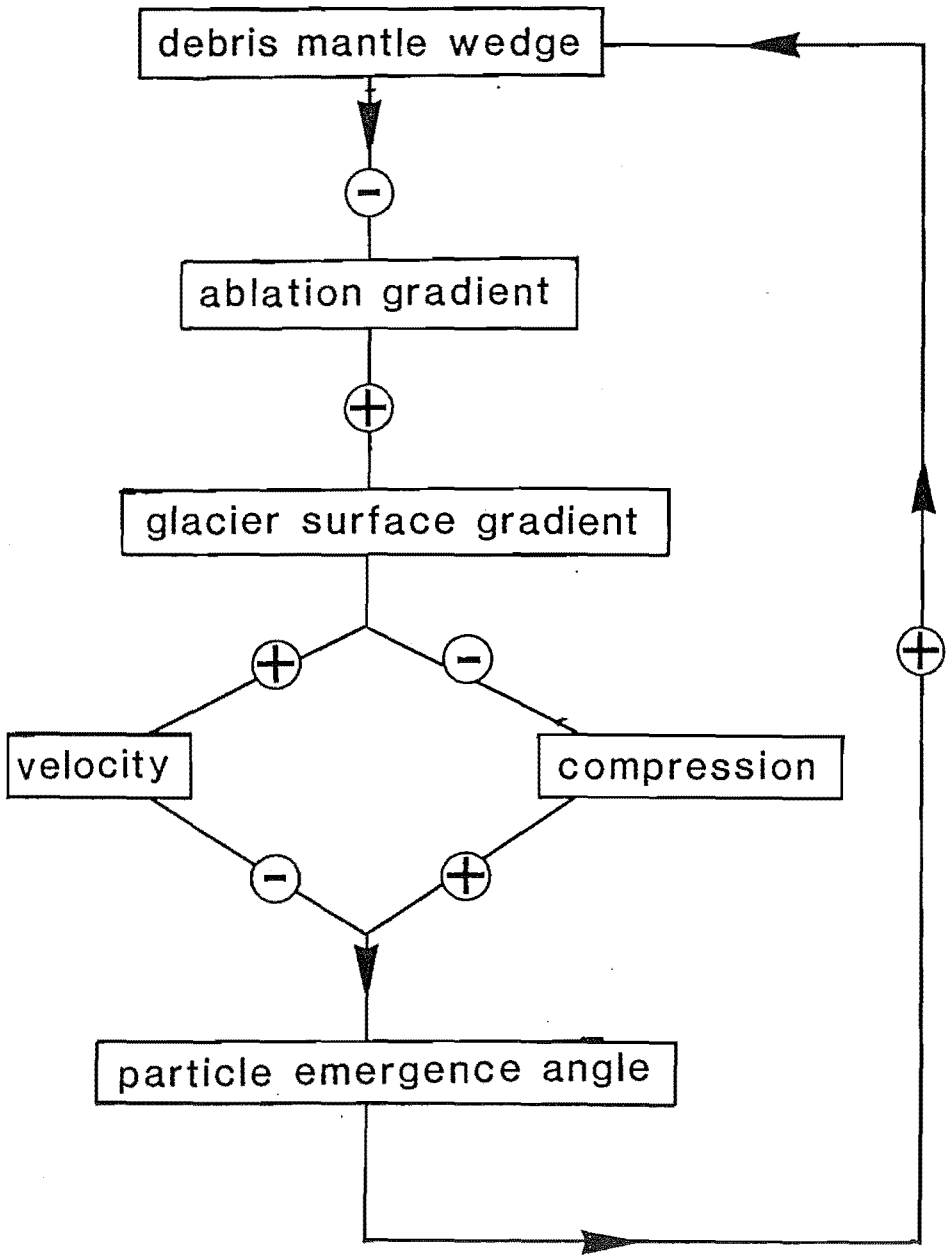

FIG. 4.14 The debris mantle feedback system, indicating positive and negative feedbacks between the debris mantle wedge and glaciological parameters. The net effect of the presence of a debris mantle is to propagate upglacier-spreading of the debris cover.

4.1.5 Can a debris mantle be an equilibrium form?

Mass flux through a glacier consists of ice and debris, each of which has a mass balance. The mass balance of glacier ice is the standard method of understanding glacier behaviour, and equilibrium involves a balance between accumulation and ablation over the glaciological year.

Equilibrium mass balance of debris prevails when debris inputs to a glacier equal outputs (deposition) over the same period. Unlike ice, rock debris does not melt at atmospheric temperatures and pressures, so that the only losses of debris from a glacier are by fluvial transport and direct deposition as till. The Tasman Glacier has a structure which favours the net accumulation of debris in the lower glacier. In the parts of the glacier where ice mass balance is strongly negative, debris mass balance is strongly positive.

The concept of mass balance can also be applied to the Tasman Glacier debris mantle itself. Inputs of debris to the mantle are by accretion to the base by melt-out of englacial debris, and to the upstream end by addition of supraglacial debris. Outputs are solely by dumping at the terminus, since no fluvial erosion of the debris mantle occurs. To have equilibrium debris mass balance, the mantle must lose as much debris by dumping as is supplied by accretion. For reasons explained in Chapter 3.2, this can rarely be the case because of the system of debris mantle dynamics. This system requires that, once initiated, the debris mantle has to thicken and spread unless a positive change in glacier mass balance occurs. Thus, if conditions allow the mantle to form in the first place, it must subsequently increase in volume. The debris mantle, by its very existence, must have a positive mass balance and cannot have equilibrium debris mass balance.

If a positive change in glacier mass balance occurs which causes a change in flowline trajectories, surface velocity, and emergence velocity, conditions may no longer favour supraglacial debris accumulation and the debris mantle will be evacuated from the glacier surface. During the transition from mantle spreading to mantle shrinkage, there will be a moment when debris accumulation equals outputs, but it is doubtful whether this state can be maintained as a true "equilibrium".

With respect to ice mass balance, the possibility exists that a debris mantle can exist during equilibrium. This is because the factors favouring debris mantle formation (Section 4.1.1) are largely independent of those which control ice mass balance. If debris sources and glacier flow structure are favourable, debris will accumulate on the glacier surface in

Glacier	Accumulation area (km^2) (Ac)	Ablation area (km^2) (Ab)	Ac:Ab area ratio	AAR
Unmantled Glaciers				
Fox	26.7	7.6	3.5:1	0.78
Franz Josef	29.4	7.0	4.1:1	0.81
Horace Walker	4.6	1.5	3.0:1	0.75
Mantled Glaciers				
Hooker	8.8	6.9	1.3:1	0.56
Mueller	7.2	10.9	1:1.5	0.46
Murchison	16.1	22.1	1:1.4	0.42
Classen	4.3	7.6	1:1.8	0.36
Godley	5.9	12.0	1:2.0	0.34
Grey-Maud	5.0	7.0	1:1.4	0.42
Balfour	3.0	4.6	1:1.6	0.39
La Perouse	5.8	4.8	1.2:1	0.55
Spencer	7.8	4.0	2.0:1	0.66
Tasman	24.7	30.2	1:1.2	0.45
				$\bar{x} = 0.46$
Patagonia Icefield (Aniya et al 1988)				
Mean of 27 unmantled glaciers.			1.7:1	0.61
Everest Area (Grove 1988: p210)				
Mean of unstated number of mantled glaciers.			1:1.4	0.41

TABLE 4.2 Comparison of accumulation and ablation areas of unmantled and debris-mantled glaciers.

the ablation zone even when the glacier is in equilibrium. The Tasman Glacier has maintained a debris mantle even during several decades of minor oscillations around an equilibrium condition in the late Nineteenth Century (Brodrick 1891; Harper 1893; Gellatly 1985c).

The implication of the presence of a debris mantle during equilibrium glacier balance is that glacier volume will increase to maintain equilibrium. This is because a debris mantle must always be thickening, and ablation rate beneath the mantle must decrease correspondingly. Since equilibrium ice mass balance demands that accumulation = ablation, ablation area must increase to compensate the decrease in ablation rate. The glacier must advance. A corollary is that if the glacier volume remains constant where an extensive debris mantle exists, the glacier must be in a state of negative mass balance.

The consequences of this lack of correspondence between glacier volume and mass balance are that observed volume changes are not necessarily indicative of the state of mass balance of the glacier. However, this relationship applies only when climatic fluctuations are minor and debris mantle effects dominate (Chapter 5). Larger climatic fluctuations overturn the debris mantle system and establish a new set of conditions of glacier volume and dynamics.

Reduced ablation rate under debris mantles causes the accumulation areas of debris-mantled glaciers to form a smaller proportion of the glacier area (accumulation area ratio, AAR) than unmantled glaciers. Potter (1972) gives a ratio of 1 : 7 for Galena Creek rock glacier, which he interprets to have a glacier ice core. If his genetic interpretation is correct, this ratio will be close to the extreme value for debris-covered glaciers. Grove (1988) describes debris-mantled glaciers in the Khumbu Himalaya as having lower AARs than unmantled glaciers. Comparison with unmantled Patagonian glaciers (Table 4.2) supports the distinction. The AARs of glaciers in the central Southern Alps are presented in Table 4.2 for comparison. In all cases AARs of debris-mantle glaciers are less than those of unmantled glaciers.

4.1.6 Relationships between debris-mantled glaciers and other landforms.

Debris-mantled glaciers are one example of a range of ice-cored landforms. Others include ice-cored moraines (Østrem 1971; Carrara 1975; Watson 1980) and some rock glaciers (Potter 1972; White 1976; Whalley 1979; Griffey & Whalley 1979; Lindner & Marks 1985; Humlum 1988; Johnson &

Lacasse 1988).

Genetic relationships between different ice-cored forms have been debated for many years, and there is no consensus even of basic definitions (eg Haeberli 1985; Martin & Whalley 1986). Several authors have proposed continua linking various ice and debris mass-movement landforms (Corte 1976a; Johnson 1980a; Shakesby et al 1987; Giardino & Vitek 1988; Kirkbride 1989) though the bases for these continua and the range of landforms they include differ from author to author.

The present author's observations in the central Southern Alps indicate that transitions from debris-mantled glaciers to ice-cored moraines and rock glaciers have occurred in the Neoglacial period (post 5,000 B.P.), but that such transitions depend on unusual local combinations of factors.

4.1.6.1 Ice-cored moraines.

Large ice-cored lateral moraines exist along the south-eastern margin of the Godley Glacier (Fig 3.24). Differential ablation between the debris-covered glacier margins and the bare ice of the glacier centre has caused the ice-cored moraines to be stranded along the valley sides during downwasting. No comparable landforms have developed where supraglacial debris covers the full width of the glacier, on the Godley or on other glaciers. The indication is that strong differential ablation between the glacier centre and margins is necessary for the formation of these ice-cored moraines.

Slumping of debris down moraine faces has exposed the ice core, which is rapidly being destroyed by ablation. Only under exceptionally thick debris covers and on slopes of suitable gradient may the ice core be preserved long enough for downslope creep to generate a rock glacier. No evidence of flow-deformation of the moraines has been observed.

Short-lived ice cores formed by the abandonment of debris-covered ice blocks during recent glacier retreat have ablated completely in less than 100 years. The resulting disintegration moraine (Eyles 1979) is visible on the forefields of the Classen and Godley Glaciers (Fig 4.15) and in the Murchison embayment of the Tasman Glacier (Fig M1).

4.1.6.2 Rock glaciers.

Rock glaciers are generated by the slow gravity-induced creep of debris-ice mixtures. Rock glaciers characteristically exhibit morphological features caused by slow creep, including frontal lobes and

Figure 4.15

transverse and longitudinal crenulations on the upper surfaces. Their constituent debris is variable, but commonly includes talus and/or till material. Interpretations of the origin and distribution of their ice content remains controversial.

Rock glaciers are documented as having commonly formed from debris-covered glaciers in some regions (White 1976; Lindner & Marks 1985; Humlum 1988), and under rather unusual circumstances in others (Whalley 1979; Griffey & Whalley 1979; Vere & Matthews 1985). Few glaciers in the Southern Alps have generated rock glaciers, for two reasons:

1. Gradients around large debris-mantled valley glaciers are rarely steep enough for ice over-topping marginal moraines to continue to flow downslope (cf Griffey & Whalley 1979; Vere & Matthews 1985; Haeberli 1985: Fig 48).

2. Debris-covered ice occurs at such low altitudes that ablation rates do not allow ice cores to survive long enough for slow creep to generate a rock glacier. For example, at 800 m altitude the annual ablation beneath 50 cm of debris is 4.5 m (Fig 2.17). An ice core 20 m thick (a probable thickness of small rock glaciers) would ablate in less than 5 years under these conditions.

Rather than being glacier-derived, many active and fossil rock glaciers known to the present author are probably of a non-glacial origin (cf. Gellatly et al 1988). Where abundant supraglacial debris occurs at higher altitudes, lower ablation rates increase the potential for glacier-derived rock glacier formation. Cirque moraines beneath large headwalls have generated rock glaciers at several sites in the Southern Alps. All of these appear to me to be associated with incorporation of glacier and/or snowbank ice within late Neoglacial end moraines.

Transitions from debris-covered glacier to rock glacier are therefore most likely close to glacier equilibrium line altitudes. Small cirque glaciers with plentiful debris supply are more likely sources than larger debris-covered tongues at lower altitudes and gradients.

4.1.7 Conclusions of Section 4.1.

1. Formation of supraglacial debris mantles is favoured by the presence of high relief and large areas of cliffs in the accumulation zone, providing debris for high-level transport through the glacier. Concave glacier long profiles assist the emergence of debris at the glacier surface.

2. The main glacial valleys in the central Southern Alps appear to

exploit strike-parallel faults in the Torlesse Group sediments and/or regional schistosity of the Haast Schists. Major valleys trend sub-parallel to the ranges which, combined with the regional precipitation gradient, causes an asymmetry of ice supply to most valley glaciers. Tributary ice falls are locations favourable to debris emergence and supraglacial accumulation.

3. The Tasman Glacier debris mantle shows a down-glacier morphological development due to differential ablation, changes in glacier surface relief, and downslope debris movements. Four zones are recognised within the debris mantle, based on the stability of the debris cover and surface relief.

4. A model of debris mantle formation identifies feedbacks between glacier dynamics and supraglacial debris accumulation which produce a distinctive evolution of glacier morphology and debris mantle spread. Redistribution of ablation and its effect on glacier surface gradient are key variables in the system.

5. Debris mantle spread is favoured by negative glacier mass balance, but may occur during equilibrium glacier mass balance where environmental conditions allow. Glacier volume is not constant during equilibrium if an extensive debris mantle is present.

6. Transitions from debris-mantled glacier tongues to related ice-cored landforms are unusual and short-lived in the field area.

4.2 DESTRUCTION OF THE DEBRIS MANTLE BY PROGLACIAL LAKE GROWTH.

Retreat of many valley glaciers in the Southern Alps has corresponded with the appearance of proglacial ice-contact lakes. Some types of lake are associated with particularly rapid retreat of glacier termini, which suggests that they play an important role in the adjustment of glacier volumes to altered climatic conditions. This section describes the growth of proglacial lakes in the Mount Cook area, and examines their role (a) as a mechanism of glacier retreat, and (b) as a sediment trap within the debris transport system.

Although it has been shown that growth of a supraglacial debris mantle has helped to preserve the contiguous ice tongue of the Tasman Glacier throughout many decades of glacier shrinkage, continued negative balance even with an extensive debris cover cannot prevent the ultimate destruction of the glacier tongue. This section describes the processes by which retreat is eventually brought about, and discusses the role of the

debris mantle in the overall mechanism of terminal retreat.

To investigate the evolution of glacier termini during retreat, an aerial photographic survey has been undertaken to calculate rates of lake growth, terminal retreat, and morphological change of the study glaciers. Direct measurement of ice-wall ablation around the Tasman Glacier terminus in 1986 supplements longer term observations of lake growth. A particular aim of this section is to investigate the extent to which the pattern of downwasting associated with debris mantle spread (Chapter 4.1) is related to certain mechanisms of proglacial lake formation.

4.2.1 Types of proglacial lake.

Three types of proglacial lake are recognised. All share a common characteristic of being ponded between the outwash head and/or terminal moraine barrier and the glacier itself.

1) Ramp-like ice front (Fig A3).

Downwasting of an inclined glacier surface behind the terminal barrier may eventually cause drowning of the terminus. The lake thus formed has a shape which reflects the topography of the glacier surface combined with the effects of local thermokarst erosion. The Hooker Glacier presently exhibits a submerged ramp-like ice front.

2) Coalescing thermokarst ponds (Fig M1).

On the Tasman Glacier, circular ponds bounded by bare ice and debris-covered slopes appear on aerial photographs since 1957. A phase of rapid growth and coalescence of the ponds commenced in the early 1970s, a phase which is still continuing. No comparable process has been documented previously, either in New Zealand or (to my knowledge) elsewhere.

3) Ice-cliff termini (Fig 4.16).

Glaciers in the Godley Valley terminate in steep (>60°) ice cliffs transverse to the glacier axis and adjacent to deep lakes. Glacier retreat operates by calving of the ice cliffs, and retreat rates of the glacier front are rapid. Possible transitions from other types to a rapidly-calving terminus are discussed below (Section 4.2.4.3).

4.2.2 Formational processes of thermokarst ponds.

Aerial photographic survey and direct measurement allow the growth of the Tasman lakes to be described over two timescales.

FIG. 4.16 Ice-cliff of the Grey and Maud Glaciers in May 1988. Note the wide exposed medial debris septum (in shadow).

4.2.2.1 Long-term growth pattern.

Thermokarst lakes on the Tasman Glacier originated by collapse of englacial conduit roofs in the 1950s (Fig M1), with subsequent backwasting of exposed ice walls (Fig 4.12). The effects of glacier hydrology on the distribution of the lakes is discussed in Section 4.2.4.1.

Five sets of aerial photographs taken between 1957 and 1986 were used to calculate the total lake area, the total area of ice slopes and the total area of debris slopes in each year (Table 4.3). The slope areas were estimated using known rates of glacier surface lowering and empirical knowledge of slope angles of bare ice and debris-covered slopes.

An overall rate of horizontal retreat of the lake shorelines of 13.4 ma^{-1} has occurred since 1973, when rapid growth commenced. This rate has probably been maintained with a fair degree of constancy since that time, despite minor changes in debris cover of the ice slopes around the lakes (Table 4.3). Because the lakes have a circular plan shape, a constant rate of shore retreat has caused an exponential increase in lake area (since $A = \pi r^2$) (Fig 4.17).

To predict future growth, the lakes may be approximated to four hypothetical circles of equal size, and with their centres evenly spaced. A constant increase in radius produces an increase in area shown by line A in Fig 4.17 (inset). At the point in time when the circles impinge, the rate of increase in area declines slightly while the total perimeter (line B) also declines. Both area and perimeter subsequently resume an increase at an increasing rate. Coalescence of the Tasman lakes occurred in the early-to mid-1980s, corresponding to a decrease in perimeter but with no discernable effect on the rate of increase in lake area. The lakes now plot at point C in Fig 4.17 (inset): thus coalescence will have only a temporary and minor effect on the growth rate.

A more major effect has been the decrease in the proportion of ice shorelines bounding the lakes, as shores have retreated to the ice margin. A growing length of lake shore is moraine with no ice core. The continued reduction in melting shorelines can be expected to cause the growth rate of the lakes to decrease.

Changes in debris cover of slopes around the lakes have been recorded from the aerial photographs. Table 4.3 shows that the proportion of debris-covered to bare ice slopes has not changed significantly during the 30-year observation period. However, the location of the debris-mantled segments varies considerably between photographs, for reasons discussed in Section 4.2.2.2.

Date of photography	Debris-covered slopes		Ice slopes		I/D	Area of lake shore slopes	Lake area
	Map area	True area	Map area	True area			
1957	141	155	48	77	0.50	233	10
1965	261	288	28	46	0.16	333	68
1971	378	418	93	152	0.36	569	91
1973	360	397	63	102	0.26	499	165
1986	293	324	76	123	0.38	447	963
					x = 0.33		

TABLE 4.3 Areas (in 10^3 m) of ice and debris-covered slopes bordering the Tasman lakes, measured from vertical aerial photographs at 1 : 13,000 scale.

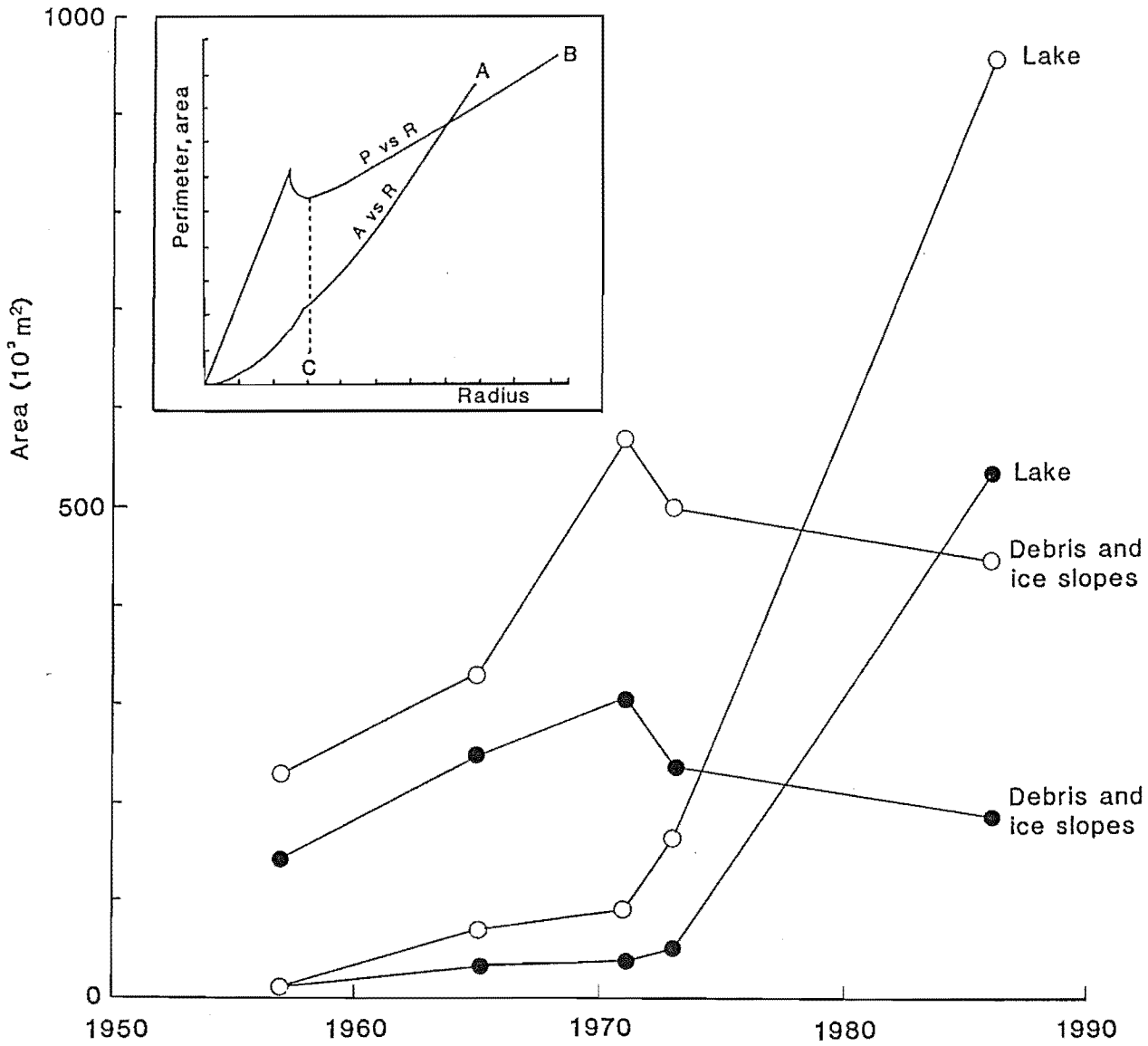

FIG. 4.17 Growth of proglacial lakes of the Tasman Glacier since 1957. Open circles refer to all lakes and shorelines, dots to the growth of four circular lakes upstream of the present river outlet of the glacier. Inset shows the increase in area, A, and perimeter, B, with increasing radius for four uniformly-spaced coalescing circles.

4.2.2.2 Short-term growth pattern.

Field observations of lake shorelines have revealed three types of slope, on the basis of debris cover and slope angle (Fig 4.18).

1. Steep, clean or sparsely dirt-covered debris-capped ice walls undercut by lake water.

2. Less steep debris-mantled and capped ice walls not undercut by lake water.

3. Intermediate forms comprising ice walls of varying angles with debris caps and basal aprons or cones, and gentler slopes of ice recently exposed by slumping of the debris cover.

Growth of the thermokarst lakes is by melting and retreat of ice slopes which form the shorelines. Claridge (1983) suggested that thermal undercutting and block collapse is the main mechanism of retreat of the lake shores (Fig 4.19). My own observations have found no evidence of significant block collapse over a three-year period. Few slope segments are sufficiently steep and high for effective block collapse, though this may not have been the case when the glacier surface was at a higher elevation.

Rather, retreat rate is dominantly a function of debris cover thickness on ice slopes. Direct measurement of lake shore retreat was made during the 1986-87 ablation season. 14 lines of painted boulders were marked at metre intervals on the debris mantle above slopes of different aspects, angles, and debris cover. All transects were laid out perpendicular to the lake shoreline. As the lake shores melted and retreated, the end of each transect was eroded and the shortening of each transect which was recorded on each visit to a site. Changes in slope angle, debris cover, and slope-foot morphology were observed.

Horizontal retreat at each transect is shown by Table 4.4. Retreat rates are plotted at the mid-point date of each measurement period in Fig 4.20. Strong seasonal variation in shoreline retreat characterises the bare ice slopes, a maximum rate of 11.5 cm d^{-1} occurring throughout January. Retreat rates increase rapidly in early summer and decline more slowly in the autumn, in a trend similar to curves of bare-ice ablation rate in Chapter 2. Retreat of debris-covered ice slopes is 2 to 3 times slower, and the seasonal trend subdued. Variability in rate between different transects increases steadily throughout the melt season: this is interpreted as partly reflecting debris thickness changes caused by mass movement, giving irregular variations in the retreat of some slopes.

FIG. 4.18 Contrasting shorelines of the Tasman proglacial lakes. Top: steep ice wall (dark colour due to mud washed down the slope from the capping debris layer), east side of lake; bottom: view south-west from site of measurement line 7 across gentle debris-covered slopes bordering the western lake shore.

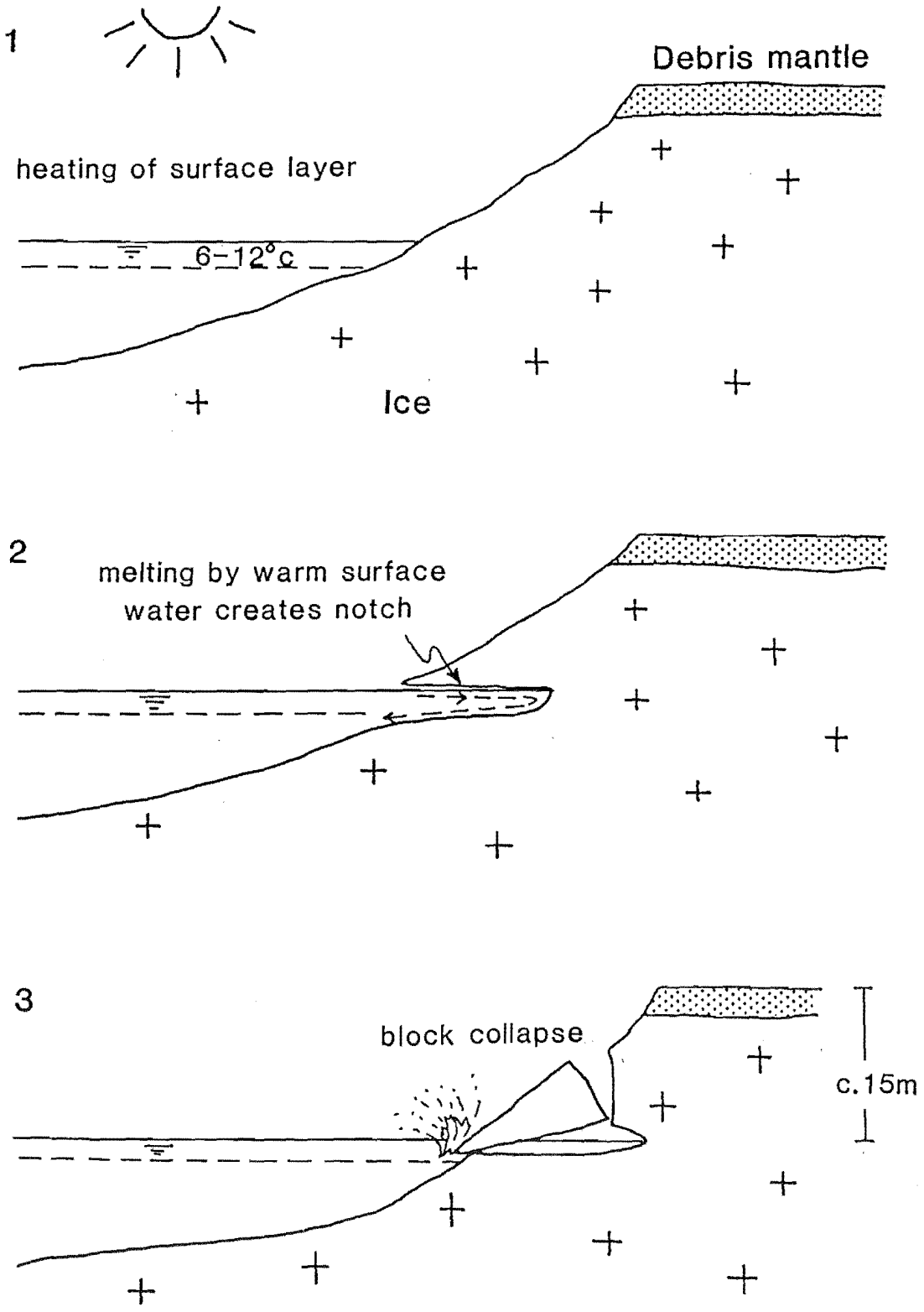

FIG. 4.19 Process of thermo-erosion and block collapse of ice shorelines (after Claridge, 1983).

Line	19 Oct - 17 Nov		17 Nov - 18 Dec		18 Dec - 29 Jan		29 Jan - 22 Mar		22 Mar - 20 Apr		20 Apr - 10 May		Total
	change	rate	change	rate	change	rate	change	rate	change	rate	change	rate	change
1	1.00	3.45	1.18	3.81	3.28	7.81	2.90	5.58	1.83	6.31	1.14	5.70	11.33
2	0.73	2.52	0.30	0.97	1.32	3.14	0.65	1.25	0.55	1.90	0.05	0.25	3.60
3	0.33	1.14	0.86	2.77	2.07	4.93	4.33	8.33	1.95	6.72	0.80	4.00	10.34
4	0.53	1.83	0.49	1.58	1.98	4.71	0.10	0.19	0.00	0.00	0.05	0.25	3.15
5	1.00	3.45	0.37	1.19	1.63	3.88	(-0.25)	(0.00)	1.41	4.85	0.51	2.55	4.92
6	0.85	2.93	1.16	3.74	0.75	1.79	0.54	1.04	0.38	1.31	0.22	1.10	3.90
7	1.23	4.24	1.11	3.57	2.77	3.98	1.10	2.11	0.40	1.38	0.16	0.80	6.77
8	0.85	2.93	0.85	2.73	2.12	3.53	1.58	3.04	0.45	1.55	0.35	1.75	6.20
9	0.95	3.26	2.42	7.81	3.98	9.84	4.54	8.73	1.36	4.69	0.50	2.50	13.75
10	2.00	6.90	3.54	11.42	5.69	13.55	5.77	11.10	2.54	8.75	1.55	7.75	21.09
11	1.43	4.93	3.45	11.14	5.08	12.09	4.76	9.16	1.64	5.67	0.71	3.53	17.07
12	1.25	4.29	2.19	7.06	4.26	10.14	5.03	9.67	2.52	8.69	1.54	7.71	16.79
13	0.47	1.62	0.95	3.06	1.15	2.74	4.31	8.29	2.22	7.65	0.13	0.65	9.23
14	1.15	3.96	0.99	3.19	2.59	6.17	3.27	6.29	0.80	2.76	0.45	2.25	9.25

TABLE 4.4 Measured lake shore retreats between October 1986 and May 1987.

Line	19 Oct - 17 Nov		17 Nov - 18 Dec		18 Dec - 29 Jan		29 Jan - 22 Mar		22 Mar - 20 Apr		20 Apr - 10 May		Mean angle
	angle	rate	angle	rate	angle	rate	angle	rate	angle	rate	angle	rate	
1	23	1.34	26	1.67	28	3.67	28	2.62	23	2.47	27	2.59	26
2	24	1.02	30	0.49	26	1.38	29	0.61	28	0.89	27	0.11	27
3	27	0.52	23	1.08	30	2.47	29	4.04	29	3.26	28	1.88	28
4	22	0.69	19	0.51	24	1.92	21	0.07	21	0.00	21	0.08	21
5	17	1.01	18	0.37	19	1.26	19	0.00	19	1.58	19	0.83	20
6	30	1.47	29	1.81	26	0.78	26	0.46	26	0.57	26	0.48	27
7	29	2.06	29	1.68	28	1.87	29	1.02	28	0.65	28	0.38	29
8	26	1.28	28	1.28	32	1.87	29	1.47	30	0.78	30	0.88	29
9	46	2.34	50	5.98	53	7.86	54	7.06	54	3.79	55	2.05	52
10	55	5.65	54	9.23	53	10.82	56	9.20	56	7.25	56	6.43	55
11	53	3.94	55	9.13	55	9.90	54	7.41	53	4.53	54	2.86	54
12	51	3.34	49	5.33	51	7.88	50	7.41	52	6.85	50	5.91	51
13	25	0.68	36	1.80	36	1.61	33	4.52	33	4.17	34	0.36	33
14	29	1.92	33	1.74	33	3.36	31	3.24	31	1.42	31	1.16	32
Means:													
Ice:	51	3.82	52	7.42	53	9.12	54	7.77	54	5.61	54	4.31	
Debris:	25	1.20	28	1.24	28	2.02	24	1.81	27	1.58	27	0.88	

TABLE 4.5 Slope angles and melt rates perpendicular to slopes of lake shore transects.

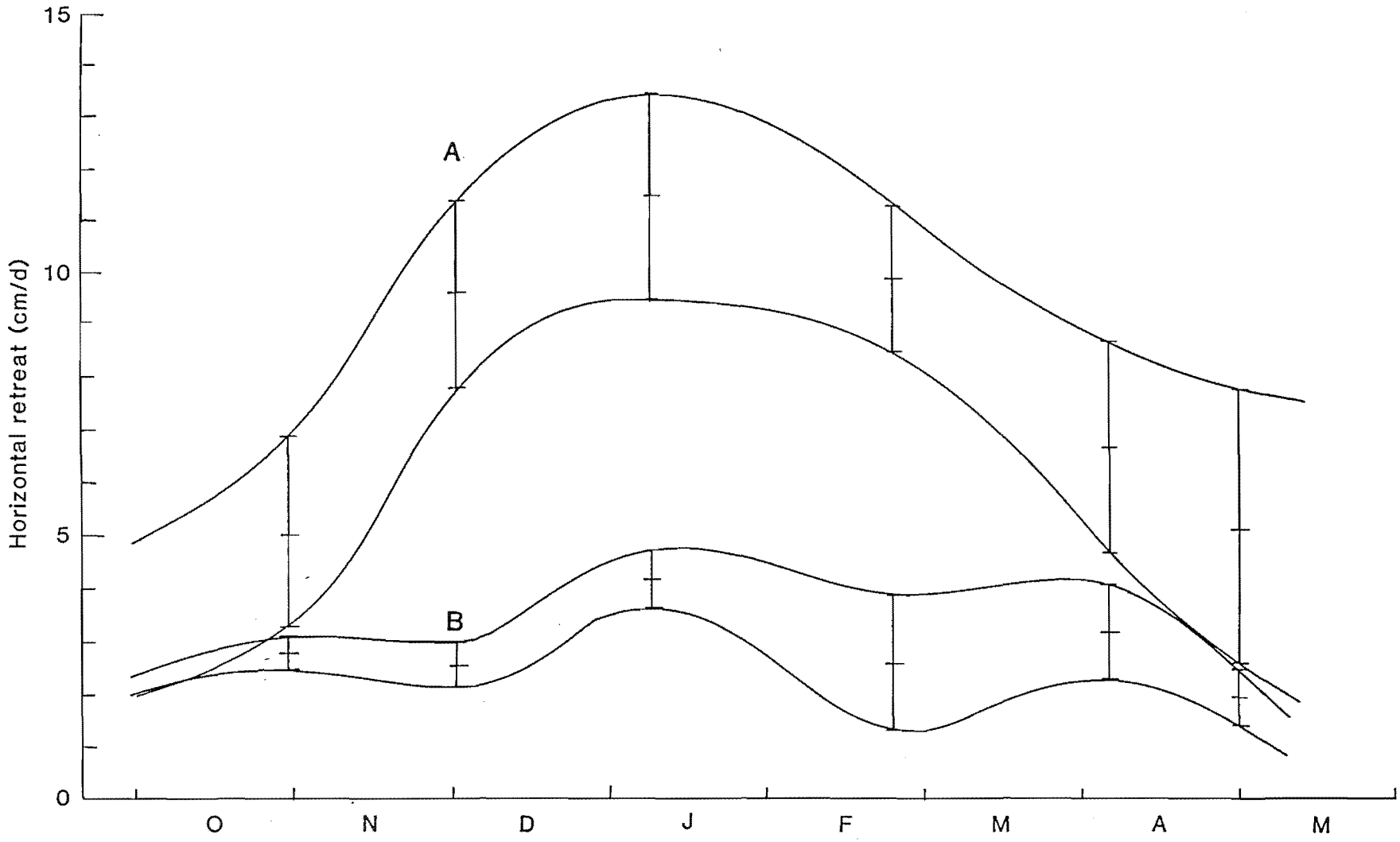

FIG. 4.20 Measured horizontal shoreline retreat of the Tasman proglacial lakes during the 1986-87 ablation season. The mean retreat ± 1 standard deviation is shown for 4 ice walls (A) and for 10 debris-covered slopes (B). Points are plotted at the mid-point of each measurement period.

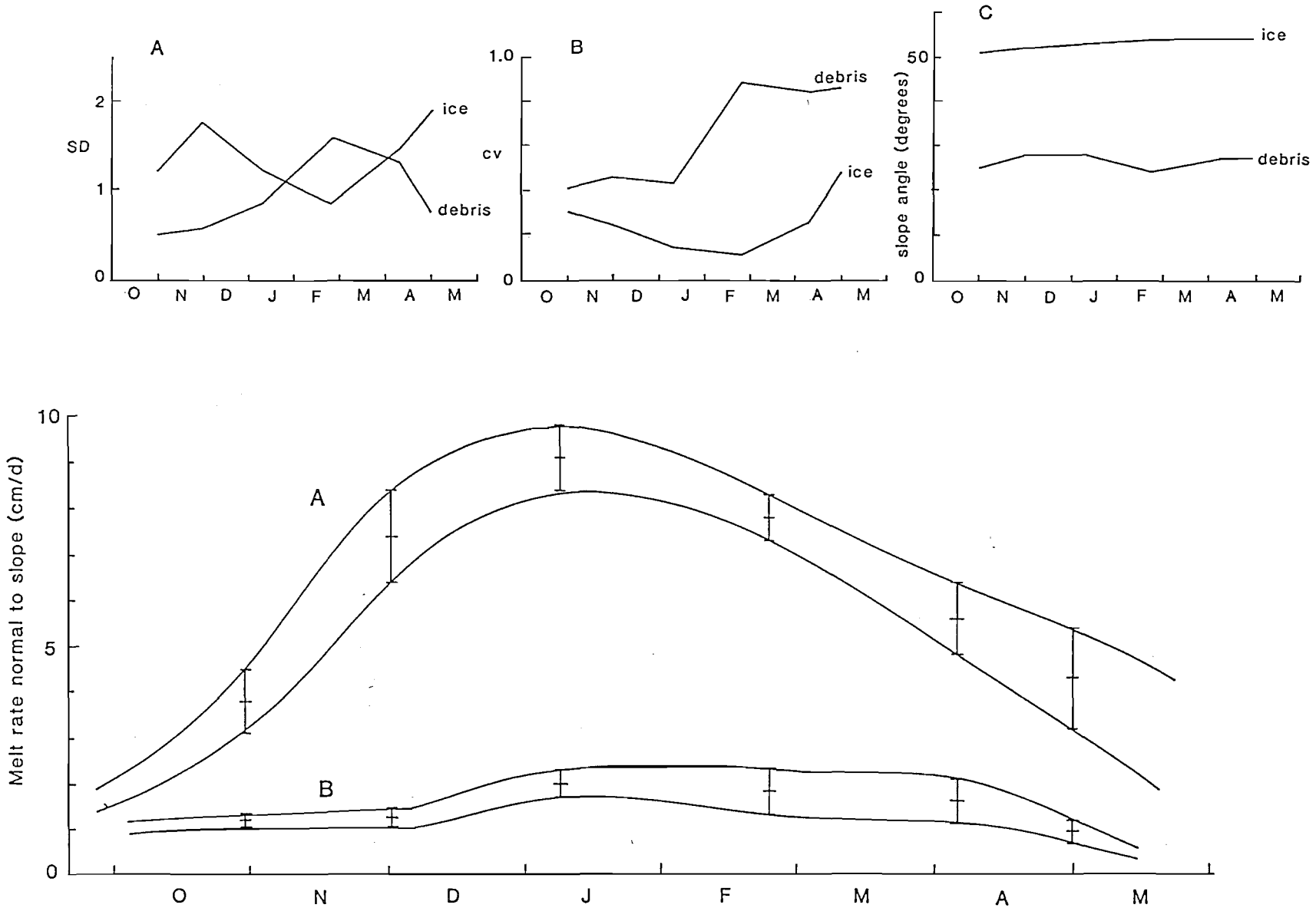

FIG. 4.21 Main graph: estimated melt rates normal to shoreline slopes. Means ± 1 standard deviation are shown for 4 ice walls (A) and for 10 debris-covered slopes (B). Insets, A: seasonal variation in standard deviations of melt rates; B: seasonal variation in co-efficients of variability of melt rates; C: mean angles of ice and debris slopes.

Period	Ice slopes			Debris slopes		
	S.D.	S.E.	cv	S.D.	S.E.	cv
19/10 - 17/11	1.19	0.69	0.31	0.49	0.16	0.41
17/11 - 18/12	1.77	1.02	0.24	0.57	0.19	0.46
18/12 - 29/01	1.25	0.72	0.14	0.86	0.29	0.43
29/01 - 22/03	0.84	0.48	0.11	1.59	0.53	0.88
22/03 - 20/04	1.46	0.84	0.26	1.32	0.47	0.84
20/04 - 10/05	1.89	1.09	0.44	0.76	0.25	0.86

TABLE 4.6 Variability of melt rates for each slope category and measurement period.

Horizontal retreat of the lake shores can be converted to melt rate perpendicular to the slope, p, by

$$p = {}^{\Delta}h \,/\, \sin\alpha \qquad (17)$$

where ${}^{\Delta}h$ = horizontal retreat rate and α = slope angle. Estimated melt rates for each transect are presented in Table 4.5. Fig 4.21 presents seasonal melt rate curves for bare-ice and debris-covered ice slopes. Because parallel retreat occurs, bare-ice slopes have consistently steeper angles (Fig 4.21C), and the difference in melt rate between the two slope groups is greater than the difference in horizontal retreat. Ice slopes melt at up to 4.5 times the rate of debris-covered slopes, a similar difference to that measured from ice-cored moraine in Antarctica (Pickard 1984).

The seasonal melt curve of debris-covered slopes (Fig 4.21) is smoother than the curve of horizontal retreats (Fig 4.20). This indicates that irregularities in the latter are at least partly due to variations in slope angle between transects. Bare-ice slopes maintain a smooth seasonal curve of melt rate. However, the decline in melt in late summer is slower than expected, compared to curves of melt rate from the glacier surface at Ball Hut, 9 km upstream. Lake water may act as a heat reservoir in late summer, from where advective heat transfer maintains rapid melting of adjacent ice slopes.

Graphs of the variability in melt rate between transects (Fig 4.21A and B, plotted from Table 4.6) show contrasts between bare-ice and debris-covered slopes. The seasonal trends in standard deviation show essentially opposite patterns for the two slope types. Variability within bare-ice slope melt rates is least in late summer, when there is maximum variability within debris-covered slope melt rates. The co-efficient of variability (cv) is dependent on melt rate for bare-ice slopes, hence at a minimum when melt rates are greatest. This is expected, given the ablation results in Chapter 2.2. In contrast, cv for debris-covered slopes rises dramatically in mid-summer and maintains a high value throughout the autumn period. The difference is probably due to thickness changes of the debris cover. The base of the debris cover on the slopes is usually clogged with mud, just as the stable debris mantle itself is. In mid-summer, when melt rates are greatest, moisture supply from melting ice to the base of the debris cover is greater than can be drained away, and the pore water pressure in the mud layer reaches a critical value for failure. Sliding of the saturated debris cover has been observed on several occasions in late summer, each time the slide occurs along the saturated,

Glacier		1920 - 1961 41 years	1961 - 1965 4 years	1965 - 1971 6 years	1971 - 1974 3 years	1974 - 1986 12 years	Total retreat (km)
Classen	retreat (km)	0.90	0.33	0.40	0.09	0.61	2.33
	rate (ma^{-1})	22.0	82.5	66.7	30.0	50.8	
Grey E.	retreat (km)	0.15	0.70	0.27	0.11	0.70	1.83
	rate (ma^{-1})	3.7	175.0	45.0	38.3	58.3	
Grey W.	retreat (km)	0.55	0.35	0.50	0.10	0.44	1.94
	rate (ma^{-1})	13.4	87.5	83.3	33.3	36.7	
Godley	retreat (km)	-	-	0.08	0.10	1.60	1.78
	rate (ma^{-1})	-	-	13.3	33.3	133.3	

TABLE 4.7 Retreats of calving glacier termini in the Godley Valley.

Date	h_v (m)	$\frac{h_v}{\text{ice depth}}$
1957	31	.20
1965	28	.19
1971	26	.18
1973	25	.17
1986	20	.14

TABLE 4.8 Mean vertical height of the glacier surface (h_v) above the Tasman lake based on the measured height in 1986 and a rate of glacier thinning of 0.38 ma^{-1}.

muddy interface between the ice and the debris cover. Slides are localised and occur irregularly, so that their effect is to increase melt rate variations spatially around the lake shore, giving the increase in cv shown by Fig 4.21B.

Changes in slope condition combined with seasonal melt changes cause, on any single slope, irregular variations in melt rate. Fig 4.22 contrasts the variation in melt rate of transects which were very similar in angle and debris cover when measurements commenced. For example, transect 7 shows the expected seasonal variation in rate, over a period in which no significant change in angle or debris cover occurred. No bare ice was visible during the whole measurement period. Transect 13 initially followed a similar trend, but in late summer a rapid increase in melting was observed. This was caused by slumping of the debris cover to expose ice over about 75 % of the slope height, a thin cover remaining at the base. Rapid melting increased the rate of fall of debris from the top of the slope which quickly buried the bare ice so that on the visit on 10th May little ice was exposed and, combined with lower air temperatures, the melt rate had been drastically reduced. These two transects typify the variability in melting caused by debris movements on the slopes. The sample of 10 debris-covered slopes gives an indication of the average variation for slopes of this type. No relationship between the pattern of ablation and slope aspect emerges. (Pickard, 1984, found this for ice-cored moraine scarps in Antarctica).

Local variations in supraglacial debris thickness above adjacent ice slopes cause changes in debris supply from above as slopes retreat. Slopes which have become buried by debris but which are bordered by bare-ice slopes may be isolated as ice-cored islands due to differential ablation between adjacent slope segments. Water depth at the slope foot is also important, because deep water prevents accumulation of a debris apron. Shallow water allows ice-contact debris cones to grow and progressively cover the ice, causing a reduction in melting and slope angle.

Retreat by subaerial ice-slope melting gives rise to shallow but extensive ice-floored lakes. Long-term lake growth is the average of highly-variable short-term melt rates of the lake shores.

4.2.3 Observations of calving termini.

The Classen, Grey/Maud, and Godley Glaciers all terminate in steep ice cliffs, retreating rapidly (Fig 4.23; Table 4.7) to calve abundant

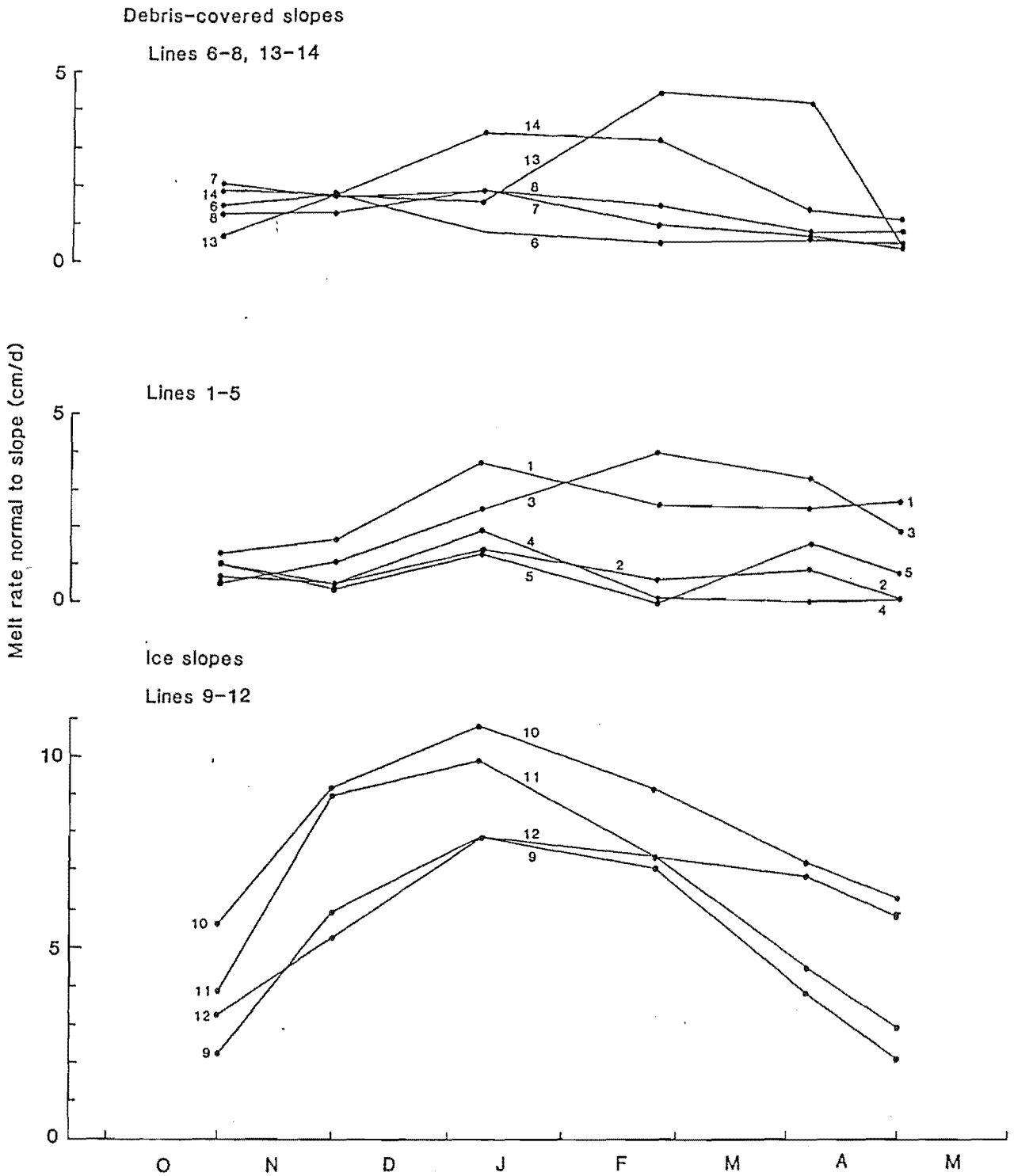

FIG. 4.22 Seasonal melt rates normal to slopes for individual measured transects. Lines 1 to 8 and 13 to 14 are debris-covered slopes, Lines 9-12 are ice walls.

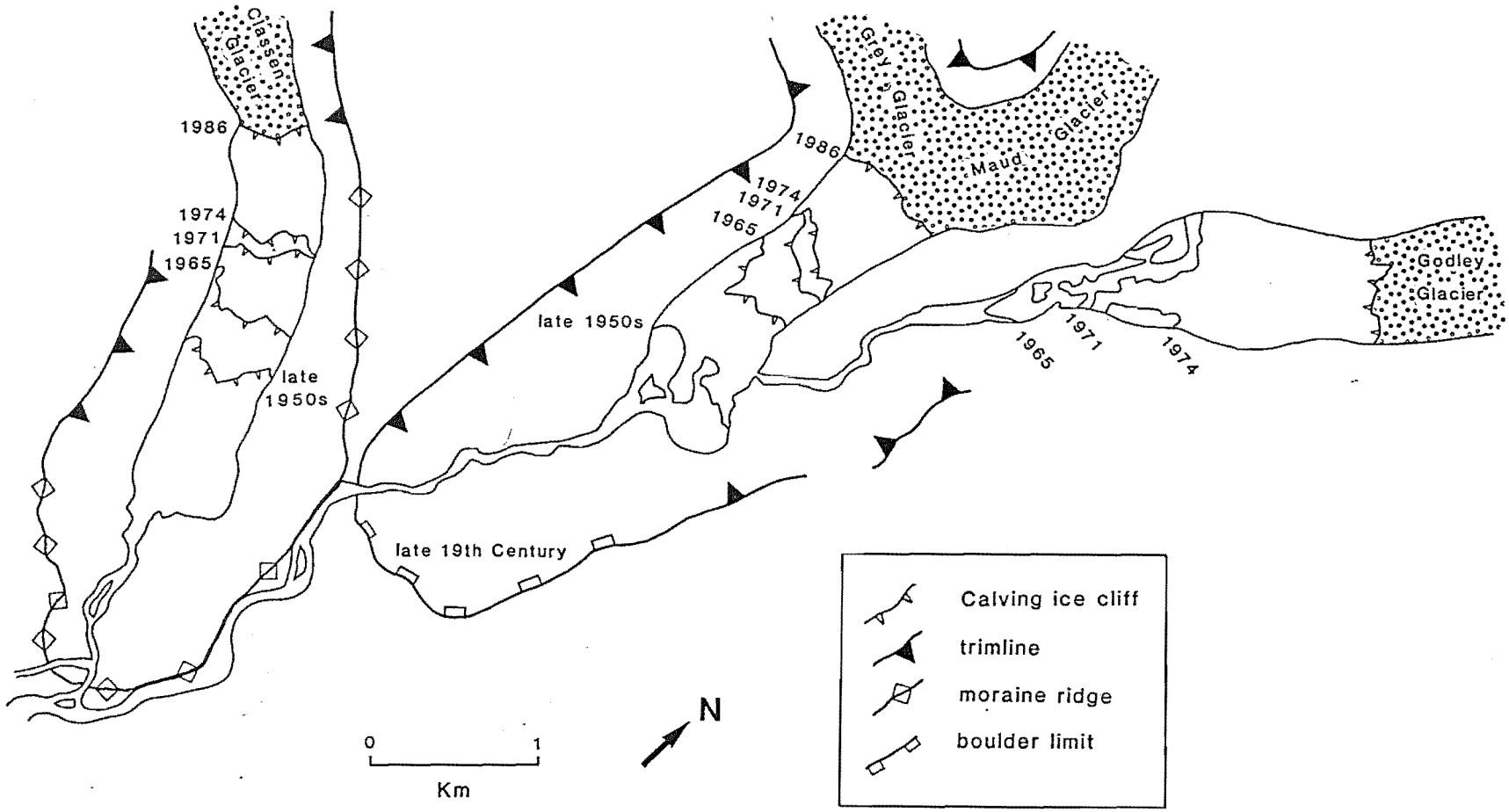

FIG. 4.23 Map indicating positions of terminal ice cliffs of glaciers in the Godley Valley at different times. Data collected from vertical aerial photographs. Trimlines, boulder limits, and moraine ridges delimit ice margin positions of the late Neoglacial maximum of the late Nineteenth Century.

icebergs into the proglacial lakes (Fig 4.15). Similarities exist with other calving termini such as the well-documented Columbia Glacier in Alaska, though recent rates of retreat in New Zealand are comparatively low. No temperate glaciers are known to have floating termini, yet drastic retreat is documented for several temperate glaciers (Meier & Post 1987). The critical factor governing calving rate is water depth at the terminus (Rasmussen & Meier 1982). Glaciers whose termini lie on a bedrock reigel or moraine shoal distal to an overdeepened basin are in a metastable state, in that they are "pinned" at the terminus. A small retreat which results in the withdrawal of the terminus into deep water usually heralds a phase of very rapid retreat, commonly of hundreds of metres to kilometres per year. The similarity in long profile of the lower Tasman and Columbia Glaciers is striking (Fig 4.24).

4.2.3.1 Calving mechanisms.

Calving is a poorly-understood process. Five possible mechanisms have been proposed (Kristensen 1983):

1. lateral spreading causing creep failure (Robin 1979);
2. Reeh-type calving due to an imbalance of hydrostatic forces along a vertical face (Reeh 1968);
3. hinge-line calving due to flexure at a grounding line (Holdsworth 1978);
4. vibrational calving due to the excitation of natural frequencies of ice;
5. collision by other icebergs and impact fracture.

Most of these processes assume that the glacier is floating, and therefore are not applicable to the study area. Others are discounted for reasons of scale and ice-front morphology. A less elaborate explanation of the timing of calving events is provided by Sikonia & Post (1980), who found a correspondence between calving rate of Columbia Glacier and meltwater run-off.

4.2.3.2 Observations of ice cliffs of the study glaciers.

Several features of calving termini give clues as to the process of calving.

Crevasses above ice cliffs form because the basal shear stress is reduced near to a partially or wholly buoyant terminus, and extensional glacier flow occurs. Such crevasses provide weaknesses for calving to exploit. Crevasses parallel to the ice front are visible on aerial

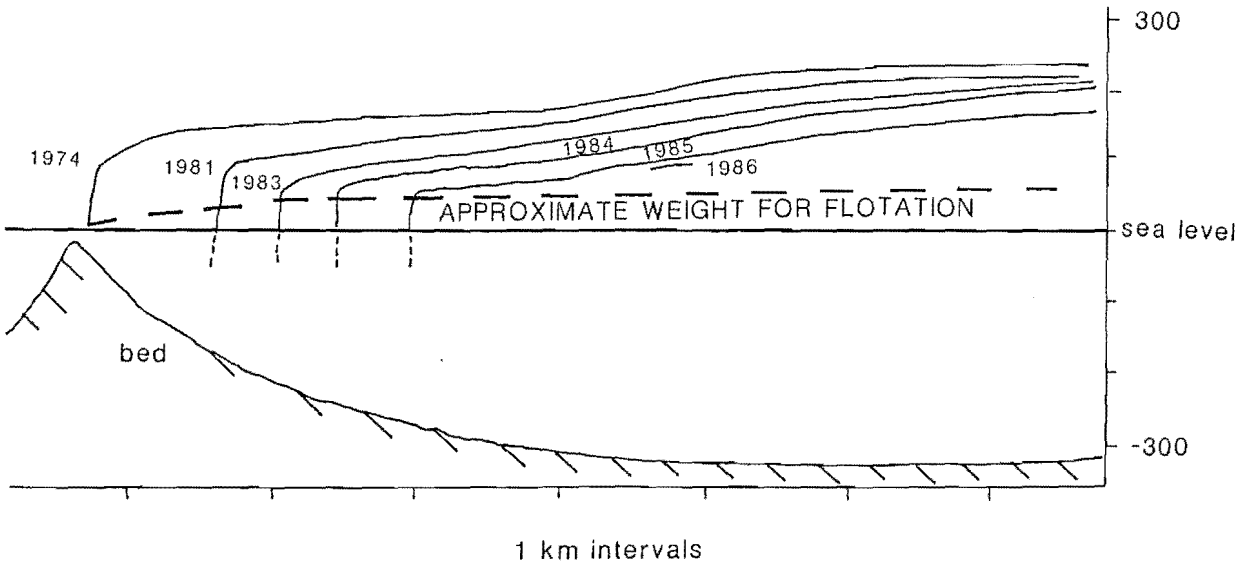

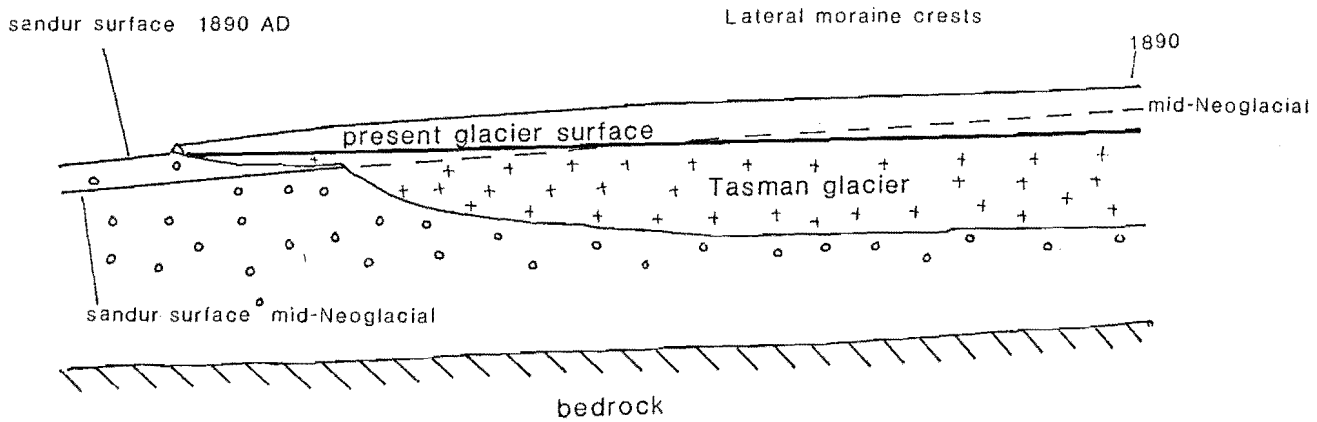

FIG. 4.24 Long-profiles of the Tasman Glacier (Broadbent 1973) and the Columbia Glacier, Alaska (Krimmel & Vaughn 1987), both showing glaciers terminating on a reverse slope in front of a deep basin.

photographs of the study glaciers, eg Classen Glacier in 1974 and 1986 (Fig 4.26). In 1986 about 10-12 crevasses were regularly spaced at intervals of about 25 m. Their concave-downstream pattern indicates extensional flow (Paterson 1981: Fig 11.4). The lack of a chaotic pattern of criss-crossing crevasses indicates that longitudinal strain is small compared to other documented examples (eg Meier & Post 1987).

Iceberg dimensions from the Godley and Classen Glaciers indicate that calving by a Reeh-type mechanism may have occurred. Reeh-type calving predicts that the size of an iceberg approximates to the floating length of a glacier, but that fracture should occur at a distance from the ice cliff which is no more than the ice depth (Reeh 1968: p.231). Thus, calving is likely when the floating length of a glacier is equal to ice thickness. Although most icebergs observed in the Godley Valley are small, examples which measure 120 x 75 m (an upright, debris-mantled berg from Godley Glacier) and 80 x 80 m (a tilted berg from the Classen Glacier) have been observed (Fig 4.15). These dimensions correspond to predicted thicknesses of these glaciers (based on gradient) of 70 m $\pm$ 35 m and 56 m $\pm$ 28 m (Chinn, unpublished data). It appears that full-depth calving has occurred on the glaciers, as well as the production of smaller bergs whose sizes are controlled by crevasse geometry. The implication is that the glacier termini are buoyant, though actual flotation is probably lacking (Fig 4.24). A similar mechanism to that proposed by Reeh (1968) may operate, but with the major difference that buoyancy forces may cause calving to occur before the terminus begins to float.

Flotation of a glacier tongue is expected to occur when less than 12 to 15% of the glacier thickness is unsupported by buoyancy (Krimmel & Vaughn 1987). The ratio of the ice cliff height to the glacier thickness has a critical ratio for buoyancy of c.0.14 to 0.12 (Fig 4.24). Cliff heights and cliff-to-glacier thickness ratios for the Tasman Glacier (which has not commenced calving) are given in Table 4.8. By 1986, the Tasman Glacier had thinned to reduce this ratio to the critical value at which calving and rapid retreat should commence. The transition to a "fast mode" of retreat is imminent.

At the Godley Glacier, the transition to a calving terminus occurred when the lake floor disintegrated in the 1970s (Fig 4.23). An irregular glacier front in 1974 subsequently straightened, to attain the most stable form with respect to the buoyant forces acting upon it. The commencement of calving on the Classen and Grey-Maud Glaciers cannot be identified precisely, but must have occurred between visits in 1914 (Williams 1967)

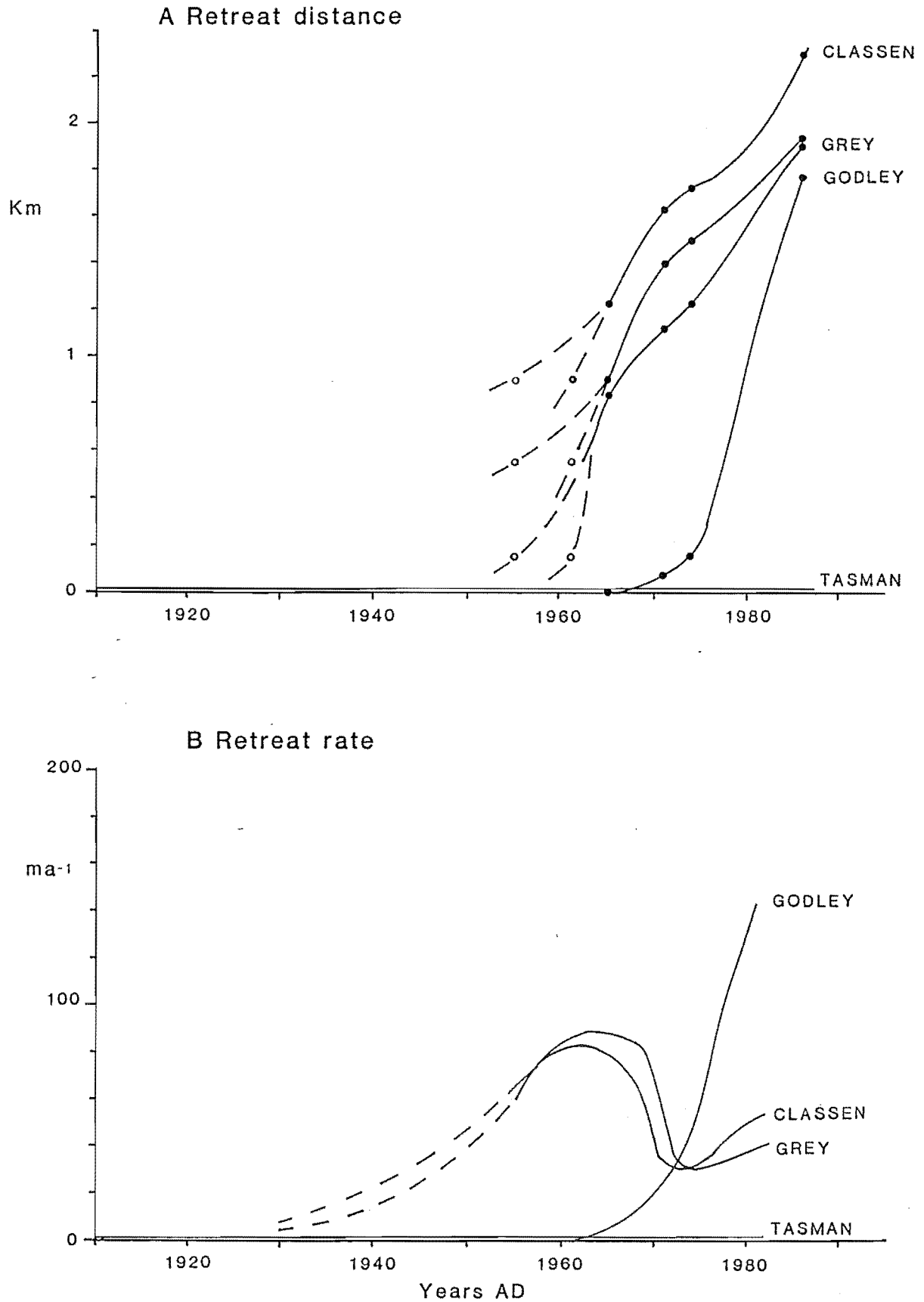

FIG. 4.25 (A) Cumulative retreat of calving glaciers in the Godley Valley compared to the Tasman Glacier. Dashed lines indicate alternative values depending on the date of the earliest photograph, which is uncertain. (B) Retreat rates of calving ice cliffs. Dashed lines are probable approximations based on verbal descriptions of the glaciers.

Classen Glacier in February 1986

0 km 1

Figure 4.16

FIG. 4.27 Ice floes on the proglacial lake of the Tasman Glacier in February 1987. On this and on other occasions there was no evidence of calving of lake shorelines, implying that the ice floes originated by disintegration of the lake floor.

and the earliest aerial photographs from the late 1950s.

Retreat rates of calving termini are up to one order of magnitude faster than retreat due to melting alone (Fig 4.25). Repeated aerial photography over a 30-year period shows the Classen and Grey-Maud Glaciers to have been retreating most rapidly in the early to mid-1960s, possibly because the termini lay in the deepest parts of the lakes at this time. Slower retreats in the late 1960s may have corresponded to a positive mass balance trend, which caused the advance of the Fox and Franz Josef Glaciers a few years earlier (Chapter 2.2). The Godley Glacier has retreated at an increasing rate since calving commenced in the early 1970s. Retreat shows no correspondence with nearby glaciers, and is probably controlled by local lake bathymetry.

The question arises: is there any field evidence that the Tasman Glacier terminus will begin to calve in the near future ? The presence of fresh ice floes in the lakes, with no ice walls around the lakes showing recent calving, is evidence for current disintegration of the ice floor of the lake. Ice floes which must have originated at the lake floor have been observed on several occasions (Fig 4.27). The ice floor is likely to be riddled with cavities and conduits which, being water-filled, have not been closed by ice flow. These cavities form weaknesses aiding fracture of the ice due to its buoyancy underwater. Break-up of the lake floor will increase water depth at the terminus and probably lead to calving. The pattern of retreat observed in the Godley Valley is therefore expected to be replicated by the Tasman Glacier, and rapid retreat, perhaps exceeding 100 ma^{-1}, may commence in the next decade. The lower gradient and greater thickness of the Tasman Glacier may result in even more rapid retreat than that observed at the Godley Glacier.

4.2.4 A model of proglacial lake evolution, and threshold conditions.

Observations of the Tasman and Godley Glaciers are here synthesised into a model of retreat of low gradient debris-mantled glaciers ponded by outwash heads (Fig 4.28). The model represents the full sequence of events which is expected to occur if the mechanism of retreat continues to its completion, at which glacier volume becomes adjusted to prevailing climatic conditions.

4.2.4.1 Lake initiation related to the glacier drainage system.

Englacial conduits fluctuate in dimension according to variations in water flux, melting of conduit walls, and closure by ice flow (Glen 1954;

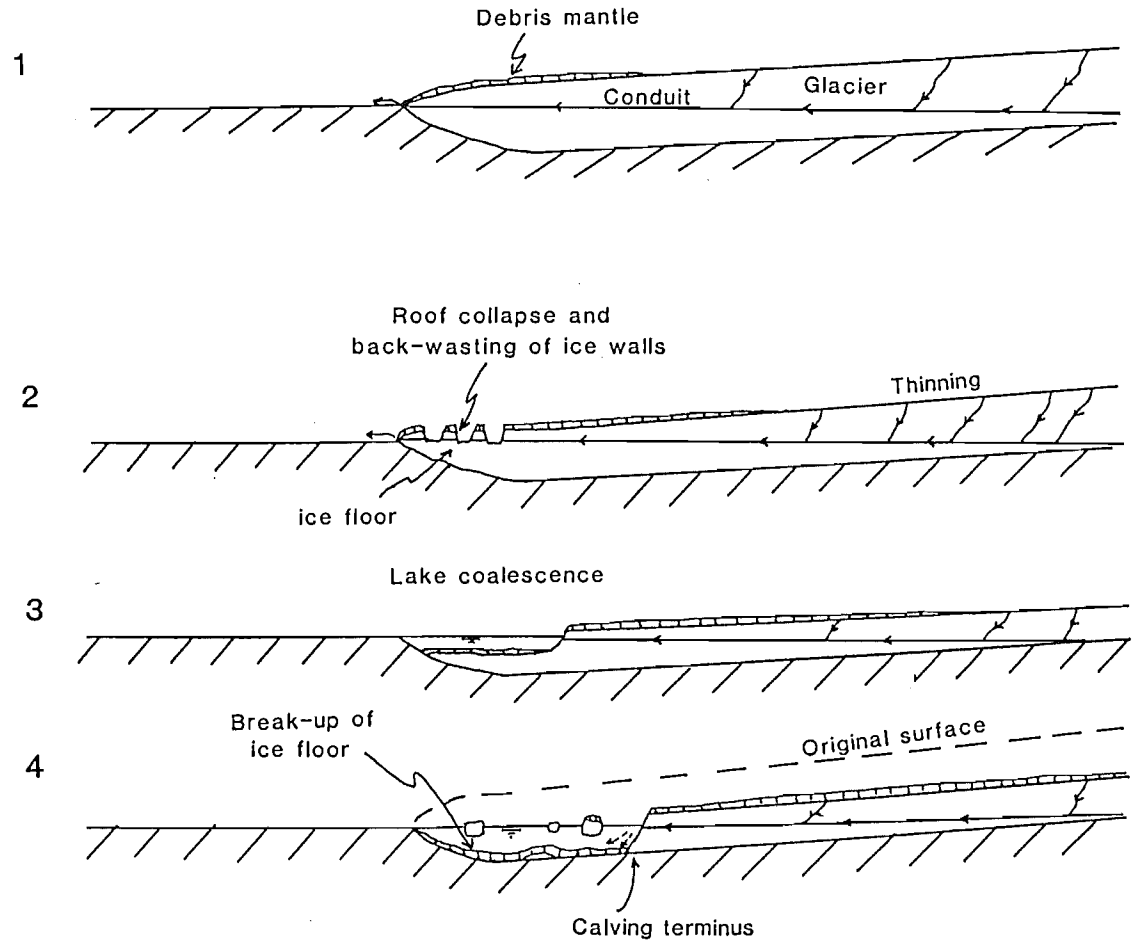

FIG. 4.28 Stages of proglacial lake formation at the Tasman Glacier.

1. Glacier at the 1890 maximum position, with englacial conduit in hydraulic equilibrium.

2. Thinning and debris-mantle spreading leads to collapse of conduit roofs, perforating the debris mantle with flooded circular holes.

3. Backwasting and coalescence of the holes leads to the formation of a single lake with an ice floor.

4. Disintegration of the ice floor increases water depth at the ice margin, where buoyancy forces cause calving and rapid retreat to commence.

The glacier is at present in a transition between stages 2 and 3.

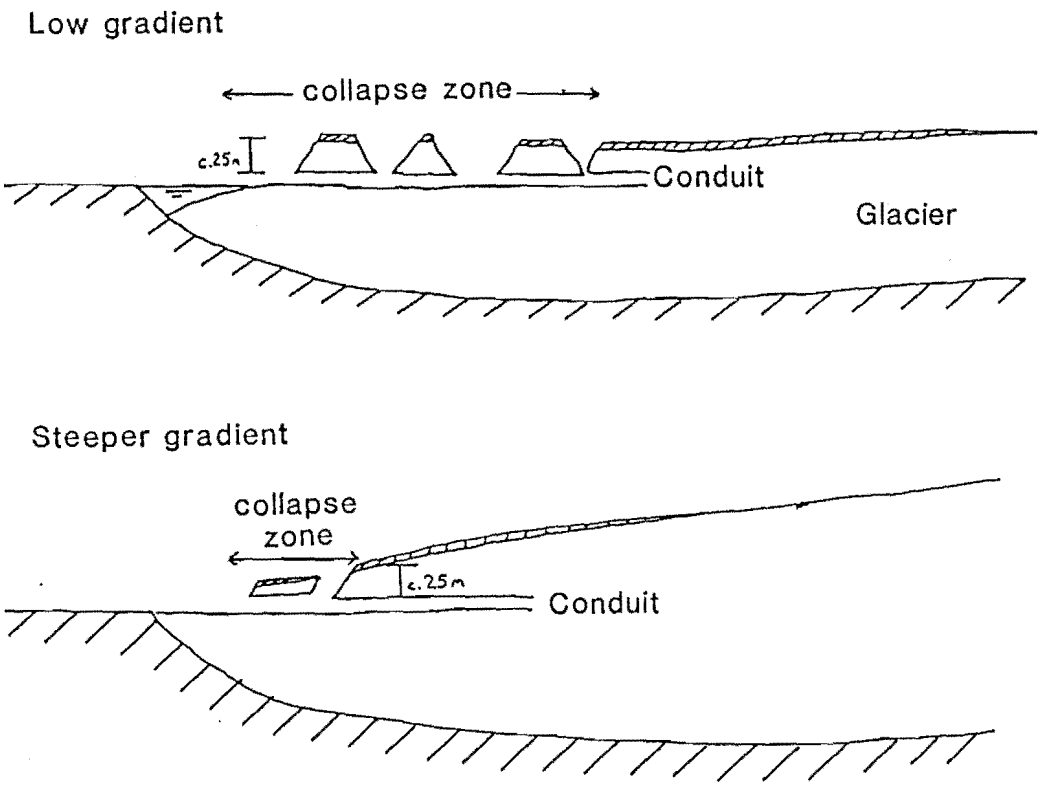

FIG. 4.29 The effect of glacier surface gradient on the extent of conduit collapse at a glacier terminus.

Shreve 1972; Röthlisberger 1972; Nye 1976). In general, conduits enlarge quickly during periods of high englacial water pressures (spring) but close slowly during winter periods of low discharge. In the ablation zones, stable conduit networks develop with respect to piezometric gradient. Conduits are predicted to flow perpendicular to equipotential surfaces in the glacier which dip upstream at approximately eleven times the surface gradient (Shreve 1972).

The situation is complicated in glaciers where the terminus is not free-draining but lies above a reigel or other reverse slope. The outwash head beneath the Tasman Glacier terminus may be likened to a bedrock reigel. Theoretical calculations predict that high-pressure flow in full conduits allows water to flow uphill to the terminus, a theory supported by observations of esker paths (Shreve 1985). Water pressures may even be sufficient to allow large subglacial lakes to persist on the upstream flanks of reigels (Lliboutry 1983).

Lliboutry (1983) believes that gradient conduits develop behind a reigel and along the lateral margins of glaciers. These conduits flow at atmospheric pressure at the highest feasible level in the glacier, in effect at the level of the top of the reigel. In the Tasman Glacier, such conditions would mean that open-channel flow (Banerjee & McDonald 1975) exists for several hundred metres upstream of the terminus, rather than full conduits under pressure.

Collapse of englacial conduits on the Tasman Glacier supports the predicted geometry of englacial drainage. Circular water-filled holes (Figs M1 and A1) originated by collapse of conduit roofs, well illustrated by the 1971 aerial photograph (Fig A1). If the conduits have maintained a level in the glacier determined by the level of the outwash head, as predicted by Lliboutry's theory, surface lowering of the glacier caused thinning of the conduit roofs to the point where they were no longer self-supporting. This point was reached when the glacier surface was c.25 m above the water level. Paige (1956) describes conduit roof collapse on the Black Rapids Glacier, Alaska, occurring at a similar point during thinning following a surge.

Differences between the Tasman and other glaciers in the Mount Cook area relate to the exceptionally low gradient of the Tasman Glacier. Conduit collapse occurred above instead of at the terminus, as in the case of the Hooker and Godley Glaciers. This is due to the angle of intersection, in a vertical plane, of glacier surface and conduit paths (Fig 4.29).

4.2.4.2 Lake growth by shoreline melting.

The protective debris mantle was perforated by tunnel collapse, exposing ice walls to ablation. Melting of the ice walls ensued, at a rate commensurate with the ablation rate of bare ice at this altitude, and circular lakes developed. Growth since 1971 corresponds to a linear retreat rate averaging 13.4 ma^{-1}. Comparison of short- and long-term growth rates reveals that the ablation rate of the ice walls has not increased since 1973, but the rapid increase in plan area of the lakes is simply due to their circular shape.

4.2.4.3 Threshold transition to rapid calving retreat.

The transition to a straight transverse ice cliff and rapid retreat by calving follows the break-up of the lake floor and retreat off the outwash head into the deep basin behind. The balance of forces acting on the terminus during the transition is not understood. Exactly when the ice floor disintegrates and a calving cliff develops is probably a function of lake depth, ice cliff height and geometry, and storm-induced lake level fluctuations. Interaction of these variables eventually causes a threshold to be crossed and there is a change of state in the mode of glacier retreat. The time taken from initial lake growth to the onset of calving was about 10 years for the Godley Glacier (Fig 4.25), and is probably about 15 years for the Tasman Glacier. I believe the latter to be very close to rapid retreat at present.

In general, calving rates are difficult to predict (Meier & Post 1987) and depend more directly on lake bathymetry than on climatic variations.

4.2.4.4 Regional gradational threshold in lake evolution.

Begin & Schumm (1984) describe how responses of examples of the same landform give a smooth function of the forcing mechanism (Fig 4.30). This reflects differences within a region in the timing and magnitude of change between individual sites. Such differences result from different sensitivies to change of individual landforms, termed "landform singularity" (Brunsden & Thornes 1979). A threshold zone separates landforms in the primary state from those in the final state: this zone defines a gradational threshold.

Although Begin & Schumm (1984) apply the concept of gradational threshold to examples from fluvial geomorphology, the present study provides an example from glacial geomorphology. A threshold marking a

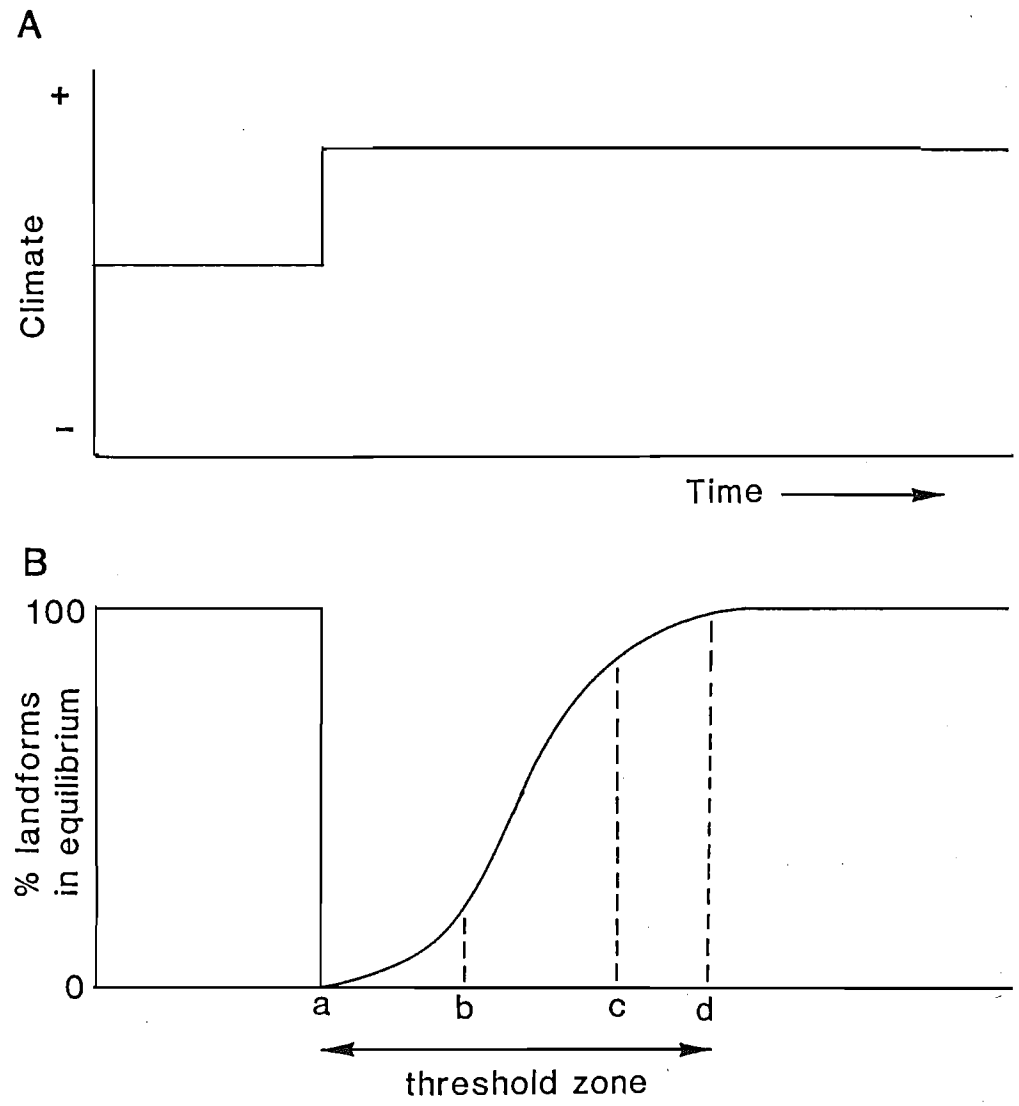

FIG. 4.30 Gradational threshold of responses of similar landforms to a step-like climatic change.

(A) Amelioration of climate at time (a) to a new constant climate.

(B) Landform response. All landforms are in equilibrium with climate before climate change at (a). A small proportion of very sensitive landforms adjust rapidly to a new equiibrium between times (a) and (b). Most landforms adjust between (b) and (c), but insensitive landforms adjust latest between (c) and (d). At (d), all landforms have attained a new equilibrium condition. The period of change between (a) and (d) represents a gradational threshold, or threshold zone.

transition from proglacial lakes growing at relatively slow rates (by shoreline melting) to those growing rapidly (by calving) is defined at each glacier by local changes in ice thickness, water depth and so on. Variations between glaciers cause landform singularity, resulting in differences in the timing of the onset of rapid retreat. Thus a gradational threshold exists.

Negative mass balance causing the present glacier shrinkage probably affected all glaciers at about the same time initially (Gellatly 1985c). The eventual onset of rapid retreat occurred first on the Classen Glacier (in the 1950s), then on the Grey/Maud Glacier (between 1961 and 1965), then on the Godley Glacier (in the mid 1970s), and soon on the Tasman Glacier (probably before 1995). Whether the same threshold will affect other glaciers is uncertain. The threshold zone spans at least 40 years due to differences between glaciers in length, gradient, debris mantle insulation, subglacial topography, and ablation rate.

The singularity exhibited by the Mount Cook glaciers makes predictions of their response difficult. Lacking detailed studies, there are uncertainties about which glaciers will cross a threshold to rapid retreat, and about the timing of changes in the mode of retreat. The prediction for the Tasman Glacier is based on information of subglacial morphology and known rates of change in the ice front, using the Godley Glacier (where the transition has already occurred) as an analogue. Insufficient data exists to predict the future behaviour of the Mueller, Hooker, and Murchison Glaciers.

4.2.4.5 Significance of the debris mantle for lake formation.

Glacier retreat would probably have resulted in the formation of a proglacial lake regardless of whether or not a debris mantle existed. However, the presence of the debris mantle on the Tasman Glacier causes a reduction in surface gradient, while delaying terminus retreat until surface lowering causes collapse of englacial conduit roofs. Without this, the proglacial lake would not have formed in the manner observed, and presumably similar lakes have not formed elsewhere for the same reasons.

Preservation of the glacier tongue has delayed the onset of retreat by nearly a century. The glacier, rather than retreating progressively and relatively slowly, has been held in a metastable state. The morphological changes caused by the debris mantle have increased the potential instability of the glacier tongue, so that its length is now so far out of equilibrium that a very rapid adjustment is almost inevitable. The

mechanisms of proglacial lake formation and rapid terminus retreat provide the means for this adjustment to take place.

4.2.4.6 Significance of proglacial lakes for catchment sediment dynamics.

The formation of proglacial lakes has important consequences for sediment transport. Prior to lake formation, there is direct transfer of large volumes of debris from glacier to proglacial outwash fan, where fluvial redistribution aggrades the fan surface. As soon as a lake exists, a sediment trap is created which abruptly interrupts the link in the transport system.

An analogy is drawn between proglacial lakes and damming of gravel bed rivers by humans. In both cases, a sediment trap is created instantaneously. This major change in the relationship of sediment and water discharges causes disequilibrium until channel systems readjust. Empirical work on artificially-dammed rivers has found that downstream effects of damming are sensitive to the dammed river's importance in the basin, relative to principal contributing areas for sediment and run-off: if the river is important, damming will be a major change to catchment sediment dynamics.

Dam construction has four effects (Williams & Wolman 1984; Andrews 1986):

1) peak discharges reduce by an average of 39% (but documented cases vary between 3% and 91%);

2) coarse sediment is trapped in the reservoir, large reservoirs generally being 100% efficient; trapping of suspended sediment depends on reservoir size, but may reach 99% in large reservoirs. Sediment starvation causes rivers to cross the threshold of critical power to become "underloaded" and erosive;

3) the river immediately downstream degrades its bed (due to (1) and (2) above), at high rates for a few months after damming (0.1 to 7.7 ma^{-1}) reducing to very low rates after 5 to 10 years;

4) the degrading reach passes downstream into a reach in quasi-equilibrium, then into an aggrading reach where sediment is redeposited. These zones may migrate over time.

Traditional theories of glacier-induced change to fluvial regime involve proglacial aggradation during glacier advance, due to abundant debris supply from glaciers, followed by degradation when this supply is cut off during retreat (Gage 1958; Suggate 1958; Wilson 1985; Maizels

1989). Wilson (1985) presents evidence from the Canterbury Plains for river aggradation during Pleistocene glacial periods, and degradation during interglacials. He ascribes the former to changes to vegetation cover and higher rates of mechanical weathering of rocks, but does not consider direct glacier-induced effects.

Current formation of proglacial lakes in the Mount Cook area is predicted to have far-reaching consequences for the proglacial fluvial system. Outwash plains which have been aggrading continuously for perhaps 5,000 years (Chapter 5) may, by analogy with effects of artificial dams, be becoming starved of bedload at the present time. The damming analogy indicates that the Tasman and Godley Rivers may begin to incise the heads of their proglacial fans in the next few decades. If glacier retreat continues, proglacial lakes will be large enough to form persistent sediment traps, and a phase of terrace-forming incision may follow.

An analogy is drawn between the present situation and the retreat of Late Pleistocene glaciers in the area. Proglacial lakes formed at that time still persist as Lakes Tekapo and Pukaki (Gage 1975), and major downstream incision occurred during glacier retreat (Maizels 1989). Terraces may have formed within a relatively short period after initial glacier retreat if measured rates of modern incision (Williams & Wolman 1984) are comparable.

4.2.5 Conclusions of Section 4.2.

Low gradient debris-mantled glaciers follow a characteristic pattern of adjustment to negative mass balance. Three phases of wasting are recognised:

1. An initial phase of downwasting, debris mantle spread, and reduced surface gradient, with no retreat of the terminus.

2. A phase of proglacial lake formation, perforating the protective debris layer and allowing growth of shallow proglacial lakes by melting. Initially, the form of the lakes mirrors the spatial distribution of englacial conduits near the glacier terminus.

3. A threshold transition to a phase of rapid terminus retreat by ice-cliff calving, until a new equilibrium is established.

All three phases are represented in the Mount Cook area at the present time. Differences in the timing and magnitude of changes between phases represent a gradational threshold. Evidence indicates that the Tasman Glacier is in a state of transition between the second and third phases, and a rapid retreat of the glacier tongue is imminent. Proglacial lakes

thus formed may persist as sediment traps aiding post-glacial incision of outwash plains.

4.3 SUMMARY OF CHAPTER 4.

Supraglacial debris-mantles occur in regions of high relief with abundant sources of debris for high-level transport, and where glacier long profiles are strongly concave to provide a flow structure aiding debris emergence. The geological structure of the central alpine region of the South Island has allowed glacial erosion to exploit structural trends sub-parallel to axial ranges, resulting in preferred orientation of valley glacier flow directions and asymmetry of ice supply to glacier tongues. This pattern provides topographic conditions favouring debris mantle accumulation.

The Tasman Glacier debris mantle shows distinct morphological zones caused by downstream changes in supraglacial debris distribution, differential ablation, and surface relief. Complex feedbacks operate during debris-mantle spread, governed primarily by the retarding effect of debris on ablation. Conditions of ice flow and debris supply allowed a debris mantle to exist during equilibrium ice mass balance on the Tasman Glacier, though negative mass balance greatly assists debris mantle formation.

Decay of low-gradient glaciers with thick mantles, typified by the Tasman Glacier, is a two-phase process of initial slow downwasting under a spreading mantle, followed by proglacial lake growth and rapid retreat of the terminus. Proglacial lakes initially form around collapsed englacial conduits perforating the protective debris mantle, causing rapid melting of bare ice walls. Subsequent break-up of the lake floor leads to a threshold transition to iceberg calving and retreat at a rate one order of magnitude faster than by melting alone. Although the presence of a debris mantle is probably not important in the formation of marginal lakes around ramp-like ice fronts such as at the Hooker Glacier, it is significant for thermokarst formation on the Tasman Glacier where gradient is less.

Glaciers in the Godley Valley are presently in the "fast mode" of retreat, whereas other glaciers in the area are at less advanced stages of decay. However, the Tasman Glacier is likely to commence rapid retreat by calving in the near future.

The style of debris mantle formation and glacier retreat described has implications for interpretations of short-term observations of glacier behaviour and their relationship to climatic change. After an initial

climatic impulse, the subsequent morphological development of the Tasman Glacier has been largely self-determined, and represents a relaxation path towards a new state of equilibrium. Observations of glacier retreat are interpreted as a response to climatic changes occurring in the first half of this century, rather than to more recent short-term fluctuations. The latter have had a minor effect on rates of change, rather than on the changes themselves.

CHAPTER 5: THE EFFECT OF GLACIER SEDIMENT BUDGET ON THE MORAINE RECORD IN THE MOUNT COOK AREA

Chapter 5 applies the processes and principles developed in earlier chapters to the glacial geological record. The aim is to investigate to what extent the debris transport system, and more specifically the sediment budget, has influenced the disposition of glacial deposits in the Tasman Valley since Late Pleistocene times. The climatic significance of the glacial record may thereby be evaluated.

The structure of Chapter 5 is as follows:

1) The empirical model of debris-mantle and glacier behaviour developed in Chapter 4 is adapted to the longer timescale involved when considering multiple glacier fluctuations. This extended model forms an a priori model for Neoglacial glacier behaviour, to be tested using geomorphic evidence from the Tasman Valley.

2) The existing glacial chronology is summarised and re-evaluated.

3) New evidence of Holocene fluctuations of the Tasman Glacier is presented.

4) Empirical observations and models of glacier behaviour are synthesised into a reconstruction of Holocene geomorphic development in the valley. The reconstruction is discussed in terms of the use of the chronology as an indicator of climatic change.

5) The chapter concludes with a comparison between the behaviour of the Neoglacial and Late Pleistocene Tasman Glacier, to assess the degree to which the former may be used as an analogue to aid interpretations of the latter.

5.1 AN A PRIORI MODEL OF GLACIER EVOLUTION IN AN AGGRADING ENVIRONMENT.

Before reconstructing the geomorphic development of the valley, it is desirable to set up a working model which develops the debris-mantle dynamic model of Chapter 4 to include the effect of multiple glacier fluctuations. The situation of a glacier whose terminus lies in a zone of long-term aggradation (ie a positive sediment budget) is described.

The model will show that glacier dynamics themselves evolve due to the changing configuration of the valley floor during aggradation. Such an evolution is a result of the sediment budget of the lower glacier and proglacial area, and is not a direct function of climate change. Such a

long-term non-climatic trend has not previously been described in the literature.

5.1.1 The development of a glacier "pond".

Fig 5.1 shows the effect of proglacial aggradation on the surface gradient of a hypothetical glacier. Differential uplift between the valley head and the lower valley is not manifested in an increase in relief. High uplift in the headwaters is compensated by the negative sediment budget and high erosion rates and results in no significant change in topographic elevation. However, at the glacier terminus, debris accumulates that has been transported both by the glacier "conveyor belt" and, (as demonstrated in Chapter 3.4), washed through the glacier in fluvial transport. Sediment is redistributed by outwash in the proglacial zone to form an aggrading fan rather than a terminal moraine. (This is an important contrast between glaciers in maritime areas with those in more arid areas, as Chernova (1981) suggests). Since no erosion occurs at the terminus, aggradation combines with the uplift rate to progressively raise the level of the outwash head, the reverse slope forming the proximal margin of the outwash plain, which may be likened to a "base level" for the glacier. The overall gradient is thereby reduced, and the lower tongue of the glacier is the zone most affected.

A glacier stillstand during aggradation allows the construction of an outwash head. Periodic advances and progressive over-riding of the outwash head would produce a gentler slope than a stillstand alone.

5.1.2 The effect of ponding on debris mantle dynamics.

Chapter 4 described how a supraglacial debris mantle operates as a self-regulating system involving the flow dynamics of the glacier tongue so that, once initiated, a debris mantle will tend to spread and thicken without further external impulse. An important feedback in this system involves the reduction of the glacier surface gradient causing longitudinal compression.

An implication of the ponding process described above is that it represents an external cause of a reduced glacier gradient. Referring again to Chapter 4, it is apparent that this will further enhance debris mantle spread in addition to the intrinsic reasons outlined in that chapter. By this is meant the propensity of the glacier to maintain a debris mantle whose dimensions fluctuate in response to mass balance changes, but which experiences an overall net growth over a period of

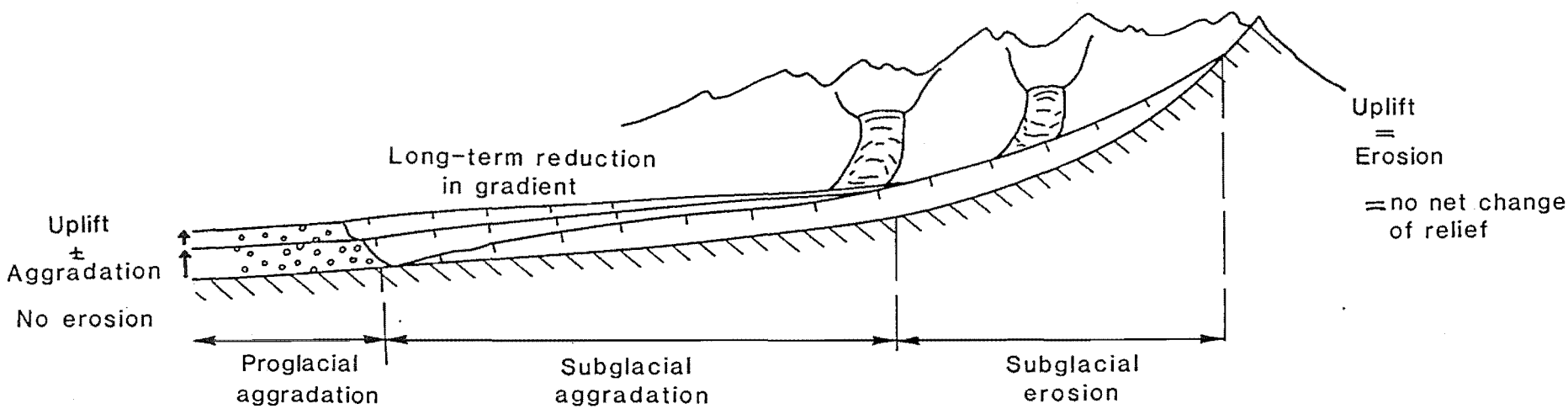

FIG. 5.1 Predicted effect of a positive proglacial sediment budget upon glacier morphology. Proglacial outwash aggradation causes ponding of the glacier and a long-term reduction in glacier surface gradient. This a priori model is based on assumptions of negative sediment budget in uplifting headwaters (causing equilibrium relief).

multiple glacier expansions and shrinkages such as those which have characterised the Neoglacial. What is not meant is the uninterrupted existence of a continuously-growing debris mantle.

It is therefore proposed that a glacier such as the Tasman, whose terminus lies in a zone of long-term aggradation, will evolve over time from a steeper and relatively "clean" glacier into a low-gradient debris-mantled glacier ponded behind an aggrading outwash fan. A stillstand is required to initiate the evolution, but thereafter the configuration of the terminal area and the flow structure will develop without any change in glacier mass balance.

The system of debris-mantle dynamics outlined in Chapter 4 may now be regarded as part of a broader system of evolution of the lower glacier which involves proglacial aggradation and ponding.

5.1.3 The effect on the glacier's response to climatic change: increasing inertia in climatic response.

As described so far, the process of glacier ponding is sensitive to being curtailed by climatically-induced mass balance change in the glacier. Either a large advance will establish a new terminus further down-valley, or else a retreat will open a proglacial lake to prevent further aggradation on the outwash surface.

However, the combined effect of an ice-contact outwash head and a supraglacial debris mantle is to reduce the sensitivity of the glacier terminus to mass balance changes. The effect is to reinforce the ponding process in both positive and negative mass balance. This works in two ways.

5.1.3.1 Glacier advance

For a given mass balance increase, the magnitude of a glacier advance is a function of the slope of the proglacial foreland (Paterson 1981: Fig 12.4). Steeper slopes encourage greater advances than gentler ones, and reverse slopes particularly reduce the horizontal advance of the terminus. Progressive aggradation of an outwash head creates a major reverse slope which acts as a barrier to glacier advance. Small or short-term positive mass balances will have difficulty over-riding the outwash barrier and the terminus will suffer increasing inertia as the barrier becomes larger. However, if the terminus over-tops the outwash head, it may then advance rapidly across the gentler slope of the fan surface.

5.1.3.2 Glacier retreat

Progressive ponding and debris-mantle spread will increase the insulation of the ablation zone. Over time, the magnitude of the negative mass balance change required to initiate retreat will become greater, and the glacier correspondingly less prone to retreat. The response lag-time will also increase. An indication of the length of this lag is given by the present glacier, which has not yet begun to retreat nearly a century after nearby debris-free glaciers commenced their retreats.

5.1.4 A comparison of "ponded" glaciers with "dam glaciers"

Ponding and thickening of a glacier tongue requires that the rate of proglacial aggradation exceeds the rate of basal till deposition, so that an outwash head is constructed. Three other possibilities may occur (Fig 5.2):

a). Proglacial aggradation = subglacial deposition, resulting in the progressive elevation of the glacier, reducing the gradient but causing no direct thickening.

b). Subglacial deposition > proglacial aggradation, resulting in the aggradation of a subglacial "carpet" of till on which the glacier rides.

c). Low outwash discharge + "dumping" of supraglacial debris, resulting in deposition of a large terminal moraine which may act as a barrier in the same way as an outwash head. Kick (1962; 1985) and Lliboutry (1977) have described how glaciers with exceptional debris loads build huge marginal moraines and ride upon rapidly-thickening beds of debris. Such glaciers have been termed "Dammgletscher". Kick suggests that surface lowering due to the recent thinning of such glaciers may have been compensated by an equivalent amount of subglacial deposition, resulting in fairly stable ice levels in spite of negative mass balance. Subsequent positive mass balances would result in a higher probability of over-topping of the marginal moraines and of till super-position than if the glacier bed was not rapidly aggrading.

Kick's descriptions (1962; 1986) indicate that this process involves both rapid termimal moraine construction and subglacial aggradation (case (b) above). Suitable environments for this occur in high altitude continental regions such as the Karakorum and Andes. These glaciers differ from the Tasman Glacier in terms of relative rates of proglacial and subglacial aggradation. Examples from the Southern Alps are small glaciers with outwash discharges unable to prevent the construction of

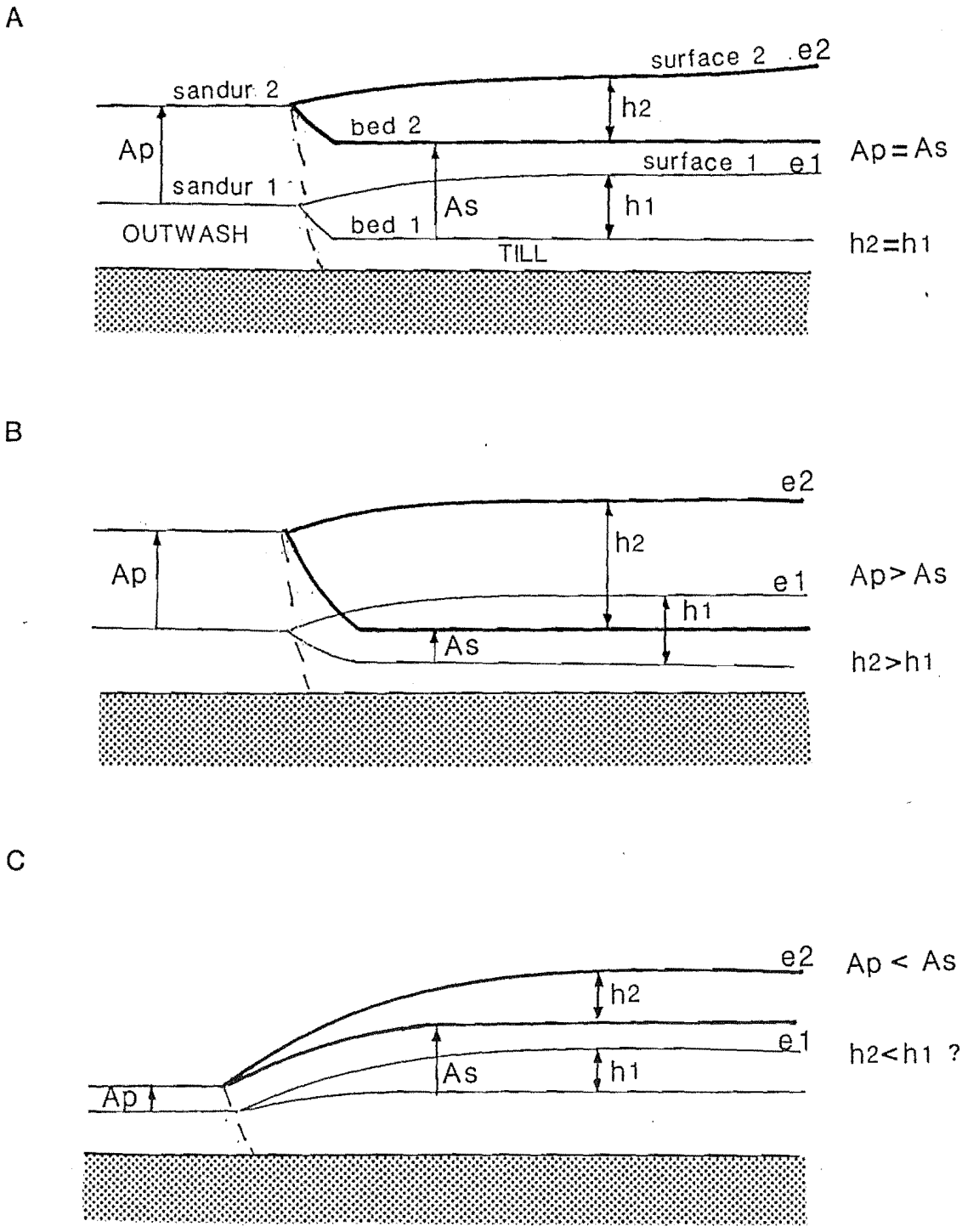

FIG. 5.2 Hypothetical effect of relative rates of subglacial and proglacial aggradation on a glacier. e1 = original surface elevation; e2 = subsequent surface elevation; h1 and h2 = original and subsequent glacier thickness; Ap = proglacial aggradation; As = subglacial aggradation.

(A) Ap = As, no change in glacier thickness but glacier elevates.

(B) Ap > As, glacier is ponded and thickens behind "dam".

(C) Ap < As, glacier rides up on an aggrading till carpet.

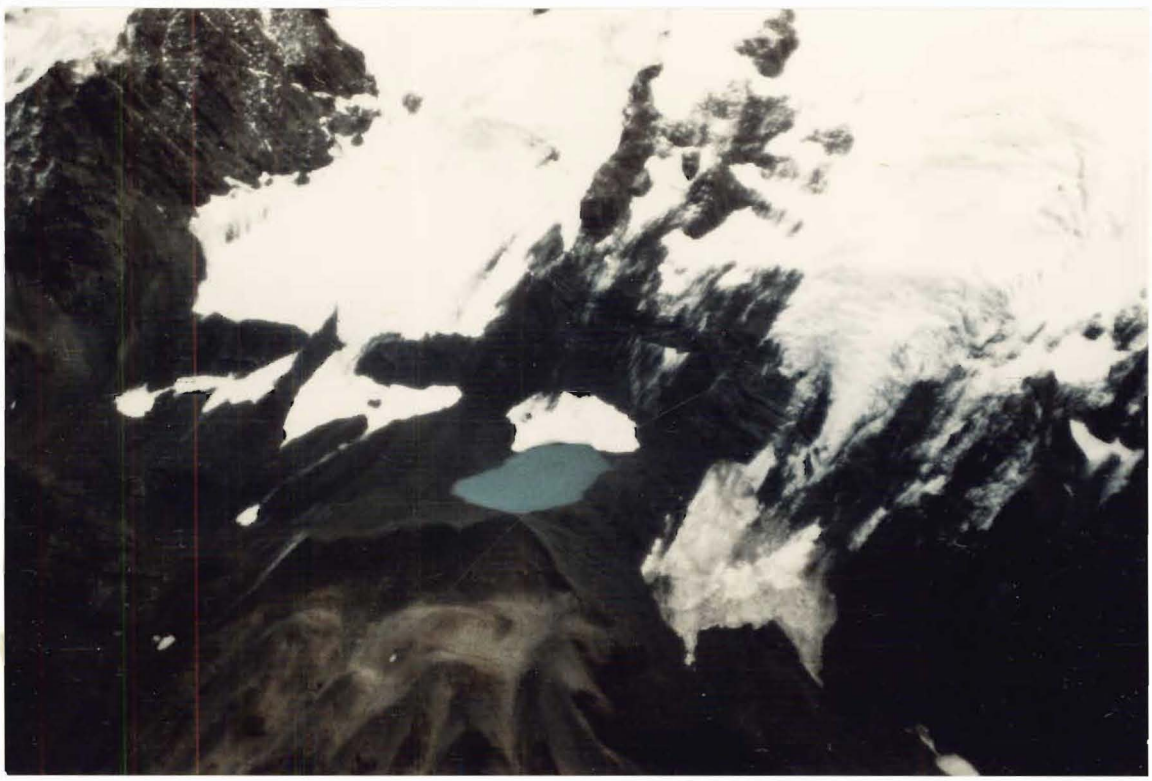

FIG. 5.3 Moraine dam at the head of Jollie Valley, eastern Liebig Range.

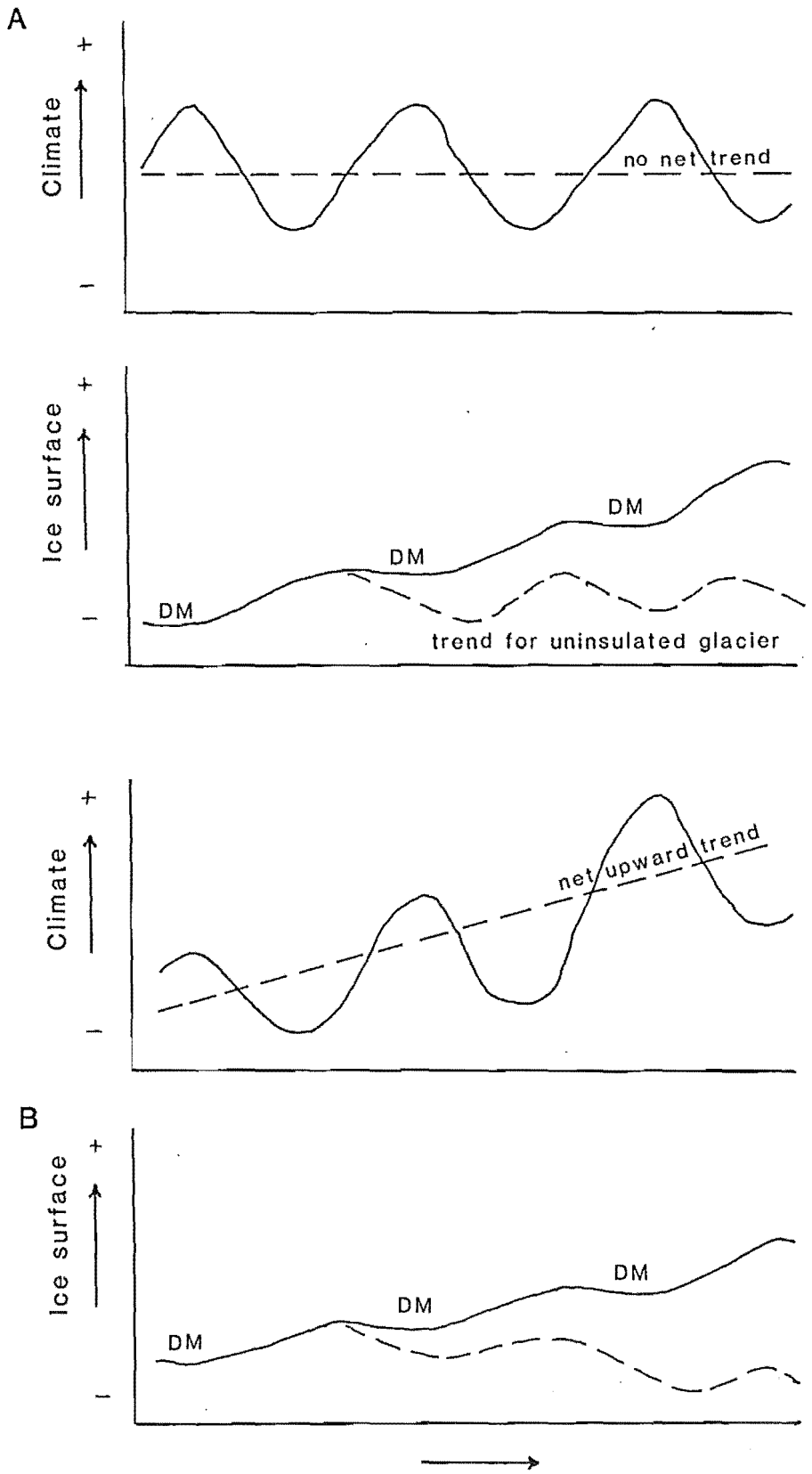

FIG. 5.3a Hypothetical explanation of the effect of a supraglacial debris mantle upon climatically-induced fluctuations of glacier surface level. (A) Climatic oscillations with no net trend result in a general increase in level of a debris-mantled glacier, due to mantle spread (DM) and insulation during negative cycles. (B) Even during a net climatic amelioration, insulation may allow a net increase in level of a debris-mantled glacier (solid line), in contrast to an unmantled glacier (dashed line).

large terminal moraine ramparts. Fig 5.3 shows an example from the Liebig Range.

5.1.5 Summary of the main features of the ponding model.

The ponding model has been developed here by **a priori** reasoning from the descriptive model of Twentieth Century glacier dynamics. The mechanisms by which a glacier may develop a ponded lower tongue and debris-mantled surface may be summarised as follows.

1. Glacier advance attains a terminal position which remains constant during a climatic stillstand. A large proglacial fan, supplied with debris transported by and washed through the glacier, aggrades in front of the more-or-less stationary terminus to construct an outwash head.

2. The glacier thickens behind the outwash head and surface gradient is reduced. Compression in the glacier tongue increases, to cause up-glacier spreading of a supraglacial debris mantle.

3. Feedbacks within the debris-mantle system (Chapter 4) allow growth to continue in the absence of a climatically-induced glacier fluctuation of sufficient magnitude to perturb the otherwise self-regulating system.

4. Progressive ponding, debris-mantle insulation and glacier thickening cause repeated over-riding and super-position of lateral moraines and a slow, non-climatic advance of the terminus (Fig 5.3a).

5. The mechanisms outlined above only occur if climatic fluctuations are too small to have a dominant influence on glacier behaviour. If the amplitude of climatic fluctuations is small, the configuration of the glacier will evolve by processes related to the distribution and flux of sediment within the glacier transport system.

An implication for the distribution of glacial deposits are that inertia of the terminal position should result in close spacing of terminal moraines. McSaveney (1975) suggests that this is indeed the case. Furthermore, the super-position of lateral moraines of debris-mantled glaciers in the Mount Cook area may also be explained by the ponding model. These, and other, lines of evidence are discussed below, following a review of the local glacial chronology.

5.2 A REVIEW OF THE HOLOCENE GLACIAL HISTORY OF THE TASMAN VALLEY.

Two main dating techniques have been employed to construct the Holocene chronology in the Mount Cook area. These are radiocarbon dating of organic matter buried beneath till during glacier advances, and rock

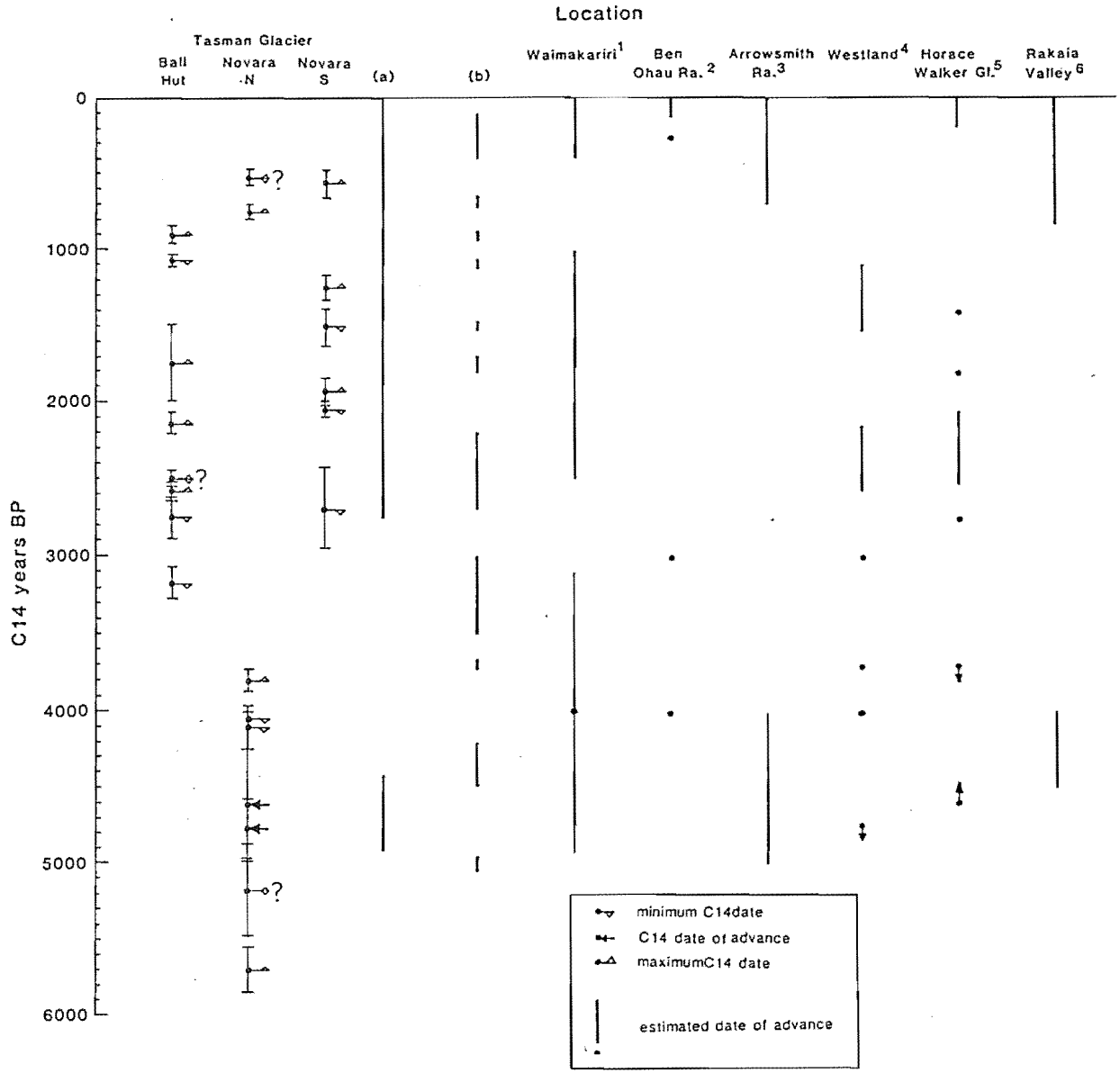

FIG. 5.4 Summary of Neoglacial chronologies from the Southern Alps.
1) Chinn 1975; 2) Birkeland 1982; 3) Burrows 1975; 4) Wardle 1973;
5) Gellatly et al 1985; 6) Burrows & Russell 1975.

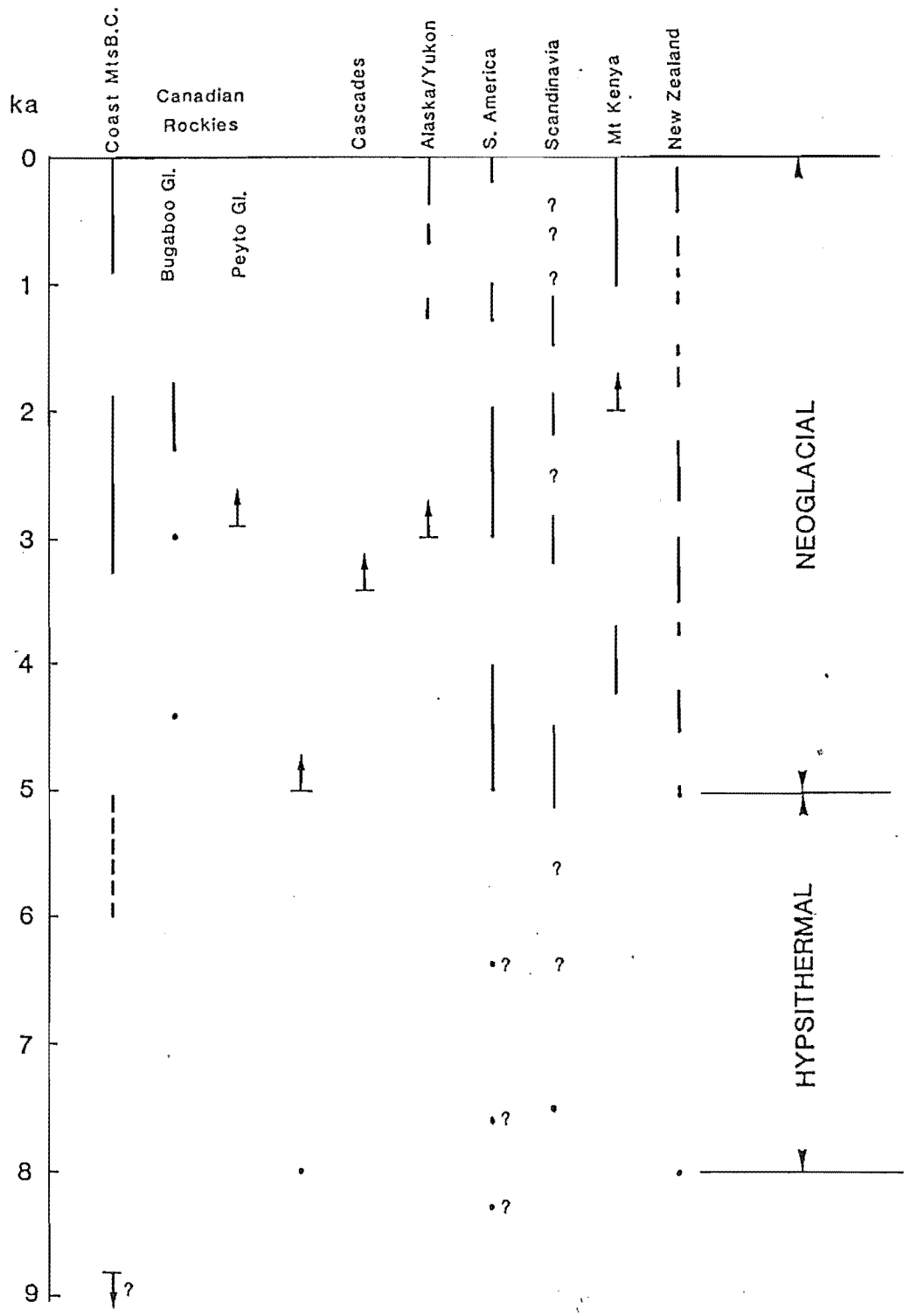

FIG. 5.5 Summary of Neoglacial glacier fluctuations throughout the world, from Davis & Osborn (1988). Arrow = maximum age of advance, ? = uncertain age of advance. Note the large number of dated events in the New Zealand (Tasman Glacier) chronology (Gellatly et al 1988).

weathering-rind thickness on moraines abandoned by retreating glaciers. Other techniques which have proved less reliable have not been extensively employed and are not reviewed in this study.

The radiocarbon-dated tills and the rind-dated moraines have not been combined into a unified chronology. Each is therefore reviewed separately in order to critically assess the precision and completeness of the glacial record before using the record to infer the influence of debris-mantle effects on fluctuations of Neoglacial glaciers in the area.

5.2.1 Radiocarbon (^{14}C)-dated chronology.

5.2.1.1 Review of the chronology

The Tasman Valley contains geomorphic evidence which has been used to construct of one of the most complete pictures of Holocene environmental change in the Southern Alps. The reconstruction has been based primarily on evidence from lateral moraines of the Tasman Glacier, supplemented by work on terminal moraines and in other smaller catchments around Mount Cook and along the Ben Ohau Range (Fig 1.3).

Lateral moraines of the Tasman Glacier are composed of multiple superposed and accreted till units (Osborn 1978; Röthlisberger & Schneebeli 1979) which have provided 48 carbon-14 dates from palaeosols preserved between the till layers (Burrows 1980; Gellatly 1985a; Gellatly et al 1985; Burrows 1989). These dates form the basis for a detailed chronology of glacier expansions over the last 5,000 years. Indeed, Gellatly et al (1988) present the Tasman chronology as the "type" sequence for New Zealand as a whole (Fig 5.4). This raises important questions concerning the representativeness of the Tasman chronology in terms of the number and magnitude of glacier expansions relative to climatic detereorations. The radiocarbon-based chronology has been supplemented by multi-parameter relative-dating techniques (Burrows 1973; Birkeland 1981; Gellatly 1982, 1984, 1985b).

Early Holocene advances in the area are represented by the Birch Hill moraines (Speight 1963; Burrows et al 1976) and by the occurrence at Sebastopol of a diamicton interpreted as till by Burrows (1979). This diamicton may have a rock-avalanche origin (McSaveney, pers. comm.). Burrows (1979, 1980) suggests that three periods of advance occurred between 11,900 and 9,500 B.P., using evidence throughout the Southern Alps. The Birch Hill moraines are believed to have been deposited around 8,000 B.P. by McSaveney & Whitehouse (1989).

A period of relatively low ice volumes in the region between c. 8,000 and 5,000 B.P. is suggested by a paucity of geomorphic evidence for glacial advances (Gellatly et al 1988). This period corresponds to the well-documented Hypsithermal interval (the Altithermal or "climatic optimum") in the Northern Hemisphere. The timing of climatic deterioration at the end of this period is not well known. Evidence from lateral moraine dates is limited by the burial of the lower proximal slopes of the moraines by scree: older dates may yet be exposed during glacier thinning. Palynological work in the South Island suggests that a pronounced cooling occurred about 5,000 B.P. on the basis of Ascarina distribution (McGlone & Moar 1977). Bowler et al. (1976) place the climatic optimum in the south-western Pacific region at 8,000 to 5,000 B.P. Elsewhere, the South American glacial record indicates the onset of the Neoglacial also at about 5,000 B.P. (Clapperton & Sugden 1988). Reviewing the global evidence, Grove (1979) tentatively suggests that the Hypsithermal period may be time-transgressive. Studies from a more recent review (Davis & Osborn 1988) are summarised in Fig 5.5. The evidence points to the onset of increased glacier volumes in the region around 5,000 B.P., a phase termed the Neoglacial by Porter & Denton (1967). Evidence presented in Section 5.3 may indicate earlier initiation of climatic deterioration.

Neoglacial (ie. post-Hypsithermal) glacier expansions are of particular interest to this study. From the Tasman Glacier radiocarbon dates, 12 periods of glacier expansion since 5,000 B.P. (Gellatly et al 1985) and 6 periods since 1,100 B.P. (Gellatly 1985a) have been recognised. The resolution of the chronology over the last millenium is presented as being precise to a decadal scale. Burrows (1989) presents 18 new dates from the Tasman Glacier and revises the chronology, concluding that reliable evidence of glacier expansions only extends back to c.3,500 B.P. The Neoglacial maximum occurred between 1862 and 1890 A.D. on the Tasman Glacier (Brodrick 1891; Gellatly 1985c) when the glacier overtopped its lateral moraines. Twentieth-Century thinning has been pronounced (Skinner 1964; Chapter 2, this study) and is a response to rising snowlines in the first half of this century. Chinn (unpublished) demonstrates that regional snowlines in New Zealand are no higher now than in the middle of the century, and Brazier et al (in prep.) find no evidence of a post-1950 warming at Franz Josef. This evidence contrasts with a recent warming trend suggested by Gellatly & Norton (1984). Glacier dynamics are such that the relaxation from this impulse is not yet completed and an increasing rate of thinning may be expected. This is not,

as Gellatly (1985c) has suggested, due to post-1950 warming, but to reduced ice velocities in the lower Tasman Glacier causing the rate of thinning to approach the ablation rate (Chapter 2).

Previous research has not addressed the question of whether the prolonged stability in glacier volume during the Neoglacial reflects a period of equivalent climatic stability followed by a rapid Twentieth-Century "amelioration" (Gellatly 1985b; Gellatly & Norton 1984) or whether the glacier's stability results from inherent dynamic properties affecting response to climatic change, as proposed by the a **priori** ponding model in Section 5.1 of this thesis.

This theme is developed in this section. Conclusions reached from the study of the recent behaviour of the glacier under various mass balance conditions are applied to the prolonged series of climatic oscillations and glacier responses which characterise the Neoglacial period. The premise that "climatic deterioration = glacier expansion = buried palaeosol" is tested and alternatives suggested which may help to understand the geomorphic evolution of the Tasman Valley. Finally, the question of its representativeness of the Southern Alps as a whole is considered.

5.2.1.2 A reappraisal of the significance of radiocarbon dates.

The 24 dates presented by Gellatly et al (1985) have been translated into a series of 12 glacier expansions by these authors. The proposed distribution of expansions (Fig 5.4) is effectively a random distribution over the 5,000 years of record. Such a distribution differs from the evidence collected in other areas of the Southern Alps (Birkeland 1982), a paradox which must be explained before the Tasman Glacier chronology can reasonably be adopted as a representative chronology. Two possibilities exist which must be considered. Either the record is more complete because the repeated overriding of moraines has allowed a more representative sample of glacier expansions to be preserved than elsewhere; or the dates have been over-interpreted and too great a significance attached to some individual dates.

The second possibility is favoured, after consideration of the list of dates and their significance (Gellatly et al 1985: Table 1). When maximum and minimum dates are plotted as such and the stratigraphic level of palaeosols examined (Fig 5.4), I would conservatively estimate that no more than 5 glacial expansions are unequivocally constrained by the suite of 24 dates. Uncertainties as to the interpretation of some dates result from

stratigraphic inversions of dated palaeosols in the Ball Hut and Novara Spur sections. The estimate of only 5 glacier expansions undoubtedly under-represents the real number of over-topping events. Of greater importance is the absence of firm evidence for expansions between 4,000 and 3,000 B.P., which is a feature of other catchments in the region (Chinn 1975; Burrows 1975; Birkeland 1982).

Burrows (1989) presents a further 18 radiocarbon dates from the Tasman Glacier, which he interprets to indicate eight periods of glacier expansion since 3,500 B.P. Burrows revises evidence of early Neoglacial advances, suggesting that when all dates are considered, the Tasman Glacier expanded on at least nine occasions since c.3,700 B.P.

It therefore appears that, until very recently, existing interpretations of periods of expansion of the Tasman Glacier were somewhat liberal and exceeded the precision of radiocarbon dates.

5.2.1.3. Implications of Neoglacial dates for glacier volume variations.

The Tasman Glacier is apparently thinner at the present than at any time in the past 3,700 years, since palaesols within this age range are exposed which (by their very existence) cannot previously have been exposed. Wholesale collapse of the valley walls due to glacier thinning (Bishop 1979; Blair 1984), which commenced in the middle of the Twentieth Century, probably has not previously occurred in the Neoglacial. This is compelling evidence for a lower ice surface at present than at any time since the Hypsithermal period.

Conversely, the glacier achieved its maximum Neoglacial thickness in the latter years of the Nineteenth Century, when it overtopped lateral moraine crests and deposited fresh till (Brodrick 1891). The glacier has therefore remained smaller than the 1890 volume and larger than the present volume for the previous 3,500 years at least, a period of remarkable stability. A general increase in ice surface elevation over the Neoglacial period is indicated by the suite of radiocarbon dates.

5.2.2 A re-appraisal of the Neoglacial weathering-rind chronology.

Moraine sequences in the Mueller, Hooker, Tasman, and Godley valleys were extensively sampled and dated using rock weathering-rind measurements by Gellatly (1984). On the basis of moraine location she identified 15 glacial depositional events and assigned rind ages to each (Fig 5.6). Correlation between glaciers was made on a moraine ridge-to-ridge basis.

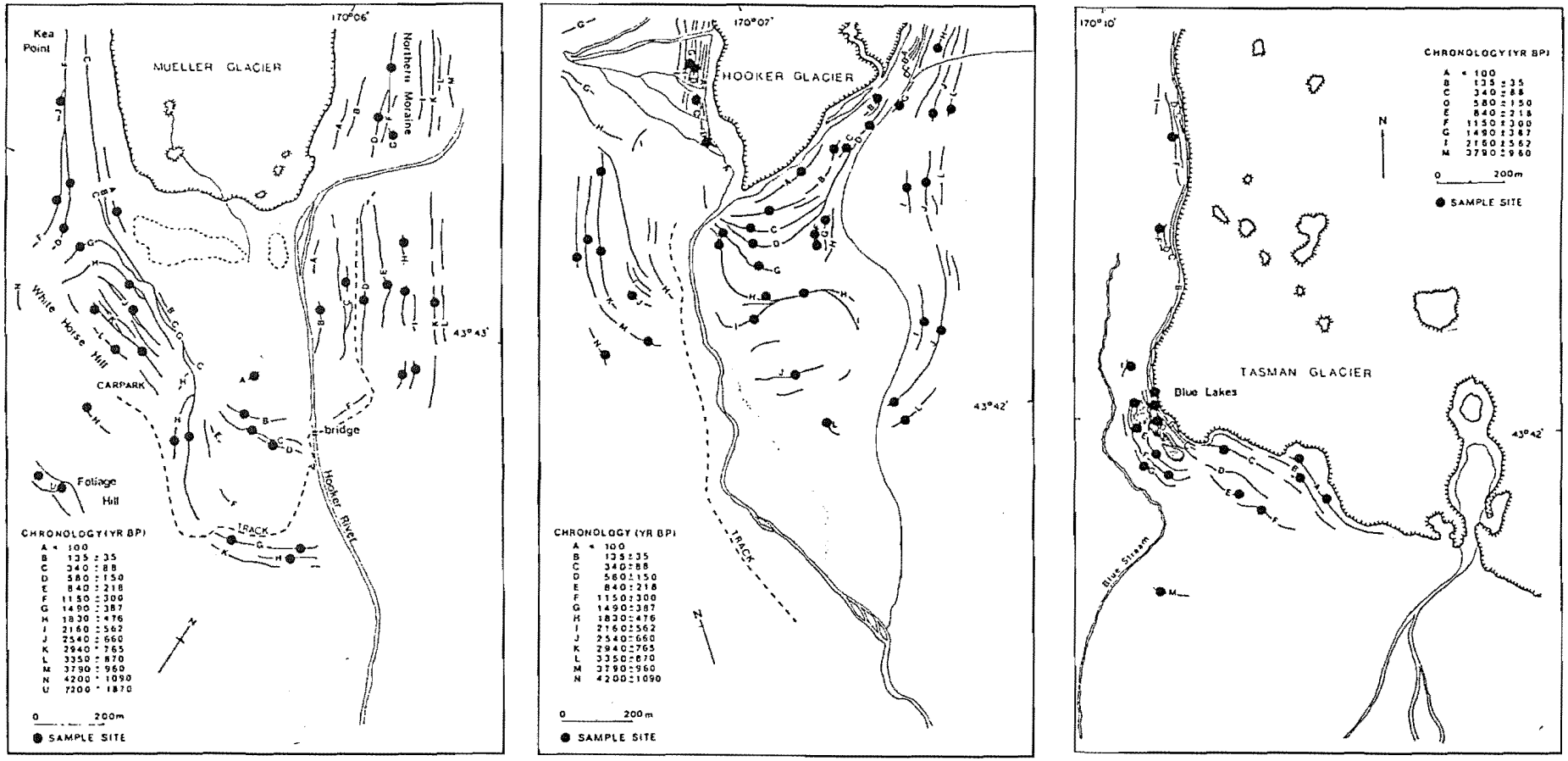

FIG. 5.6 Neoglacial moraine sequences at five glacier termini in the Mount Cook National Park, from Gellatly (1984).

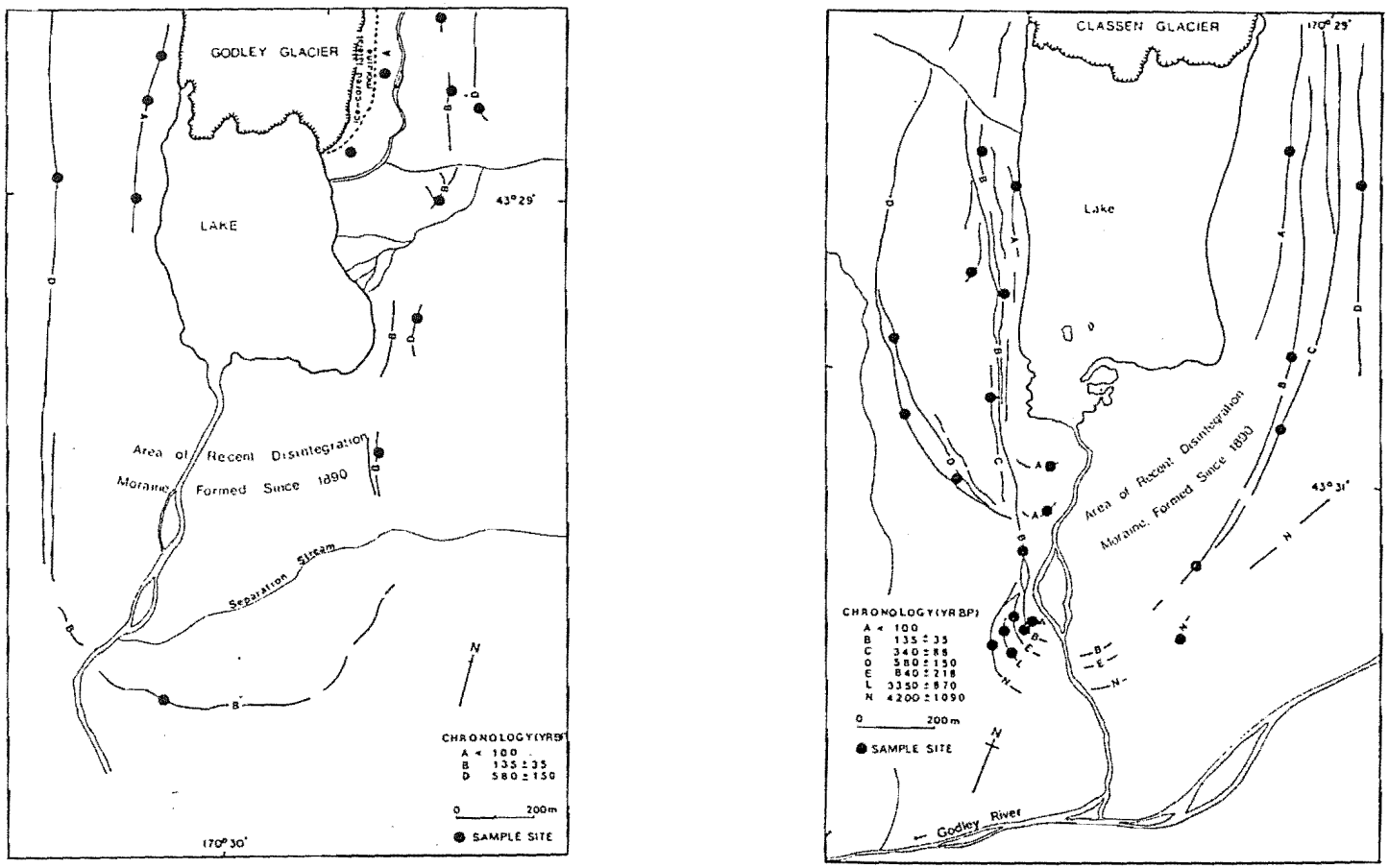

FIG. 5.6 (continued).

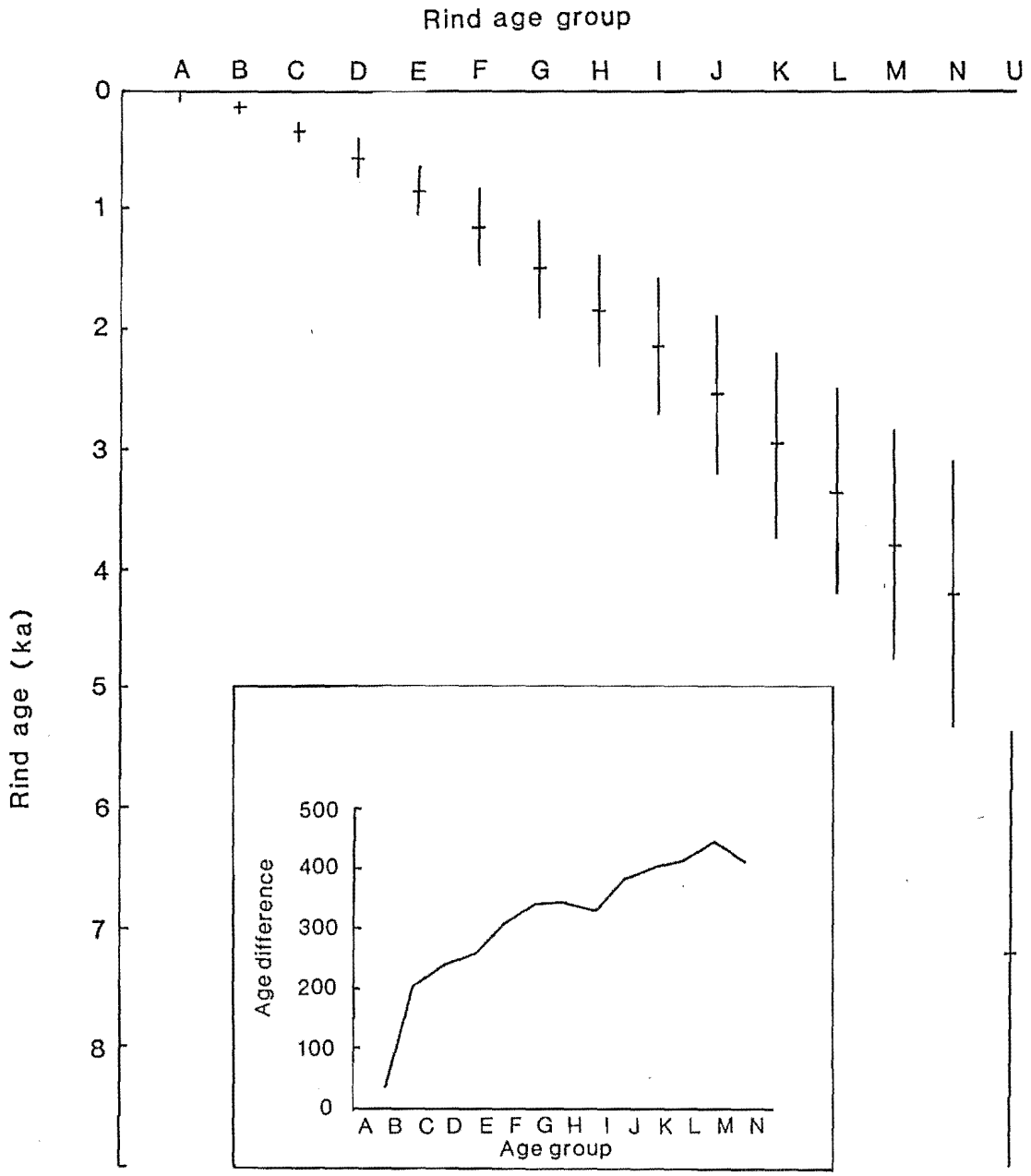

FIG. 5.7 Weathering rind age-distribution chart, using data from Gellatly (1984). Bars represent ± 1 standard error for each age category. Letters refer to the age categories given by Gellatly (1984). INSET: Graph of age differences between groups, for Neoglacial period.

Fourteen moraines were deposited since 4,200 B.P., a significant revision of earlier work in the area which had identified Neoglacial moraines no older than 830 B.P. (Burrows 1973), 1100 B.P (Burrows 1980) and 1465 B.P. (Birkeland 1982).

The general correspondence between the rind chronology and the radiocarbon chronology confirms the duration of Neoglacial fluctuations in the area. Glacier termini have oscillated over a narrow zone for at least 4,200 years while the glacier surfaces have risen and fallen correspondingly. Exact matching of the two chronologies, one dating over-riding events (^{14}C) and the other the commencement of retreats (rinds) is prevented by lack of precision of both techniques. Nevertheless, the narrow spacing of terminal moraines contrasts with the spread of equivalent-age moraines in other areas. This invites a detailed study of possible debris-mantle induced effects on glaciers at Mount Cook.

The chronology has been presented as very detailed and complete, with correlations of individual moraine ridges being made (Fig 5.6). If this precision is justified, there exists considerable scope for detailed examination of the frequency of climatic oscillations and of responses of debris-mantled glaciers over the Neoglacial period.

The analysis presented below tests the completeness and precision of the weathering-rind record.

5.2.2.1 Completeness of the record

The age difference between adjacent moraine ridges increases in an approximately linear trend between 135 and 4,200 B.P. (Fig 5.7 inset). Two interpretations of this trend are possible.

1. Assuming the moraine record is complete, there has been an increase in the frequency of climatic oscillations over the last 4,200 years. There is no established precedent or physical reason why this should be the case.

2. Erosion censoring has resulted in preservation of a smaller proportion of older ridges, due to some combination of outwash erosion and burial beneath the aggrading sandar surfaces. The dataset of moraine ages follows an age distribution characteristic of many landforms whose preservation potential decreases with time (McSaveney, in preparation). Furthermore, if Gellatly et al's (1985) chronology is accepted (but see Burrows 1989), there is evidence in radiocarbon-dated lateral moraines for glacier advances around 5,000 B.P. (Fig 5.4). These advances are absent from the weathering-rind-dated terminal moraine sequences, suggesting that

younger advances have over-ridden the earliest Neoglacial terminal positions.

The terminal moraine sequences under-represent the number of glacier advances occuring during the Neoglacial, even in apparently-complete sequences such as those at the Mueller and Hooker Glaciers. However, loss of evidence is predictable given the trend to the curve of moraine age differences in Fig 5.7. Allowance for this may be made when making palaeoclimatic interpretations.

5.2.2.2 Precision of the moraine dates

A thorough presentation of rind ages given by Gellatly (1984: Table 1) allows differences in age between moraines to be tested statistically. A precondition of this analysis is that individual moraines are of different ages simply because they are located in different places. This test objectively assesses the confidence with which inter-valley correlations may be made, and searches for statistical groupings of moraines which would indicate periods of increased glacier activity.

A one-tailed t-test has been used to compare each age category, denoted by letters A to N in Figs 5.6 and 5.7, with every other category. The significance levels of differences between categories are tabulated in Table 5.1. For clarity, these are presented graphically for selected significance levels in Fig 5.8. In each graph in Fig 5.8, a single vertical line links all categories which are not statistically different at the given significance level.

The results reveal several points of interest.

1. There is greater similarity between categories with increasing age. Therefore, the discriminating power of the dating technique is reduced on progressively older deposits. Mid-Neoglacial moraines are statistically indistinguishable from the adjacent 3 or 4 moraines in both younger and older directions at the 0.10 significance level.

2. There are no clusters of moraines of similar age, separate from moraines of distinctly different age. Instead, the tie-lines in Fig 5.8 show a smooth overlap through all categories, indicating that periods of moraine deposition have occurred at fairly regular intervals over the last 4,200 years. This is in marked contrast to other Neoglacial chronologies which have moraines whose ages cluster (Fig 5.4).

A	B	C	D	E	F	G	H	I	J	K	L	M	N
	B	.025	.01	.01	.01	.01	.01	.01	.01	.01	.01	.01	.01
		C	.10	.01	.01	.01	.01	.01	.01	.01	.01	.01	.01
			D	-	.10	.025	.01	.01	.01	.01	.01	.01	.01
				E	-	.10	.05	.05	.025	.025	.01	.01	.01
					F	-	-	.10	.05	.05	.025	.025	.025
						G	-	-	.10	.10	.05	.025	.025
							H	-	-	-	.10	.05	.025
								I	-	-	-	.10	.10
									J	-	-	-	-
										K	-	-	-
											L	-	-
												M	-
													N

TABLE 5.1 Matrix of significance levels of differences in age between moraine age categories.

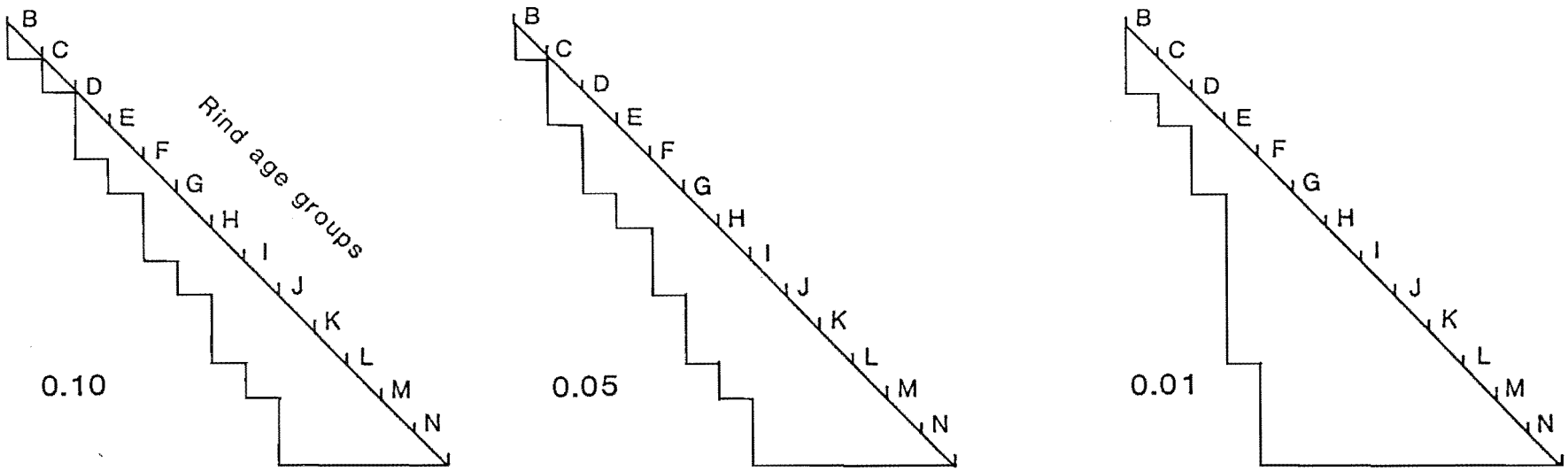

FIG. 5.8 Similarity diagrams of age categories for different significance levels. Vertical bars are tie-lines joining all age categories which are statistically indistinguishable at the given significance level.

5.2.2.3 General interpretation of the record

The Mount Cook Neoglacial chronology is one of the best in the world in terms of the number of dated depositional events that it includes. The importance of Gellatly's (1984) chronology is the recognition of a prolonged period of small oscillations in terminal position. If younger moraines are preserved more or less in their entirety, the frequency of these oscillations is about 200 to 250 years. Early Neoglacial moraines are not preserved and the older existing moraines probably represent about half of the glacier fluctuations which occurred around that time, because they are separated by intervals of 400-500 years.

Correlations between valleys must be treated with circumspection because of the incomplete record and the uncertainty with which a moraine is ascribed an age. Difficulties in correlating individual moraines partly result from the short intervals between depositional events throughout the Neoglacial. For example, there is less than 90% certainty that moraine H in the Mueller Valley correlates with moraine H in the Hooker Valley (Fig 5.6). In fact, it could correlate with either F,G,I,J, or K with equal certainty (Fig 5.8). There is even a 50 % probability that moraine H in the Mueller Valley has no existing correlative in the Hooker Valley. Realistically, correlations may only be made with a resolution of many hundreds of years in the early and middle Neoglacial period.

In conclusion, comparison of glacier fluctuations between different valleys on the scale of centuries is not possible for most of the Neoglacial period. Such temporal resolution is unfortunately necessary to interpret detailed effects of debris-mantle insulation on Neoglacial glacier behaviour. However, interpretations of a more general nature are possible, and are discussed below.

5.2.2.4 Comparison between chronologies of the Mount Cook glaciers.

Most of the debris-mantled valley glaciers in the field area have significant gaps in their moraine records (Fig 5.9). Only the Mueller Glacier has a "type" sequence of 14 Neoglacial terminal moraines, and the Hooker Glacier has all but moraine E (c.840 B.P.) present. In contrast, major gaps occur in moraine sequences of the Tasman, Classen and Godley Glaciers.

Over-riding by younger advances can be inferred in cases where missing moraines are bounded by older moraines (Fig 5.10). The magnitude of the over-riding advance can also be inferred. In cases where older moraines

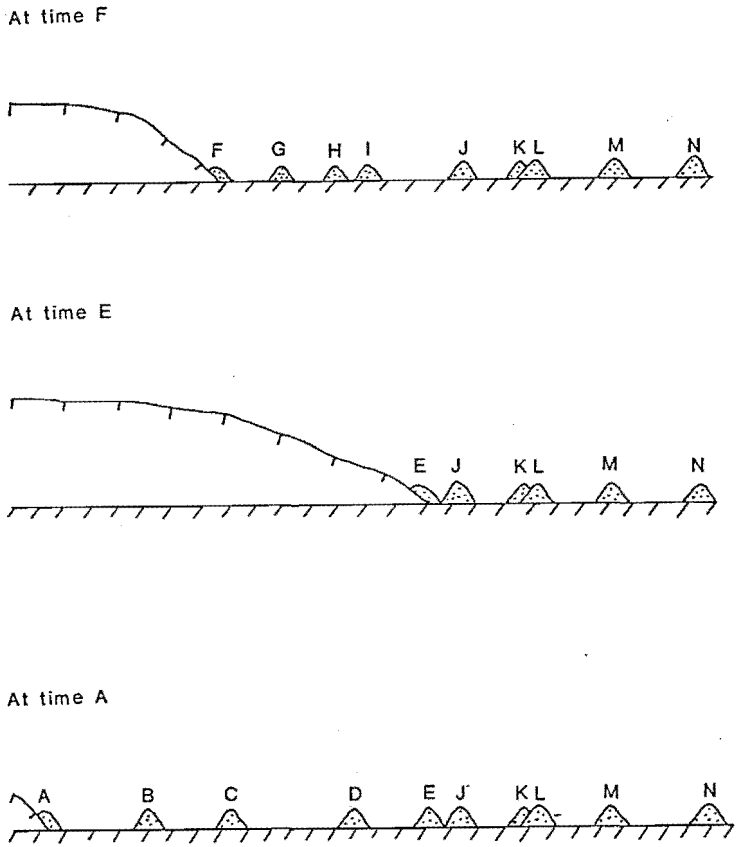

FIG. 5.9 The hypothetical effect of a glacier readvance on a generally recessional series of moraines. An advance after time F obliterates moraines deposited at time F, G, H and I to cause a gap in the moraine sequence.

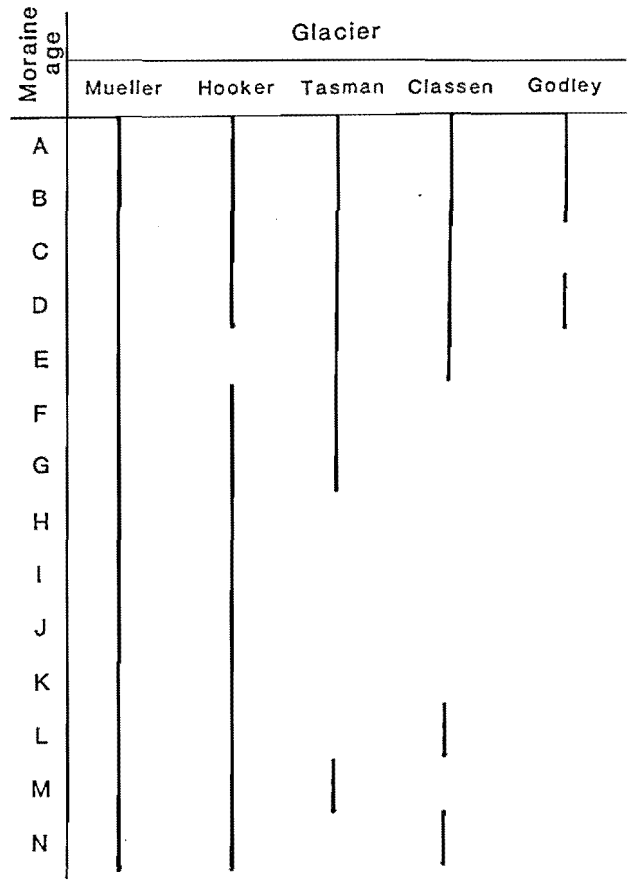

FIG. 5.10 Distribution of moraine ages for major glaciers in the Mount Cook area, using Gellatly's (1984) weathering-rind ages.

are not preserved, their absence may be due to over-riding, or to erosion or burial by outwash streams.

Using the chronology proposed by Gellatly (1984), an inferred over-riding event of the Tasman Glacier occurred about 1490 B.P. which obliterated all moraines post-dating the 3,350 B.P. moraine. Similar events occurred on the Classen Glacier about 840 B.P. and 580 B.P., and on the Godley Glacier about 580 B.P. Given the resolution of the dating discussed above, differences in timing are probably apparent rather than real, and only one over-riding event may have occurred sometime between about 600 and 1500 B.P. Alternatively, more over-riding events have occurred but are obscured by uncertain correlations between valleys. Despite imprecise dating of moraines, I suggest that more than one over-riding event probably occurred at some glacier termini. This contrasts with the general decline in the magnitude of advances during the Neoglacial in catchments without debris-mantled glaciers (see Section 5.5.2). In conclusion, the presence of debris mantles is inferred to introduce variation in response to climatic change between glaciers in the same area.

This situation is similar to that in the Karakorum Mountains described by Kick (written communication, 1988). Kick observes that debris-mantled glaciers in the region attained "Little Ice Age" maxima at quite different times (Table 5.2). This contrasts with the European Alps, where glaciers are relatively free of supraglacial debris and "Little Ice Age" maxima occurred around 1855 A.D. $\pm$10 years. Kick suggests that differences in debris-mantle insulation is a likely cause of this contrasting variability in response (see Section 5.5 below).

5.3 NEW EVIDENCE FOR HOLOCENE GLACIER FLUCTUATIONS.

Several localities around the margin of the Tasman Glacier present morphological and sedimentological evidence for glacier fluctuations and deposition. This evidence supplements the purely stratigraphic approach on which the existing Neoglacial chronology is based. Much of the evidence involves interpretation of sediment-landform associations (Eyles 1983) combined with an understanding of recent glacier behaviour, developed in earlier chapters. Each locality where new evidence has come to light is discussed before the evidence is synthesised into a new interpretation of Holocene fluctuations of the glacier.

	Glacier	Date of last maximum*
Europe	all	1855 ± 10 years A.D.
Himalaya	most	post-1890
	Chogo Lungma	1913
	Fedchenko	1913
New Zealand	Tasman	1890
	Godley	1890

* maximum length, not necessarily maximum volume.

TABLE 5.2 Dates of last maximum extent of glaciers in different regions.

5.3.1 The geomorphology of the Murchison Embayment.

The informally-named Murchison Embayment is 2 km^2 area of ice-free ground bounded by the present glacier margin to the west and a large Neoglacial moraine loop to the east (Figs 5.11, A1 and M1). The moraine was deposited where the Tasman Glacier invaded the lower part of the Murchison Valley. The embayment is the only area where the Tasman ice margin has retreated significantly from its Neoglacial maximum position to reveal over-ridden landforms and till sections, exposed by ice retreat since the 1950s.

5.3.1.1 Landform stratigraphy.

A flight of four till-mantled benches has been exposed (Fig 5.13). The benches are traceable northwards into boulder layers in the moraine wall below Trig. V (Fig 5.12). Younger palaeosols occur at higher levels in the moraine wall (Gellatly et al 1985), therefore it follows that the till benches become progressively younger in a distal (eastward) direction. Together with the presence of flutes on the risers and treads of the benches (Fig 5.11) it is clear that each bench has been overridden by the Murchison lobe of the Tasman Glacier prior to the formation of the succeeding bench. The flutes are unlike "true" flutes described by Boulton (1976) and Åmark (1980), being larger, poorly-defined on the ground, and formed of (or mantled by) ablation till. Nevertheless their "controlled" geometry (sensu Gravenor & Kupsch 1959) indicates deposition (or at least reworking) by sliding ice. The staircase of till benches indicates a general trend of increasing ice levels and over-riding during their formation.

The glacier over-topped the highest moraine crest bounding the embayment in the late Nineteenth Century. Ice walls and meltwater conduits existed at the northern corner of the embayment at this time (Brodrick 1891). Ice-margin retreat since 1957 has been mapped from aerial photographs (Fig 5.14). The 20th Century is probably the first time the till benches have been exposed since being over-ridden. Recent recessional moraines are superimposed on the exhumed embayment floor. Absence of ice beneath debris in the embayment is indicated by the clarity of shallow lakes which occupy depressions in the till sheets and disintegration ridges. The disintegration ridges are similar to features described by Gravenor & Kupsch (1959) and appear to have been formed by the dumping of supraglacial debris in open full-depth crevasses close to the retreating ice-margin. Although the position of the lakes is now

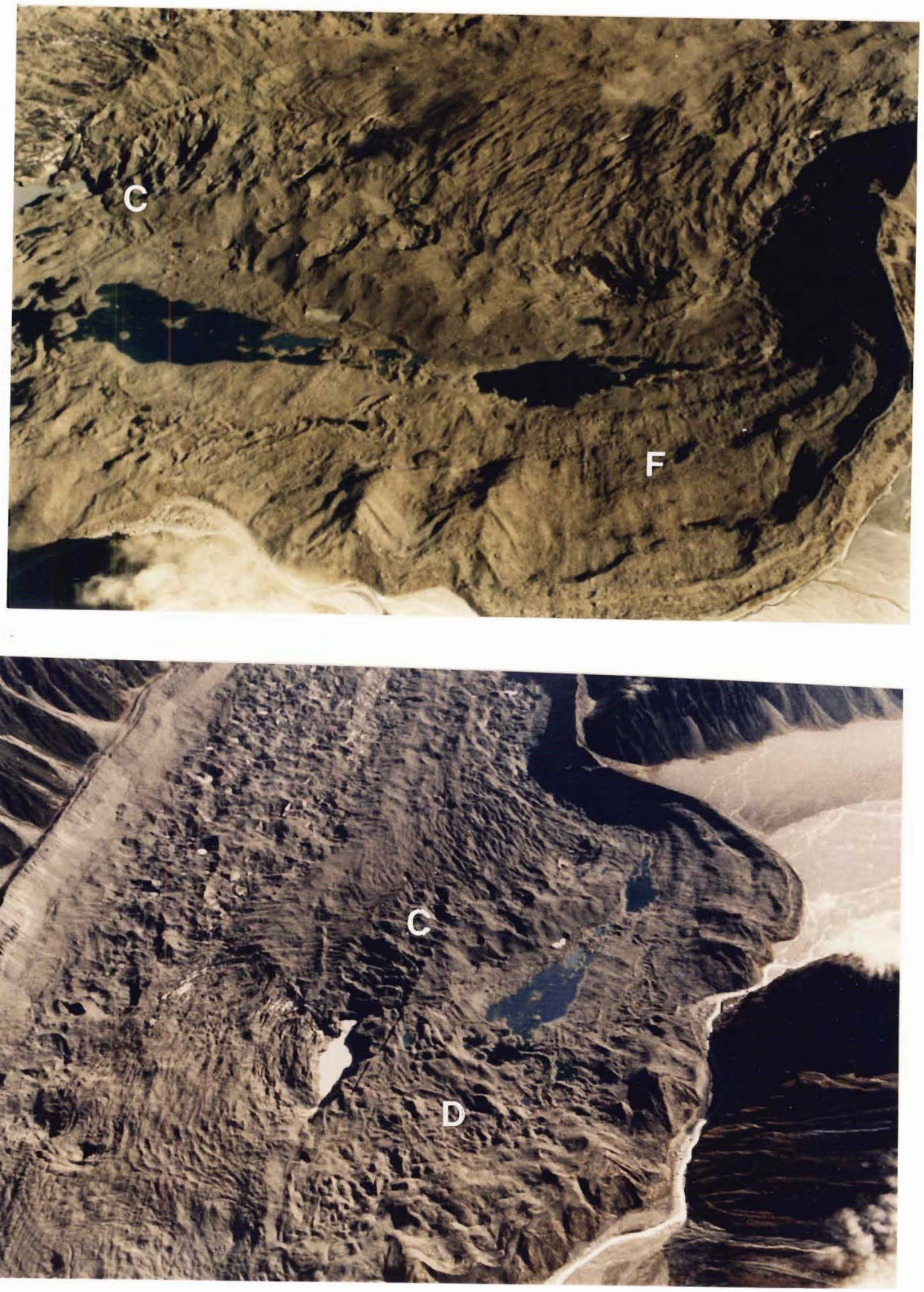

FIG. 5.11 Oblique aerial photographs of the Murchison embayment and the Tasman Glacier debris mantle. Note crevassed ice margin (C), fluted till (F), and disintegration topography (D) in the embayment (April 1988). (Photos by T. Chinn).

FIG. 5.12 View northwards across the Murchison embayment. Till-mantled benches (middle distance) merge with bouldery horizons in the far moraine wall (in shadow).

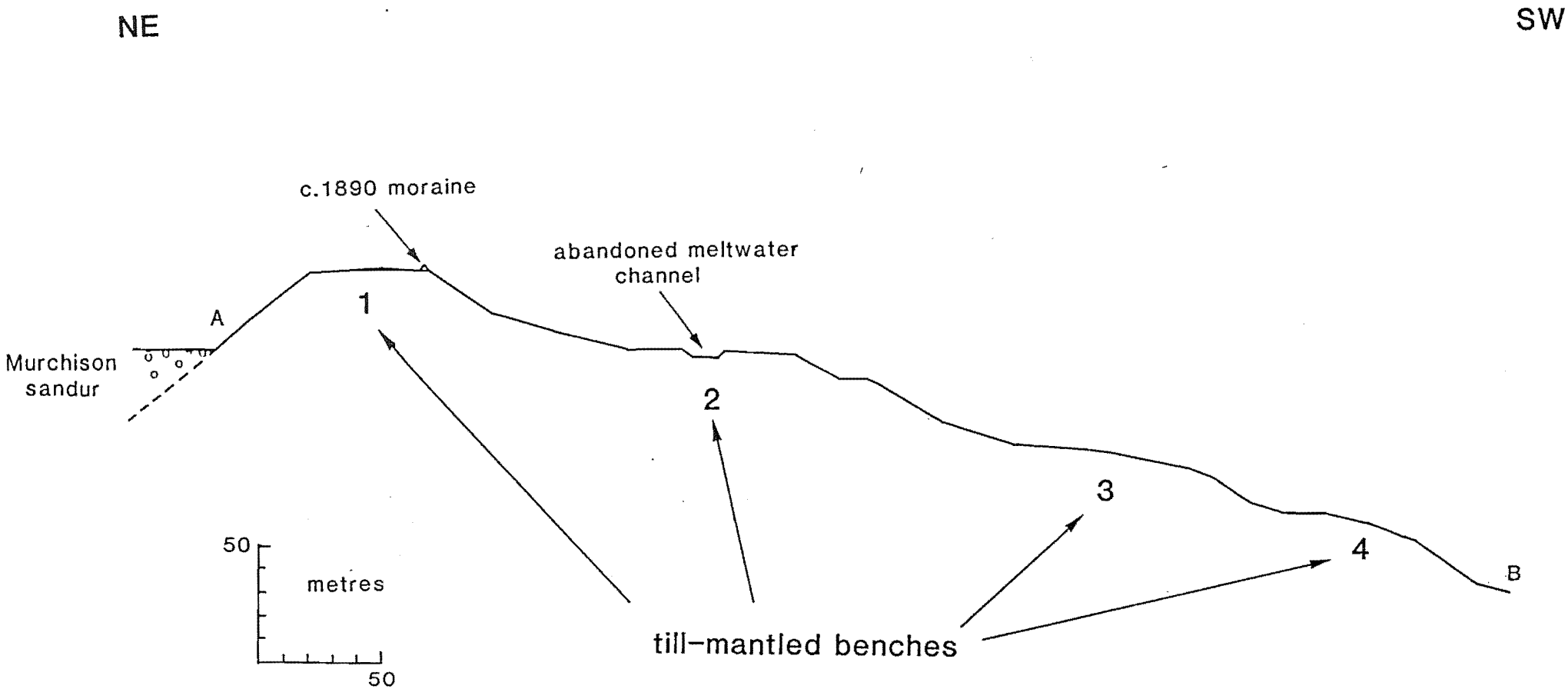

FIG. 5.13 Profile of the Murchison embayment till benches (Line A-B in Fig 5.11). Measured using abney level and 30m tape measure.

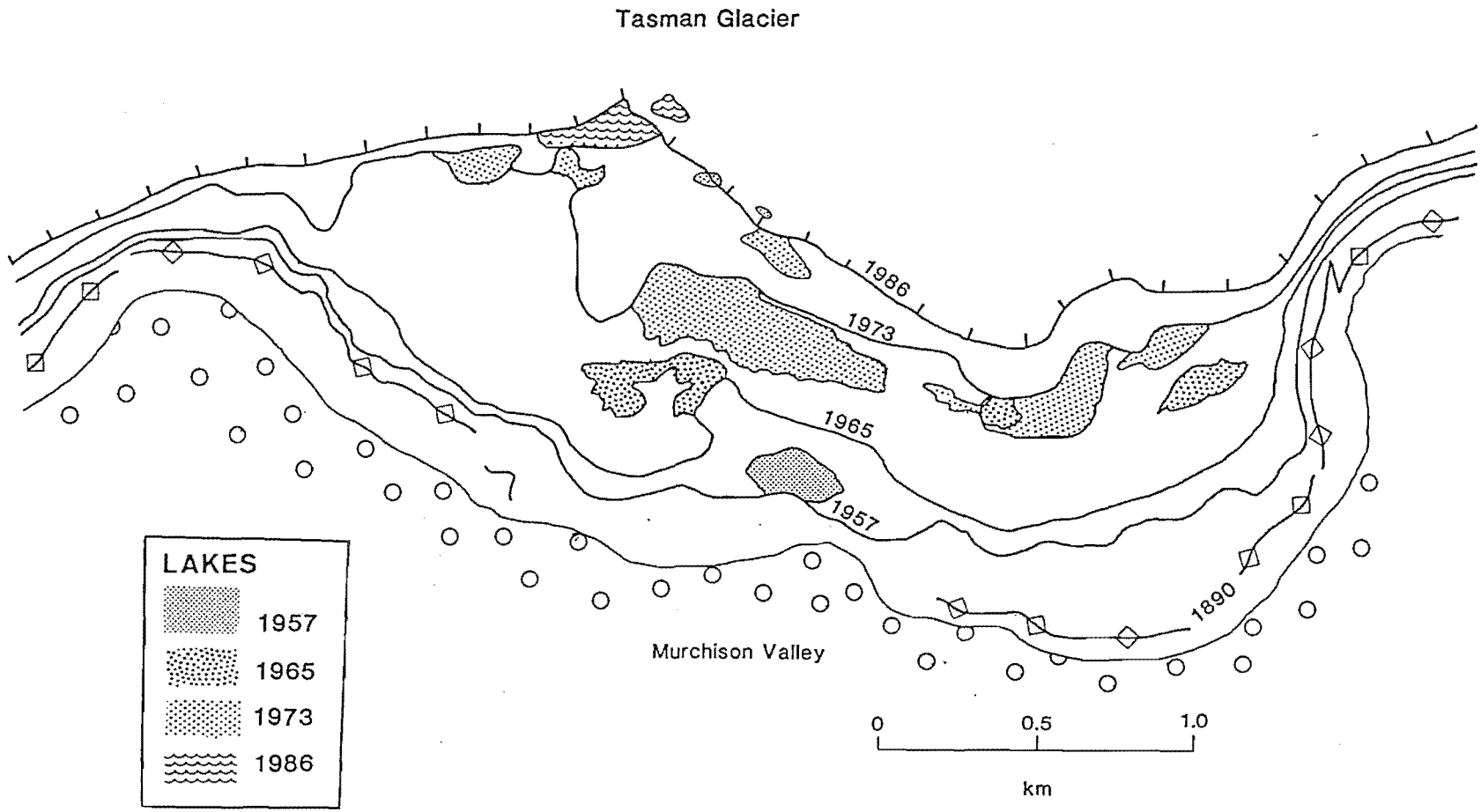

FIG. 5.14 Retreating ice margin positions and ice-contact lakes in the Murchison embayment. Data from aerial photographs.

stable, during retreat of the ice margin across a reverse slope over the last 30 years ephemeral lakes were repeatedly ponded against the ice margin and drained as outlets became available. Although too short-lived to accumulate lacustrine sediments, ephemeral lakes may have acted as heat reservoirs aiding ablation, in the manner described in Chapter 4.2.

In contrast to this area of "controlled" topography, the southern part of the embayment contains assorted "uncontrolled" landforms (Fig 5.11). Conical mounds, ring-ridges and short sinuous ridges interspersed with water-worked gravels were deposited by ice melting in situ. The difference between "controlled" and "uncontrolled" deposition appears to relate to the slope of the embayment floor: to the north it is relatively steep; to the south it is virtually level, causing crevasse-bounded ice blocks to become isolated during glacier retreat. Ablation and dumping of supraglacial debris formed a variety of disintegration features.

The age of the embayment moraines is inferred from nearby moraine-wall radiocarbon dates (Burrows 1989), and by direct observation using aerial photographs. The outer (main) moraine ridges relate to the Neoglacial maximum of the late 19th Century, but internally may contain tills as old as 1,600 B.P. The lower over-ridden bench is about 1,600 years old, the inner two benches about 3,300 and 3,500 years old. Superimposed on these large landforms are the small, young disintegration ridges and hummocks, which are the morphological expression of the till sheet deposited this century.

5.3.1.2 Till stratigraphy exposed in section.

Sections forming the cliff of the present ice-marginal lake have recently become exposed for the first time and are rapidly collapsing (Figs M1 and 5.15). About 50 m of stratified gravels and sand form steep cliffs. Couplets of relatively boulder-rich and sand-rich textures define the stratification. Their lateral continuity decreases (or at least becomes obscure) with depth. The gravels are weathered to yellow-brown, except for the uppermost couplet of fresh grey till deposited in the last few decades. The contrast in the degree of weathering between the topmost till couplet and the rest of the section represents a significant disconformity (Fig 5.16). An orange-brown weathered horizon occurs near the base of the section.

The section contains two dominant facies (Fig 5.15):

FACIES 1 comprises diamict units which are relatively consistent in thickness and lateral continuity. Units are typically 1-3 m thick and

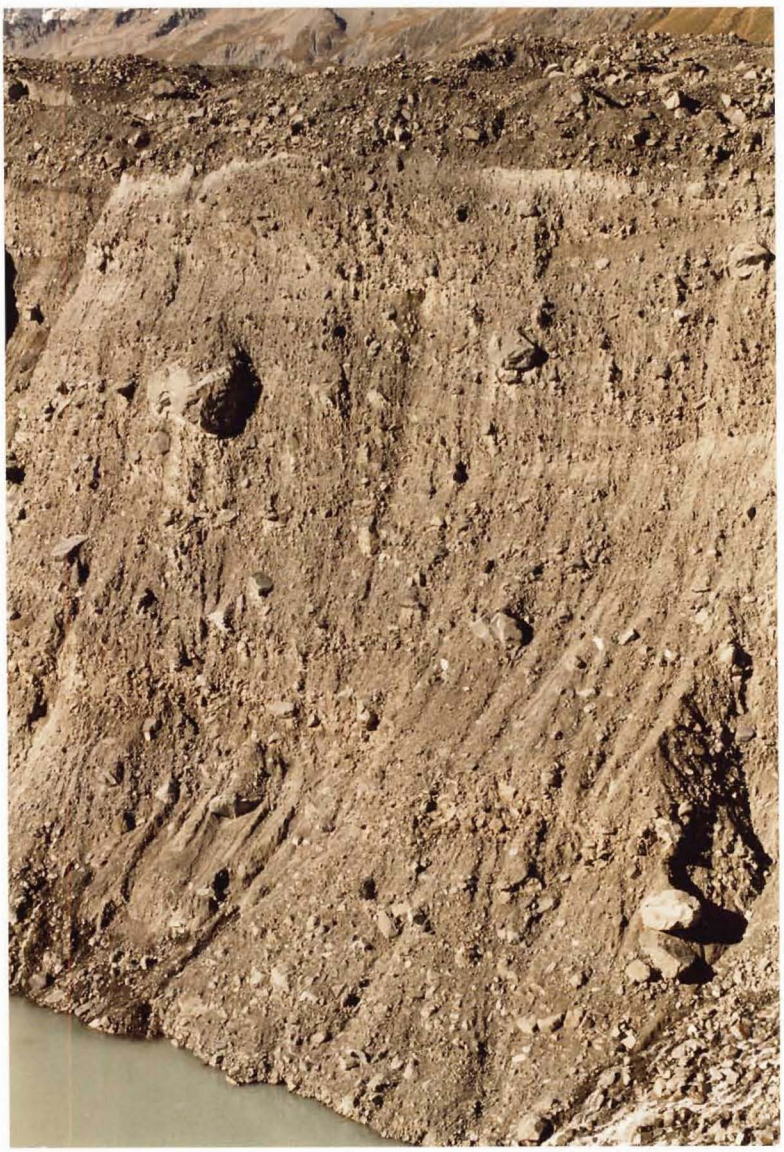

FIG. 5.15 Till cliffs recently exposed by glacier retreat from the Murchison embayment. At least 7 couplets of till horizons are discernible. For location see Fig M1.

FIG. 5.16 Till exposure in fault scarp immediately east of till cliff in Fig 5.15. Colour change reflects different degree of weathering between very recent till cap and earlier Neoglacial tills.

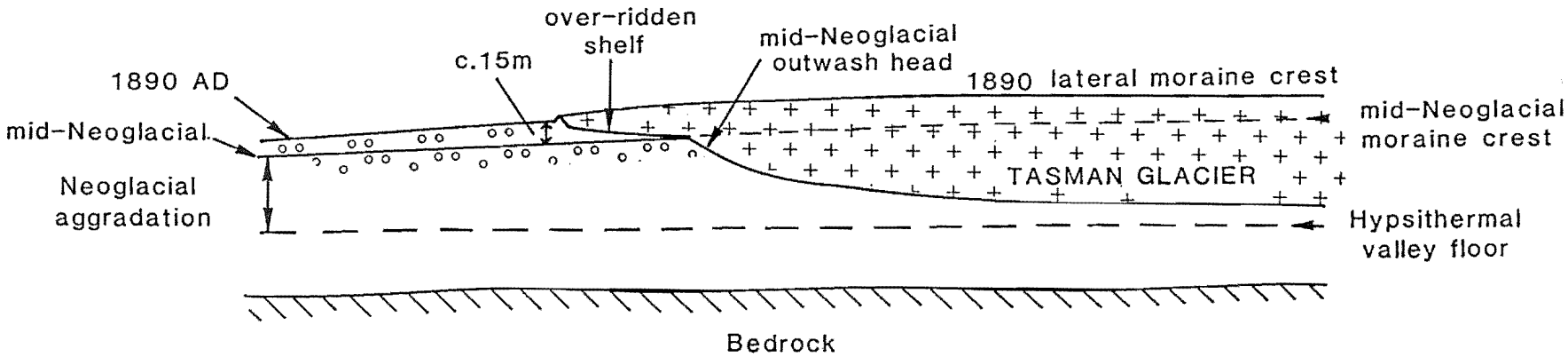

FIG. 5.17 Interpretation of the long profile of the Tasman Glacier terminal area, based on geophysical profiles (Broadbent 1973).

extend over several 10s of metres. The diamict contains very angular to sub-rounded clasts in a compact silty matrix. A sample of 50 clasts from one unit gave a mean roundness of 2.56, and several striated clasts were found. Matrix-support predominates except in pebbly horizons common in some units where a clast-supported framework is found. The units are often horizontal in three-dimensions, but may drape subjacent undulations. Upper and lower contacts are sharp.

The contrasting interbeds of massive pebbly diamicton with matrix-supported pebbly silt and the lateral continuity of the beds are similar to basal melt-out tills described by Lawson (1979; 1981). The roundness of the clasts is very close to that of traction-zone material described in Chapter 3.4. A basal melt-out origin of facies 1 is therefore preferred.

FACIES 2 consists of discontinuous massive diamictons of highly variable thickness. Angular clasts in a clast-supported framework predominate. The matrix is sandy, and weak stratification occasionally occurs in pebbly laminae. Lower contacts are sharp, upper contacts are sharp and often erosional.

Facies 2 is interpreted as supraglacial melt-out till deposited by dumping, due to its similarity to recently-deposited supraglacial ablation till in the locality.

If the genetic interpretations of the tills are correct, the alternating sequence of eroded ablation tills and basal melt-out tills forces an interpretation of a depositional history which includes periods of sub-aerial exposure. Combined with the much greater degree of weathering compared to the 20th Century tills, it is concluded that the tills exposed in the sections must pre-date the earliest dated Neoglacial moraines.

A maximum age is constrained by the end of the Hypsithermal. This date is poorly known in New Zealand, but is thought to have occurred around 5,000 B.P. (Section 5.2.1.1). If the tills forming the benches pre-date the earliest-known Neoglacial lateral moraine dates, about seven till couplets visible in Fig 5.15 must represent seven previously-unrecognised glacier fluctuations at the start of the Neoglacial. They were therefore deposited during glacier expansions before 3,500 B.P. This period is envisaged as being one of a succession of advances and retreats of a lobe of ice into an embryonic embayment, where till deposition was rapid.

The disconformity below the most recent tills indicates an absence of basal tills of middle and late Neoglacial age. Glaciers are known to

deposit marginal moraines at the same time that they erode their beds (Rothlisberger & Schneebeli 1979: Figs 15 and 25), but it is unlikely that the Tasman Glacier has not been depositing basal till during the last 3,500 years. Either tills of this age have been eroded completely, or other explanations must be considered.

Alternative interpretations.

Two alternatives must be considered which may allow a different age to be assigned to the tills.

1. If earlier phases of moraine wall collapse have occurred but left no evidence, the glacier may have been smaller than at present during the last 3,500 years. Sub-aerial exposure may therefore have occurred in the Murchison embayment during retreats from the moraine benches. The till sequence may then represent topographically-lower but stratigraphically-equivalent deposition during retreat phases in the last 3,500 years. I find it unlikely that wholesale valley-side collapse, similar to that caused by present low ice levels, can have occurred during the last 3,500 years without leaving evidence. This interpretation is therefore unlikely.

2. The origin of the tills exposed in section may have been mis-interpreted. Chinn (written communication) has suggested that the till couplets may be basal melt-out (facies 2) overlying lodgement till (facies 1). The alternative explanation of facies 1 is easier to accept than that of facies 2. If future work reveals this to be correct, there is no need to invoke periods of subaerial exposure during deposition, and the tills are stratigraphic equivalents of the moraine walls, laid down by alternating phases of mobile (during expansions) and immobile (during retreats) basal ice. Again, an age of post-3,500 B.P. is implied. This interpretation is regarded as unlikely in the light of existing (though limited) sedimentological evidence.

In conclusion, the Murchison embayment provides convincing evidence of a dominantly aggradational glacial-geomorphic system during the last 3,500 years, and perhaps over the whole Neoglacial period. Several features predicted by the **a priori** ponding model (Section 5.1) are identified:

1) Progressive over-riding of terminal positions associated with gradual advance of the glacier.

2) Limited retreat between advances during the last 3,500 years at least.

3) Abundant supraglacial melt-out tills, indicative of high supraglacial debris loads throughout the Neoglacial.

The recent exposure of the till cliffs in the embayment is a cautionary tale in dealing with glaciers in an aggrading system: much evidence relating to the Neoglacial (and perhaps even the Hypsithermal) must await exhumation as current glacier shrinkage continues. It is also instructive to note that much of this evidence is likely to be preserved in unusual toporaphic settings, united by the common characteristic of protection from fluvial erosion.

5.3.1.3 Summary of the Murchison embayment evidence.

The landforms and stratigraphy of the embayment are indicative of progressive over-riding of ice marginal positions over a period of at least 3,500 years, and possibly of 5,000 years. The development of the embayment is linked to aggradation at the terminus of the glacier over the same period (see below). Observations of the geomorphic development of the embayment therefore allow interpretations to be drawn about the timing and rate of aggradation at the terminus.

5.3.2 Subglacial morphology.

The long profile of the lower 2 km of the glacier bed has been constructed from geophysical surveys (Broadbent 1973). Fig 5.17 shows a shallow shelf of ice behind the present terminus, extending westward around the glacier margin (Fig 2.4). By comparison with the exhumed benches in the Murchison embayment, these shelves are interpreted as over-ridden outwash heads or moraines. Moraine ridges (Fig 5.6) date the timing of the over-riding event at about 1,500 B.P., more recent than over-riding events in the Murchison embayment.

Morphology of the glacier bed provides further evidence of an expanding glacier during the Neoglacial period.

5.3.3 Implications of new evidence for the a priori model.

The proglacial area of the Tasman Valley has maintained a positive sediment budget throughout the Holocene. An absence of terracing, a flat sandur surface bounded laterally by sharp breaks of slope, and a large proglacial fan, are evidence for continuing aggradation. The burial of the early Holocene Birch Hill moraines (Speight 1940) indicate net deposition since at least 8,000 B.P. Estimated aggradation is 40 m over 3,000 years on the Murchison sandur (Fig 5.13), and 15 m since the mid-Neoglacial (c.1,500-2,500 years) at the terminus (Fig 5.17). Ponding of the Tasman Glacier has been caused by aggradation at the terminus, in turn giving

increasing ice levels and encroachment of an ice lobe into both the Murchison embayment and at Blue Lakes. Aggradation of the Murchison sandur is a result of damming by the embayment moraines, which ultimately reflect the degree of aggradation at the terminus.

5.4 TESTING THE MODEL: THE GEOMORPHIC DEVELOPMENT OF THE TASMAN VALLEY SINCE THE MID-HOLOCENE.

The following reconstruction combines geomorphic and stratigraphic observations with intuitive reasoning within the time control based on the existing radiocarbon chronology. The result is a synthesis of events since the Hypsithermal Interval in the mid-Holocene, presented in the form of "images" of the valley at selected times. As in all such reconstructions, the evidence becomes sketchier and the interpretations more speculative with increasing distance from the present.

A positive sediment budget has caused net aggradation in the lower Tasman Glacier and the proglacial area throughout the last 3,500 to 5,000 years (Section 5.3). Within this framework, the following stages in the evolution of the valley are recognised.

5.4.1 Hypsithermal c.8,000 - 5,000 B.P.(Fig 5.18A).

Glaciers had retreated from their early Holocene maxima of about 8,000 B.P., represented by the Birch Hill moraines. This maximum must have been a prolonged stillstand, the moraines being large and remnants still surviving in valley-floor locations, protruding through the thick aggradational deposits of Neoglacial riverbed. By analogy with the configuration of the Pukaki-age and modern glacier termini, a Birch Hill age outwash head may have ponded a lake in the trough vacated by the retreating glacier after the 8,000 B.P. maximum. No direct evidence for this lake exists, nor is the location of the glacier terminus during the Hypsithermal known. Proxy evidence for a prolonged interval of warmer temperatures than the present (McGlone & Moar 1977; McGlone & Topping 1978) allow speculation that the glacier terminus lay a some distance upstream of its present location. A glacier in equilibrium with present snowline altitudes might terminate in the vicinity of Novara Spur. A slightly warmer climate than at present would presumably correspond to smaller glaciers, so that a terminal position in the Hypsithermal upstream of the Murchison junction is probable. There is a remote possibility that ice existed throughout the Hypsithermal interval,

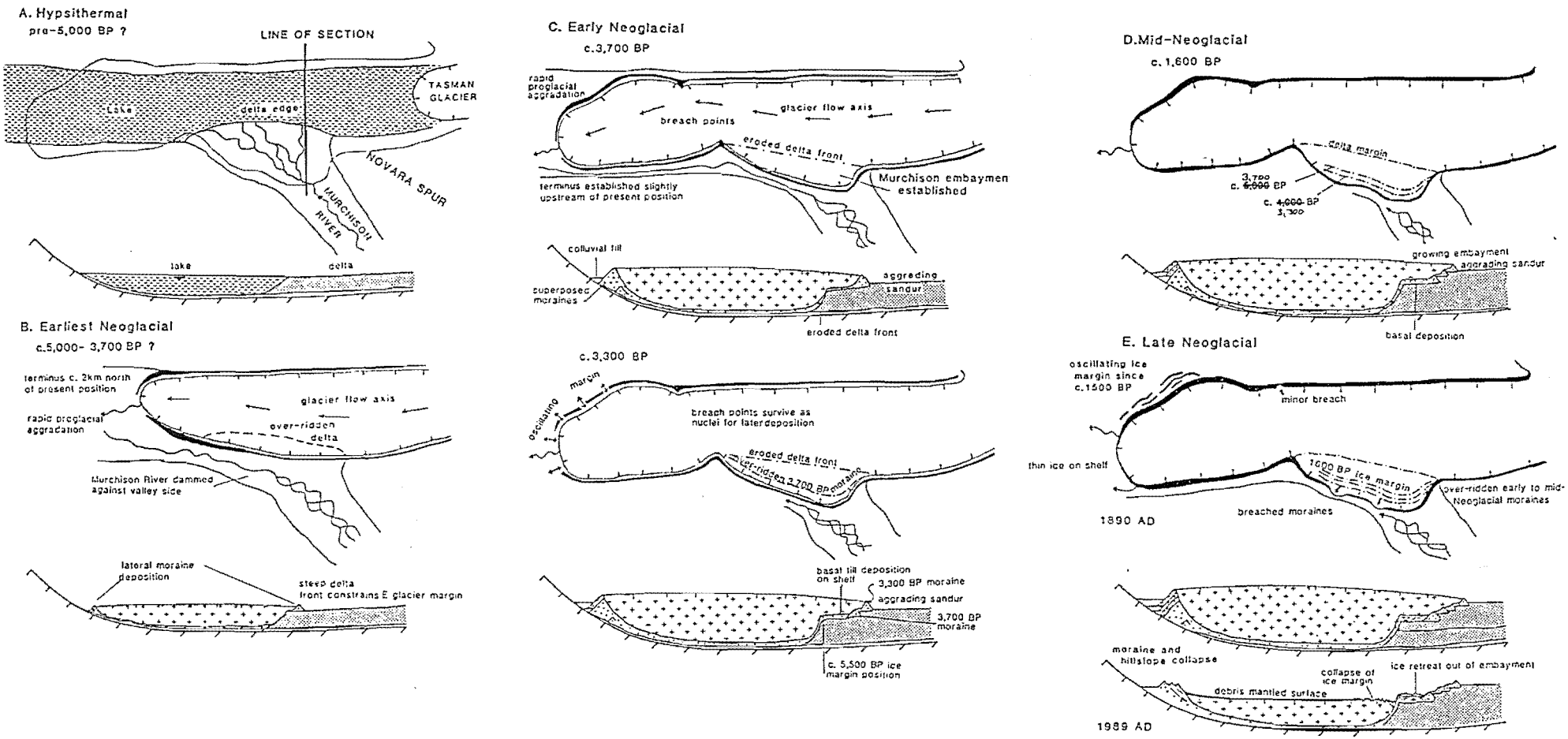

FIG. 5.18 Reconstruction of events in the lower Tasman Glacier since the Hypsithermal interval. See text for discussion.

buried beneath ablation till and outwash from the Murchison River. I regard this possibility as less likely than a Hypsithermal lake, though it may have had similar morphological consequences.

The Murchison River, unconstrained by a glacier in the main valley, would have prograded a steep-fronted delta into the lake. This interpretation (rather than a low-angle alluvial fan invading a sub-aerial outwash plain) is favoured because the sharp, very steep contact between the present glacier margin and the cliff of horizontally-bedded tills (Fig 5.12) seems to demand that a steep slope existed at this place before the Neoglacial readvances. It is difficult to reconcile this steep contact with any other interpretation, with the possible exception of buried ice in the main valley. The persistence of a subglacial obstruction at the mouth of the Murchison Valley during the Neoglacial is consistent with other lines of evidence described below.

5.4.2 Earliest Neoglacial c.5,000 - c.3,700 B.P. (Fig 5.18B).

In the centuries prior to 3,700 B.P. (the oldest accepted moraine wall date so far obtained) the earliest mid-Holocene readvances occurred. The exact timing is not known. The glacier in equilibrium would have been smaller than at present, due to its steeper surface gradient combined with its lower surface elevation. Two distinct kinks in the eastern and western lateral moraines of the Tasman Glacier may be derived from the latero-terminal moraine segments of the early Neoglacial glacier. The latero-terminal segments of moraines tend to be larger (and with a greater preservation potential) than the true lateral or terminal ridges due to englacial sediment routeways in the ablation zone (Boulton & Eyles 1979; Matthews & Petch 1982) and to meltwater destruction of the terminal moraine (Speight 1940; Chernova 1981). The lateral-moraine kinks by the Tasman Glacier are interpreted as the latero-terminal moraines of a smaller glacier, that were subsequently breached but remained as nucleii for later till accretion. (A comparable situation existed at the Mueller terminus where breaching occurred about 3,000 B.P.).

The early Neoglacial glacier would have just over-topped the Murchison delta, and been forced to flow towards the western valley wall by the presence of the delta. This may be responsible for the particularly large eastern moraine kink surviving in a location protected from faster-flowing ice. The asymmetry imposed on the glacier by the obstructing delta is illustrated by Fig 5.18B, and deflection of the thread of maximum velocity in the early Neoglacial has persisted to this day.

c.3,700 B.P. (Fig 5.18C).

Glacier advance established a configuration similar to the present day, as indicated by buried soils 60-70m below the crests of the lateral moraines (Gellatly et al 1985; Burrows 1989). Older moraines were breached where they offered least resistance: at the terminus itself. A lobe of ice extended round the "corners" of the latero-terminal barriers to occupy space in front of them, and to establish a new terminus close to its present position. Thereafter, a prolonged stillstand allowed the proglacial fan to aggrade in front of a more-or-less stable outlet position. This had a consolidating effect on the position of the glacier terminus in the manner described in Section 5.1. Aggradation formed a steep reverse slope or outwash head at the terminus which reduces the amount of any advance for a given increase in ice discharge, due to simple geometric relationships (Section 5.1.3.1). The glacier would be pre-disposed to debris mantle accumulation. Proglacial aggradation and outwash head construction would increase compression in the lower glacier and enhance the flow structure favouring debris-mantle growth. In this way, the debris mantle would have become increasingly significant during the Neoglacial. Increased insulation would have increased the lag between reduced ice discharges and the onset of retreat, making the glacier less likely to respond to negative mass balance by retreating. Put another way, the reduction in ice discharge needed to cause a retreat has become greater over time. Therefore, since about 5,000 B.P. the terminus of the glacier has become increasingly prone to an inertia under both positive and negative mass balance fluctuations. Such temporal evolution in the sensitivity of glacier response is a direct result of the strongly positive sediment budget in the lower glacier and proglacial area, resulting in the combined and complementary effects of proglacial aggradation and debris mantle development.

The Murchison embayment became established about 3,700 B.P. as a lobe of Tasman ice over-topped the delta front to build a moraine loop in front of a shallow shelf of ice.

c.3,300 B.P.

The pattern established around 3,700 B.P. continued. Further proglacial aggradation increased the ponding effect at the terminus and ice levels followed a rising oscillatory trend (cf. Fig 4.14). The oscillations are climatically-induced fluctuations: the overall rising

trend is a product of the increased ponding effect and debris mantle insulation and does not reflect a general climatic deterioration. In the Murchison embayment, an over-riding event took place about 3,300 B.P. and established a new moraine loop outside and above the 3,700 B.P. moraine. The latter was planed-off during over-riding, and is currently exposed as the lowermost moraine bench in Figs 5.12 and 5.13.

More till was accreted at the breach points in the main lateral moraines, which continued to laterally-constrain glacier flow. The old Murchison delta, now buried and mantled by till, formed the shelf which is the floor of the embayment on which thinner, slower-moving ice has periodically deposited the basal tills now seen in section (Fig 5.15). Behind the bounding moraine of the embayment, the Murchison sandur was forced to aggrade due to damming by the moraine.

5.4.3 Mid-Neoglacial c.1,600 B.P. (Fig 5.18D).

Little change in areal pattern occurred during the mid-Neoglacial. Continued vertical trends of proglacial aggradation and ice ponding and generally rising ice levels led to a further expansional event in the embayment. The c.3,300 B.P. moraine was over-ridden to form the second moraine bench (Fig 5.13) and a new moraine rampart established, again in a higher and more distal position.

5.4.4 Late Neoglacial 1890 A.D.

Further glacier expansions after c.1,600 B.P. over-rode the contemporary Murchison embayment moraine and construction of the present moraine took place during periodic advances up to 1890 A.D. This moraine was partially breached in several places but never completely over-ridden (Fig 5.11). At the terminus, shallow ice-covered marginal shelves (Fig 2.4 probably relate to over-riding and advance at about the same time. Moraine dates (Gellatly et al 1985) marginal to these shelves indicate oscillations of the ice margin since c.1,500 B.P., made possible by the gentle slope on which the ice margin lay. The glacier flow axis was still affected by the buried obstruction.

1986 A.D.

From the late Nineteenth Century ice maximum, the glacier has thinned and the ice margin retreated out of the Murchison embayment into the main channel. Moraine benches and till cliffs have been exposed during this period, their preservation being aided by the lack of surface drainage and

protection from the Murchison River.

Extensive collapse of valley-side moraines is in progress (Bishop 1979; Blair 1984), while a heavily debris-covered (but mobile) ice tongue occupies the main channel. Ice discharges are declining and becoming less able to sustain the glacier tongue. Crevassing and thermokarst erosion of the ice margin is rapidly destroying the protective debris mantle.

5.4.5 The Twenty-First Century.

If current trends continue, in a few decades' time the lower glacier tongue will have completely broken up in the manner of the Godley Glacier in the 1970s and 1980s. Because it occupies a deeper trough of lower gradient, the Tasman Glacier will retreat further and perhaps more quickly than the Godley Glacier (Chapter 4.2).

Although the lateral support provided by the glacier to the hillsides will disappear, it will be replaced by water of similar density to ice, but much lower viscosity. The lake surface will be at a lower elevation, and net loss of support will result in continued major slope instabilities in both the drift mantle and in bedrock. Lateral moraines perched on steeper valley-side slopes will rapidly erode to leave steep rock faces above the lake. The high discharge of the Hochstetter icefall will probably remain sufficient to dam the valley for another century at least, and will supply all of the ice reaching the terminus.

5.4.6 Conclusion: the applicability of the a priori model to the Tasman Glacier.

The a priori model of glacier ponding, debris mantle spread, and glacier response (Section 5.1.5) predicted that such glaciers should show the following features:

1) evidence of continued proglacial aggradation;

2) evidence of repeated elevation of the glacier surface over several mass-balance cycles.

Field evidence supports the model closely. Evidence in support of a ponding/ debris-mantle model of behaviour for the Tasman Glacier includes:

1) absence of a terminal moraine, indicating meltwater redistribution of debris delivered from the glacier preventing the formation of a moraine;

2) an extensive aggrading proglacial foreland, with no evidence of terracing;

3) a large outwash head revealed by geophysical survey;

4) overlap of the glacier margins to deposit super-posed lateral moraines and to create shallow subglacial marginal shelves.

It is concluded that the a **priori** model is confirmed, and may be applied to the Tasman Glacier over the Neoglacial period. To what extent this behaviour is applicable over the whole region demands that the Tasman Glacier chronology is compared with chronologies of other glaciers.

5.5 REGIONAL OVERVIEW: A COMPARISON OF THE NEOGLACIAL CHRONOLOGIES OF DEBRIS-MANTLED AND DEBRIS-FREE GLACIERS IN THE SOUTHERN ALPS.

This section contrasts the records of Neoglacial fluctuations of debris-mantled and unmantled glaciers in the Southern Alps. On the basis of observed differences, an assessment is made of the suitability of chronologies of each type of glacier as an indicator of climatic change.

5.5.1 Behavioural comparisons in historic times

The glaciological significance of the Tasman Glacier's debris mantle is to preserve the glacier tongue by insulating ice from melting, thereby preventing (or at least delaying) retreat of the terminus. There has been a regional trend of glacier retreat over the last century in the Southern Alps (Wardle 1973; Burrows 1975; Burrows et al 1979; Bishop & Forsyth 1988). McSaveney (1975) contrasted the Cameron Glacier, which has no extensive debris mantle, with the Tasman Glacier to demonstrate the extent to which the debris mantle of the latter had prevented retreat up to the 1970s. A detailed examination of the significance of debris-mantle insulation in historic times is undertaken here.

General relationships between snowline elevation changes and glacier lengths may be understood with reference to a simple model. Departures from the "expected" behaviour of glaciers in the region, possibly caused by debris insulation, may then be identified.

Fig 5.19 illustrates schematically the relationship between relief, snowline elevation, and the vertical descent of glaciers. For simplicity, summit levels are represented as a horizontal ridge with an altitude of 20 units. The snowline gradient is imposed on this idealised mountain range. (The same effect on glacier descents would result from a horizontal snowline on rising summit levels). The ratio, r, of the vertical range in altitude of accumulation areas to glacier descents varies, but typically lies between 0.4 and 0.6 depending on the area/altitude distribution of individual glaciers. A value for this ratio of $r = 0.5$ is used in this

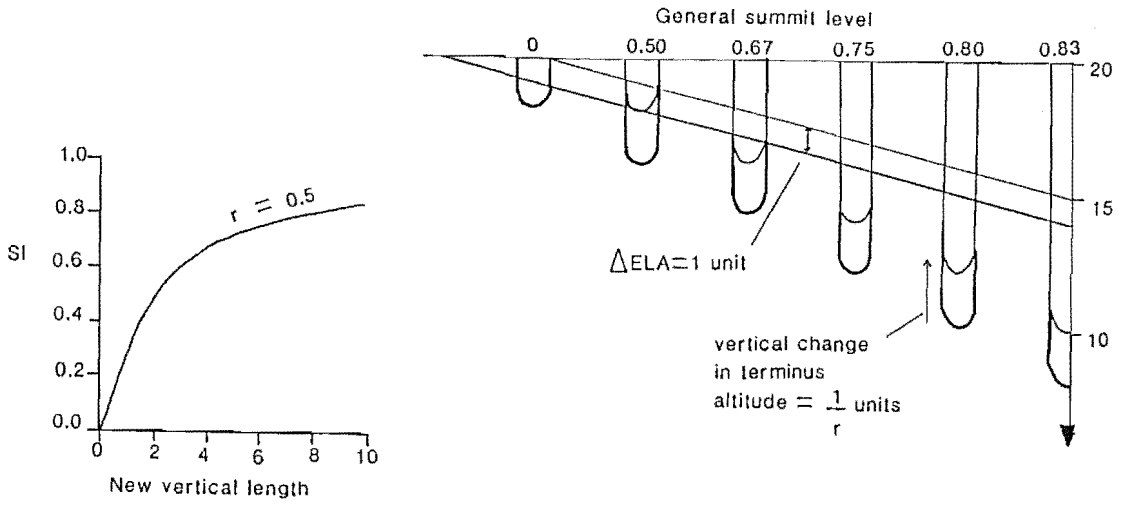

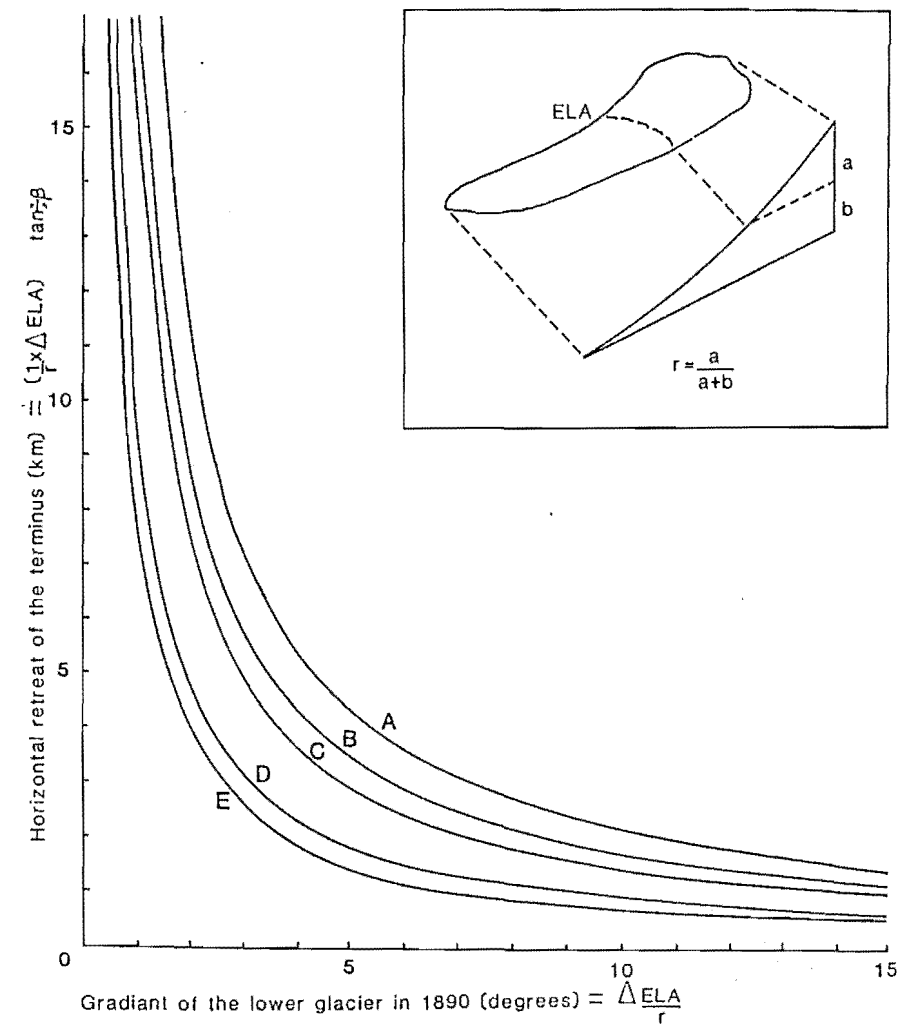

FIG. 5.19 Top: Diagram illustrating relationship between summit level, equilibrium line altitude (ELA), and vertical descent of glaciers. Bottom: Relationship between glacier shortening index (SI) and glacier length, for 5 different values of r (inset) and ELA.

A r = 0.4 ELA = 150 m
B r = 0.5 ELA = 150 m
C r = 0.6 ELA = 150 m
D r = 0.5 ELA = 80 m
E r = 0.6 ELA = 80 m

model. The higher that summit levels project above the snowline elevation, the greater is the descent of glaciers from those summits. Thus, a glacier with an equilibrium-line elevation (ELA) of 17 units will terminate at 14 units, one with an ELA at 18 units will terminate at 16 units, and so on.

A step-like rise in snowline elevation of one unit follows. To maintain the ratio r = 0.5, all glaciers retreat by the same vertical magnitude of 2 units. All glaciers whose initial length was 2 units or less disappear. With increasing length, the proportion of the glacier which disappears becomes less. This may be expressed as

$$\left(\frac{l_0 - l_1}{l_0}\right) = l_0 - \left(\frac{1}{r} \cdot \Delta ELA\right) \qquad (18)$$

The retreat of any glacier may be expressed as a shortening index, S_i, where

$$S_i = l_0 / l_1 \qquad (19)$$

where l_0 is the original vertical descent (length) of the glacier, and l_1 the new equilibrium length. The relationship between S_i and l_1 is asymptotic (Fig 5.19), demonstrating the greater proportionate effect of the ELA line rise on the map lengths of smaller glaciers (since map length is generally a function of vertical descent).

The next step is to calculate an expected horizontal retreat of glaciers in the Southern Alps, caused by the ELA rise since the late 19th Century. Observed retreats of both debris-mantled and unmantled glaciers may then be compared with their expected values. The year 1890 is chosen as a datum year when most glaciers were close to a maximum extent (and therefore close to an equiibrium mass balance condition) and terminal positions are well-documented.

The change in ELA since 1890 has been estimated by Porter (1975a), who suggests a figure of 140 $\pm$ 50 m for the Mount Cook area, based on reconstructed glacier dimensions. For Europe, Oerlemans (1988) presents the measured ELA rise of four glaciers, which average 82 m with a standard deviation of 25 m. Porter's figure is rounded to 150 m and used in this study. Based on this figure and on the ratio r = 0.5, it is predicted that the altitude of glacier termini will have risen by 150 / 0.5 = 300 m. This is converted to a horizontal distance Δ T where

$$\Delta T = \frac{(1/r . \Delta ELA)}{\tan \beta} \qquad (20)$$

Horizontal retreat is proportional to the tangent of the gradient of that part of glacier lost during retreat, β . Retreat is therefore sensitive to glacier gradient, as shown by the asymptotic curves in Fig

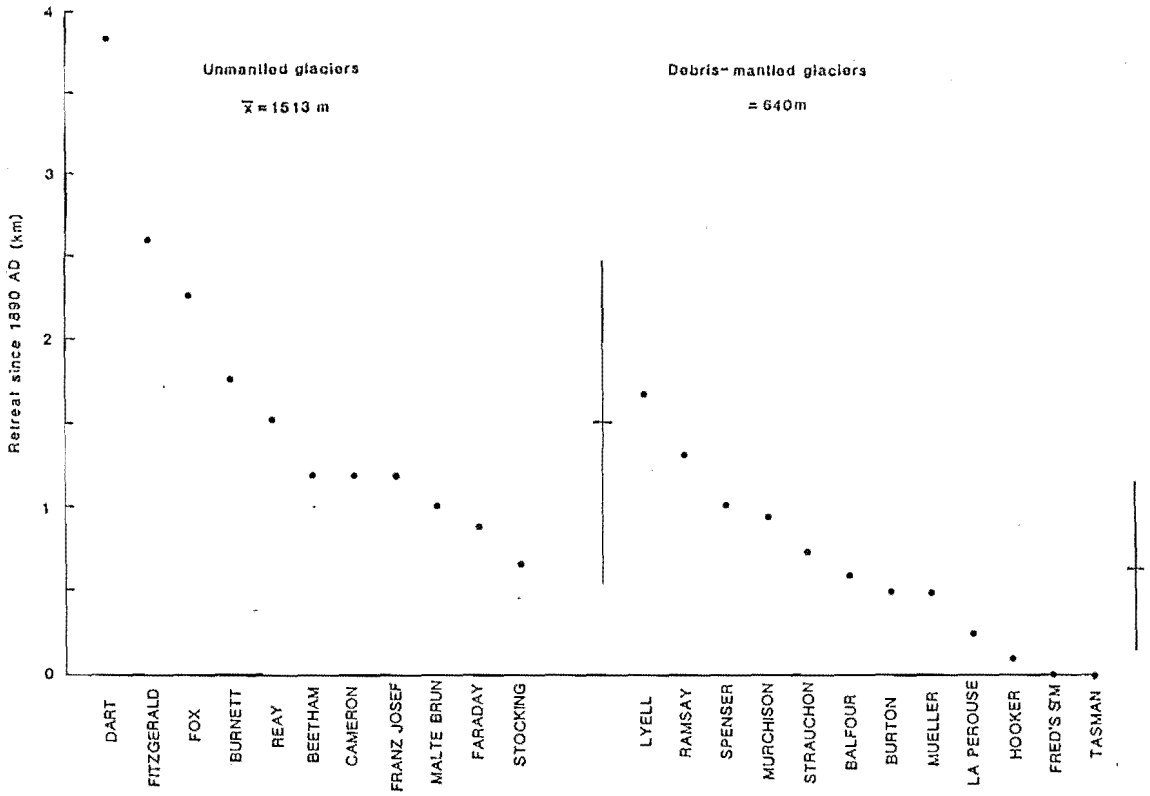

FIG. 5.20 Glacier retreats since the late Nineteenth Century for unmantled and debris-mantled glaciers in the Southern Alps. Bars indicate mean retreat ± 1 standard deviation.

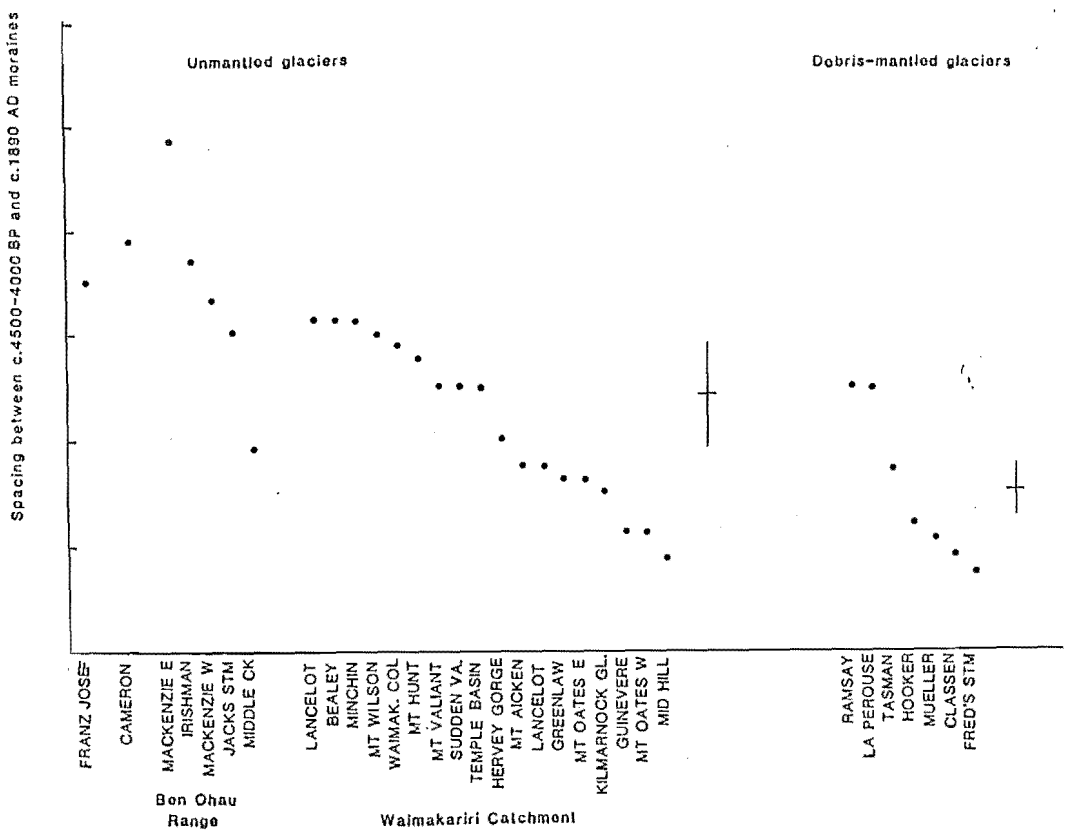

FIG. 5.21 Glacier retreats since the early Neoglacial period for unmantled and debris-mantle glaciers in the Southern Alps. Bars indicate mean retreat ± 1 standard deviation.

5.19. Curve C has been used to calculate the expected retreat of the glaciers listed in Table 5.3. Comparison with measured retreats shows that debris-mantled glaciers have retreated shorter distances than predicted. A check on the method is provided by the unmantled Franz Josef and Malte Brun Glaciers, whose retreats have been close to the predicted values. Retreats of 12 debris-mantled glaciers are significantly less than retreats of 12 unmantled glaciers (Fig 5.20), using a one-tailed t-test. The level of significance is 0.02.

The difference between the expected and actual retreats of debris-mantled glaciers varies (Table 5.3), indicating differing degrees of debris-mantle insulation between glaciers. The 7 debris-mantled glaciers in Table 5.3 for which data exists are "over-long" by an average of 3.7 km.

The Tasman Glacier is in a potentially extremely unstable condition. The very low surface gradient results in the lower 8 km being vulnerable to retreat. Chapter 4 demonstrated that the "over-long" tongue of ice is presently poised on a threshold between slow and drastic retreat.

An implication of this analysis is that for unit increases in ELA, map lengths of glaciers increase exponentially with decreasing glacier gradient (Fig 5.19). Because smaller glaciers usually have steeper gradients than larger ones, a unit increase in ELA is effective in causing very large retreats of low-gradient glacier tongues. The small, steep cirque glaciers of the present day are therefore relatively insensitive to climatic amelioration compared to the large valley glaciers of the Late Pleistocene. A given increase in mean annual temperature in the Pleistocene would have caused much greater glacier retreats than an equivalent rise at the present day. This may explain rapid retreats and the large decrease in ice-covered area at the close of the Pleistocene (Porter 1975a).

5.5.2 Neoglacial fluctuations

The difference between the Twentieth-Century retreats of debris-mantled and unmantled glaciers indicates that insulation of ice has been significant on a timescale of 10^2 years. To discover whether the difference is detectable over longer timespans of the Neoglacial period, changes in the lengths of mantled and unmantled glaciers are compared. Chronologies from catchments where supraglacial debris mantles have not been present show, almost without exception, a general declining trend in the magnitude of readvances since c.5,000 B.P. Chronologies used in this

TABLE 5.3 Predicted and observed retreat of glaciers in the central Southern Alps since the late Nineteenth Century.

Glacier	Gradient of lower 250 m	Expected retreat	Si	Observed retreat	Si
Classen	5.0^{o}	2.9		*	*
Grey	3.7^{o}	3.9		*	*
Godley	3.9^{o}	3.6		*	*
Murchison	2.7^{o}	5.5	0.68	0.95	0.95
Tasman	1.7^{o}	8.4	0.71	0.00	1.00
Hooker	3.6^{o}	4.0	0.66	0.10	0.99
Mueller	4.4^{o}	3.3	0.73	0.50	0.96
Burton	8.1^{o}	1.7	0.76	0.51	0.93
La Perouse	3.9^{o}	3.6	0.65	0.25	0.98
Balfour	6.2^{o}	2.3	0.77	0.60	0.94
Franz Josef	5.9^{o}	2.4	0.80	2.50	0.79
Malte Brun	13.3^{o}	1.3		1.10	

* indicates drastic retreat associated with calving terminus

study are those of the Waimakariri Valley (Chinn 1975), the Cameron Valley (Burrows 1975), the Ben Ohau Range (Birkeland 1982), and the Franz Josef Glacier (Wardle 1973).

A null hypothesis is proposed, that there is no difference in horizontal spacing of early Neoglacial and late Neoglacial moraines between debris-mantled and unmantled glaciers. If debris mantles have prevented retreat of some glaciers during negative mass-balance phases, the null hypothesis would be rejected. In other words, repeated mass-balance cycles of insulated glaciers would produce a closer spacing of moraines compared to moraines of uninsulated glaciers.

Data collection is hindered by the small number of catchments containing dated early Neoglacial moraines. There is a bias towards the Arthur's Pass area where many such moraines have been mapped (Chinn 1975). A sample of 26 unmantled and 7 debris-mantled glaciers have moraines of approximately equivalent ages. The horizontal spacing of moraines introduces a loss of information, because it is used as a surrogate for vertical glacier descent (Section 5.5.1). Variations in glacier gradient make the dataset somewhat "noisy". Results are shown in Fig 5.21. The samples differ at a 0.01 significance level (using the t-test), but only if the apparently anomalous case of the Lyell Glacier is omitted. This glacier has retreated over 3 km since the early Neoglacial, when other mantled glaciers have retreated less than about 1 km.

If adjustment was made to the dataset for glacier gradient, distinction between the two categories of glacier would be further enhanced because the Arthur's Pass and Ben Ohau range glaciers are steeper than the debris-mantled valley glaciers in the sample. Even without this refinement, a significantly closer spacing of glacier maxima for debris-mantled glaciers than for unmantled glaciers during the Neoglacial period is demonstrated. It is concluded that the existence of debris mantles over a c.5,000 year period has significantly influenced the magnitude of response of many glaciers to climatic change.

5.5.3 The suitability of different glaciers as indicators of climatic change.

It has been demonstrated that glaciers without debris mantles followed a trend of repeated advances of decreasing magnitude over the last 5,000 years. Moraines from these glaciers have provided relatively few radiocarbon dates. Debris-mantled glaciers have apparently experienced much smaller frontal oscillations, some glaciers even reaching their

Neoglacial maxima in the last few centuries. Many radiocarbon dates have been obtained from the moraines of debris-mantled glaciers.

The abundance of radiocarbon dates has lead Gellatly et al (1988) to treat the Mount Cook chronology as the "type" Holocene glacial sequence for New Zealand. Such emphasis on the chronology of a single glacier must be qualified before it is accepted. Although many more dated events occur in the Mount Cook area than in other catchments in the region, the climatic significance of these events is questioned.

The crucial point is to assess to what extent the dated expansion of a debris-covered glacier indicates a climatic cooling. Small expansions may be caused by a short-term climatically-induced changes in mass balance. This study demonstrates that they may equally be a response to progressive aggradation and ponding of the terminus under conditions of constant climate. Also, the increase in debris mantle extent and a corresponding reduction in ablation rate restricts the effect of negative balance phases and may even lead to small expansions during conditions of approximately equilibrium mass balance.

Furthermore, if a tongue of debris-covered, insulated ice is preserved during negative balance, the magnitude of the succeeding expansion will be affected. More energy would be required for a terminus to readvance to a former maximum position than for a kinematic wave propagated through an existing tongue of ice to cause over-riding of the former maximum position.

Debris-mantled and ponded glaciers are useful for providing an abundance of datable material in their moraines. Ironically, this abundance is a result of non-climatic influences on ice levels, which have encouraged over-topping of marginal moraines during relatively insignificant advances with a dubious relationship with climatic change. Adjacent debris-mantled glaciers differ greatly in the number and age-distribution of their Neoglacial moraines. Their chronologies provide dates indicating of general phases of glacier fluctuation. The magnitude and timing of individual climatic impulses cannot be reconstructed from their moraine distributions.

Conversely, the magnitudes of fluctuations of unmantled glaciers and glaciers without outwash-head barriers tends to reflect the magnitude of climatic changes more faithfully. Problems arise from a relative absence or inaccessibility of datable material, which limits reconstruction of the timing of events. However, general correspondence between chronologies of geographically-widespread glaciers suggests that moraines of unmantled

glaciers in the Southern Alps are more representative of the number and magnitude of significant climatic changes in the Holocene.

5.6 CONCLUSIONS OF CHAPTER 5

1. The existing chronology of Holocene glacier fluctuations at Mount Cook is broadly representative of the timing of events but has not considered non-climatic influences on the magnitude of glacier fluctuations.

2. The Tasman Glacier, and by inference other similar glaciers, have been affected by proglacial ponding and debris mantle development since the mid-Holocene. This has been a result of the strong positive sediment budget in the lower glacier and proglacial zone. The effect has been to reduce the sensitivity of glacier response to the low-amplitude climatic fluctuations which have characterised the Neoglacial period.

3. This behaviour contrasts with that of glaciers without debris mantles whose termini are more responsive to mass balance change. The difference in response has lead to over-ridden and clustered Neoglacial terminal moraines around mantled glaciers, but widely-spaced moraines around unmantled glaciers.

4. Moraines deposited by mantled glaciers record a greater proportion of ice-marginal fluctuations than those of unmantled glaciers.

5. However, moraines of unmantled glaciers give a better indication of the general climatic trends of the Neoglacial than do those of mantled glaciers.

6. The 20th-Century shrinkage of the Tasman glacier is the greatest since the start of the Neoglacial and indicates a significant climatic warming in the context of the whole Holocene.

CHAPTER 6: LATE PLEISTOCENE SEDIMENT-LANDFORM ASSOCIATIONS: EVIDENCE FOR AND AGAINST THE PONDING MODEL

The behaviour of the Neoglacial Tasman Glacier during a prolonged period of aggradation has been reconstructed with reasonable confidence (Chapter 5.4). This is because the general form, size and dynamics of the glacier since c.5,000 B.P. have not been greatly different from the present day. The main uncertainties revolve around the timing of events rather than the nature of events themselves.

If the model of ponding, debris mantle development and an increasingly unresponsive terminus can be applied to the glacier at the close of the Pleistocene, inferences may be made about mechanisms and rates of glacier retreat. However, the uniformitarian approach adopted for the Neoglacial cannot be applied with the same degree of confidence to the Late Pleistocene. Several characteristics distinguish the glacier during the Tekapo and Mount John advances (Mansergh 1973) from the Neoglacial glacier. Collectively, these reduce the likelihood that glacier dynamics evolved in the same way in the much larger glacier of the Pleistocene.

1. Relative relief between the summit elevations and the glacier surface was less, due to ice levels up to 700 m higher than at present (Porter 1975a). Tributary icefalls, though more numerous, were graded to a higher level, were less steep, and flow was less compressive where tributaries entered the trunk glacier. Tributaries from the Ben Ohau Range did not enter via icefalls at all (Porter 1975a).

2. The relative discharge of ice to debris in high-level transport through the valley would have been greater. Rockfall rates were probably not significantly greater than at present. Although the area of debris sources was greater, ice discharges would have been proportionately greater still. The result would have been a lower englacial debris concentration.

3. Unlike the present glacier, which is confined by a narrow valley, the Pleistocene glacier was able to spread laterally across the gentle slope forming the eastern margin of the ablation zone (Fig 6.1). Downstream from the former equilibrium line the valley progressively widens. Longitudinal compression in the glacier tongue could therefore have been accommodated by lateral expansion rather than by ice thickening (and increased upward flow component) alone. Particle trajectories would not have steepened so rapidly or to such an extent during increased compression compared to the Neoglacial glacier.

FIG. 6.1 Oblique aerial photograph looking west across Lake Pukaki.
Foreground: Late Pleistocene lateral moraines spread acrossgentle ground.
Background: Lateral moraines /kame terraces constructed on the steep western front of the Ben Ohau range.

6.1 TILL SEDIMENTOLOGY.

The modern glacier is depositing large volumes of supraglacial melt-out till by sub-aerial dumping and in ice-marginal lakes. These tills are exclusively very blocky and contain dominantly angular clasts. The texture results partly from the eluviation of fines from interstices during a long residence period as a supraglacial debris mantle, followed by further sorting and/or eluviation during deposition by dumping. The high porosity and coarse clast-supported texture of the tills prevents resedimentation as flow tills (Lawson 1982).

Comparisons with Late Pleistocene tills are limited by the paucity of good exposures of the latter. Sections along the Lake Pukaki shoreline are generally in proximal ice-contact lacustrine facies and most till present has been reworked and mixed with mass-movement and fluvial material. Of several sections which have been examined, only three are relevant to this study.

6.1.1 Powerhouse section (S100/874 825) (Fig 6.2 and 6.3)

A roadcut through a latero-terminal moraine of Tekapo age has revealed a section of reworked ablation till, which shows close similarities with modern lateral moraines. The till is weakly stratified with a low dip towards the former glacier, indicating resedimentation on the proximal face of a moraine. The till has variable clast and matrix support and consists of poorly-sorted coarse gravel and sand. Clasts up to 50 cm b-axis are abundant and are dominantly angular. Sub-angular to sub-rounded clasts are common, and their roundness and lack of striations indicates water-working rather than sub-glacial abrasion (Chapter 3.4). Clusters of water-worked debris (Fig 6.3) may have been rounded in an englacial position as well as (or instead of) in ice-marginal streams. From the topographic position of the moraine, the former seems more likely.

Debris with few coarse clasts and better-developed bedding occurs in small pockets (Fig 6.3). The lack of current indicators and poor sorting suggests deposition in small ice-marginal ponds. No palaeosols were found in the moraine.

The section indicates that the glacier at this site was depositing supraglacial melt-out till in Tekapo times. Abundant supraglacial debris at the ice margin is not, however, an indicator that the glacier was extensively debris-mantled.

FIG. 6.2 Till section on Pukaki lakeshore road 2 km south of Tekapo B Powerhouse.

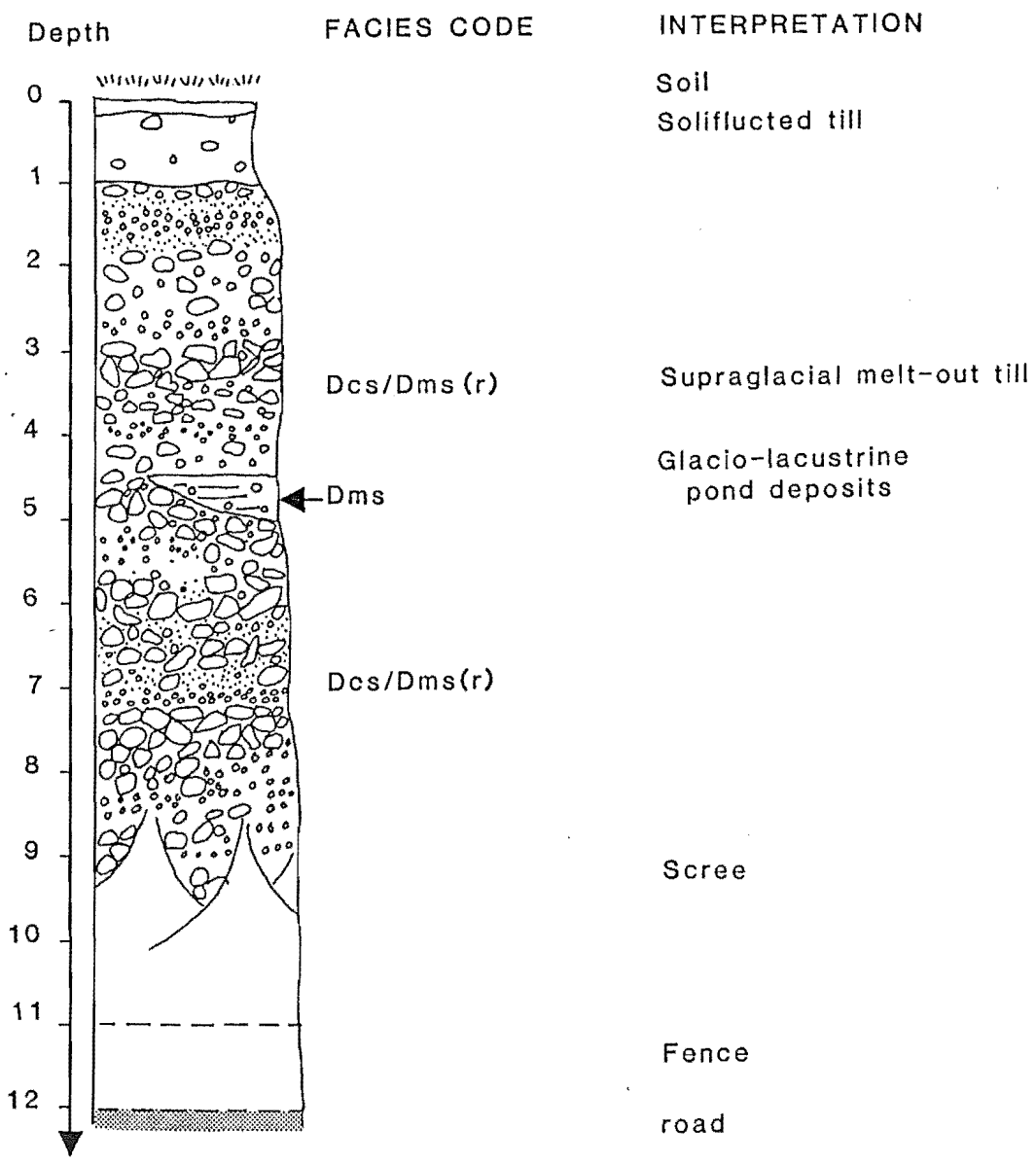

FIG. 6.3 Lithofacies column of the Powerhouse section, Lake Pukaki shore. Facies codes refer to Eyles (1983):

1st letter	2nd letter	3rd letter
D = diamict	m = matrix support	s = stratified
S = sand	c = clast support	m = massive
F = mud	l = laminated	d = deformed
(r) = resedimented		

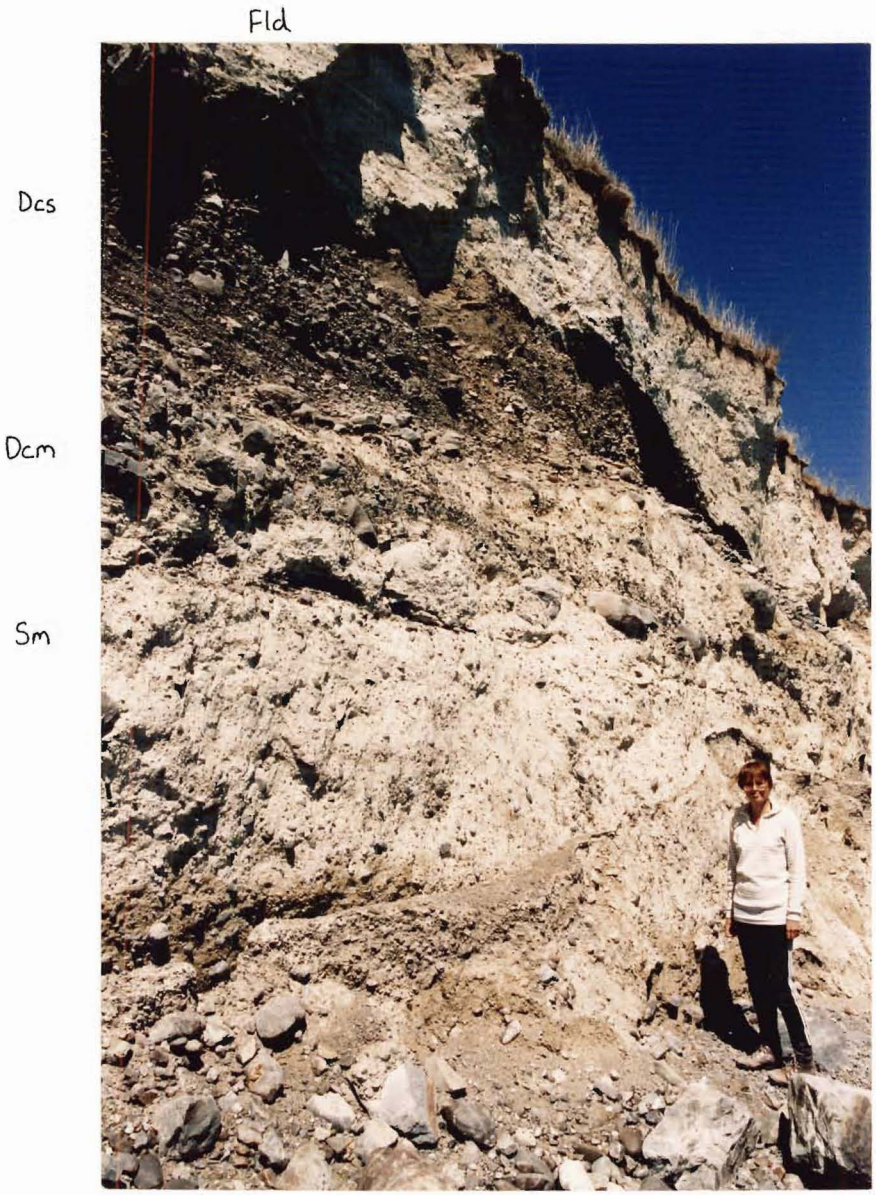

FIG. 6.4 Till section on south shore of Lake Pukaki below Trig UU.

6.1.2 Trig UU section (S100/838 778) (Fig 6.4 and 6.5).

Again cut in the proximal slope of the Tekapo-age moraine, the section comprises three distinct till units and two proglacial units. Fine sandy tills with dispersed rounded and striated clasts form the lower two units. Tills are massive and structureless except for a few faint millimetre-scale silty lenses. Both tills are interpreted as basal (probably lodgement) tills. They are separated by an erosional contact which undulates 2 to 3 m over 12 m distance.

Above the basal tills and in sedimentary contact with them lies up to 1 m of laterally-discontinuous massive clast-supported gravel. Angular clasts predominate. The lateral discontinuity and erosional upper contact suggest that much of this unit may be missing. It is interpreted as supraglacial melt-out till deposited by direct dumping.

Coarse, stratified clast-supported gravels lie above the erosional contact. Decimetre-scale scale cross-bedding within occasional sandy layers give a south-westerly palaeocurrent, approximately paralleling (and presumably ponded by) the former ice-margin. Clasts are sub-angular to sub-rounded and smaller than in the underlying till. The unit was laid down in an ice-marginal melt-water channel flowing across and eroding the till beneath.

Distinct lenses of fine pale sand and silt are interbedded in the upper metre of the glacio-fluvial gravels. A sharp, very irregular contact separates the gravels from overlying laminated silts and fine sands with pebble lenses and occasional coarser clasts. The lamination is wavy, locally contorted and with de-watering structures indicating rapid sedimentation and syn-depositional deformation. The unit appears to have been deposited in a small ice-contact lake. The highly irregular lower contact superficially resembles a loaded contact, but this is unlikely where fine sediment overlies coarse gravel. The irregularities are taken to reflect an undulating eroded top to the lower unit when the lake formed.

The significance of the section is that it shows episodic sedimentation in an environment dominated by flowing water and temporary standing water bodies. In general, there is little evidence of supraglacial dumping. This would not be expected in a terminal ice-contact location in any case. The basal tills exposed at this site are typical of many exposures around the shoreline of Lake Pukaki, and such tills appear to comprise a greater proportion of the deposits around the ice margin

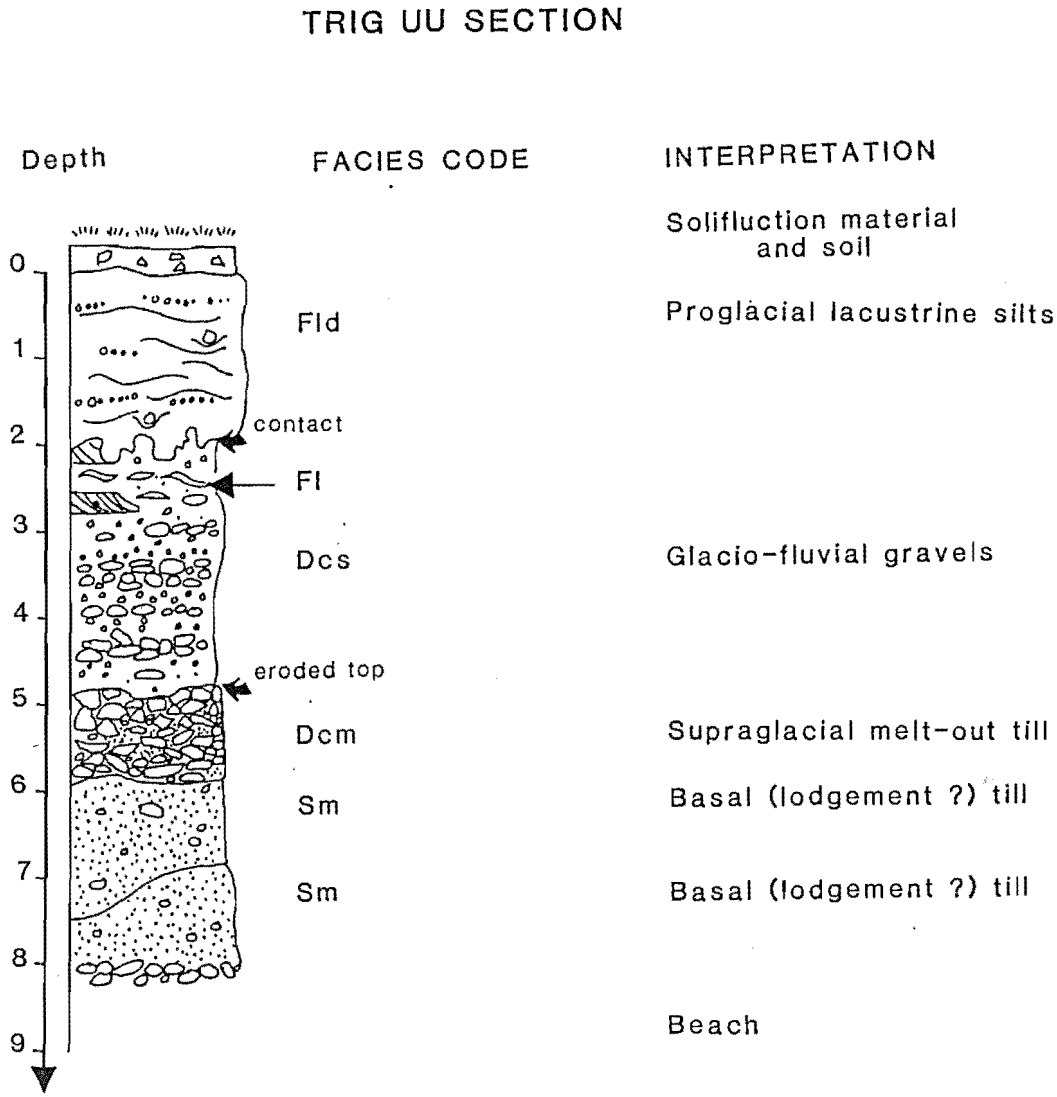

FIG. 6.5 Lithofacies column of the Trig UU section, Lake Pukaki shore. Facies code as for Fig 6.3.

FIG. 6.6 Pukaki Dam section. Pale-yellow lacustrine silts overlie grey outwash gravels. Height of section c. 30 m.

than around the present Tasman Glacier. To what extent this reflects a dominance of exposures at a lower stratigraphic level is debatable; nevertheless, even basal tills in the Murchison embayment (Section 5.3.1.2) appear to be "blockier" than their Pleistocene equivalents. This presumably reflects greater transport distance of debris in the Pleistocene glaciers.

6.1.3 Pukaki Dam section (S100/817 755) (Fig 6.6).

The sedimentology, stratigraphy and geomorphic setting of the exposure is discussed in detail by Speight (1942), whose interpretations are accepted without modification.

The moraine is unusual in having lacustrine silts at high level in a moraine ridge. The lake in which deposition occurred can only have been dammed by ice. The moraine is a relatively thin deposit resting upon outwash gravels exposed at the base of the section. This serves to emphasise that many Pleistocene "terminal moraines", often considered to be dams ponding large ribbon lakes in the South Island (Gage 1975), are really thin water-worked till deposits super-posed on spectacular outwash heads. At this site, the moraine indicates that the glacier terminus advanced after a prolonged stillstand, during which the outwash head was constructed.

6.1.4 General conclusions.

Sedimentological evidence throws little light on mechanisms of glacier retreat. Most preserved deposits and exposed sections are within deposits formed during glacier advance, and give an indication of the type of debris in transport. Although angular, blocky debris characteristic of the high-level transport zones is common, it does not have the overwhelming areal dominance typical of Neoglacial sequences. Pleistocene tills in general appear to have finer textures resulting from longer transport distances and/or a higher proportion of the glacier debris load in the basal traction zone.

6.2 LANDFORM ASSOCIATIONS.

A potentially stronger line of evidence lies in the distribution of landforms which reflect changes in glacier size, geometry and activity. Four associations of landforms are described which are useful in assessing the applicability of the proglacial ponding and debris mantle growth/

downwasting model.

6.2.1 Outwash heads

Superb examples of outwash heads are displayed at Lake Pukaki, Lake Alexandrina (Fig 6.7) and Lake Tekapo (Speight 1942). These ice-contact positions mark prolonged stillstands of an ice margin and aggradation of thick proglacial fan gravels analagous to the Neoglacial proglacial fans. The Pukaki outwash head is 180 m high (Irwin 1970) and was occupied by ice during both Mount John and Tekapo times, a period of at least 2,000 years. Most aggradation appears related to the Mount John terminal moraine, with the smaller Tekapo moraine accreted to the proximal slope. The outwash head obviously presented a formidable barrier to the younger readvance.

The process of ponding of the glacier by proglacial aggradation (Section 5.1) appears to have operated at these ice margins. However outwash heads, while spectacular, are no larger than their Neoglacial equivalents. Given the much longer Pleistocene glaciers, a unit increase in the outwash head elevation would have had proportionately less effect on reducing the gradient of the glacier, as the model describes. Thus the feedback between aggradation, glacier gradient, longitudinal compression and englacial debris emergence would have been less strong in the Pleistocene glacier than in the Neoglacial glacier. This is not to say that the process did not occur: only that a longer timescale would have been needed to acheive the same effect on glacier dynamics. A longer timescale would have allowed other (climatic) processes to have exerted a stronger influence on glacier dynamics than the influence of proglacial aggradation.

6.2.2 Push-moraine associations.

Low, continuous and gently curving ridges which parallel former ice margins are common distal to the outwash heads (Fig 6.8). No similar features have been found around Neoglacial glaciers in the region. Their morphology and geometry accords with Boulton's (1986) descriptions of annual push moraines formed by winter readvances of maritime glaciers during general retreat phases. Several implications may be drawn from these landforms on the basis of Boulton's findings:

1. the glaciers experienced at least one short-term advance which over-topped the outwash head and spread several hundred metres down the outwash surface;

2. the ice margin was responsive to short-term changes in temperature

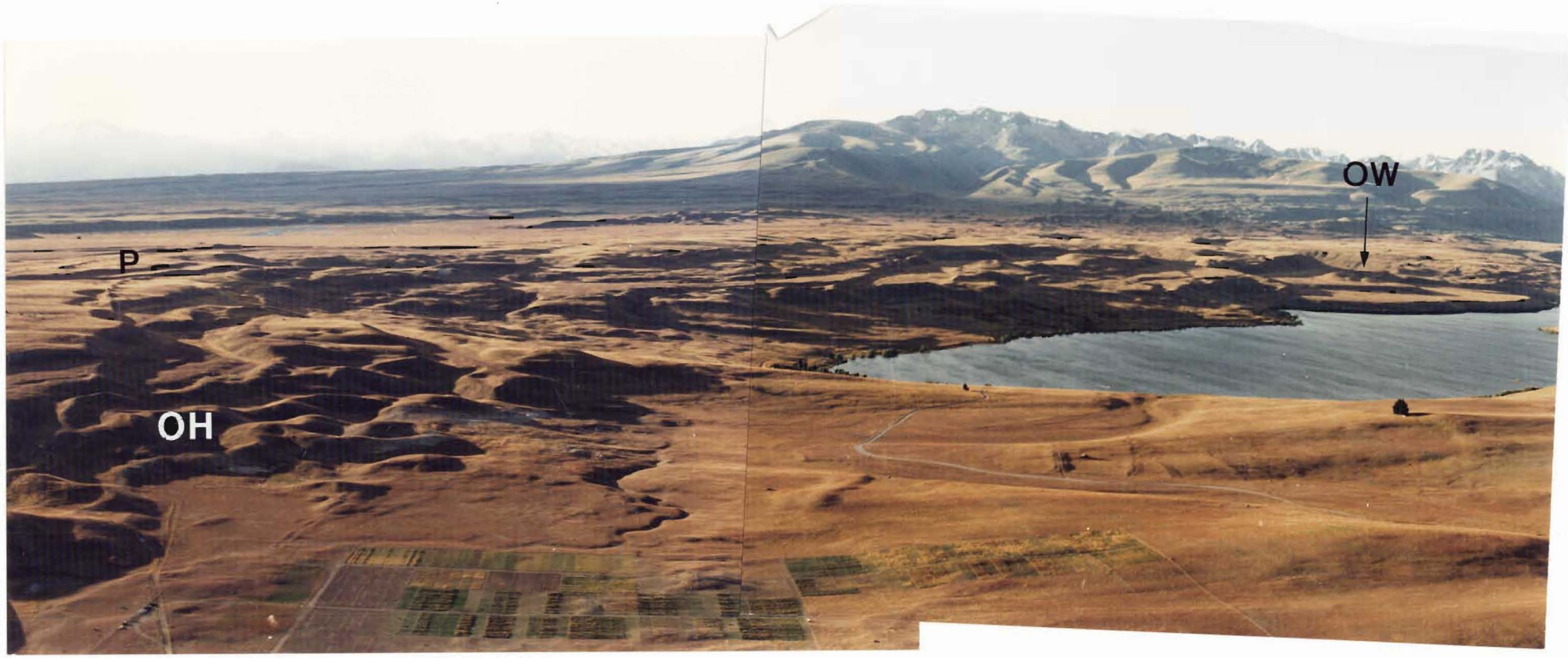

FIG. 6.7 Ice-contact landforms of Tekapo age (c. 12,000 B.P.) at Lake Alexandrina. View south-west from Mount John Observatory. Note small push-moraines (P), outwash head with superimposed ice-disintegration moraines (OH), and ice-marginal outwash channel (OW).

FIG. 6.8 Oblique aerial view of Mt John (MJ) and Tekapo (TK) age terminal moraines at Lake Tekapo. Note small parallel push-moraines (P) superimposed on large Mt John moraine.

and formed a coherent lobate front;

3. the ice was actively moving during retreat and no stagnation occurred. No disintegration topography is associated with the push moraines, but a streamlined substrate occurs between parallel moraines which delineates the direction of ice movement;

4. moraine spacing indicates retreat rates of the order of tens to a hundred metres per year. Together with their generally feeble development, this indicates slow-moving ice and cold winters (Boulton 1986);

5. the outwash and basal till substrate was deformable. This observation has far-reaching implications for reconstructions of the Late Pleistocene glaciers in terms of the appicability of different flow laws and basal shear stress regimes;

At Lake Tekapo (Fig 6.8) the push moraines occur distal to subdued mounds of the Mount John terminal moraine. It appears that here, and possibly in other localities as well, the Tekapo readvance was sufficient to over-ride the Mount John outwash head and moraine barrier but insufficient to obliterate it.

These feeble Pleistocene moraines contrast with the much larger bouldery ridges deposited where modern glaciers have over-ridden outwash heads (eg the Godley and Classen Glaciers and the Tasman Glacier in the Murchison embayment). An implication is that the modern glaciers are not close analogues of the Pleistocene. The Pukaki and Tekapo ice margins seem much closer to maritime lobate ice margins, such as Breidamurkurjokull in Iceland (Price 1969; Boulton 1986).

6.2.3 Lateral moraine and kame terrace associations.

If the glacier had undergone a sequence of slow downwasting followed by rapid terminal retreat, as predicted by the model in Chapter 4.2, evidence of stable ice levels may be expected at elevations below the Tekapo-age maximum lateral-moraine and kame-terrace complex (Mathews 1967; Porter 1975a). Such a trimline would also be expected to depict a lower surface gradient than that existing at the ice maximum (Chapter 4.1). An extensive search along the western side of the Tasman Valley above Lake Pukaki has failed to reveal any convincing evidence supporting a stillstand in ice levels. The tributaries of the Ben Ohau Range contain aggadational fills relating to the Tekapo ice maximum (especially Jacks Stream, see Porter 1975a) and incised fan and cone remnants related to uplift west of the Ostler Fault, which bounds the eastern front of the Ben Ohau Range.

6.3 SUMMARY OF THE LATE PLEISTOCENE LANDFORM EVIDENCE AND CONCLUSIONS CONCERNING GLACIER RETREAT MECHANISMS.

Superbly-preserved ice-marginal landforms and limited till exposures provide little evidence of the mechanism of ice retreat from the Tekapo-age maximum in the Tasman Valley. The landform evidence unfortunately relates to glacier fluctuations close to the maximum positions, and there is little which allows retreat mechanisms to be reconstructed to test the debris-mantle model presented in Chapter 4.2

Therefore it is difficult to invoke the ponding model with any degree of confidence. Similarities between the Neoglacial and Late Pleistocene outwash heads indicate that a prolonged stillstand and proglacial aggradation occurred during Mount John time, but there is no conclusive evidence for or against this stillstand being due to climatic stability or to a ponded glacier of low sensitivity to climatic impulses. Push-moraine evidence points to a terminus responsive to seasonal (or at least short-term) fluctuations when close to its maximum, quite unlike the Neoglacial Tasman Glacier.

The Lake Pukaki basin was deep enough (Irwin 1970) for a calving terminus to develop during retreat and a rapid retreat is to have been expected. Whether or not a period of slow downwasting beneath a debris mantle preceded retreat is uncertain. Reasons why the Late Pleistocene glacier would have been less prone to debris mantle development than the Neoglacial glacier have been presented.

In conclusion, there is no reason to invoke the model of glacier ponding and debris mantle spread to explain any features of Late Pleistocene glacier retreat in the Tasman Valley. This is not to say that such mechanisms did not occur to some extent: but no features exist which cannot be explained by "normal" processes of retreat.

CHAPTER 7: CONCLUSIONS AND OVERVIEW

Individual chapters have concluding sections summarising their findings: these are not repeated here in full. This chapter assesses the extent to which the four broad objectives of the thesis (Chapter 1.1) have been achieved.

The objectives were:

1) to establish a dynamic model explaining the form and observed changes of the Tasman Glacier;

2) to assess the significance of valley glaciers in the region on the sediment transport system;

3) to interpret Neoglacial landform development in the light of current glacier dynamics;

4) to assess the wider spatial and temporal context of the results of this study.

Chapter 7.1 deals with the objectives (1), (2), and (3). Chapter 7.2 is an overview of the whole study and a discussion of the wider implications of this work.

7.1 MODEL OF CURRENT GLACIER BEHAVIOUR.

An empirical model of recent behaviour of the Tasman Glacier has been formulated. The model synthesises piecemeal scientific observations made since 1890 with glaciological monitoring over a two-year period.

Twentieth-Century glaciological changes are explained by a feedback system between debris cover, ablation, glacier long profile, ice flow, and particle trajectories. Modelling of medial moraine dynamics indicates that the system is aided by negative mass balance, but, once initiated, can be largely self-propagating. The insulation of ice provided by an extensive debris mantle is identified as being of prime importance, and feedbacks result in spreading and thickening of the debris mantle further increasing insulation. Debris-mantle dynamics during negative mass balance have led to thinning of the Tasman Glacier with no retreat of the terminus.

Debris-mantle accumulation is a function of deep valley incision and of concave glacier long profile. The first of these observations confirms previous work that extraglacial debris-source area controls supraglacial debris accumulation. The second has not previously been recognised in this context: concave long profiles are associated with strongly-compressive ablation zones and steep upward particle trajectories. Extensive debris

mantles form mostly by coalescence of medial moraines derived from rock outcrops above equilibrium lines, rather than by erosion of recently-exposed moraines bordering the ablation area. As such, debris supply to the high-level transport zone is largely independent of glacier mass balance.

Negative mass balance leads to a two-phase retreat mechanism. The Tasman Glacier initially downwasted slowly under a spreading debris mantle, with no retreat of the terminus. From comparisons with other glaciers in the area, it is postulated that a threshold separates the initial phase from a second phase of rapid retreat by calving into a proglacial lake. The model is of predictive value: a transition to drastic retreat of the Tasman Glacier appears to be imminent.

7.2 GLACIERS IN THE SEDIMENT TRANSPORT SYSTEM.

Estimated denudation of cirques in the Tasman Valley is c.5-6 mma^{-1}. Efficient evacuation of debris from glacier accumulation zones results in a negative sediment budget in source areas. Downglacier, this passes into a strongly-positive budget where debris accumulates in the lower glacier tongue and proglacial outwash system, causing supraglacial debris-mantle spread and proglacial aggradation.

The Tasman Glacier is the dominant transporting agent for debris through the upper Tasman Valley. Debris discharges in the three transport zones of the glacier have been quantified, and found to reduce downglacier and during the Twentieth Century. Towards the terminus, the internal drainage system of the glacier increases its importance as a transporting agent at the expense of "glacial" transport. The glacier assumes a more passive role, slow-moving debris-covered ice forming a reservoir of accumulating debris through which debris is transported and modified by powerful englacial streams.

During glacier decay, the role of the glacier changes (Fig 7.1). As positive balance changes to negative, the transporting efficiency of the glacier reduces and the sediment budget in the lower tongue becomes more positive. With proglacial lake formation, the proglacial zone is starved of coarse debris and erodes, while the lower glacier continues to accumulate sediment. Drastic retreat releases sediment from the glacier, causing a sudden negative change to the glacier sediment budget and lacustrine deposition.

Spatial and temporal changes in sediment budget reflect glacier mass

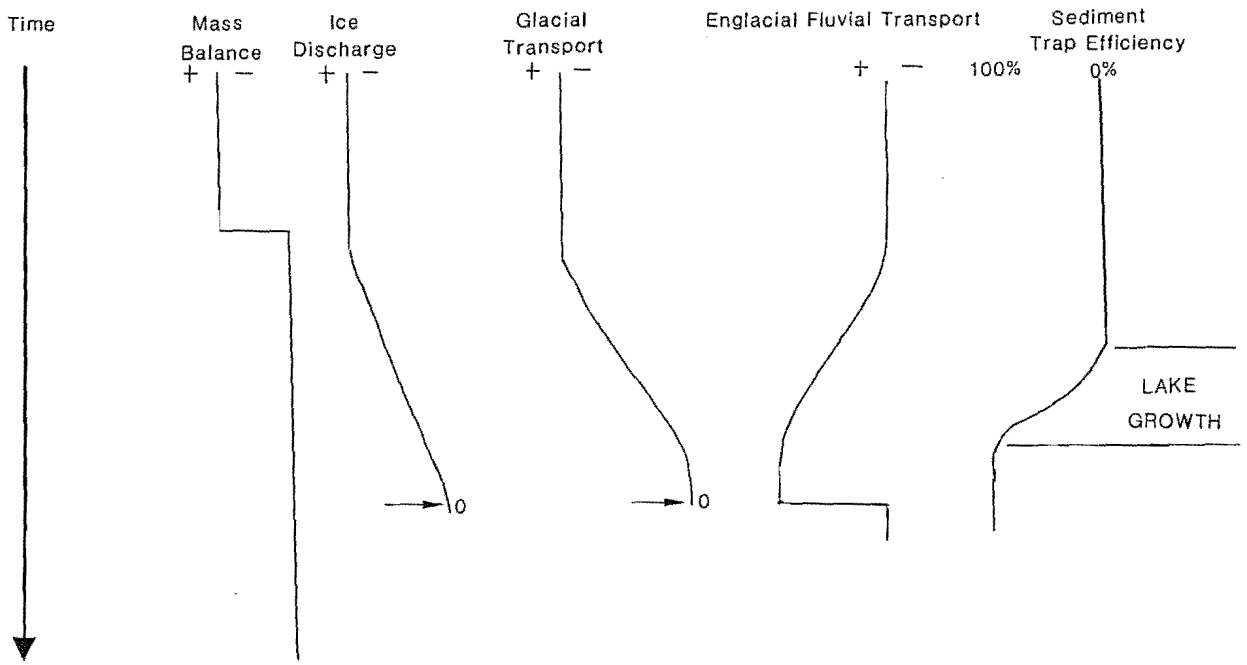

FIG. 7.1 Changing glacial influence on the sediment transport system during glacier decay.

balance. Broadly speaking, sediment budget varies inversely with glacier mass balance, while mechanisms of glacier retreat create localised variations in sediment accumulation and deposition.

7.3 NEOGLACIAL LANDFORM DEVELOPMENT.

The empirical model of Twentieth-Century behaviour of the Tasman Glacier forms the foundation of a reconstruction of Neoglacial behaviour, covering 5,000 years of glacier fluctuations. In the absence of detailed observations of advancing glaciers, deductive reasoning was used to transform the empirical (Twentieth Century) model into an a priori model for behaviour during multiple oscillations. Independent geomorphic and chronological evidence have been used to reconstruct changes in the morphology of the Tasman Glacier since the Hypsithermal interval. The reconstruction was used to test the a priori model. The predicted and inferred behaviour of the Tasman Glacier are found to correspond closely.

An important contrast exists between the Tasman Glacier and unmantled glaciers in the region. Depositional landforms of the Tasman Glacier are consistent with a history of increasing ice levels and glacier length. Unmantled glaciers have responded quite differently to the same climatic impulses, their moraines indicating retreat and thinning from early- and mid-Neoglacial maxima. Although an extreme example, the behaviour of the Tasman Glacier is comparable to that of other debris-mantled glaciers in the region.

The striking difference is attributed to the overwhelming effects of an aggradational depositional system in the ablation zone and proglacial sandur. Persistent insulating debris mantles on the Tasman and similar glaciers, during negative, (to a lesser extent) equilibrium, and perhaps even positive mass balances have been sufficient to delay retreat, or even to cause advance, of glacier termini throughout the Neoglacial. Moraine records of unmantled glaciers indicate an oscillating warming trend of Neoglacial climate. Reduction of ablation by debris mantles is concluded to have been sufficiently great throughout the period to have more than compensated for the effect of climatic amelioration.

The resulting stability of the Tasman Glacier terminus has allowed the glacier to deliver sediment to a narrow proglacial zone over a long period of time. Redistribution by outwash streams has constructed a large outwash head in this zone. Persistent accumulation of sediment in the lower glacier and proglacial zone is manifested in a dominance of depositional

landforms and considerable vertical aggradation of the valley floor.

Current glacier retreats in the region are significant, in that no comparable retreat has occurred in the last 3,700 years at least, and possibly since the earliest Neoglacial advances c.5,000 B.P. By implication, Twentieth Century glacier mass balances are concluded to be more negative than at any time in the Neoglacial period. This conclusion is significant as an interpretation of minimum glacier volumes, unlike most palaeo-environmental interpretations which are based on glacier maxima.

7.4 OVERVIEW.

The Tasman Glacier behaves as a pond of ice, dammed by an outwash head and supplied by steep, fast-flowing tributaries. Mass inputs and outputs and the dynamics of the system are such that an extensive debris mantle is a normal feature of this type of glacier, and this type of glacier is a normal feature of its climatic and tectonic environment, regardless of minor mass-balance fluctuations. The study of the Tasman Glacier has identified the importance of sediment budget as both a cause and effect of glacier behaviour. Sediment budget reflects the combined effects of climatic and tectonic environment, and an attempt to assert the dominance of one over the other would be inappropriate.

I envisage the tectonic environment as a fundamental control, plate convergence providing the relief and setting the stage on which climatically-determined processes may act. The tectonic setting provides the uplift of metasediments whose induration and highly-fractured structure aid the production of coarse debris.

Climate controls processes rather than rates of erosion of the mountains. Denudation appears to be a function of precipitation (Hicks et al, in press) and uplift rate (Adams 1980; Wellman 1979). In the extreme maritime environment of the Southern Alps, superhumid unglacierized ranges may erode as rapidly as the heavily-glacierized Mount Cook area. Climate and relief happen to combine to create glaciers which remove rock debris in some areas; rock fall, slopewash, and rivers perform the same role just as effectively in others.

The interaction of climatic and tectonic effects has implications for the use of glaciers as climatic indicators in the Central Southern Alps. Glaciers without debris mantles, and the associated mass-balance complications that debris mantles introduce, are more faithful indicators

of short-term climatic change. Their lengths fluctuate, in response to mass-balance change, with short relaxation times. These glaciers have become progressively shorter since the mid-Neoglacial period, with the result that dateable buried organic matter is sparse in their moraines. Debris-mantled ice ponds, conversely, respond partly to climatic fluctuations and partly to changes in thickness and extent of their debris covers. The Tasman Glacier has a history of expansion due to conditions which have become increasingly conducive to debris-mantle growth during the Neoglacial period. Buried organic material is abundant because the lower glacier lies in an aggradational system. While providing many radiocarbon dates from lateral moraines, the climatic significance of dates from such a system is difficult to assess.

In the Tasman Valley, a pattern of landform construction around stable glacier termini, punctuated by drastic changes in terminal position, may have been repeated many times throughout the Pleistocene. Each cycle may have involved ice-ponding and debris-mantle insulation, as I have proposed, progressively increasing the stability of glacier termini against climatic perturbations. When a climatic upheaval of sufficient magnitude caused a threshold to be crossed (either ice over-topping the outwash head, or thinning leading to drastic retreat), change would have been rapid and large. When a new stillstand occurred, the ponding process would have recommenced. By this "stick-slip" movement of glacier termini, in response to threshold conditions, the relationship between climatic change and glacier response is complicated. Only the more significant climatic ameliorations and deteriorations will have left their mark in the geomorphic record, and the magnitudes of changes of ponded, mantled glaciers may not correspond to those of unmantled glaciers.

I have shown that such behaviour has characterised the Neoglacial valley glaciers of the Mount Cook area, and possibly glaciers in the latest Pleistocene. I believe that older, larger glaciers which expanded into piedmont lobes may not have involved a dynamic system as conducive to debris mantle accumulation, owing to their less confined nature.

This study has implications for glaciers in other parts of the world. A review of the literature revealed that debris mantles are found in most alpine regions, and the system of debris mantle dynamics operating on the Tasman Glacier and its related problems of interpretation of glacier chronology may be generally applicable. The global trend of Twentieth-Century glacier wasting appears to have introduced a bias in the literature towards an association of supraglacial debris accumulation and

negative mass balance. I have suggested that extensive supraglacial debris accumulations may be a normal product of the sediment budget of many valley glaciers, not just a result of negative balance.

7.5 DIRECTIONS FOR FUTURE RESEARCH.

Long-term study of glaciological change in New Zealand suffers from the piecemeal nature of the data base. There is a need for a long-term monitoring of glacier mass balance to serve as a reference study and to provide a context for the short-term studies which continue to be carried out.

This study has identified specific topics which remain poorly understood, but which have potential for fruitful reserch in the future.

1) Thermal properties of supraglacial debris need to be quantified more precisely, especially thick debris covers. Technological advances in remote data collection now make it possible to monitor debris-mantle temperature profiles and moisture movements, and ablation rates beneath debris covers. Much more data is needed to develop a fuller understanding of debris mantle insulation and its glaciological effects.

2) Sub-glacial and englacial processes remain poorly understood. Two areas where advances are needed are (a) in the area of englacial sediment transport by streams, which is probably very important in many glaciers in humid environments, and (b) the effects of substrate conditions on glacier flow, particularly substrate deformation and its effect on glacier profiles in the Pleistocene in New Zealand.

3) Seismic effects on glacier debris transport have not been investigated. The frequency of major earthquakes in the area is longer than the time taken for mass exchange to completely replace the ice of the Mount Cook glaciers. Sufficient time has elapsed since the last major earthquake on the Alpine Fault that none of the present glaciers have extensive supraglacial rock avalanche deposits triggered by large earthquakes. Such events very probably happened in the past, but their effects on glacier ablation and fluctuations remain unknown.

REFERENCES.

ACKERT, R.P. 1984: Ice-cored lateral moraines in Tarfala Valley, Swedish Lappland. Geografiska Annaler 66A 79-88.

ADAMS, J. 1979: Age and origin of the Southern Alps, in Walcott, R.I. & Cresswell, M.M. (eds) The Origin of the Southern Alps Royal Society of New Zealand Bulletin 18, 73-78.

ADAMS, J. 1980: Contemporary uplift and erosion of the Southern Alps, New Zealand: summary. Bulletin of the Geological Society of America 91 2-4.

ADDISON, K. 1981: The contribution of discontinuous rock mass failure to glacial erosion. Annals of Glaciology 2 3-10.

AGASSIZ, L. 1840: Etudes sur les Glaciers. (Studies on Glaciers), translated and edited by A.V. Carozzi, 1967. Hefner Publishing Company, 213pp.

AHLMANN, H.W. 1948: Glaciological research on the North Atlantic coasts. Royal Geographical Society Research Series 1 83pp.

ALEAN, J. 1985: Ice avalanche activity and mass balance of a high-altitude hanging glacier in the Swiss Alps. Annals of Glaciology 6 248-249.

ALLIS, R.G. 1981: Continental underthrusting beneath the Southern Alps of New Zealand. Geology 9 303-307.

ÅMARK, M. 1980: Glacial flutes at Isfallsglaciaren, Tarfala, Swedish Lappland. Geologisk Foren, Stockholm Forrhandl 102 251-259.

ANDERSON, J.B. 1983: Ancient glacial marine deposits: their spatial and temporal distribution, in Molnia, B.F. (ed.) Glacial Marine Sedimentation. Plenum, New York 3-92.

ANDERTON, P.W. 1970: Deformation of surface ice at a glacier confluence, Kaskawulsh Glacier, in Bushnell, V.C. & Ragle, R.H. (eds.) Icefield Ranges Research Project. Scientific Results Vol.2 American Geographical Society/ Arctic Institute of North America, 59-76.

ANDERTON, P.W. 1975: The Tasman Glacier, 1971-73. Hydrological Research: Annual Report No.33 Ministry of Works and Development, National Water and Soil Conservation Organisation, 28pp.

ANDERTON, P.W. & CHINN, T.J. 1978: The Ivory Glacier, New Zealand: an I.H.D. representative basin study. Journal of Glaciology 20 67-84.

ANDREWS, E.D. 1986: Downstream effects of Flaming Gorge reservoir on the Green river, Colorado and Utah. Geological Society of America Bulletin 97 1012-1023.

ANDREWS, J.T. 1972: Glacier power, mass balance, velocities and erosion potential. Zeitschrift für Geomorphologie Supplementband 13 1-17.

ANDREWS, J.T. 1975: Glacial Systems: An Approach to Glaciers and their Environments. Duxbury Press, Massachusetts, 191pp.

ANIYA, M. 1988: Glacier inventory for the northern Patagonia Icefield, Chile, and variations 1944/45 to 1985/86. Arctic and Alpine Research 20 179-187.

ANIYA, M.; CASASSA, G,; & NARUSE, R. 1988: Morphology, surface characteristics, and flow velocity of Soler Glacier, Patagonia. Arctic and Alpine Research 20 414-421.

ANONYMOUS, 1969: Mass balance terms. Journal of Glaciology 8 3-7.

ASCHENBRENNER, B.C. 1956: A new method of expressing particle sphericity. Journal of Sedimentary Petrology 26 15-31.

BALLANTYNE, C.K. 1978: Variations in the size of coarse clastic particles over the surface of a small sandur, Ellesmere Island, N.W.T., Canada. Sedimentology 25 141-147.

BALLANTYNE, C.K. 1979: Patterned ground on an active medial moraine, Jotunheimen, Norway. Journal of Glaciology 22 396-401.

BALLANTYNE, C.K. 1982: Aggregate clast form characteristics of deposits near the margins of four glaciers in the Jotunheimen Massif, Norway. Norsk Geografisk Tidsskrift 36 103-113.

BALLANTYNE, C.K. 1984: The Late Devensian periglaciation of upland Scotland. Quaternary Science Reviews 3 311-343.

BALLANTYNE, C.K. & KIRKBRIDE, M.P. 1986: Characteristics and significance of some Lateglacial protalus ramparts in Upland Britain. Earth Surface Processes and Landforms 11 359-371.

BALLANTYNE, C.K. & KIRKBRIDE, M.P. 1987: Rockfall activity in upland Britain during the Loch Lomond Stadial. Geographical Journal 153 86-92.

BANERJEE, I. & MCDONALD, B.C. 1975: Nature of esker sedimentation, in Jopling, A.V. & McDonald, B.C. (eds.) Glaciofluvial and Glaciolacustrine Sedimentation. SEPM Special Publication 23 123-154.

BARNES, P.; TABOR, D. & WALKER, J.C.F. 1971: The friction and creep of polycrystalline ice. Proceedings of the Royal Society of London, Series A 324 127-155.

BARRETT, P.J. 1980: The shape of rock particles, a critical review. Sedimentology 27 291-303.

BEGIN, Z.B. & SCHUMM, S.A. 1984: Gradational thresholds and landform singularity: significance for Quaternary studies. Quaternary Research 21 267-274.

BELL, J.M. 1910: A geographical report on the Franz Josef Glacier. New Zealand Geological Survey, Wellington 1910, 14pp.

BIRKELAND, P.W. 1973: Use of relative dating methods in a stratigraphic study of rock glacier deposits, Mount Sopris, Colorado. Arctic and Alpine Research 5 401-416.

BIRKELAND, P.W. 1981: Soil data and the shape of the lichen growth-rate curve for the Mount Cook area (Note). New Zealand Journal of Geology and Geophysics 24 443-445.

BIRKELAND, P.W. 1982: Subdivision of Holocene glacial deposits, Ben Ohau Range, New Zealand, using relative dating methods. Geological Society of America Bulletin 93 433-449.

BIRNIE, R.V. 1978: Rock debris transport and deposition by valley glaciers in South Georgia. Unpublished PhD thesis, University of Aberdeen, 421pp.

BISHOP, B.C. 1957: Shear moraines in the Thule area, northwest Greenland. Snow, Ice, and Permafrost Research Establishment. Research Report 17.

BISHOP, D.G. 1979: Alpine huts: havens or headaches? New Zealand Alpine Journal 32 76-78.

BISHOP, D.G. & FORSYTH, P.J. 1988: Vanishing Ice: a study of the Dart Glacier. John McIndoe & Sons and New Zealand Geological Survey 56pp.

BLAIR, R.W. Jnr. 1984: Geological survey of alpine hut sites. Unpublished report to Mount Cook National Park, 30pp.

BLUCK, B.J. 1964: Sedimentation of an alluvial fan in Southern Nevada. Journal of Sedimantary Petrology 34 395-400.

BOOTH, D.B. 1986: Mass balance and sliding velocity of the Puget Lobe of the Cordilleran Ice Sheet during the last glaciation. Quaternary Research 25 269-280.

BOOTHROYD, J.C. & NUMMEDAL, D. 1978: Proglacial braided outwash: a model for humid alluvial fan deposits, in Miall, A.D. (ed.) Fluvial Sedimentology Canadian Society of Petroleum Geologists Memoir 5 641-668.

BOULTON, G.S. 1967: The development of a complex supraglacial moraine at the margin of Sørbreen, Ny Friesland, Vestspitsbergen. Journal of Glaciology 6 717-735.

BOULTON, G.S. 1968: Flow tills and related deposits on some Vestspitsbergen glaciers. Journal of Glaciology 7 391-412.

BOULTON, G.S. 1970: On the origin and transport of englacial debris in Svalbard glaciers. Journal of Glaciology 9 213-229.

BOULTON, G.S. 1974: Processes and patterns of glacial erosion, in Coates, D.R. (ed.) Glacial Geomorphology State University, New York, 41-87.

BOULTON, G.S. 1976: The origin of glacially-fluted surfaces-observations and theory. Journal of Glaciology 17 287-309.

BOULTON, G.S. 1978: Boulder shapes and grain-size distributions as indicators of transport paths through a glacier and till genesis. Sedimentology 25 773-799.

BOULTON, G.S. 1979: Processes of glacial erosion on different substrata. Journal of Glaciology 23 15-37.

BOULTON, G.S. 1986: Push-moraines and glacier-contact fans in marine and terrestrial environments. Sedimentology 33 677-698.

BOULTON, G.S. & EYLES, N. 1979: Sedimentation by valley glaciers; a model and genetic classification, in Schlüchter, Ch. (ed.) Moraines and Varves A.A. Balkema, Rotterdam 11-23.

BOULTON, G.S. & HINDMARSH, R.C.A. 1987: Sediment deformation beneath glaciers: rheology and geological consequences. Journal of Geophysical Research 92 B9 9059-9082.

BOULTON, G.S. & JONES, A.S. 1979: Stability of temperate ice caps resting on beds of deformable sediment. Journal of Glaciology 24 29-43.

BOULTON, G.S. & VIVIAN, R. 1973: Underneath the glaciers. Geographical Magazine 45 311-316.

BOWLER, J.M.; HOPE, G.S.; JENNINGS, J.B. & WALKER, D. 1976: Late Quaternary climates of Australia and New Guinea. Quaternary Research 6 359-394.

BOZHINSKIIY, A.N.; KRASS, M.S. & POPOVNIN, V.V. 1986: Role of debris cover in the thermal physics of glaciers. Journal of Glaciology 32 255-266.

BRADLEY, W.C., FAHNESTOCK, R.K. & ROWEKAMP, G.T. 1972: Coarse sediment transport by flood flows on Knik River, Alaska. Geological Society of America Bulletin 83 1261-1284.

BROADBENT, M. 1973: A preliminary report on seismic and gravity surveys on the Tasman Glacier 1971-2. Geophysics Division, Department of Scientific and Industrial Research, Wellington, K/6/2/1.

BRODRICK, T.N. 1891: Report on the Tasman Glacier. Journal of the House of Representatives of New Zealand Session 2 Volume 1 C1-A Appendix 4 39-43.

BRODRICK, T.N. 1894: Ice motion of the Canterbury glaciers. New Zealand Alpine Journal 1 307-316.

BRODRICK, T.N. 1906: Glacier Movements. Journal of the House of Representatives of New Zealand Session 2 Volume 1 C1-A Appendix 2 16-17.

BRUNSDEN, D. & THORNES, J.B. 1979: Landscape sensitivity and change. Transactions, Institute of British Geographers, New Series 4 463-484.

BUDD, W.F.; KEAGE, P.L. & BLUNDY, N.A. 1979: Empirical studies of ice sliding. Journal of Glaciology 23 157-169.

BURROWS, C.J. 1973: Studies of some glacial moraines in New Zealand- 2. Ages of moraines of the Mueller, Hooker and Tasman Glaciers. New Zealand Journal of Geology and Geophysics 16 831-855.

BURROWS, C.J. 1975: Late Pleistocene and Holocene moraines of the Cameron Valley, Arrowsmith Range, Canterbury, New Zealand. Arctic and Alpine Research 7 125-140.

BURROWS, C.J. 1979: A chronology for cool climate episodes in the Southern Hemisphere 12,000 - 1,000 B.P. Palaeogeography, Palaeoclimatology, Palaeoecology 27 287-347.

BURROWS, C.J. 1980: Radiocarbon dates for post-Otiran glacial activity in the Mount Cook region, New Zealand. New Zealand Journal of Geology and Geophysics 23 239-248.

BURROWS, C.J. 1989: Aranuian radiocarbon dates from moraines in the Mount Cook region, New Zealand. New Zealand Journal of Geology and Geophysics 32 205-216.

BURROWS, C.J. & GELLATLY, A.F. 1982: Holocene glaciers in New Zealand, in Karlén, E. (ed.) Holocene Glaciers. Striae 18 41-47.

BURROWS, C.J. & RUSSELL, J.B. 1975: Moraines of the upper Rakaia Valley. Journal of the Royal Society of New Zealand 5 463-477.

BURROWS, C.J.; CHINN, T.J. & KELLY, M. 1976: Glacial activity in New Zealand near the Pleistocene-Holocene boundary in the light of new radiocarbon dates. Boreas 5 463-477.

BURROWS, C.J. & HEINE, M. 1979: The older moraines of the Stocking Glacier, Mount Cook region. Journal of the Royal Society of New Zealand 9 5-12.

CARRARA, P.E. 1975: The ice-cored moraines of Akudnirmuit Glacier, Cumberland Peninsula, Baffin Island, N.W.T., Canada. Arctic and Alpine Research 7 61-67.

CHERNOVA, L.P. 1981: Influence of mass balance and run-off on the relief-forming activity of mountain glaciers. Annals of Glaciology 2 69-71.

CHINN, T.J. 1975: Late Quaternary snowlines and cirque moraines within the Waimakariri watershed. Unpublished MSc thesis, University of Canterbury, 213pp.

CHINN, T.J. 1981: Use of rock-weathering rind thickness for Holocene absolute age dating in New Zealand. Arctic and Alpine Research 13 33-45.

CHINN, T.J. & DILLON, A. 1987: Observations on a debris-covered polar glacier "Whisky Glacier", James Ross Island, Antarctic Peninsula, Antarctica. Journal of Glaciology 33 1-11.

CHORLEY, R.J. & KENNEDY, B.A. 1971: Physical Geography: a Systems Approach. Prentice-Hall 370 pp.

CLAPPERTON, C.M. 1972: The Pleistocene moraine stages of west central Peru. Journal of Glaciology 11 255-263.

CLAPPERTON, C.M. 1975: The debris content of surging glaciers in Svalbard and Iceland. Journal of Glaciology 14 395-406.

CLAPPERTON, C.M. & SUGDEN, D.E. 1988: Holocene glacier fluctuations in South America and Antarctica. Quaternary Science Reviews 7 185-198.

CLAPP, F.G. 1904: Relations of gravel deposits in the northern part of glacial lake Charles, Massachusetts. Journal of Geology 12 198-214.

CLARIDGE, D. 1983: A geophysical study of the termini of the Mount Cook National Park glaciers. Unpublished MSc thesis, University of Auckland.

CLARK, S.P.1966: Thermal Conductivity: Section 21, in Handbook of Physical Constants; Revised Edition. Geological Society of America Memoir 97 459-482.

CLAYTON, L. 1964: Karst topography on stagnant glaciers. Journal of Glaciology 5 107-112.

CLAYTON, L. 1967: Stagnant glacier features of the Missouri Coteau in North Dakota, in Clayton, L. & Freers, T.F. (eds.) Glacial geology of the Missouri Coteau and adjacent areas North Dakota Geological Survey Miscellaneous Series 30 25-52.

COOK, J.H. 1924: The disappearance of the last Glacial Ice Sheet from eastern New York. New York State Museum Bulletin 251 158-176.

COOK, J.H. 1946a: Ice contacts and the melting of ice below a water level. American Journal of Science 244 502-512.

COOK, J.H. 1946b: Kame complexes and perforation deposits. American Journal of Science 244 573-583.

CORTE, A.E. 1976: Rock glaciers. Biuletyn Peryglacjalny 26 175-197.

CORTE, A.E. 1978: Guide for compilation and assemblage of data for a world glacier inventroy. Debris covered glaciers, rock glaciers and ice cored moraines. Based on the inventory of the dry central Andes at 31°-32° SL. Mendoza, Argentina.

DALE, M.L. & BALLANTYNE, C.K. 1980: Two statistics for the analysis of orientation data in geography. Professional Geographer 32 184-191.

DANSGAARD, W.; CLAUSEN, H.B.; GUNDESTRUP,N.; HAMMER, C.U.; JOHNSEN, S.F.; KRISTINDOTTER, P.M. & REED, N. 1982: A new Greenland deep ice core. Science 218 1273-1277.

DAVIS, P.T. & OSBORN, G. (eds.) 1988: Holocene Glacier Fluctuations. Quaternary Science Reviews 7.

DOMACK, E.W.; ANDERSON, J.B.& KURTZ, D. 1980: Clast shape as an indicator of transport and depositional mechanisms in glacial marine sediments: George V continental shelf, Antarctica. Journal of Sedimentary Petrology 50 813-820.

DOWDESWELL, J.A. 1982: Relative dating of Late Quaternary glacial deposits using cluster and discriminant analysis, Audobon Cirque, Mt. Audobon, Colorado Front Range. Boreas 11 151-161.

DOWDESWELL, J.A. 1986: The distribution and character of sediments in a tidewater glacier, Southern Baffin Island, North West Territories, Canada. Arctic and Alpine Research 18 45-56.

DOWDESWELL, J.A.; HAMBREY, M.J. & WU, R. 1985: A comparison of clast fabric and shape in Late Precambrian and modern glacigenic sediments. Journal of Sedimentary Petrology 55 691-704.

DRAKE, L.D. 1970: Rock texture: an important factor for clast shape studies. Journal of Sedimentary Petrology 40 1356-1361.

DRAKE, L.D. 1972: Mechanisms of clast attrition in basal till. Geological Society of America Bulletin 83 2159-2166.

DREIMANIS, A. 1976: Tills: their origins and properties, in Leggett, R.F. (ed.) Glacial Till. Royal Society of Canada Special Publication 12 11-49.

DREIMANIS, A. 1989: Tills: their genetic terminology and classification, in Goldthwait, R.P. & Matsch, C.L. (eds.) Genetic Classification of Glacigenic Deposits. A.A. Balkema, 17-84.

DREWRY, D.J. 1972: A quantitative assessment of dirt cone dynamics. Journal of Glaciology 11 431-446.

DREWRY, D.J. 1986: Glacial Geologic Processes. Edward Arnold, 276 pp.

DRISCOLL, F.G. 1980a: Formation of the Neoglacial surge moraines of the Klutlan Glacier, Yukon Territory, Canada. Quaternary Research 14 19-30.

DRISCOLL, F.G. 1980b: Wastage of Klutlan ice-cored moraines, Yukon Territory, Canada. Quaternary Research 14 31-49.

DROZDOWSKI, E. 1977: Ablation till and related indicatory forms at the margins of Vestspitsbergen glaciers. Boreas 6 107-114.

ELLIS, J.M. & CALKIN, P.E. 1983: Environments and soils of Holocene moraines and rock glaciers, central Brooks Range, Alaska, in Evenson, E.B.: Rabassa, J. & Schlüchter, Ch. (eds) Tills and Related Deposits. A.A. Balkema (publ) 315-328.

DU FAUR, F. 1915: The Conquest of Mt Cook. Allen and Unwin , London 250pp

ENGELHARDT, H.F.; HARRISON, W.D. & KAMB, W.B. 1978: Basal sliding and conditions at the glacier bed as revealed by bore-hole photography. Journal of Glaciology 20 469-508.

ESPIZÙA, L.E. 1983: Glacier and moraine inventory on the eastern slope of Cordon del Plata and Cordon del Portillo, central Andes, Argentina, in Evenson, E.B., Rabassa, J. & Schlüchter, Ch. (eds.) Tills and Related Deposits. Balkema, 381-395.

EVENSON, E.B. & CLINCH, J.M. 1987: Debris transport mechanisms at active alpine glacier margins: Alaskan case studies, in Kujansuu, R. & Saarnisto, M. (eds.) INQUA Till Symposium. Geological Survey of Finland Special Paper 3 111-136.

EVENSON, E.B.; SCHLÜCHTER, Ch. & RABASSA, J. (Eds.) 1983: Tills and Related Deposits. Proceedings of INQUA Symposium on the Genesis and Lithology of Quaternary Deposits, USA 1981/ Argentina 1982. A.A. Balkema, 454pp.

EYLES, N. 1976a: Morphology and development of medial moraines: comments on the paper by R.J. Small and M.J. Clark. Journal of Glaciology 17 161-162.

EYLES, N. 1976b: Morphology and development of medial moraines: further comments on the paper by R.J. Small and M.J. Clark. Journal of Glaciology 17 164-165.

EYLES, N. 1979: Facies of supraglacial sedimentation on Icelandic and alpine temperate glaciers. Canadian Journal of Earth Sciences 16 1341-1361.

EYLES, N. (ed.) 1983: Glacial Geology: An Introduction for Engineers and Earth Scientists Pergamon Press, 409pp.

EYLES, N. & ROGERSON, R.J. 1977: Glacier movement, ice structures, and medial moraine form at a glacier confluence, Berendon Glacier, British Columbia, Canada. Canadian Journal of Earth Sciences 14 2807-2816.

EYLES, N. & ROGERSON, R.J. 1978a: A framework for the investigation of medial moraine formation: Austerdalsbreen, Norway, and Berendon Glacier, Canada. Journal of Glaciology 20 99-113.

EYLES, N. & ROGERSON, R.J. 1978b: Sedimentology of medial moraines on Berendon Glacier, British Columbia, Canada; implications for debris transport in a glacierized basin. Geological Society of America Bulletin 89 1688-1693

FAHNESTOCK, R.K. 1963: Morphology and hydrology of a glacial stream- White River, Mount Rainier, Washington. United States Geological Survey Professional Paper 422A 70pp.

FIELD, B.D. 1976: Geology of the central Liebig Range, Mount Cook. Unpublished MSc thesis, University of Auckland, 118 pp.

FINDLAY, R.H. & SPÖRLI, K.B. 1984: Structural geology of the Mount Cook Range and Main Divide, Hooker Valley region, New Zealand. New Zealand Journal of Geology and Geophysics 27 257-276.

FLEISHER, P.J. 1986: Dead ice sinks and moats: environments of stagnant ice deposition. Geology 14 39-42.

FLINT, R.F. 1929: The stagnation and dissipation of the last ice sheet. Geographical Review 19 256-289

FLINT, R.F. 1942: Glacier thinning during deglaciation: Part 2: glacier thinning inferred from geologic data. American Journal of Science 240 113-136.

FLINT, R.F. 1971: Glacial and Quaternary Geology John Wiley & Sons, 2nd Ed. 892pp.

FLINT, R.F. & DEMOREST, M. 1942: Glacier thinning during glaciation: Part 1. American Journal of Science 240 29-66.

FOOKES, P.G.; DEARMAN, W.R. & FRANKLIN, J.A. 1971: Some engineering aspects of rock weathering with field examples from Dartmoor and elsewhere. Quarterly Journal of Engineering Geology 4 139-185.

FRASER, H.J. 1935: Experimental study of the porosity and permeability of clastic sediments. Journal of Geology 43 910-1010.

GAGE, M. 1951: The dwindling glaciers of the upper Rakaia Valley, Canterbury, New Zealand. Journal of Glaciology 1 504-507.

GAGE, M. 1958: Late Pleistocene galciations of the Waimakariri Valley, Canterbury, New Zealand. New Zealand Journal of Geology and Geophysics 1 123-155.

GAGE, M. 1966: The climate of New Zealand during cool phases of the Pleistocene, in Pleistocene and Post-Pleistocene Climatic Variations in the Pacific Area. Tenth Pacific Science Congress of the Pacific Science Association, University of Hawaii, 83-94.

GAGE, M. 1975: Glacial Lakes, Chapter 2 in Jolly, V.H. & Brown, J.M.A. (eds.) New Zealand Lakes Auckland University Press/ Oxford University Press, 57-69.

GAIR, H.S. 1967: Sheet 20 Mount Cook (1st Edition). Geological Map of New Zealand 1:250,000 Department of Scientific and Industrial Research, Wellington.

GELLATLY, A.F. 1982: The use of lichenometry as a relative-age dating method with specific reference to Mount Cook National Park, New Zealand. New Zealand Journal of Botany 20 343-353.

GELLATLY, A.F. 1984: The use of rock weathering-rind thickness to re-date moraines in the Mount Cook National Park, New Zealand. Arctic and Alpine Research 16 225-232.

GELLATLY, A.F. 1985a: Glacier fluctuations in the central Southern Alps, New Zealand: documentation and implications for environmental change during the last 1,000 years. Zeitschrift für Gletscherkunde und Glazialgeologie Band 21 S 259-264.

GELLATLY, A.F. 1985b: Phosphate retention: relative dating of Holocene soil development. Catena 12 227-240.

GELLATLY, A.F. 1985c: Historical records of glacier fluctuations in Mount Cook National Park. Geographical Journal 151 86-99.

GELLATLY, A.F. & NORTON, D.A. 1984: Possible warming and glacier recession in the South Island. New Zealand Journal of Science 27 381-388.

GELLATLY, A.F.; RÖTHLISBERGER, F. & GEYH, M.A. 1985: Holocene glacier variations in New Zealand (South Island). Zeitschrift für Gletscherkunde und Glazialgeologie, Band 21 S 265-273.

GELLATLY, A.F.; CHINN,T.J.H. & ROTHLISBERGER, F. 1988: Holocene glacier variations in New Zealand: a review. Quaternary Science Reviews 7 227-242.

GIARDINO, J.R. & VITEK, J.D. 1988: The significance of rock glaciers in the glacial-periglacial landscape continuum. Journal of Quaternary Science 3 97-103.

GIBBONS, A.B.; MEGEATH, J.D. & PEARCE, K.L. 1984: Probability of moraine survival in a succession of glacial advances. Geology 12 327-330.

GLAZYRIN, G.E. 1975: The formation of ablation moraines as a function of the climatological environment. Proceedings of the Moscow Symposium, August 1971: IAHS-AISH Publication 104 106-110.

GLEN, J.W. 1952: Experiments on the deformation of ice. Journal of Glaciology 2

GLEN, J.W. 1954: The stability of ice-dammed lakes and other water-filled holes in glaciers. Journal of Glaciology 2 316-318.

GLEN. J.W. 1958: The flow law of ice. A discussion of the assumptions made in glacier theory, their experimental foundations and consequences. International Association of Scientific Hydrology Publ. 47 171-183.

GOLDTHWAIT, R.P. 1951: Development of end moraines in east-central Baffin Island. Journal of Geology 59 567-577.

GOLDTHWAIT, R.P. 1960: Study of an ice cliff in Nunartarssuaq, Greenland. U.S. Army Cold Regions Research and Engineering Laboratory. Technical Report 39.

GOLDTHWAIT, R.P. (ed.) 1975: Glacial Deposits. Benchmark-Halstead Press, 464pp.

GOLDTHWAIT, R.P. & MCKELLAR, I.C. 1962: New Zealand Glaciology, in Antarctic Research Geophysical Monograph 7 American Geophysical Union, 209-216.

GOLDTHWAIT, R.P. & MATSCH, C.L. (eds.) 1988: Genetic Classification of Glacigenic Deposits. A.A. Balkema, 294pp.

GOLUBEV, G.N. & KOTLYAKOV, V.M. 1978: Glacial landscapes and their spatial variability in the temperate and sub-polar latitudes. Arctic and Alpine Research 10 277-282.

GOMEZ, B. & SMALL, R.J. 1985: Medial moraines of the Haut Glacier d'Arolla, Valais, Switzerland: debris supply and implication for moraine formation. Journal of Glaciology 31 303-307.

GORDON, J.E. & BIRNIE, R.V. 1986: Production and transfer of subaerially generated rock debris and resulting landforms on South Georgia: an introductory perspective. British Antarctic Survey Bulletin 72 25-46.

GRAVENOR, C.P. & KUPSCH, W.O. 1959: Ice disintegration features in western Canada. Journal of Geology 67 48-64.

GRAVENOR, C.P.; VON BRUNN, V. & DREIMANIS, A. 1984: Nature and classification of waterlain glacigenic sediments, exemplified by Pleistocene, Late Palaeozoic, and Late Precambrian deposits. Earth Science Reviews 20 105-166.

GRIFFEY, N.J. & WHALLEY, W.B. 1979: A rock glacier and moraine-ridge complex, Lyngen Peninsula, north Norway. Norsk Geografisk Tidsskrift 33 117-124.

GRIFFITHS, G.A. 1981: Some suspended sediment yields from some South Island catchments, New Zealand. Water Resources Bulletin 17 662-671.

GRIFFITHS, G.A. & MCSAVENEY, M.J. 1983: Distribution of mean annual precipitation across some steepland regions of New Zealand. New Zealand Journal of Science 26 197-209.

GRINDLEY, G.W. 1963: Structure of the Alpine Schists of South Westland, New Zealand. New Zealand Journal of Geology and Geophysics 6 872-930.

GROVE, J.M. 1972: The incidence of landslides, avalanches, and floods in western Norway during the Little Ice Age. Arctic and Alpine Research 4 131-138.

GROVE, J.M. 1988: The Little Ice Age. Methuen, 498pp.

GUNN, B.M. 1965: Flow rates and secondary structures of Fox and Franz Josef Glaciers, New Zealand. Journal of Glaciology 5 173-190.

GUSTAVSON, T.C. 1974: Sedimentation on gravel outwash fans, Malaspina Glacier foreland, Alaska. Journal of Sedimentary Petrology 44 374-389.

HAEBERLI, W. 1985: Creep of mountain permafrost: internal structure and flow of alpine rock glaciers. Mitteilungen der Versuchsanstalt für Wasserbau, Hydrologie und Glaziologie Nr.77 142pp.

HALLET, B. 1976: Deposits formed by subglacial precipitation of $CaCo_3$. Geological Society of America Bulletin 87 1003-1015.

HALLET, B. 1979: A theoretical model of glacier abrasion. Journal of Glaciology 23 39-50.

HALLET, B. 1981: Glacial abrasion and sliding: their dependence on the debris concentration in basal ice. Annals of Glaciology 2 23-28.

HAMBREY, M.J. & MULLER, F. 1978: Structures and ice deformation in the White Glacier, Axel Heiberg Island, North West Territories, Canada. Journal of Glaciology 20 41-66.

HARPER, A.P. 1893: Exploration and character of the principal New Zealand glaciers. Geographical Journal 1 32-42.

HARPER, A.P. 1934: Glacier retreat. New Zealand Alpine Journal 5 173-175.

HARPER, A.P. 1935: Glacier retreat. New Zealand Alpine Journal 5 322-326.

HARPER, A.P. 1946: Memories of Mountains and Men. Simpson & Williams, Christchurch, 208pp.

HARTSHORN, J.H. 1952: Supraglacial and proglacial geology of the Malaspina Glacier, Alaska, and its bearing on the glacial features of New England. Geological Society of America Bulletin 63 1259-1260.

HARTSHORN, J.H. 1958: Flow till in south-east Massachusetts. Bulletin of the Geological Society of America 69 477-482.

HARRINGTON, H.J. 1952: Glacier wasting and retreat in the Southern Alps of New Zealand. Journal of Glaciology 2 140-144.

HASTENRATH, S. 1987: On the relation of net balance, ice flow, and surface lowering of Lewis Glacier, Mount Kenya. Journal of Glaciology 33 315-318.

HAY, J.E. & FITZHARRIS, B.B. 1988: The synoptic climatology of ablation on a New Zealand glacier. Journal of Climatology 8 201-215.

HEALY, T.R. 1975: Thermokarst: a mechanism of de-icing ice-cored moraines. Boreas 4 19-23.

HESSELL, J.W.D. 1983: Climatic effects on the recession of the Franz Josef Glacier. New Zealand Journal of Science 26 315-320.

HICKS, M. ; McSAVENEY, M.J. & CHINN, T.J.H. (in press): Sedimentation rates in Ivory Lake- a proglacial lake in the high-rainfall zone of the Southern Alps, New Zealand. Arctic and Alpine Research.

HIGGINBOTTOM, I.E. & FOOKES, P.G. 1971: Engineering aspects of periglacial features in Britain. Quarterly Journal of Engineering Geology 3 85-117.

HODGE, S.M. 1974: Variations in the sliding of a temperate glacier. Journal of Glaciology 13 349-369.

HOEK, E. & BRAY, J.W. 1981: Rock Slope Engineering. Institute of Mining and Metallurgy, London, 358pp.

HOLDSWORTH, G. 1969: Structural glaciology of Meserve Glacier. Antarctic Journal of the United States 4 126-128.

HOLDSWORTH, G. 1978: Some mechanisms for the calving of icebergs, in Husseiny, A.A. (ed.) Iceberg Utilization Pergamon Press, Oxford, 160-175.

HOLLIN, J.T. & CAMERON, R.L. 1961: I.G.Y. glaciological work at Wilkes Station, Antarctica. Journal of Glaciology 3 833-842.

HOOKE, R. Le B. 1973: Flow near the margins of the Barnes ice cap, and development of ice-cored moraines. Geological Society of America Bulletin 84 3929-3948.

HOOKE, R. Le B. 1977: Basal temperatures in polar ice sheets: a qualitative review. Quaternary Research 7 1-13.

HOOKE, R. Le B.; DAHLIN, B.B. & KAUPER, M.T. 1972: Creep of ice containing dispersed fine sand. Journal of Glaciology 11 327-336.

HOOKE, R. Le B.; WOLD, B. & HAGEN, J.O. 1985: Subglacial hydrology and sediment transport at Bondhusbreen, southwest Norway. Geological Society of America Bulletin 96 388-397.

HUDLESTON, P.J. 1976: Recumbent folding in the base of the Barnes ice cap, Baffin Island, Northwest Territories, Canada. Geological Society of America Bulletin 87 1684-1692.

HUMLUM, Ø. 1981: Observations on debris in the basal transport zone of Myrdalsjokull, Iceland. Annals of Glaciology 2 71-77.

HUMLUM, Ø. 1988: Rock glacier appearance level and rock glacier initiation line altitude: a methodological approach to the study of rock glaciers. Arctic and Alpine Research 20 160-178.

IKEN, A.; FLOTRON, A; HAEBERLI, W. & ROTHLISBERGER, H. 1979: The uplift of Unteraargletscher at the beginning of the melt season - a consequence of water storage at the bed? Journal of Glaciology 23 430-431 (Abstract).

IRWIN, J. 1970: Lake Pukaki, Provisional Bathymetry 1:31680. New Zealand Oceanographic Institute Chart, Lake Series.

JOHNSON, P.G. 1971: Ice-cored moraine formation and degradation, Donjek Glacier, Yukon Territory, Canada. Geografiska Annaler 53A 198-202.

JOHNSON, P.G. 1974: Mass movement of ablation complexes and their relationship to rock glaciers. Geografiska Annaler 56A 93-101.

JOHNSON, P.G. 1980a: Rock glaciers: glacial and non-glacial origins. IASH Publication 126 285-293.

JOHNSON, P.G. 1980b: Glacier-rock glacier transition in the southwest Yukon Territory, Canada. Arctic and Alpine Research 12 195-204.

JOHNSON, P.G. & LACASSE, D. 1988: Rock glaciers of the Dalton Range, Kluane Ranges, south west Yukon Territory, Canada. Journal of Glaciology 34 327-332.

KAMB, B. 1970: Sliding motion of glaciers: theory and observation. Review of Geophysics and Space Physics 8 673-728.

KAMB, B. & LACHAPPELLE, E.R. 1964: Direct observation of the mechanism of glacier sliding over bedrock. Journal of Glaciology 5 159-172.

KAYE, C.A. 1960: Surficial geology of the Kingston Quadrangle, Rhode Island. United States Geological Survey Bulletin 1071-1 344-396.

KERSTEN, M.S. 1966: Thermal properties of frozen ground, in United States National Research Council Building Research Advisory Board; Proceedings of the International Conference on Permafrost. National Research Council Publication 1287 301-305.

KEYS, J.R.; ANDERTON, P.W. & KYLE, P.R. 1977: Tephra and debris layers in the Skelton Névé and Kempe Glacier, South Victoria Land,, Antarctica. New Zealand Journal of Geology and Geophysics 20 971-1002.

KICK, W. 1962: Variations of some central Asiatic glaciers. IASH Publication 58 223-229.

KICK, W. 1985: Geomorphologie und rezente Gletscherandrungen in Hochasien. Geographie: Naturwissenschaft und Geistewissenschaft. Regensburger Geographische Schriften Heft 19/20, 53-77.

KICK, W. 1986: Hundert jahre Sachéngletscher am Nanga Parbat-kein ausnahmeverhalten ? Internationales Symposium über Tibet und Hochasien, 8-11 Oct 1985. Gottinger Geographische Abhandlungen. Heft 81 8-11.

KIRKBRIDE, M.P. 1989: About the concepts of *continuum* and *age*. Boreas 18 88-89.

KNIGHTON, A.D. 1973: Grain size characteristics of supraglacial dirt. Journal of Glaciology 12 522-524.

KRAUS, H. 1966: Freie und bedeckte Ablation. Ergebn. Forschung - Unternehmen Nepal Himalaya. Leifg. 3 203-236.

KRENEK, L.O. 1958: The formation of dirt cones on Mount Ruapehu, New Zealand. Journal of Glaciology 3 312-314.

KRIMMEL, R.M. & VAUGHN, B.H. 1987: Columbia Glacier, Alaska: changes in velocity 1977-1986. Journal of Geophysical Research 92 B9 8961-8968.

KRISTENSEN, M. 1983: Iceberg calving and deterioration in Antarctica. Progress in Physical Geography 7 313-328.

KRUMBEIN, W.C. 1941: Measurement and geological significance of shape and roundness of sedimentary particles. Journal of Sedimentary Petrology 11 64-72.

KUHN, M. 1984: Mass budget imbalances as criteria for a climatic classification of glaciers. Geografiska Annaler 66A 229-238.

LANE, E.W. & CARLSON, E.J. 1954: Some observations on the effect of particle shape on the movement of coarse sediments. American Geophysical Union Transactions 35 453-462.

LAWSON, D.E. 1979: Sedimentological analysis of the western terminus region of the Matanuska Glacier, Alaska. Cold Regions Research and Engineering Report 79-9 122pp.

LAWSON, D.E. 1981: Distinguishing characteristics of diamictons at the margin of Matanuska Glacier, Alaska. Annals of Glaciology 2 78-84.

LAWSON, D.E. 1982: Mobilisation, movement, and deposition of active subaerial sediment flows, Matanuska Glacier, Alaska. Journal of Geology 90 279-300.

LEES, G. 1964: A new method for determining angularity of particles. Sedimentology 3 2-21.

LEVSON, V.M. & RUTTER, N.W. 1989: A lithofacies analysis and interpretation of depositional environments of montane glacial diamictons, Jasper, Alberta, Canada, in Goldthwait, R.P. & Matsch, C.L.(eds.) Genetic Classification of Glacigenic Deposits. A.A. Balkema, 117-141.

LEWIS, W.V. 1940: Dirt cones on the northern margins of Vatnajokull. Journal of Geomorphology 3 16-26.

LILLIE, A.R. 1962a: Geology of the southern part of the Mount Cook Range. New Zealand Journal of Geology and Geophysics 5 320-321.

LILLIE, A.R. 1962b: Geology of the Malte Brun Range, central Alps, New Zealand. New Zealand Journal of Geology and Geophysics 5 256-268.

LILLIE, A.R. 1964: Fold patterns in the New Zealand Alps indicative of drag along the axial belt. Report of the 22nd Session, International Geological Congress part 14 171-182.

LINDNER, L. & MARKS, L. 1985: Types of debris slope accumulations and rock glaciers in South Spitsbergen. Boreas 14 139-153.

LINDSAY, J.F. 1970: Depositional environment of Paleozoic glacial rocks in the central Transantarctic Mountains. Geological Society of America Bulletin 81 1149-1171.

LISTER, H. 1981: Particle size, shape and load in a cold and temperate valley glacier. Annals of Glaciology 2 39-44.

LLIBOUTRY, L. 1964: Traite de Glaciologie Masson, Paris, 2 volumes (478pp. and 162pp.)

LLIBOUTRY, L. 1968: General theory of subglacial cavitation and sliding of temperate glaciers. Journal of Glaciology 7 21-58.

LLIBOUTRY, L. 1977: Glaciological problems set by the control of dangerous lakes in Cordillera Blanca, Peru. 2. Movement of a covered glacier embedded within a rock glacier. Journal of Glaciology 18 255-274.

LLIBOUTRY, L. 1978: Glissement d'un glacier sur un plan parsémé d'obstacles hemispheriques. Annales Geophysiques 34 147-162.

LLIBOUTRY, L. 1983: Modifications to the theory of intraglacial waterways for the case of subglacial ones. Journal of Glaciology 29 216-226.

LLIBOUTRY, L. 1986: Discharge of debris by Glacier Hatunraju, Cordillera Blanca, Peru. Journal of Glaciology 32 133.

LLIBOUTRY, L.; ARNAO, B.M.; PAUTRE, A. & SCHNEIDER, B. 1977a: Glaciological problems set by the control of dangerous lakes in the Cordillera Blanca, Peru. 1. Historic failures of morainic dams, their causes and prevention. Journal of Glaciology 18 239-254.

LLIBOUTRY, L.; ARNAO, B.M. & SCHNEIDER, B. 1977b: Glaciological problems set by the control of dangerous lakes in Cordillera Blanca, Peru. 3. Study of moraines and mass balances at Safuna. Journal of Glaciology 18 275-290.

LOCKE, W.W. 1986: Fine particle translocation in soils developed on glacial deposits, southern Baffin Island, NWT, Canada. Arctic and Alpine Research 18 33-43.

LOOMIS, S. 1970: Morphology and ablation processes on glacier ice, in Bushnell, V.C. & Ragle, R.H. (eds) Icefield Ranges Research Project Scientific Results Vol. 2 27-31.

McGLONE, M.S. & MOAR, N,T. 1977: The Ascarina decline and post-glacial climatic change in New Zealand. New Zealand Journal of Botany 15 485-489.

McGLONE, M.S. & TOPPING, W.W. 1977: Aranuian (post-glacial) pollen diagrams from the Tongariro region, North Island, New Zealand. New Zealand Journal of Botany 15 749-760.

McKELLAR, I.C. 1962: Tasman Glaciological Observations, 5-18 November 1962. Unpublished report to the New Zealand Geological Survey.

McKELLAR, I.C. 1965: Tasman Glaciological Observations, 1-8 April 1965. Unpublished report to the New Zealand Geological Survey.

McKELLAR, I.C. 1966: Tasman Glaciological Observations, 26-27 October 1966. Unpublished report to the New Zealand Geological Survey.

McKELLAR, I.C. 1967: Ice ablation on the Tasman Glacier, New Zealand. Unpublished report, 16pp.

McKENZIE, G.D. 1969: Observations on a collapsing kame terrace in Glacier Bay National Monument, south-east Alaska. Journal of Glaciology 8 413-425.

McKENZIE, G.D. & GOODWIN, R.G. 1987: Development of collapsed glacial topography in the Adams Inlet area, Alaske, U.S.A. Journal of Glaciology 33 55-59.

McSAVENEY, M.J. 1975: The Sherman Glacier rock avalanche of 1964: its emplacement and subsequent effects on the glacier beneath it. Unpublished PhD thesis, Ohio State University, 403 pp.

McSAVENEY, M.J. 1978a: Sherman Glacier rock avalanche, Alaska, U.S.A. Chapter 6 in Voight, B. (ed.) Rockslides and Rock Avalanches 1, Natural Phenomena Elsevier 197-258.

McSAVENEY, M.J. 1978b: Magnitude of erosion across the Southern Alps. Proceedings of a Conference on Erosion Assessment and Control in New Zealand. New Zealand Association of Soil Conservators, 7-24.

McSAVENEY, M.J. & WHITEHOUSE, I.E. 1989: An early Holocene glacial advance in the Macauley River valley, central Southern Alps, New Zealand. New Zealand Journal of Geology and Geophysics 32 217-223.

McSAVENEY, M.J. & GAGE, M. 1968: Ice flow measurements on the Franz Josef Glacier, New Zealand, in 1966. New Zealand Journal of Geology and Geophysics 11 564-592.

MAIZELS, J.K.1977: Experiments on the origin of kettle holes. Journal of Glaciology 18 291-304.

MAIZELS, J. 1989: Differentiation of late Pleistocene terrace deposits using geomorphic criteria: Tekapo Valley, South Island, New Zealand. New Zealand Journal of Geology and Geophysics 32 225-242.

MANNERFELT, C.M. 1981: Stagnation or activity in the last ice remnants? Geografiska Annaler 63A 139-147.

MANSERGH, G. 1973: Excusion 7: The Central South Island. Guidebook for the 9th INQUA Congress, Christchurch, New Zealand.

MARANGUNIC, C. 1972: Effects of a landslide on the Sherman Glacier, Alaska. Institute of Polar Studies, Report No.30 Ohio State University Research Foundation.

MARCUS, M.G.; MOORE, R.D. & OWENS, I.F. 1985: Short-term estimates of energy transfers and ablation on the lower Franz Josef Glacier, South Westland, New Zealand. New Zealand Journal of Geology and Geophysics 28 559-567.

MARTIN, H.E. & WHALLEY, W.B. 1987: Rock glaciers Part 1: rock glacier morphology: classification and distribution. Progress in Physical Geography 11 260-282.

MATHEWS, W.H. 1959: Vertical distribution of velocity in Salmon Glacier, British Columbia. Journal of Glaciology 3 448-454.

MATHEWS, W.H. 1967: Profiles of Late Pleistocene glaciers in New Zealand. New Zealand Journal of Geology and Geophysics 10 146-164

MATTHEWS, J.A. 1987: Regional variation in the composition of Neoglacial end moraines, Jotunheimen, Norway: an altitudinal gradient in clast roundness and its possible palaeoclimatic significance. Boreas 16 173-188.

MATTHEWS, J.A., CORNISH, R. & SHAKESBY, R.A. 1979: "Saw-tooth" moraines in front of Bodalsbreen, Southern Norway. Journal of Glaciology 22 535-546.

MATTHEWS, J.A. & PETCH, J.R. 1982: Within-valley asymmetry and related problems of lateral moraine development at certain Jotunheimen glaciers, southern Norway. Boreas 11 225-247.

MEIER, M.F. & POST, A. 1987: Fast tidewater glaciers. Journal of Geophysical Research 92 B9 9051-9058.

MELLOR, M. & TESTA, R. 1969: Effect of temperature on the creep of ice. Journal of Glaciology 8 131-145.

MORAN, S.R.; CLAYTON, L.; HOOKE, R.L.; FENTON, M.M. & ANDRIASHEK, L.D. 1980: Glacier-bed landforms in the prairie region of North America. Journal of Glaciology 25 457-476.

MORLAND, L.W. 1976: Glacier sliding down an inclined wavy bed with friction. Journal of Glaciology 17 463-477.

MORLAND, L.W. & BOULTON, G.S. 1975: Stress in an elastic hump: the effects of glacier flow over elastic bedrock. Proceedings of the Royal Society (London) Series A 344 157-173.

MULLER, F. & KEELER, C.M. 1969: Errors in short-term ablation measurements on melting ice surfaces. Journal of Glaciology 8 91-106.

NAKA(W)O, M. 1979: Supraglacial debris of G2 Glacier in Hidden Valley, Mukut Himal, Nepal. Journal of Glaciology 22 273-283.

NAKA(W)O, M. & TAKAHASHI, S. 1982: A simplified model for estimating glacier ablation under a debris layer. in Proceedings of the Exeter Symposium on Hydrological Aspects of Alpine and High Mountain Areas, IAHS Publication 138 137-145.

NAKA(W)O, M. & YOUNG, G.J. 1981: Field experiments to determine the effect of a debris layer on ablation of glacier ice. Journal of Glaciology 2 85-91.

NAKA(W)O, M. & YOUNG, G.J. 1982: Estimate of glacier ablation under a debris layer from surface temperature and meteorological variables. Journal of Glaciology 28 29-34.

NAKA(W)O, M.; IWATA, S.; WANATABE, O. & YOSHIDA, M. 1986: Processes which distribute supraglacial debris on the Khumbu Glacier, Nepal Himalaya. Annals of Glaciology 8 129-131.

NIELSEN, E. & POST, A.S. 1953: The Castner Glacier Region, Alaska. Journal of Glaciology 2 277-280.

NYE, J. 1952a: The mechanics of glacier flow. Journal of Glaciology 2 82-93.

NYE, J. 1952b: A comparison between the theoretical and the measured long profile of the Unteraar Glacier. Journal of Glaciology 2 103-107.

NYE, J. 1959a: The deformation of a glacier below an ice-fall. Journal of Glaciology 3 387-408.

NYE, J. 1959b: A method of determining the strain rate tensor at the surface of a glacier. Journal of Glaciology 3 409-419.

NYE, J. 1969: The effect of longitudinal stress on the shear stress at the base of an ice sheet. Journal of Glaciology 8 207-213.

NYE, J. 1970: Glacier sliding without cavitation in a linear viscous approximation. Proceedings of the Royal Society (London) Series A 315 381-403.

NYE, J. 1976: Water flow in glaciers: Jokulhlaups, tunnels and veins. Journal of Glaciology 17 181-207.

ODELL, N.E. 1948: Stagnant glacier in British Columbia. Journal of Glaciology 1 191.

ODELL, N.E. 1960: The mountains and glaciers of New Zealand. Journal of Glaciology 3 739-744.

OGILVIE, I.H. 1904: The effect of superglacial debris on the advance and retreat of some Canadian glaciers. Journal of Geology 12 722-743.

OSBORN, G.D. 1978: Fabric and origin of lateral moraines, Bethartoli Glacier, Garwhal Himalaya, India. Journal of Glaciology 20 543-553.

ØSTREM, G. 1959: Ice melting under a thin layer of moraine and the existence of ice cores in moraine ridges. Geografiska Annaler 41A 228-230.

ØSTREM, G. 1965: Problems of dating ice-cored moraines. Geografiska Annaler 47A 1-38.

ØSTREM, G. 1971: Rock glaciers and ice-cored moraines, a reply to D. Barsch. Geografiska Annaler 54A 76-84.

ØSTREM, G. 1975: Sediment transport in glacial meltwater streams, in Jopling, A.V. & McDonald, (eds.) Glaciofluvial and Glaciolacustrine Sedimentation. SEPM Special Publication 23 .

ØSTREM, G. & STANLEY, A. 1969: Glacier mass-balance measurements- a manual for field work and office work. Canadian Departments of Mines and Resources and Norwegian Water Resources and Electricity Board, 107pp.

PAIGE, R.A. 1956: Subglacial stoping or block caving: a type of glacier ablation. Journal of Glaciology 2 727-729.

PATERSON, W.S.B. 1970: The sliding velocity of Athabasca Glacier, Canada. Journal of Glaciology 9 55-64.

PATERSON, W.S.B. 1981: The Physics of Glaciers. Pergamon, 2nd Edition 380 pp.

PESSL, F. & FREDERICK, J.E. 1981: Sediment source for meltwater deposits. Annals of Glaciology 2 92-96.

PICKARD, J. 1983: Surface lowering of ice-cored moraines by wandering lakes. Journal of Glaciology 29 338-342.

PICKARD, J. 1984: Retreat of ice scarps on an ice-cored moraine, Vestfold Hills, Antarctica. Zeitschrift für Geomorphologie N.F. 28 443-453.

PORTER, S.C. 1975a: Equilibrium-line altitudes of Late Quaternary glaciers in the Southern Alps, New Zealand. Quaternary Research 5 27-47.

PORTER, S.C. 1975b: Glaciation limit in New Zealand's Southern Alps. Arctic and Alpine Research 7 33-37.

PORTER, S.C. & DENTON, G. 1967: Chronology of Neoglaciation in the North American Cordillera. American Journal of Science 265 177-210.

PORTER, S.C. & OROMBELLI, G. 1980: Catastrophic rockfall of of September 12, 1717 on the Italian flank of the Mont Blanc massif. Zeitschrift für Geomorphologie N.F. 24 200-218.

PORTER, S.C. & OROMBELLI, G. 1981: Alpine rockfall hazards. American Scientist 69 67-75.

POSAMENTIER, H.W. 1978: Thoughts on ogive formation. Journal of Glaciology 20 218-220.

POST, A. 1967a: A non-earthquake origin for supraglacial debris on Martin River and Sioux Glaciers, Alaska. Journal of Glaciology 6 953-956.

POST, A. 1967b: Effects of the March 1964 Alaska earthquake on glaciers. United States Geological Survey Professional Paper 544-D 42pp.

POST, A. 1972: Periodic surge origin of folded medial moraines on Bering Piedmont Glacier, Alaska. Journal of Glaciology 11 219-226.

POTTER, N. 1972: Ice-cored rock glacier, Galena Creek, Northern Absaroka Mountains, Wyoming. Geological Society of America Bulletin 83 3025-3058.

POWERS, M. 1953: A new roundness scale for sedimentary particles. Journal of Sedimentary Petrology 25 117-119.

PRICE, R.J. 1969: Moraines, sandar, kames and eskers near Breidamerkùrjükull, Iceland. Institute of British Geographers Transactions 46 17-43.

RASMUSSEN, L.A. & MEIER, M.F. 1982: Continuity equation model of the predicted drastic retreat of Columbia Glacier, Alaska. United States Geological Survey Professional Paper 1258-A 23pp.

RAY, L.L. 1935: Some minor features of valley glaciers and valley glaciation. Joural of Geology 43 297-322.

REEH, N. 1968: On the calving of ice from floating glaciers and ice sheets. Journal of Glaciology 7 215-232.

REHEIS, M.J. 1975: Source, transportation and deposition of debris at Arapaho Glacier, Front Range, Colorado, U.S.A. Journal of Glaciology 14 407-420.

RISK, G.F. 1971: A resistivity sounding downstream from the terminal moraine of the Tasman Glacier. Unpublished report to the Superintendent, Geophysical Survey, 6pp.

ROBIN, G. de Q. 1979: Formation, flow and disintegration of ice shelves. Journal of Glaciology 24 259-271.

ROGERSON, R.J. 1986: Mass balance of four cirque glaciers in the Torngat Mountains of northern Labrador, Canada. Journal of Glaciology 32 208-218.

ROGERSON, R.J.; OLSON, M.E. & BRANSON, D. 1986: Medial moraines and surface melt on glaciers of the Torngat Mountains, Northern Labrador, Canada. Journal of Glaciology 32 350-354.

RÖTHLISBERGER, F. & SCHNEEBELI, W. 1979: Genesis of lateral moraine complexes, demonstrated by fossil soils and trunks; indicators of postglacial climatic fluctuations, in Schlüchter, C. (ed.) Moraines and Varves. Proceedings of the INQUA Symposium on Genesis and Lithology of Quaternary Deposits. Balkema, Rotterdam 387-419.

RÖTHLISBERGER, H. 1972: Water pressure in intra- and sub-glacial channels. Journal of Glaciology 11 177-203.

RÖTHLISBERGER, H. 1987:
Journal of Geophysical Research 92 B9

RUBULIS, S. 1983: Deposition in a thermokarst sinkhole on a valley glacier, Mount Tronador, Argentina, in Evenson, E.B., Rabassa, J. & Schlüchter, C. (eds.) Tills and Related Deposits A.A. Balkema, Rotterdam, 245-253.

SALINGER, M.J.; HEINE, M.J. & BURROWS, C.J. 1983: Variations of the Stocking (Te Wae Wae) Glacier, Mount Cook, and climatic relationships. New Zealand Journal of Science 26 321-338.

SALISBURY, R.D. 1894: Superglacial drift. Journal of Geology 2 613-632.

SAMES, C.W. 1966: Morphometric data of some recent pebble associations and their application to ancient deposits. Journal of Sedimentary Petrology 36 126-142

SARA, W.A. 1968: Franz Josef and Fox Glaciers 1951-1967. New Zealand Journal of Geology and Geophysics 11 768-780.

SARA, W.A. 1970: Glaciers of Westland National Park. Department of Scientific and Industrial Research Information Series No.75, 47pp.

SAUNDERS,I. & YOUNG, A. 1983: Rates of surface processes on slopes, slope retreat and denudation. Earth Surface Processes and Landforms 8 473-501.

SCHLÜCHTER, Ch. (Ed.) 1979: Moraines and Varves. Proceedings of the INQUA Symposium on Genesis and Lithology of Quaternary Deposits, 1978. A.A. Balkema, 441pp.

SCHYTT, V. 1967: A study of "ablation gradient". Geografiska Annaler 49A 327-332.

SCHUMM, S.A. 1979: Geomorphic thresholds: the concept and its applications. Transactions, Institute of British Geographers 4 485-515.

SELBY, M.J. 1980: A rock mass strength classification for geomorphic purposes: with tests from Antarctica and New Zealand. Zeitschrift für Geomorphologie N.F. 24 31-51.

SEPPÄLÄ, M. 1976: Stone roundness of moraines connected with Taku Glacier, south-eastern Alaska. Bulletin of the Geological Society of Finland 48 87-94.

SEREBRYANNY, L.R. & ORLOV, A.V. 1982: Genesis of marginal moraines in the Caucasus. Boreas 11 279-289.

SHAKESBY, R.A.; DAWSON, A.G. & MATTHEWS, J.A. 1987: Rock glaciers, protalus ramparts and related phenomena, Rondane, Norway: a continuum of large scale talus-derived landforms. Boreas 16 305-317.

SHARP, M. 1985: Sedimentation and stratigraphy at Ekjabakkajükull- an Icelandic surging glacier. Quaternary Research 24 268-284.

SHARP, M. & GOMEZ, B. 1986: Process of debris comminution in the glacial environment and implications for quartz sand-grain micromorphology. Sedimentary Geology 46 33-47.

SHARP, R.P. 1947: The Wolf Creek Glaciers, St. Elias Range, Yukon Territory. Geographical Review 37 26-52.

SHARP, R.P. 1949: Studies of superglacial debris of valley glaciers. American Journal Of Science 247 289-315.

SHAW, J. & ARCHER, J. 1979: Deglaciation and glacio-lacustrine sedimentation conditions, Okanagan Valley, British Columbia, Canada, in Schlüchter, Ch. (ed.) Moraines and Varves A.A. Balkema, - .

SHREVE, R.L. 1972: Movement of water in glaciers. Journal of Glaciology 11 205-214.

SHREVE, R.L. 1985: Esker characteristics in terms of glacier physics, Katahdin esker system, Maine. Geological Society of America Bulletin 96 639-646.

SHUMSKIY, P.A. 1978: Dynamic Glaciology. Amerind Publishing Company, New Delhi (translated by U. Radok and V.J. Vinocuroff).

SIKONIA, W.G. & POST, A. 1980: Columbia Glacier, Alaska: recent ice loss and its relationship to seasonal terminal embayment, thinning, and glacier flow. United States Geological Survey Hydrologic Investigations Atlas 619 3 sheets.

SKINNER, B.E. 1964: Measurement of Twentieth Century ice loss on the Tasman Glacier, New Zealand. New Zealand Journal of Geology and Geophysics 7 796-803.

SLATT, R.M. 1971: Texture of ice-cored deposits from ten Alaskan valley glaciers. Journal of Sedimentary Petrology 41 828-834.

SMALL, R.J. 1983: Lateral moraines of the Glacier de Tsidjiore Neuve: form, development and implications. Journal of Glaciology 29 250-259.

SMALL, R.J. & CLARK, M.J. 1974: The medial moraines of the lower Glacier de Tsidjiore Neuve. Journal of Glaciology 13 255-263.

SMALL, R.J.; CLARK, M.J. & CAWSE, T.J.P. 1979: The formation of medial moraines on alpine glaciers. Journal of Glaciology 22 43-52.

SMITH, N.D. 1985: Proglacial Fluvial Environment, in Ashley, G.M., Shaw, J. & Smith, N.D. (eds.) Glacial Sedimentary Environments Society of Economic Palaeontologists and Mineralogists Short Course No.16.

SMYTH, M.A. 1984: An assessment of methodologies for dating and correlating moraines. Unpublished BSc Honours thesis, University of St. Andrews.

SNEED, E.D. & FOLK, R.L. 1958: Pebbles in the lower Colorado River, Texas: a study in particle morphogenesis. Journal of Geology 66 114-150.

SOONS, J.M. 1971: Recent changes in the Franz Josef Glacier. Proceedings of the 6th New Zealand Geography Conference, Christchurch, 1970, Volume 1 195-200.

SOUCHEZ, R.A. & LORRAIN, R.D. 1975: Chemical sorting effect at the base of an alpine glacier. Journal of Glaciology 14 261-265.

SPEIGHT, R. 1940: Ice wasting and glacier retreat in New Zealand. Journal of Geomorphology 3 131-143.

SPEIGHT, R. 1942: A detail of the Pukaki moraine. Transactions and Proceedings of the Royal Society of New Zealand 72 148-159.

SPEIGHT, J.G. 1963: Late Pleistocene historical geomorphology of the Lake Pukaki area, New Zealand. New Zealand Journal of Geology and Geophysics 6 160-188.

SPÖRLI, K.B. & LILLIE, A.R. 1974: Geology of the Torlesse Supergroup in the northern Ben Ohau Range, Canterbury, New Zealand. New Zealand Joural of Geology and Geophysics 17 115-141.

SPÖRLI, K.B.; STANAWAY, K.J. & RAMSAY, W.R.H. 1974: Geology of the Torlesse Supergroup in the southern Liebig and Burnett ranges, Canterbury, New Zealand. Journal of the Royal Society of New Zealand 4 177-192.

STEPHENS, G.C.; EVENSON, E.B.; TRIPP, R.B. & DETRA, D. 1983: Active alpine glaciers as a tool for bedrock mapping and mineral exploration: a case study from Trident Glacier, Alaska, in Evenson et al (eds) Tills and Related Deposits, Balkema.

STURM, M.; BENSON, C. & MACKEITH, P. 1986: Effects of the 1966-8 eruptions of Mt. Redoubt on the flow of Drift Glacier, Alaska, U.S.A. Journal of Glaciology 32 355-362.

SUGDEN, D.E. 1978: Glacial erosion by the Laurentide ice sheet. Journal of Glaciology 20 367-392.

SUGDEN, D.E.; CLAPPERTON, C.M.; GEMMELL, J.C. & KNIGHT, P.G. 1987: Stable isotopes and debris in basal ice, South Georgia, Southern Ocean. Journal of Glaciology 33 324-329.

SUGGATE, R.P. 1952: Franz Josef Glacier, March, 1951. New Zealand Journal of Science and Technology 299-304.

SUGGATE, R.P. 1958: Late Quaternary deposits of the Christchurch metropolitan area. New Zealand Journal of Geology and Geophysics 1 103-122.

SUTHERLAND, D.G.; BALLANTYNE, C.K. & WALKER, M.J.C. 1984: Late Quaternary glaciation and environmental change on St. Kilda, Scotland, and their palaeoclimatic significance. Boreas 13 261-272.

SWITHINBANK, C.W.M. 1950: The origin of dirt cones on glaciers. Journal of Glaciology 1 461-465.

TARR, R.S. & MARTIN, L. 1914: Alaskan Glacier Studies. National Geographical Society, Washington, 498 pp.

THIEL, D.V. 1986: A preliminary assessment of glacier ice profiling using VLF surface impedance measurements. Journal of Glaciology 32 376-381.

THOMPSON, L.G. 1977: Variations in microparticle concentration, size distribution and elemental composition found in Camp Century, Greenland and Byrd Station, Antarctica, ice cores. Proceedings of the Grenoble Symposium, 1975 IAHS-AISH Publication 178 351-364.

THOMPSON, L.G. & MOSLEY-THOMPSON, E. 1987: Evidence of abrupt climatic change during the last 1,500 years recorded in ice cores from the tropical Quelccaya Ice Cap, Peru, in Berger, H. & Labeyrie, L.D. (eds) Abrupt Climatic Change. D. Reidel, 99-110.

THOMPSON, L.G.; MOSLEY-THOMPSON, E. & ARNAO, B.M. 1984: El Niño-Southern Oscillation events recorded in the stratigraphy of the tropical Quelccaya Ice Cap, Peru. Science 226 50-53.

TRICART, J. 1956: Etude éxperimentale du problème de la gélivation. Biuletyn Peryglacjalny 4 285-318.

TUTHILL, S.J. 1966: Earthquake origin of the superglacial drift on the glaciers of the Martin River area, south-central Alaska. Journal of Glaciology 6 83-88.

VERE, D.M. & MATTHEWS, J.A. 1985: Rock glacier formation from a lateral moraine at Bukkeholsbreen, Jotunheimen, Norway: a sedimentological approach. Zeitschrift für Geomorphologie N.F. 29 397-416.

VIVIAN, R. 1975: Les Glaciers des Alpes Occidentales. Allier, Grenoble, 513pp.

VOIGHT, B. (ed.) 1978: Rockslides and Avalanches, 1 Natural Phenomena. Elsevier, 833 pp.

WADELL, H. 1932: Volume, shape and roundness of rock particles. Journal of Geology 40 443-451.

WARDLE, P. 1973: Variations of glaciers of Westland National Park and the Hooker Range, New Zealand. New Zealand Journal of Botany 11 349-388.

WARREN WILSON, J. 1953: The initiation of dirt cones on snow. Journal of Glaciology 2 281-287.

WASHBURN, A.L. 1979: Geocryology: a Survey of Periglacial Processes and Landforms. Edward Arnold, 2nd Edition 406pp.

WATERHOUSE, J.B. 1966: The Häckel Syncline and neighbouring folds of the upper Tasman Glacier. Transactions of the Royal Society of New Zealand 14 183-195.

WATERHOUSE, J.B. 1972: Folds of the Mt Cook National Park and their origin under a wrench regime acting in a subduction zone. Journal of the Royal Society of New Zealand 2 413-430.

WATERHOUSE, J.B. 1985: Preliminary account of geology of Malte Brun Range, New Zealand. Australian Geologist Newsletter 57 7-8.

WATSON, R.A. 1980: Landform development on moraines of the Klutlan Glacier, Yukon Territory, Canada. Quaternary Research 14 50-59.

WEERTMAN, J. 1957: On the sliding of glaciers. Journal of Glaciology 3 33-38.

WEERTMAN, J. 1961: Mechanism for the formation of inner moraines found near the edge of cold ice caps and ice sheets. Journal of Glaciology 3 965-978.

WEERTMAN, J. 1964: The theory of glacier sliding. Journal of Glaciology 5 287-303.

WEERTMAN, J. 1969: The stress dependence of the secondary creep rate at low stresses. Journal of Glaciology 8 494-495.

WEERTMAN, J. 1971: In defence of a simple model of glacier sliding. Journal of Geophysical Research 76 6485-6487.

WELLMAN, H.W. 1979: An uplift map for the South Island of New Zealand, and a model for uplift of the Southern Alps, in Walcott, R.I. & Cresswell, M.M. (eds.) The Origin of the Southern Alps Royal Society of New Zealand Bulletin 18, 13-20.

WENTWORTH, C.K. 1922: A method of measuring and plotting the shapes of pebbles. Bulletin of the U.S. Geological Survey 730C 91-114.

WHALLEY, W.B. 1979: The relationship of glacier ice and rock glacier at Grubengletscher, Kanton Wallis, Switzerland. Geografiska Annaler 61A 49-61.

WHITE, S.E. 1976: Rock glaciers and block fields, review and new data. Quaternary Research 6 77-97.

WHITEHOUSE, I.E. 1982: Erosion on Sebastopol, Mt Cook, New Zealand, in the last 85 years. New Zealand Geographer 38 77-80.

WHITEHOUSE, I.E. 1983: Distribution of large rock avalanche deposits in the central Southern Alps, New Zealand. New Zealand Journal of Geology and Geophysics 26 271-279.

WHITEHOUSE, I.E. 1987: Geomorphology of a compressional plate boundary, Southern Alps, New Zealand, in Gardiner, V. (ed.) International Geomorphology 1986 Part 1 John Wiley & Sons Ltd., 897-924.

WHITEHOUSE, I.E. & GRIFFITHS, G.A. 1983: Frequency and hazard of large rock avalanches in the central Southern Alps, New Zealand. Geology 11 331-334.

WHITEHOUSE, I.E. & McSAVENEY, M.J. 1983: Diachronous talus surfaces in the Southern Alps, New Zealand, and their implications to talus accumulation. Arctic and Alpine Research 15 53-64.

WHITEHOUSE, I.E.; McSAVENEY, M.J.; KNUEPFER, P.L.K. & CHINN, T.J.H. 1986: Growth of weathering rinds on Torlesse Sandstone, Southern Alps, New Zealand, in Coleman, S.M. & Dethier, D.P. (Eds.) Rates of Chemical Weathering of Rocks and Minerals. Academic Press, 419-435.

WHITTEN, D.G.A. & BROOKS, J.R.V. 1985: The Penguin Dictionary of Geology. Penguin Books, 495pp.

WILLIAMS, E.R. 1967: Expedition in the Godley in 1917. The Press, Christchurch, 23 December 1967 p.5.

WILLIAMS, G.P. & WOLMAN, M.G. 1984: Downstream effects of dams on alluvial rivers. United States Geological Survey Professional Paper 1286 83pp.

WILSON, D.D. 1985: Erosional and depositional trends in rivers of the Canterbury Plains, New Zealand. Journal of Hydrology (N.Z.) 24 32-44.

WRIGHT, C.S. & PRIESTLEY, R.E. 1922: Glaciology. British (Terra Nova) Antarctic Expedition 1910-1913. Harrison & Sons, London, 581 pp.

APPENDIX 1 Location of survey stations.

Theodolite and E.D.M. surveys of ablation stakes and cairns used existing Trigonometric points where possible. These points are marked on NZMS 1 series topographic maps. Elsewhere, new stations were established and marked with a view to resurveys in the future. Details of survey stations used in surveys of each transect are given below.

	NZMS 1 Map ref.	Altitude	Comments
CELMISIA TRANSECT			
TRIG X	S79/810339	793.39 m	Thick scrub
TRIG W	S79/834415	1146.66 m	Level section of spur
Blue Lakes	S79/825359	813.70 m	Tourist viewpoint
BALL HUT TRANSECT			
TRIG W	S79/834415	1146.66 m	(as above)
TRIG V	S79/869424	1151.87 m	knob below Novara Spur
DE LA BECHE TRANSECT			
De la Beche Ridge	S79/892541	1579.69 m	rock knob above hut
Beetham	S79/901528	1637.53 m	outcrop just above trimline

Newly established stations were all marked with a cairn built over a rock bolt and paint mark. Details of Trig. point locations are available from the Department of Survey and Lands Information, Worcester Street, Christchurch.

APPENDIX 2 Survey methods

Field measurement of marker positions was made using a Wild T1-A optical theodolite and a Wild DI 4L Electronic Distance meter mounted on the theodolite. Each marker (cairn or stake) to be surveyed was visited by a field assistant with nine prisms set up on a tripod. Vertical and horizontal angles and distances were measured for each marker in a transect and from two survey stations at least 1 km apart. Radio contact between markers and stations is essential.

Intersection of angles and distances was carried out by Mr Derek Brown (DOSLI, Christchurch) using standard programs. Points were fixed relative to the DOSLI co-ordinate system. EDM data was found to be more precise than theodolite data, and adjustment made accordingly when angular miscloses were large (using a Bowditch correction). No temperature or pressure adjustments were made to the field measurements. Full details of the field data may be obtained from DOSLI, Christchurch.

Summary of data from McKellar (1966), adjusted to annual ablation rates based on seasonal variation established in this study

Altitude (m)	Period	Daily rate cm	Annual ice loss (m) 1964-5
1630	14/11-10/4	2.84	4.36
	14/11- 10/4	2.62	4.70
1580	14/11-9/10	1.71	5.90
	" "	1.47	5.00
1550	" 10/4	3.95	5.80
	" "	3.57	5.25
1240	15/4-3/4	2.75	10.25
1180	14/4-6/4	3.25	12.00
1070	17/4-8/4	3.69	13.45
1040	" 2/4	3.63	13.20

	1965-6
1630	5.10
	6.10
1580	5.00
	7.36
1550	5.60
1530	6.10
	7.30
1250	11.50
1230	11.45
	10.00
1180	10.00
	12.20
1120	13.60
	14.20
	14.40
1070	14.40
1030	13.00

APPENDIX 4 Corrections made to ablation stake measurements

Muller & Keeler (1969) found that short ablation stakes tend to transmit heat to the bottom of their holes and cause melting there. The observed emergence of the stake is then no longer a measure of the surface lowering of the glacier, since the base of the stake is not fixed in position relative to the glacier. On the Tasman Glacier, I experimented to assess the significance of this "melt-subsidence" effect for the 2 m long stakes being used.

Holes were drilled to different depths at the same site, and stakes placed. Remeasurement between 1 and 5 days later allowed the emergence of deeply-placed stakes (2 m) to be compared to that of stakes whose bases lay closer to the ice surface. The experiment was carried out over 5 periods at the Ball Hut transect and over 1 period at the De la Beche transect. The results indicate that melt-subsidence causes an underestimate of glacier ablation when less than c.1 m of stake remains below the ice surface. The scatter of points is great, however, due to other problems of short-term measurements (particularly "weathering crust" formation: Muller & Keeler 1969).

Although a well-constrained relationship between the underestimate of ablation and the buried stake length has not been acheived, intuitively the error will be greater when less stake length remains in the hole. The line shown in the diagram has therefore been adopted to make some allowance for the melt-subsidence effect. All field measurements have been adjusted if less than 1 m of stake remained in the hole when remeasured. The underestimate is generally less than 10%, but occasionally up to 20%.

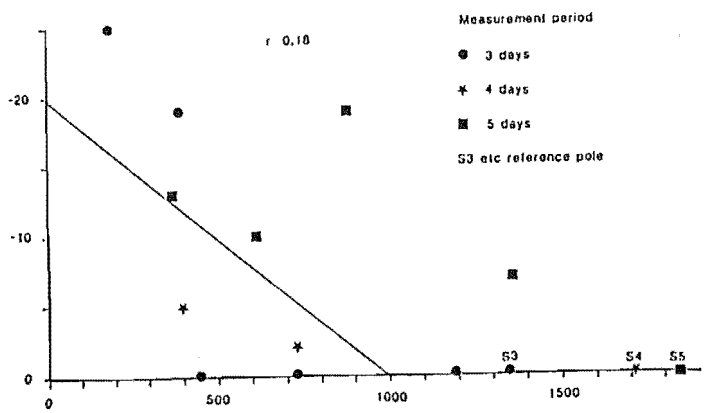

APPENDIX 5 Calculation of ice level changes.

The figure illustrates the geometry of two cases, one where the ice surface is rising and one where it is falling. Using the notation shown, if the surface is rising, the change in elevation, (d-h), is given by

$$(d - h) = l.\tan B$$

If the surface is rising, the change in elevation becomes (d+h), and:

$$(d + h) = l.\tan B$$

using these equations, the change in ice surface elevation for each marker on the Tasman Glacier is listed below.

Transect 3 De la Beche

Values in metres: (d+h) = positive value, (d-h) = negative value

(a) Nov 85 - May 86 (b) May - Dec 86

	174 days	213 days	annual change
P2	- 2.51	+ 5.06	+ 3.41
P3	- 3.05	+ 6.02	+ 4.23
P4	- 3.76	+ 5.58	+ 1.67
P5	- 4.98	+ 5.56	- 0.75
P7	- 4.43	+ 8.33	+ 4.98

$$\text{annual change} = \frac{a}{174} + \frac{b}{213} \times 365$$

Transect 2 Ball Hut

	Elevation (m)			Horizontal	Slope	Elev. change	Annual
	May	Dec	Change	movement (m)		(l.tan B) + d	change*
F1	977.6	978.4	+ 0.8	37.79	2.3	+ 2.32	+ 1.00
P1	960.2	964.0	+ 3.8	46.39	"	+ 5.66	+ 2.45
P4	955.9	959.3	+ 3.4	45.58	"	+ 5.23	+ 2.26
P3	964.9	968.8	+ 3.9	47.21	"	+ 5.79	+ 2.50
F2	975.9	978.8	+ 2.9	51.05	"	+ 4.95	+ 2.14
F3	966.9	970.5	+ 3.6	47.14	"	+ 5.49	+ 2.38
F4	980.6	981.4	+ 0.8	42.38	"	+ 2.50	+ 1.08
MEAN.....							+ 1.98

* based on ratio of winter surface rise to summer fall of 0.75, determined at De la Beche transect.

Transect 1 Celmisia Flat.

At transect 1, the glacier slope and velocity are negligible. Annual elevation changes quoted in Chapter 2.2 were calculated by weighting the measured elevation change with respect to the length of the measurement period, with the same seasonal adjustment as for the other transects.

APPENDIX 6 Calculation of englacial debris concentration.

From an examination of the 1986 debris mantle thickness and from the map of debris mantle spreading (Fig 4.), the thickness of debris in 1986 at the lowest point of bare ice in previous years was estimated. These points are the location of the furthest down-glacier extensions ofbare ice recorded on maps and aerial photographs.

Between each pair of dates, the debris mantle spred upglacier by d in n years. Assuming a constant downglacier thickening in the debris mantle, it follows that the debris has thickened by Δh at each point formerly occupied by bare ice.

From the known bare-ice ablation gradient, the annual loss at each point (a) is estimated. The englacial debris concentration, c, required to produce the observed thickening in supraglacial debris is given by;

$$c = \frac{\Delta h}{n \times a}$$

Values of c calculated by this method are probably minima because no account has been taken for reduced ablation beneath debris thicker than c.10 cm. Thinner debris will have had a compensating effect by increasing ablation, however. Calculations of c cover 4 periods;

	h (m)	a (m)	n (yr)	c	c (vol.%)
1971-86	0.1	16	15	0.00042	0.042
1965-86	0.125	16	21	0.00037	0.037
1947-86	0.2	15	39	0.00034	0.034
1890-86	0.3	13	96	0.00024	0.024

The decrease in c over time is apparent, being a product of the assumption that debris cover does not reduce ablation beneath. Thus the highest estimate of c will be closest to the true value

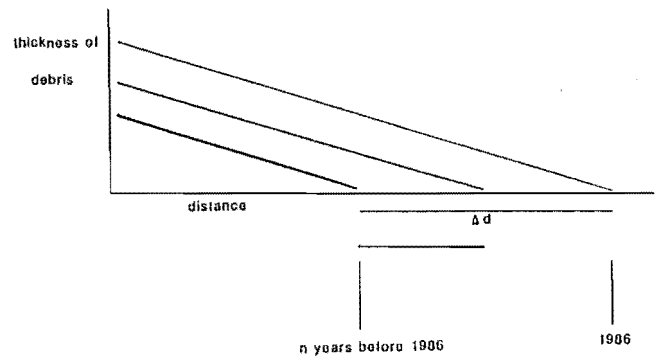

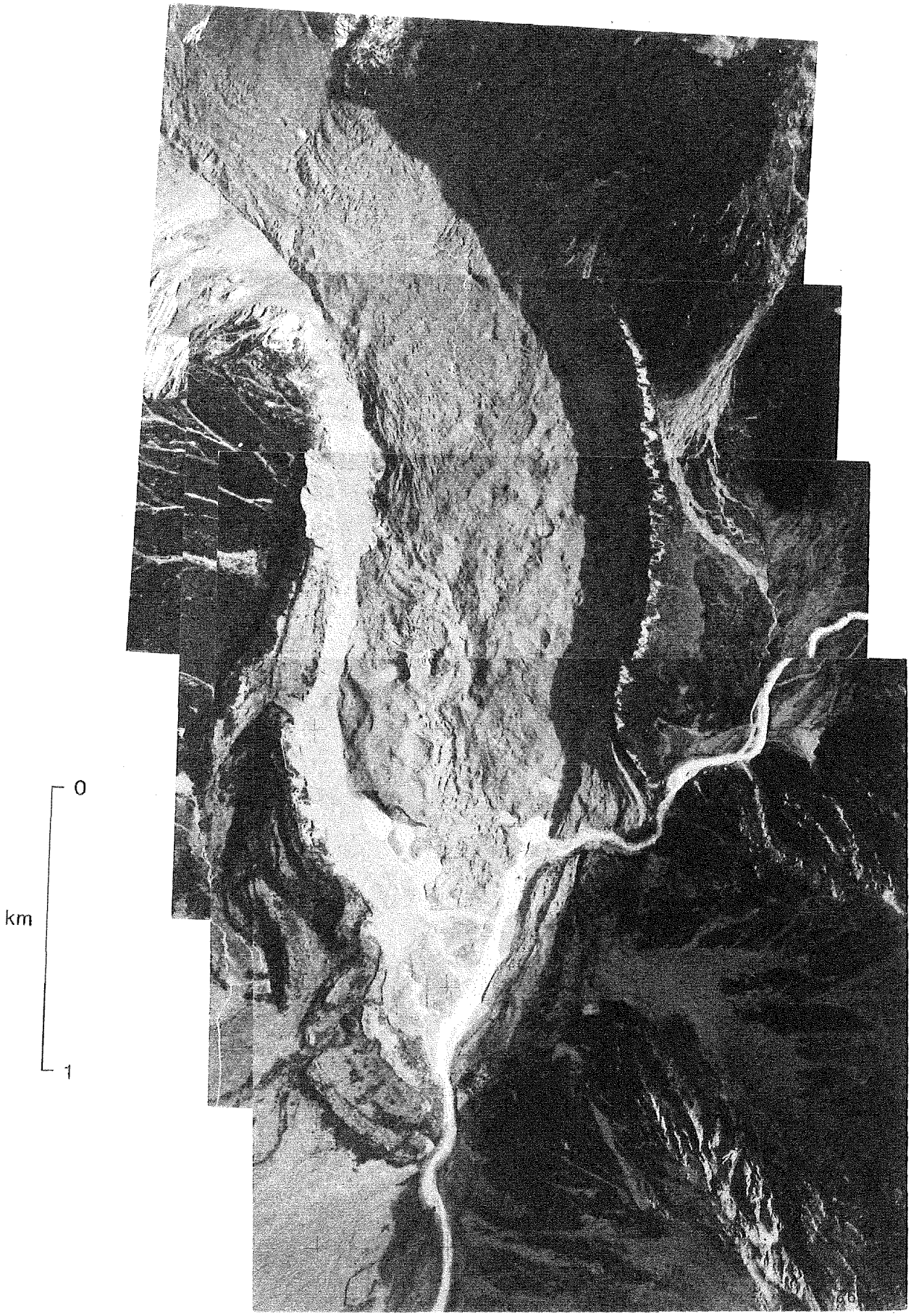

Figure A 2

MUELLER GLACIER February 1986

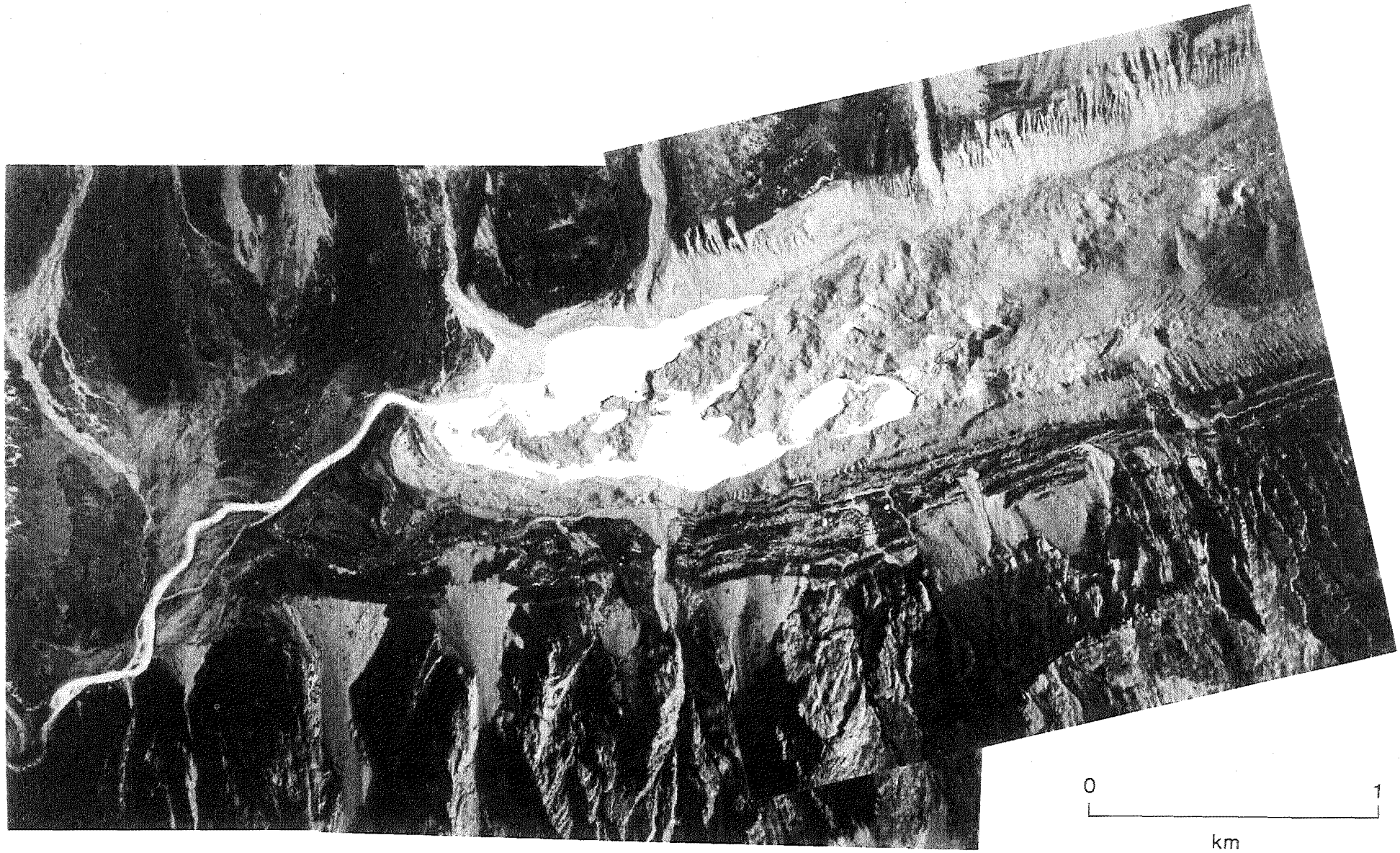

Figure A 3

HOOKER GLACIER

February 1986

ACKNOWLEDGEMENTS

Many people have assisted in the completion of field work and the writing of this thesis. I am particularly grateful to Professor Jane Soons for her supervision, and for helpful advice at all stages of the thesis. Lengthy discussions and debates with Trevor Chinn and Dr. Mauri McSaveney stimulated many thoughts and ideas, both in the office and in the field. Professor Jim Cole was a source of constant encouragement.

Field assistants who have accompanied me include; John Atkinson; Paul Augustinus; Vanessa Brazier; Derek Chinn; Trevor Chinn; Mary-Rose Fowlie; Mark Lawrence; Caroline Lucas; Myles McCauley; Rob McCone; Veijo Pohjola; Derek Shaw; and Mary-Ann Waters. Mark also kindly devoted time to help in the final stages of compiling the thesis.

The staff of the Department of Conservation at Mount Cook National Park have freely given help and shown interest in the study, particularly Martin Heine, Ray Bellringer, and Alan Wilson. I am very grateful to Ray Slater and his staff for this help.

Several visiting geomorphologists and glaciologists have also given useful advice, and Dr George Denton and Dr Mike Hambrey spent time with me in the field. Drs Willi Kick kindly provided information on Asian glaciers for comparison with New Zealand work. Thanks also to participants of the 1988 I.G.S. tour for a stimulating week in the Southern Alps.

The secretarial and technical staff of the Department of Geology have assisted with many practical and logistical aspects of the thesis. Albert Downing very efficiently printed the photographs. I also thank Derek Brown of the Department of Survey and Lands Information for his assistance with processing survey data, and for his general enthusiasm for the project. Thanks also to Tracey for the final printing of this thesis.

I am also grateful to Dr David and Iola Shelley and to Professor Tony Crawford for their hospitality on my arrival in New Zealand, and to all the other lecturing staff who have offered advice and encouragement.

Finally, thanks to Nes for her practical help in the final stages of the thesis, and for her patience, encouragement and support throughout.

I dedicate the thesis to my parents.